2021

Proceedings of the 1st NSE Minna Branch Engineering Conference

The Nigerian Society of Engineers

Minna Branch

1st NSE Minna Branch Engineering Conference

Conference theme

Role of Engineering in Sustainable Development Goals

Nigerian

Society of

Engineers

Minna Branch

The Nigerian Society of Engineers
Minna Branch
1st NSE Minna Branch Conference 2021

Conference theme

Role of Engineering in Sustainable Development Goals

Conference Date: Wednesday 9th to Thursday 10th June 2021

Conference Overview

Primarily, Engineering innovations are concerned with improving human living standards, protecting and restoring the environment. To this end, sustainable Engineering strives to design or operate systems for efficient usage of resources. As a major stakeholder in sustainable development, the NSE Minna Branch, in partnership with COREN, NITDA, NASENI and SEDI-Minna, is organizing the 1st National Conference. The theme focuses on the roles of Engineering in attaining the 17 sustainable development goals within and outside Nigeria.

Local Organizing Committee	
Engr. Prof. Abdulkarim Ambali Saka, MNSE	Chairman
Engr. Prof. Abdulsalami Sanni Kovo, MNSE	Co-Chairman
Engr. Dr. Abubakar Sadiq Ahmad, MNSE	Secretary
Engr. Prof. Abdulrahman Salawu Asipita, MNSE	Member
Engr. Dr. Caroline Alenoghena, MNSE	Member
Engr. Dr. Elizaberth J. Eterigho, FNSE	Member
Engr. Dr. Muhammadu M. Masin, MNSE	Member
Engr. Dr. Mohammed Liman Yerima, MNSE	Member
Engr. David Bala Jiya, MNSE	Member
Engr. Muhammad N. Abdullahi, MNSE	Member
Engr. Abubakar Takuma, MNSE	Member
Engr. Solomon Joseph Ibrahim, MNSE	Member

Executive Committee Members NSE Minna Branch	
Engr. Dr. Elizaberth J. Eterigho, FNSE	Chairman
Engr. Dr. Muhammadu M. Masin, MNSE	Vice Chairman
Engr. Dr. Mohammed Liman Yerima, MNSE	General Secretary
Engr. Muhammad N. Abdullahi, MNSE	Asst. Gen Sec.
Engr. Mohammed Danjuma Abubakar, MNSE	Treasurer
Engr. Hadiza Danyaya, MNSE	Financial Secretary
Engr. Dr. Abubakar Sadiq Ahmad, MNSE	Tech. Secretary
Engr. Omotoso Oladipo, MNSE	Asst. Tech. Secretary
Engr. Solomon Joseph Ibrahim, MNSE	Publicity Secretary
Engr. Prof. Mohammed Baba Ndaliman, MNSE	Ex-offcio I
Engr. Hauwa Abubakar Gimba, MNSE	Ex-offcio II

The Nigerian Society of Engineers
Minna Branch
1st NSE Minna Branch Conference 2021

Conference theme

Role of Engineering in Sustainable Development Goals

Conference Date: Wednesday 9th to Thursday 10th June 2021

Conference Editorial Committee

Engr. Dr. Abubakar Sadiq Ahmad, MNSE *Department of Electrical and Electronics Engineering, FUT Minna, Nigeria.*	*Chief Editor/* *Tech. Sec*
Engr. Prof. Abdulkarim Ambali Saka, MNSE *Department of Chemical Engineering, FUT Minna, Nigeria.*	*Chief Editor* *SIPET*
Engr. Prof. Abdulsalami Sanni Kovo, MNSE *Department of Chemical Engineering, FUT Minna, Nigeria.*	*Co-Chief Editor* *SIPET*
Engr. Dr. Caroline Alenoghena, MNSE *Department of Telecomunication Engineering, FUT Minna, Nigeria.*	*Chief Editor* *SEET*
Engr. Dr. Bala A. Salihu, MNSE *Department of Telecomunication Engineering, FUT Minna, Nigeria.*	*Co-Chief Editor* *SEET*
Engr. Prof. Abdulrahman Salawu Asipita, MNSE *Department of Materials and Metallurgy Engineering, FUT Minna, Nigeria.*	Member
Engr. Prof. Oluwafemi Ayodeji Olugboji, MNSE *Department of Mechanical Engineering, FUT Minna, Nigeria.*	Member
Engr. Prof. Abdulkarim Nasir, MNSE *Department of Mechanical Engineering, FUT Minna, Nigeria.*	Member
Engr. Dr. Musa Alhassan, MNSE *Department of Civil Engineering, FUT Minna, Nigeria.*	Member
Engr. Dr. Abraham U. Usman, MNSE *Department of Telecomunication Engineering, FUT Minna, Nigeria.*	Member
Engr. Dr. Sunday Albert Lawal, MNSE *Department of Mechanical Engineering, FUT Minna, Nigeria.*	Member
Engr. Dr. Olatomiwa Lanre, MNSE *Department of Electrical and Electronics Engineering, FUT Minna, Nigeria.*	Member
Engr. Dr. David Micheal, MNSE *Department of Telecomunication Engineering, FUT Minna, Nigeria.*	Member
Engr. Dr. Henry Ohize *Department of Electrical and Electronics Engineering, FUT Minna, Nigeria.*	Member
Engr. Dr. Umar Suleiman Dauda, MNSE *Department of Electrical and Electronics Engineering, FUT Minna, Nigeria.*	Member
Engr. Dr. Adedipe Oyewole, MNSE *Department of Mechanical Engineering, FUT Minna, Nigeria.*	Member
Engr. Dr. Elizaberth J. Eterigho, FNSE *Department of Chemical Engineering, FUT Minna, Nigeria.*	Member
Engr. Dr. Taiye Adejumo, MNSE *Department of Civil Engineering, FUT Minna, Nigeria.*	Member
Engr. Dr. Solomon Dauda, MNSE *Deparment of Agricultural and Bioresources Engineering FUT Minna, Nigeria*	Member
Engr. Dr. Alkali Babawuya, MNSE *Department of Mechatronics Engineering, FUT Minna, Nigeria.*	Member
Engr. Dr. Muhammadu Muhammadu Masin, MNSE	Member

The Nigerian Society of Engineers
Minna Branch
1st NSE Minna Branch Conference 2021

Conference theme

Role of Engineering in Sustainable Development Goals

Conference Date: Wednesday 9th to Thursday 10th June 2021

Department of Mechanical Engineering, FUT Minna, Nigeria.

Engr. Dr. Mohammed Liman Yerima, MNSE
Department of Materials and Metallurgy Engineering, FUT Minna, Nigeria.   Member

Engr. Abdullazeez Yusuf, MNSE
Department of Civil Engineering, FUT Minna, Nigeria.   Member

Engr. Mahmud Abubakar, MNSE
Department of Civil Engineering, FUT Minna, Nigeria.   Member

Engr. Jibril Abdullahi Bala, MNSE
Department of Mechatronics Engineering, FUT Minna, Nigeria.   Member

The Nigerian Society of Engineers
Minna Branch
1st NSE Minna Branch Conference 2021

Conference theme

Role of Engineering in Sustainable Development Goals

Conference Date: Wednesday 9th to Thursday 10th June 2021

TABLE OF CONTENT

The Nigerian Society of Engineers
Minna Branch
1st NSE Minna Branch Conference 2021

Conference theme

Role of Engineering in Sustainable Development Goals

Conference Date: Wednesday 9th to Thursday 10th June 2021

The Nigerian Society of Engineers
Minna Branch
1st NSE Minna Branch Conference 2021

Conference theme

Role of Engineering in Sustainable Development Goals

Conference Date: Wednesday 9th to Thursday 10th June 2021

The Nigerian Society of Engineers
Minna Branch
1st NSE Minna Branch Conference 2021

Conference theme

Role of Engineering in Sustainable Development Goals

Conference Date: Wednesday 9th to Thursday 10th June 2021

The Nigerian Society of Engineers
Minna Branch
1st NSE Minna Branch Conference 2021

Conference theme

Role of Engineering in Sustainable Development Goals

Conference Date: Wednesday 9th to Thursday 10th June 2021

University Research and Innovation for Regional Economic Development: Panacea for Eradication of Extreme Poverty in Nigeria

OKOPI ALEX MOMOH

Executive Secretary,

Nigerian Society of Engineers, National Engineering Centre, Abuja

okopimomoh@yahoo.com +2348037196213

ABSTRACT

The natural and human resources endowment of Nigeria is enormous. Paradoxically, the nation remains largely poor due to inadequate exploitation of these resources. Every region of the country is richly endowed with resources for sustainable economic development. However, there has not been a sustained and collective advocacy for collaboration and synergy for sustainable regional development in Nigeria. This paper studied and recommended the Triple Helix Collaboration Model among Government, Industry and the Academia where Government provides the necessary infrastructure and enabling environment for investment by Industry while the Academia provides the intellectual properties for enterprise development through licensing of patents. This will lead to focused applied research by our tertiary institutions for regional economic development, open more opportunities for Nigerian Engineers to be actively involved in regional economic development activities through job and employment creation and create more visibility for Nigerian Engineers. The proposed model will also lead to establishment of Innovation hubs and Industrial parks to stimulate manufacturing contribution to the nation's Gross Domestic Product (GDP) which is currently only at 6%.

KEYWORDS: *Regional development, Research, Entrepreneurial University, Triple Helix Model, Intellectual Property, Innovation, Commercialization, Manufacturing*

1. INTRODUCTION

Every region of Nigeria is endowed with enormous human and natural resources. Paradoxically the country is regarded as the poverty capital of the world. The national focus on resource utilization has only been on sale of crude oil as the main source of national revenue. Most of the county's other exports are raw materials without value addition. The country exports crude oil and imports refined petroleum products. Similarly, jewelries are imported from exported raw gold and many other such commodities because of lack of in-country processing capabilities. With technology advancing rapidly towards clean energy globally, emergence of electric cars and huge global investments in renewable energy systems, the future of crude oil as a national revenue source is becoming very bleak. The need to develop other resources has become very paramount.

The global economy has become a knowledge - driven economy. Internationally, regional economic development has been founded on innovation and research activities. The Regional Innovation System (RIS) has become popular among academics, political decision makers and regional stakeholders of innovation. Academic institutions conduct substantial volumes of research that are funded by government, industry, and philanthropic organizations. In Nigeria, the Tertiary Education Trust Fund (TETFUND) spends a lot of money on Institution Based Research both in Universities and Polytechnics. For Nigeria to utilize the potentials of university research, there is a need for universities to conduct scholarly activities that translate both basic and applied research into commercially viable processes and technologies (Sanberg et al 2014). In developed and newly industrializing nations, there is pressure on university-based research by way of increased emphasis on the commercialization of research (Ogbogu & Caulfield 2015, Hand et al 2013, Caulfield 2012, Rasmussen 2008, Downie & Herder 2007).

Commercialization of research which is a primary means through which research results are utilized to generate products and services, should also be a key component of the research mission such that novel ideas, techniques and products can be generated for the marketplace for the benefit of relevant stakeholders and society in general. Societal expectations of tertiary institutions now go beyond

The Nigerian Society of Engineers
Minna Branch
1st NSE Minna Branch Conference 2021

Conference theme

Role of Engineering in Sustainable Development Goals

Conference Date: Wednesday 9th to Thursday 10th June 2021

just teaching and research. The missions of higher education institutions are expanding to include economic development, of which translation of research is a major part ((Hand et al, 2013). The greatness of a university is not just in its ability to attract research grants and contracts but also in how the university impacts and changes the world and society at large (Caulfield, 2012).

The United States of America former President Obama's enthusiastic endorsement of the use of academic research to drive economic growth in his State of the Union Addresses (Obama 2014, Obama 2015a,) and in other speeches (Macilwain 2010, Obama 2011, Obama 2015b) is one high profile example of government policy commitment to commercialization of research outputs. President Obama's remark that "Twenty-first century businesses will rely on American science and technology, research and development" (Obama 2015a) is a propelling policy commitment to the use of research for industrialization. According to Claulfield and Ogbogu (2015), other world leaders who have made similar policy commitments include the former Prime Minister of Canada, Stephen Harper who was of the view that scientific research should be used to power commerce. In the industrialized countries of America, Canada and Europe, there is a growing political view that universities ought to play a central role in the growth of economies (Petersen & Krisjansen 2015, Philpott et al 2010) or to accord with national or regional economic priorities (Claulfield & Ogbogu 2015, Simons 2015, Caulfield 2010). In these countries, if researchers want funding, they must frame their work in line with the commercialization ethos (Claulfield & Ogbogu 2015).

The paper discusses the research and innovation commercialization lessons from some developed and newly industrializing nations as classical examples of how the application of technologies drives economic and industrial development of nations. It typically highlights a rich variety of policy initiatives at the State and Regional levels in America as best practice examples to foster knowledge-based growth and development.

According to Vanderford and Marcinkowski (2015), United States-based institutions generated over 24,000 disclosures, obtained over 5,000 new patents, executed over 5,000 licensing agreements, formed over 800 start-up companies, and generated $2.75 billion in license income in 2013. The Bayh-Dole Act in America has stimulated a substantial acceleration in the patenting and licensing of university-developed technologies. The Canadian government in its 2006 to 2008 budgets provided additional $2.2 billion in new funding for science and technology initiatives with commercialization efforts at Canadian universities developing into an integral part of research and innovation activities.

According to Dodd (2017) the Hebrew University of Jerusalem, an institution which boasts of Albert Einstein as one of its founders, has earned **over** $20 billion in commercialization revenue over the years. The reasons for the Hebrew University of Jerusalem's success in research and commercialization include incentives to its researchers to commercialize and counting of patents for promotion. Patents are counted as part of the portfolio of a professor to be promoted in addition to publications. Researchers, departments and faculties, are also rewarded when technology is commercialized. Since the establishment of Hebrew University of Jerusalem in 1964 the university's technology transfer arm, the *Yissum Research Development Company*, has registered over 9300 patents covering 2600 inventions, licensed 800 technologies and spun off 110 companies.

According to Leichman (2018), "Universities are reinventing themselves as microenvironments for innovation and entrepreneurship. A university that can't demonstrate its impact on industry and the marketplace will become less relevant in the future,"

Comparatively, Nigerian tertiary institutions and research institutes do not make significant contributions to the socio-economic development of the nation through commercialization of research results despite the high number of students' research projects and relatively huge sums of money spent on research annually.

2. **UNIVERSITIES AS INNOVATION AND ENTREPRENEURSHIP DRIVERS FOR REGIONAL ECONOMIC DEVELOPMENT**

A major factor in the rise of the United States as a technological power has been attributed to a long tradition of close ties and frequent collaboration between companies and universities. Underlying the success of regional innovation clusters such as Silicon Valley, Route 128, and the Research Triangle of North Carolina are local universities with a longstanding mission of spurring economic development by developing and transferring technology to local industries and stimulating the creation of new businesses in university-centered incubators and science parks. Technology-intensive companies commonly locate their operations near the best universities in particular fields of science and Engineering to enable their internal research departments to work with "star" scientists and to recruit promising students.

Start-up companies spinning off from universities most commonly establish operations near those institutions. The Association of University Technology Managers (AUTM) reported in 2002 that in the fiscal year 2000, at least 368 new companies were formed based on university research and that most of them settled "near the institution where the technology was born (AUTM, 2002). "The presence of research universities is now widely viewed as a necessary condition to bring about innovation-based economic development of regions." (Wessner,2013). Illustrating the impact, a single research university can have on a region, in 2004 alone MIT produced 133 patents, launched 20 startup companies, and spent $1.2 billion in sponsored research. Data from 1994 showed that, at that time, MIT graduates had founded over 4,000 companies employing 1.1 million people generating $232 billion in sales worldwide (Daniel, 2011). In the Boston area, MIT is flanked by other great research universities, including Harvard, Tufts, the University of Massachusetts, Boston University, and others. Since the early 1970s, spinoffs from these institutions have created a thriving pharmaceutical industry where virtually none had previously existed (Stevens, 2011).

According to San Diego (2017**),** the licensing of university research has made significant contributions to US gross domestic product (GDP), industry gross output, and jobs over the last two decades**.** The report, "The Economic Contribution of University/Nonprofit Inventions in the United States: 1996- 2015," documents the sizeable return that US taxpayers receive on their investment in federally funded research. It shows that, during a 20-year period, academic patents and the subsequent licensing to industry bolstered US industry gross output by up to $1.33 trillion, US GDP by up to $591 billion, and supported up to 4,272,000 jobs.

3. THE EMERGENCE OF THE ENTREPRENEURIAL UNIVERSITY

With a knowledge-based economy in a globalization-governed world, higher education institutions bear the responsibility of producing graduates with a long list of technical and professional skills (Nasr, 2014). These graduates must be equipped with fundamental knowledge and skills to solve problems never seen before in a world that is open and competitive.

According to O'Connor et al (2012), the traditional higher education paradigm has evolved and is now characterized by a strong focus on the development of academic entrepreneurship through the commercialization of higher education research with campus and graduate enterprise development. Higher education encompasses several roles from teaching to scientific research and translation of research results into economic development through knowledge transfer (Etzkowitz *et al*, 2000). This is referred to as an **Entrepreneurial University Education***,* whose purpose is to transform academic knowledge into economic and social utility (Clark, 1998). With a focus on effective knowledge transfer and the creation of new campus businesses, the **Entrepreneurial University** also enhances the competitive advantage of existing enterprise entities both in and outside the institution. **Entrepreneurial Universities** include teaching and research activities as core to their mission whilst also focusing on academic entrepreneurship as a key contributor to economic development. Essentially, an Entrepreneurial University should comprise (i) spin-offs and spin-ins; (ii) Entrepreneurial Education; (iii) links with SMEs and industry; (iv) the development of diverse income streams; and (v) campus incubators.

Van der Sijde and Ridder (1999) argued that the best guarantee for sustainability of entrepreneurship within a higher education institution is to change it

The Nigerian Society of Engineers
Minna Branch
1st NSE Minna Branch Conference 2021

Conference theme

Role of Engineering in Sustainable Development Goals

Conference Date: Wednesday 9th to Thursday 10th June 2021

into an entrepreneurial organization; that is, what holds for the integration of entrepreneurship in the academic curricula also holds for the commercialization of research via spin-off companies.

4. **COMMERCIALIZATION OF UNIVERSITY RESEARCH AND INNOVATION FOR ECONOMIC DEVELOPMENT**

Most research universities in the developed countries establish Technology Transfer Offices to commercialize their research results in the form of patents, licenses, and start-ups of new companies. Some examples of university innovation statistics are given below.

4.1 University Innovation Statistics

4.1.1 University of Minnesota Key Performance Indicators

Table 1. University of Minnesota Key Performance Indicators: 2016–2020

	2016	2017	2018	2019	2020
LICENSES & REVENUE					
New Licenses	194	213	230	223	235
Current Revenue Generating Agreements	528	545	575	571	601
STARTUPS					
Startup Companies Formed	17	18	13	19	19
INVENTIONS & PATENTS					
Invention Disclosures	402	406	400	391	397
New Patent Filings	202	232	179	163	152
New Patent Filing Rate*	50%	57%	45%	42%	38%
Issued Patents (US and Foreign)	168	147	186	187	182
MN-IP					
MN-IP Research Agreements	81	72	86	103	73
Companies w/ MN-IP Research Agreements	62	51	58	77	69
Sponsored Research Commitments	$12.2	$20.9	$21.3	$22.5	$27.9

Dollar amounts in millions
Technology Commercialization, Wellspring Sophia; UMN Enterprise Financial System
*New Patent Filing Rate is number of new patents filed during the fiscal year divided by number of new disclosures in the same time period

Source: The University has spun out 170 companies since 2006, with operations across a diversity of fields and 74 percent being Minnesota-based.
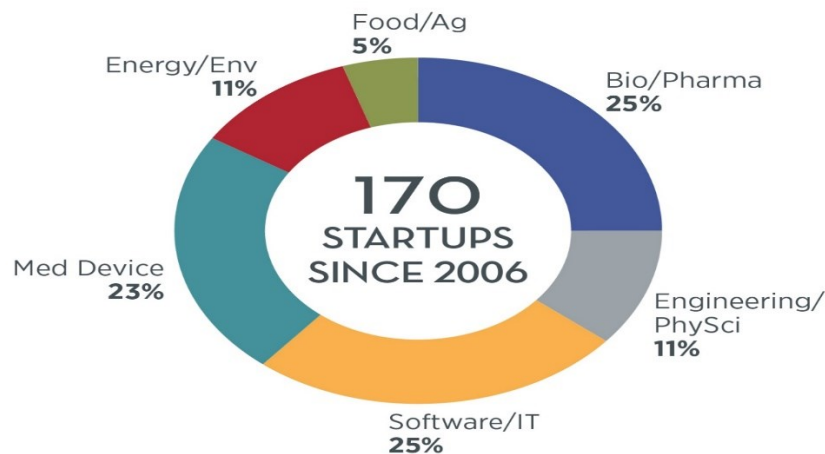
University of Minnesota

The Nigerian Society of Engineers
Minna Branch
1st NSE Minna Branch Conference 2021

Conference theme

Role of Engineering in Sustainable Development Goals

Conference Date: Wednesday 9th to Thursday 10th June 2021

4.1.2 Harvard University Key Performance Indicators

Table 2: Harvard University Key Performance Indicators: 2014–2018

S/N	Description	2014	2015	2016	2017	2018
1	New Patent Applications Filed	246	243	294	274	234
2	U.S. Patents Issued	87	125	122	151	181
3	Licenses	43	50	51	46	51
4	Total Commercialization Revenue (MM)	$17.3	$16.1	$37.8	$35.4	$54.1
5	Startup Companies	10	14	14	14	21
6	Industry-Sponsored Research Agreements	98	75	71	81	77
7	Industry-Sponsored Research (MM)	$48.6	$42.9	$48.4	$51.0	$53.0
8	Material Transfer Agreements	2,243	2,332	2,240	2,285	2,640

The Harvard University fiscal year runs from July 1 to June 30; hence, Fiscal Year 2018 includes July 1, 2017 - June 30, 2018.

4.1.3 North Carolina State University

Table 3: North Carolina State University Key Performance Indicators: 2014–2018

S/N	DESCRIPTION	2014	2015	2016	2017	2018
1	**DISCLOSURES**					
2	Inventions	204	196	225	217	210
3	Software	22	41	36	18	18
4	Plant Variety	13	20	17	20	25
5	Copyright	14	29	13	14	19
6	Trademark	5	4	0	0	0
7	Tangible Research Materials	0	1	0	6	3
8	**Total**	**258**	**291**	**290**	**275**	**275**
9	**PATENT ACTIVITY**					
10	New Patents Filed	186	181	229	241	264
11	U.S. Patents Issued	40	20	53	43	44
12	Foreign Patents Issued	42	24	12	16	28
13	**Total Patents Issued**	**82**	**43**	**65**	**59**	**72**
14	**COMMERCIALIZATION AGREEMENTS**					
15	Patent License	40	27	42	46	39
16	Software License	1	4	3	3	6
17	Plant License	27	37	45	38	49
18	Copyright License	0	7	10	2	1
19	Tangible Research Materials License	2	3	1	2	3
20	Options	75	61	63	78	43
21	**Total**	**145**	**139**	**164**	**169**	**141**
22	**MISCELLANEOUS AGREEMENTS**					
23	MTA	165	201	203	241	258
24	CDA	395	377	404	367	362
25	Other	184	233	306	297	272
26	**Total**	**744**	**811**	**913**	**905**	**892**
27	**REVENUE**					
28	Royalties ($ millions)	$7.5	$7.6	$3.8	$4.4	$5.3
29	**NEW VENTURE DEVELOPMENT**					
30	Startup Companies	10	12	12	15	20

Source : https://otd.harvard.edu/about/productivity-highlights/

The Nigerian Society of Engineers
Minna Branch
1st NSE Minna Branch Conference 2021

Conference theme

Role of Engineering in Sustainable Development Goals

Conference Date: Wednesday 9th to Thursday 10th June 2021

5. UNIVERSITY INNOVATION FOR REGIONAL ECONOMIC DEVELOPMENT

5.1 Stanford University and Silicon Valley

California's Silicon Valley is an important point of reference in State and regional initiatives to develop innovation clusters. Stanford University played a historic role in the establishment of Silicon Valley and in sustaining the survival and flourishing of high technology industries in the surrounding region. The university is credited with creating firms that accounted for half the revenues generated in the Valley between 1988 and 1996 and with an exemplary contribution to local labor market needs (Moore & Davis, 2001). Stanford is known for its startup culture in a region in which most successful firms began as start-ups. It is almost an unwritten rule in Stanford University that you must start a company to be a successful professor (Upstarts and Rabble Rousers, 2006). As of 2011 nearly 5,000 companies existed which could trace their roots to Stanford, including Hewlett-Packard, Cisco Systems, Sun Microsystems, Yahoo, and Google (Wessner, 2013c). "Stanford and MIT were both committed to an endogenous strategy of encouraging firm formation from academic knowledge." "The examples of Massachusetts Institute of Technology and Stanford University in stimulating regional high-technology development are often highlighted for emulation (Wessner, 2013).

Stanford's Office of Technology Licensing opened in 1970, and in four subsequent decades disclosed roughly 8300 cumulative inventions and executed over 3500 licenses. Notable inventions licensed by the office include FM sound synthesis (created by a small Yamaha music chip developed by the music department), recombinant DNA technology, functional antibodies, and digital subscriber line (DSL) technology commercialized by Texas Instruments (Katherine, 2011). The University's very well-known licensee is Google, which was created by two Stanford graduate students (Larry Page and Sergey Brin) over a four-year period. Stanford's experience is an example of what a university can do to make technology transfer effective (Katherine, 2011).

5.2 University of Akron

The University of Akron Research Foundation (UARF), a not-for-profit organization to facilitate the transfer of research results from the university to public and commercial use was established by University of Akron in 2001. Between 2001 and 2012, the Foundation created fifty (50) start-up companies from university-based patents with annual research activity of $50 million. The "Akron Model" for the remaking of University of Akron as a major stakeholder in the turnaround of Ohio's economy was anchored on the mission:

*The university through its research foundation and other avenues is leveraging its talent for local companies and entrepreneurs, serving as something of a research arm or problem-solver in the regional economy (*Wessner, 2013e)

5.3 THE NEW YORK NANOTECHNOLOGY INITIATIVE

The New York State's nanotechnology R&D initiative offers a classical example of how the initiative of a single U.S. State can transform the global competitive map in a strategic economic area. New York has been able to alter the competitive landscape in the semiconductor industry through large-scale investments, particularly in university research infrastructure, and collaborative arrangements with the private sector and regional development organizations, leading to offshore flow of U.S. investment and jobs in the sector (Zimpher, 2013). The epicenter of New York's semiconductor effort is the State University of New York at Albany with SUNY Albany as one of six "NY Innovation Hubs" established to link university-based research to regional innovation, and sustained investments in the university's research infrastructure. It is one of the foremost centers of nanotechnology research in the world and a regional economic driver (Zimpher, 2013)

6. MANAGEMENT OF UNIVERSITY RESEARCH AND INNOVATION FOR REGIONAL ECONOMIC DEVELOPMENT IN NIGERIA

According to (Uche 2017), the lack of attention to commercialization of research outputs explains the dearth of local solutions to the nation's economic problems and the country's over dependence on imported products. According to Ahaneka (2016), "Considerable research findings abound in Nigerian universities serving no further purpose for society at

The Nigerian Society of Engineers
Minna Branch
1st NSE Minna Branch Conference 2021

Conference theme

Role of Engineering in Sustainable Development Goals

Conference Date: Wednesday 9th to Thursday 10th June 2021

large because of lack of linkage with industry. This raises the urgent necessity of moving beyond basic research to applied research and innovation, which in addition to creating knowledge/technology would lead to discovering solution and promote global competitiveness of our industries". Zaku (2011) charged Nigerian scientists to embark on demand driven research which would facilitate the speedy commercialization of Research and Development outputs through industry linkages.

Nigerian universities and other research institutes do not make significant contributions to the socio-economic development of the nation despite the high number of students and academic staff who engage in research projects because of lack of attention to commercialization of research outputs and innovation. Another factor hindering commercialization of research output is irrelevant research carried out that do not reflect the needs of the nation. Most research work in Nigerian tertiary institutions are not formulated and carried out with commercialization focus. The Tertiary Education Trust Fund (TETFUND) spends a lot of money to fund research in tertiary institutions but there has been no defined national focus on commercialization of research projects.

Number of Universities in Nigeria

S/N	REGION	STATE	NUMBER OF UNIVERSITIES			TOTAL
			FEDERAL	STATE	PRIVATE	
1	NORTH CENTRAL	Benue	2	1	1	4
2		Kogi	1	2	1	4
3		Kwara	1	1	7	9
4		Plateau	1	1	2	4
5		Nasarawa	1	1	3	5
6		Niger	1	1	1	3
7	**SUBTOTAL**		7	7	15	29
8	NORTHEAST	Adamawa	1	1	1	3
9		Bauchi	1	1	-	2
10		Borno	2	1	-	3
11		Gombe	1	2	-	3
12		Taraba	1	1	1	3
13		Yobe	1	1	-	2
14	**SUBTOTAL**		7	7	2	16
	NORTHWEST	KADUNA	3	1	2	6
		KANO	2	2	2	6
		KATSINA	1	1	1	3
		KEBBI	1	1	-	2
		JIGAWA	1	1	1	3
		SOKOTO	1	1	-	2
		ZAMFARA	1	1	-	2
	SUBTOTAL		10	8	6	24
	SOUTHEAST	ABIA	1	1	3	5
		ANAMBRA	1	1	4	6
		EBONYI	1	1	1	3
		ENUGU	1	1	4	6
		IMO	1	2	3	6
	SUBTOTAL		5	6	15	26
	SOUTHSOUTH	**AKWA IBOM**	1	1	3	5

The Nigerian Society of Engineers
Minna Branch
1st NSE Minna Branch Conference 2021

Conference theme

Role of Engineering in Sustainable Development Goals

Conference Date: Wednesday 9th to Thursday 10th June 2021

	BAYELSA	1	3	-	4
	CROSS RIVER	1	1	1	3
	DELTA	2	1	5	8
	EDO	1	2	5	8
	RIVERS	1	2	3	6
SUBTOTAL		7	10	17	34
SOUTHWEST	EKITI	1	1	1	3
	LAGOS	2	1	6	9
	OGUN	1	3	12	16
	ONDO	1	3	3	7
	OSUN	1	1	8	10
	OYO	1	2	7	10
SUBTOTAL		7	11	37	55
FCT	**FCT**	1	-	6	7
GRAND TOTAL		**44**	**49**	**98**	**191**

Summary of Number of Universities in each Region:

North Central: 29

Northeast   16

Northwest   24

Southeast   26

South south   34

Southwest   55

FCT   7

Total   191

7. NIGERIAN SOCIETY OF ENGINEERS ADVOCACY FOR REGIONAL ECONOMIC DEVELOPMENT USING THE TRIPLE HELIX MODEL OF UNIVERSITY – INDUSTRY – GOVERNMENT COLLABORATION

The Nigerian Society of Engineers is leading a strong advocacy for regional economic development in Nigeria. NSE is worried that with the enormous human and natural resources in all the regions of the country, the nation remains poor and is classified as the poverty capital of the world. Engineers must rise and begin to harness their creativity and innovation for economic and social development of the nation.

NSE is convinced that Nigeria can develop rapidly if the innovation potentials of her tertiary education research are properly harnessed by focusing on research that translates rural area endowments into commercially viable enterprises and adopting deliberate policies for commercialization of research results and innovation. NSE has therefore proposed to lead the advocacy for sustainable regional economic development through regional resources documentation and conferences, summits, or town hall meetings. Under the advocacy plan, there is a Study/Planning Team for each region to document its natural resources endowment, identify investment potentials, appropriate technologies for exploitation, collaboration/partnership models and plan the engagement with stakeholders (Conference, Summit, Town Hall Meetings).

The advocacy plan will focus on the Triple Helix Collaboration Model among Government, Industry, and the Academia for Government to provide necessary infrastructure and enabling environment for investment by the private sector while the academia provides the intellectual properties for enterprise development through licensing of patents. The group studies on regional development will also consider potentials for establishment of Innovation hubs and Industrial parks to stimulate manufacturing contribution to the nation's Gross Domestic Product (GDP) which is currently only at 6%. NSE will use its network of eighty-one (81) Branches and twenty - five (25) Professional Institutions across the country for the advocacy programme.

Expected Outcome of the Advocacy Programme

The Nigerian Society of Engineers
Minna Branch
1st NSE Minna Branch Conference 2021

Conference theme

Role of Engineering in Sustainable Development Goals

Conference Date: Wednesday 9th to Thursday 10th June 2021

1. Our universities and other tertiary institutions will begin to cultivate a new culture of creating businesses from intellectual properties and research works through licensing of patents or establishing start-up companies, thus becoming entrepreneurial institutions instead of conducting research for mere academic promotions. They will become key architects and drivers of regional development.

2. Tertiary institutions will begin to focus research on developing appropriate technologies for exploitation of local resources and engage in contract research for industries and government.

3. Students in tertiary institutions will focus on generating ideas that create businesses for them instead of seeking for employment after graduation.

4. Tertiary institutions will start to generate more internal revenues from licensing of patents and creation of spin-off industries to make them less dependent on government and prevent incessant strikes over funding.

5. Enhanced quality of education and training

6. The Organized Private Sector will get opportunities to access intellectual properties for business development to create more jobs and employment.

7. A more stable regional and national economies will emerge.

8. There will be drastic reduction in crime and criminality.

9. Gross Domestic Product (GDP) will be enhanced with significant increase in manufacturing contribution.

10. National earnings will improve with country-wide improvement in standard of living over time.

11. States will be made to focus on providing relevant infrastructures and creating enabling environments for investment. There will be enhancement of innovation infrastructure and opening of public and community space for accelerated development.

12. State governments will earn more revenue from taxes and have leaner civil service as more people will be employed by the private sector.

13. There will be less dependence on foreign goods thereby preserving the scarce foreign reserve for more critical transactions.

14. Promotion of regional attractiveness for foreign direct investment.

8. DISCUSSION

The study has shown the immense contributions of focused research and commercialization of innovations to economic and industrial development. America's Silicon Valley, Route 128, and the Research Triangle with strong collaboration with universities as innovation drivers is a major lesson for Nigeria on how university research and innovation drive economic development.

The development of State and regional innovation clusters in America around top rate universities in specific economic sectors with high impacts on enterprise development and employment generation is a classic example of the kind of initiatives State governments in Nigeria should be taking. Government policies, regulatory frameworks, and commitment to commercialization of research and innovation are essential for accelerated growth and development. The self – sustenance of the university system has been exemplified by the entrepreneurship and enterprise development culture of Stanford University, MIT, University of Akron, University of Minnesota, Harvard, North Carolina State University and Hebrew University of Jerusalem. Our universities can also become top rate universities and achieve these results if they follow the examples.

9. CONCLUSION

The Key Performance Indicators of university of Minnesota, North Carolina University, Harvard University and U.S.A National Institutes of Health provide great lessons for Nigerian Universities on intellectual property generation and commercialization. Regional universities have contributed immensely to the economic and industrial development of America and other developed countries. States in collaboration with universities and other research organizations and the organized private sector are the prime drivers of innovation clusters for sustainable economic development. University research is often business focused with commercialization as the third primary function of universities in addition to teaching and research. Many universities in developed countries are self-sustaining through the force of commercialization of intellectual properties. Nigerian tertiary institutions can use collaborative research to harness States' and regional comparative

The Nigerian Society of Engineers
Minna Branch
1st NSE Minna Branch Conference 2021

Conference theme

Role of Engineering in Sustainable Development Goals

Conference Date: Wednesday 9th to Thursday 10th June 2021

advantages to create industries and jobs for the Nigerian economy. In comparative terms, Nigerian Universities and research organizations are not doing enough in intellectual property generation and commercialization of innovations. Rural development in Nigeria can be significantly influenced by commercialization of research and innovation based on rural area resource endowment with active collaboration among Government, research organizations and the private sector.

10. RECOMMENDATIONS

The Nigerian Society of Engineers advocacy plan for regional economic development through the adoption of the Triple Helix collaboration model among Universities, Industries and Government in each region of Nigeria to drive sustainable economic development of the regions, should be aggressively pursued.

The Research and Development (R & D) mandates of our tertiary institutions should focus on creating productive and innovative enterprises from their regional resource endowments. Virtually every State in the country has a university and a Polytechnic. Research in these institutions should focus on problem solving and business development for the growth of regional economies.

Commercialization of research should be made an explicit role of our tertiary institutions in addition to teaching and research. Our Universities, Polytechnics and Research Institutes must become drivers of regional economic growth and development.

The National Universities Commission (NUC) should develop a template for the establishment of research and innovation commercialization unit in every university to coordinate intellectual property generation, patenting and licensing for start-up companies and create the essential linkage with the private sector and government on the Triple Helix for commercialization of research results.

Regional Universities should facilitate the creation of regional innovation centres to exploit endowments of common regional interest for accelerated development.

REFERENCES

Ahaneka J (2016), Commercialization of Research is Key to Nigeria's Development. http://247ureports.com/commercialization-of-research-is-key-to-nigerias-development/. 247ureports.com

Caulfield T, Ogbogu U (2015). The commercialization of university-based research: Balancing risks and benefits. BMC Med Ethics V.16; 2015. Published online 2015 Oct 14. Accessed November 15, 2017

Caulfield T (2012). Talking science - commercialization creep. Policy Options. 20–23

Caulfield T (2010). Stem cell research and economic promises. J Law Med Ethics. 38:303–313.

Daniel, D. (2011). University of Texas at Dallas, "Making the State bigger: Current Texas University Initiatives," National Research Council. Clustering for 21st Century Prosperity: Summary of a Symposium. Wessner C, editor. Washington, DC: The National Academies Press; 2011.

Dodd (2017). Hebrew University of Jerusalem Earned $US20b Revenue from Commercializing its Research. http://www.cfhu.org/news/hebrew-university-of-jerusalem-earned-us20b-revenue-from-commercialising-its-research

Downie J, Herder M (2007). Reflections on the commercialization of research conducted in public institutions in Canada. McGill Health Law Publication.1:23–44.

Hand E, Mole B, Morello L, Tollefson J, Wadman M, Witze A (2013). A back seat for basic science. Nature. 2013; 496:277–279.

Katherine, K (2011). Office of Technology Licensing,Stanford University. 40 Years of Experience with Technology Licensing; Building Hawaii's Innovation Economy: Summary of a Symposium; January 13–14, 2011. National Research Council;

Leichman, A. K (2018). Why Israel rocks at commercializing academic innovations - Universities worldwide are looking to emulate Israel's tech-transfer magic. https://www.israel21c.org/why-israel-rocks-at-commercializing-academic-innovations/

Macilwain C (2010). Science economics: what science is really worth. Nature. 2010;465:682–684.

The Nigerian Society of Engineers
Minna Branch
1st NSE Minna Branch Conference 2021

Conference theme

Role of Engineering in Sustainable Development Goals

Conference Date: Wednesday 9th to Thursday 10th June 2021

Moore, G. & Davis, K. (2001).SIEPR Discussion Paper No. 00-45. Stanford Institute for Economic Policy Research; Jul 15, 2001. Learning the Silicon Valley Way; p. 11.

Obama (2015a). Remarks by the President in State of the Union Address, Jan 20, 2015 [https://www.whitehouse.gov/the-press-office/2015/01/20/remarks-president-state-union-address-january-20-2015]. Access date: November 15, 2017.

Obama (2015b). Remarks by the President on Precision Medicine, Jan 30, 2015 [https://www.whitehouse.gov/the-press-office/2015/01/30/remarks-president-precision-medicine]. Access date: November 15, 2015.

Obama (2014). President Barack Obama's State of the Union Address, Jan 28, 2014 [https://www.whitehouse.gov/the-press-office/2014/01/28/president-barack-obamas-state-union-address]. Access date: November 15, 2017.

Obama (2011). Remarks by the President in State of the Union Address, Jan 25, 2011 [http://www.whitehouse.gov/the-press-office/2011/01/25/remarks-president-state-union-address]. Access date: November 15, 2017.

Ogbogu U, Caulfield T.(2015) "Science powers commerce": mapping the language, justifications, and perceptions of the drive to commercialize in the context of Canadian research. Canadian Journal of Comparative and Contemporary Law. 2015;1:137–158.

Ohio's Third Frontier (2012). Rebuilding Ohio's Innovation Economy;" Annual Report

Petersen A, Krisjansen I (2015). Assembling "the bioeconomy": exploiting the power of the promissory life sciences. Journal of Sociology. 2015;51:28–46.

Philpott K, Dooley L, O'Reilly C, Lupton G (2011). The entrepreneurial university: examining the underlying academic tensions. Technovation. 2011;31:161–170.   doi: 10.1016/j.technovation.2010.12.003.]

Rasmussen E (2008). Government instruments to support the commercialization of university research: lessons from Canada. Technovation. 2008;28:506–517.

Remarks by the President on Precision Medicine, Jan 30, 2015 [https://www.whitehouse.gov/the-press-office/2015/01/30/remarks-president-precision-medicine]. Access date: October 8, 2015.

Remarks by the President in State of the Union Address, Jan 25, 2011 [http://www.whitehouse.gov/the-press-office/2011/01/25/remarks-president-state-union-address]. Access date: October 8, 2015.

Sanberg P R, Garib M, Harker P T, Kaler E W, Marchase R B, Sands T D, Arshadi N,

Uche O (2017), How university research can transform from paper to products https://techpoint.ng/2017/07/06/university-research-commercialization/

Upstarts and Rabble Rousers (2006). Stanford Fetes 4 Decades of Computer Science. San Francisco Chronicle. Mar 20, 2006.

Vanderford N.L & Marcinkowski E (2015). A case study of the impediments to the commercialization of research at the University of Kentucky

Wessner, C. W (2013) Committee on Competing in the 21st Century: Best Practice in State and Regional Innovation Initiatives. National Research Council (US), Washington (DC)

Wessner, C. W (2013a). The University City Science Center: An Engine of Growth for Greater Philadelphia. Sep, 2009. pp. 6pp. 23–28.

Wessner, C. W (2013b). "Arkansas Workforce and Wind power". Committee on Competing in the 21st Century: Best Practice in State and Regional Innovation Initiatives. National Research Council (US), Washington (DC) (http://www.tekes.fi/en),

Wessner, C. W (2013c). Sowing the Seeds of a Startup: StartX Seeks to Propel Young Entrepreneurs to Forefront of their Field. San Jose Mercury News. Dec 29, 2011.

Wessner, C. W (2013d). P&G Floats Idea for Soap. Committee on Competing in the 21st Century: Best Practice in State and Regional Innovation Initiatives. National Research Council (US), Washington (DC)

Zaku A B (2011). Commercialization of Research Findings Key to VISION 20-20. The Nigerian Voice online. Access date: November 15, 2017

The Nigerian Society of Engineers
Minna Branch
1st NSE Minna Branch Conference 2021

Conference theme

Role of Engineering in Sustainable Development Goals

Conference Date: Wednesday 9th to Thursday 10th June 2021

Zimpher, N. L (2013). "The Power of SUNY," National Research Council Symposium, "New York's Nanotechnology Model: Building the Innovation Economy" Troy, New York, April 4, 2013

The Nigerian Society of Engineers
Minna Branch
1st NSE Minna Branch National Conference 2021

Conference theme
Role of Engineering in Sustainable Development Goals

A Topsis-Based Methodology for Prioritizing Maintenance Activities Suitable for A Municipal Water Works

Case Study: Chanchaga Water Works, Minna

Musa Kotsu, U. G Okoro and I. A. Shehu

Mechanical Engineering Department,

Federal University of Technology, PMB 65 Minna, Niger State, Nigeria

Corresponding author email: musakotsu@gmail.com, +2347053965955

ABSTRACT

Maintenance is performed in the industry to ensure that physical assets continue to function to designed capacity. In most instances, scheduled maintenances are hardly fully implemented owing to maintenance budget fluctuations/constraints. Budget shortage has negative impact on maintenance strategies and results in the undesirable deterioration of production plant's components and increasing risk of accidents and downtimes. In most traditional practices, the choice, of which maintenance location that should be addressed urgently and which to delay, to the subjective discretion of the maintenance manager. One of the dangers of such discretional judgment in maintenance is that the risk of delayed maintenance is different for different components even for the same plant: a low-risk component could be chosen ahead of a high-risk one which jeopardized the overarching objectives of conducting the maintenance activities. The paper developed and implemented a methodology to minimize the impact of budget fluctuation by quantifying the risk of not performing a maintenance activity and identifying the priority of maintenance activities based on the quantified risk. TOPSIS algorithm uses a value system to estimate the risks that are not only relevant to failure of the system but also concern with the repair of the various sub- system of the plant under various criteria and to integrate the scores to arrive at a prioritization metric as an alternative to risk priority number of the traditional failure mode and effect analysis (FMEA). The framework is implemented on a real case study of Municipal water works and the conclusions proved well for wider applications in varied and allied industrial settings. Last, From the result obtained, the alternative A4 (reservoir) has the highest relative coefficient of 0.904049 which shows that it suffers most criticality than the other Alternatives, this occur as a result of abandonment of this component over dedicates because it has not been develop any fault and for that reason much attention were been diverted to those components like; pumping machine and others, since they always develop faults. The Alternative A5which is fire hydrant with relative closeness of 0.704793 becomes the second component that suffers high criticality due to the unavailability of this component across the metropolis; there is a need for the management to build more of it across the metropolis that will help reduce the loads on this existing one. Follow by valve with closeness coefficient of 0.483325, pipe with 0.47755 and finally pumping machine with 0.061847.

KEYWORDS: *Maintenance, TOPSIS, Delayed Maintenance, Water Supply and Decision Making*

1. INTRODUCTION

Water is life: adequate supply of water is central to life and civilization. The five basic human needs namely air, water, food, light, and heat. Water is common factor to other four. It is therefore not an understatement to say water is life, because it forms an appreciable proportion of all living things including man. In fact, water is very critical to human life. Water constitutes about 80% of animal cells. The human body by weight consists of about 70% water and several body functions depend on water (United Nations report, 2006).According to the popular Nigerian musician Fela Kuti who in his song "water no get enemy" reiterated that all human activities cling on water and that man will go to any length to search for water in times of scarcity and this has proven the slogan "water is life" right. In the third world countries of the world with Nigeria inclusive, the problem of portable water supply in Minna metropolis have poised a lot of challenges with task of collecting water falling largely on women and children and their journey to collect

water is long, tiring and often dangerous, it prevents millions of mothers from working and lifting their families out of poverty. It keeps millions of children out school and from playing, depriving them of the wellbeing and education necessary to become healthy adults.

According to United Nations Report, (2012), 783 million people, or 11% of the global population, remain without access to an improved source of portable water supply. Water is fundamental to our way of life at whatever point in the socio-economic spectrum a community may be situated. The essential paradox of water supply in developing countries is that, in one sense, everyone has a water supply, in another sense, most people have not. Water is essential for life and all human communities must have some kind of water source. It may be dirty, it may be in adequate in volume and it may be several hours walk away but, nevertheless some water must be available. However, if reasonable criterion of adequacy in term of the quantity, quality and availability of water then most people in developing countries do not have an adequate supply (Cairncross and Feachem,1988) More so, delivery of safe reliable supply of drinking water to consumers tap depends on the integrity of the distribution system. The pipe networks, extending over large areas encompasses multiple connections and points of access typically constituting the bulk of water utility assets. Proper management of water system is crucial for ensuring sustainability of a given water resource, maintaining high quality water resources, and maximizing the utility's ability to respond to profound operating conditions (punmia et al, 2001). To survive in the modern economy, water production companies must be careful in making decisions. Improper decisions increase companies' costs in terms of resource wastage as well affect the consumers' satisfaction. Modern water production companies are now facing some great problems like budget deficient as a result of modern economy, time consumption and lack of advanced knowledge as well experience. The difficulty of the component's evaluation problem has driven the researcher to develop a model for helping decision makers/maintenance managers. The specific objective of this research model is to

help decision maker in dealing with difficulty arising from maintenance significant in components criticality problem. The strategic decision, backed by the company is to be implemented effectively to increase water production capacity and safety as a whole. The identification of most critical component among eligible alternatives is a very powerful decision. As decisions regarding components are crucial elements in a company's quality success or failure. In order to identify the most critical component among the various alternatives the decision maker must consider meaningful criteria and possess special knowledge of the components properties. But those criteria should be considered those maximize the water production capacity. A thorough evaluation and identification of the component that suffers the must criticality among the existing components will be carried out and the most critical component would be suggested to the Niger State Water works which will help the management to find a lasting solution to the problem of inadequate water supply in Minna metropolis. In this study, the evaluation criteria for the identification of component's criticality decision ware selected from the studies and the discussions with the company's workers in deferent areas. To evaluate the component criticality, deferent methods have been widely applied in the literature: Simple Additive Weighting Method (SAW), Simple Multi-Attribute Rating Technique (SMART), Elimination and Choice Translation Reality (ELECTHRE) and The Analytical Hierarchy Process (AHP) are some of these methods.

In this research work a prototype frame work using TOPSIS method has been employed to evaluate the component criticality to prompt the water production capacity.

2.0 METHODOLOGY
TOPSIS: Means Technique for order of preference by similarity to ideal solution. This is one of the multiple – criteria decision making technique that deals with the selection of the best alternative usually have the closest distance to the ideal solution and farthest distance from the negative ideal solution.

The Nigerian Society of Engineers
Minna Branch
1st NSE Minna Branch National Conference 2021

Conference theme
Role of Engineering in
Sustainable Development Goals

TOPSIS allows trade-offs between criterions, where a poor result in one criterion can be negated by good result in another criterion. This provides a more realistic form of modeling than non-compensatory methods. TOPSIS Technique has been commonly used to solve decision making problems. This technique is based on the comparison between all the alternatives included in the problem. This proposed technique is highly useful in large-scale decision-making problems found in water quality assessment, disaster risk assessment, real estate management, sustainability assessment, environmental risk assessment, supplier selection.

TOPSIS also has the following advantages:

i. Simplicity
ii. Rationality
iii. Good computational efficiency and has ability to measure relative performance for each alternative in a simple mathematical form (Chen and Hwang,1992).

2.1. ANALYSIS PROCEDURES BY THE USES OF THE TOPSIS METHOD

In the TOPSIS method, the process of rating particular alternatives and comparing them with others, there is a distance expressed in the n-dimensional, Euclidean distance (n- number of criteria) between the value vectors describing particular alternatives and vectors responding to ideal and negative-ideal variants. The most reasonable alternative is the one with the value vector of simultaneously the shortest distance from the vector of negative-ideal solution.

The decisive steps, covered by the analysis of TOPSIS method are followed:

i. Creation of a decision matrix,
ii. Creation of normalized decision matrix
iii. Creation of weight, normalized decision matrix
iv. Indication of the ideal and negative-ideal solution
v. Calculation of the distance of each alternative for ideal and negative ideal solution.

vi. Calculation of the similarity indicators of particular alternatives for the ideal solution
vii. Creation of the final alternatives, ranking in the decreasing order of the similarity value indicator (Jahanshahloo et al ,2006).

2.2 CLASSICAL VERSION OF THE TOPSIS METHOD

As it was mentioned in the previous part of the paper, the foundations of the TOPSIS method were presented in the work of (Hwang andYoon, 1981). The basis of the analysis is the decision matrix $Q_{m,n}$ including ratings of considered alternatives $i = 1, 2, ..., m$ in the context of the accepted criteria $j = 1, 2, ..., n$: On the basis of which there have been calculated normalized ratings of particular alternatives.

$$\mathbf{Q}_{m,n} = \begin{bmatrix} Q_{1,1} & Q_{1,2} & \cdots & Q_{1,n} \\ Q_{2,1} & Q_{2,2} & \cdots & Q_{2,n} \\ \cdots & \cdots & \cdots & \cdots \\ Q_{m,1} & Q_{m,2} & \cdots & Q_{m,n} \end{bmatrix} \tag{1}$$

$$n_{i,j} = \frac{Q_{i,j}}{\sqrt{\sum_{i=1}^{m} Q_{i,j}^2}} \tag{2}$$

In the phase of normalized rating, it is possible to use the formulas (Ishizaka, Nemery, 2013):

$$n_{i,j} = \frac{Q_{i,j}}{Q_{\max}} \tag{3}$$

----- for the criterion

$$n_i = \frac{Q_{\min}}{Q_{i,j}} \tag{4}$$

Then, there is an identification of the ideal solution conducted (V+) and negative-ideal solution (V–) with the use of corrected assessments. The ideal solution is defined as:

$$V^+ = \left\{ v_1^+, v_2^+, ..., v_n^+ \right\} \tag{6}$$

$$V^- = \left\{ v_1^-, v_2^-, ..., v_n^- \right\} \tag{7}$$

In the above equations

j v+ and j v− are the values defining ideal and

$$d_i^+ = \sqrt{\sum_{j=1}^{n} \left(v_{i,j} - v_j^+ \right)^2} \tag{8}$$

negative ideal solutions in the context of criterion(j), however, Cbenefits, Ccosts are respectively benefits and costs criteria subsets. After indication of the ideal and negative ideal solution there are the distances calculated di + and di − between them and consecutive alternatives:

On the basis of di+ and di − there is a ranking the coefficient of the particular alternatives indicated:

$$d_i^- = \sqrt{\sum_{j=1}^{n} \left(v_{i,j} - v_j^- \right)^2} \tag{9}$$

$$R_i = \frac{d_i^-}{d_i^- + d_i^+} \tag{10}$$

The procedure ends with the establishment of the alternatives ranking in the decreasing order of the Ri value rating (Hwang and Yoon, 1981).

2.3 ENTROPY METHOD

The entropy method is the method used for assessing the weight in a given problem because with this method, the decision matrix for a set of candidate materials contains a certain amount of information. The entropy works based on a predefined decision matrix. Entropy in information theory is a criterion for the amount of uncertainty represented by a discrete probability distribution, in which there is agreement that a broad distribution represents more uncertainty than does a sharply packed one (Dong et al. 2005). The entropy method for assessing the relative importance of criteria is calculated using material data for each criterion, the entropy of the set of normalized outcomes of the jth criterion is given by

$$E_j = -\left[\sum_{i=1}^{m} p_{ij} \ln(p_{ij}) \right] / \ln(m) \; ; \; j = 1, 2,$$

....n and i=1,2 ...m   (11)

The pij form the normalized decision matrix and is given by

$$p_{ij} = \frac{r_{ij}}{\sum_{i=1}^{m} r_{ij}} \; ; \; i = 1, 2, ..., \text{ and}; \; j = 1,$$

2,. . . , n   (12)

$$w_j = \frac{1 - E_j}{\sum_{j=i}^{n} (1 - E_j)}$$

Where rij is an element of the decision matrix, k is a constant of the entropy equation and j E as the information entropy value for jth criteria. Hence, the criteria weights, j w is obtained using the following expression

$$w_j = \frac{1 - E_j}{\sum_{j=i}^{n} (1 - E_j)}$$

J=1,2,…………..   (13)

Whereby (1-Ej) is the degree of diversity of the information involved in the outcomes of the Jth criterion (Dong et all.2005)

2.4 FIGURES AND TABLES

The following components are to be consider in this research work

i. Pumping machines
ii. Pipes lines
iii. Valves
iv. Power source
v. Reservoir

(i) PUMPING MACHINE

Pumps are used to increase the energy in a water distribution system (Mays, 2006). There are many different types of pumps. They include positive displacement pumps, kinetic pumps, turbine pumps, horizontal centrifugal pumps, vertical centrifugal pumps. However, the most commonly used type of pumps in water distribution system is the centrifugal pumps. This is because of their low cost, system piping consists of the transmission system which are the raising mains and the distribution system which are the distribution mains. The transmission system consists of components that are designed to convey large quantity of water over a great distance from water works to the service reservoirs. simplicity, and reliability in the range of flows and head encountered.

Plate I A centrifugal pump of 355kw

(ii) PIPE LINES

The water system piping consists of the transmission system which are the raising mains and the distribution system which are the distribution mains. The transmission system consists of components

that are designed to convey large quantity of water over a great distance from water works to the service reservoirs.

Plate II an asbestos cement pipe

(iii) VALVES

Valves are used for various purposes in water distribution systems, including isolation, air release, drainage, and checking and pressure reduction.

The valves were air release valves, sluice valve and butterfly valves. Sluice and gate valves are extensively used in the distribution to shut off the supplies whenever desired.

Plate III. A Butterfly valve

(vi). STORAGE AND DISTRIBUTION RESERVOIRS

Punmia et al., (2001) described storage and distribution reservoirs as important units in a modern distribution system. Clear water storage is required for storage of filtered water until it is pumped into the service reservoirs or distribution reservoirs. Bhargava and Gupta (2004) gave the

The Nigerian Society of Engineers
Minna Branch
1st NSE Minna Branch National Conference 2021

Conference theme
Role of Engineering in
Sustainable Development Goals

functions and economic benefits of service reservoir to include:

The service reservoirs absorb the hourly fluctuation in and allow the pumps to operate at a constant rate. This improves the efficiency and reduces the cost of operation;

Plate IV. A clear water storage reservoir

(iv) Hydrants

There is only one functional hydrant throughout the distribution system. A fire hydrant which is an active protection measure and a source of water provided in most urban, suburban and rural areas with municipal water service to enable fire-fighters to tap into the municipal water supply to assist in extinguishing a fire. Looking at the importance of fire hydrant, there is the need for the Water Board to install more fire hydrants at strategic positions in the water distribution system.

Plate V: fire Hydrant

2.5 THE EXISTING CRITERIA FOR THIS RESEARCH WORK

Scoring Scheme for Maintenance Significant Factors

A number of issues are related to the failure of an item, its repair and subsequent use. The factors linked to failure of an item are identified as occurrence of failure, Severity, and reliability respectively. The issue of repair can be identified to

have closer association with service time and the ability to organize the resources for repair, which are classified as maintainability and lead time to get spares. When the equipment is put to use, a measure of safety and economic loss can be relevant. This concern can be taken care of by measures like economic safety factor. Thus, the five factors that are to be considered in this research work are as follows: chance of failure (occurrence), reliability importance measure, maintainability, lead time for spare parts, economic safety factor.

The evaluation of each attribute is obtained in different ways by defining a rational method to quantify the single criterion for each cause of fault, based on a series of tables. In particular, every factor is divided into several classes that are assigned a different score (in the range from 1 to 9) to take into account the different criticality levels. The scores have then been defined in accordance with the experiences of the maintenance personnel. A technical data used to assign the different scores is discussed below (marivappan, 2004).

a. CHANCE OF FAILURE (O)

It is concerned with the frequency with which a failure mode occurs; higher value indicates higher criticality of the item. Probability of occurrence of failure was evaluated as a function of Mean Time Between Failures (MTBF).

TABLE 1: CHANCE OF FAILURE (O

Occurrence	MTBF	Score
Almost never	>2 years	1
Rare	2-3 years	2
Very few	2-3 years	3
Few	3/4- 1 years	4
Medium	6-9 months	5
Moderately high	4-6 months	6
High	2-4 months	7
Very high	1-2 months	8
Extremely high	<30 days	9

Adapted from (marivappan, 2004).

b. RELIABILITY IMPORTANCE MEASURE (RI)

Here, the Biranbaum's measure of Reliability Importance (RI) is used to assess the change in top

Conference theme

Role of Engineering in Sustainable Development Goals

event occurrence for a given change in the probability of occurrence of input event. Birnbaum's measure of a component represents the probability that a system will be in a critical state due to the failure of that component at time t. The guidelines to assign the score for reliability importance of a component are presented in Table 2.

Table 2: Reliability Importance Measure(RI)

Criteria %	Criteria for Reliability importance	Score
Less than 10	Negligible	1
10-20	Slight	2
20-30	Little	3
30-40	Minor	4
40-50	Moderate	5
50-60	Significant	6
60-70	High	7
70-80	Very high	8
More than 80	Extremely high	9

Adapted from (marivappan, 2004).

c. MAINTAINABILITY (M)

Maintainability is defined as the probability that an equipment/ component/ system can be restored back to its original/desired condition within the specified time interval. A low value of this index indicates lower chance of putting the equipment back to its original/desired condition. Thus, higher maintenance criticality index is associated with lower maintainability value. The scores assigned to different levels of maintainability index are listed in Table 3.3

Table 3: Maintainability (M)

Criteria	Maintainability	Score
$Mt > 0.8$	Almost certain	1
$0.7 < Mt \leq 0.8$	Very high	2
$0.6 < Mt \leq 0.7$	High	3
$0.5 < Mt \leq 0.6$	Moderately high	4
$0.4 < Mt \leq 0.5$	Medium	5
$0.3 < Mt \leq 0.4$	Low	6
$0.2 < Mt \leq 0.3$	Very low	7
$0.1 < Mt \leq 0.2$	Slight	8
$Mt < 0.1$	Extremely low	9

Adapted from (marivappan, 2004).

d. SPARE PARTS (SP)

A large number of spare parts are required for maintenance. Their chances of availability and importance level for the functioning of the equipment have substantial effect on the maintenance criticality of that equipment. The scoring scheme for their combinations is shown in Table 4 below.

Table 4: Spare parts score (SP)

Criteria	Easy	Difficult	scarce
	Availability		
Desirable	1	4	7
Essential	2	5	8
Vital	3	6	9

Adapted from (marivappan, 2004).

e. ECONOMIC SAFETY LOSS (ES)

The economics of safety also need to be considered while defining the maintenance criticality of a component. Table 5 below.

Table 5: Economic safety loss (ES)score

Status of the equipment/ sub system	Score
With no moving parts	3
With one moving part/critical category	6
With more than one moving parts/critical category	9

Adapted from (marivappan, 2004).

Table 6: The collected Data

Components (Alternatives)	Chance of failure (O)	Reliability importance Measure (RI)	Maintainability (M)	Spare Part (SP)	Economy safety loss (ES)
Pump	5	5	5	6	6
Pipe	3	4	5	6	3
Valve	4	3	5	6	3
Reservoir	2	1	5	3	3
Fire Hydrant	1	1	5	5	3

The Nigerian Society of Engineers
Minna Branch
1st NSE Minna Branch National Conference 2021

Conference theme
Role of Engineering in
Sustainable Development Goals

The Table 6 above describes the details of five different components data collected from Niger state water works Minna. The components: pump, pipe, valve, reservoir and fire Hydrant are the alternatives and represented as A1, A2, A3, A4 and A5 respectively WHILE the criteria are: chance of failure, Reliability importance measure, Maintainability, spare parts and Economic loss functions are represented as C1, C2, C3, C4 and C5 respectively. Therefore, the Table 6 will result to the Table 7 below.

TABLE 7: DECISION MATRIX

Components	Criteria	Criteria	Criteria	Criteria	Criteria
Alternative	C1	C2	C3	C4	C5
A1	5	5	5	6	6
A2	3	4	5	6	3
A3	4	3	5	6	3
A4	2	1	5	3	3
A5	1	1	5	6	3

TABLE 8: NORMALIZED DECISION MATRIX

	C1	C2	C3	C4	C5
A1	0.6742	0.693375	0.447214	0.503509	0.70710678
A2	0.40452	0.55547	0.447214	0.503509	0.35355339
A3	0.53936	0.416025	0.447214	0.503509	0.35355339
A4	0.26968	0.138675	0.447214	0.251754	0.35355339
A5	0.182574	0.19245	0.5	0.485643	0.5

TABLE 9: ENTROPY VALUE EJ

	C1	C2	C3	C4	C5
Ej	-3.19651	-3.08055	-3.5339	-3.4707	-3.50134

TABLE 10: WEGTHS CRITERIA VALUES WJ

	C1	C2	C3	C4	C5
Wj	0.192651	0.187327	0.208139	0.205238	0.206645

Table 11: WEIGHTED NORMALIZED DECISION MATRIX

	C1	C2	C3	C4	C5
A1	0.129885	0.129888	0.093083	0.103339	0.14612008
A2	0.077931	0.10391	0.093083	0.103339	0.07306004
A3	0.103908	0.077933	0.093083	0.103339	0.07306004
A4	0.051954	0.025978	0.093083	0.05167	0.07306004
A5	0.035173	0.036051	0.10407	0.099672	0.1033225

TABLE 12: IDEAL SOLUTION AND NEGATIVE IDEAL SOLUTION

	C1	C2	C3	C4	C5
A+	0.035173	0.025978	0.093083	0.05167	0.07306004
A-	0.129885	0.129888	0.10407	0.103339	0.14612008

TABLE 13: SEPARATION FROM POSITIVE AND NEGATIVE IDEAL SOLUTION

	S+	S-
A1	0.166659	0.010987
A2	0.102818	0.093982
A3	0.100467	0.093982
A4	0.016781	0.15811
A5	0.058671	0.140074

TABLE 14: RELATIVE CLOSENESS TO THE IDEAL SOLUTION

	CI	RANK
A1	0.061847	5
A2	0.47755	4
A3	0.483325	3
A4	0.904049	1
A5	0.704793	2

3. RESULT AND DISCUSSION

This research work is a case study of Niger State Chanchaga water works, Minna, therefore, the company need to prioritise the existing components in order to treat the most critical components before those with less criticality should be treated last. From the result obtained, the alternative A4 is the reservoir has the highest relative coefficient of 0.904049 which shows that it suffers most criticality than the other Alternatives, this occur as a result of abandonment of this component over dedicates because it has not been develop any fault and for that

The Nigerian Society of Engineers
Minna Branch
1st NSE Minna Branch National Conference 2021

Conference theme
Role of Engineering in
Sustainable Development Goals

reason much attention were been diverted to those components like; pumping machine and others, since they always develop faults.

The Alternative A5 which is fire hydrant with relative closeness of 0.704793 becomes the second component that suffers high criticality due to the unavailability of this component across the metropolis; there is a need for the management to build more of it across the metropolis that will help reduce the loads on this existing one. The Alternative A3 which is valve, it has the relative closeness coefficient of 0.483325 and that make it to be the third Alternative that suffers much criticality. This incident occurs as a result of lack of proper attention because most of the parts in this component need repair and replacements.

The Alternative A2 which is pipe has relative closeness coefficient of 0.47755 which has become the fourth Alternative which shows that it has less criticality since this particular component is a fixed component and the leakages can easily be detected and repaired. the Alternative which is pumping machine has the most least relative closeness coefficient of 0.061847 which shows that special attention always been giving to this particular component simply because of the awareness of its functionality therefore, as a result of this constants attention to pumping machine had made it to suffers the least criticality.

Finally, the Alternatives, A4, A5 andA3 which are reservoir, fire hydrant and valve are suffering highest criticality which needs to be treated first before these Alternatives, A2 and A3 which are pipe and pump have less criticality and should be treated last.

4. CONCLUSION

This study describes the role of maintenance as a support function and its impact on production efficiency with respect to the life length and performance of production equipments which is fundamental in achieving production profitability.

Maintenance is performed to ensure that physical assets continue to function to the capacity for which they were designed. The benefits of a well-maintained plant include a lower rate of failures and downtime, cost efficiency and higher productivity. This proper decision paves way for the company to deliver its service to the consumers effectively. Several factors are considered in other to identify the component that suffers the highest criticality. But the consideration of this several criteria makes the process of selecting of the most critical component more difficult. for that reason, this paper has presented a prototype frame work using the TOPSIS classical interval version method as an effective tool for supporting component's criticality selection decision.

In this research, the weights of the different criteria are calculated using ENTROPY method of determining the weighted criteria values under the objective weighting method and for identifying the most critical component one of the well-known MCDM methods namely TOPSIS method has been used. For both methods, the results are calculated by using Microsoft office Excel.

REFRENCES
Carnacross, S. and Feachem, R.G. (1988) Environmental Health Engineering in the Tropics: An Introductory text. John Wiley & Sons. Great Britain.

Jahanshahloo, G.R; Lotfi, F. H; Izadikhah, M. (2006). An algorithmic method to extend TOPSIS for decision making problems with interval data, Applied Mathematics and Computation 175.2: 1375-1384.

Marivappan , V. (2004) some studies on RCM, PhD thesis, IIT, Bombay.

Mays, L.W. (2006) Water resources engineering First edition. John Wiley & Sons, Inc .Hobooken. 74

Chen, C.T. Extensions of the TOPSIS for group decision-making under fuzzy environment. Fuzzy Sets Syst. 2000, 114, 1–9.

Jahanshahloo, G.R.; Lotfi, F.H.; Izadikhah, M. Extension of the TOPSIS method for decision-makingproblems with fuzzy data. Appl. Math. Comput. 2006, 181, 1544–1551.

Yoon, K.; Hwang, C.L. Multiple Attribute Decision Making: Methods and Applications; Springer:Berlin/Heidelberg, Germany, 1981.

Dong, S.J; Jine, S.J; Eui, H.K. (2005). Development of Integrated Materials Database System for Plant Facilities Maintenance and Optimisation. Key Engineering Materials, Switzerland: Trans Technical Publications 297-300: 2681-2686.

Bhargava, D.S. and Gupta, P.K. (2004) Variation effect on the economical design of service reservoirs.Indian Journal of Engineering and Material Sciences.Vol II, pp 107-112 www.niscair.res.in

Punmia, B.C., Jain, A.K., and Jain, A.K. (2001) Water supply engineering, second edition Laxima Publications (P) Limited. New Delhi, India.

United Nations. (2012). Millennium Development Goals (MDGs) Report. New York: United Nations. Retrieved October 8, 2012, from http://www.undp.org/content/dam/undp/library/MDG/english/The_MDG_Report_2012.pdf

United Nations, (2006) Development programmed UN PLZA, NEW YORK,10017, USA

The Nigerian Society of Engineers
Minna Branch
1st NSE Minna Branch National Conference 2021

Conference theme
Role of Engineering in Sustainable Development Goals

The Effectiveness of Flood Early Warning by Nigerian Meteorological Agency for Sustainable Econimic Development

Abdullahi Hussaini and Mansur Bako Matazu

Nigerian Meteorological Agency, Abuja

Corresponding Author: usaini2000@yahoo.com, gsm: +2348033115536

ABSTRACT

This study assessed the effectiveness of the flood early issued by Nigerian Meteorological Agency (NIMET) for the sustainable development of the economic sectors in Nigeria. The information used in this study was obtained from the NIMET. The flood early warning issued by NIMET prior to the 2012 devastating flood that destroyed so many lives and properties and displaced many people was used the index for comparison. The predicted 2012 rainfall across the country during the Seasonal Rainfall Prediction (SRP) was used to compare with the actual rainfall using paired t- test two sample for means and the result indicated no significance difference between the predicted rainfall by NIMET and the actual rainfall recorded in 2012. Also, the month-to-month Standardized Precipitation Index (SPI) for Drought and Flood Monitoring of 2012 as analyzed by NIMET was used to further affirm the effectiveness of flood early warning by NIMET. The results from this study indicated that NIMET has indeed issued an effective early flood warning prior to the 2012 devastated flood. This study recommended that NIMET should be adequately funded to acquire the latest state of the art instruments, the decentralization of its SRPs which has now become Seasonal Climate Prediction (SCP) to the various geopolitical zones, proper circulation of its climate predictions, training and retraining of staff and the establishment of more meteorological stations.

KEYWORDS: *Flood Early Warning System, Nigeria, NIMET, Socio-economic Sectors, Sustainable Development.*

1. INTRODUCTION

Having effective flood early warning systems is widely accepted as one component of managing risk from disasters. The Hyogo Framework for Action (2010 – 2015) made early warning a priority for action and the post 2015 framework for Disaster Risk Reduction is expected to strengthen early warning systems and tailor them to user's needs, including social and cultural requirements. As such, the primary objective of a flood warning system is to reduce exposure to flooding (Linham and Nicholls, 2010). The SDGs are global goals for achieving environmental and human development by the year 2030 (Bebbington and Unerman 2018). Nigeria has challenges to achieving them because of the issue of recurrent flooding. Sustainable development and the sustainable development goals (SDGs) Sustainable Development is; "Development that meets the needs of the present without compromising the ability of future generations to meet their own needs." This is the most widespread and accepted definition of sustainable development, adopted from the UN Report of the World Commission on Environment and Development: Our Common Future, known as the Brundtland Report after the Chair, Gro Harlem Brundtland (Brundtland Report, 1987). The United Nation Sustainable Development Disasters like flooding have disproportionate impact across populations all over the world. The differences in impact are attributed to the fact that countries of the world are at different levels of development and do not face the same challenges (Mata-Lima et al. 2013; Reckien et al. 2017). Indeed, flooding disrupts various aspects of life.The National Emergency Management Agency, NEMA (2013) reported that about 7.7 million people in Nigeria had been affected by flooding between the period July to October, 2012 when 363 were killed and 18,282 injured. The devastating flood event occurred due to heavy downpours in many parts of the country. The flood of August, 2012 along Rivers Niger and Benue that submerged most parts of Lokoja town blocked the major road linking the Northern and South-eastern part of the country. Also the released water from Lagdo Dam in the Cameroun Republic affected

parts of Adamawa State in Nigeria. The Nigerian Meteorological Agency (NiMet), has the mandate to provide timely and reliable weather and climate information to all sectors of the economy, serves as a decision support tool for Nigerians, as it provides key information to ease decision-making processes, especially for strategic planning, policy making, and for operators of various sectors of the economy which rely on climate information for their daily operations. Some of these sectors include: Agriculture, Telecommunication, Water resources management, Transportation, Power, Health and Disaster risk management among others. Over the years, it has proven to be very resourceful as it has helped in cutting down losses resulting from extreme weather conditions to the barest minimum and also improved productivity to optimal levels. This has gone a long way in providing information to the activities leading to a sustainable development in all the socio-economic sectors.

1.1 Study area

The country Nigeria is situated between Latitudes 4°N and 14°N and between Longitudes 3⁰E and 15⁰E (see Fig 1). It is bordered on the north, east, and west by Niger, the Cameroon, and Benin Republic, respectively (Nigeria's First National Communication, 2003; Nwilo and Badejo 2006; Oguntunde, Abiodun and Lischeid, 2011). Nigeria, a sub-Saharan West African country, is on the Gulf of Guinea, east of the Greenwich and north of the equator. The country is made up of 36 states and the Federal Capital Territory (FCT), Abuja. It maintains a large expanse of coastline, over 853 km in magnitude, with hydrological features which include the Rivers Niger and Benue, both of which confluence at Lokoja, and flows further southwards through the Niger Delta into the Atlantic Ocean.

1.1.1 Climate and vegetation

Nigeria is located within the lowland humid of the tropics and is generally characterized by a high temperature experienced continuously throughout the year. Nigeria falls within the Tropical Continental Climate. Temperatures across the country is relatively high with a very narrow variation in seasonal and diurnal ranges (22°C-36°C). However, there are clear differences in temperatures between the country's South and North. While the far south of the country has the mean maximum temperature of 32°C, the North has a mean maximum temperature of 41°C. Conversely, the mean minimum temperature in the northern region is under 13°C, indicating a much higher annual range and the mean temperature for the southern region of Nigeria is 21°C. The mean minimum temperature for the entire country is 27°c in the absence of altitudinal variations (Nigeria's First National Communication, 2003).
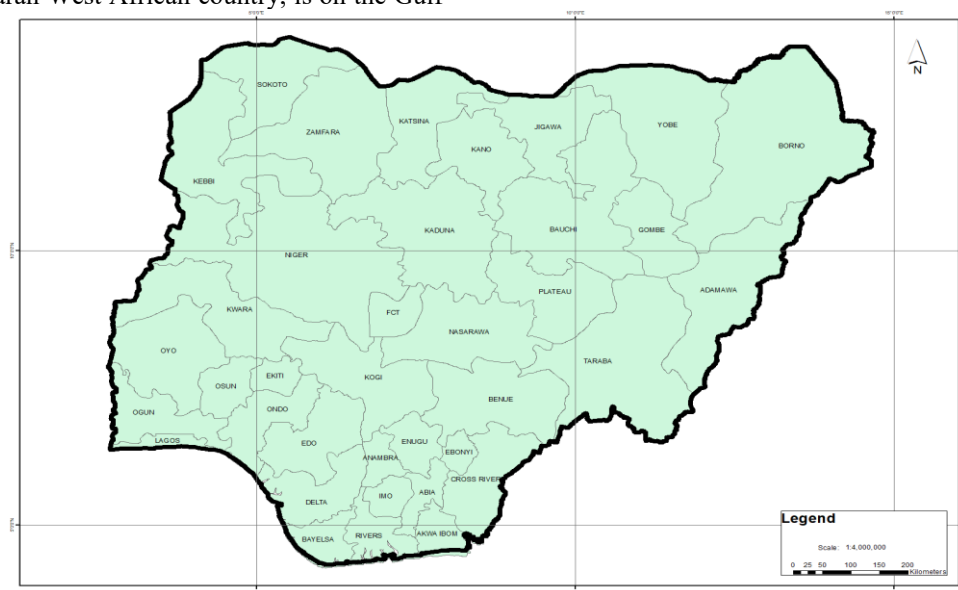

Figure 1: The Study Area

The Nigerian Society of Engineers
Minna Branch
1st NSE Minna Branch National Conference 2021

Conference theme

Role of Engineering in
Sustainable Development Goals

Annual rainfall generally decreases from the coast inland from an average of about 3000 mm in Warri on the coast to less than 500 mm in Nguru in the Sahel of the north-east. However, rainfall is mostly seasonal- in the south, the wet season extends from March to October, while it is May to September in the north (Ojo, 1977; Iloeje, 1981). The southern two thirds of the country is characterised by double maxima rainfall regime. The period of the maximum in the north may have shifted from August to July and the primary rainfall peak in the south from July to September. Also, the high intra-annual variability of Nigeria's rainfall is becoming more prominent (Odekunle and Adejuwon, 2007). This comes with long dry spells during the growing seasons causing crop failures. Recent studies have also revealed declining trends in rainfall (Odjubo, 2010). Also, some northern states in Nigeria receive less than 75 per cent of their mean annual rainfall and this is significant and calls for proactive actions (Nigeria's First National Communication on Climate Change, 2003). It could be argued that, this trend is most likely than not, to get worse in the future as a result of climate change. According to the United Nation Development Programme (UNDP, 2011), Nigeria is exposed to the dangers of climate change, like other countries globally.

Vegetation: The identified vegetation zones that are common in Nigeria are; Mangrove and Freshwater swamps along the coast, giving way northwards to Rain Forest, Guinea savannah, Sudan savannah, and Sahel savannah. It has been observed also, that, the actual vegetation cover in all the vegetation zones have shown heavy imprint of centuries of human activities (National Adaptation Strategy and Plan of Action on Climate Change for Nigeria (NASPA-CCN, 2011). This suggests that there are significant human impacts on the environment.

2. MATERIALS AND METHODS
Materials used for this research work were the products of interview from the Director General and Chief Executive Officer of the Nigerian Meteorological Agency, the Directorate of Applied Meteorological Services, the Directorate of Engineering and Technical Services and the Directorate of Training and Research. Content analysis was used in getting vital information from the interviews. Rainfall information from the Data Management Unit (DMU) of NIMET was collected during the interview. The 2012 SRP prediction by NIMET was used to determine the effectiveness of the early warning issued by NIMET on Flood. Also information on the 2012 Flood and Drought Bulletins using Standard Precipitation Index was analyzed.

3. DISCUSSION OF RESULTS
The results of this study are discussed in 3.1, 3.2 and 3.3.

3.1 Using the 2012 Seasonal Rainfall Prediction to show the effectiveness of flood the early warning system by NIMET
The Seasonal Rainfall Prediction (SRP) released by NIMET in early July 2012, clearly forecast that excessive rainfall and flooding were very likely to occur during July, August and September 2012 in many parts of the country.

Table 1 presents the predicted and actual rainfall data of 2012 by NIMET

Paired t- test two sample for means was to show if there is any significant difference between the predicted rainfall and the actual rainfall using these hypotheses:
Ho: There is no significant difference between the predicted rainfall and the actual rainfall in 2012
H1: There is significant difference between the predicted rainfall and the actual rainfall in 2012
After running the variables on an excel package using 0.05 level of significance the following result was arrived as presented in Table 1

The calculation in Table 2 has clearly indicated that t statistis (-4.31554) is lower than t critical (2.04523) and therefore Ho (Null Hypothesis) is accepted. This has shown that there is no significant difference between the predicted rainfall by NIMET and the actual rainfall and this has further shown that the flood warning system emanating from NIMET is effective based on the Seasonal Rainfall Prediction and the Flood and Drought Monitoring Bulletins

3.2 The 2012 Standard Precipitation Index (SPI) Month to Month Analysis
The cumulative 12-month SPI analysis for stream-flow and lake storage monitoring reveals apparent wetness intensification over some stations in the North like Bauchi, Jos and Kano in particular while Potiskum, Sokoto and it environ experienced mild dryness. In the same vein, most Southern parts of the

country also witnessed normal to extreme wet condition especially over Calabar. This was as a result of the effect of October, 2011 to September, 2012 cumulative rainfall on the stream-flow and lake storage in the country (Figure. 2).

Table 1: 2012 Predicted Rainfall and Actual Rainfall

Station	Predicted Rainfall (mm)	Actual Rainfall (mm)
Abeokuta	1035.0	1364.2
Abuja	1424.0	1672.2
Akure	1284.0	1389.3
Bauchi	886.0	1545.8
Benin	1985.0	2464.7
Bida	995.0	1349.7
Calabar	2635.0	4044.9
Enugu	1693.0	2137.7
Gusau	811.0	754.6
Ibadan	1275.0	1377.2
Ijebu-ode	1395.0	1584.4
Ikeja	1279.0	1557.0
Ilorin	1095.0	1079.0
Iseyin	1069.0	1299.7
Jos	1057.0	1468.0
Kaduna	1082.0	1448.2
Kano	799.0	1689.5
Katsina	462.0	698.7
Lokoja	1040.0	1343.3
Maiduguri	430.0	868.8
Minna	1046.0	1543.2
Nguru	336.0	654.1
Oshogbo	1227.0	1526.7
Owerri	2233.0	2260.7
Port Harcourt	2131.0	2248.6
Sokoto	522.0	613.4
Uyo	2061.0	4627.2
Warri	2649.0	2893.6
Yelwa	883.0	952.2
Yola	742.0	930.7

Source: Author's field work, 2019

Table 2: Result of the t-test: Paired Two Sample for Means

	Predicted Rainfall (mm)	Actual Rainfall (mm)
Mean	1252.033	1646.243
Variance	378128.2	832734.1
Observations	30	30
Pearson Correlation	0.855876	
Hypothesized Mean Difference	0	
Df	29	
t Stat	-4.31554	
P(T<=t) one-tail	8.44E-05	
t Critical one-tail	1.699127	
P(T<=t) two-tail	0.000169	
t Critical two-tail	2.04523	

Reduced rainfall is expected in the month of October especially over the far North; indications of approaching end of the rainy season due to southward movement of the Inter-Tropical Discontinuity (ITD). Meanwhile, Central and the Southern states may continue to experience normal rainfall with considerable reduced intensity rate. Increased river and stream flows which favours positive marine and hydropower related activities is therefore expected particularly coastal regions of the country. Few cases of flash flood may not be ruled out particularly in flood prone areas.

Conference theme
Role of Engineering in Sustainable Development Goals

The Nigerian Meteorological Agency has called on the various stakeholders to make necessary arrangements to mitigate the effect of the flood that may occur due to the excessive rainfall expected in 2012.

Normal – to – above normal rainfall amount was predicted for 2012. In the update released in early July 2012, it was clearly predicted that excessive rainfall and flooding were very likely to occur during July, August and September 2012 in many parts of the country as was observed. In 2012, there was a fair agreement between the observed and the predicted length of rainy season. However, the observed was higher than the predicted over Borno, Kano, Plateau, Adamawa and Taraba States in the North and parts of the Southern States.
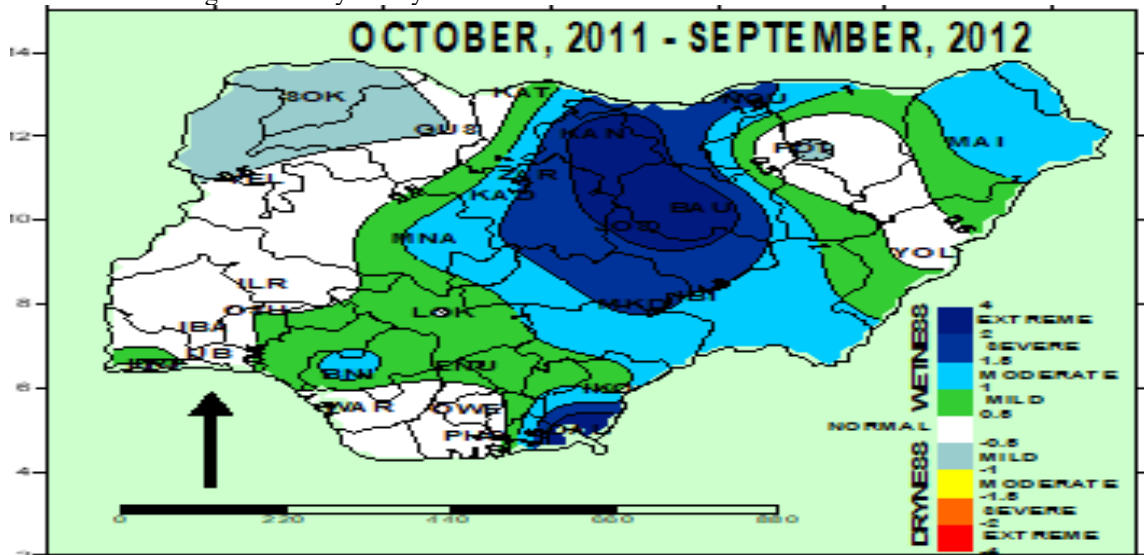
Figure. 2: 12-month SPI, October, 2011 – September, 2012
Source: Authors' fieldwork (2019) (from NIMET Hydro Unit)
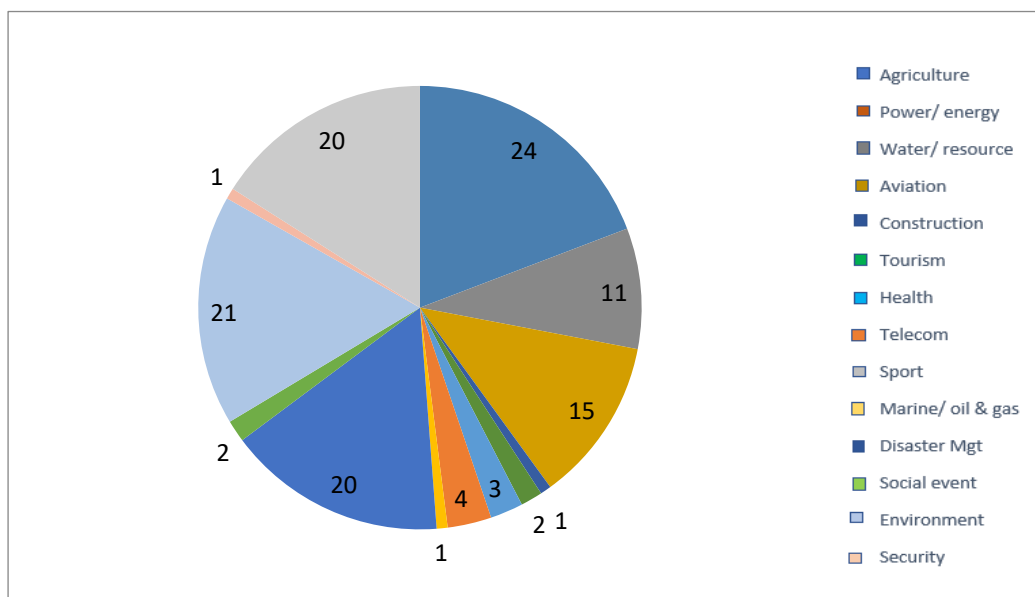
Figure 3: Sector of the Economy Participants

The Nigerian Society of Engineers
Minna Branch
1st NSE Minna Branch National Conference 2021

Conference theme
Role of Engineering in
Sustainable Development Goals

3.3 Establishment of Scientific Mechanism from Stakeholder's Feedback of Seasonal Rainfall Prediction (SRP) 2019.

Figure 3 presents the feedback received from the different sector of the economy in relation to the 2019 SRP

The Seasonal Rainfall Prediction (SRP) is a product of the Nigerian Meteorological Agency with broad methodology centered on Agricultural, Environment and Disaster Management principles and it is no doubt that a large section of those that participated in the unveiling of the product in 2019 were from the Agricultural sector. It is also worth saying that the versatility of the product is seen by the cross-section participation of most sectors in the national economy and everyday life. The figure above shows the percentage number of participant's respondents' questionnaire for the 2019 Seasonal Rainfall Prediction. Agriculture, Disaster Management and Environment had the highest number of questionnaire respondents (19% and 16% each respectively).

4. CONCLUSION

It was established by this research study through the predicted and the actual rainfall amount of 31 selected cities in 2012 obtained from NIMET using paired t-test, that there is no significant difference between the predicted and the actual rainfall recorded during 2012 and this has confirmed the effectiveness of NIMET's flood warning in 2012. This study has also indicated that NIMET has issued flood early warnings prior to the 2012 flood in Nigeria. An effective flood early warning system is surely a way of averting disasters before they occur and this will go a long in reducing the impact on all the socio-economic sectors.

4.1 Recommendations

i. NIMET should aggressively broaden its internal revenue generation away from aviation and agro meteorology to all sectors of the economy.
ii. Factory training on flood warnings equipment should be instituted. Observers, Forecasters, Meteorologist and Engineers should be trained and retrained.
iii. The establishment of Meteorological Stations at every 100km should be actualized as this will improve NIMET Seasonal Rainfall Predictions and Flood Monitoring.

REFERENCES

Bebbington, J., and J. Unerman. (2018). "Achieving the United Nations Sustainable Development Goals." Accounting, Auditing & Accountability Journal 31: 2–24. doi:10.1108/ AAAJ-05-2017-2929.

Brundtland, G. H. (1987). Report of the World Commission on environment and development "our common future.": United Nations.

Iloeje, N.P. (1981). A New Geography of Nigeria. New Revised Edition, Longman, Great Britain.

Linham, M. and Nicholls, R.J. (2010). Technologies for Climate Change Adaptation: Coastal erosion and flooding. TNA Guidebook Series.UNEP/GEF. Available from: http://tech-action.org/Guidebooks/TNAhandbook-CoastalErosionFlooding.pdf

Mata-Lima, H., A. Alvino-Borba, A. Pinheiro, A. Mata-Lima, and J. A. Almeida. (2013). "Impacts of Natural Disasters on Environmental and Socio-economic Systems: What Makes the Difference?" Ambiente & Sociedade 16: 3

National Adaptation Strategy and Plan of Action on Climate Change for Nigeria (NASPA-CCN) (2011) Report www.naspanigeria.org/ (Accessed 02/02/2012)

Nigeria's First National Communication (2003) www.unfccc.int/nationa_reports/items/1408.pl (Accessed 02/02/2018)

Nigeria's First National Communication (2003) www.unfccc.int/nationa_reports/items/1408.pl (Accessed 02/02/2018)

Nigerian Emergency Management Agency (NEMA) (2013) Report on flood disasters in Nigeria. Abuja: Government Press.

Nwilo, P. C. and Badejo, O. T. (2006). Impacts and Management of Oil Spill Pollution along the Nigeria Coastal Areas FIG Publications No. 36, 119-133

Odjugo P.A.O. (2010). Regional Evidenece of Climate Change in Nigeria, *J. Geogr. Reg. Plann.*, 3(6): 142-150.

Oguntunde, P.G., B.J. Abiodun and G. Lischeid, (2011). Rainfall trends in Nigeria, 1901-2000. *J. Hydrol.*, (411), 207-218.

Ojo, O. (1977). The Climates of West Africa, Heinemann, London.

Reckien, D., F. Creutzig, B. Fernandez, S. Lwasa, M. TovarRestrepo, D. McEvoy, and D.

Satterthwaite. (2017). "Climate Change, Equity and the Sustainable Development Goals: An Urban Perspective." Environment and Urbanization 29 (1): 159–182. doi:10.1177/ 0956247816677778.

United Nations-Water (2011). Cities coping with water uncertainties. Media Brief, UN-Water Decade Programme on Advocacy and Communication, 2011.

The Nigerian Society of Engineers
Minna Branch
1st NSE Minna Branch National Conference 2021

Conference theme
Role of Engineering in Sustainable Development Goals

Evaluation of Hydraulic Model for Water Allocation in a Large Rice Irrigation Scheme, Malaysia

Habibu Ismail [a, *], Md Rowshon Kamal [b], N.J. Shanono [c] and S.A. Amin [d]

[a] Department of Agricultural and Bio-Resources Engineering,
Ahmadu Bello University, Zaria Nigeria; habfta@yahoo.com

[b] Department of Biological and Agricultural Engineering, Faculty of Engineering,
Universiti Putra Malaysia, 43400 UPM Serdang, Selangor, Malaysia; rowshon@yahoo.com;

[c] Department of Agricultural and Environmental Engineering,
Bayero University, Kano Nigeria; njshanono.age@buk.edu.ng

[d] Department of Agricultural and Bioresource Engineering,
ATBU Bauchi Nigeria; aasanusi@atbu.edu.ng

* Correspondence: habfta@yahoo.com; Tel.: +2348038758660

ABSTRACT

The productivity of agro-hydrological watersheds and water availability in various irrigation schemes has been affected by spatial and temporal variability in climate. Water shortage is a crucial issue for Tanjung Karang Rice Irrigation Scheme Malaysia due to imbalanced water supplied to the water demand. Hydrologic Engineering Centers River Analysis System (HEC-RAS) model was evaluated for effective water supply in the scheme. The water schedule has been analyzed using the simulated available water for supply by the model. Results of R^2, Nash-Sutcliffe Efficiency (NSE), Percentage bias (PBIAS) and Root mean square error – standard deviation ratio (RSR) for calibration and validation periods were 0.66, 0.64, 0.94 and 0.60; and 0.65, 0.59, 1.77 and 0.64, respectively. The simulated water supply to the scheme using the developed HEC-RAS model was found to be improperly allocated compared to the water demand, thereby wasting excess water in the low-demand periods and shortage supply in high-demand. This suggests for a storage facility in the area, which could be used to store excess water and use during the high-demand periods.

KEYWORDS: *adaptive water allocation; HEC-RAS; Hydraulic modelling; irrigation.*

1 INTRODUCTION

An appropriate water allocation in irrigation scheme is one of the important factors considered for improving irrigation management of the scheme (Rowshon et al., 2011). Water scarcity has been a significant constraint in recent decades for socio-economic growth around the globe. The issue is probable to be exacerbated by fast population growth, a drier environment, and increased water requirements (Ipcc, 2007). Globally, irrigated agriculture as the biggest water consumer is subject to water allocation reductions, owing to fast development in water demand for non-agricultural environmental industries (e.g. residential, industrial, recreational, ecological and use) in both developed and developing areas (Levidow et al., 2014). In addition, ineffective use of irrigation water, especially in many irrigated fields has created issues with irrigation water non-uniformity, desertification and degradation of water quality. Water management in irrigation areas is adequately improved with the use of tools to integrate various resources for planning and decision-making. The use of prediction tools is an effective alternative in evaluating difficult tasks in a system.

It is difficult to manually estimate and regulate flow at various parts of a canal in a big irrigation scheme, resulting in insufficient supply and demand. The Bernam River Basin serves as the primary source of irrigation for Malaysia's Tanjung Karang Rice Irrigation Scheme. The hydraulic analysis of this river basin is very important for adequate plan of water schedules in the scheme. There is usually an imbalance between water supply from upstream and water demand at the scheme's intake (Nawabs, 2018). As a result, there is either a water shortage during periods of high demand or water waste during periods of low demand. Various computerized hydraulic models were applied in various irrigation systems to address similar challenges. For instance, DUFLOW, MODIS, CANAL and CARIMA models were respectively evaluated by Clemmens (1993),

Conference theme
Role of Engineering in Sustainable Development Goals

Schuurmans (1993), Holly and Parish (1993) and Rogers and Merkley (1993). MIKE 11 and MIKE SHE models were also applied by Singh (1997). An irrigation canal was evaluated by Kumar (2002) using CANALMAN model. The HEC-RAS is a hydraulic simulation tool that has the capability of producing river geometry using spatial data via the model's GIS component (HEC-GeoRAS), which is particularly useful in canals with limited data. Nevertheless, information on applying the HEC-RAS model to model the hydraulics of an irrigation system is sparse (Javan, 2005), with essentially no studies on water allocation for irrigation schemes. Therefore, this study evaluated HEC-RAS model for adequate water allocation at the study area.

2   METHODOLOGY

2.1   STUDY AREA

Tanjung Karang Rice Irrigation Scheme (TAKRIS) is located at latitude 30 25/ to 30 45/ N and longitude 1000 58/ to 1010 15/ E within the State of Selangor of Peninsular Malaysia on a coastal plain in Kuala Selangor District as shown in Figure 1. The area being near the coast is generally flat with minimal slope falling towards the coast direction. The runoff of the Upper Bernam river basin is the main source of irrigation water for the scheme (Amin et al., 2011; Dlamini, 2017). The diversion of water for irrigation is from the Basin at the BRH, situated at about 130 km upstream from the estuary of the Bernam River, and it reaches the scheme at TRH through a feeder canal.
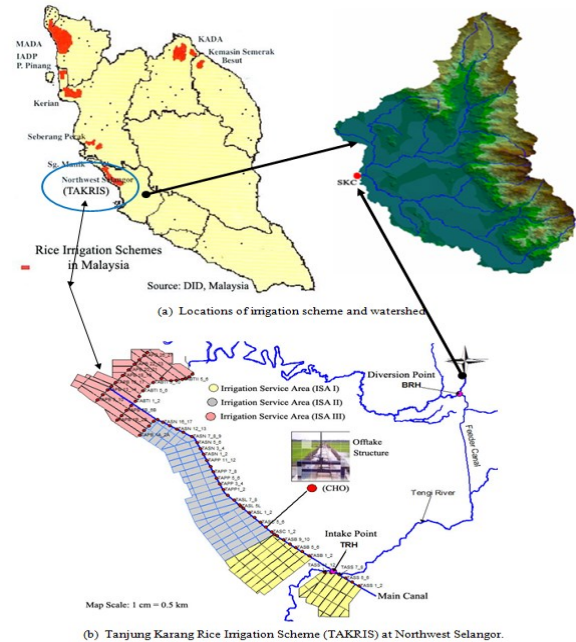
Figure 1: Tanjung Karang Rice Irrigation Scheme (TAKRIS)

2.2   HYDRAULIC MODELING OF THE RIVER

HEC-RAS model is one of the most accurate and widely applied models in river analysis system (Harrower et al., 2012; Henry & Walton, 2008; Khatibi et al., 2011; Sami et al., 2016) and was adopted in the present study. HEC-RAS is a computer program that models the hydraulics of water flow through natural rivers and other channels. It was developed by the US Department of Defense, Army Corps of Engineers in order to analyze and manage rivers (Henry & Walton, 2008). The latest HEC-RAS 5.0 version 2016 with Geospatial Hydrologic Modeling extension (Arc-Hydro and HEC-GeoRAS) was used which is available for public domain from the HEC website www.hec.usace.army.mil (2016).

2.3   INPUT DATA AND MODEL SETUP

To create river system interconnectivity, prior to using the HEC-RAS model, a 30 m x 30 m Digital Elevation Model (DEM) of the river area was employed; cross-section data reach lengths, etc., were obtained using HEC-GeoRAS. The total cross-section features of the channel were obtained and uploaded into the HEC-RAS model after pre-

processing steps with HEC-GeoRAS. The contraction and expansion coefficients employed in the model were chosen based on Usace-Hec (2016).

In order to perform an unsteady flow simulation in a river, the river system should be evaluated first with steady flow model (Usace-Hec, 2016). Thus, twelve multiple profiles were used, to cover the range (10 to 120 m3/s) of flows the unsteady flow experiences within the study location. The model was run and adjustments were made thereafter, the unsteady flow model was applied.

2.4 HEC-RAS CALIBRATION AND VALIDATION

The HEC-RAS model's most variable calibration parameter is channel resistance, (i.e., Manning's n). Its values can be derived using HEC-GeoRAS and a land use map of the area. However, due to a lack of land use data spanning the entire river area Chow (1959), n values were chosen as an initial estimate of the acceptable channel resistance. Moreover, flow for one month was selected to run the unsteady-flow mode using the adjusted n values. The n values were further refined until a good fit was obtained between the simulated and observed-values using 2001 to 2003 daily discharge data of the river, that was taken at the downstream side located at the intake of the scheme. Subsequently, the validation of the calibrated model executed with the 2004 daily discharge data.

2.5 STATISTICAL EVALUATION OF MODEL

The model's performance was assessed using the most widely used statistical measures as: (i) Coefficient of Determination, R^2

$$R^2 = \left(\frac{\Sigma_{i=1}^{n}\left(P_i^{obs}-P_i^{mean}\right)\left(P_i^{sim}-P_i^{mean}\right)}{\left[\Sigma_{i=1}^{n}\left(P_i^{obs}-P_i^{mean}\right)^2 \Sigma_{i=1}^{n}\left(P_i^{obs}-P_i^{sim}\right)^2\right]^{0.5}} \right)^2$$

(1)

(ii) Nash-Sutcliffe Efficiency NSE

$$NSE = 1 - \frac{\sum_{i=1}^{n}(Qo_i - Qs_i)^2}{\sum_{i=1}^{n}(Qo_i - \overline{Qo})^2}$$

(2)

(iii) Percentage bias PBIAS

$$PBIAS = \frac{\Sigma_{i=1}^{N}(Q_{oi}-Q_{si})}{\Sigma_{i=1}^{N}Q_{oi}} \text{ x } 100 \text{ \%}$$

(3)

(iv) Root mean square error (RSME) – standard deviation (STDEV) ratio (RSR)

$$RSR = \frac{RMSE}{STDEV} = \frac{\sqrt{\Sigma_{i=1}^{n}(Q_{obs}-Q_{sim})^2}}{\sqrt{\Sigma_{i=1}^{n}(Q_{obs}-\overline{Q_{obs}})^2}}$$
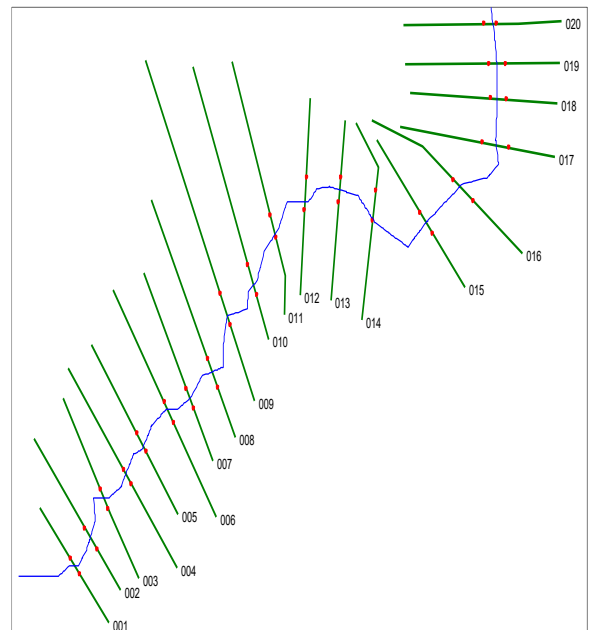
(4)

Where, Qo,i, Qs,i are the i th observed and simulated discharges respectively; $(\overline{Qo})$ = mean observed discharge;

Piobs and Pisim are observed and simulated flows, respectively; Pmean is the mean of observed flow; n is the total number of reference data points.

3 RESULTS AND DISCUSSION

3.1 HYDRAULIC MODELING OF THE RIVER

The topology of the river was generated and extracted using a DEM of the area, originating from the water source and ending at the scheme's intake. As indicated in Figure 2, the river reach was segmented into 59 cross-sections perpendicular to the direction of flow.
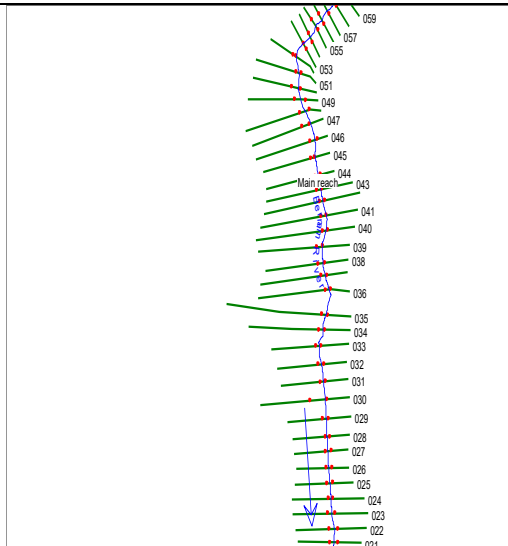

(a)

The Nigerian Society of Engineers
Minna Branch
1st NSE Minna Branch National Conference 2021

Conference theme
Role of Engineering in
Sustainable Development Goals

(b)

Figure 2: River geometry traits at the study location: (a) Cross-sections at Tengi river; (b) Cross-sections at Bernam river/feeder canal

The estimated coefficients of Manning's roughness for the main channel and both left and right overbanks are 0.045 and 0.05, respectively. The contraction coefficient was set at 0.1, while the expansion coefficient was set to 0.3. (Figure 3).
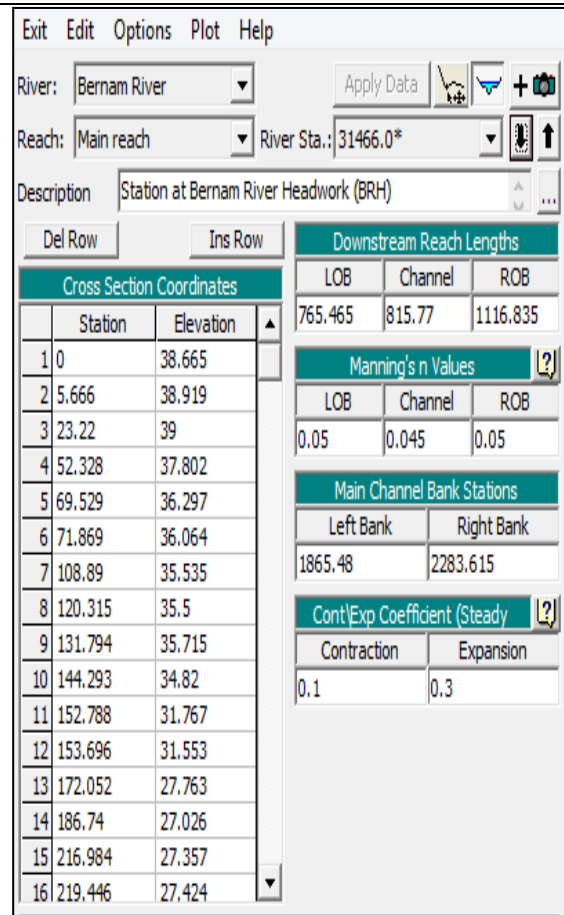
(b)

Figure 3: River cross-section data: (a) TRH; (b) BRH
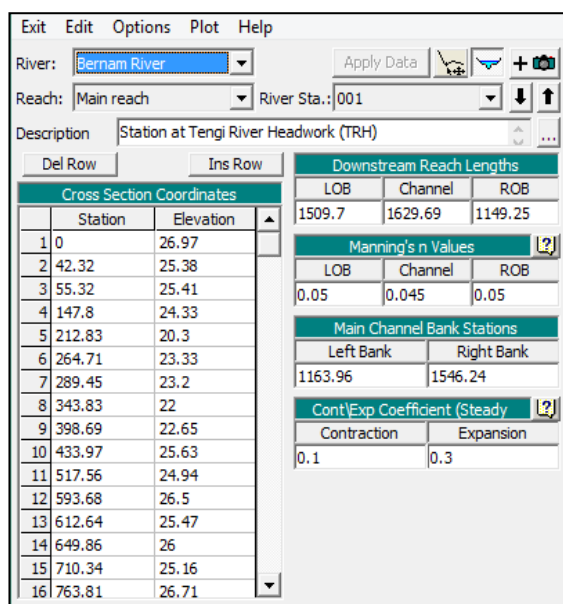
3.1 CALIBRATION AND VALIDATION OF HEC-RAS MODEL

The results of R^2, NSE, PBIAS and RSR during the calibration and validation periods were 0.66, 0.64, 0.94 and 0.60; and 0.65, 0.59, 1.77 and 0.64, respectively as shown in Figure 4. Since the results are more than 0.5, it indicates that the model simulation is satisfactory (Moriasi et al., 2007).

(a)
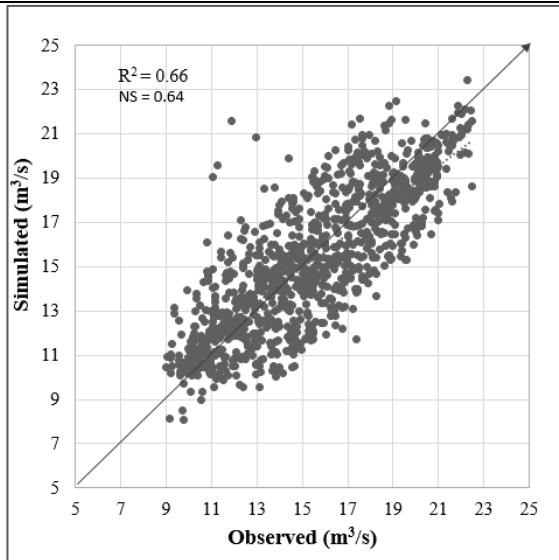
(a)
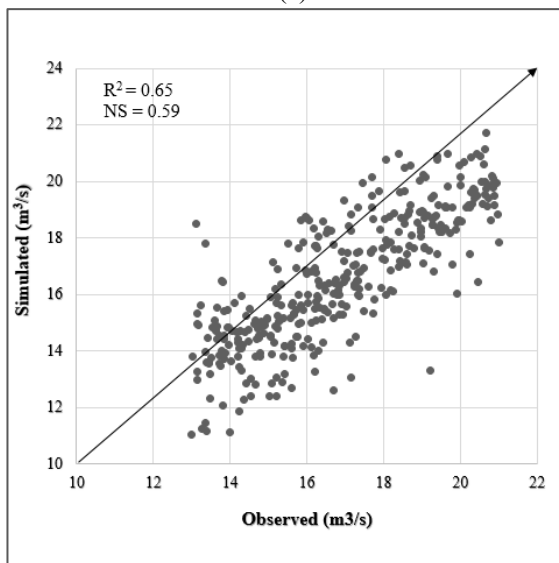
(b)

Figure 4: Simulated and observed daily streamflow for HEC-RAS model: (a) calibration; (b) validation

3.2   DEMAND AND SUPPLY

The daily water demand was compared with the available water for supply simulated using the developed HEC-RAS model for the Scheme as shown in Figure 5. The upstream water supply to the scheme is not managed relative to the amount of water required. As a result, the simulated supply to the scheme fluctuates over the seasons, with over-

supply in certain periods and under-supply in others in relation to the project's required supply. A balanced water supply-demand should always be attained for effective water management. Such balancing is attained with the operational actions, most of which necessitate the use of prediction tools (De Souza Groppo et al., 2019). This strongly suggests that a developed hydraulic model for the scheme could improve water allocation by ensuring the right supply of the desired needed water in the scheme, avoiding over-supply in low-demand periods and under-supply in high-demand periods.
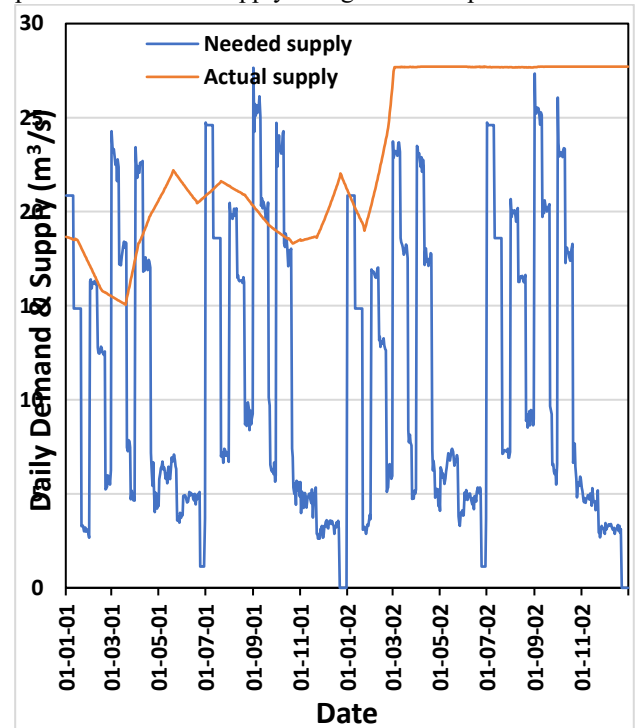
Figure 5: Water Demand and Supply in Tanjung Karang Rice Irrigation Scheme for 2001-2002

4   CONCLUSION

The runoff of the Upper Bernam river basin is the main source of irrigation water for the Tanjung Karang Rice Irrigation Scheme, which is the fourth largest rice producing schemes in Malaysia. The flow estimation in the area is using a rating curve, which is not reliable and irregular. HEC-RAS Model evaluation for effective water allocation in the scheme was satisfactory. Results of R^2, Nash-Sutcliffe Efficiency (NSE), Percentage bias (PBIAS) and Root mean square error – standard

The Nigerian Society of Engineers
Minna Branch
1st NSE Minna Branch National Conference 2021

Conference theme
Role of Engineering in
Sustainable Development Goals

deviation ratio (RSR) for calibration and validation are 0.66, 0.64, 0.94 and 0.60; and 0.65, 0.59, 1.77 and 0.64, respectively. Water supplied to the scheme as simulated using the developed HEC-RAS was found to be improperly allocated compared to the needed supply, thereby wasting excess water in the period of low-demand and shortage supply in the period of high-demand. This suggests for a storage facility in the area, which could be used to store water at low-demand period and use during high-demand. A proper water allocation of the scheme should be scheduled based on the actual scheme water demand using the developed HEC-RAS model.

REFERENCES

de Souza Groppo, G., Costa, M.A., & Libânio, M. (2019). Predicting water demand: a review of the methods employed and future possibilities. *Water Supply*.

Clemmens A.J. (1993). Description and evaluation of program: DUFLOW (ASCE). *Journal of Irrigation and Drainage Engineering, 119*, 724–734.

GP, R.D.C.M. (1993). Description and evaluation of program USM (ASCE). *Journal of Irrigation and Drainage Engineering, 119*, 693–702.

IPCC. (2007). Climate Change 2007: Sysnthesis Report. . *Contribution of Working Groups I, II and III to the Fourth Assessment Report of the Intergovernmental Panel on Climate Change. IPCC, Geneva, Switzerland,*, 104pp.

JB., H.F.M.P. (1993). Description and evaluation of program CARIMA (ASCE). *Journal of Irrigation and Drainage Engineering, 119*, 703–713.

JAVAN, M.A.S.M. (2005). Performance assessment of Doroodzan irrigation network by steady state hydraulic modeling. *Irrigation and drainage systems, 19*, 189–206.

Kumar, P., M. A., Raghuwanshi N.S. & Singh R. (2002). Application of unsteady flowhydraulic-model to a large and complex irrigation system (Elsevier). *Agricultural WaterManagement, 54* 49–66.

Levidow, L., Zaccaria, D., Maia, R., Vivas, E., Todorovic, M., & Scardigno, A. (2014). Improving water-efficient irrigation: Prospects and difficulties of innovative practices. *Agricultural water management, 146*, 84-94.

NAWABS. (2018). National Water Balance Management System (Nawabs) Bagi Lembangan Sungai Bernam. *Progress report, II*.

Rowshon, M., Amin, M., & Shariff, A. M. (2011). GIS user-interface based irrigation delivery performance assessment: a case study for Tanjung Karang rice irrigation scheme in Malaysia. *Irrigation and drainage systems, 25*(2), 97-120.

Singh R., R. J. C., Yde L., Jorgensen G.H. & Thorsen M. . (1997). Hydraulic-hydrologicalsimulations of canal-command for irrigation water management. *Irrigation and DrainageSystems, 11*, 185–213.

W., S. (1993). Description and evaluation of program MODIS (ASCE). *Journal ofIrrigation and Drainage Engineering, 119*, 735–742.

The Nigerian Society of Engineers
Minna Branch
1st NSE Minna Branch National Conference 2021

Conference theme
Role of Engineering in Sustainable Development Goals

Ultrasonic Motion Detector, A Panacea For Theft Related Security Challenges in the 21st Century

ADEBISI J.A.[*] and ABDULSALAM K. A.
Electrical Electronics and Computer Engineering, University of Lagos
jadebisi@unilag.edu.ng; kabdulsalam@unilag.edu.ng

ABSTRACT

The rate of theft, following various prison break and escape of bandits in police custody across the nation is alarming. Most of escapees have been found wanting in various theft scenes in recent times hence this study. This work considers using an Ultrasonic motion detector as a technique for addressing security challenges, especially in Nigeria. This monitoring approach emits sound energy and react to changes based on frequency shift in reflected energy. This design uses signal interference methodology by a moving body such that the presence of an intruder is being monitored in real time. Wide range of components such as power supply, sensor unit, control and alarm units, Display units were used for the design. The receiver feedback is fed to a conditioning circuit of the signal, which consists of an Amplifier, Schmitt trigger and a phase locked loop (PLL). The signal level is raised by an amplifier, the Schmitt trigger converts the output from the amplifier into a square wave form which equally eliminates the noise. The PLL was used to detect forty (40) kHz bursts in the signal received. The designed circuit was simulated on PROTEUS to ensure its effectiveness before the model construction. Results shows that the 40 kHz signal burst released from the transmitter and the receiver converts the reflected ultrasounds to electrical signals of the same 40 kHz frequency, which is effective up to a distance of 30 centimetres based on the test result.

KEYWORDS: *Amplifier, Motion-detector, Security, Ultrasonic.*

1 BACKGROUND OF STUDY

Today motion sensor technologies are fast becoming popular. It is required to measure the distance at which detection is made within specified range without any physical contact. This study discussed the development of a system based on a microcontroller device as a receiver, processor and transmitter of information due to the incessant security challenges especially in small neighbourhood and rural communities Nigeria. This challenge requires a 21st century approach beyond community policing and other security measures. It aimed at designing and constructing a simple and cheap ultrasonic motion detector such that unwanted theft related movement can be detected within a given range, perform distance calculation and raise an alarm on intruder. Motion is the movement of a body from one point to another David and Cheeke (2002). Geisheimer, (2002); further described motion as a change in position of an object over time. There are basically four major types of motion Random Motion (motion with no pattern), Oscillatory Motion (movement synonymous swinging pendulum), Rotational Motion (motion in a circular path or along a fixed point) and Translational Motion: (rigid objects). Walking people generate unique footstep acoustic Ekimov, (2006) and doppler signatures that can be used in security systems for human detection and recognition to differentiate them from other moving objects.

Vibrations can be generated from human footsteps and sound by interaction of the foot on a supporting surface. Human footstep acoustic signatures have broadband frequency response from a few Hertz up to ultrasonic frequencies (Adebisi, et al, 2018). These frequencies are band by a force normal to the supporting surface and is concentrated in a low-frequency range below 500 Hz. They can be used for seismic security detectors. Different walking styles (regular, soft and stealth) (Houston K.M. and McGaffigan, 2003) The maximum ranges for this kind of footstep recognition are determined by varied vibration signatures in the low-frequency band. Ultrasonic sensors can also detect, sounds of man, animal or any kind of moving objects which have a sound and can result to slow or fast movement. Ultrasonic waves have a frequency of roughly 20 KHz and are sound waves that are above

the range of human hearing. Ultrasonic frequencies are those that exceed 20 kHz. Ultrasonic frequency are mostly the ones above 20 KHz. Mostly they comprise of one or more transducer which transforms sound energy into electrical and vice-versa, a covering which, protects the transducer, connectors, and if possible, some electronic circuit for signal processing.

When a noticeable shift is observed from a moving person in the case of human motion, which is the target of this work; a frequency of sound is experienced (Ekimov A. S., 2006) Any unusual shift in frequency, which is generally recognized owing to predetermined frequency, is detected by a circuit in the device. A minor frequency shift, such as that caused by an insect or rat, is overlooked. Although application of motion detectors can also be found in complex security situations such as banks, offices and shopping malls however this study concentrates more on neighbourhood and private property protection measures as a form of intruder alarm in such situation. The prevailing motion detectors can stop serious accidents by sensing the persons who are in close proximity to the detector. The main element in the motion detector circuit is the dual infrared reflective sensor or any other detecting sensor.

1.2 THE JOURNEY OF ULTRASONIC MOTION DETECTOR

The first motion detector was invented in the early 1950s by Samuel Bango's which was a burglar alarm. He applied the fundamentals of a radar to ultrasonic waves at a frequency to detect fire or thief and that which human beings cannot hear. The motion detector that he developed was based on the principle of Doppler Effect. When James Prescott Joule in 1886 investigated that a ferromagnetic bar expands when it is weakly magnetized but contracts when magnetic saturation is reached as such mechanical changes that arise due to changes that occur in the magnetic field are referred to as magneto static effects (this phenomenon was later widely investigated by George Washington Pierce).When these changes are linear in nature they are known as Joule effect which is of great necessity in the production of oscillation for commercial application. The piezo electric or pressure electrical was first discovered and studied by Pierre Curie a French scientist in the early 1880's of which he was

able to discover that asymmetrical crystals such as Rochelle salt and quartz generate an electric charge on their surfaces when mechanical stress is applied. When pressure is applied to such its crystal surfaces becomes electrically charged (i.e., one side become positive and the other becomes negative).

During World War II ("Radar During World War II., 2007) the use of ultrasonic pulses for detection of energy vessels came to maturity. Ultrasonic waves have also been used for purposes other than echo-elation. Strong and rapid vibrations can shake grime loose and therefore they have been used in industries to clean parts and assemblies. It has also been used to penetrate steel girders in search of gas bubbles and other flaws just as it is customary to regard light and heat as radiation, invisible, ultra-violet and infrared sections of the electromagnetic spectrum. Sound can also be regarded as mechanical vibrations having frequencies from few cycles to ultrasonic vibrations. This fascinating word of silent sounds that are not audible by human ear starts from 20 kHz and extends to about 500 KHz.

1.3 THEORETICAL FRAMEWORK

A typical security system which uses sensing ability is otherwise known as a motion detector, it has the ability to detect movements through sensors and usually triggers alarm or sometimes stimulate other circuits for additional operations. Albeit the application of motion detectors are common for indoor protections which scope has gradually been expanded to cater for outdoor security concerns and large communities. one major advantage identified with indoor applications is the effective close control. When used in homes for security purposes, movements are being detected in a locked space with an area of little distance. Detectors for large range silos can protect areas with dimensions as large as 24mx37m (80ft by120ft) (Dorp, 2003). Places like museums where long time and historical assets are being kept is a critical area of application when it comes to motion detectors. They can guide against break-in at defenseless points. Some of these areas include the brick partitions, entrance frames, windows to mention a few among other openings. Further efforts could also be put in place as special detectors to handle inner exhibits such as gold and diamonds or where similar items are kept. Narrow

The Nigerian Society of Engineers
Minna Branch
1st NSE Minna Branch National Conference 2021

Conference theme
Role of Engineering in
Sustainable Development Goals

area coverage becomes very important such that; in a slightest touch motions can be detected, and such intrusion could be captured accurately. There are two major categories of motion related detectors as captured by (Ekimov A. S., 2006) they are namely, no outgoing signals (Passive detectors) and sending of energy waves (Active detectors). Human, animal or moving object produces sound.

Depending on the ways sounds are being created, they can trigger physical movement which might be slow movement or fast one. They can be detected by an ultrasonic sound detector or an equivalent device. Most of these sound waves are above the range of human hearing thus having a frequency of about 20 kHz. It is worthy to note that frequencies above 20kHz are regarded as (Geisheimer, 2002) (Theraja, 2002). In general, an ultrasonic sensor naturally encompasses of one or more ultrasonic transducer which converts sound energy into electrical and vice-versa.

1.4 TYPES OF MOTION DETECTORS

Common motion detectors are: Passive Infrared [PIR], and Microwave, Video motion detector, Radar motion detector and Photo electric motion detectors. Passive infrared motion detectors are electronic devices which are sensitive to infrared wavelengths of energy. They facilitate the detector to recognise the level of heat that is always present in the area based on impostor entry. On the other hand, Microwave motion detectors transmit electric signal within a designated area in an electronic field. The video Motion Detectors [VMD] use Closed Circuit Television (CCTV) systems which are very common as a form of capturing images in sequence to be watched at later time. It has wide motion capacity and its highly effective in surveillance and alarm signal.

Furthermore, an active sensor RADAR (Radio Detector and Ranging) which has passed through considerable enhancement and uses ultrahigh frequency radio waves to notice intrusion within an area under watch. RADAR is frequently used to conceal openings such as wall cracks doorways or hallways related to as basic outlines or a trip wire; an alarm is triggered once the ray is interrupted. Photoelectric motion detectors, which consist of two machineries (the transmitter and the receiver) is the

last: the former uses a Light Emitting Diode (LED) as a source of light while the later uses Photoelectric cell. LED transmits a steady infrared beam of light to the later. The photoelectric cell is responsible for sensing the points when beam is present. An alarm signal is generated if at least 90% of the signal being transmitted by the photo electric cell is not received for as brief as 75 milliseconds (time of intruder crossing the beam). When there is a change of up to 1,000 times per second in a manner that is similar to that of the receiver's anticipation for the prevention of a bypass attempt using an alternative light source; then the sensor can be bypassed at the angle of beam and a perfect match of the modulation frequency is obtained. This occurs when the beam is modulated at a very high frequency.

1.5 ULTRASONIC MOTION DETECTOR

This is a key concept of this work. It is a detector that uses ultra-sound with a very high frequency to detect motion. In this case a transmitter sends out sound waves of a frequency that is too high for the human ear to hear, a receiver picks up the sound waves reflected from the area under protection. The motion of someone or something in the space between the receiver and transmitter will cause a change or shift in the frequency of sound (the "Doppler Effect" also known as the frequency shift is a reaction of the sound waves behaviour when compacted by a moving object) a circuit in the device detect any unusual shift in frequency. A small shift in frequency such as that produced by an insect or rodent is ignored but when a larger shift such as one produced by a moving person is detected the device triggers the alarm. (Adebisi et al., 2021)

2.0 EMPIRICAL REVIEW

James M. Sabatier et al., (2006) discussed a method for the detection of human movement using passive and active ultrasonic methods. They work on the probability of human presence detection to reduce false alarms. They used footstep acoustic signatures for regular, soft and stealthy walking styles of a man and was measured as shown in figure 2.1.

A digital data acquisition boards (DAQ) has a specimen rate of 32 kHz and a 64 KHz distortion minimization and filter acquired signals from the accelerometer and the ultrasonic ceramic sensor

The Nigerian Society of Engineers
Minna Branch
1st NSE Minna Branch National Conference 2021

Conference theme
Role of Engineering in
Sustainable Development Goals

(UCS) was used while the full circle represents the ten footsteps for each walking style were taken and combined in one data file.

Satish Pandey et al., (2008) discussed a short-range ultrasonic obstruction, its detection and its practical implementation. This work considered the distance measurement in this device. They used an ultrasonic transducer pair sounds that detect obstructions based on sound and sensing waves. The creation of 40 KHz signal burst used in the transmitter circuitry was achieved with the use of ATmega8 AVR microcontroller. It further used it to process the received signal for gauging the period of flight of replicated waves and precise range of the hitch.

Iin Shrivastava, A.K et al., (2010) they used separate ultrasonic transmitter, receiver and a microcontroller to measure the distance of an obstacle the measurement system is mounted at a small distance between them and a Phillips P89C51RD2 microcontroller-based system. This system was tested for use in robotic sewer inspection system which is under development. The Ultrasonic wave propagation velocity in air is approximately 340 m/s time delay at 15°C of air or atmospheric temperature which is same as sonic velocity. To be accurate the ultrasound velocity is governed by the medium and its temperature. Hence the velocity in the air is calculated using Equation 2.1:

V= 340 + 0.6(t-15) m/s (Eq 2.1)

Where t is the temperature in ^{0}C

The distance can then be calculated as Distance (cm) = **(Travel Time*10^{-6} * 34300) / 2**

Their study assumed room temperature of 20°C is assumed; hence the velocity of ultrasound in the air is taken as 343 m/s.

Shamsul Arefin et al., (2013), This research uses a circuit to calculate the distance based on the speed of sound at 25°C ambient temperature and shows it on LCD display. The technique of distance measurement using ultrasonic in air include continuous wave & pulse echo technique. In this model, the target needs to have a proper orientation on how the pulse can be perpendicular to the direction of propagation of the pulses. The

amplitude of the received signal gets significantly attenuated and is a function of the nature of the medium and the distance between the transmitter and target.

Jeneeth Subashini et al., (2014) This project uses an ultrasonic sensor with very limited feature. They considered detection in a room of an area of 35 m2 with the ultrasonic transducers at an angle of 450. The detection of movement is also possible within the coverage area of about ±4m. however it comes with a challenge of limited area of within a room.

Nadee et al., (2015) studied a systematic approach to reduce the falling risk in the area where closed-circuit television (CCTV) is not available by the usage of ultrasonic sensors for its detection. The ultrasonic sensors having a transmitter and a receiver is connected to an Arduino microcontroller to send the signal via Wi-Fi to computer. The sensors are positioned to array on top and wall of room. Then the threshold signal was analysed to find the action such as stand, sit and fall by comparison between top and side signal. The various side signals
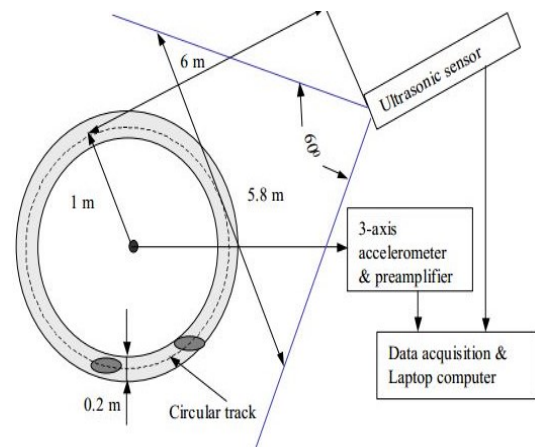

Figure 2.1: Setup for measurements of vibration and sound frequency response. Source: Ekimov, (2006)

indicate the failure.

3.0 DESIGN METHODOLOGY

The design of the work comprises of several components as shown in the design block diagram in figure 3.1. It includes the Arduino Microcontroller, Ultrasonic Sensors, Display unit, Alarm unit and Power unit. A code was written in C language to generate 40 kHz signal burst and the equivalent

The Nigerian Society of Engineers
Minna Branch
1st NSE Minna Branch National Conference 2021

Conference theme
Role of Engineering in
Sustainable Development Goals

drawn-out Intel hex file i.e. dot hex repository. On a successful signal surge generation, a 40 KHz electrical signal was produced due to the transfer from the ultrasonic transmitter which the receiver changes to the reproduced ultrasounds. The same to electrical signals of the 40 kHz frequency. These signals involve strengthening and managing to suit the purpose due to their weak nature.
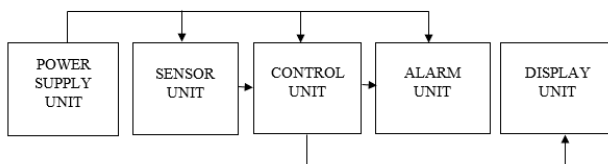
Figure 3.1 Block diagram of the ultrasonic motion detector

A conditioning circuit for signals, contains an amplifier, Schmitt trigger, and PLL, receives the receiver output. Schmitt trigger converts the signal into square wave form, which removes noise. To detect 40 kHz bursts in the received signal, PLL is used. When they are identified, the PLL switches from a high to a low logic state. This output is then passed into the microcontroller, which starts up and calculates the time of flight and determines the distance at which the motion was detected before displaying it on the screen. This work considered both hardware (transducer, microcontroller, signal conditioning, power supply, voltage regulator, electrolyte capacitor, transmitter and the receiver etc) and software components include the c-programming IDE and proteus used for the simulation.

3.1 THE MICROCONTROLLER
To manufacture an ultrasonic sound wave, an Arduino Uno microcontroller based on the ATmega328 was utilized to generate bursts of 40 kHz electrical pulse signal with the needed time delay included. Similarly, each time the signal burst is detected on the receipt of signal at the receiver a Phase Locked Loop (PLL) is activated. The microcontroller computes the time difference between the broadcast and received signal as soon as its burst is recognized. This can be achieved by separating the time break into 50% of the genuine

period of flight and since the pace of sound in air is a recognized measure; the range of the impediment can be determined more clearly. It was also employed for signal creation and calculating the distance at which motion was detected. To enable real time functions, data acquisition and data logging, for sending and receiving data, the microcontroller can be connected to a PC through its serial connection.

3.2 THE TRANSMITTER AND RECEIVER
Transmitter circuit consist of a signal generator, inverters, and an ultrasonic component, all connected to a Microcontroller, produce a 40 KHz electrical signal burst with a NOT gate. Due to the piezoelectric effect, the transducer will produce an oscillating acoustic output, resulting in ultrasonic sound waves. On the contrary, is the receiver, which receives an ultrasonic sound wave at the same frequency of the transmitter and convert this sound wave to an electrical charge. The design receives the same level of frequency. The Receiver circuit consists of signal amplification and conditioning for detection at required frequency for certain components. The PLL (LM567) is a tone decoder that is set to lock onto a signal of 40 kHz. When there is no echo, the tone decoder output is HIGH, and when there is an echo, it swings LOW. The tone decoder's output is routed into a microcontroller, which determines when an echo has been received. A low amplitude signal is usually the case which is less power and sometimes may contain unnecessary noise signals from atmospheric sources.

Other components used are the voltage regulator, A 7805 voltage regulator was used to regulate the filtered DC signal to fix a 5v to feed the microcontroller, transmitter circuit and receiver circuit for proper operation. Resistors, TL084 CN Amplifier: The FET-input operational amplifier family is intended to provide more options than any other operational amplifier family previously established. The analogue output of a FET input amplifier comprises a variety of voltage components, some of which may be undesired noise signals.

The Schmitt trigger is used to detect and transform the needed signal components into square wave form. To reduce false triggering, it uses regenerative comparison. Schmitt triggers have a noise-

cancelling positive feedback mechanism. It also contains upper and lower threshold points that can be used to filter out undesired voltage levels in the received signal. Hysteresis voltage is defined as the difference between the upper and lower threshold voltages. Another important component is the **Phase Locked Loop – LM 547:** a frequency decoder and a tone with synchronous AM lock detection and power output circuitry that is quite stable. The presence of a self-biased input is obvious when a sustained frequency is observed within the detection band, the principal duty of this, is to drive a load. Four external components individually affect the bandwidth center frequency and output delay.

3.3 RELATED FORMULATIONS
In the negative feedback mode of procedure is an operational amplifier gain and it is provided by:

$$A_V = R_f/R_1 \qquad (1)$$

while the Phase locked loop (PLL) tone detector, the centre frequency of a current controlled oscillator is defined as its free-running frequency when an input signal is lacking, and it is given by:

$$F_o = 1/(1.1R_1C_1) \qquad (2)$$

Detection Bandwidth for PLL: This is a frequency range centered on Fo within which an input signal exceeding the threshold voltage (typically 20mVRMS) causes the output to be logically zero. The loop capture range corresponds to the detection bandwidth.

$$BW \text{ (in \% of } F_o) = 1070V_1/(F_oC_1) \qquad (3)$$

Velocity of Sound in Air: The velocity of sound V in gas such as air for frequencies above 200 Hz is given by:

$$V = \sqrt{(\gamma\rho / e)}, \text{ which is 332 m/s} \qquad (4)$$

For 1 μsec, the velocity is 34 mm.

3.4 CIRCUIT CONSTRUCTION
Details of the circuit diagram showing all components interconnections and operations as shown in figure 3.2.
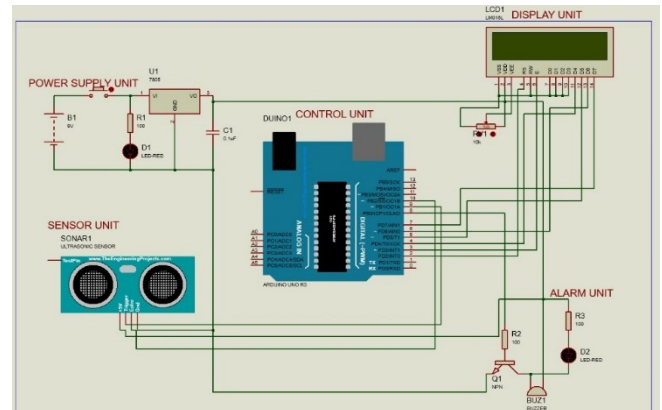

Figure. 3.2 Circuit diagram of the ultrasonic motion detector

4.0 RESULT DISCUSSION
Following successful simulation and hardware construction the circuit. The model was tested appropriately, all basic interconnections including polarity checks, individual segment checks and the interoperability validation of the entire circuitry was also not left out. The circuit was powered with a constant 6v dc supply to the component with the help of the voltage regulator and that the capacitor filtered and smoothens the voltages to avoid fluctuation. This model was evaluated under several theft scenarios based on the distance and sensitivity/sound intensity. The receiving ultrasonic transducer received the signal from the transmitting transducer causing continuous ultrasound between transducer so any break in transmission triggers the alarm. These sections were tested one after another and were given a considerable time under test to respond as desired as shown in table 4.1.

TABLE 1: TEST RESULTS

Serial Number	Ranges of Distance(m)	Sensitivity/Sound intensity
1	0-6	Very high
2	7-12	high
3	13-18	high
4	19-24	Relatively high
5	25-30	low
6	31 and above	No response at all

Other components such as resistors and capacitors were verified appropriately with their required values. Figures 4.2 and 4.3 depicts graphs showing the sensitively i.e., the degree at which this ultrasonic detector can be used to track intruders in case of theft or related scenarios per distance. It can be observed that the close the range the better the performance, a very good performance strength was recorded up to 20 metres, beyond 20m the sound detector and alarm system capacity reduced drastically and fade away till 30m and beyond as shown in figure 4.3. After extensive testing, the system was proven to be quite effective in detecting all motion within a range of 0-30 meters, with a success rate of about 90%.
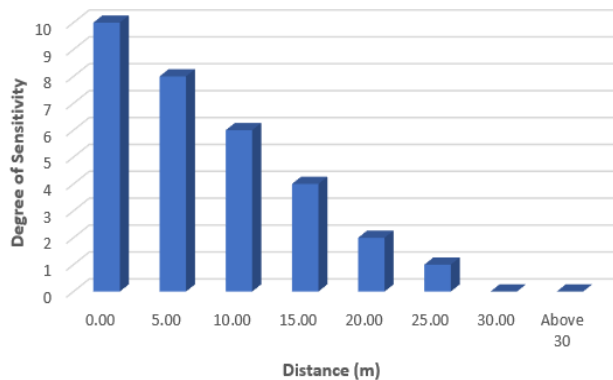
Table 4.2: Evaluation result showing strenght of model
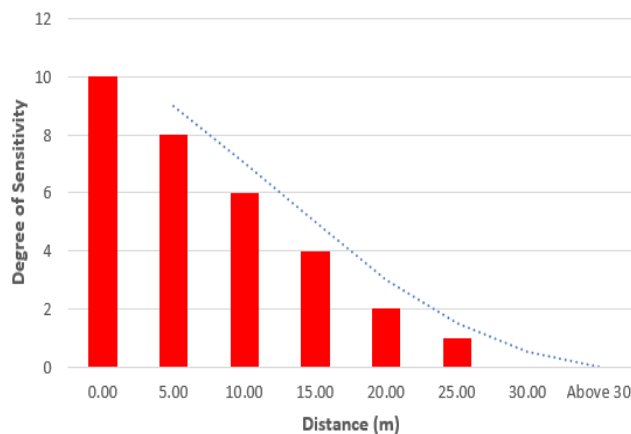
Table 4.3: Evaluation result showing the trend of strenght

5.0 APPLICATON TO SECURITY CHALLENGES

Nowadays, solutions to security challenges through network innovations and communication have moved on and the multiplicity of technologically-inclined security applications have improved. The increase of security challenges especially in nigeria can be addressed through the result of this work. This motion detector has a very high frequency to detect motion and can be deployed to offices, prisons and other sensitive locations where security issues has become a very serious matter. In addition, is the high tone alert which can awaken other security apparatus in case there is a breach of such where they are installed. This will quikly mobilize additional measures to abat the challenge as may be required. In future, this work will be improved upon to have a cloud-backup such that location data and signal reports can be incorporated as soon as there is an alert, this can equally be accessed remotely even from sensitive bush locations to track kidnappers, bandits and other threat to the peace of a community, state and nation at large. However, the secure design consideration was based on a notice/awareness security principle.

6.0 CONCLUSION

Conclusively, the outcome of this research and demonstration of an ultrasonic motion sensor for security system, human or object interference within a space has been designed, implemented and evaluated based on two major parameters; it can be deduced that the use of a GSM and camera provides better quality for any security purpose however; considering the peculiarity of remote areas, and basic theft activities in the face of poverty. The result of this project becomes more viable. This system has undergone an amount of research with different authors presenting different methods, implementation and design with motion detection, obstacle detection and distance measurements as one necessary requirements to satisfy one requirement or the other. However, the lacuna in the reviewed work has been considered approprioatly to address some of the current security issues being faced by Nigeria today. This proposed design uses a microcontroller to generate signal that helps to detect motion, obstacle and calculate the

distance at which the detection was made and intruders can be arrested for justice accordinly. The implemenation is affordable and will in turn contribute to security of lives and properties from the grassroot.

REFERENCES

Adebisi, J. A., Afolabi, B. S., & Akhigbe, B. I. (2018). A

Value-based approach to modelling interoperability in Knowledge Organization Systems. *In Challenges and Opportunities for Knowledge Organization in the Digital Age* (pp. 720-728). Ergon-Verlag.

Adebisi, J. A., Abdulsalam, K. A., & Adams, I. O. (2021).

Multi-Power Source and Cloud-Backup Enabled Security Framework for Surveillance in Nigeria. *In IOP Conference Series: Earth and Environmental Science* (Vol. 730, No. 1, p. 012005). IOP Publishing.

David, J. N cheeke (2002). "Fundamentals of Ultrasonic
    Waves" CRC Press, Florida, USA.

Ekimov, A., & Sabatier, J. M. (2006). Broad frequency

acoustic response of ground/floor to human footsteps. *In Data Mining, Intrusion Detection, Information Assurance, and Data Networks Security* 2006 (Vol. 6241, p. 62410L). International Society for Optics and Photonics.

Ekimov, A., & Sabatier, J. M. (2006). Vibration and

sound signatures of human footsteps in buildings. *The Journal of the Acoustical Society of America,* 118(3), 762-768.

Geisheimer, J. L., Greneker III, E. F., & Marshall, W. S.

(2002). High-resolution Doppler model of the human gait. *In Radar Sensor Technology and Data Visualization* (Vol. 4744, pp. 8-18). International Society for Optics and Photonics.

He, H., & Liu, J. (2008). The design of ultrasonic distance

measurement system based on S3C2410. *In 2008 International Conference on Intelligent Computation Technology and Automation (ICICTA)* (Vol. 2, pp. 44-47). IEEE.

Houston, K. M., & McGaffigan, D. P. (2003, September).

Spectrum analysis techniques for personnel detection using seismic sensors. *In Unattended Ground Sensor Technologies and Applications V* (Vol. 5090, pp. 162-173). International Society for Optics and Photonics.

Jeneeth Subashini, b. C. (2014). Implementation, working

and results of circuit detection of intruder(s) movement using ultrasonic sensors. *International journal of computer science and information technology research.* 2(3), pp: (520-526).

Nawer, A., Hossain, F., & Anwar, M. G. (2015).

Ultrasonic Navigation System for the visually impaired & blind pedestrians. Am. J. Eng. Res. (AJER), 4(2), 13-18.

Nadee, C., & Chamnongthai, K. (2015, June). Ultrasonic

array sensors for monitoring of human fall detection. *In 2015 12th international conference on electrical engineering/electronics, computer, telecommunications and information technology* (ECTI-CON) (pp. 1-4). IEEE.

Pandey, S., Mishra, D., Srivastava, A., Srivastava, A., &

Shukla, R. K. (2008). Ultrasonic Obstruction Detection and Distance Measurement using AVR Microcontroller. *Sensors & Transducers Journal*, 95(8), 49-57.

Sabatier, J. M., & Ekimov, A. E. (2006). Ultrasonic

Methods for Human Motion Detection. *In Battlefield Acoustic Sensing for ISR Applications.* (pp. 9-1 – 9-12). Retrieved from http://www.rto.nato.int/abstracts.asp.

Sharma, A., Patidar, R., Mandovara, S., & Rathod, I. (2013). Blind Audio Guidance System. *International Journal of Emerging Technology and Advanced Engineering*, 3, 17-19.

Shamsul Arefin, T. M. (2013). Design of an Ultrasonic

Distance Meter. International Journal of Scientific & Engineering Research. 4(3), pp. 90-101.

Shrivastava, A. K., Verma, A., & Singh, S. P. (2010).

Distance measurement of an object or obstacle by ultrasound sensors using P89C51RD2.

International Journal of Computer Theory and Engineering, 2(1), 64-68.

Shefali Malhotra, S. B. (2016). "Blockage detection in
    seeder". *World Conference on Futuristic Trends in Research and Innovation for Social Welfare* (Startup Conclave).

Theraja, B. L., & Theraja, A. K. (2005). A textbook of
    Electrical Technology vol 1-IV. S. Chand and Company limited: New Delhi, India 2002, pp. 1712 – 1716.

The Nigerian Society of Engineers
Minna Branch
1st NSE Minna Branch National Conference 2021

Conference theme
Role of Engineering in Sustainable Development Goals

A Brief Review of Proposed Models for Jamming Detection in Wireless Sensor Network

Grace AUDU, Michael DAVID and Abraham U. USMAN
grace.audu@st.futminna.edu.ng

ABSTRACT

Wireless sensor network (WSN) consists of a group of sensor nodes usually deployed in a hostile environment used for sensing, processing, transmitting and receiving data from the area. Sensor Nodes are characterized by limited memory, limited power and short transmission range, which exposes them to attacks like jamming. In this paper, we review different jamming attacks in WSN. We also review several proposed methods for detecting jamming. We have provided a comparative conclusion to aid researchers studying this field.

KEYWORDS: *Jamming, Jamming detection, Denial of Service Attacks, Wireless Sensor Network.*

I. INTRODUCTION

Wireless sensor network (WSN) consists of a group of sensor nodes usually deployed in a hostile environment used for sensing, processing, transmitting and receiving data where they are deployed to a base station (Osanaiye et al 2015).

WSNs have different applications. They find application were collecting data remotely is needed. These areas include military, environmental monitoring, health, controlling traffic, agriculture, and industries (Kumari et al, 2015). WSN have constrained power, storage, bandwidth and short communication distance. These constraints in addition to the open and shared wireless transmission medium makes sensor nodes prone to security attacks. Denial of Service (DoS) is one of the common attacks in WSN. These attacks occur in physical, link and network layer. At the physical layer, the most common DoS attack is jamming. Jamming occurs when a rogue node intentionally transmits a high-range signal to disrupt the normal transmission of information between legitimate nodes by reducing the signal to noise ratio. This attack affects the functionality of the network as it truncates the delivery of desired packets to the intended receiver hence impeding network capabilities (Bhushan & Sahoo ,2018). The major goal of jamming is to affect the long-term availability of sensor nodes. The jammer depletes the resources of sensor nodes by transmitting electromagnetic signals at high power towards the communication channel of the sensor nodes thereby prohibiting data from reaching its destination (Upadhyaya et al.2019).

Jamming can be perpetrated by listening passively to the communication channel in order to transmit at the same frequency as the legitimate sensor node. Jammers have high energy efficiency and are not easily detected (Pelechrinis et al., 2011)

Jamming attack may be mitigated by increasing the robustness of the legitimate signal or by implementing frequency hopping. Due to the limited resources of WSN applying those solution is difficult. WSN, hence the need for detecting jamming. In this paper we describe types of jamming attacks, metrics used for detecting jamming and review the different proposed methods to detect jamming.

WIRELESS SENSOR NETWORK ARCHITECTURE

The WSN architecture is made up of five layers (Akyildiz & Vuran, 2010)**.** These includes:

Physical layer: is responsible for transmission, modulation and receiving techniques.

Link layer: ensures bit are transferred without errors and it controls access to the channel.

Network layer: routes the data supplied by the transport layer.

Transport layer: This layer is needed when the network is going to be access by external networks; it helps to maintain the flow of data to prevent congestion.

Application Layer: provides software for numerous applications depending on the sensing task.

Jamming attack occurs at the physical and link layer.

II. JAMMING ATTACKS IN WIRELESS SENSOR NETWORK

Constant Jammer: constant jammer transmits random bits continuously on the channel to disrupt communication on the channel. This could lead to depletion of the legitimate node's energy. The constant jammer does not follow any

Medium Access Control (MAC) layer procedure before continually transmitting series of radio signals to interrupt legitimate signal transmission in the network. This jammer continuously transmits random bits that occupy the transmission path of the network, hence disrupting legitimate data transmissions initiated by nodes (Misra et al., 2010).

Deceptive jammer: A deceptive jammer continuously injects legitimate bit sequences into the communication channel without gaps in between. The sensor nodes believe that a legitimate transmission is going on, hence they remain in the listening state. Detecting deceptive jammers is difficult since they are aware of the network protocol (Misra et al., 2010).

Random Jammer: Random jammers moves from active mode to sleep mode and vice versa to save energy. During the active state, the attacker jams the network for a specific time then it turns off its transmitter and goes to sleep mode. The attacking node begins to transmit the malicious signal again, after a while then goes back to sleep mode; the sequence continues (Misra et al., 2010).

Reactive Jammer: Reactive jammers constantly sense the channel to listen for when packets are being transmitted. Once they detect a packet transmission on the channel, they begin to transmit malicious signals to disrupt the legitimate signal. This type of jammer reduces the rate of power dissipation and are hard to detect (Misra et al., 2010).

a. PROPOSED METHODS FOR DETECTING JAMMING IN WIRELESS SENSOR NETWORK

Research on jamming detection in WSNs has been ongoing for a while. A lot of proposed methods for detecting jamming involves either the use of dedicated tools or algorithms installed on the sensor nodes. Most of these proposed methods make use of information gathered a priori about some metrics of the node when it is jammed or normal. Some of these metrics include received signal strength(RSS), packet delivery ratio(PDR), packet inter arrival time(PIAT), packet sent ratio, bad packet ratio(BPR) signal to noise ratio(SNR), consumed energy, clear channel assessment.

Osanaiye et al. (2015) proposed an approach for detecting jamming attacks that uses the cluster-based topology. The EMWA algorithm used for detecting jamming is only installed on the cluster head and base station. The base station detects jamming in the member nodes while base stations detect jamming in the cluster head. In order to minimize overhead they used only metric packet IAT to detect jamming. In order to detect changes in traffic flow during situations of both non-jamming and jamming, a trace-driven experiment using EWMA was carried out. Results obtained from their work shows that their proposed model can detect jamming attack efficiently with little or no overhead in WSN from the 20th jammed packet.

Bikalpa et al. (2019) in their work proposed a node-centric approach. To reduce overhead in nodes in this detection method, network information for detecting jamming are passively gathered by anchor nodes placed in the network. Using random forest algorithm, the information gathered a prior about the network is used differentiate when the network is jammed or not. Their work achieved 89.7% and 98.6% accuracy using RSSI from five anchor nodes for real and simulated data respectively.

In their work, Youness et al., (2020) used four metrics BDR, PDR, RSS and clear channel to identify the presence of jamming attack. They generated a large set of data in a real environment simulation and gathered measurements of these parameters when the network was jammed and when it was normal. They then used these data sets to train, validate, and test the machine learning algorithms. The simulation results showed that the proposed detects jamming attacks with an accuracy of 97.5%.

Ganeshkumar et al. (2016) proposed a framework that also uses cluster-based topology for jamming detection. They used statistical tests to compute the detection metrics normal threshold. The cluster head verifies if a packet received is from a legitimate node. The framework validates whether the node is a legitimate node by using the cluster head code. Lastly, the auditing algorithm on the CH estimates the metrics (PDR, RSSI) and makes decision about "jammed situation" or "non-jammed situation. Their proposed framework detects jamming with an accuracy of 99.88%.

A fuzzy logic–based algorithm was proposed by Vijayakumar et al. (2018) for jamming detection in cluster-based wireless sensor networks. The detection metrics is checked by the cluster head to check for jamming. An accuracy of 99.89% was gotten from their simulation. The jamming detection metrics are checked by the cluster head at the lower level and by the base station at the higher level. There by reducing the overhead cost on the member nodes.

Mistra et al., (2010) proposed the use of a fuzzy inference-based system for jamming at the base stations using three metrics. These metrics include received signal strength, total packets received during a period and the number of dropped packets during that period. The power received signal is measured at the base during the jamming attack to find the difference in value between the normal RSS.The total packets received during a specific period and the packet sent over the period is used at the base station to determine the packet drop per terminal (PDPT) and signal-

to-noise ratio (SNR). These metrics are then inputted to obtain the jamming index from the fuzzy inference system. The jamming index varies from 0 to 100. The system's true-detection rate is as high as 99.8%. In a Table 1, we present a summarize Comparison of Proposed Methods for Jamming detection in Wireless Sensor Network.

TABLE 1: Comparison of Proposed Methods for Detecting Jamming in Wireless Sensor Network

REFERENCE	MACHINE LEARNING OR NON-MACHINE LEARNING METHOD	ALGORITHM USED	Metrics	WSN STRUCTURE	ACCURACY
Osanaiye *et al* (2015)	Non-Machine Learning Method	EMWA	IAT	Cluster	100% >20 Jammed packets
Bikalpa *et al.* (2019)	Machine Learning method	Random forest	RSS	Flat	89.7% for real data and 98.6 for simulated data
Youness *et al.*, (2020)	Machine Learning method	Random forest	BPR, PDR, RSS	Flat	97.5%.
Ganeshkumar *et al.*, (2016)	Non-Machine Learning Method	Auditing algorithm	PDR and RSSI	Cluster	99.88 %.
Vijayakumar *et al.*,(2018	Non-Machine Learning Method	Fuzzy logic–based jamming detection algorithm	PDR and RSSI	Cluster	99.89 %.
Misra *et al.*, 2010	Non-Machine Learning Method	Fuzzy logic	PDR, RSS	Cluster	99.89 %.

A fuzzy inference-based system to detect jamming attacks in the base stations using three metrics measured from each sensor node in the network was proposed by Mistra et al., (2010). These metrics are the total packets received during a specific period, the number of dropped packets during that period and the received signal strength (RSS). The base station computes the power received during the jamming attack to find any difference in value between the current RSS and the normal RSS. These values are used by the base station to compute the packet drop per terminal (PDPT) and signal-to-noise ratio (SNR) which is further used as inputs for the fuzzy inference system to obtain the jamming index. The jamming index varies from 0 to 100 and is used to determine the intensity of the jamming attack, which can range between a situation of 'no jamming' to absolute jamming'. The system with its high robustness, ability to grade nodes with jamming indices, and its true-detection rate as high as 99.8%, is worthy of consideration for information warfare defense purposes. In a Table 1, we present a summarize Comparison of Proposed Methods for Detecting Jamming in Wireless Sensor Network.

III. CONCLUSION

In this paper, we presented a brief survey about jamming detection in wireless sensor networks. Different jamming attacks occurring in WSNs are described in detail. Different metrics used for detecting jamming was described. The different types of jamming are described, and detection techniques of jamming has been is pointed out. Our future work will focus on improving jamming detection.

ACKNOWLEDGEMENTS

REFERENCES

O.A. Osanaiye, S.A. Attahiru, & Gerhard P. Hancke (2018). A Statistical Approach to Detect Jamming Attacks in Wireless Sensor Network. *Sensors*, 1691(18) 1-15

Saru Kumari, Muhammad Khurram Khan, and Mohammed Atiquzzaman. (2015). User authentication schemes for wireless sensor networks. *Ad Hoc Netw*. 27, C (April 2015), 159–194.DOI:https://doi.org/10.1016/j.adhoc.2014.11.018

B. Upadhyaya, S. Sun and B. Sikdar (2019). Machine Learning-based Jamming Detection in Wireless IoT Networks. *2019 IEEE VTS Asia Pacific Wireless Communications Symposium (APWCS),*1-5.

Bhushan, B. & Sahoo, G. (2018). Recent Advances in Attacks, Technical Challenges, Vulnerabilities and Their Countermeasures in Wireless Sensor Networks. *Wireless PersCommun* 98, 2037–2077. https://doi.org/10.1007/s11277-017-4962-0

Y. Arjoune, F. Salahdine, S.Islam, E. Ghribi & N. Kaabouch(2020). A Novel Jamming Attacks Detection Approach Based on Machine Learning for Wireless Communication. *The 34th International Conference on Information Networking (ICOIN 2020)* ffhal02509430f, 1-5.

Ganeshkumar, P. , Vijayakumar, K. , & Anandaraj, M. (2016). A novel jammer detection framework for cluster-based wireless sensor networks. *J Wireless Com Network, 2016 (1)*. doi: 10.1186/s13638-016-0528-1

K. P. Vijayakumar,P. Ganeshkumar, M. Anandaraj, K. Selvaraj & P. Sivakumar(2018). Fuzzy logic–based jamming detection algorithm for cluster based wireless sensor network. Int Journal of Communication Systems 31(10), 1-21.

Misra, S., Singh, R. & Mohan, S.V.R (2010). Information Warfare-Worthy Jamming Attack Detection Mechanism for Wireless Sensor Networks Using a Fuzzy Inference System. *Sensors* 2010, *10*, 3444-3479. https://doi.org/10.3390/s100403444

Osanaiye, O., Choo, K.K.R. & Dlodlo, M. (2016). Distributed denial of service (DDoS) resilience in cloud: Review and conceptual cloud DDoS mitigation framework. J. Netw. Comput. Appl. 2016, 67, 147–165. Journal of Network and Computer Applications 67, 147-165 https://doi.org/10.1016/j.jnca.2016.01.001

Pelechrinis, K.; Iliofotou, M.; Krishnamurthy, S.V. (2011). Denial of service attacks in wireless networks: The case of jammers. *IEEE Commun. Surv. Tutor. 2011*, 13, 245–257.

Ian F. Akyildiz & Mehmet Can Vuran(2010). WSN Architecture and Protocol Stack. *Wireless Sensor Networks* 10-15

Conference theme
Role of Engineering in Sustainable Development Goals

Design and Implementation of a Fire/Gas Safety System with SMS and Call Notification

M. A. Kolade, K.A. Abu-bilal, U.F. Abdu-Aguye, Z.Z Muhammad, and Kassim A. Y
Department of Telecommunications Engineering,
Ahmadu Bello University Zaria, Nigeria

Email: medinatapampa@yahoo.com

ABSTRACT

Swift and effective communication have a tremendous effect on the outcome of the safety and incidences. With the increase in domestic use of Liquefied gas in developing country coupled with poor infrastructures and low level of literacy, it is paramount to incorporate prompt safety measures to safeguard life and properties. The availability and wide acceptance of mobile phones in the countries make them a suitable communication means, for swift and effective remote monitoring and control. Design and implementation of a fire and gas detection system with SMS and call notification was carried out in this paper. This system is divided into three units, the control unit, sensing unit, and the alert unit. The designed system uses a micro-controller and GSM module, to translating and relate the output from the sensors. The codes used by the micro-controller were developed in Arduino IDE (Independent Development Environment) using Arduino language. The prototype of the system was developed using MQ9 and KY-026 for the gas and fire sensor respectively located at specific locations in the home. The GSM module was used to enable remote communication to the user mobile phone. It receives the information from the micro-controller and then acts as programmed. The prototyped system was subjected to load and no-load test in which the system was found to be working normally in accordance with the design specifications. When the system was subjected to reliability test, an index of 0.85 was obtained based on the failure rate of each of the component used in fabricating the system. The design system has the potential of reducing loss of lives and property to fire outbreak and gas leakages, due to its remote and surrounding alerting capabilities.

KEYWORDS: *Mobile phone, GSM module (SIM800), Arduino UNO, Gas Sensor, Fire Sensor.*

1. INTRODUCTION

Gas leakages and fire incidence are common occurrence in today's world especially in developing country where safety is least considered coupled with low level of literacy. Where fire or gas leakage is been detected early and responded to as appropriately, probability of getting out of control can be litigated. (1) designed a GSM based low-cost gas Leakage, explosion, and fire alert system with advanced security. The system is designed such that in case fire or gas leakage occurs a buzzer is turned on, an LCD outputs a message indicating the reason for the alarm and an SMS is sent to the home owner. (2) Also propose such a system, where a gas sensor is used to detect gas leakage and subsequently, turn the exhaust fan on. [4] Developed a similar system with an addition to monitor rapid temperature increase in a home. (3) Also improved on subsequent systems with a system equipped to open an exit windows to allow for diffusion of the concentrated air in case of gas leakage similar to (2),

(5) in another related system, in the event of a fire, the system is equipped with a solenoid valve controlled water/carbon dioxide reservoir to douse the fire, as well as an alert system.

It is evident from the reviewed literatures that a lot of research has been done on fire and gas leakage detection systems with some going further to control the situation. Most of the implemented systems are to turn on buzzer and send SMS to the homeowner, without additional steps to ensure the sent SMS are viewed with required urgency. Hence a need for a system with an increase the probability of sent SMS been read received the required urgency which is directly related to swift response from the homeowner.

2. MATERIALS AND METHORDS

In this section, the details of the design, hardware's and software's materials used in the implementation of the system are summarized.

2.1 The Design Structure

Figure 1 shows the block diagram of the Fire/Gas Safety System. It consists of a power supply unit which supplies required power to other subsystems. The control unit consist of a programmable microcontroller - Arduino UNO, fire sensor – KY-026 and gas sensor – MQ-9 and the alert unit which consist of the GSM-module and the buzzer. The GSM module serves as the communication bridge between the microcontroller and the user's phone. SMS messages and call from the system in case of emergency are sent to the user's phone through the GSM module. The system is divided into two sections: Hardware and software.
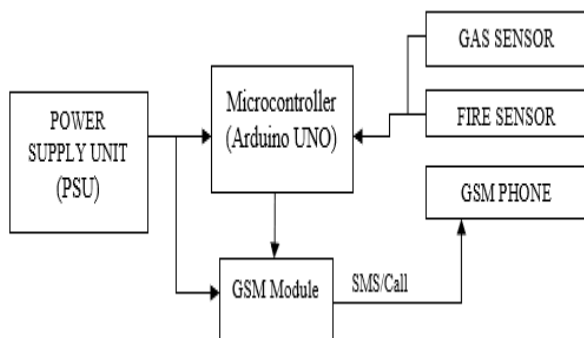
Figure 1: Block Diagram of the Fire/Gas Detection System

2.2 Hardware Design and Selection

The hardware components used are Arduino UNO, KY-026, MQ-9, GSM module SIM800, 240V/12V 3A transformer, four diodes 1N4001, filtering capacitor 2000uf and 5V 2A regulator LM78S05 and buzzer.

Detailed analysis of the various hardware units is given below.

2.2.1 Power Supply Unit

This unit is made up of several sections, the system component's power requirement is considered in this design. The control unit requires a 5V 500mA for the Arduino UNO, while SIM800 requires between 3.4V - 4.4V and 1A current for reliable operation. The fire and smoke sensors both require 3.5V - 5V and current of about 200mA. The power supply should be able to provide the combine current of 2A. Figure 2 shows the block diagram of the power supply unit.
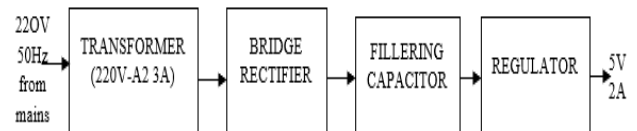

Figure 2: Block Diagram of the Power Supply Unit

The power supply unit consists of a stepdown transformer that has an output of 14V AC with output current of about 1A, a full bridge rectifier, a voltage regulator (7805) and a filter. The power requirement of the security system is 5V.

The transformer design and selection: The 220V AC from the mains is stepped down to 14V AC with the help of the transformer. The peak voltage output of the transformer is calculated using equation (1).

$$V_{peak} = \sqrt{2} \times V_{rms} \qquad (1)$$
Where, $V_{rms} = 14V$

$$V_{peak} = \sqrt{2} \times 14$$

$$V_{peak} = 19.80V$$

Rectifier diode design and selection: Four 1N4001 diode connected in bridge were used for the full wave rectification of the output voltage from the transformer. IN4001 was chosen because its PIV (Peak Inverse Voltage) is 50V which is greater than V_{peak} which is approximately 20V. The value of the rectified voltage is calculated as follows.

$$V_{dc} = (2 / \pi) \times V_{peak} \qquad (2)$$
But $\quad V_{peak} = 19.80V$
$$V_{dc} = (2/\pi) \times 19.80$$
$$V_{dc} = 12.61V$$

Voltage regulation and filter design: For the section of the home security system which requires a 5V power supply, a 5V regulator (LM7805) was used. The choice is based on the IC's ability to keep its output voltage stable at 5V and it can provide up to 1A load current. LM7805 also have attached heat sink to conduct the generated heat away from it under working condition. For the filter section it is preferable to choose a filtering capacitor that holds the peak-to-peak ripples (RF) at approximately 70% - 80% of the peak voltage. The smaller the ripple factor the better the performance of the filter.

Conference theme

Role of Engineering in Sustainable Development Goals

Therefore, using design specifications, the value of the capacitor can be calculated as follows:

From the relations:

$$Q = C \times V \tag{3}$$
$$Q = I \times T \tag{4}$$
$$f = \frac{1}{T} \tag{5}$$

$$I_{min} = I_{dc} = 1A$$

Here, C is filtering capacitor, Q is charge in colombs, I is current taken by the load, T is period in seconds and f is frequency in Hz. Using, equations (3) and (4) and substituting for T from equation (5), yields:

$$C = \frac{I}{Vf} \tag{6}$$

But V is the peak-to-peak voltage, and RF is the ripple factor. To calculate its value, the relation of equation (7) is used

$$V = RF \times V_{rms} \tag{7}$$

V_{rms} is given by $\sqrt{2} \times V_m$ where V_m is the system required voltage 5V, the mains frequency is 50Hz and the RF is 70%.

Therefore

$$V = 0.7 \times \sqrt{2} \times 5$$
$$V = 4.949 \text{ Volts}$$
$$\text{And } C = \frac{1}{4.949 \times 50}$$
$$C = 4040\mu f$$

The standard available value used is 4400µf, where two 2200µf are connected in parallel. Figure 3 shows the circuit diagram of the power supply unit of the fire/gas detection system.
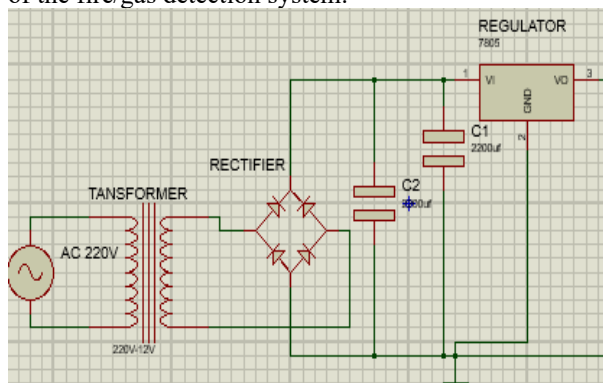

Figure 3: Circuit Diagram of Power Supply Unit

2.2.2 Control Unit: This unit is made up of three main components which are: Arduino UNO, fire sensor and smoke sensor.

Arduino UNO: is a board embedded with ATmega328 a microcontroller, ATmega328 is an integrated circuit (IC) containing all the main parts of a typical computer, which are: Processor, Memories, Peripherals, Inputs, and Outputs (6). It will provide required computing resource to achieve the aim. All communication and controls in this system pass through the microcontroller. The Arduino UNO has 14 digital input/output pins (of which 6 can be used as PWM-Pulse Width Modulation- outputs), 6 analogue inputs, a 16 MHz ceramic resonator, a USB connection, a power jack, an In-Circuit Serial Programming (ICSP) header, and a reset button. It contains everything needed to support the microcontroller. Arduino UNO board is shown in Figure 4.
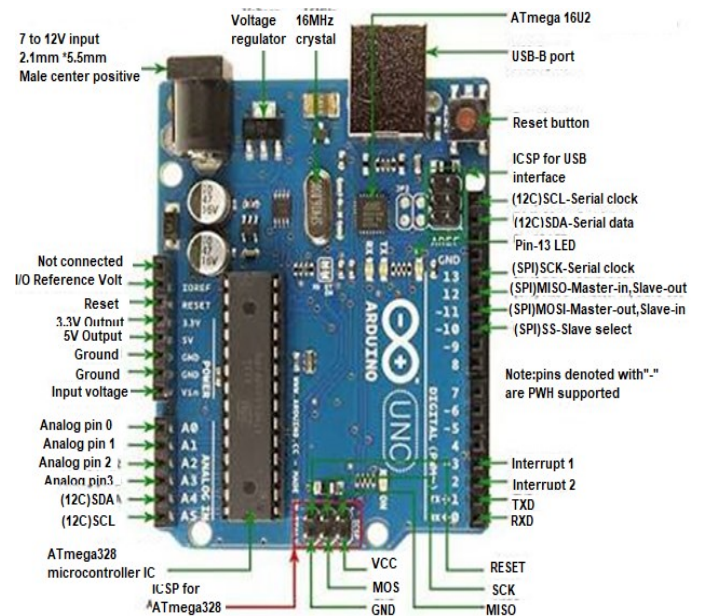

Figure 4: The Arduino UNO Board

Fire Sensor KY-026: The KY-026 consist of a 5mm infra-red receiver LED, a LM393 dual differential comparator a 3296W trimmer potentiometer, six resistors and two indicator LEDs. (7) The board features an analogue and a digital output. Its operating voltage ranging between 3.3V to 5V and Infrared Wavelength detection of about 760nm to 1100nm.The connected photo diode is sensitive to the spectral range of light, which is created by open flames. Digital Out: After detecting a flame, a signal will be outputted. The sensor has 3 main components on its circuit board. First, the

sensor unit at the front of the module, which measures the area physically and sends an analogue signal to the second unit, the amplifier. The amplifier amplifies the signal, according to the resistant value of the potentiometer, and sends the signal to the analogue output of the module. The third component is a comparator which switches the digital out and the LED if the signal falls under a specific value. You can control the sensitivity by adjusting the potentiometer. A KY-026 Fire Sensor is shown in Figure 5.
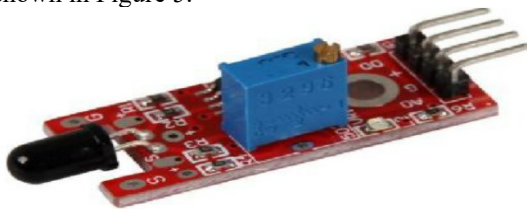

Figure 5: Fire Sensor KY-026

Gas Sensor MQ-9: (7) MQ-9 consist of a sensitive material (SnO_2), which has lower conductivity in clean air, the sensors conductivity increases as concentration of carbon monoxide and hydrocarbon in the air increases. Detection is made by method of cycle high and low temperature. It has a working voltage of 5V, a with wide 2-20kΩ range of resistance and able to detect concentration of about 200ppm minimum and 10000ppm maximum. (7) A relationship between the voltage output and gas concentration level for various common gases is shown in table 1.

Table 1: Output Voltage against Gas Detected Concentration Level
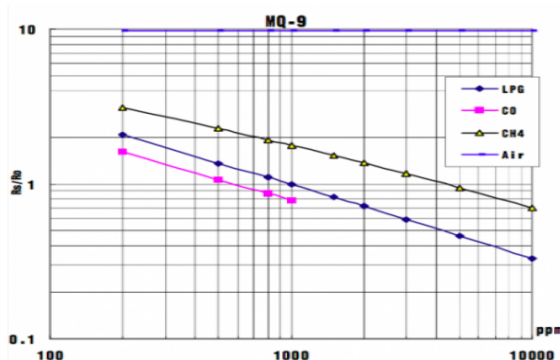
2.2.3. The Alerting Unit

The alerting or output unit comprises of the GSM module and buzzer, both are to relate information from the controller, they are the link between the user and the system's control section.

GSM Module SIM800: SIM800 is a cellular communication module that can make calls, send email, SMS, and even connect to the internet. The module operates like a mobile phone, but it needs external peripherals to function properly. Figure 6 show the image of a SIM800 board.
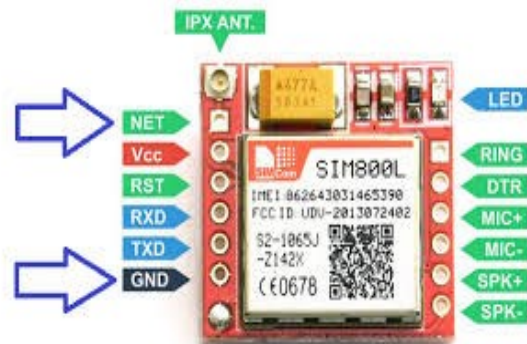

Figure 6: SIM800 Board

The module has audio channels which include a microphone input and a receiver output, a SIM card interface, and it is Quad band hence can connect to any global GSM network with any 2G SIM. The receiver pin (RXD) of the module is connected to transmitter pin (02) of Arduino while the transmitter pin (TXD) of the module is connected to the receiver pin (01) of Arduino, V_{cc} pin of the module is connected to the LM78S05 in voltage divider circuit and GND pin to the ground. Communication speed (baud rate) depends on the board to be paired with, baud rate of 115200 was chosen, this rate allows for successful communication between SIM800 and Arduino UNO.

Buzzer:

A buzzer is an electronics component usually used to add sound feature to systems, the buzzer is associated with switching ON or turning OFF at required time and adequate interval. The buzzer is powered with 5V DC and controlled through the Arduino. It has two terminals, the positive terminal is identified by (+) symbol or longer terminal lead, while the negative terminal is identified by (-) symbol or shorter terminal lead.

The hardware of the system unit comprises of LEDs-which serves as indicators, resistors, GSM module (SIM800), fire sensor, gas sensor, buzzer, and Arduino UNO. The receiver pin Pin 0 of Arduino is connected to the transmitter pin Pin Tx of SIM800 and the receiver pin Pin Rx of SIM800 is connected to transmitter pin pin1 of the Arduino, the signal pin GPIO of SIM800 is connected to pin 9 of Arduino, analog pin (A01) of the Arduino is connected to the signal pin SIC of MQ-9, while the analog pin (A02) of Arduino is connected to the analog signal pin A0 of KY-026 as showed in Figure 6. Power requirement of SIM800 is 3.3V 20mA, 3.3V for KY-026 and 5V for MQ-9. LED1 is connected to digital pin10, LED2 is connected to digital pin13. The LEDs were connected in a series connection with resistors in a simple way to stabilize the current flowing through them. Also, the buzzer is connected to pin4 of the microcontroller through an amplifying transistor, which controls the switch ON and OFF the buzzer. Figure 7 the circuit diagram of the alert units and control unit.
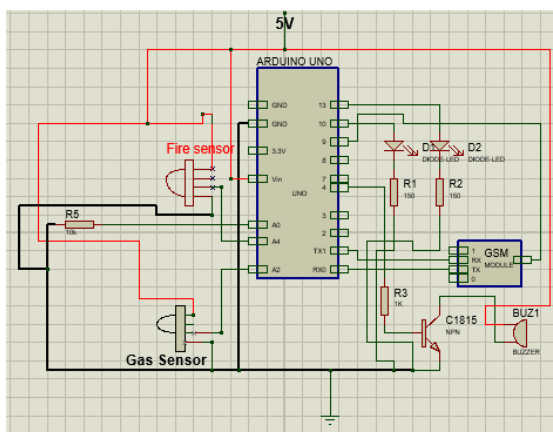

Figure 7: Circuit Diagram of GSM, Fire Sensor and Gas Sensor connected to Arduino UNO

Design and calculations:
Led design
LEDs voltage drop V_f is between 1.8V - 2.5V (a worst case is used in the design, 2.5V) and operating current I is 20mA, while V_s (supply voltage) is equal to 5V (from Arduino pin). Using these values, the value of the current limiting resistors can be obtained.
Ohms law, equation (8) was used to calculate the value of the Resistors R (R_1 and R_2), as shown.

$$R = \frac{(V_S - V_f)}{I} \qquad (8)$$

$$R = \frac{(5 - 2.5)}{(20 \times 10^{-3})}$$

$$R = 125\Omega$$

From the obtained value of 125 ohms a standard value of **150 Ω±20%** was chosen for R_1 and R_2.
Buzzer circuitry:
The home-based alert system (buzzer) requires an amplifying circuit. The amplification circuit requires a multipurpose NPN transistor (C1815) with a base resistor R_3 required to provide base current for the transistor. The value of the resistor (R_3) was calculated using equations (9):

$$R = \frac{(V_S - V_f)}{I} \qquad (9)$$

Where V is the powered voltage from the Arduino UNO 5V, V_{be} is the base-emitter voltage 0.7V and I_b is the base current (500uA)

$$R_3 = \frac{5 - 0.7}{0.005}$$

$$R_3 = 860\Omega$$

From the obtained value of 860 ohms a standard value of **1k Ω±20%** was chosen. The complete circuit diagram of the whole system with the power supply is shown in figure 8.
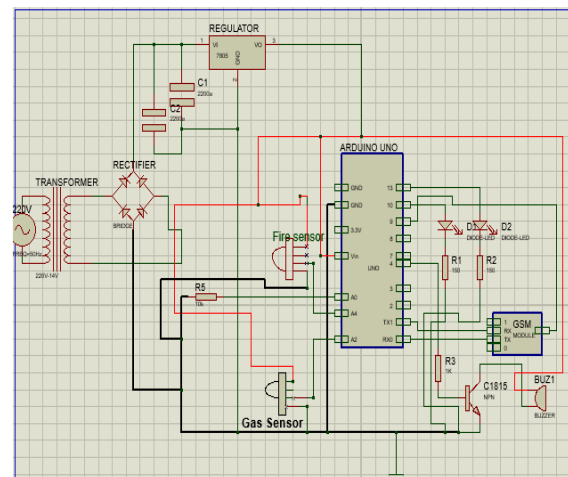

Figure 8: Circuit Diagram of the Complete System

2.3 Writing Source code for the microcontroller Arduino UNO
The source code is written to satisfy the requirement of system whose main controller is an Arduino UNO. The program was written in the Arduino IDE.

The Nigerian Society of Engineers
Minna Branch
1st NSE Minna Branch National Conference 2021

Conference theme
Role of Engineering in
Sustainable Development Goals

The flowchart of Figure 9 was used to develop the program.

2.3.1 Software Design Methodology

The software used in this work to control and synchronize the activities of all system parts to function as a unit is implemented using the flowchart in Figure 8. The software codes were written in Arduino integrated development environment (IDE) with Arduino programming language.
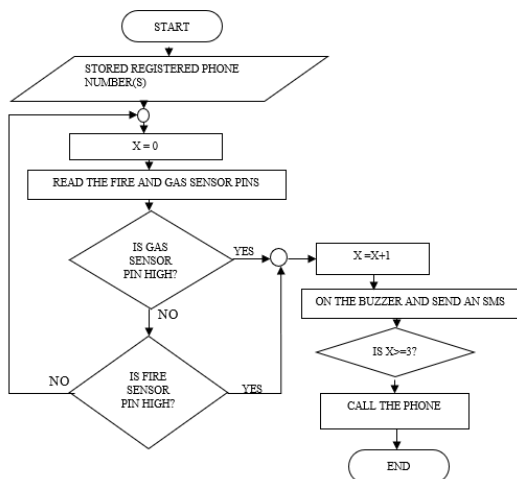

Figure 9: Flow Chart of the System Control

3.   RESULTS AND DISCUSSION

3.1 Testing of the designed circuit and components

All the components used were tested to ensure workability before and after physical construction of the system's porotype to ensure that all contacts and connections were made properly. Test was conducted at unit levels. The tests conducted were categories into hardware and software test.

The hardware unit was initially designed and simulated using circuit wizard and proteus, this is to ascertain the circuit is working properly based on design specifications. After which the components are put onto breadboard for further testing and finally soldered on the Vero-board. Figure 10 shows simulation of the power supply unit.
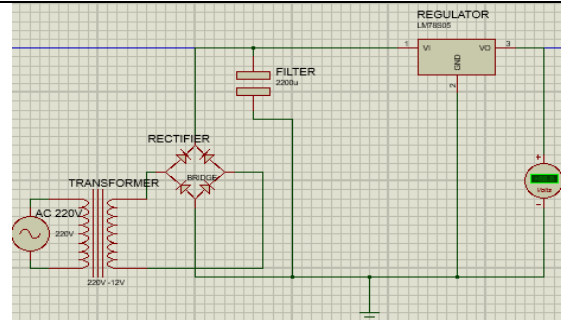

Figure 10: Screen Shot of the Power Supply during Simulation

Controller Unit

The controller unit comprises of the microcontroller board, fire detector, gas detector and the GSM module. Software was uploaded on the microcontroller and the response to stimuli from both the fire and gas detectors was monitor via the communication 3 port (COM3) of the computer. This test makes it possible to understand what is happening inside the microcontroller. The GSM module has in it a registered subscriber identification module (SIM) card. Once the GSM module is connected to power, a blinking green led (with about 2 seconds interval) on it indicates a successful connection to network. Software was also written in the microcontroller to output status of network connection. The software is presented in appendix A. Figure 11 presents the COM3 output during a stage of the test period.
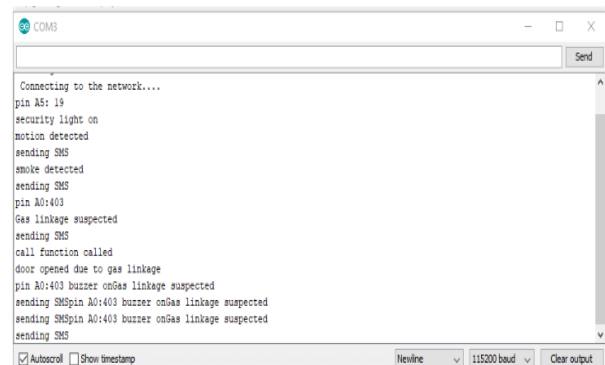

Figure 11: Software Test Result

3.3 Fire Sensor/Gas Sensor

The sensors were both tested with same situation while connected to a DC battery, a beep from both

sensors, indicate they are both in good condition, their functionality is ensured.

3.4 System Test

The full system test was to ensure proper response is given by the developed system in a case of fire outbreak or gas leakage when required by the homeowner. The system was initially designed and simulated in proteus environment, to ensure the system is working perfectly based on design specifications. The system was constructed on a breadboard; this was to ensure proper arrangement in other to ensure a potable system. Finally, the system was implemented and tested on a Vero-board.

3.4.1. Simulation Test

This simulation was carried out using Circuit Wizard, this helped in design of the circuit and testing it with software uploaded, to ascertain the circuit is working properly based on design specifications. After which the components are put onto breadboard for further testing and finally soldered on the Vero-board.

3.4.2. No - Load Test

This test was carried out when the circuit has been developed on a Vero board. A state at which the system is not faced with any control responsibility, this is the verification stage. Physical inspection was done to ensure all components and connections were in place. This was done by checking all closed tracks, jumper wires etc. for open or short circuit. Power was fed to the circuit for a minute. Fingertip was then used to sense the temperature of the components if any was overheating. Also, code inspection was carried out to ensure optimal use of memory, by employing DRY (Don't Repeat Yourself) technique. DRY technique is a principle in software development implemented to reduce software duplication. Being satisfied with this test result, load test then followed.

3.4.3. Load Test

At this stage, power consumption was monitored to ensure power specifications are met, with the voltmeter, the current consumption of the circuit was taken note of - when a response is required and when not. The response time to control was also monitored. For the software aspect, the performance

of the code was scrutinized, the software was compiled and executed, parameters such as memory usage, CPU usage, response time and overall performance for the software were analyzed. Voltage test then followed. This was performed with a digital multi-meter. Voltage and current level at different points on the board was taken and compared with design specification. Figure 11 shows the test diagram used during voltage and current consumption test.
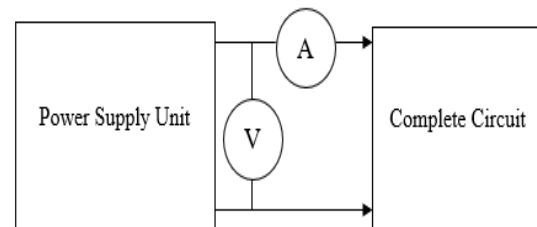

Figure 11: Test Diagram for Voltage and Current Consumption

The current consumption test of the system was carried out using two instances, when response is required and when not. This test was repeated several times and an average value computed. The voltage at the Arduino power pin was also monitored, to ensure conformance with design specifications. Results of the voltage and current test carried out are presented in Table 2 and Figure 12 shows a test instance.

Table 2: Voltage and Current Consumption Readings.

S/N	No load current (A)	Load current (A)	Voltage (V)
1	0.234	0.45	5.12
2	0.232	0.43	4.97
3	0.201	0.46	5.09
4	0.200	0.42	5.00
5	0.221	0.41	5.05
Average	0.217	0.434	5.056

Figure 12: System Current Load Test

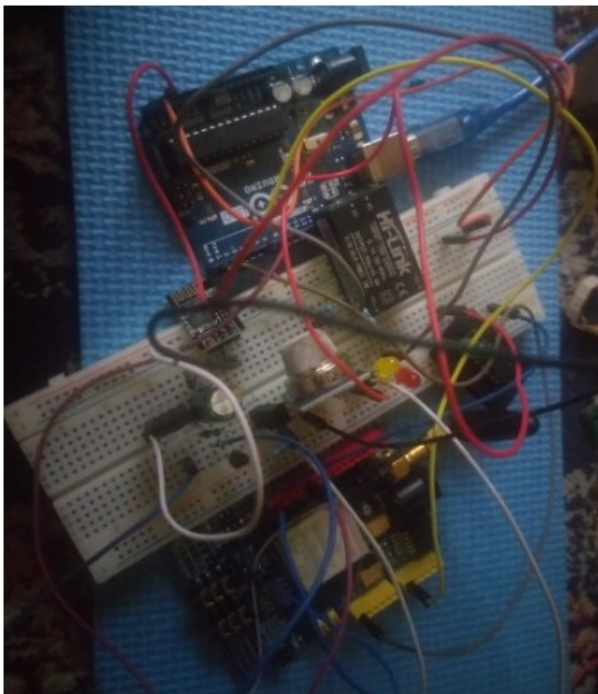**Figure 13:** System on the Breadboard

Figure 14: The System Prototype

3.4.4. Reliability Test

The reliability test of the developed system was done using Part Count Failure Rate Techniques where reliability of a system is approximate as a relation of the units of parts used in the system design. Computation was done using relation with time to failure test. During this test, values of data are recorded which can be put into cumulative function, F(t). Reliability is express explicitly by equation (9) (8):

$$F(t) = 1 - R(t) \qquad (9)$$

The method used in calculating the reliability of system requires information like part category, part quantities and quality factor. The system failure rate is defined in equation (10) (9). Where F_i is given as failure rate of ith part, n is number of part category, N_i is quantity of the part and π_{Q_i} is the quality factor of the ith part:

$$F = \sum_{i=1}^{n} N_i F_i \pi_{Q_i} \qquad (10)$$

The failure rate of each unit was computed using equation (10) with data from reliability prediction of electronic equipment handbook table obtained from (9) and (10). The calculated failure rate of the security system is presented in Table 3. Equation (10) was used to compute the value of the reliability of the system.

From Table 3: the Calculated Failure Rate of the individual components was used to determine that of

The Nigerian Society of Engineers
Minna Branch
1st NSE Minna Branch National Conference 2021

Conference theme
Role of Engineering in
Sustainable Development Goals

Table 3: Calculated Failure Rate of Fire/Gas Safety System

S/N	Components	Fi/ 10^6 hours	N (category)	Ni (units)	π_{Q_i}	F10^{-5}/ 10^6 hours
1	Resistors	0.000196	1	3	0.03	1.764
2	Capacitors	0.000002	1	2	0.01	0.004
3	ICs	0.73	1	1	0.0043	313.9
4	Microcontrollers	0.015	1	1	2.4	3600
5	Semiconductors	0.0038	2	6	8.0	364.8
6	Mechanical device	0.083	1	1	0.103	854.9
7	Modules	0.028	2	3	0.26	4368
8	Inductive devices	0.0030	`1	1	0.30	90
9	Connector	0.040	1	2	0.659	5272
10	Contact/Hand soldering	0.0064	1	27	0.0013	22.464
11	Total failure rate of the system					14887.504

the system. The failure rate was then used to obtain the system reliability using equation (9) as shown below.

$$R(t) = 1 - 0.14887504$$

$$R(t) = 0.85115196$$
$$R(t) \approx 0.85$$

4. CONCLUSION

The detailed procedure for the design and implementation of a fire and gas safety system with SMS and call notification was outline in this work. The designed system was simulated using proteus, the simulated system was then fabricated using hardware components. The fabricated prototyped system worked normally as designed. The system is light in weight (that is portable) and has a reliability index of 0.85 when subjected to reliability test. The design system has the potential of reducing loss of lives and property to fire outbreak and gas leakages, due to its remote and surrounding alerting capabilities.

REFERENCES

P. Ghosh and P. K. Dhar, "GSM Based Low-cost Gas Leakage, Explosion and Fire Alert System with Advanced Security," 2019 International Conference on Electrical, Computer and Communication Engineering (ECCE), Cox'sBazar, Bangladesh, 2019, pp. 1-5, doi: 10.1109/ECACE.2019.8679411.

M. A. F. Malbog, H. D. Grimaldo, L. L. Lacatan, R. M. Dellosa and Y. D. Austria, "LPG Leakage and Flame Detection with SMS Notification and Alarm System: Rule-Based Method," 2020 11th IEEE Control and System Graduate Research Colloquium (ICSGRC), Shah Alam, Malaysia, 2020, pp. 323-327, doi: 10.1109/ICSGRC49013.2020.9232494.

A. Y. Nasir, Adoyi Boniface, A.M. Hassan, N. M. Tahir "Development of a Gas Leakage Detector with Temperature Control system, 2019" Journal of Multidisciplinary Engineering Science and Technology (JMEST) ISSN: 2458-9403 Vol. 6 Issue 12.

Rupali S. Gajare, Dr. P. M. Mahajan, "Home and Industrial Safety System for fire and gas Leakage detection, 2018", International Research Journal of Engineering and Technology (IRJET) e-ISSN: 2395-0056 www.irjet.net p-ISSN: 2395-0072

Lacatan, Luisito & Dellosa, Rhowel & Malbog, Mon Arjay & Austria, Yolanda. (2020). LPG Leakage and Flame Detection with SMS Notification and Alarm System: Rule-Based Method. 10.1109/ICSGRC49013.2020.9232494

Arduino IDE available: www.arduino.org/downloads

MQ-9 data sheet assessed 06/12/2020 https://www.mouser.com/catalog/specsheets/Seeed_101020045.pdf

"Proteus PCB Design & Simulation Software-Labcenter Electronics", labcenter.com, 2017. www.labcenter.com/ [Accessed: 26- jan-2020]

Walls, L., and Quigley, J. (2000). *Learning to Enhance Relaibility of Electronic Systems through Effective Modeling and Risk Assessment*. Available online: http://ieeexplore.ieee.org /document/816334

Military handbook on reliability prediction of electronic equipment (1990) (Available online: https://snebulos.mit.edu/projects/reference/MIL-STD/MIL-HDBK-217F-Notice2.pdf)

D. Kumar, Saurav, A. Yadav and Sharmila, "Easy to wear child guarding gadget," *2019 4th International Conference on Internet of Things: Smart Innovation and Usages (IoT-SIU)*, Ghaziabad, India, 2019, pp. 1-6, doi: 10.1109/IoT-SIU.2019.8777635.

Kyeongha Kwon, Seung Yun Heo, Injae Yoo, Anthony Banks, Michelle Chan, Jong Yoon Lee, Jun Bin Park, Jeonghyun Kim, John A Rogers (2019). Designed an automatic door system using a unique wireless ID by using infrared ray or Bluetooth technology. *Science Advances eaay2462*

Walls, L., and Quigley, J. (2000). *Learning to Enhance Relaibility of Electronic Systems through Effective Modeling and Risk Assessment*. Available online: http://ieeexplore.ieee.org/document/816334

Warrendale P.A. (1987). *Electronics Reliability Subcommittee*. Automotive electronics reliability handbook. Society of Automotive Engineers, Inc.page169,328-9

J. Chou (2000). *Hazardous Gas Monitors: A Practical Guide to Selection, Operation and Application*. Co-published by McGraw-Hill and SciTech Publishing

Non-linear Scaling in Global Optimisation. Part I: Implementation and Validation

[1, 2]*Abubakar, H. A., [2, 3]Misener, R. and [2]Adjiman, C. S.

[1]Department of Chemical Engineering, Ahmadu Bello University, Zaria
[2]Department of Chemical Engineering, Imperial College London
[3]Department of Computing, Imperial College London
*Corresponding Author: abuabib2006@gmail.com

ABSTRACT

Mathematical representation of practical optimisation problems that arise in many engineering applications in nature are non-linear. These problems, which could comprise polynomial and signomial functions, can be solved to absolute global optimality using global optimisation solvers. The challenge is that some of these real-life problems can be badly scaled because they are inherently multi-scales in nature   Current state of the art approaches of solving a badly scaled problem either disregard the inherent disparity in the numerical scales of the problem or does not take into consideration the nonlinearity in the problem. Ignoring the disparity in the numerical scales by not scaling generates numerical instability that often results in a solution that is not the global optimum. On the other hand, neglecting the non-linearity in the problem by applying linear scaling many a time results in a solution that is infeasible to the original problem. We implemented a scaling algorithm that takes into account the non-linearity in a problem and validated its suitability for global optimisation test problems that contain polynomial and signomial functions. Analysis of the results of the test problems considered showed that the implemented scaling technique has the potential of preventing global optimisation solvers from developing numerical instabilities when solving badly scaled problems.

KEYWORDS: *Scaling, nonlinear, global optimisation, instability, NLP.*

1   INTRODUCTION

Many practical engineering problems involve choosing the best among different alternative ways of achieving a set goal. A number of these problems contain nonlinearity and are common in numerous applications, such as process synthesis, molecular products design, facility location and allocation, facility planning and scheduling, and topology of transportation network (Adjiman et al., 2021; Floudas, 1995; Floudas, 2000; Grant et al., 2018; Li and Yang, 2021; Misener and Floudas, 2010; Niebling and Eichfelder, 2019; Sahinidis, 2019). For this reason, several computational frameworks and solvers have been developed in recent time to solve this important group of problems to global optimum. These problems may sometime contain terms (or functions) with extreme coefficient and/or variables with wide disparity in their order of magnitudes, implying that they are badly scaled. Numerical solution of a badly-scaled problem entails a solver dealing with numbers of widely different order of magnitudes, which tend to generate instability in the numerical process and could have negative impact on the final solution.

Real numbers are represented on a computer using floating point, in which only a fixed and finite number of digits are used (Burden et al., 2015). This representation introduces round-off errors that become significant when carrying out computational arithmetic. Significant round-off errors have very high likelihood of resulting in wrong results, and an instance where this occurrence is very frequent is when carrying out arithmetic operations involving numbers of widely different order of magnitudes (Chapra and Canale, 2010).

One of the methods used in mitigating the numerical difficulty that solvers encounter when solving badly scaled problems is scaling (Neumaier, 1997; Ploskas and Samaras, 2013; Tomlin, 1975). Scaling ensures that the variables in a given problem are of similar order of magnitude and eliminates wide variation in coefficients of terms in the problem. Linear systems scaling is a well-researched topic in the literature and many scaling techniques and routines have been developed and implemented in linear optimisation

solvers (Elble and Sahinidis, 2012). For nonlinear systems, there is paucity of study on scaling. The few studies on scaling polynomial systems in the literature were carried out by Watson et al (1985), Morgan (1987) and Domes and Neumaier (2008). In Domes and Neumaier (2008), a scaling algorithm, linear programing (SCALELP) algorithms, for scaling polynomial systems was presented. The algorithm was demonstrated, using some examples, to be very stable for problems where previously known non-linear scalling algorithms performed poorly and are therefore recommended to be suitable for general purpose scaling.

Although the SCALELP algorithm was proposed to be suitable for general purpose scaling and has been reportedly implemented in GLoptLab (Domes, 2009), no study has been carried out in the literature that tests the suitability of the algorithm for scaling problems that require the use of a global optimization solver. Furthermore, the impacts the algorithm would have on the performance of the solver has not been assessed. In this study, which is the first part of a two-part paper, the validity of the scaling algorithm for global optimisation problem is assessed. We explored the idea of scaling directly the non-linear system rather than the linearised system in the solution process.

2 NONLINEAR SCALING: THEORY AND IMPLEMENTATION

The performance of a solver used in an optimisation problem may be dependent on the formulation of the problem, and an important issue in the formulation of problems is scaling (Liberti, 2008; Nocedal and Wright, 2006). To ensure numerical stability, it is important to incorporate scaling into designing algorithms since computer arithmetic is not scale invariant (Gill et al, 1986; Nocedal and Wright, 2006).

Scaling involves the modification of the coefficients matrix that characterise a system in such a way that extreme variations that could lead to numerical instabilities during computations is eliminated (Morgan, 1987). By scaling, the variables and equations in a given problem are modified using variable and equation/constraint scaling factors, respectively, in such a manner that the variables become similar in their order of magnitudes and the equations become well conditioned relative to the variable's perturbation and well balanced relative to one another (Gill et al, 1986).

2.1 NONLINEAR SCALING THEORY

A general polynomial system denoted as $f(x) = 0$ can be compactly written as

$$At(x) = 0 \qquad (2.1)$$

where

$$f(x) = [f_1(x), f_2(x), \dots . f_M(x)]^T$$

$$t(x) = [t_1(x), t_2(x), \dots . t_K(x)]^T$$

with

$$f_m(x) = A_{M,1}t_1(x) + A_{M,2}t_2(x) + \cdots A_{M,K}t_K(x) = 0$$

$$(2.2)$$

and

$$t_k(x) = \prod_{i=1}^{I} x_i^{P_{k,i}} = x_1^{P_{k,1}} \times x_2^{P_{k,2}} \times \cdots x_I^{P_{k,I}} \forall k = 1 \dots . K \quad (2.3)$$

where , I, K, and M are the number of variables, terms and equations in the polynomial systems, respectively; x is a vector of the systems variables with component $x_i \forall = 1 \dots . I$; $t(x)$ is a vector of all the terms in the polynomial systems; P is a $K \times I$ matrix of power of variables in the terms, whose coefficients are denoted as $P_{(k,i)} \forall k = 1 \dots . K, i = 1 \dots . I$; A is a $M \times K$ matrix of coefficient of terms represented as $A_{m,k} \forall m = 1 \dots . M, k = 1 \dots . K$.

Using (2.2) and (2.3), the system of polynomial functions can be written as

$$f_m(x) = \sum_{k=1}^{K} A_{m,k} \prod_{i=1}^{I} [x_i]^{P_{k,i}} \forall m = 1 \dots \dots M$$

$$(2.4)$$

Performing variable and equation/constraint scaling on (2.4) using the variables and constraints scaling factors represented as $v = \begin{bmatrix} v_1 \\ v_2 \\ \vdots \\ v_I \end{bmatrix}$ and $c = \begin{bmatrix} c_1 \\ c_2 \\ \vdots \\ c_M \end{bmatrix}$, respectively, the scaled form of (2.4) denoted as f_m^s becomes

$$f_m^s(x) = \sum_{k=1}^{K} c_m A_{m,k} \prod_{i=1}^{I} [v_i x_i]^{P_{k,i}} \forall m = 1 \dots \dots M$$

$$(2.5)$$

Thus, the scaled coefficients of A are given as

$$A^s_{m,k} = c_m A_{m,k} \prod_{i=1}^I [v_{i_i}]^{P_{k,i}} \quad \forall\ m = 1 \dots\dots M, k = 1 \dots\dots K \ (2.6)$$

The scalar $\prod_{i=1}^I [v_i]^{P_{k,i}} \ \forall\ k \in \{1, \dots. K\}$ in (2.6) could be called the column or term scaling factors. For a particular term (function or column), it has the same value irrespective of the equation where it appears and is only dependent on the variable scaling factors of the term constituent variables. This concept of term scaling factor is the key difference between non-linear and linear scaling techniques.

Expressing the scaling factors and the coefficient of terms as a power of base β such that

$$\begin{cases} c^\beta_m = \log_\beta c_m \ \forall\ m \in \{1, \dots. M\} \\ v^\beta_i = \log_\beta v_i \ \forall\ i \in \{1, \dots. I\} \\ A^\beta_{m,k} = \log_\beta |A_{m,k}| \ \forall\ (m,k) \in Q \end{cases}$$
$$(2.7)$$

it can be shown that (2.6) gives

$$A^s_{m,k} = \beta^{E_{m,k}}$$

where **E** is a set of exponents of non-zero scaled coefficients given as

$$E_{m,k} = c^\beta_m + A^\beta_{m,k} + \sum_{i=1}^I [v^\beta_i P_{k,i}] \ \forall\ m \in \{1,2 \dots. M\}, k \in \{1,2 \dots. K\}$$
$$(2.8)$$

Equation (2.8) is the relation that is used in the determination of the scaling factors. Its manipulation distinguishes between different non-linear scaling techniques. The manipulation of (2.8) results in an optimisation problem in which the scaling factors are the variables. The linear program for SCALELP together with its post-processing linear program implemented in this study are provided in (2.9) and (2.10), respectively. Further details on the formulation of the optimisation problems for the nonlinear scaling techniques, with illustrative examples, are available in Abubakar (2014).

$$\max \ objv := \sum_{m=1}^M [n_m c^\beta_m] + + \sum_{k=1}^K \sum_{i=1}^I [h_k v^\beta_i P_{k,i}]$$
$$st: \ c^\beta_m + A^\beta_{m,k} + \sum_{i=1}^I [v^\beta_i P_{k,i}] \ \forall\ (m,k) \in Q$$
$$v^\beta_i{}^{Lb} \le v^\beta_i \le v^\beta_i{}^{Ub} \quad \forall\ i \in \{1,..I\}$$

$$(2.9)$$

where n and h are the number of nonzero entries in each row and column of A, respectively; c^β and v^β are constraints and variables scaling factors expressed as power of base β, respectively; $v^\beta_i{}^{Lb}$ and $v^\beta_i{}^{Ub}$ are the lower and upper bounds on $v^\beta_i \forall\ i \in \{1,..I\}$ and are computed from the variable bounds as follow:

$$\begin{cases} sf_{min} = eps * \min(1, 1/\max(|x^{Lb}|), \min(|x^{Ub}|)) \\ v^\beta_i{}^{Lb} = \log_\beta \left(\max_i(x_i{}^{Lb}, sf_{min}) \right) \\ v^\beta_i{}^{Ub} = \log_\beta \left(\min_i(x_i{}^{Ub}, sf_{min}{}^{-1}) \right) \end{cases}$$

$$\begin{cases} \min objv = \sum_{m=1}^M [c^{\beta^*}_m c^\beta_m] + \sum_{i=1}^I [v^{\beta^*}_i v^\beta] \\ st.\ c^\beta_m + A^\beta_{m,k} + \sum_{i=1}^I [v^\beta_i P_{k,i}] \ \forall\ (m,k) \in Q \\ \sum_{m=1}^M [n_m c^\beta_m] + + \sum_{k=1}^K \sum_{i=1}^I [h_k v^\beta_i P_{k,i}] \ge objv^* \\ v_i \begin{cases} \le 0 \ \forall\ v^{\beta^*}_i < 0 \\ \ge 0 \ \forall\ v^{\beta^*}_i > 0 \\ = 0 \ \forall\ v^{\beta^*}_i = 0 \end{cases} \\ c^\beta_m \begin{cases} \le 0 \ \forall\ c^{\beta^*}_m < 0 \\ \ge 0 \ \forall\ c^{\beta^*}_m > 0 \\ = 0 \ \forall\ c^{\beta^*}_m = 0 \end{cases} \end{cases}$$
$$(2.10)$$

where sf_{min} is the minimum scaling factor and eps is machine precision; x^{Lb} and x^{Ub} are the lower and upper bounds on variables in the polynomial system; c^{β^*} and v^{β^*} are the solutions to the constraints and variables scaling factors expressed as power of base β in (2.9), respectively; $objv^*$ is the solution of objv functon in (2.9).

2.2 SCALING CODE IMPLEMENTATION

We implemented the scaling code in MATLAB installed on a workstation running a Microsoft Windows 7 operating system. The implementation is divided into two parts; generation and solution of linear programmes (2.9) and (2.10), and computation of scaling factors and scaled coefficient matrix using (2.7) and (2.6), respectively. The code takes as inputs, power of variables matrix (**P**), coefficient matrix (**A**) and the bounds on the variables, $x_i{}^b \ \forall\ i = \{1, \dots. I\}$, and outputs the row scaling factors, variable scaling factors and the scaled matrix ($\mathbf{A^S}$).

The starting point in the code implementation is writing the constraints, along with the objective function, in a given optimization problem in the form

Conference theme
Role of Engineering in Sustainable Development Goals

of (2.4), from which the input data are then generated. Figure 2.1 shows the steps taken in generating outputs from a given inputs. It is noteworthy that constraints (2.8) are generated only from the nonzero entries in **A** which corresponds to the finite entries in $\mathbf{A}^\beta$. This additional freedom differentiates the implementation carried out in this study from that reported in Domes and Neumaier (2008) wherein they used only the finite, non-zero entries in matrix $\mathbf{A}^\beta$. In addition, we imposed restriction on the minimum acceptable value of sf_min to ensure that the minimal scaling factor is not less than the precision of the machine used, eps. Following the generation of the objective function, the constraints and the bounds on the variable, MATLAB linear programming solver, linprog function, is called to solve the built (2.9) and (2.10) linear programs.

Finally, the scaling factors (**v** and **c**) and the scaled coefficient matrix ($\mathbf{A}^S$) are computed, and the results released as the outputs of the scaling code.
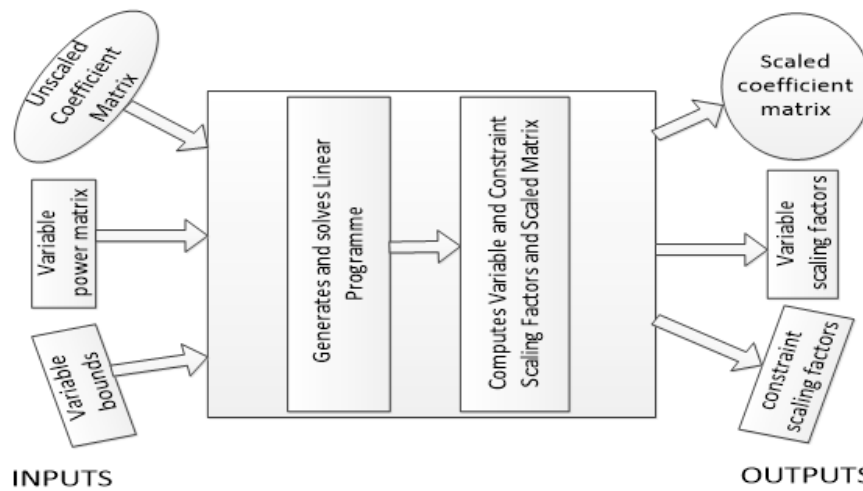

Figure 2.1: Algorithmic steps for the computation of scaling factors and scaled coefficient matrix from a given inputs.

3 SCALLING CODE VALIDATION AND TESTING

We confirm the validity of the implemented code by scaling a number of test cases, including the chemical

Test Case 1

equilibrium problem (CEP) used as an example problem in Domes and Neumaier (2008) and taken as test case 1 in this study. The inputs generated from the polynomial system of the CEP problem, and the outputs of the scaling code are given as follow:

$$A = \begin{pmatrix} X_1 & X_2 & X_3 & X_4 & X_5 & X_6 & X_7 & X_8 & X_9 & X_{10} & - & X_1^2 & X_2^2 & X_4^2 & X_1X_3 & X_1X_2 & X_1X_2^2 \\ 0 & 1 & 0 & 0 & 0 & 2 & 0 & 0 & 1 & 2 & -1.10^{-5} & 0 & 0 & 0 & 0 & 0 & 0 \\ 0 & 0 & 1 & 0 & 0 & 0 & 0 & 1 & 0 & 0 & -3.10^{-5} & 0 & 0 & 0 & 0 & 0 & 0 \\ 1 & 0 & 1 & 0 & 2 & 0 & 0 & 2 & 1 & 1 & -5.10^{-5} & 0 & 0 & 0 & 0 & 0 & 0 \\ 0 & 0 & 0 & 1 & 0 & 0 & 2 & 0 & 0 & 0 & -1.10^{-5} & 0 & 0 & 0 & 0 & 0 & 0 \\ 0 & 0 & 0 & 0 & 0.5140437.10^{-7} & 0 & 0 & 0 & 0 & 0 & 0 & -1 & 0 & 0 & 0 & 0 & 0 \\ 0 & 0 & 0 & 0 & 0 & 0.1006932.10^{-6} & 0 & 0 & 0 & 0 & 0 & 0 & -1 & 0 & 0 & 0 & 0 \\ 0 & 0 & 0 & 0 & 0 & 0 & 0.7816278.10^{-15} & 0 & 0 & 0 & 0 & 0 & 0 & -1 & 0 & 0 & 0 \\ 0 & 0 & 0 & 0 & 0 & 0 & 0 & 0.1496236.10^{-6} & 0 & 0 & 0 & 0 & 0 & 0 & -1 & 0 & 0 \\ 0 & 0 & 0 & 0 & 0 & 0 & 0 & 0 & 0.6194411.10^{-7} & 0 & 0 & 0 & 0 & 0 & 0 & -1 & 0 \\ 0 & 0 & 0 & 0 & 0 & 0 & 0 & 0 & 0 & 0.2089296.10^{-14} & 0 & 0 & 0 & 0 & 0 & 0 & -1 \end{pmatrix}$$

Variable Bounds

Conference theme

Role of Engineering in Sustainable Development Goals

$$X0 = [0\ 5.10^{-5}; 0\ 10.10^{-5}; 0\ 5.10^{-5}; 0\ 10^{-5}; 0\ 2.5.10^{-5};\ 0\ 5.10^{-6}; 0\ 5.10^{-6}; 0\ 2.5.10^{-5}; 0\ 5.10^{-5}; 0\ 5.10^{-5}]^T$$

Variables' power matrix

$$P = \begin{bmatrix}
X_1 & X_2 & X_3 & X_4 & X_5 & X_6 & X_7 & X_8 & X_9 & X_{10} \\
1 & 0 & 0 & 0 & 0 & 0 & 0 & 0 & 0 & 0 \\
0 & 1 & 0 & 0 & 0 & 0 & 0 & 0 & 0 & 0 \\
0 & 0 & 1 & 0 & 0 & 0 & 0 & 0 & 0 & 0 \\
0 & 0 & 0 & 1 & 0 & 0 & 0 & 0 & 0 & 0 \\
0 & 0 & 0 & 0 & 1 & 0 & 0 & 0 & 0 & 0 \\
0 & 0 & 0 & 0 & 0 & 1 & 0 & 0 & 0 & 0 \\
0 & 0 & 0 & 0 & 0 & 0 & 1 & 0 & 0 & 0 \\
0 & 0 & 0 & 0 & 0 & 0 & 0 & 1 & 0 & 0 \\
0 & 0 & 0 & 0 & 0 & 0 & 0 & 0 & 1 & 0 \\
0 & 0 & 0 & 0 & 0 & 0 & 0 & 0 & 0 & 1 \\
0 & 0 & 0 & 0 & 0 & 0 & 0 & 0 & 0 & 0 \\
2 & 0 & 0 & 0 & 0 & 0 & 0 & 0 & 0 & 0 \\
0 & 2 & 0 & 0 & 0 & 0 & 0 & 0 & 0 & 0 \\
0 & 0 & 0 & 2 & 0 & 0 & 0 & 0 & 0 & 0 \\
1 & 0 & 1 & 0 & 0 & 0 & 0 & 0 & 0 & 0 \\
1 & 1 & 0 & 0 & 0 & 0 & 0 & 0 & 0 & 0 \\
1 & 0 & 2 & 0 & 0 & 0 & 0 & 0 & 0 & 0
\end{bmatrix}$$

Outputs

Variable scaling factors

$$v = [1.1336.10^{-6};\ 1.587..10^{-6}; 3.0.10^{-5}; 2.442.10^{-9}; 2.5.10^{-5}; 2.5.10^{-5}; 5.10^{-6}; 2.5.10^{-5}; 5.10^{-5}; 2.5.10^{-5}]$$

Constraint scaling factor

$$c = [2.10^4; 3.333.10^4; 3.333.10^4; 2.10^4; 1.10^5; 7.7814.10^{11}; 3.9725.10^{11}; 1.6769.10^{17}; 2.9404.10^{10}; 3.2287.10^{11}; 3.5042.10^{17}]$$

Scaled coefficient matrix

A^s

X_1	X_2	X_3	X_4	X_5	X_6	X_7	X_8	X_9	X_{10}	$-$	X_1^2	X_2^2	X_4^2	X_1X_3	X_1X_2	$X_1X_2^2$
0	0.0317	0	0	0	1	0	0	1	1	−0.2000	0	0	0	0	0	0
0	0	1	0	0	0	0	0.8333	0	0	−1	0	0	0	0	0	0
0.0227	0	0.6	0	1	0	0	1	1	0.5	−1	0	0	0	0	0	0
0	0	0	$2.442.10^{-4}$	0	0	1	0	0	0	−1	0	0	0	0	0	0
0	0	0	0	1	0	0	0	0	0	0	−1	0	0	0	0	0
0	0	0	0	0	1	0	0	0	0	0	0	−1	0	0	0	0
0	0	0	0	0	0	$6.554.10^{-4}$	0	0	0	0	0	0	−1	0	0	0
0	0	0	0	0	0	0	0.1100	0	0	0	0	0	0	−1	0	0
0	0	0	0	0	0	0	0	1	0	0	0	0	0	0	−0.5807	0
0	0	0	0	0	0	0	0	0	0.0183	0	0	0	0	0	0	−1

From the output results, it is clear that there is disparity in the magnitude of the scaled nonzero entries when compared with the results of Domes and Neumaier (2008). Despite the observed differences in the magnitude of the results, we are convinced that the code outputs are correct as the original coefficient matrix are easily recovered using the scaling factors. In addition, as required of the scaling code output, the scaled coefficient matrix entries are small, bounded in absolute value by 1, and of similar order of magnitudes. The difference in the magnitude of the entries

when compared with the results of Domes and Neumaier (2008) could be due to the restriction imposed on the minimum scaling factor and the finite entries (including zeros) used in generating the constraints.

Further validations of the non-linear code were carried using optimisation problems whose solutions are known a priori and its suitability for scaling other nonlinear functions different from polynomials verified. We considered a number of test cases containing polynomial

and signomial functions. For a given test case, the original problem was solved in GAMS to confirm the primal solution. The test case was then scaled using the scaling code prior to using GAMS in solving it. From the solution to the scaled problem in GAMS, the solution to the original problem was recovered using the variable scaling factors obtained from the scaling code and the recovered solution compared with the known primal solution. The following are the unscaled and scaled test cases solutions.

Test Case 2
Unscaled problem
$1.5.10^{-5}X_1^2 - 200X_2 + X_3 = 15.6$
$X_1X_2^2 - 3X_3 = -9$
$X_1 + 80X_2 + X_3 = 1208$
solution $= [1200; 0.05; 4]$

Scaled problem
$0.4772X_1^2 - X_2 + 0.1429X_3 = 0.7432$
$X_1X_2^2 - X_3 = -1$
$0.6764X_1 + 0.0070X_2 + 0.0025X_3 = 1$
$v = [817.1506; 0.1105; 3]$
$c = [0.0476; 0.1111; 8.2781.10^{-4}]$
solution $= [1.4685; 0.4764; 1.3333]$
Recovered solution $\approx [1200; 0.05; 4]$

Test Case 3
Unscaled problem
$X_1^2 - 50X_2 + 1.125.10^{-5}X_3 = 16.00275$
$8.10^{-4}X_2^2 + 5X_1^2 - 0.001X_3 = 79.2$
$X_2 - X_3 + 12.5X_1^3 = 0.000125$
solution: $X = [4; 1.25.10^{-4}; 800]$

Scaled problem
$0.0625X_1^2 - 0.0983X_2 + 7.0300.10^{-7}X_3 = 1$
$X_2^2 + 0.0631X_1^2 - 1.2626.10^{-5}X_3 = 1$
$0.0025X_2 - 0.0800X_3 + X_1^3 = 1.10^{-5}$
$v = [1; 0.0315; 1]$ $c = [0.0625; 0.0126; 0.0800]$
solution: $X = [4; 0.00397; 800]$
Recoverd solution: $X \approx [4; 1.25.10^{-4}; 800]$

Test Case 4
Unscaled problem
$100X_2^2 + X_1 = 33$
$X_2X_1^2 + 200X_2X_1^{-2/3} + X_2^{-2} = 59$
solution: $X = [8; 0.5]$;

Scaled Problem

$X_2^2 + 0.1597X_1 = 1$
$0.2705X_2X_1^2 + 0.6429X_2X_1^{-2/3} + 0.0295X_2^{-2} = 1$
$v = [5.2712; 0.5745]$ $c = [0.0303; 0.0169]$
solution $= [1.5177; 0.8704]$
Recovered solution: $X \approx [8; 0.5]$

Test Case 5
Unscaled problem
$\min_{X_1} 0bjv = X_1^2 - 3X_1$
$St. X_1^2 + 100X_1 - 525 = 0$
$0 \le X_1 \le 100$
solution: $[X_1; 0bjv] = [5; 10]$

Scaled Problem
$\min_{X_1} 0bjv = X_1^2 - 0.75X_1$
$St. 0.0305 X_1^2 + 0.7619X_1 - 1 = 0$
$0 \le X_1 \le 1.3125$
$v = [4; 16]$ $c = [0.0625; 0.0019]$
solution: $[X_1; 0bjv] = [1.25; 0.625]$
Recovered solution: $[X_1; 0bjv] \approx [5; 10]$

Test Case 6
Unscaled problem
$\min_{X_1} objv = 0.25X_1^2 + 500X_2$
$St. 5X_1 + X_2^2 - 44 = 0$
$X_1 + 2X_2 \le 12$
$X_2 - X_1 \le 4$
$0 \le X_1 \le 9; 0 \le X_2 \le 6.7$
solution: $[X_1; X_2; objv] = [8; 2; 1016]$

Scaled Problem
$\min_{X_1} 0.8264objv = 0.0065X_1^2 + X_2$
$St. X_1 + 0.8182X_2^2 - 1 = 0$
$0.7333X_1 + X_2 \le 1$
$0.6818X_2 - X_1 \le 0.4545$
$0 \le X_1 \le 1.0227; 0 \le X_2 \le 1.1167$
$v = [8.8; 6; 2.4793.10^3]$ $c = [0.0625; 0.0019]$
solution: $[X_1; X_2; objv] = [0.9091; 0.3333; 0.4098]$
Recovered solution: $[X_1; X_2; objv] \approx [8; 2; 1016]$

Results of Test cases 2-5 confirmed the validity of the scaling code for applications involving general signomial functions and for global optimisation problems. In all cases, the recovered solution to the scaled test problem is the same as that obtained for the original unscaled problem and the primal solution. It can be seen that scaling resulted

in decreased search space for the variables. The bound on the variable in test case 5 decreased by two orders of magnitude. Similarly, for test case 6, the bound on the variables decreased by an order of magnitude. Reduction in search space could decrease the CPU time in arriving at the solution of an optimisation problem. Furthermore, the results showed that the applicability of the non-linear scaling code is not limited to polynomial systems, but can be applied to any nonlinear system, in so far, the system can be written in the form of (2.4). The restriction that the system under consideration must be written in the form of (2.4) limits the direct applicability of the non-linear scheme to a system containing logarithmic, trigonometric, hyperbolic or exponential functions.

Table 3.1: Effect of Scaling Algorithm on the Condition Number And the Size (2-Norm) of the Coefficient Matrices of the Test Cases.

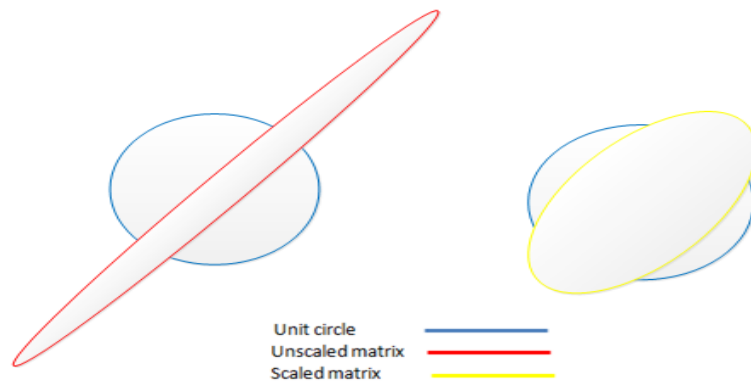| Test Examples	Matrix Norms		Condition numbers	
	unscaled	scaled	unscaled	scaled
Case 1	3.8273	2.7518	3.8273	4.9164
Case 2	8.10^4	1.6212	$6.3788.10^3$	2.5982
Case 3	$1.2107.10^3$	2.0140	384.0625	2.2220
Case 4	208.8052	1.6709	1.9933	1.9680
Case 5	534.4402	1.6740	163.4826	1.4452
Case 6	500.0061	2.1261	$2.1315.10^3$	3.5102

Unit circle
Unscaled matrix
Scaled matrix

Figure 3.1: Geometric interpretation of the observed reduction in condition number of coefficient matrix using 2-norm in $\mathbb{R}^2$.
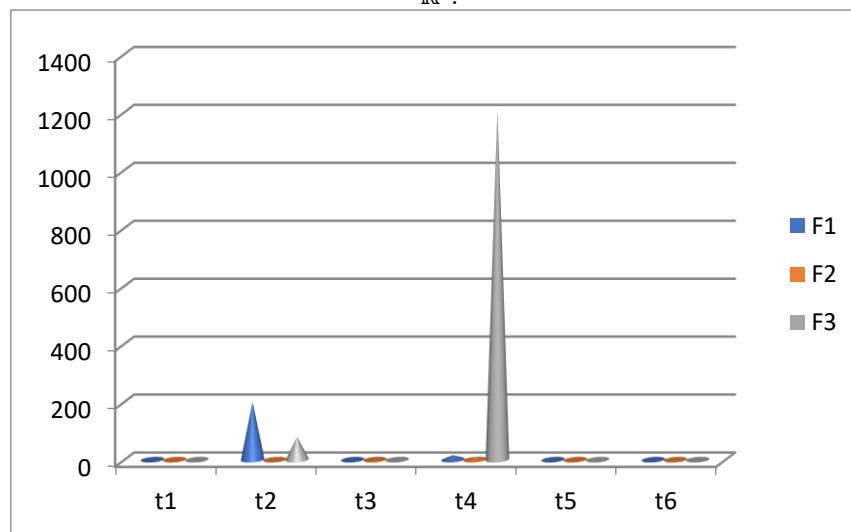
(a)
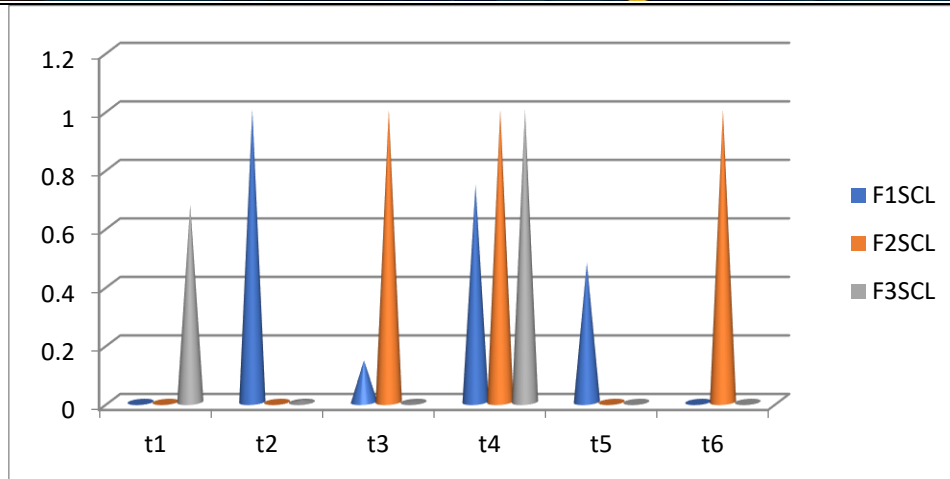
(b)

Figure 3.2: Variations between the absolute value of nonzero entries in coefficient matrix of Test case 2 (a) before scaling (b) after scaling. The vertical (legend) and horizontal axes represent the functions and terms in the test case as captured by (2.5) and 2.2, respectively.

The norm and condition number of the coefficient matrix of the test cases are shown in Table 3.1. The norm is a measure of the size of a coefficient matrix while the condition number measures how 'well-scaled' the coefficient matrix is. Geometrically, condition number indicates the relative maximum stretching and shrinking impacts a matrix has on any nonzero vector, see Figure 3.1. A high magnitude of condition number shows that the coefficient matrix is poorly scaled. From Figure 3.2, the scaling code decreased the size of the coefficient matrices, thereby improving the degree of the 'well-scaledness' of the matrices. In contrast, it is seen that scaling of test case 1 resulted in increased magnitude of its condition number. This could be related to the nature of the problem, wherein the observed extreme values in the coefficient of the terms in the polynomial system for the problem are due to equilibrium constants used in the problem formulation but not because the variables are of widely different order of magnitudes. Therefore, it is likely that the increase in condition number is due to change in variable scales that occurred to ensure that the scaled coefficients are bounded in absolute value by 1.

4   CONCLUSION

A general-purpose non-linear scaling algorithm developed by Domes and Neumaier (2008) has been implemented in MATLAB and its suitability for scaling optimisation problems validated.

Furthermore, it was shown that the applicability of the code is not limited to polynomial functions but can also be used for problems containing general signomial functions. Hence, its suitability for global optimisation problems or solver confirmed. From the decreased variability in the scaled coefficients, the reduction in the scaled variable search space and the reduced condition number of the scaled coefficients matrix of the test cases considered, it is evident that the implemented scaling code has the potential of improving the performance of global optimisation solvers**.**

REFERENCES

Abubakar, H. A. (2014). Managing disparate numerical scales in global optimisations. MSc thesis, Imperial College London.

Adjiman, C. S., Sahinidis, N. V., Vlachos, D. G., Bakshi, B.,.Maravelias, C. T. and Georgakis, C. (2021). Process Systems Engineering Perspective on the Design of Materials and Molecules. I*nd. Eng. Chem. Res.* 60, 14, 5194–5206

Burden, R.L. and Faires, J.D.(2011). Numerical Analysis, 9th Ed., Pacific Grove, Calif

Chapra, S.C. and Canale, R.P. (2010). Numerical Methods for Engineers, 6th ed., International ed., McGraw-Hill Higher Education, Boston, London.

Domes, F.: GloptLab (2009). A Configurable Framework for the Rigorous Global Solution of

Quadratic Constraint Satisfaction Problems. *Optim. Methods Softw*. 24, 727–747

Domes, F. and Neumaier, A. (2008). A Scaling Algorithm for Polynomial Constraint Satisfaction Problems. *J. Glob. Optim.,* 42:327–345

Elble, J. M. and Sahinidis, N.V. (2012). Scaling Linear Optimisation Problems Prior To Application of the Simplex Method, *Comput Optim Appl.*, 52, 345–371

Floudas, C.A. (1995). Nonlinear and Mixed-Integer Optimisation: Fundamentals and Application, Oxford University Press, New York.

Floudas, C.A. (2000): Global optimisation in design and control of chemical process systems, *J. Process Control* 10, pp. 125–134

Gill, P.E., Murray, W. and Wright, M.H. (1986). Practical Optimisation, Academic press, London, UK.

Grant, E., Pan, Y., Richardson, J., Martinelli, J. R., Armstrong, A., Galindo, A. and Adjiman, C. S. (2018). Multi-objective computer-aided solvent design for selectivity and rate in reactions. *Computer Aided Chemical Engineering*. 44, 2437-2442

Hickey, T. and Ju, Q. (2001). Interval Arithmetic: From Principles to Implementation, *Journal of the ACM*, 48 (5), 1038–1068.

Li, G. and Yang, X. (2021). Convexification Method for Bilevel Programs with a Nonconvex Follower's Problem. *Journal of Optimization Theory and Applications*, 188, pg. 724–743

Misener, R. and Floudas, C.A. (2010): Global Optimisation of Large-Scale Generalized Pooling Problems: Quadratically Constrained MINLP Models, *Ind. Eng. Chem. Res*., 49, 5424–5438

Morgan, A. (2009). Solving Polynomial Systems Using Continuation for Engineering and Scientific Problems, *Society for Industrial and Applied Mathematics, Philadelphia*, Prentice-Hall, chapter 5, 107-119

Neumaier, A. (1997). Scaling and Structural Condition Number, *Linear Algebra Appl*., 263, 157-165

Niebling, J., Eichfelder, G. (2019). A branch-and-bound-based algorithm for nonconvex multiobjective optimization. *SIAM J. Optim.*, 29(1), 794–821

Nocedal, J. and Wright, S. J. (2006). Numerical Opimization, 2nd edition, springer science, USA

Ploskas, N. and Samaras, N. (2013). The Impact of Scaling on Simplex Type Algorithms, *ACM* digital Library

Sahinidis, N. V (2019). .Mixed-integer nonlinear programming 2018. *Optimization and Engineering* (2019) 20:301–306

Tomlin, J. (1975). On scaling linear programing problems, *Mathematical Programing study*, 4, 146-166

Watson, L.T., Billups, L.C. and Morgan, A.P. (1985). HOMPACK: A Suite of Codes For Globally Convergent Homotopy Algorithms. http://deepblue.lib.umich.edu/bitstream/handle/2027.42/8204/ban6930.0001.001.pdf;jsessionid=4845D7244E05308ECF4988DCEBD9BEC8?sequence=5

The Nigerian Society of Engineers
Minna Branch
1st NSE Minna Branch National Conference 2021

Conference theme
Role of Engineering in Sustainable Development Goals

An Automatic Bus Route Monitoring System for the Federal University of Technology, Minna

Hamza Farouk[1], Michael David[2], Nathaniel Salawu[3], Ebune Emmanuel Opaluwa[4], Mamud Michael Oluwasegun[5], and Akabuike Kingsley Ikenna[6]

Telecommunication Engineering Department,
Federal University of Technology, PMB 65 Minna Niger State, Nigeria.
Faroukhamza2@gmail.com[1], +2348121695567; mikeforheaven@futminna.edu.ng[2]

ABSTRACT

Transportation between both university campuses has become a tedious and tiring activity because of the existing disconnect between the university's transport system and the commuters due to the rapid increase in student population. The major factor responsible for this disconnect is the information gap between the passengers and the bus(es) en-route. This study therefore, proposes to bridge this gap by designing and implementing a system to monitor bus route and create awareness to the waiting passengers at the bus park via an audio system communicating remotely with the distant bus in transit via GPRS technology. Results obtained prove the efficiency of the project, in helping commuters make better decisions.

KEYWORDS: *Bus tracking, Bus route, GPRS, GPS, Latitude, Longitude*

1 INTRODUCTION

As cities continue to grow in size, challenges arise in the design of urban mobility infrastructure, and one of the key challenges of rapidly growing cities is to provide effective public transport services to satisfy the increasing demands for mobility (James & Nair, 2017). The Federal University of Technology Minna (FUTMinna) with its rapid growth rate, is attest to the problem stated in above (James & Nair, 2017). The university has two campuses located approximately 20km apart. As a result, providing an "effective" means of transportation to cater for the entire population of her students proves to be a herculean task.

There have been series of solutions proposed to increase the efficiency of public transportation around the world, ranging from systems using either or a combination of Global System for Mobile Communication (GSM), General Packet Radio Service (GPRS), Global Positioning System (GPS) technologies, and Radio Frequency Identification (RFID) (Shyam, Kumar, Shashi, & Kumar, 2015), (Raad, Deriche, & Sheltami, 2021), (Kumbhar, Survase, Mastud, Salunke, & Sirdeshpande, 2016), (Ahmed et al., 2019), (Dhende, Kaotekwar, Kokane, & Karambelkar, 2017).

1.1 REVIEW OF RELATED WORKS

Vehicle tracking systems have been in existence and employ various technologies to achieve their respective aims or goals. They have been deployed worldwide, and there is a high possibility of having improvement on existing methods and/or devising new methods to achieve the goal of near-perfect transportation and traffic management systems.

A. Developing a Smart Bus for Smart City using IOT Technology.

The proposed method in (Kadam, Patil, Kaith, & Patil, 2018) employed a combination of GPS, Bluetooth, GPS, and GPRS technologies to track a bus. The bus trackers on board were equipped with two pairs of IR sensors connected to an Arduino Uno microcontroller via Bluetooth. The Arduino Uno was equipped with a GSM/GPRS web module for purpose of web connectivity. The IR sensors on the bus were used to carryout headcount of passengers boarding and alighting from the bus and this information, alongside the exact (live) location of the bus as computed by the GPS was updated to a cloud server where processing was done and further transmitted to an application hosted on an android device. The estimated time of arrival (ETA) was calculated using the Euclidean Distance Formula and was also displayed on the android application alongside the number of passengers aboard as at the time of query.

B. Intelligent Bus Monitoring System

The proposed method achieved its aim by implementing a system consisting of a GPS/GSM modem, PIR sensors, DC motors, switches, and a smartphone, all of which were coordinated by an ARM cortex microprocessor. Tracking of the bus was done both offline via GSM and online via GPRS and GPS modules. Upon detection of an accident, the system updated the exact location of the vehicle via GPS/GSM technology and sent a message to relevant authorities informing them of the accident and the location of the vehicle. The system also proposed a smartphone application to remotely monitor and obtain the exact location of the bus, obtain an estimated arrival time, and also number of passengers and available seats aboard at any time to help users facilitate decision making (Shinde & Ansari, 2017).

C. UiTM Campus Bus Tracking System Using Arduino Based and Smartphone Application

The system discussed herein employed GPS, Wi-Fi, and web technologies, all coordinated by an Arduino microcontroller board. The installed GPS unit attached to the microcontroller received the coordinates (longitude and latitude) from GPS satellites and sent them to the Arduino microcontroller for processing. The Arduino Uno then updated the data in the local server. The mobile smartphone application, which was wirelessly linked with the microcontroller's local server, was allowed to read the data on the server after proper authentication and relay it to users via its user-friendly user interface. The system also provided an LCD display which displayed the real-time location of the bus as obtained from the Arduino microcontroller (Kamisan, Aziz, Ahmad, & Khairudin, 2017).

D. College Bus Tracking Android Application using GPS

The implemented system was divided into the Hardware Unit and the Monitoring Unit. The monitoring unit of the system made use of a SIM 900 GSM module as a modem for data transmission to the server using GPRS, and a GPS module which obtained location data from GPS satellites. Both modules coordinated by an Arduino microcontroller. The location data on reception by the GPS tracker was sent to the microprocessor and then to the GSM module whose task was to communicate and store the data on the database. On the monitoring system which was majorly software, a user-friendly Android application (written in Android Studio) was developed and interfaced with the hardware unit and the server via the internet. The major function of the application was to download the location data (longitude and latitude) from the server and display the real-time location of the bus. The obtained information was displayed on Google Map with the aid of Google Maps API (Kumar, Aishwarya, & Mounika, 2016).

2 METHODOLOGY

This paper proposes a cost-effective method of tracking vehicles (campus shuttle buses) that run between both campuses of the university. The system, sub-divided into two; the Bus Segment and the Bus Park Segment, replaces the conventional GPRS and GPS live-tracking approach to bus tracking by comparing the coordinates (Longitude and Latitude) of pre-defined locations along the route with the real-time location of the bus while in motion. For the purpose of this paper, the route of concern will be the Bosso – Gidan-Kwano route, and the predefined locations and their coordinates are listed below:

i. Bosso Campus
ii. Kure Market
iii. Kpakungun
iv. NECO Office
v. GidanKwano

The onboard NEO-6 GPS sensor tracks the real-time coordinates of the vehicle and relays the information to the Atmega 328 microcontroller, which communicates with the Bus Park Segment via the A6 GSM module. The communication is made over GSM by sending SMS to the inserted SIM card on the GSM module of the Bus Park Segment. The received information is decoded and a signal is sent to the Mini mp3 player for playback to the audience at the bus park.

2.1 BUS SEGMENT

This unit consists of an Atmega 328 microcontroller, a bulk converter, an A6 GSM module, a NEO-6 GPS module, filtering and

coupling capacitors, resistors, and LEDs. The A6 module captures the real time coordinates of the bus in motion or at rest and sends it to the GSM module for transmission via SMS to the Bus Park Segment. The block diagram of this segment is shown in Figure 1.0 alongside the flow diagram of operations of the segment in Figure 2.
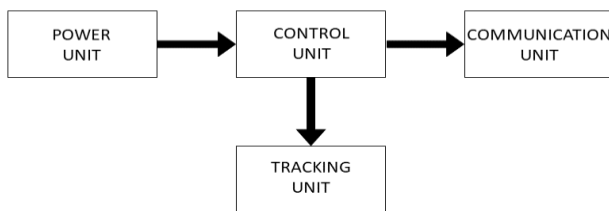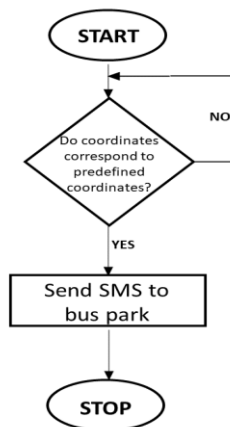

Figure 1: Block diagram of the bus segment

Figure 2: Flow diagram of the bus segment

2.2 BUS PARK SEGMENT

This segment of the system consists also of an Atmega328 microcontroller, an A6 GSM module, a bulk converter, a DF mini player, a 4-ohm speaker, filtering and coupling capacitors, indicator LEDs, and resistors, all powered by a two 3.75V battery units connected in series to give a 7.5V power supply. The A6 GSM module receives the information from the Bus Park segment and communicates it to the DF mini mp3 player board connected to the microcontroller.

The DF mini player is a serial MP3 module with an integrated MP3 and WMV decoder chip also equipped with a micro SD card driver, FAT16 and FAT32 file system support. It converts the received

message into audio format and delivers particular messages audio messages via the speakers. The block diagram and the flow diagram of the segment are shown in Figure 3 and Figure 4 respectively.
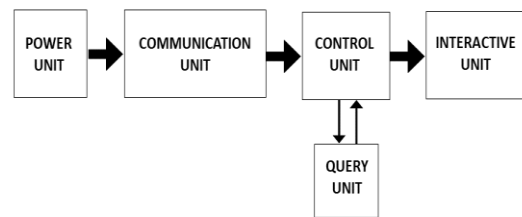
Figure 3: Block diagram of the bus park segment
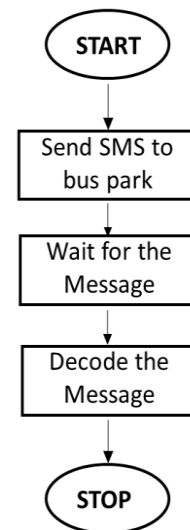
Figure

2.3 ALGORITHM

STEP 1: INITIALIZE SYSTEM
STEP 2: GPS RECEIVE VEHICLE COORDINATES
STEP 3: COMPARE WITH PREREGISTERED COORDINATES
STEP 4: CHECK FOR A MATCH IN THE COORDINATES
STEP 5: IF THERE IS A MATCH, SEND SMS TO BUS PARK UNIT. IF NONE, NO SMS IS SENT
STEP 6: BUS PARK UNIT PLAYS THE CORRESPONDING AUDIO MESSAGE TO THE COORDINATES THAT WERE RECEIVED

3 RESULTS AND DISCUSSION

The following images show the results obtained when the bus arrived each of the predefined locations. However, this is a proposed work as at the time of writing this paper and modifications are currently ongoing.

3.1 RESULTS FROM BUS SEGMENT

Figure 5: Final construction indicating the bus segment is completely initialized

Figure 6: Final construction indicating the bus segment GSM signal strength

The Bus Segment is a device that tracks the bus location in real time. The LEDs in Figure 5 shows the signal level of the device.
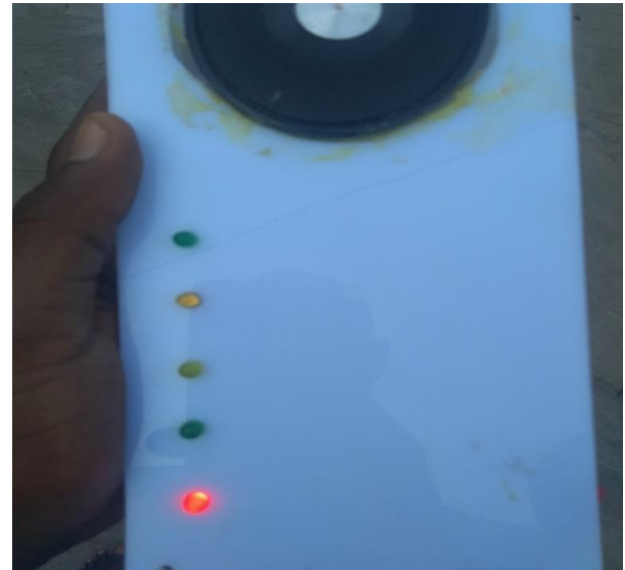
3.2 RESULTS FROM BUS PARK SEGMENT

Figure 7: system indicating the bus is or has gone beyond Bosso campus

Figure 8: system indicating the bus has reached Kure Market

Conference theme
Role of Engineering in Sustainable Development Goals

Figure 9: system indicating the bus has reached Kpankungu Roundabout

Figure 11: system indicating the bus has reached Gidan Kwano Gate

Figure 10: system indicating the bus has reached NECO Office

Figures 7, 8, 9, 10, and 11 are images from the Bus Park Segment, it houses a speaker that announce the real time location of the bus when the system is queried and also LEDs to show the matched location of the bus. Figure 12 shows the result displayed the when system was queried at particular interval

BUS SEGMENT

The steps taken to test the operation of the bus segment are as follows;

STEP 1: switch on the bus segment via the switch at the side of the casing. When the system is on, the five LEDS on the bus segment comes on in sequence to indicate the adequate power supply is circulating in the circuit. Four of the LEDS represent the GSM while the last led is for the GPS.

STEP 2: the LEDS remains on until the GSM module on-board initializes this usually takes up to 3 seconds. After its eventual initialization, the LEDS turn off in sequence to indicate a successful initialization.

STEP 3: the controller queries the GSM module to know how much of signal strength is available,

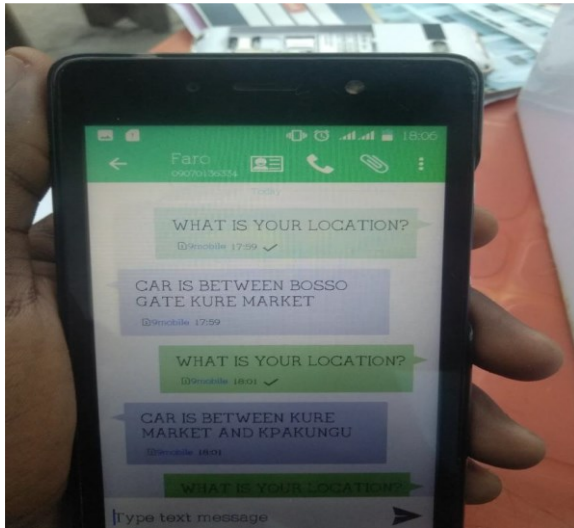based on the received value, the controller turn on four LEDS.

Figure 12: Showing Result when system was queried at particular interval

STEP 4: the system waits for the GPS to connect to the satellite, after successful connection, the GPS starts blinking at a constant interval. This is only visible through the transparent casing but when the GPS start receiving real coordinates from the satellite, the GPS LED starts to blink at constant interval.

STEP 5: the bus segment sends an SMS to the bus park segment to notify of its connection.

STEP 6: the bus segment starts comparing the received coordinate to that of the predefined coordinates. These are school gate Bosso campus, Kure market, Kpakungun roundabout, NECO office and school gate Gidan Kwano campus.

STEP 7: when there is match in the coordinates the bus segment sends a message to the bus park segment. The programmed messages are Bosso gate for school gate Bosso, Kure for Kure market, Kpakungun for Kpakungun roundabout, NECO for NECO office and gk gate for school gate Gidan Kwano.

BUS PARK SEGMENT

The steps taken to test the operation of the bus segment are as follows;

STEP 1: the switch of the bus park segment at the side of the casing was pushed. When the system came on, the five LEDS on the bus segment comes

on in sequence to indicate the adequate power supply is circulating in the circuit. All the LEDS in this case are for the GSM.

STEP 2: the LEDS remains on until the GSM module on-board initializes this usually takes few seconds. After its eventual initialization, the LEDS turn off in sequence to indicate a successful initialization.

STEP 3: the system announced the welcome message- "Good Morning Fellow Students. I am Hamza the school bus monitoring system welcome to the school bus park. System trying to locate bus" Was made by the speaker. This message rounds up the initialization process of this segment.

STEP 4: the system waited for the messages from the bus segment to know the location of the bus. Throughout the course of journey, the following sounds were heard- "bus is at school gate Bosso campus", "bus has reached Kure market", "bus has Kpakungun roundabout," "bus has reached NECO office", "bus has reached school gate Gidan Kwano campus" and as the announcement is made the LEDS were coming up respectively.

STEP 5: the system awaits SMS query from students. During the course of the journey the bus park segment was queried severally and the following messages were received. - bus is at bus park Bosso campus, bus is between school gate Bosso campus and Kure market, bus is between Kure market and Kpakungun roundabout, bus is between Kpakungun roundabout and NECO, bus is between NECO and school gate and bus is at bus park Bosso campus.

4   CONCLUSION

This project is aimed at providing a solution to an inherent problem in the FUT Minna transportation system. It has been tested to be working and hopefully the University will consider it for implementation in other to serve it desired purpose. It is a low power solution that can save student a lot of energy and resource. The system when fully implemented will give the University bus system a modern look and the technology with which University is recognized for it will be clearly evident even in the bus transit system. Further work on the developed solution is still on going and more detail results will be showed cased in our next publication.

However, an improvement is ongoing presently, working on the limitations and shortcomings to give a better result.

ACKNOWLEDGEMENTS

REFERENCES

Ahmed, A., Parvez, M. R., Hasan, M. H., Nur, F. N., Moon, N. N., Karim, A., . . . Jonkman, M. (2019). *An intelligent and secured tracking system for monitoring school bus.* Paper presented at the 2019 International Conference on Computer Communication and Informatics (ICCCI).

Dhende, S., Kaotekwar, V., Kokane, V., & Karambelkar, V. (2017). Intelligent bus system using rfid, zigbee and gprs. *International Research Journal of Engineering Technology, 4*(4), 3.

James, J. G., & Nair, S. (2017). *Efficient, real-time tracking of public transport, using lorawan and rf transceivers.* Paper presented at the TENCON 2017-2017 IEEE Region 10 Conference.

Kadam, A. J., Patil, V., Kaith, K., & Patil, D. (2018). *Developing a Smart Bus for Smart City using IOT Technology.* Paper presented at the 2018 Second International Conference on Electronics, Communication and Aerospace Technology (ICECA).

Kamisan, M., Aziz, A., Ahmad, W., & Khairudin, N. (2017). *UiTM campus bus tracking system using Arduino based and smartphone application.* Paper presented at the 2017 IEEE 15th Student Conference on Research and Development (SCOReD).

Kumar, G. K., Aishwarya, C., & Mounika, A. S. (2016). College Bus Tracking Android Application using GPS. *International Journal of New Innovations in Engineering and Technology, 4*(4), 40-44.

Kumbhar, M., Survase, M., Mastud, P., Salunke, A., & Sirdeshpande, S. (2016). Real time web based bus tracking system. *International Research Journal of Engineering and Technology, 3*(2), 632-635.

Raad, M. W., Deriche, M., & Sheltami, T. (2021). An IoT-Based School Bus and Vehicle Tracking System Using RFID Technology and Mobile Data Networks. *Arabian Journal for Science and Engineering, 46*(4), 3087-3097.

Shinde, N., & Ansari, S. (2017). Intelligent bus monitoring system. *International Journal of Computer Applications, 975*, 8887.

Shyam, N., Kumar, N., Shashi, M., & Kumar, D. (2015). SMS Based Kids Tracking and Safety System by using RFID and GSM. *IJISET-International Journal of Innovative Science, Engineering & Technology, ISSN*, 2348-7968.

The Nigerian Society of Engineers
Minna Branch
1st NSE Minna Branch National Conference 2021

Conference theme
Role of Engineering in Sustainable Development Goals

Reformation of Engineering Education for Health, Wealth and Sustainable Development in Nigeria

Oluwadare Joshua OYEBODE

Civil and Environmental Engineering Department, Afe Babalola University,
Ado-Ekiti (ABUAD), Ekiti State, Nigeria

Email: oyebodedare@yahoo.com

ABSTRACT

Reformation of engineering education is a principal requirement for health, wealth and sustainable development in Nigeria and most nations of the world. This paper focuses on the reformation of engineering education in order to attain public health, wealth creation and sustainable development in Nigeria. Methodology includes literature review, consideration of recent trends in engineering education and clear discussion of engineering education. Nigerian engineering teaching methods and outputs and challenges facing engineering education in Nigeria were carefully examined. Findings revealed that there is an urgent need for the reformation of engineering education in order to ensure adequate public health, wealth and sustainable development in Nigeria. Engineering curriculum requires periodic review and there must be substantial linkages between academia and engineering industry. This will enhance engineering productivity, generation of employment, increased output through innovations, job creation, efficient utilization of available resources and the facilitation in the transfer of technological advancement. Recommendations include enforcement of policies that will enhance reformation of engineering education and sustainable development in Nigeria, collaboration of academia, government, regulatory bodies, stakeholders, professionals, engineers and industries in with the curriculum review and project implementation.

KEYWORDS: *Engineering, Regulatory Bodies, Reformation of Education, Sustainable Development, Wealth*

1. INTRODUCTION

Engineering education has a lot of roles to play in the achievement of sustainable development goals. The real problem facing humanity today in terms of achieving sustainable development is how to motivate people to change underlying behaviors and activities that are problematic. Human beings are very resentful to change. In other words, people should be encouraged to channel their energy towards contributing more to assist alleviate poverty by acquiring relevant education and skills so as to market developmental efforts that do not pollute good ideas and wasting scarce resources to destroy lives and edifices built over the years.

Quality education is a critical requirement for national growth industrialization and citizens in most nations of the world. Education is of great importance to every nation as it is quite obvious that the functionality of an individual in any nation is largely dependent on the quality of education that is imparted on that individual.

There is a general consensus among scholars that education is the most potent instrument for the overall development of any nation (Njoku and Onyegbula, 2017). There is often no productive human capital without a functional education, countries that are at the forefront of technological advancement equally having the most educated population. Educated people possess more skills and are able to perform their jobs effectively. They are also better suited to more complex jobs, which are often associated with high rates of pay and greater economic benefits (Adedeji and Campbell, 2013).

The Nigerian education system has a foothold over most of the framework adopted globally, because the six years spent on education compared to other countries with a 5-year secondary education. Engineering education which is majorly taught at the higher institution has become a key aspect of education in Nigeria. Engineering education is based on conceptualizing, creating and maintaining processes or systems that are needed by humans or

the society. This paper shall examine if this engineering teaching trend is sustainable. Present approaches to engineering education in Nigeria, the factors behind the observed success, challenges and proffer some solutions and methods to improving engineering education should be carefully checked in Nigeria. The present and future of engineering education is also examined with some recommendations for a sustainable teaching method that would meet the future need of the nation.

2.0 OVERVIEW OF ENGINEERING EDUCATION IN NIGERIA

Engineering education was neglected among other fields of education in Nigeria until around the middle of the 19th century. Nigeria, however, realized that this field is one of the major bedrocks of any nation and established a number of Technical Colleges, Polytechnics and Faculties of Engineering in Universities just after the independence of the country. As a result of the importance and technicality of engineering education, the study of any engineering degree in Nigeria is structured for a five-year period, with the primary year spent studying general sciences. To become a totally qualified engineer, a graduate of any Engineering degree must practice for a minimum of four years, among other requirements before becoming a registered engineer with the Council for the Regulation of Engineering in Nigeria (COREN).

The Nigerian engineering education performed well by meeting the immediate need of the early post-independence period. The educational performance at that point was also commended, especially giving the very fact that the majority engineering teachers worked with the knowledge of the industry. However, in recent times, the standard of engineering education in Nigeria is of major concern more especially to the industries as it seems the standard is falling.

Corruption is an act which deviates from the formal rules of conduct governing the actions of someone in a position of public authority because of private regarding motives such as wealth, power or status (Keeper, 2010).

There is inadequate access to spotless modern energy services is a massive challenge facing Nigerian because energy is fundamental for socioeconomic development and poverty eradication (Oyedepo, 2012).

There is urgent need for revitalization of engineering education (Oyebode, 2020).

Drawing is very important for all engineering fields as engineers we all know that drawing is engineering language. This encompasses the architectural, civil, electrical, structural, mechanical and all engineering professions (Oyebode, 2015).

Technological advancements serve as a main key to a nation's development. Proper engineering knowledge (acquired through appropriate structures) plays a major role in the attainment of a high level of technological advancement (Akintola, 2002).

There is a worldwide campaign for efficient teaching methods for engineering education in Nigeria, especially with the arrival of information and telecommunication technologies (Oloyede et al., 2017).

Education is often seen as a prerequisite for quality manpower development and creation of wealth, a sure path to success in life and service to humanity (Ogunyinka et al., 2015).

Thus, creating a barrier between the talents required by the labor markets and what's obtainable by the graduates. This results in the decision for improvement of the prevailing classical course delivery methods toward meeting the market needs. However, over the years, extensive information technology, vanguard technological ideas and developmental initiative are happening within the planet as a result of engineering innovations; however, there are not any major changes within the engineering education, lecturing style, and attitude within the same time-frame in Nigeria.

3.0 SITUATION AND CHALLENGES FACING ENGINEERING EDUCATION IN NIGERIA

Challenges facing engineering education include curriculum issues, lack of basic knowledge by the engineering students, an explosion in enrolled students, difficulty in students' recruitments, inadequate facilities for teaching of engineering education, lack of or inadequate university industry

linkages, inadequate funding of education, inadequate mentoring of engineering lecturers, lack of special remunerations to engineers, teacher-to-student ratio and thus the utilization of ineffective teaching methods.

Furthermore, lack of basic infrastructure, lack of necessary support from non-academic staff, poor access to internet services, irregular power supply, lack of fantastic leadership and mentoring schemes are among other challenges facing engineering education in Nigeria. The system of education in Nigeria today is more of socializing with less emphasis on diligence both on the students and lecturers. These challenges are having a big impact on the standard of Education in Nigeria.

However, this paper shall focus mainly on the three areas namely: the curriculum, equipment and thus the teaching methods utilized in Engineering Education in Nigeria. In discussing things, this paper shall explore a number of these situations and suggest some solutions to sustainable engineering education in Nigeria.

3.1 Teaching and Learning Methods

Teaching is that the process of transferring knowledge. It should be delivered during a scientific, interactive, organized and purposive manner. The first purpose of teaching at any level is to bring a fundamental change in students' learning. it's therefore, expected that teaching will cause desirable change within the learners' behavior. Learners during this context, we are pertaining to the scholars. Therefore, teaching should be seen because the integral a part of any educational policy framework implementation because it would have an immediate impact on the students' learning. There are many teaching methods available, and a couple of these methods are tested in diverse environments and proven effective in several scenarios. These include discovery method spaced lecture, group work, dialogue, scaffolding and constructivism etc. The project method on the other hand involves active participation of the scholar in such how that a cooperative (group) study of a real-life situation within the category is undertaken, under the supervision of the teacher. However, the concerned, feelings and reactions of the scholars during this situation are taken into consideration during the course of interacting with each other. This

might even be mentioned because the "Role-Play Method". Simulation method may be a more practical oriented approach of teaching where students are exposed to devices and equipment physically. This method is taken into account because the most effective in Science and Engineering related subjects as it's hastens and stimulates the understanding of learners. Numerous learning methods are identified and related to specific teaching methods. Today, in Nigeria, mostly, engineering lecture rooms are faced with an identical scenario because it was in decades ago. The teaching methodology remains the traditional approach where an educator delivers lectures by standing within the classroom, dictating notes or deriving equations from the 'old' notebook', recycling examples, assignments and projects. This sort of approach does not allow skills acquisition, critical thinking and creativity needed during a challenging multi-disciplinary course like engineering. Notably, some enhancements are observed following the diffusion of ICT into the teaching, and learning process and this creates some quite modification on teaching methodology. Moreover, there are quite number of methods that might be used/or integrated in to the pedagogies. These methods are expected to enhance students' learning. it had been discovered that the bulk engineering students are visual, sensing, inductive, active, and artistic whereas the teaching methods used are mostly passive, auditory, abstract, deductive and sequential. Thus, resulting in incompatibility between the teaching and therefore the learning process, and hence, resulting to poor performance among engineering students.

Furthermore, lack of basic infrastructure, lack of necessary support from non-academic staff, poor access to internet services, irregular power supply, lack of good leadership and mentoring schemes are among other challenges facing engineering education in Nigeria. The system of education in Nigeria today is more of socializing with less emphasis on hard work both on the part of the students and the lecturers. These challenges are having a significant impact on the quality of Education in Nigeria as discussed.

However, this paper shall focus mainly on the three areas that have to do with content delivery namely: the curriculum, equipment and the teaching methods

The Nigerian Society of Engineers
Minna Branch
1st NSE Minna Branch National Conference 2021

Conference theme
Role of Engineering in
Sustainable Development Goals

used in Engineering Education in Nigeria. In discussing the situation, this paper shall explore some of the present situations and suggest some solutions to sustainable engineering education in Nigeria.

3.1 Teaching and Learning Methods

Teaching is the process of transferring knowledge. It should be delivered in a systematic, interactive, organized and purposive manner. The primary purpose of teaching at any level is to bring a fundamental change in students' learning. It is therefore, expected that teaching will cause desirable change in the learners' behavior. Learners in this context, we are referring to the students. Therefore, teaching should be seen as the integral part of any educational policy framework implementation as it would have a direct impact on the students' learning. There are many teaching methods available, and some of these methods have been tested in diverse environments and proven effective in different scenarios. These include discovery method spaced lecture, group work, dialogue, scaffolding and constructivism etc. However, in Nigeria, the most widely used teaching methods are: lecture method, discussion method, project method, simulation method and problem-solving method. The lecture method is also commonly referred to as "talk chalk method" which involves the teacher explaining the ideas with giving examples and occasionally, writes on the chalk board. The project method on the other hand involves active participation of the student in such a way that a cooperative (group) study of a real-life situation in the class is undertaken, under the supervision of the teacher. The drama method, may also be classified as group method as it involves a group-oriented approach. However, the concerned, feelings and reactions of the students in this situation are taken into consideration during the course of interacting with one another. This may also be referred to as the "Role-Play Method". Simulation method is a more practical oriented approach of teaching where students are exposed to devices and equipment physically. This method is considered as the most efficient in Science and Engineering related subjects as it's hastens and stimulates the understanding of learners. So many learning methods have been identified and associated with specific teaching methods. Today, in Nigeria,

mostly, engineering lecture rooms are faced with a similar scenario as it was in decades ago. The teaching methodology is still the conventional approach where a teacher delivers lectures by standing in the classroom, dictating notes or deriving equations from the 'old' notebook', recycling examples, assignments and projects. This type of approach does not allow skills acquisition, critical thinking and creativity needed in a challenging multi-disciplinary course like engineering. Notably, some enhancements have been observed following the diffusion of ICT into the teaching, and learning process and this creates some sort of modification on the process. Moreover, there are quite a number of methods that could be used/or integrated in to the teaching method. These methods are expected to improve students' learning. It was discovered that most engineering students are visual, sensing, inductive, active, and creative whereas the teaching methods used are mostly passive, auditory, abstract, deductive and sequential. Thus, leading to incompatibility between the teaching and the learning process, and hence, resulting to poor performance among engineering students.

3.2 ENGINEERING EDUCATION CURRICULUM

Curriculum is one of the most important components of implementing any education policy as it describes the syllabus, teaching methods employed and ultimately, it would determine the learning experience. Engineering curriculum is expected to be dynamic to reflect the change in emerging engineering and societal problems. Curriculum is a reflection and a product of the society and can contribute to changing the society. Therefore, it is important in the process of the curriculum development and education process to reflect labor market issues. Furthermore, for sustainable development, engineering curriculum has to be innovative project-based and has to be linked with our local industries. The knowledge passed through the modern-day engineering curriculum must be flexible, dynamic and encompass a broad knowledge within a specialized field of knowledge. The traditional mode of engineering curriculum cannot provide these and the present-day work environment requires specialized individuals. Therefore, there is a need to have different tracks or specialization within the same subject area. This method is been adopted in the United Kingdom and

even Nigeria where the students spend three years obtaining a specialized degree while the fourth year is being spent in the industry. The program is designed in such a way that critical thinking, independent problem solving and creativity are rewarded and encouraged which leads to creativity and problem-solving skills. These skills are important for independent learners to develop and possess while overcoming challenges that are associated with modern day engineering. Therefore, the curriculum must allow for attitudes that can bring out the skills and knowledge gained. Attitude is also important because team work is an essential feature in solving engineering challenges. The curriculum must encourage more team work because the reality is that most projects in the field of engineering today and in the future require team work from diverse range of knowledge culture, social and religious backgrounds.

Unfortunately, lots of names have been associated with the engineering education in Nigeria. The static nature of Nigerian engineering curriculum has made it to be described as obsolete. This is because there is a huge gap between the general education knowledge provided by the universities and technical skills required by the industries. As such, the graduates are not meeting the needs of the labor markets, thus, necessitating the need for retraining programs by the employers. The current engineering education is also described as out of touch especially with what is going on in the industry. This also defeats the aim of the 21st-century engineering education which is supposed to provide knowledge, skills and attitude. Some authors also describe the present-day engineering training as that of the era of the parents of the present-day engineers. Although, individual efforts towards realizing dynamic engineering curriculum are acknowledged due to recent growth in number of lecturers acquiring higher degrees from abroad. Also, with the recent improvements on internet access in the Nigerian Universities, have provided access to a wider range of information and educational resources, this has further broadened the need and call for a review of the system. Despite all these, there is no significant improvement in terms of the curriculum. Based on the findings from a survey conducted, 94% of the lecturers who have obtained postgraduate degree outside Nigeria and realized the need for improved

curriculum attended a conference or seminar where improved engineering curriculum is encouraged said they cannot implement what they have learnt. This is because of the lack of the necessary infrastructure and work load. Therefore, equipment and better infrastructure is an important aspect of the improved curriculum. Furthermore, It was also discovered that human attitude towards making the change must also be encouraged. Conferences are expected to expose lecturers to latest discovery and stimulate discussions among teachers and students about the latest discovery in modern engineering world. The problem of changing existing curriculum is not only peculiar to Nigeria but across the world. This is because the global problem with engineering education has to do with the challenges of the 21st-century workplace and the permeating nature of product and services provided by engineers. Therefore, the lack of willingness to adopt changes in engineering curriculum as the field of engineering is changing is a global problem. A general reason for refusing changes in engineering education has to do with the fact that this field is changing very fast and before a curriculum change can be made, some more advance changes are already recorded on the field. However, changing this attitude must be encouraged in Nigeria as it is been presently done around the globe.

3.3 EQUIPMENT AND INFRASTRUCTURE
Apart from the global problems, engineering education in Nigeria is facing some peculiar problems like lack of equipment and infrastructure. Most engineering faculties in Nigeria complain about the lack or inadequate availability of necessary basic equipment and Infrastructure. This is because of inadequate funding to our universities. Most students and lecturers respectively complain about the level of available equipment and infrastructure in our engineering departments. Lack of equipment and necessary infrastructure like classrooms and teaching aid equipment is seen as the major barrier to teaching and learning of engineering in Nigeria.

4.0 THE WAY FORWARD
Engineering students must be ready to learn new skills discretely and also very quickly to satisfy up with the ever-changing requirements of the engineering field. Majority of the engineering

departments in Nigerian university are not customer-focused as a result of either lack of funds or the very fact that the amount seeking admission year in year out far exceeds the number of places available. a transparent understanding of the necessity of the customer, the scholars (who are the foremost important customer), their parents, the society and therefore the industry that might eventually employ these students would go an extended way in ensuring that some level of quality is achieved. to satisfy up with the demand of the industry and to be ready to still compete favorably round the world, variety of changes need to be implemented to enhance the standard of engineering education in Nigeria. Consequently, some major changes that require immediate attention and the way to travel about these changes are discussed below:

4.1 Degree Specialization and choice to Spend a Full Year within the industry

The reality facing engineering education today is significantly different from that of the past, and therefore the future would be distinct from that of today. to satisfy the longer-term need of engineering education, significant changes are required. the necessity of today is different, and therefore the relevance and direction of a number of the modules or departments in some faculty of engineering need to be questioned. for instance, up until the first 90s, an EE graduate in Nigeria is predicted to figure for an electrical company or somewhere similar. However, the truth of today is that electrical engineers are now computer engineers, telecommunication engineers and even biomedical engineers where different knowledge of biology, telecommunications computer-oriented language and programming are all essential to having the ability to perform well. Therefore, this five-year engineering learning structure within the university without specialization would not meet the necessity of future engineers. There is a requirement to breakdown the areas of specialization and stop the thought of generalization.

4.2 Continuous Modification within the Curriculum of Engineering Education

To meet up with the longer-term demand, there has got to be machinery in situ to accommodate the rapid technological changes that are now being experienced. Any curriculum that might meet the

necessity of the economic practice has got to change continuously. New technology is developing at a rate where if care is not taken before a change has been implemented the technology would have changed. the matter related to these changes are often solved by providing long life learning, where essential skills are those taught. Knowledge skills and attitude must even be emphasized. Teamwork must be encouraged because the processes and systems that engineers would need to conceive, create and operate are quite complex. Hence, it's important that engineers must learn to unravel problems in teams. Furthermore, the test to students must be challenging but fair. Knowledge is that the database of an engineer, skills are the tools to manipulate the knowledge to satisfy a goal dictated or strongly influenced by attitude. Presently, there's a growing acceptance of online degrees from foreign universities. an honest number of the undergraduate students say they might be happy to possess a web degree from a university outside Nigeria if going forward for a master's degree as an alternate to travelling outside Nigeria. The rationale provided is that they believe they might be recuperating knowledge from the web degrees than attending a standard university in Nigeria. This is often an enormous sign that conventional universities in Nigeria must still evolve and improve upon the content. With technological advancement, the planet is now a worldwide village, and giving the universal nature of education, if care is not taken, with the way technology is advancing, there's a likelihood that within the near future technical course like engineering would be taught online to incorporate access to varied practical and this may need some negative impacts on the enrolments of student in our universities. This practical could be designed using software to simulate the important environment.

4.3 Teaching what is necessary within the world

Engineering Education has been described as a three-legged stool counting on science mathematics and technique. Even as a stool cannot stand on two legs, adopting a correct technique is as important because the other two. The technique needed within the field of engineering cannot be fully taught within the four walls of the classroom. There is a requirement for interaction and reinforcement of the essential fundamentals that an engineer would wish

when on the sector. Engineering education must provide increased practical experience. This helps the students' ability to find out the abstract and theory that forms much of the engineering fundamentals. It also helps their ability to understand the applicability and practical usefulness of an honest theory. an answer to the present would be emphasizing more on the basics of science with integrated knowledge while longer would be spent that specialize in the important world. Consistent with a search which studied successful young engineers across the sector of engineering, the study showed that success within the field of engineering lies within the combination of generic skills with technical capabilities with emotional intelligence and focused thinking. The research also showed that less emphasis should get on assessment of predictable skills as more of technical expertise should be examined. This suggests that lecturers should adopt the utilization of application-based test such the important world capability is tested. Furthermore, emphasis has been made on the very fact that the important world must be taught majorly the fundamentals, problem-solving skills, engineering ethics, and therefore the connection between technology and the society while reducing the number of years spent within the class room. Teaching what's necessary within the world requires more equipment and infrastructures. Therefore, government and therefore the management of our universities must provide more in terms of kit and infrastructure.

4.4 Use of Innovative approaches to teaching and learning

The use of innovative approaches to teaching and learning is extremely essential. Results indicate that 96% of the scholars who have studied within the university abroad are satisfied with the standard of engineering education they received or obtained. However, only 14% of the scholars were satisfied with the standard of engineering education in Nigeria. Additionally, 100% of the scholars agreed that the staff outside Nigeria who are always using teaching aids are better at explaining things, provide better concentration, participation in school and students were ready to retain what's being taught for much longer compared to the normal method of teaching utilized in the Nigeria. 100% of the scholars also confirmed that the very fact that

teaching materials are available online before and after lectures makes learning easier. This means that education is global, and lecturers should be encouraged to form their notes available online. The utilization of technological teaching aids is long overdue. This has got to tend proper attention by both the management and staff of our universities. Some lecturers are not taking adequate advantage of the small aids like projectors and electronics boards presently available. This might be as a result of lack of data about the usage of that equipment. Therefore, adequate retraining program must even be administered to form sure that this will be put to proper use.

5.0 CONCLUSIONS

Engineering education is very critical for the achievement of sustainable development goals. Quality research, industrial training, effective teaching, community development and substantial collaboration between tertiary institutions and industry are major requirement for realization of sustainable development goals. Most challenges traceable to teaching and learning can be overcome through strategic approach and effective funding. Employability, entrepreneurial skills and global competitiveness are required by engineering graduates to realize success both at under-graduate and post-graduate levels and for effective professional practice within industries. Engineering curriculum requires periodic review and there must be substantial linkages between academia and engineering industry. This will enhance engineering productivity, generation of employment, increased output through innovations, job creation, efficient utilization of available resources and the facilitation in the transfer of technological advancement.

6.0 RECOMMENDATIONS

There is need for enforcement of policies that will enhance reformation of engineering education, lifelong learning initiatives and sustainable development in Nigeria, collaboration of academia, government, regulatory bodies, stakeholders, professionals, engineers and industries in with the curriculum review and project implementation. Resilient infrastructures should be provided in engineering institutions for effective sanitation, industrialization and innovation. Lecturers and staff need to recommit themselves towards the

development of sound engineers through the provision of adequate resources for teaching as well as well-equipped learning and training schools and centers. Regulatory bodies should ensure that students are trained to be more skillful and independent as this will ensure achievement of sustainability in the education system in Nigeria.

ACKNOWLEDGEMENTS

REFERENCES

Adedeji, O., and Campbell, O. (2013). The role of higher education in human capital development. *Available at SSRN 2380878*.

Akintola, A. A., Aderounmu, G. A., and Owolarafe, O. K. (2002). Problems of engineering education and training in developing countries: Nigeria as a case study. *European journal of engineering education*, *27*(4), 393-400.

Keeper, D. G. (2010). Systemic corruption in Nigeria: A threat to sustainable development. In *Proceedings of the first International Technology Education and Environment Conference*.

Njoku, J. U., and Onyegbula, J. C. (2017). Human Capital development as a strategy for sustainable development in the Nigerian education system. *African Research Review*, *11*(2), 178-189.

Ogunyinka, E. K., Okeke, T. I., and Adedoyin, R. C. (2015). Teacher education and development in Nigeria: An analysis of reforms, challenges and prospects. *Education Journal*, *4*(3), 111-122.

Oloyede, A. A., Ajimotokan, H. A., and Faruk, N. (2017). Embracing the future of engineering education in Nigeria: teaching and learning challenges. *Nigerian Journal of Technology*, *36*(4), 991-1001.

Oyebode, O. J. (2020). Revitalization of the Quality Engineering Education in Nigeria: Special attention to Funding and Implementation Strategies. *IJCEP*, *38*, 47.

Oyebode, O. J., Adebayo, V. B., and Olowe, K. O. (2015). Assessment of the use of AutoCAD package for teaching and learning engineering drawing in Afe Babalola University Ado-Ekiti. *Assessment Of the Use Of Autocad Package For Teaching And Learning Engineering Drawing In Afe Babalola University Ado-Ekiti*, *4*(9), 1-8.

Oyedepo, S. O. (2012). Energy and sustainable development in Nigeria: the way forward. *Energy, Sustainability and Society*, *2*(1), 1-17.

A Review of Different Biomass Based Materials used to Produce Activated Carbon for Water Treatment.

Korie C.I, Afolabi E.A, Kovo A.S., Muktar A.

Department of Chemical Engineering, Federal University of Technology, Minna.

ABSTRACT

Water treatment for industrial wastewater is very necessary, as it prevents effluents from posing hazardous influences to the environment. Adsorption and Adsorbents are part of the techniques used to treat effluents. Adsorbents can be developed with various materials, but it is important to focus on adsorbents that are not expensive, do not require a lot of processing but have high adsorption capacity. Activated carbon from agricultural waste is becoming an increasingly interesting area for research as it fits into the sphere of inexpensive adsorbents. Activated carbon is formed through two stages; firstly, the pyrolysis or carbonization of the precursor and secondly activation via steam or various reagents. The preparation of high-quality activated carbon is dependent on the production process; operation parameters like time, temperature, and impregnation ratio have influence on its quality. This article seeks to show the viability of low-cost adsorbent when activated carbon is prepared from biomass and used as adsorbents during water treatment of heavy metal, oil spills organic contaminants and dyes.

KEYWORDS: Activated carbon, adsorption, water treatment, biochar, biomass

1   INTRODUCTION

Industrialization has its advantages, but it is usually at costs that are environmentally detrimental. Processes that deal with converting raw materials to finished goods on a large scale, comes with its share of problems. A lot of which revolves around water effluents. As such, it has become equally important to determine ways to implement water treatment procedures. Textile industries discharge colored effluents into water bodies and battery manufactures discharge effluents consisting of heavy metals that have an impact the quality of the water. Other ways water might be contaminated include oil spills that may happen at any of its extraction, production, distribution, and transportation stages. Contaminated water bodies do not only affect sea life, they have the ability to affect human life as well. Adsorption is usually the most preferred option for treating contaminated water because of its low cost, it needs no skill for utilization, is flexible and highly effective. Additionally, adsorption works to remove organic and inorganic pollutants from effluents in a green way; this means that bio-hazardous side products will not be developed.

Low costs adsorbents do not need a lot of processing before it is used. They are usually low-cost because they are abundant whether it be natural, a side product, or waste from industries. It is noteworthy to add that additional processing is fine,

if it can make up for increased adsorption capacity. There are different types of adsorbents: organic polymers (synthetic), natural sorbents, and mineral materials (inorganic) (Bailey, S.E. et al, 1999). Heavy research on the area of implementing bio adsorbents as treatment options is ongoing. It has been discovered that bio adsorbents are lightweight, have good adsorption selectivity, considerable adsorption efficacy, outstanding adsorption recyclability, and can be easily operated, plus it has an inexpensive preparation technique. As such, it is necessary to explore all the probable agro and horticulturally based adsorbents in order to determine their viability for removing contaminants.

1.1   ACTIVATED CARBON

Of the many adsorbents used to treat inorganic and organic pollutants in polluted water, plant or lignocellulose wastes, activated carbons, biopolymers and clays are very well known adsorbents. Activated carbon has the higher popularity out of all the adsorbents that researchers use for water treatment. However, the higher the quality, the more expensive it is. Small-scale industries are looking for cheaper ways to prepare activated carbon; hence, the movements towards agricultural waste produce. Activated carbon is formed firstly through pyrolysis or carbonization of the precursor to get biochar and secondly activation via an activating agent. There are two types of

activation. For chemical activation, a catalyst is used to speed up the process; as such, less temperature is used. Common activators used for this process are H3PO4, ZnCl2, KOH, K2S, H2SO4, and KCNS (Zor et al., 1998). This process minimizes tar formation and volatilization. Chemical activation is one process, but two separate temperatures are used (Smisek and Cerny, 1970). Physical activation requires a higher temperature and more time and ultimately might produce tar and increase volatilization; chemical activation offers better results and gets recommendations. Chemical activation is also advantageous as the activation targets the carboxyl and hydroxyl groups that are important for adsorption to oil spills. A lot of research on how activated carbon is prepared from biomass and how effective this type of adsorbent is on treating effluents form organic and inorganic sources is ongoing

1.2   WATERMELON RIND

(Jimoh et al, 2014) studied about preparing activated carbon using watermelon peel. They focused on activating temperature of 200°C and varied this temperature to about 350°C. The time for activation was also varied from 15 to 60 minutes. The researchers discovered peak conditions at 300°C and 60 minutes. The researchers impregnated the sample with different reagents at different molar concentrations ranging from 0.5 to 1.5 m. HCL, H2SO4, and zncl2 were used to get optimal outcomes (1.0m sulphuric acid). The process was characterized using proximate-ultimate analysis and FTIR analysis. (Oghenejoboh, 2018) researched on adsorbing nickel (ii) ion from wastewater with activated carbon from watermelon rind. The temperature and time implemented from carbonization was 380°C for 120 minutes. Impregnation was done using 1.0m zinc chloride. (Mohd Azmier Ahmad, 2017) carried out research on producing activated carbon to removal synthetic dye. The optimal and time and temperature for the production of char was 1 hour and 700°C. The activated agent used was KOH. The proximate analysis was used for characterization and a carbon yield of 32% was discovered. Additionally, the sample was characterized via BET and the surface area was recorded as 776.65 m2/g. (Qiu-Feng Lu, 2018) produced activated carbon at optimal conditions via pyrolysis. The gas used was nitrogen, it's heating rate at heating rate of 5 °C and optimum

temperature and time for activated carbon at 700 °C for 1 h under nitrogen flow. The reagent used was hydroxide with optimum impregnation ratio of 1:2. This sample was characterized with BET and it was discovered to have a surface area of 1303.3 m2 g-1

1.3   ORANGE PEELS

(Foo, K. Y. et al, 2012) researched on preparing activated carbon from orange peels using microwave assisted K2CO3 activation. Optimum operation parameters were determined from microwave power, chemical impregnation ratio, and irradiation time. The biomass was characterized using some analytical methods such as zeta potential measurement, scanning electron microscopy, nitrogen adsorption isotherm, elemental analysis, Fourier transform infrared spectroscopy and surface acidity/basicity. The carbon yield for the optimal condition of orange peel was 80.99%. (Fernandez, M. E., 2014) also prepared activated carbon from orange peels to be used for the adsorption of basic dye. The parameters considered were impregnation ratio of 2:1 in a H3PO4 acid solution, time of 2h and temperature of 110°C. Additional preparation on this activated carbon using furnace temperature of 475°C, heating rate of 3°C /min and time of 0.5 h was initiated. (EdaKöseoğlu et al, 2015) produced activated carbon via chemical activation with reagents like zinc chloride (ZnCl2) and potassium carbonate (K2CO3). The optimum impregnation ratio was at 1:1 and temperature range used for this process was from 500–1000°C. BET was used to get the surface area for K2CO3 and ZnCl2 which were 1352 m2 g−1 and 1215 m2 g−1, respectively.

1.4   RICE HUSK

(Md. Ahiduzzaman, 2016) developed biochar and activated carbon using rice husk. The temperature was varied from 600 to 900 °C and heating time from 30 to 120 mins at an interval of 30min. Activation of biochar to activated carbon happened with the reagent zinc chloride at 6500C for 2hrs. (Y.C. Sharma 2009) also prepared activated carbon using rice husks. The precursor was activated using a muffle furnace at 450°C For 1 hr. It was carbonized in the absence of oxygen as such nitrogen (99.99%) with a flow of 150ml/min was maintained throughout the process. (Rostamian, R., 2018) prepared biochar and activated carbon using pyrolysis by varying temperature from 400 to 800 °C. Two activation methods were used; physical activation with steam and chemical activation with

The Nigerian Society of Engineers
Minna Branch
1st NSE Minna Branch National Conference 2021

Conference theme
Role of Engineering in
Sustainable Development Goals

potassium hydroxide (KOH). BET characterization was used to determine the surface area, and it was discovered that the chemical activation process provided a higher surface area (2201 m 2 g -1) and total pore volume (0.96 cm 3 g -1) than the physical adsorption process. (Sobhanardakani, S. et al, 2013) developed activated carbon from rice husk which was used for heavy metal removal. The researchers performed characterizations on the physical and chemical properties of the activated carbon. It was discovered that rice husk was an effective adsorbent due to its reduction of particle size. The particle size used for this process was maintained by passing the rice husk through a 1-mm sieve.

1.5   COCONUT SHELL

(M.K.B. Gratuito et al, 2008) used coconut shell in producing activated carbon. The chemical method of activation was used constraints like impregnation ratio of 1 to 2 with a 0.5 interval of phosphoric acid (H3PO4) was used. Activation time ranging from 10 to 30 min and activation temperature ranging from 400 to 500 °C was implemented.

(Tan, I et al, 2008) used coconut husk to prepare activated carbon by combining two activation methods; potassium hydroxide (KOH) and carbon dioxide (CO2). The parameters temperature, CO2 activation time, impregnation ratio was used to determine optimal conditions which were gotten at 750°C, 2.29 h and 2.91. (Anirudhan, T. S et al, 2011) used coconut husk to prepare activated carbon to remove heavy ions. The operational parameter for activation using sulphuric acid was investigated using an impregnation time of 2 hrs. The optimal parameters for activation via steam activation were 400°C and 1 hr. Carbon yield of 40.0% was recorded.

1.6   BAGASSE

(Mohan et al, 2002) used bagasse to develop activated carbon to remove cadmium and zinc. The carbon was activated with chemical activation with temperature ranging from 150–1651°C for 24 h using sulfuric acid and physical activation using parameters temperature at 800–8501°C for 30 minutes. The activated carbon was characterized using an SEM photograph to determine the porosity levels and surface texture. (Demiral, H et al, 2010), used sugar beet bagasse to produce activated carbon to remove nitrate from wastewater. The activated carbon was prepared using chemical activation and zinc chloride as the reagent. Pyrolysis was used with nitrogen and flow

at 100 ml/min, the temperature ranged from 500 to 700°C. (Bernardo, E. C. et al, 1997) produced activated carbon from cane bagasse to use to decolorize of molasses' wastewater. Pyrolysis temperature of 300°C was used with nitrogen gas to prepare biochar and activated carbon was produced with steam at 800°C. The authors characterized the activated carbon using proximate analyses and this indicated that bagasse was an adequate precursor for activated carbon because ash content was low. BET was sued to determine surface area of the activated carbon and got a value greater 400 m2 g−1. (Hakan Demiral et al, 2008) used olive bagasse to produce activated carbon using steam as an activating agent. This was used to remove chromium (IV) from wastewater. The optimal parameters were discovered at 500◦C and 1 h. Activation temperature was at 850◦C for a time of 0.5 h. Characterization on the sample was initiated to discover if the sample would be perfect for adsorption. BET for surface area was done on the sample and the value gotten was 718 m2/g.

1.7   PALM PRODUCTS

(Nor AdillaRashid et al, 2017) used palm kernel shell to produce activated carbon via physical activation method using carbon dioxide (CO2) using direct activation at 850 °C for 1 h. The sample was characterized and it was discovered that palm kernel shell is a good adsorbent for carbon dioxide. (Adinata, D. et al, 2007) developed activated carbon via chemical activation, using palm shell as precursor and potassium carbonate (K2CO3) as the activating chemical. Parameters like activation temperature and impregnation ratio were varied; 600–1000°C and 0.5–2.0. The results showed that the yield reduced as impregnation ratio and temperature increased, and CO2 adsorption increased. The optimal conditions for producing activated carbon using this sample was at a temperature 800 °C, time 2 h and IR of 1.0. The characterization at optimal conditions for BET specific surface area gave a value of 1170 m2/g.

1.8   WOOD-BASED BIOMASS

(Liu, Q. S et al, 2010) used bamboo to produce activated carbon via chemical activation. The researchers used microwave-induced activation and phosphoric acid and considered how parameters like IR, radiation time and microwave power would

The Nigerian Society of Engineers
Minna Branch
1st NSE Minna Branch National Conference 2021

Conference theme
Role of Engineering in
Sustainable Development Goals

activate activation of the sample; they discovered optimum conditions at 1:1, 20 min and 350 W respectively. The activated had a carbon yield of 48% and BET surface area of 1432 m2/g. (Wang, T et al, 2009) produced activated carbon from wood using zinc chloride and microwave for activation. The operational parameters varied to determine influence was particle size, which was 0.3–3.3 mm, IR of 0:1 to 3:1. The microwave radiation power was optimized at 700 W under a nitrogen flow of 20 ml/min. (Xing et al, 2014) used steam activation to develop activated carbon and characterized this activated carbon to determine how these parameters would affect adsorption capacity. The researchers discovered that the higher the temperature the lower the adsorption capacity because elements like pore volume and surface area are reduced.

The optimal conditions for activation were activation time of 120 min, temperature of 850°C, and steam flow rate of 0.2-cm3 min−1. BET surface area and total pore volume were 1210 m2 g−1 and 0.542 cm−3 g−1 respectively.

1.9   AGRO STALKS

(IşılayOzdemir et al, 2014) used chemical activation method to prepare activated carbon from grape stalk with ZnCl2 in CO2 atmosphere. The operational parameters ware temperature, time, and impregnation ratio. These parameters were discovered to have an outcome on surface area and pore structure which was determined by characterizations on BET, SEM-EDX and particle size distribution and proximate-ultimate analysis. The optimum parameters for this procedure were temperature, carbonization, impregnation time and impregnation ratio of 700°C, 120 min, 36 h and 2:1 respectively. The BET area was recorded as 1411 m2/g. (Deng, H. et al, 2009) produced activated carbon from cotton stalk with Zinc chloride and microware. This was used to treat methylene blue. The parameters investigated for the development of activated carbon from the sample was microwave radiation time microwave power, and impregnation ratios and the optimal values discovered for these parameters were 9 min, 560 W, and 1.6 g/g respectively. Characterization for activated carbon produced a carbon yield of 37.92%.

1.10   DATE STONES

(Bouchelta, C. et al, 2008) produced activated carbon using steam activation as a method and date stones as the precursor. Pyrolysis temperature of 700

°C and 100cm3 min−1 flow rate for nitrogen was used for step one and step two involved steam activation at 700 °C for 6 h. The researchers characterized the activated carbon via scanning electron microscopy (SEM), Fourier transform infrared spectroscopy (FTIR) X-ray diffraction (XRD), and nitrogen adsorption (BET). The characterization for optimal conditions showed the surface area and microporus volume as 635m2 g−1 and 0.716 cm3 g−1 respectively. The proximate-ultimate analysis showed that cellulose and hemicellulose were present in the raw material, and that carbon and graphite were present after pyrolysis. (FawziBanat et al, 2013) used date pits to produce activated carbon and compared adsorption capacity of the raw and activated date pits when treating dye effluent waters. The researchers considered the effect of parameters like activation temperature; solution pH, solution salinity adsorbent particle size, and solution temperature on the removal of methylene blue removal. Solution PH was an important parameter for dye removal. Characterization using BET, FT-IR analysis, SEM-EDX and particle size distribution shows how elements like surface area, pore volume; pore diameters have been modified to affect activated carbon adsorption capacity. (Hadoun, H. et al, 2013) used H3PO4 as an activating agent to produce activated carbon from date stems. The parameters varied for this process was temperature, which was varied at 450, 550, and 650°C. Impregnation ratio of 2/1 of the activating agent was used to produce the activated carbon. The Researchers characterized the activated carbon to determine it met with standards of other activated carbon being used for adsorption. One of the characterizations was BET which was used to find the surface area and pore volume; surface area for the AC with these three varying temperatures 450, 550 and 650°C respectively was recorded at 682, 1455, 1319 m2/g and the pore volumes were recorded at 0,343, 1,045 and 0.735 cm3/g.

1.11   OTHER BIOMASS

(Selvaraju, G et al, 2017) worked on producing activated carbon from artocarpus integer (breadfruit) fruit processing waste. The researchers favored steam activation with peak temperature of 750°C and time of 60 min. BET analysis on this AC showed that the surface area was at 1411 mg/g. Other analysis like Fourier Transform Infrared, Scanning

Electron Microscope (SEM), Spectroscope (FTIR), and X-ray powder Diffraction (XRD) showed that the AC had the functional groups needed for adsorption purposes and a high micro-porous and amorphous structure (P. Sugumaran et al, 2012) used Delonix regia fruit pod and banana empty fruit bunch as precursors when activating carbon via chemical activation. A TGA analysis showed maximum loss at 500 °C, as such the samples went through pyrolysis at 400°C and 450°C respectively. IR was used as an activation factor and BET was implemented immediately after for analysis. The fruit pod treated with H3PO4 had a higher surface area than its untreated counterpart did but a lower pore volume than its untreated counterpart.

(M.K. Rai et al, 2016) used mango seed as a precursor of activated carbon to remove Cr (VI) from aqueous solutions. This was a one step chemical activation process with H3PO4 and a temperature of 600 °C for 1 hour. The sample was characterized BET surface area analyzer, FTIR spectroscopy, using elemental analyzer, and SEM analysis. (M. Benadjemia et al, 2011) produced activated carbons via the pyrolysis of artichoke leaves to remove of methyl blue dye from wastewater. The activating agent used was phosphoric acid at a temperature of 500 °C and IR was varied at 100, 200, and 300 wt.%. (HasanSayğılı et al, 2016) produced activated carbon from tomato processing solid with chemical activation. The production variables for this process were carbonization temperature, impregnation ratio, and carbonization time. The peak conditions determined for the production of activated carbon for this process were; 600 °C carbonization temperature 6:1 impregnation ratio, and 1 h carbonization time. Characterization using proximate analysis showed that the sample had a carbon content percentage of 53.92% and a yield of 38.20%. BET was another analysis implemented to show surface area recorded at 1093 m2/g/ (Syed, S. P, 2011) developed activated carbon from kapok hull to remove malachite green from wastewater. The sample was treated with sulphuric acid using an impregnation ratio 1:1 for 24hr. The sample was washed using distilled water and kept in an air oven 383K for 12 hours. Temperature and time were varied to study the changes in yield. The optimal temperature and time were recorded at 823K for an hour. Particle size was also utilized to study changes in yield using particle sizes of 250,150 and 100 BSS mesh numbers. XRD and SEM were the characterization used to determine the structural and morphological changes. (Tang et al, 2012) produced activated carbon, using Ramulus mori as a precursor and ammonium hydrogen phosphate as a chemical activation agent. Investigation on operational parameters was carried out. The optimal temperature for carbonization was 400°C, time was 90 min, impregnation ratio of hydrogen phosphate to carbonized sample was 1:2, 800°C for activating temperature, and 120 min for time. The sample was characterized the yield of activated carbon was recorded as 26.56%. It was discovered that hydroxyl and carbonyl group exist on the surface of the activated carbon. (Ceyhan, A. A. et al, 2013) used EAS biomass to produce activated carbon using a pyrolysis temperature of range of 150 to 350°C and heating rate of 5oC/min. The sample was treated with zinc chloride with impregnation ratios of 1:1, 1:2, 1:3, and 1:4 and a pre-treatment temperature rate of 30, 50, and 80oC for 3hrs. The time for activation was 3h. (Angın, D., et al, 2013) used safflower seed press cake biochar to produce activated carbon. The influence on activation temperature and IR was determined. This was a two-step chemical activation process using zinc chloride and the activated carbon developed was used to treat methylene blue dye. The activated carbon was characterized and carbon content of 76.29% was recorded. The BET surface area was as 801.5 m2 g−1and total pore volume 0.393 cm3 g−1. (Ioannidou, O. A., et al, 2010) prepared activated carbon using agricultural residues for the treatment of pesticides. The precursors used were olive kernels, corncobs, soya stalks and rapeseed stalks. The influences of operational parameters were investigated. The optimal parameters for the pyrolysis stage at 800oC for temperature and 60 min for time with a flow rate of 15 mL /min and heating rate of 27 oC/ min for nitrogen. The biochar was activated using physical activation at the same temperature for pyrolysis with a time range of 30 min under steam flow 40 g /min at 0.5 bar. (Qian, Q. et al, 2007) used cattle-manure compost to produce activated carbon via chemical activation using zinc chloride as an activating agent. Operational parameters such as IR, Temperature and time were investigated to determine their influence on production. The activated carbon was characterized using BET to determine the surface area and pore volume which were 2170 m2/g and 1.70 cm3/g. The

sample was also characterized using Thermogravimetric analysis (TGA). The activated carbon was used to treat phenol. (Ahmadpour, et al, 1997) developed activated carbon from macadamia nutshell using chemical activation. The parameters varied were particle size variance of 212-300 pm and 500-600 pm. Two different reagents - ZnCl and KOH – were utilized in the activation of the carbonized precursor. The results for the experiment depict that using a lower temperature (500°C) for ZnCl would favor adsorption capacity. KOH on the other hand recorded favorable conditions such as high surface area and micropore volume when higher temperatures were used. (Pallarés, J. et al, 2018) worked on the production of activated carbon using barley straw as a precursor. The activation method used was physical activation method and the activating agents were steam and carbon dioxide. The operational parameters were investigated to determine influence. It was discovered that temperature and heating rate for the carbonization process were important factors. Additionally, activation temperature and time were necessary operational parameters for the process. The peak conditions discovered for activated carbon using barely straw was 800 °C for temperature and time was 1 h for carbon dioxide and 700 °C and a hold time of 1 h for steam activation. The BET surface area was 789 m2/g and micropore volume was 0.3268 cm3/g for carbon dioxide activation and 552 m2/g and 0.2304 cm3/g for steam activation. (Zhong, Z. Y., et al, 2012) used peanut hull to produce activated carbon via chemical activation using phosphoric acid for Remazol Brilliant Blue R adsorption purposeses. The particle size was set at 2.0 mm. The sample was characterized via proximate analysis and the results for cellulose 16.91%, moisture 10.85%, lignin 27.43%, hemicellulose 10.11%, and ash 2.62%. The operational time for the impregnation was set at 24 h. (Theydan, S. K. et al, 2012) developed activated carbon from pits using FeCl3 as a chemical activating agent. The IR for the process was 100ml of the activating agent to 1.5 g/g. this was run for 24h at 30 ∘C. The sample was carbonized at a temperature 700 ∘C for an activation time of 1 h. (Bello, O. S. et al, 2008) produced activated carbon from periwinkle shells for the adsorption of methylene blue via physicochemical activation. The activation agents used were carbon dioxide (CO2) and potassium hydroxide (KOH) . The operational

parameters for the activation were determined at at 850 °C for 2 h. (Demirbas, E. et al, 2008) developed activated carbon from apricot stone to use for removal of basic dye. The operational parameters investigated for influence were particle size, at 0.5 to 2.0 mm. The sample was activated with concentrated H2SO4 at 250 C for 24 h. The activated carbon sample was characterized for surface area and this was determined at 560 m2 /g. (Baccar, R. et al, 2013) produced activated carbon from olive-waste cakes to use in the adsorption of tannery dye. The operational parameters utilized to investigate production influence were particle size ranging between 100 and 160 μm. BET (Brunauer–Emmett and Teller) was used to calculate the surface area, pore volume and pore diameter as 793m2 g−1, 0.49cm3 g−1 and 4.2nm, respectively (Cafer Saka, 2012) produced activated carbons from acorn shell using zinc chloride (ZnCl2) as an activating agent. The precursor was carbonized at 600 °C in nitrogen gas atmosphere and the samples were characterized. The parameters investigated for influence were duration time, activation temperature, IR and impregnation time. The BET surface area was recorded as 1289 m2/g. The sample was also characterized by FT-IR spectroscopic method to determine surface chemical characteristics. (Kong, J. et al, 2013) used leather waste to produce activated carbon via physical and chemical activation means. The conditions investigated for activation optimization were carbonization time, carbonization temperature, and impregnation ratio.

The researchers characterized using thermal gravimetric analysis of LW-H4P2O7 showed that using H4P2O7 as the activating agent encourages the development of carbonaceous material. Other types of characterization on the activated carbon were scanning electron microscopy (SEM), X-ray diffraction (XRD), and Fourier transform infrared spectroscopy (FT-IR).

1.12 FIGURES AND TABLES

TABLE 1: SUMMARY OF THE REVIEW ON BIOMASS BASED ACTIVATED CARBON

Author(s)	Research Work
(Jimoh et al, 2014)	Study on the production of activated carbon from watermelon Peel. The impregnation was done using different reagents at different molar

Author(s)	Research Work	Author(s)	Research Work
	concentrations. H2SO4, HCL and zncl2. The best results were gotten from 1.0m sulphuric acid.		mixture was heated in an electric furnace at 475°C at a heating rate of 3°C /min and time of 0.5 h.
(Oghenejoboh, 2018)	Research on adsorbing nickel (ii) ion from wastewater with activated carbon from watermelon rind. The temperature and time implemented from carbonization was 3800c for 120 minutes. Impregnation was done using 1.0m zinc chloride.	(EdaKöseoğlu et al, 2015)	Production of activated carbon from orange peels using potassium carbonate (K2CO3) and zinc chloride (ZnCl2). The temperature range used for this process was from 500–1000°C and the impregnation ratio was at 1:1.
(Mohd Azmier Ahmad et al, 2017)	Research on producing activated carbon for the removal of synthetic dye. The optimal time and temperature for the production of char was 700 °C and held for 1 h. KOH was used to activate the precursor.	(Md. Ahiduzzaman, 2016)	Research on preparing biochar and activated carbon with rice husk. The parameters considered were temperature and time. The temperatures range varies from 600 to 900°C; the heating time ranged from 30 to 120 min. Activation temperature and time for chemical activation with zinc chloride was 650°C for 2hrs.
(Qiu-Feng Lu et al, 2018)	Research on preparing activated carbon at optimal conditions of 700 °C for temperature, 5 °C min-1 for heating rate and 1 h for time with nitrogen flow. The carbon was activated with IR potassium hydroxide of 1:2		
		(Y. C. Sharma, 2009)	Preparation of activated carbon using rice husks. Rice husk was activated using a muffle furnace at 450 C for 1 hr. It was carbonized in the absence of oxygen as such nitrogen (99.99%) with a flow of 150ml/min was maintained throughout the process.
(Foo, K. Y., 2012)	Study on preparing activated carbon from orange peels using chemical agent K2CO3 and microwave. The carbon yield for the optimal condition of orange peel was 80.99%.		
(Fernandez, M. E., 2014)	Study on preparation of activated carbon from orange peels to be used for the adsorption of basic dye. The preparation method was implemented by mixing the precursor with H3PO4 acid with IR of 2:1, time at 2 h at 110°C for temperature. This	(Rostamian, R., 2018)	Preparation of biochar and activated carbon by varying temperature at 400, 600, and 800°C. Chemical activation was with potassium hydroxide (KOH) and physical activation was with steam.
		(Sobhanardakani, S. et al, 2013)	Development of activated carbon from rice husk to remove heavy metals from

The Nigerian Society of Engineers
Minna Branch
1st NSE Minna Branch National Conference 2021

Conference theme
Role of Engineering in
Sustainable Development Goals

Author(s)	Research Work
	wastewater. It was discovered that rice husk was an effective adsorbent due to its reduction of particle size. The particle size used for this process was maintained by passing the rice husk through a 1-mm sieve.
(M.K.B.Gratuito et al, 2008)	Research on using coconut shell to produce activation via chemical activation. Parameters like IR with phosphoric acid (H_3PO_4) were varied at 1 to 2 with a 0.5 interval. Other parameters used were activation temperature from 400 to 500°C with a 50°C temperature interval and time at 10 to 30 min.
(Tan, I et al, 2008)	Research preparing activated carbon from coconut husk using potassium hydroxide (KOH) as a chemical activation method and carbon dioxide (CO_2) gasification as a physical activation method. Parameters with peak results were activation temperature of 750 °C, and time of 2.29 h for the physical activation method and IR of 2.91 for the chemical activation method.
(Anirudhan, T. S et al, 2011)	Preparing activated carbon to remove heavy metal ions from wastewater using coconut hull as a precursor. The operational parameters for activation using sulphuric acid were investigated using a impregnation time of 2 hrs. The optimal temperature for activation via steam

Author(s)	Research Work
	activation was 400°C and time of 1 hr.
(Mohan et al, 2002)	Research on producing bagasse-based activated carbon to remove zinc and cadmium via chemical activation using sulphuric acid. A temperature range of 150– 165°C for a period of 24 h is utilized and thermal activation is used for the product at 800–850°C for 30 min.
(Demiral, H et al, 2010)	Research on producing activated carbon from sugar beet bagasse for the removal of nitrate from aqueous solutions by activated carbon. The dried bagasse was activated with $ZnCl_2$ in two stages. IR was varied from 1 to 3 and the mixture was passed through a vertical furnace in the absence of air with temperature of 500, 600 and 700°C and flow rate of 100ml/min.
(Bernardo, E. C. et al, 1997)	Production of activated carbon from cane bagasse to use to decolorize of molasses' wastewater. The sample was passed through pyrolysis at 300°C using nitrogen and inert athmosphere and activated with steam at 800°C in a horizontal electric furnace.

2   CONCLUSIONS

It can be concluded that biomass from activated carbon is an effective way to treat effluents from various sources. Additionally, the carbonization process is usually dependent on temperature and time. Temperature is an important variable for pore volume evolution. The process of activating carbon can also be optimized by varying the impregnation ratio of carbonized biomass to activating agent. It is

necessary to characterize the activated carbon to determine how well the resulting structures will interact with metal ions, dyes, or organic contaminants.

REFERENCES

Ahmad, M. A., Ahmad, N., & Bello, O. S. (2017). Statistical optimization of adsorption process for removal of synthetic dye using watermelon rinds. Modeling Earth Systems and Environment, 3(1), 25.

Ahiduzzaman, M., & Islam, A. S. (2016). Preparation of porous bio-char and activated carbon from rice husk by leaching ash and chemical activation. SpringerPlus, 5(1), 1248.

Ahmadpour, A., & Do, D. D. (1997). The preparation of activated carbon from macadamia nutshell by chemical activation. Carbon, 35(12), 1723-1732.

Angın, D., Altintig, E., & Köse, T. E. (2013). Influence of process parameters on the surface and chemical properties of activated carbon obtained from biochar by chemical activation. Bioresource Technology, 148, 542-549.

Anirudhan, T. S., & Sreekumari, S. S. (2011). Adsorptive removal of heavy metal ions from industrial effluents using activated carbon derived from waste coconut buttons. Journal of Environmental Sciences, 23(12), 1989-1998.

Baccar, R., Blánquez, P., Bouzid, J., Feki, M., Attiya, H., & Sarrà, M. (2013). Modeling of adsorption isotherms and kinetics of a tannery dye onto an activated carbon prepared from an agricultural by-product. Fuel processing technology, 106, 408-415.

Banat, F., Al-Asheh, S., & Al-Makhadmeh, L. (2003). Evaluation of the use of raw and activated date pits as potential adsorbents for dye containing waters. Process Biochemistry, 39(2), 193-202.

Bello, O. S., Adeogun, I. A., Ajaelu, J. C., & Fehintola, E. O. (2008). Adsorption of methylene blue onto activated carbon derived from periwinkle shells: kinetics and equilibrium studies. Chemistry and Ecology, 24(4), 285-295.

Bernardo, E. C., Egashira, R., & Kawasaki, J. (1997). Decolorization of molasses' wastewater using activated carbon prepared from cane bagasse. Carbon, 35(9), 1217-1221.

Bailey, S.E., Olin, T.J., Bricka, R.M., and Adrian, D.D., (1999). A Review of Pontentially Low-Cost Sorbents for Heavy Metals. Water Res. 33(11): 2469-2479 pp

Benadjemia, M., Millière, L., Reinert, L., Benderdouche, N., & Duclaux, L. (2011). Preparation, characterization, and Methylene Blue adsorption of phosphoric acid activated carbons from globe artichoke leaves. Fuel Processing Technology, 92(6), 1203-1212.

Bouchelta, C., Medjram, M. S., Bertrand, O., & Bellat, J. P. (2008). Preparation and characterization of activated carbon from date stones by physical activation with steam. Journal of Analytical and Applied Pyrolysis, 82(1), 70-77.

Ceyhan, A. A., Şahin, Ö., Baytar, O., & Saka, C. (2013). Surface and porous characterization of activated carbon prepared from pyrolysis of biomass by two-stage procedure at low activation temperature and it's the adsorption of iodine. Journal of Analytical and Applied Pyrolysis, 104, 378-383.

Demiral, H., & Gündüzoğlu, G. (2010). Removal of nitrate from aqueous solutions by activated carbon prepared from sugar beet bagasse. Bioresource technology, 101(6), 1675-1680.

Demiral, H., Demiral, I., Tümsek, F., & Karabacakoğlu, B. (2008). Adsorption of chromium (VI) from aqueous solution by activated carbon derived from olive bagasse and applicability of different adsorption models.

Demirbas, E., Kobya, M., & Sulak, M. T. (2008). Adsorption kinetics of a basic dye from aqueous solutions onto apricot stone activated carbon. Bioresource technology, 99(13), 5368-5373.

Deng, H., Yang, L., Tao, G., & Dai, J. (2009). Preparation and characterization of activated carbon from cotton stalk by microwave assisted chemical activation—application in methylene blue adsorption from aqueous solution. Journal of Hazardous Materials, 166(2-3), 1514-1521.

Fernandez, M. E., Nunell, G. V., Bonelli, P. R., & Cukierman, A. L. (2014). Activated carbon developed from orange peels: Batch and dynamic competitive adsorption of basic dyes. Industrial Crops and Products, 62, 437–445.

Foo, K. Y., & Hameed, B. H. (2009). Value-added utilization of oil palm ash: A superior recycling

of the industrial agricultural waste. Journal of Hazardous Materials, 172(2-3), 523-531.

Fu, K., Yue, Q., Gao, B., Sun, Y., & Zhu, L. (2013). Preparation, characterization and application of lignin-based activated carbon from black liquor lignin by steam activation. Chemical engineering journal, 228, 1074-1082.

Gratuito, M. K. B., Panyathanmaporn, T., Chumnanklang, R. A., Sirinuntawittaya, N. B., & Dutta, A. (2008). Production of activated carbon from coconut shell: Optimization using response surface methodology. Bioresource Technology, 99(11), 4887-4895.

Gin, W. A., Jimoh, A., Abdulkareem, A. S., & Giwa, A. (2014). Production of activated carbon from watermelon peel. Int. J. Scient. Eng. Res, 5, 66-71.

Hadoun, H., Sadaoui, Z., Souami, N., Sahel, D., & Toumert, I. (2013). Characterization of mesoporous carbon prepared from date stems by H3PO4 chemical activation. Applied Surface Science, 280, 1-7.

Ioannidou, O. A., Zabaniotou, A. A., Stavropoulos, G. G., Islam, M. A., & Albanis, T. A. (2010). Preparation of activated carbons from agricultural residues for pesticide adsorption. Chemosphere, 80(11), 1328-1336.

Kong, J., Yue, Q., Huang, L., Gao, Y., Sun, Y., Gao, B., ... & Wang, Y. (2013). Preparation, characterization and evaluation of adsorptive properties of leather waste based activated carbon via physical and chemical activation. Chemical Engineering Journal, 221, 62-71.

Köseoğlu, E., & Akmil-Başar, C. (2015). Preparation, structural evaluation and adsorptive properties of activated carbon from agricultural waste biomass. Advanced Powder Technology, 26(3), 811-818.

Liu, Q. S., Zheng, T., Wang, P., & Guo, L. (2010). Preparation and characterization of activated carbon from bamboo by microwave-induced phosphoric acid activation. Industrial Crops and Products, 31(2), 233-238.

Lin, X. Q., Yang, N., Lü, Q. F., & Liu, R. (2019). Self-Nitrogen-Doped Porous Biocarbon from Watermelon Rind: A High-Performance Supercapacitor Electrode and Its Improved Electrochemical Performance Using Redox Additive Electrolyte. Energy Technology, 7(3), 1800628.

Madhumitha, S., Vanitha, B., & Balaganesh, P. (2016). Preparation of Activated Carbon from Watermelon peel (CITRUS LANATUS) and preliminary studies on its characteristics.

Mohan, D., & Singh, K. P. (2002). Single-and multi-component adsorption of cadmium and zinc using activated carbon derived from bagasse—an agricultural waste. Water research, 36(9), 2304-2318.

Oghenejoboh, K. M. (2018). Biosorption of nickel (II) ion from synthetic wastewater on watermelon rind activated carbon using reponse surface methodology (RSM) optimization approach. Nigerian Journal of Technology, 37(3), 647-655.

Ozdemir, I., Şahin, M., Orhan, R., & Erdem, M. (2014). Preparation and characterization of activated carbon from grape stalk by zinc chloride activation. Fuel processing technology, 125, 200-206.

Pallarés, J., González-Cencerrado, A., & Arauzo, I. (2018). Production and characterization of activated carbon from barley straw by physical activation with carbon dioxide and steam. Biomass and bioenergy, 115, 64-73.

Qian, Q., Machida, M., & Tatsumoto, H. (2007). Preparation of activated carbons from cattle-manure compost by zinc chloride activation. Bioresource technology, 98(2), 353-360.

Rashidi, N. A., & Yusup, S. (2017). Potential of palm kernel shell as activated carbon precursors through single stage activation technique for carbon dioxide adsorption. Journal of cleaner production, 168, 474-486.

Rai, M. K., Shahi, G., Meena, V., Meena, R., Chakraborty, S.,ingh, R. S., & Rai, B. N. (2016). Removal of hexavalent chromium Cr (VI) using activated carbon prepared from mango kernel activated with H3PO4. Resource-Efficient Technologies, 2, S63-S70.

Rostamian, R., Heidarpour, M., Afyuni, M., & Mousavi, S. F. (2018). Characterization and Sodium Sorption Capacity of Biochar and Activated Carbon Prepared from Rice Hus.

Saka, C. (2012). BET, TG–DTG, FT-IR, SEM, iodine number analysis, and preparation of activated carbon from acorn shell by chemical activation with ZnCl2. Journal of Analytical and Applied Pyrolysis, 95, 21-24.

Sayğılı, H., & Güzel, F. (2016). High surface area mesoporous activated carbon from tomato processing solid waste by zinc chloride activation: process optimization, characterization and dyes adsorption. Journal of Cleaner Production, 113, 995-1004.

Selvaraju, G., & Bakar, N. K. A. (2017). Production of a new industrially viable green-activated carbon from Artocarpus integer fruit processing waste and evaluation of its chemical, morphological and adsorption properties. Journal of Cleaner Production, 141, 989–999.

Smíšek, M., & Černý, S. (1970). Active carbon: manufacture, properties and applications (Vol. 12). Elsevier Publishing Company.

Sobhanardakani, S., Parvizimosaed, H., & Olyaie, E. (2013). Heavy metals removal from wastewaters using organic solid waste—rice husk. Environmental Science and Pollution Research, 20(8), 5265-5271.

Sugumaran, P., Susan, V. P., Ravichandran, P., & Seshadri, S. (2012). Production and characterization of activated carbon from banana empty fruit bunch and Delonix regia fruit pod. Journal of Sustainable Energy & Environment, 3(3), 125-13

Syed, S. P. (2011). Study of the removal of malachite green from aqueous solution by using solid agricultural waste. Research Journal of Chemical Sciences Vol, 1(1).

Tan, I. A. W., Ahmad, A. L., & Hameed, B. H. (2008). Preparation of activated carbon from coconut husk: Optimization study on removal of 2, 4, 6-trichlorophenol using response surface methodology. Journal of hazardous materials, 153(1-2), 709-717.

Tang, Y. B., Liu, Q., & Chen, F. Y. (2012). Preparation and characterization of activated carbon from waste ramulus mori. Chemical Engineering Journal, 203, 19-24

Theydan, S. K., & Ahmed, M. J. (2012). Adsorption of methylene blue onto biomass-based activated carbon by FeCl3 activation: Equilibrium, kinetics, and thermodynamic studies. Journal of Analytical and Applied Pyrolysis, 97, 116-122.

Üner, O., Geçgel, Ü., & Bayrak, Y. (2015). Preparation and characterization of mesoporous activated carbons from waste watermelon rind by using the chemical activation method with zinc chloride. Arabian Journal of Chemistry.

Venkata Ramana, D. K., & Min, K. (2016). Activated carbon produced from pigeon peas hulls waste as a low-cost agro-waste adsorbent for Cu (II) and Cd (II) removal. Desalination and Water Treatment, 57(15), 6967-6980.

Wang, T., Tan, S., & Liang, C. (2009). Preparation and characterization of activated carbon from wood via microwave-induced ZnCl2 activation. Carbon, 47(7), 1880-1883

Zhang, Y. J., Xing, Z. J., Duan, Z. K., Li, M., & Wang, Y. (2014). Effects of steam activation on the pore structure and surface chemistry of activated carbon derived from bamboo waste. Applied Surface Science, 315, 279-286.

Zhong, Z. Y., Yang, Q., Li, X. M., Luo, K., Liu, Y., & Zeng, G. M. (2012). Preparation of peanut hull-based activated carbon by microwave-induced phosphoric acid activation and its application in Remazol Brilliant Blue R adsorption. Industrial Crops and Products, 37(1), 178-185.

Zor, S., Yazici, B., Erbil, M., Galip, H., 1998. The electrochemical degradation of linear alkylbenzene sulfonate Ž . Ž. LAS on platinum electrode. Water Res. 323, 579586.

Conference theme

Role of Engineering in Sustainable Development Goals

Risk Analysis of Power Transmission Infrastructure for Sustainable Development: A Case Study of the Nigerian 330 kV-41 Bus Network

Jethro Shola[1]*, Emmanuel Sunday Akoji[2], UmbugalaKigbu F.[3]*, Yusuf Isah[4], & A. A. Sadiq[5]

[2,4,5]Department of Electrical and Electronics Engineering, Federal University of Technology, Minna

[1]* Transmission Company of Nigeria, PMB 193 Abuja

[3]*Federal Institute of Industrial Research (FIIRO) PMB 21023 Lagos

*Corresponding Authors email: kigbu4ril@gmail.com

ABSTRACT

This study was aimed at risk assessment of the electrical power system network in Nigeria. The Nigeria 330kV 41-Bus network was employed in this study, sampling five transmission stations of Birnin Kebbi, Gwagwalada, Benin, Onitsha and Ikeja. The traditional modelling risk assessment index was employed in this study, using mathematical relationships to determine the failure rate, reliability, probability of failure and risk index of the five transmission stations sampled. The results obtained from the analysis were presented in tabular and graphical forms. From the analysis, it was discovered that Birnin Kebbi Transmission Station has the highest reliability of 98% while Gwagwalada Transmission Station has the least reliability of 75%. It was also found in the study that Ikeja Transmission Station has the highest risk index of 83.39. This shows that failure of the transmission station will have the highest impact on the economy of the country. This is largely due to the power delivered by the transmission station and the number of consumers the station serves. Therefore, among other, it was recommended that since Ikeja supplies enormous power and the probability of failure of the station is high, the equipment used for power transmission should be made adequate to forestall imminent failure, resulting to high-risk index.

KEYWORDS: *Failure Rate, Reliability, Risk Assessment, Sustainable Development, Transmission Stations,*

1   INTRODUCTION

The importance of electrical power in human life cannot be overemphasized and the impact of power outage had been demonstrated through history. Recently, from February 13 to February 17 2021, a large winter storm and associated cold wave caused over 5 million inhabitants to lose power across the United States, with Texas alone having over 4.3 million customers without power (Brian and Nauren, 2021). On 9th January. 2021 in Pakistan, power outage occurred leaving around 200 million people without electrical supply (Masood, 2021). In Nigeria, power outage had led to the crippling of industries in various sectors such as agriculture, mining and industrial sector of the economy (Aliyu *et al*., 2013). Inadvertently, the poor reliability of electrical power supply in Nigeria has made it one of the best markets for generator dealers across the world and the overall effect of this anomaly is an increase in pollution, increase in noise level, inflation, dwindling economy, death of indigenous and small-medium scale business among others.

Sustainable Development Goals (SDGs) number 7, aims to ensure access to affordable, *reliable*, sustainable and modern energy for all. In particular, SDG-7 seeks to by the end of 2030, expand transmission infrastructure and upgrade technology for supplying modern and sustainable energy services for all in developing countries (like Nigeria), in particular least developed countries, small island developing States and land locked developing countries, in accordance with their respective programmes of support.

Access to reliable power in Nigeria is majorly hindered by component outage which results in system collapse, such as the outage of transmission line. The problem of power outage in Nigeria is continually worsening as the day goes by. This made Awosope (2014), to opine that unreliable power system network in Nigeria has become a tool with which the politicians used in their electoral campaign to score political points. However, results are not achieved because of the lack of experience on the side of the politicians on how the power sector works,

coupled with political maneuvering in the country, leading to politicians with no competence in the field of electrical engineering which were often times appointed to head the sector (Airoboman *et al*., 2016).

The power system network in Nigeria is basically categorized into three which are the generating stations, the transmission network and the distribution network. Major problem occurs in the transmission network as it is the link between the power generating stations and the distribution network. However, the risk assessment of the electrical power network in Nigeria has often focused on the voltage stability of 330kV transmission power grid in the country. Voltage instability in the electrical power system network is caused by contingencies; faults occurring in the generating station or in the transmission line leading to power outage.

Risk assessment is the procedure in which the risks posed by inherent hazards involved in processes or situations are estimated either quantitatively or qualitatively. Rausand (2013) in his book, Risk Assessment: Theory, Methods, and Applications, opined that risk assessment is the combined effort of identifying and analyzing potential (future) events that may negatively impact individuals, assets, and/or the environment (i.e., hazard analysis); and making judgments "on the tolerability of the risk on the basis of a risk analysis" while considering influencing factors (i.e., risk evaluation). From the above context, it is understood that risk assessment brings about the likelihood of a hazard occurring which impacts sustainable development. The cost of such hazard on a system, can be assessed using quantitative or qualitative approach.

Qualitative risk assessment typically means assessing the likelihood that a risk will occur based on subjective qualities and the impact it could have using predefined ranking scales on sustainable development. The impact of risks is often categorized into three levels: low, medium or high. The probability that a risk will occur can also be expressed the same way or categorized as the likelihood it will occur, ranging from 0% to 100%. Quantitative risk assessment, on the other hand, attempts to assign a specific financial amount (as a measure of sustainability) to adverse events, representing the potential cost if that event actually occurs, as well as the likelihood that the event will occur in a given year (Rosencrance, 2020).

Power outages and unreliability of the electrical power system network in Nigeria had forces the closure of many companies in the different sectors of the Nigeria economy with others forced to relocate to other countries with more stable and reliable power supply. In order to mitigate the consequences of power outage and unreliability of the power system network in Nigeria, there is need to carry out a risks assessment in the electrical power system. This will help identify the factors causing outage in the power system network, the cost of risks in the power system network and suggest mitigation process to be pursued.

In this paper, the assessment of the risk in a Nigerian 41-bus, 330kV power grid system is studied and discussed. Risk assessment index ranking from 0 to 1 was used in the assessment of risks occurring in the electrical power distribution network for a year under review. This study is aims at carrying out risk assessment of the electrical power system network in Nigeria through the following:

i. Determine the failure rate of randomly chosen five transmission stations in the Nigeria electrical power system network.
ii. Examine the reliability of randomly chosen five transmission stations in the Nigeria electrical power system network.
iii. Calculate the availability of randomly chosen five transmission stations in the Nigeria electrical power system network.
iv. Determine the risk index associated with failure of transmission stations in the Nigeria electrical power system network

2 METHODOLOGY

In paper, the traditional component failure model will be employed in the assessment of the risks in the case study power system network of Nigeria. For power transmission system risk evaluation using this model, only failures of transmission components are considered, whereas generating units are assumed to be 100% reliable. Key transmission components include overhead lines, cables, transformers, capacitors, and reactors (Guo, 2014).

Three key parameters were used for the risk assessment which are the failure rate of the transmission line, the reliability of the transmission line, probability of failure on the transmission line and risk index of the transmission line using the Nigerian 330kV, 41-bus network shown in Figure 1(Onohaebi, 2017).

The Nigerian Society of Engineers
Minna Branch
1st NSE Minna Branch National Conference 2021

Conference theme
Role of Engineering in
Sustainable Development Goals

The data for the year 2017 was obtained from five randomly chosen transmission stations:

A. Birnin Kebbi Transmission Station,
B. Gwagwalada Transmission Station,
C. Benin Transmission Station,
D. Onitsha Transmission Station and
E. Ikeja Transmission Station

Load point indices is used to calculate the reliability, availability as well as the failure rate.

Equations (1) to (11) were used in the risk assessment of the power system network using five transmission stations (Raza, 2019). The results obtained were graphically interpreted using Microsoft Excel 2016.
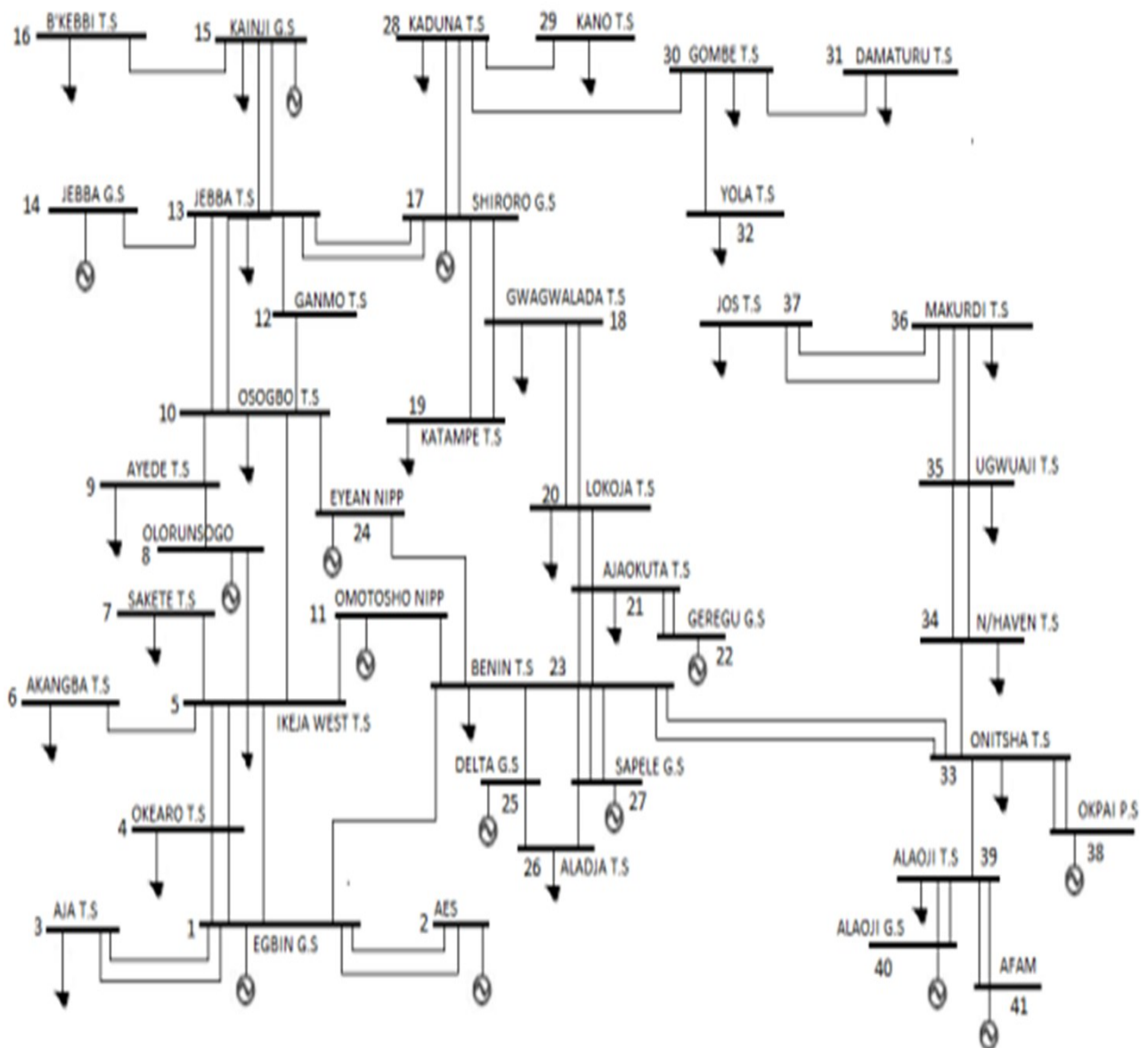

Figure 1: Nigerian 330kV 41-bus Network (**Source:** Onohaebi, 2017).

1ˢᵗ NSE Minna Branch Engineering Conference 2021

2.1 RELIABILITY INDICES

1. **Mean Time Between Failures (MTBF):** This is the average intervals between successive failures in a system measured in hours per year. The Mean Time Between Failures (MTBF) is calculated thus:

$$MTBF = \frac{8760 - Downtime\ (DT)}{Number\ of\ Outage\ (NO)} \qquad (1)$$

Where 8760 is the total hour of operation in a year (24 hours x 365 days).

2. **Mean Time To Repair (MTTR):** This is the average time required to repair a system and bring it back to its operational state (hours per year). The MTTR is calculated thus:

$$MTTR = \frac{Downtime\ (DT)}{Number\ of\ Outage\ (NO)} \qquad (2)$$

3. **Failure rate (λ):** The frequency of component failure per unit time. It is usually denoted by the Greek letter λ (Lambda). In reliability engineering calculations, failure rate is considered as forecasted failure intensity given that the component is fully operational in its initial condition. The formula for failure rate is given as:

$$\lambda = \frac{1}{MTBF} \qquad (3)$$

4. **Repair rate (μ):** The frequency of successful repair operations performed on a failed component per unit time. It is usually denoted by the Greek letter μ (Mu). The repair rate is determined using the formula of equation (4).

$$\mu = \frac{1}{MTTR} \qquad (4)$$

5. **Reliability:** Reliability is calculated as an exponentially decaying probability function which depends on the failure rate. Since failure rate may not remain constant over the operational lifecycle of a component, the average time-based quantities such as MTBF can be used to calculate Reliability. The mathematical function is specified as:

$$Reliability\ (R) = e^{-\lambda} \qquad (5)$$

Reliability (R) is complementary to probability of failure (P), hence,

$$R = 1 - Probability\ of\ Failure\ (P) \qquad (6)$$

6. **Probability of Failure (P):** This is used in determining the likelihood that failure will occur in the transmission line. The probability of failure is used for the risk index of the failure in the transmission line. The formula for calculating the probability of failure is given as:

$$Probability\ of\ Failure\ (P) = \frac{\lambda}{\lambda + \mu} \qquad (7)$$

From Equation (6), probability of failure can also be calculated as

$$Probability\ of\ Failure\ (P) = 1 - R \qquad (8)$$

7. **Availability (A):** Availability is an important metric used to assess the performance of repairable systems, accounting for both the reliability and maintainability properties of a component or system.

While there are many types of availability, such as Instantaneous (or Point) Availability, Average Uptime Availability (or Mean Availability), Steady State Availability, Inherent Availability, Achieved Availability and Operational Availability, this article focused on Operational Availability. Operational availability is a measure of the "real" average availability over a period of time and includes all experienced sources of downtime, such as administrative downtime, logistic downtime, etc. The operational availability is the availability that the consumer of electricity supplied by the transmission stations actually experiences.

Operational availability is the ratio of the system uptime to total time. Mathematically, it is given by:

$$Availability\ (A) = \frac{Uptime}{Total\ Time} \qquad (9)$$

It should also be noted that uptime can be computed using Equation (10).

$$Uptime = Total\ Time - Downtime \qquad (10)$$

Risk Index (R_{index}): The risk index is a scale which is used in determining the severalty of the risk of failure in the transmission line. The risk index can quantitatively capture probabilities (likelihood) of occurrence of contingencies and their impact. In simplified terms, risk index is the product of event likelihood and its severity. The severity in the transmission line is the power loss during the risk occurrence.

Conference theme
Role of Engineering in Sustainable Development Goals

In mathematical terms

$$Risk\ Index\ (R_{index}) = Prob.of\ Failure\ (P) \times Severity\ (S)\ (11)$$

Table 1 is the summary of data obtained for the five-transmission station whose risk of power failure occurrence was investigated in this study.

3   RESULTS AND DISCUSSION

Equations (2) to (11) were used in the analysis of the data obtained as shown in Table 1 and the results are shown in Table 2.

Figure 2 shows the Failure Rate of the various transmission stations. From the graph, it is seen that Benin Transmission station has the highest failure rate of 0.092 (9.2%) followed by Gwagwalada Transmission Station with failure rate of 0.071

(7.1%) while Birnin Kebbi Transmission Station has the least failure rate of 0.013 (1.3%).

The reliability graph of **Figure 3** indicates that Birnin Kebbi has a reliability of 0.98 (98%), followed by Onitsha Transmission Station with reliability of 0.95 (95%). The transmission station with the least reliability is Gwagwalada Transmission Station 0.75 (75%)

Table 1: Data of Selected Transmission Stations

Transmission Station	Number of Outages (NO)	Downtime (DT)	Uptime (UT)	Power (MW)
Birnin Kebbi	112	159.1	8600.9	276
Gwagwalada	476	2122.2	6637.8	117.4
Benin	625	1984.9	6775.1	134
Onitsha	280	398	8362	326
Ikeja	293	1045.8	7714.2	698.5

Source: (Asibeluo and Madueme, 2018)

Table 2: Result of the Risk Assessment of Power System Network in Nigeria

Trans. Station	Num of Outages (NO)	Down Time (DT)	Severity (S)	MTBF	MTTR	Failure Rate (λ)	Repair rate (μ)	Probability of Failure (P)	Reliab (R)	Availab (A)	Risk Index (R$_{index}$)
Birnin Kebbi	112	159.1	276	76.794	1.4205	0.01302	0.70396	0.018162	0.98184	0.9818	5.01274
Gwagwalada	476	2122.2	117.4	13.945	4.4584	0.07171	0.2243	0.24226	0.75774	0.7577	28.44136
Benin	625	1984.9	134	10.84	3.1758	0.09225	0.31488	0.226587	0.77341	0.7734	30.36263
Onitsha	280	398	326	29.864	1.4214	0.03349	0.70352	0.045434	0.95457	0.9545	14.81142
Ikeja	293	1045.8	698.5	26.328	3.5693	0.03798	0.28017	0.119384	0.88062	0.8806	83.38942
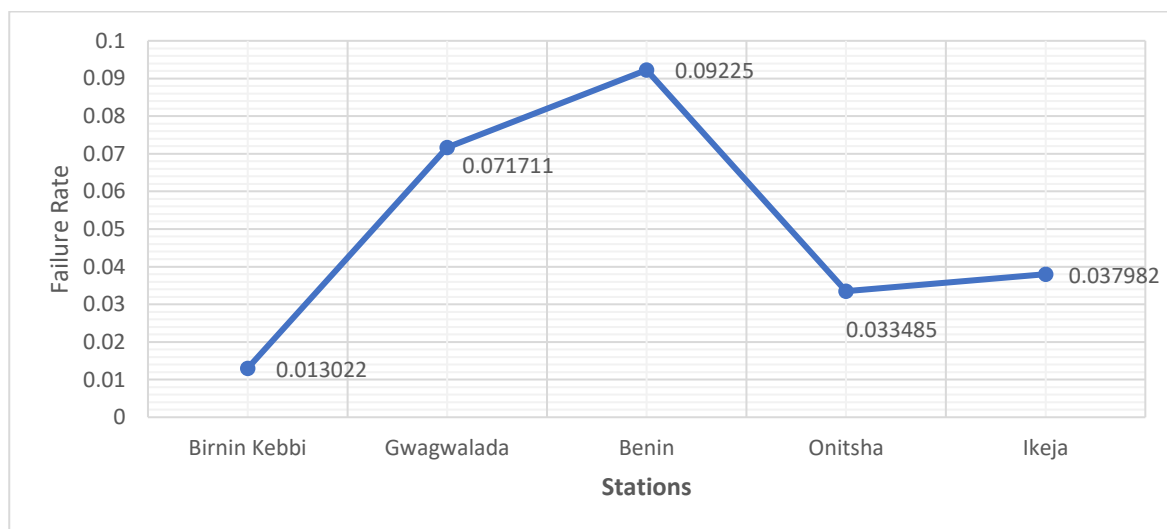
Figure 2: Failure Rate of Selected Power System Network in Nigeria

The Nigerian Society of Engineers
Minna Branch
1st NSE Minna Branch National Conference 2021

Conference theme
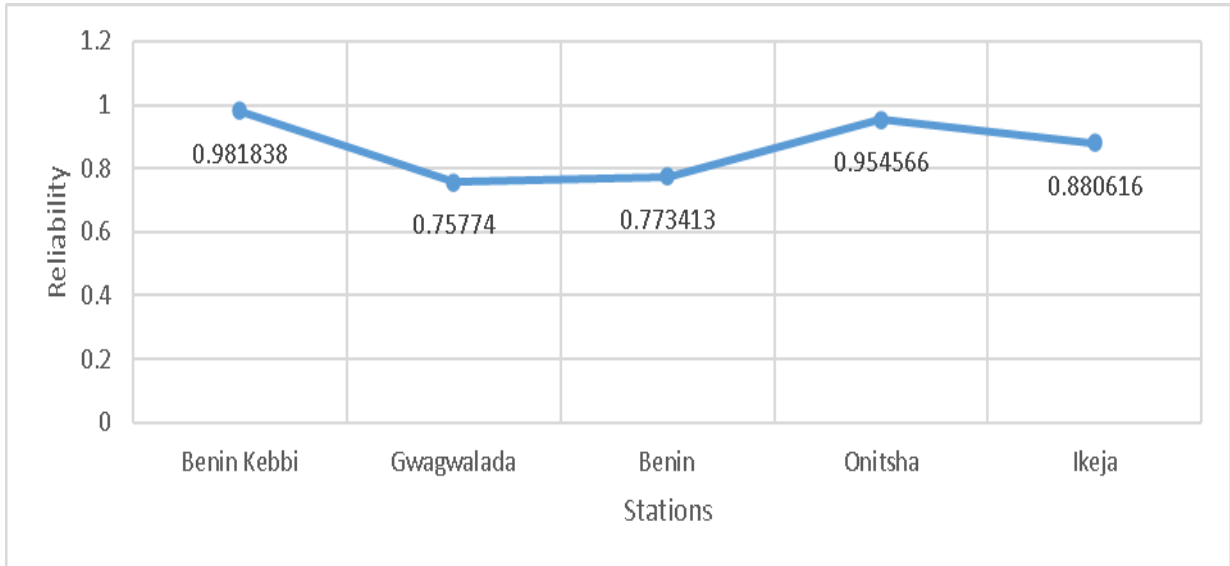Role of Engineering in
Sustainable Development Goals

Figure 3: Reliability of Selected Transmission Stations in Nigeria

The probability of failure graph of Figure 4 indicates that the transmission station with the high probability of failure is Gwagwalada Transmission Station with probability of 0.242 (24.2%) followed by Benin Transmission Station with probability of 0.226 (22.6%). Birnin Kebbi Transmission Station has the least probability of failure with probability of 0.018 (1.8%).
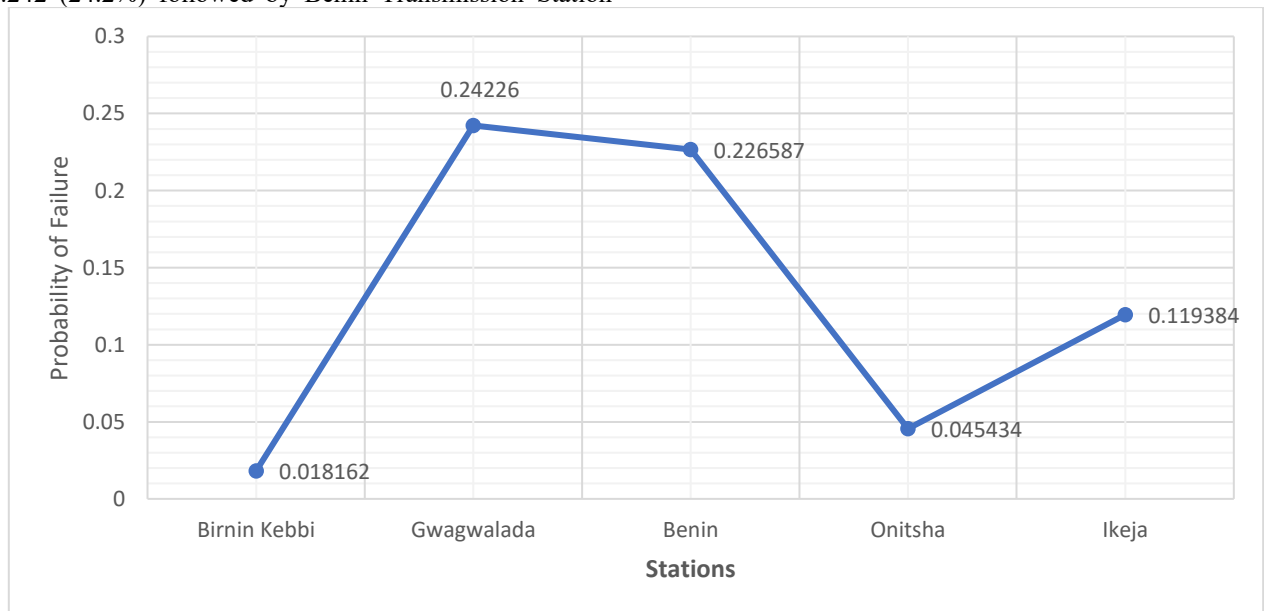

Figure 4: Probability of Failure of Selected Transmission Stations in Nigeria

Figure 5 shows the availability of the studied power stations in Nigeria. From the graph, it is observed that Birnin Kebbi has the highest availability score of 0.98 (98%) among the selected power stations in Nigeria. This is largely due to its least downtime and severity index as shown in Table 2. Birnin Kebbi is followed by Onitsha with availability of 0.95 (95%) and then Ikeja having availability of 0.88 (88%). Gwagwalada has the least availability 0.75 (75%) and from the bottom is followed by Benin with availability of 0.77 (77%).

The risk index graph of **Figure 6** shows that the Ikeja Transmission Station has the highest risk index and followed by Benin Transmission Station. The implication

Conference theme

Role of Engineering in Sustainable Development Goals

of this is that failure occurrence on the Ikeja Transmission Station would have the highest impact on the economy of the country compared to other transmission station in Nigeria. This is largely due to the power delivered to by the Ikeja Transmission Station and the population the station serves.

Lagos being the economic hub of the Nigeria economy is served by this transmission station and this accounts for the

enormous risk in the power system network serving the state.

From Figure 2 to Figure 6, it is seen that Birnin Kebbi Transmission Station is more stable than other transmission stations in the study. Benin has the least failure rate (Figure 2), hence its reliability is high (98.2%) with lowest probability of failure (1.8%). Due to the stability of Birnin Kebbi Transmission Station, its risk index is the lowest (5.01).
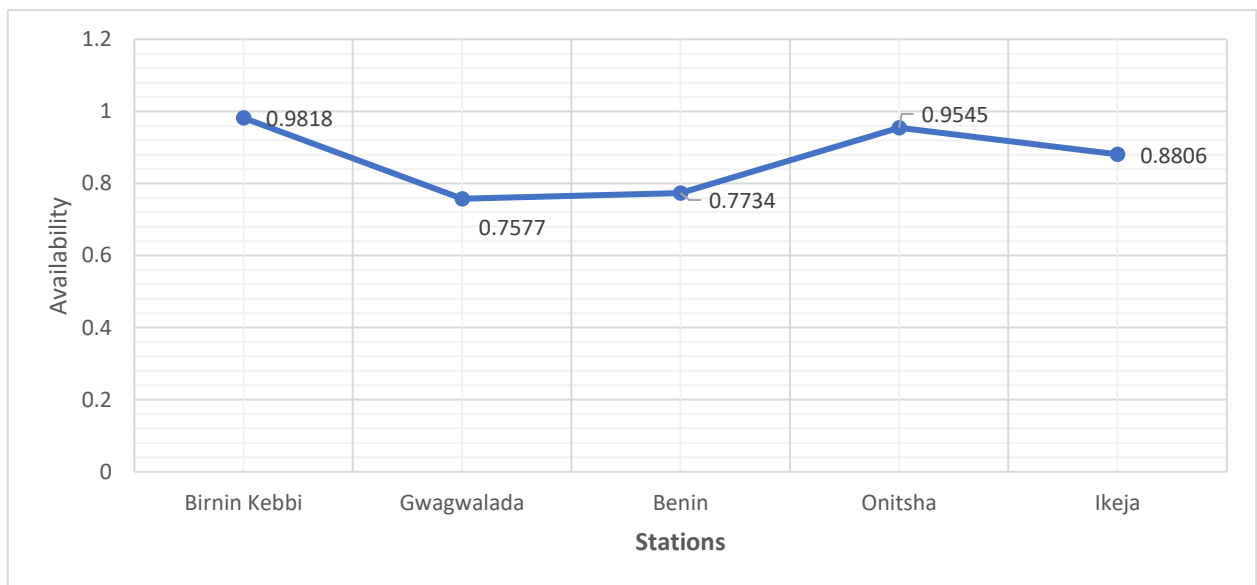
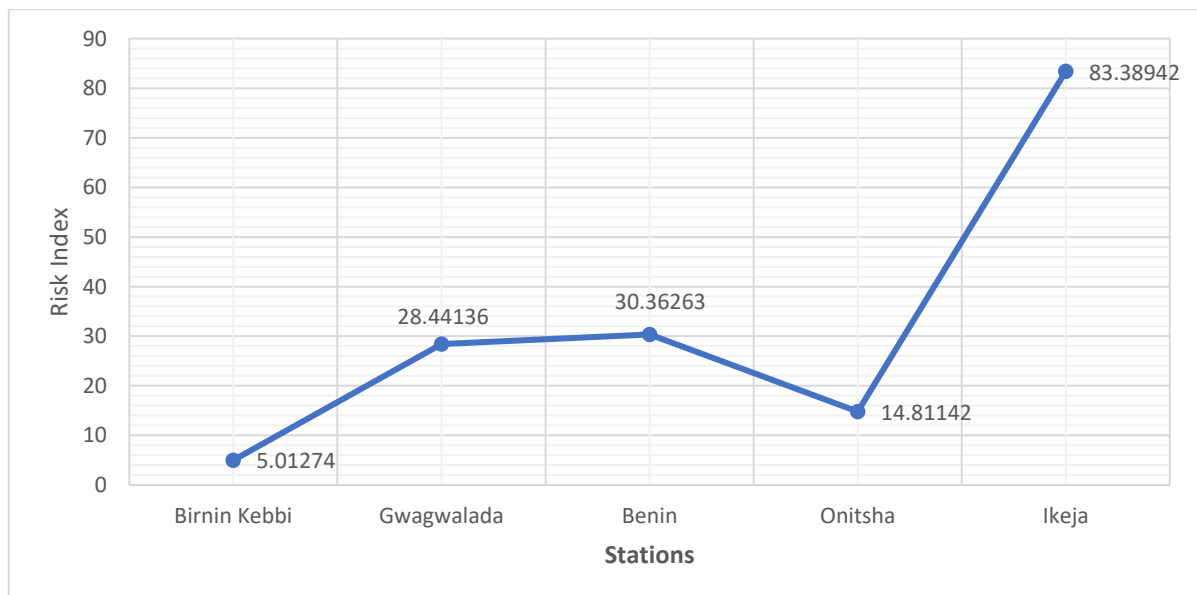**Figure 5:** Availability of Selected Power System Network in Nigeria

Figure 6: Risk Index of Selected Power System Network in Nigeria

The Nigerian Society of Engineers
Minna Branch
1st NSE Minna Branch National Conference 2021

Conference theme
Role of Engineering in
Sustainable Development Goals

The results of the analysis of the selected power stations indicates that Gwagwalada Transmission Station has the least availability. This can be attributed to the high downtime recorded by the station and the least repair rate of 0.22. The less available of the Gwagwalada transmission station can also be linked to the least severity of failure of the station, hence, less attention is given to it compared to other stations.

Further analysis of the results shows that though Ikeja Transmission Station has moderate failure rate (3.8%) and high reliability of 88.06%, the risk index of the transmission station is very high in comparison to other transmission station.

4   CONCLUSION

This study was carried out for the risk assessment of electrical power system network in Nigeria. Five transmission stations were used for this study, as the generating stations and distribution system in the country is considered fairly stable over the transmission station. From the analysis of the results obtained, it was discovered that Birnin Kebbi Transmission Station has the highest reliability of 98%. The high reliability of Birnin Kebbi Transmission Station is linked to its high availability (98% availability) due to its least number of outages and downtime.

Gwagwalada Transmission Station has the least reliability of 75% and this is linked to its least availability among the selected transmission power stations. Though Gwagwalada Transmission Station did not record the highest number of outages, it recorded the highest number of downtime and least repair rate. This suggests that the transmission station receives less attention for repair when compared to other transmission stations selected in this study irrespective of the fact that it supplies the Nigeria seat of power, Federal Capital Territory.

It was also found in the study that Ikeja Transmission Station has the highest risk index of 83.39. This shows that failure of the transmission station will have the highest impact on the economy of the country. This is largely due to the power delivered by the transmission station and the number of consumers the station serves.

5   RECOMMENDATION

Based on the findings of this study, it is recommended that:

i.   Proactive measures should be put in place to reduce the down time of Ikeja Transmission Station as failure of the transmission has the greatest impact in our country.

ii.   Benin and Gwagwalada Transmission stations should be adequately maintained to decrees the failure rate and down time of the transmission stations as the rate of failure of the two stations are high compared to other stations.

iii.   Equipment in Benin and Gwagwalada Transmission stations should be overhauled as the reported mean time between failures of the two stations are low, indicating frequent failure and down time for the stations while attention should also be given to the two stations to increase their availability to consumers.

iv.   Because Ikeja supplies enormous power and the probability of failure of the station is high as well as the risk index, the equipment used for power transmission should be made adequate to forestall imminent failure, resulting to high risk.

REFERENCES

Rausand M (2013). "Chapter 1: Introduction". Risk Assessment: Theory, Methods, and Applications. John Wiley & Sons. pp. 1–28.

Masood, S, (2021). "Much of Pakistan Loses Power in Massive Blackout". The New York Times.

Brian, K. S. and Nauren S. M. (2021). "5 Million Americans Have Lost Power from Texas to North Dakota After Devastating Winter Storm"

Aliyu, A., Ramli, A., Saleh, M. (2013). Nigeria electricity crisis: Power generation capacity expansion and environmental ramifications. Energy, 61(8), 354-367

Awosope, C.A (2014) "Nigeria Electricity Industry: Issues, Challenges and solutions". Public lecture Series Vol. 3, No. 2.

Airoboman, A.E. Ibhaze, A.E, Amaize, P.A and Okakwu, I.K (2016) "Restructuring the Electrical Power Sector for Sustainable Development" (CU-ICADI) International

Conference on African Development Issues May 9–11 2016, Ota, Nigeria. pp.1-4

Guo, L., Qiu, Q., and Liu, J. (2014). Power transmission risk assessment considering component condition. J. Mod. Power Syst. Clean Energy 2, 50–58

Onohaebi, S. O. (2017) Power Transmission constraints and faults analysis in Nigeria Power System

Raza, M. (2019). System Reliability and Availability Calculations. https://blogs.bmc.com/system-reliability-availability-calculations/?print=pdf

Morteza, A., Habib, R. and Yaser, D. (2014). "Reliability-Centered maintenance for circuit breakers in transmission networks" IET Generation, Transmission & Distribution. pp. 1583-1590.

Asibeluo, U. N. and Madueme, T. C. (2018): Risk-Based Security Assessment of Power System Voltage Drop: A Case Study of Nigerian 330kv 41-Bus Transmission Grid. Nigerian Journal of Technology (NIJOTECH) Vol. 37, No. 3, July 2018, pp. 735 – 741

Rosencrance, L. (2020). risk analysis. Accessed on 15th March, 2021 from https://searchsecurity.techtarget.com/definition/risk-analysis?amp=1

Non-linear Scaling in Global Optimisation. Part II: Performance Evaluation

[1, 2]*Abubakar, H. A., [2, 3]Misener, R. and [2]Adjiman, C. S.
[1]Department of Chemical Engineering, Ahmadu Bello University, Zaria
[2]Department of Chemical Engineering, Imperial College London
[3]Department of Computing, Imperial College London
*Corresponding Author: abuabib2006@gmail.com

ABSTRACT

Numerous real-life engineering problems that arise in many areas of applications such as process synthesis, molecular products design, scheduling and planning of batch processes, among others, are non-linear and can be solved to guarantee global optimum using global optimisation solvers. However, these solvers sometimes develop numerical instability when solving problems that are badly scaled resulting in either no solution, infeasible solution or a solution that is not the global optimum. One of the approaches of preventing such numerical instability is scaling. In this study, we examined the impact of a scaling algorithm that accounts for nonlinearity in a problem on the performance of three global optimisation solvers, SCIP, BARON and ANTIGONE using two real life global optimisation test problems. The original and transformed forms of the test problems, whose solutions are known a priori, are scaled using the scaling code implemented and validated in the part I of this paper. The scaled and unscaled versions of the original and transformed problems are solved in GAMS using the aforementioned global optimisation solvers and the solution analysed under four performance criteria. For the test problems considered, the implemented algorithm demonstrates its effectiveness in preventing the global optimisation solvers from developing numerical instability when solving extremely badly-scaled forms of the problems and is therefore recommended for large scale global optimisations applications.

KEYWORDS: Scaling, Nonlinear, Global Optimisation, Instability, NLP.

1   INTRODUCTION

A great number of scientific or industrial problems encountered in practice involve selecting the best among different alternative decisions. These problems can be formulated as an optimisation problem and are generally nonlinear and nonconvex (Adjiman et al., 2021; Adjiman et al, 1998a; Grant et al., 2018; Niebling and Eichfelder, 2019). Their nonconvex nature add complexity to the problems as they possess two or more local optimal solutions, and choosing the global optimum is not trivial (Boukouvala et al., 2016; Ryoo and Sahinidis, 1995; Sahinidis, 2019; Tawarmalani and Sahinidis, 2004). However, global optimisation strategy can effectively handle this type of problem.

Many important classes of problem demand the use of global optimisation method. Typical examples are nonconvex continuous, mixed-integer, bilevel, differential-algebraic, and non-factorable problems (Floudas and Gounaris, 2008; Li and Yang, 2021). For these problems, a number of solvers have been developed to solve them to guarantee global optimum. Commonly used deterministic global optimisation solvers include Solving Constraint

Integer Programs (SCIP) of Bussieck and Vigerske (2012), Branch-and-Reduce Optimisation Navigator (BARON) of Sahinidis (1996), Convex Over and Under ENvelopes for Nonlinear Estimation (COUENNE) of Belloti et al (2009) and Algorithms for coNTinuous / Integer Global Optimisation of Nonlinear Equations (ANTIGONE) of Misener and Floudas (2013), among many others.

Despite the advancement in global optimisation theory and the numerous numbers of solvers available, some problems are known to be difficult to solve numerically and are common in many application areas, such as waste minimization and treatment, phase and chemical equilibrium, and controller design. These problems inherently operate on many numerical scales, hence could be termed badly scaled problems.

One of the approaches of tackling the challenges that solvers encounter when solving badly scaled non-linear problems is scaling. However, the state-of-the-art approaches of solving a badly scaled problem either disregard the inherent disparity in the numerical scales of the problem or does not take into consideration the nonlinearity in the problem. Ignoring the disparity in the

numerical scales by not scaling generates numerical instability that often results in a solution that is not global optimum. On the other hand, neglecting the non-linearity in the problem by applying linear scaling many a time results in a solution that is infeasible to the original problem.

Other alternative approaches of preventing the numerical difficulties that come from the solution of these problems, such as extended precision (Chapra and Canale, 2010) and interval arithmetic (Zilinskas and Zilinskas, 2006) are computationally demanding, thereby may not be reasonable when compared to scaling.

Scaling involves the modification of the coefficients matrix that characterise a system in such a way that extreme variations that could lead to numerical instabilities during computations is eliminated (Morgan, 1987). By scaling, the variables and equations in a given problem are modified using variable and equation/constraint scaling factors, respectively, in such a manner that the variables become similar in their order of magnitudes and the equations become well conditioned relative to the variable's perturbation and well balanced relative to one another.

Scaling ensures that the approaches employ in determining and verifying the feasible points of constraint satisfaction problems do not develop numerical challenges (Domes, 2009). The same benefit is obtainable in constrained optimisation problems since the former are also optimisation problems with no given or constant objective function. Domes and Neumaier (2011) showed how scaling can be helpful in the calculation of interval hull of an ill conditioned strictly convex quadratic constraint by directed Cholesky factorization. It was demonstrated that by scaling of the constraint symmetric matrix, the condition number of the matrix decreased by six orders of magnitude.

Linear systems scaling is a well-researched topic in the literature and many scaling techniques and routines have been developed and implemented in linear optimisation solvers (Elble and Sahinidis, 2012). In solving linear optimization problems, scaling is widely used to reduce the condition number of the constraint matrix (Ploskas and Samaras, 2013). It may decrease the computational effort in arriving at a solution and possibly improve the numerical behaviour of the solver used (Elble and Sahinidis, 2012).

A major issue in nonlinear systems involving multivariable polynomials is the occurrence of variables of that operates on widely different numerical scales, which can have negative impacts on the results of solving the systems (Domes and Neumaier, 2008). Unlike in linear systems, there are limited studies that have been carried out on scaling nonlinear systems. For scaling of polynomial systems, the few studies in the literature were carried out by Watson et al (1985), Morgan (1987) and Domes and Neumaier (2008). In Domes and Neumaier (2008), a scaling algorithm, linear programing (SCALELP)

algorithms, for scaling polynomial systems was presented. The algorithm was demonstrated, using some examples, to be very stable for problems where previously known nonlinear scalling algorithms performed poorly and are therefore recommended to be suitable for general purpose scaling. In this study, we assessed the impact of a scaling algorithm implemented and validated in part I of this paper on the performance of SCIP, BARON and ANTIGONE by solving two test problems in process design under four criteria. These criteria are the CPU time taken in arriving at solution, number of iterations carried out in reaching the solution, number of nodes explored and the quality of solutions.

2   PROBLEM DESCRIPTIONS

Following the validation of the suitability of the scaling technique for optimisation problems containing signomial and polynomial functions (see part I of this paper), the performance of the validated scaling techniques is assessed using practical global optimisation problems that contain these functions. The following two test problems in geometric programming are considered.

2.1   TEST PROBLEM 1:   ALKYLATION PROCESS DESIGN

The goal in this optimisation problem is to find the optimal operating conditions that is required to maximise a profit function in an alkylation process, shown in Figure 2.1. The model for this process was originally formulated by Bracken and McCormick (1968) and then reformulated in Dembo (1976) as a signomial problem. The reformulated model is available in Floudas et al (1999) as a test problem. In this study, we reintroduced the equality constraints and the variables eliminated from the original model during the reformulation process, and then transformed the model into a form that is suitable for the scaling code (see (2.4) in part I of the paper).
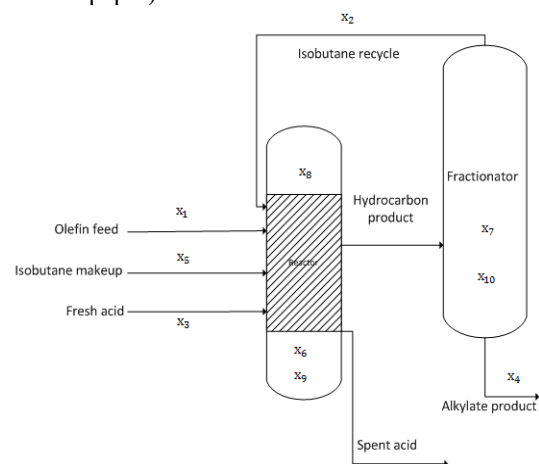

Figure 2.1: Alkylation process optimisation

Conference theme

Role of Engineering in Sustainable Development Goals

Cost parameters

$$\begin{bmatrix} \text{Alkylate product value} := \$0.063 \text{ per octane. barrel} \\ \text{Olefin feed cost: } \$5.04 \text{ per barrel} \\ \text{Isobutane recycle costs} := \$ 0.035 \text{ per barrel} \\ \text{Acid addition cost} := \$10.00 \text{ per thousand pounds} \\ \text{Isobutane makeup cost} := \$ 3.36 \text{ per barrel} \end{bmatrix}$$

Process variables

$$\begin{bmatrix} x_1: \text{Olefin feed (barrel per day)} \\ x_2: \text{Isobutane recycle (barrel per day)} \\ x_3: \text{Acid addition rate (thousands of pounds per day)} \\ x_4: \text{Alkylate yield (barrel per day)} \\ x_5: \text{Isobutane makeup (barrel per day)} \\ x_6: \text{Acid strength (wt\%)} \\ x_7: \text{Octane number} \\ x_8: \text{External isobutane} - \text{to} - \text{olefin ratio} \\ x_9: \text{Acid dilution factor} \\ x_{10}: \text{F} - 4 \text{ performance number} \end{bmatrix}$$

Optimisation problem

Objective

profit per day maximisation

$$\min \ objv = \left(\underbrace{10x_3}_{\substack{\text{Acid} \\ \text{addition} \\ \text{cost}}} + \underbrace{5.04x_1}_{\substack{\text{Olefin} \\ \text{feed} \\ \text{cost}}} + \underbrace{0.035x_2}_{\substack{\text{Isobutane} \\ \text{recycle} \\ \text{cost}}} + \underbrace{3.36x_5}_{\substack{\text{Isobutane} \\ \text{make up} \\ \text{cost}}} + \underbrace{3000}_{\substack{\text{fixed} \\ \text{cost}}} \right) - \underbrace{0.063x_4x_7}_{\substack{\text{Alkylate} \\ \text{Value}}}$$

$$\underbrace{\hspace{8cm}}_{\text{Total cost}}$$

Subject to

Mathematical model

Alkylate yield
$$\begin{bmatrix} 0.0059553571x_8{}^2 + 0.88392857x_4x_1{}^{-1} - 0.1175625x_8 \leq 1 \\ 1.1088x_1x_4{}^{-1} + 0.1303533x_1x_4{}^{-1}x_8 - 0.0066033x_1x_8{}^2x_4{}^{-1} \leq 1 \end{bmatrix}$$

Octane number
$$\begin{bmatrix} 0.00066173269x_8{}^2 - 0.019120592x_8 - 0.0056595559x_6 + 0.017239878x_7 \leq 1 \\ 56.85075x_7{}^{-1} + 1.08702x_8x_7{}^{-1} + 0.32175x_6x_7{}^{-1} - 0.03762x_8{}^2x_7{}^{-1} \leq 1 \end{bmatrix}$$

Acid dilution factor
$$\begin{bmatrix} 2462.3121x_3x_4{}^{-1}x_6{}^{-1} - 25.125634x_3x_4{}^{-1} + 0.006198x_{10} \leq 1 \\ 161.18996x_{10}{}^{-1} + 5000x_3x_4{}^{-1}x_{10}{}^{-1} - 489510x_3x_4{}^{-1}x_6{}^{-1}x_{10}{}^{-1} \leq 1 \end{bmatrix}$$

F4 performance number
$$\begin{bmatrix} 44.333333x_7{}^{-1} + 0.33x_{10}x_7{}^{-1} \leq 1 \\ 0.022255x_7 - 0.00759474x_{10} \leq 1 \end{bmatrix}$$

External isobutane to olefin ratio
$$\begin{bmatrix} x_1x_8x_2{}^{-1} - x_5x_2{}^{-1} = 1 \end{bmatrix}$$

Isobutane makeup
$$[0.819672131x_1x_4{}^{-1} + 0.819672131x_5x_4{}^{-1} = 1$$

Bounds

Acid strength
$$\begin{bmatrix} 98000x_3x_4{}^{-1}x_6{}^{-1}x_9{}^{-1} - 1000x_3x_4{}^{-1}x_9{}^{-1} = 1 \end{bmatrix}$$

Variable bounds

$$\begin{bmatrix} 1500 \le x_1 \le 2000 \\ 1 \le x_2 \le 16000 \\ 1 \le x_3 \le 120 \\ 3000 \le x_4 \le 3500 \\ 1 \le x_5 \le 2000 \\ 85 \le x_6 \le 93 \\ 90 \le x_7 \le 95 \\ 3 \le x_8 \le 12 \\ 1.2 \le x_9 \le 3.6 \\ 145 \le x_{10} \le 162 \end{bmatrix}$$

2.2 TEST PROBLEM 2: OPTIMAL REACTOR DESIGN

The goal is to determine the optimal operating conditions to maximise profit from a steady enzymatic reaction process operating at fixed feed flow rate in two continuous stirred tank reactors arranged in series, see Figure 2.2. This entails determining the holding time and the temperature for each reactor that maximised the final conversion of the substrate (SS) to product (δ). The higher the conversion of SS, the more the yield of δ, and the greater is the total profit. The model for this process was formulated as a geometric programming problem in Rijckaert (1973). The model, available as a test problem in Dembo (1976) and Floudas et al (1999), is presented here.

Rate expression $\left[rr = \dfrac{\theta_2(T) C_{EE0} C_{SS}}{\theta_{mk}(T) + a C_{SS}} \right.$

With
$$\begin{cases} \theta_2(T) = 1.7.\,10^{13} e^{\frac{-1830}{RT}} \\ \theta_{mk}(T) = 4e^{\frac{-3240}{RT}} + 2e^{\frac{-830}{RT}} \\ a = 0.1 \\ C_{EE0} = 10^{-13} \text{mol/l} \\ C_0 = 10 \text{mol/l} \end{cases}$$

Optimisation problem

Objective

Reactor cost $:= 0.4$ per (holdup time)$^{0.67}$. cost of pro

Where $T, \theta, C_{SS}, C_{EE0}$ and C_0 denote reactor temperature, reaction rate constants, outlet substrate concentration, total enzyme concentration and feed concentration, respectively.
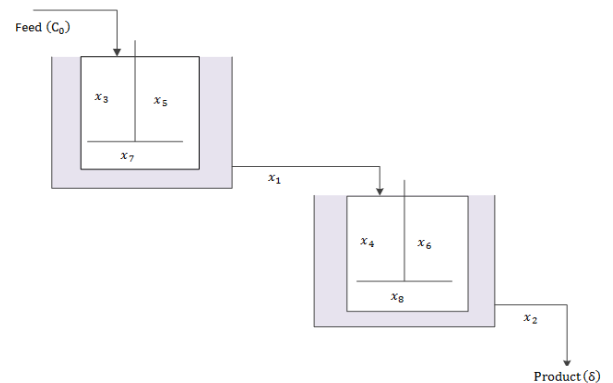

Figure 2.2: An enzymatic reaction process in a CSTR cascade

Process variables

$$\begin{bmatrix} x_1 \text{: Concentration of } \delta \text{ in reactor } 1 \text{(mol/L)} \\ x_2 \text{: Concentration of } \delta \text{ in reactor } 2 \text{ (mol/L)} \\ x_3 \text{: Exponential function of T in reactor } 1(-) \\ x_4 \text{: Exponential function of T in reactor } 2(-) \\ x_5 \text{: denominator of reaction rate in reactor } 1 \text{ (mol/L. s)} \\ x_6 \text{: denominator of reaction rate in reactor } 2 \text{ (mol/L. s)} \\ x_7 \text{: reaction rate in reactor } 1 \text{ (mol/L. s)} \\ x_8 \text{: reaction rate in reactor } 2 \text{ (mol/L)} \end{bmatrix}$$

Profit per unit cost of product maximisation

$$\min \text{ objv} = - \left[\underbrace{(x_1 + x_2)}_{\substack{\text{Product} \\ \text{value per} \\ \text{unit cost}}} - \underbrace{\left(\underbrace{0.4 \left(\frac{x_1}{x_7}\right)^{0.67}}_{\substack{\text{cost of} \\ \text{reactor 1}}} + \underbrace{0.4 \left(\frac{x_2}{x_8}\right)^{0.67}}_{\substack{\text{cost of} \\ \text{reactor 2}}} + \underbrace{10}_{\substack{\text{fixed} \\ \text{cost}}} \right)}_{\text{Total cost per unit cost of product}} \right]$$

Subject to:

Mathematical model

$$\text{Reaction rate} \begin{bmatrix} 0.0588x_5x_7 + 0.1x_1 \leq 1\} \text{ reactor 1} \\ 0.0588x_6x_8 + 0.1x_1 + 0.1x_2 \leq 1\}\text{reactor 2} \end{bmatrix}$$

$$\begin{matrix} \text{Denominator of} \\ \text{reaction rate} \end{matrix} \begin{bmatrix} 4x_3x_5^{-1} + 2x_3^{-0.71}x_5^{-1} + 0.0588x_7x_3^{-1.3} \leq 1\} \text{ reactor 1} \\ 4x_4x_6^{-1} + 2x_4^{-0.71}x_6^{-1} + 0.0588x_8x_4^{1.3} \leq 1\} \quad \text{reactor 2} \end{bmatrix}$$

$$\begin{matrix} \text{variable} \\ \text{bounds} \end{matrix} [0.1 \leq x_i \leq 10 \quad \forall\, i \in \{1 \ldots\ldots.8\}$$

3   RESULTS AND DISCUSSION

The impact of the nonlinear scaling code, validated in part I of the paper, on the performance of global optimisation solvers is analysed using a two-stage approach. First, the scaled and unscaled versions of original test problem described in section 2.0 are solved in GAMS as shown in Figure 3.1. In the second stage, the original problems are transformed such that the problems become extremely badly scaled, and the unscaled and scaled forms of the resulting problems solved. Global optimisations solvers, SCIP, BARON and ANTIGONE are utilised for solving the problems and the solutions compared under four performance measures: numerical value or quality of the solutions, CPU time, iteration number and number of nodes explored. Details of the statistics of the test problems are shown in Table 3.1.

3.1 ORIGINAL TEST PROBLEMS

Tables 3.2-3.3 show optimisation results for the test problems under the four performance measures aforementioned.   For a given test problem, we determined if the solution quality has changed by computing the percentage deviation between the scaled and unscaled solution value of the variables. If at least one of the variables deviations is greater than 10%, the solution is considered to have unchanged. For the CPU time, iteration number and number of nodes explored, they are considered to have changed when the change in their values is at least an order of magnitude.

From the results presented in Tables 3.2 and 3.3, it is seen that in both test problems, there is no change in the solution values of the variables. The solvers all arrived at the same solution before and after scaling. Hence, scaling has no impact on the solution quality. For the other three performance criteria, the impact of scaling, though negligibly small, is dependent on the solvers. While

ANTIGONE showed no improvement, scaling has impact on the performance of SCIP and BARON. For SCIP, significant reduction in the number of nodes explored before a solution is found is noticeable. Similarly, for BARON, improvement is observed in the number of iterations carried out before solution is found, particularly in test problem 1.
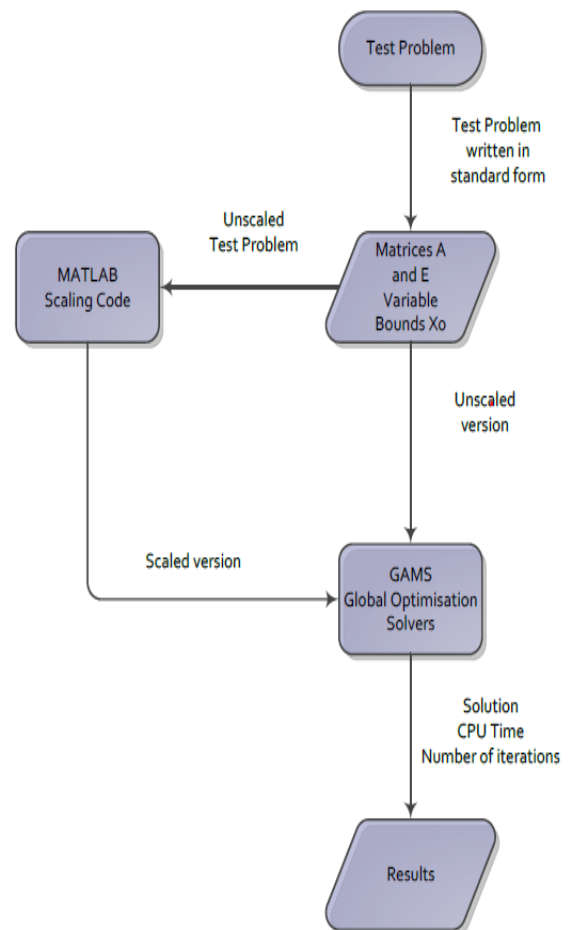

Figure 3.1: Performance measure assessment procedure.

TABLE 3.1: STATISTICS OF THE TEST CASES

Test Problems	No. of Variables	No. of Equations	No. of Terms (Number of nonlinear terms)	No. non-zero entries
1	8	15	29 (20)	59
2	9	5	20 (10)	21

Conference theme
Role of Engineering in Sustainable Development Goals

TABLE 3.2: OPTIMISATION RESULTS FOR THE SCALED AND UNSCALED VERSIONS OF TEST PROBLEM 1

Measures	Solvers					
	ANTIGONE		BARON		SCIP	
	unscaled	scaled	unscaled	scaled	unscaled	scaled
Solution						
x_1	1698.18	1698.18	1698.18	1698.18	1698.18	1698.18
x_2	15829.86	15829.86	15829.86	15829.86	15829.86	15829.85
x_3	53.67	53.67	53.67	53.67	53.67	53.67
x_4	3031.30	3031.30	3031.30	3031.30	3031.30	3031.30
x_5	2000.00	2000.00	2000.00	2000.00	2000.00	2000.00
x_6	90.11	90.11	90.11	90.11	90.11	90.11
x_7	95.00	95.00	95.00	95.00	95.00	95.00
x_8	10.50	10.50	10.50	10.50	10.50	10.50
x_9	1.55	1.55	1.55	1.55	1.55	1.55
x_{10}	153.54	153.54	153.54	153.54	153.54	153.54
$objv$	1227.23	1227.23	1227.23	1227.23	1227.23	1227.22
CPU time(s)	0.10	0.10	1000.00	0.13	0.61	0.24
No. of iterations	4	4	322056	1	2379.00	1812
No. of node explored	0	0	1	0	940	71

TABLE 3.3: OPTIMISATION RESULTS FOR THE SCALED AND UNSCALED VERSIONS OF TEST PROBLEM 2

Measures	Solvers					
	ANTIGONE		BARON		SCIP	
	unscaled	scaled	unscaled	scaled	unscaled	scaled
Solution						
x_1	6.3458	6.3458	6.3458	6.3458	6.3458	6.3458
x_2	2.3410	2.3410	2.3410	2.3410	2.3410	2.3410
x_3	0.6709	0.6709	0.6709	0.6709	0.6709	0.6709
x_4	0.5347	0.5347	0.5347	0.5347	0.5347	0.5347
x_5	5.9528	5.9528	5.9528	5.9528	5.9528	5.9528
x_6	5.3164	5.3164	5.3164	5.3164	5.3164	5.3164
x_7	1.0440	1.0440	1.0440	1.0440	1.0440	1.0440
x_8	0.4201	0.4201	0.4201	0.4201	0.4201	0.4201
$objv$	3.9180	3.9180	3.9180	3.9180	3.9180	3.9180
CPU time(s)	0.4610	0.5410	0.9800	0.4100	1.9800	0.9600
No. iterations	4	4	25	3	26551	10968
No. nodes	3	3	1	1	1431	758

The Nigerian Society of Engineers
Minna Branch
1st NSE Minna Branch National Conference 2021

Conference theme
Role of Engineering in
Sustainable Development Goals

3.1 TRANSFORMED TEST PROBLEMS

Test problems in section 2 are transformed into their badly scaled forms by modifying the units of the variables in such a way that they become widely different in their order of magnitudes. For the two test problems, identified variables with units are transformed into new units to get a scaling factor SF that was used to scale the variables. Essentially, (3.1) is used to substitute for old variables x in terms of the new variables x*. Table 3.4 shows the variables that are transformed in the test problems and their corresponding scaling factor.

Tables 3.5 and 3.6 represent the results of the numerical investigation performed on the modified test problems. The results confirmed the implemented and validated scaling technique to be invaluable for global optimisation solvers when solving extremely badly scaled problems as all the solvers developed numerical instability before scaling. The instability results in no solution reported as seen in the results of all the solvers for the two test problems. However, with the problems scaled prior to being solved, the three solvers obtained the same solution as in the original test problems in about the same iteration number, CPU time and number of nodes explored (see Tables 3.2 and 3.3).

$$x = SF\ x^* \qquad (3.1)$$

Table 3.4: Scaling factors for the transformed variables.

Test problem 1		Test problem 2	
x	SF	x	SF
x_1	$1.16 \cdot 10^{-8}$	x_1	$1.00 \cdot 10^6$
x_2	$1.59 \cdot 10^5$	x_2	1.00
x_3	1000.00	x_5	1.00
x_4	$1.59 \cdot 10^5$	x_6	1.00
x_5	$1.16 \cdot 10^{-8}$	x_7	$1.67 \cdot 10^{-11}$
$objv$	$1.16 \cdot 10^{-8}$	x_8	$6.00 \cdot 10^7$

TABLE 3.5: OPTIMISATION RESULTS FOR THE SCALED AND UNSCALED VERSIONS OF BADLY SCALED TEST PROBLEM 1.

Measures	Solvers					
	ANTIGONE		BARON		SCIP	
	unscaled	scaled	unscaled	scaled	unscaled	scaled
Solution						
x_1	1759.72	1698.18	0.00	1698.18	0.00	1698.18
x_2	16000.00	15829.86	0.00	15829.86	0.00	15829.85
x_3	56.59	53.67	0.00	53.67	0.00	53.67
x_4	3081.74	3031.30	0.00	3031.30	0.00	3031.30
x_5	2000.00	2000.00	0.00	2000.00	0.00	2000.00
x_6	90.37	90.11	0.00	90.11	0.00	90.11
x_7	95.00	95.00	0.00	95.00	0.00	95.00
x_8	10.23	10.50	0.00	10.50	0.00	10.50
x_9	1.55	1.55	0.00	1.55	0.00	1.55
x_{10}	153.54	153.54	0.00	153.54	0.00	153.54
$objv$	-2377.23	1227.23	0.00	1227.23	0.00	1227.22
CPU time(s)	0.11	0.12	0.13	0.14	0.01	0.62
No. of iterations	NA	5	NA	1	0.00	8595
No. of node	0	0	0	1	0	291

The Nigerian Society of Engineers
Minna Branch
1st NSE Minna Branch National Conference 2021

Conference theme
Role of Engineering in
Sustainable Development Goals

TABLE 3.6: OPTIMISATION RESULTS FOR THE SCALED AND UNSCALED VERSIONS OF BADLY SCALED TEST PROBLEM 2.

Measures	Solvers					
	ANTIGONE		BARON		SCIP	
	unscaled	scaled	unscaled	scaled	unscaled	scaled
Solution						
x_1	0.0000	6.3458	0.0000	6.3458	0.0000	6.3458
x_2	0.0000	2.3410	0.0000	2.3410	0.0000	2.3410
x_3	0.0000	0.6709	0.0000	0.6709	0.0000	0.6709
x_4	0.0000	0.5347	0.0000	0.5347	0.0000	0.5347
x_5	0.0000	5.9528	0.0000	5.9528	0.0000	5.9528
x_6	0.0000	5.3164	0.0000	5.3164	0.0000	5.3164
x_7	0.0000	1.0440	0.0000	1.0440	0.0000	1.0440
x_8	0.0000	0.4201	0.0000	0.4201	0.0000	0.4201
$objv$	0.0000	3.9180	0.0000	3.9180	0.0000	3.9180
CPU time(s)	0.0000	0.4710	0.0100	0.3900	0.0100	0.8000
No. iterations	NA	4	NA	3	0	9063
No. nodes	0	3	0	1	0	594

4   CONCLUSION

The impact of nonlinear scaling algorithm, implemented in the part I of this paper, on the performance of ANTIGONE, BARON and SCIP was analysed using two real life global optimisation problems in the area of process design. The scaling code proved very effective in preventing the solvers in running into numerical problem when solving the badly scaled forms of the problems. For problems that are not obviously badly scaled to the extent that the solvers may developed instability problem, as was the case of the original test problems, the scaling technique shows potential to help a solver reduce CPU time, number of iterations and nodes explored in arriving at solution. It is therefore highly recommended for large scale global

REFERENCES

Adjiman, C.S., Dallwig, S., Floudas, C.A. and Neumaier, A. (1998). A global optimisation method, αBB, for general twice-differentiable constrained NLPs–I: Theoretical advances. Comput. Chem. Eng. 22, 1137-1158

Adjiman, C. S., Sahinidis, N. V., Vlachos, D. G., Bakshi, B., Maravelias, C. T. and Georgakis, C. (2021). Process Systems Engineering Perspective on the Design of Materials and Molecules. I*nd. Eng. Chem. Res.* 60, 14, 5194–5206

Bracken, J. and McCormick, G. P. (1968). Selected Applications of Nonlinear Programming, Wiley, New York.

Boukouvala, F., Misener, R. and Floudas, C.A (2016). Global optimization advances in Mixed-Integer Nonlinear Programming, MINLP, and Constrained Derivative-Free Optimization, CDFO. *European Journal of Operational Research*, 252 (3).

Bussieck, M. R. and Vigerske, S. (2012). MINLP Solver Software. In J. J. Cochran, L. A. Cox, P. Keskinocak, J. P. Kharoufeh, and J. C. Smith, editors, Wiley *Encyclopedia of Operations Research and Management Science*. John Wiley & Sons, Inc.

Chapra, S.C. and Canale, R.P. (2010). Numerical Methods for Engineers, 6th ed., international ed., McGraw-Hill Higher Education, Boston, London.

Dembo, R. S. (1976). A Set of Geometric Programming Test Problems and Their Solutions. *Math. Prog.* 10, 192-213

Domes, F.: GloptLab (2009). A Configurable Framework for the Rigorous Global Solution of Quadratic Constraint Satisfaction Problems. *Optim. Methods Softw*. 24, 727–747

Domes, F. and Neumaier, A. (2008). A Scaling Algorithm for Polynomial Constraint Satisfaction Problems. *J. Glob. Optim*., 42:327–345

Domes, F. and Neumaier, A. (2011). Rigorous Enclosures of Ellipsoids and Directed Cholesky Factorization, *SIAM J. Matrix Anal. Appl*. 32, 262–285

Elble, J. M. and Sahinidis, N.V. (2012). Scaling Linear Optimisation Problems Prior To

Application of the Simplex Method, *Comput Optim Appl.*, 52, 345–371

Floudas, C.A. and Gounaris, C.E. (2008). A Review of Recent Advances in Global Optimisation. *J. Glob. Optim*. 45, 3–38

Floudas, C.A., Pardalos, P.M., Adjiman, C.S., Esposito, W.R., Gumus, Z.H., Harding, S.T., Klepeis, J.L., Meyer, C.A., and Schweiger, C.A. (1999). Handbook of Test Problems in Local and Global Optimisation, Kluwer Academic Publishers, Dordrecht

Grant, E., Pan, Y., Richardson, J., Martinelli, J. R., Armstrong, A., Galindo, A. and Adjiman, C. S. (2018). Multi-objective computer-aided solvent design for selectivity and rate in reactions. *Computer Aided Chemical Engineering*. 44, 2437-2442

Li, G. and Yang, X. (2021). Convexification Method for Bilevel Programs with a Nonconvex Follower's Problem. *Journal of Optimization Theory and Applications*, 188, pg. 724–743

Misener, R. and Floudas, C. A. (2013): ANTIGONE :http://www.gams.com/dd/docs/solvers/antigone , version 1.0

Morgan, A. (2009). Solving Polynomial Systems Using Continuation for Engineering and Scientific Problems, Society for Industrial and Applied Mathematics, Philadelphia, Prentice-Hall, chapter 5, 107-119

Niebling, J., Eichfelder, G. (2019). A branch-and-bound-based algorithm for nonconvex multiobjective optimization. *SIAM J. Optim*. **29**(1), 794–821

Ploskas, N. and Samaras, N. (2013). The Impact of Scaling on Simplex Type Algorithms, ACM digital Library

Rijckaert, M.J. (1973). Engineering Applications of Geometric Programming", in: Avriel, M. Rijckaert, M.J. and Wilde, D.J., eds., *Optimization and Design*, Prentice-Hall, Eaglewood Cliffs, New Jersey, 196-220

Ryoo, H. S. and Sahinidi, N. V. (1995). Global Optimisation of Nonconvex NLPs and MINLPs With Applications in Process Design, *Computers chem. Engng*, 19, 551-566

Sahinidi, N. V. (1996). BARON: A General-Purpose Global Optimisation Software Package, *Journal of Global Optimisation*, 8, 201-205

Sahinidis, N. V (2019). Mixed-integer nonlinear programming 2018. *Optimization and Engineering* (2019) 20:301–306

Tawarmalani, M. and Sahinidis, N.V. (2004). Global Optimisation of Mixed-Integer Nonlinear Programs: A Theoretical and Computational Study. Mathematical Programming, 99, 563-591.

Watson, L.T., Billups, L.C. and Morgan, A.P. (1985). HOMPACK: A Suite of Codes for Globally Convergent Homotopy Algorithms. http://deepblue.lib.umich.edu/bitstream/handle/ 2027.42/8204/ban6930.0001.001.pdf:jsessionid =4845D7244E05308ECF4988DCEBD9BEC8?s equence=5

Zilinskas, A. and Zilinskas, J. (2006). On efficiency of tightening bounds in interval global optimization, Lecture Notes in Computer Science 3732: 197–205.

A Review of Different Proposed Image Detection Techniques for Road Anomalies Detection.

A. M. Oyinbo[1], A. S. Mohammad[2], S. Zubair[3], and E. MICHAEL[4]

[1,2,3,4] Department of Telecommunication Engineering,
Federal University of Technology Minna – Nigeria.

[1]oyinbo.pg822514@st.futminna.edu.ng, [2]abu.sadiq@futminna.edu.ng, [3]zubairman@futmina.edu.ng,
[4]electmike84@gmail.com

ABSTRACT

Road anomalies such as, potholes, speed bumps and cracks have been one of the major problems faced by road users globally, contributing to vehicular accidents on roads, quick wear and tear of vehicles, among others. Overtime, advancement in vehicular technology and sensors, has led to the establishment of automated approach for detecting road anomalies. Though, these approaches can be categorized into 3D reconstruction-based approach, 2D vision-based approach and the vibrational-based approach. These techniques are geared towards enabling vehicles in detecting road anomalies and notifying drivers of such, thereby reducing the rate of accidents on roads caused by these anomalies. Also, these approaches can be incorporated into vehicular Ad-hoc network, where automated vehicles can be able to navigate through road terrains with pothole anomalies. However, the 2D vision-based approach has received wide acceptance among the academia and the industry due to its advantages over the 3D reconstruction-based, such as, lower cost of implementation. Also, it has advantage over the vibrational-based approaches in terms of better detection accuracy. In this regard, this paper presents a mini-survey of various 2D vision-based techniques proposed in the literature for road surface condition monitoring and anomaly detection. The merits and drawbacks of these techniques are highlighted. Furthermore, open research issues are presented. Our effort forms part of a larger goal aimed at improving and developing robust vision-based approaches for road anomaly detection, as well as giving researchers a pathway in similar pursuits.

KEYWORDS: *Anomalies, Detection, Image, Potholes, Road and Cracks.*

1. INTRODUCTION

Road network plays important crucial role in any nation's economy (Aldagheiri, 2009), contributing to its economic growth and development with social benefits. Road networks provides access to employment, social, health and educational services (Fan & Chan-Kang, 2005). Roads open up more areas and stimulate economic and social development. For these reasons, road infrastructure is one of the most important of all public assets (Lemer, 1999). This is attributed to the fact that, it is one of the major means of transportation (Adeniyi, 2012), that allow the vehicular movement of goods, services and human from one location to another. However, it is important to ensure that these roads are in good conditions at all times by continuous monitoring of its surfaces and repairs of areas with anomalies.

Road anomalies on asphalt road occur as a result of the road exceeding their maximum lifespan. The use of poor quality materials for construction, poor drainage system (Onoyan-Usina,2013), excess road traffic and failure to comply with the standard road construction specification (Bello-Salau *et al.,* 2014). These anomalies are usually observed in form of potholes, speed bumps and cracks (Akarsu *et al.*, 2016). The adverse effects of these anomalies on roads cannot be over emphasized, ranging from discomforts experienced by drivers while plying such roads, vehicular damages, road traffic accidents, among others. Though, prevalent among these anomalies in developing nations like Nigeria is the potholes anomalies, which has contributed greatly to the rate of road traffic accident (Ryu *et al.,* 2015).

Pothole has been one of the major problems faced by road users globally, and has been a contributing factor to vehicle accidents on roads, quick wear and tear of vehicles, among others. This is such a serious issue that several organizations and countries always try to show the effect of potholes on the economy at large. For example, the American Automobile Association estimated that about 16 million drivers had suffered damage from potholes in the last five years before the year 2016 within the United States alone (Byun *et al.,* 2018). Britain also made their estimation cost of fixing potholes on their roads to amount

up to 12 billion pounds annually. While India has a record of over 3000 deaths in road accidents caused by potholes on their roads annually (Byun *et al.,* 2018). Nigeria is not left out, Federal Road Safety Corps (FRSC) of Nigeria on January of 2019, estimated that a total of 7,827 persons were involved in road accidents within a month ("540 killed in road crashes in January - FRSC - Premium Times Nigeria," 2019), and some of these accidents can be attributed to the presents of these road anomalies on roads across the country.

In order to reduce these menace and safe guard lives and properties on roads, most countries have set aside road maintenance agencies to occasionally check, repair and maintain road infrastructures across the country. This involves personnel of these agencies, manually inspecting roads for road defect repairs, which leads to waste of time, money, resources and man power. In other to tackle these, there is a need of equipping vehicles with the capability of detecting and informing drivers and appropriate road maintenance agencies of the presence of these road anomalies. Furthermore, another approach is, also incorporating this technology into vehicular Ad hoc Network (VANETs) as shown in figure 1.1. Whereby, vehicles have the ability to detect and communicate with each other about possible road anomalies encountered at different road locations and possible ways of avoiding such anomalies.
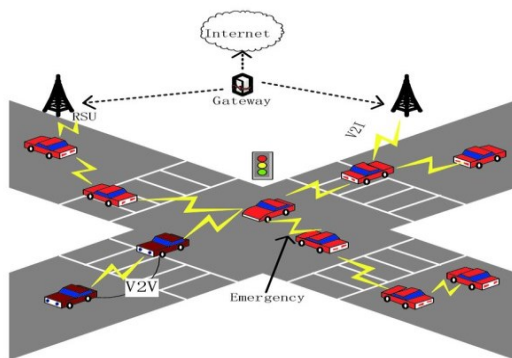

Figure 1.1: vehicular Ad hoc Network (VANETs). (Wang, 2017).

In this regard, this paper examines the different 2D vision-based approaches proposed for the detection of road anomalies based on its intrinsic advantages in terms of higher detection accuracy than the vibrational-based approach, and it cost effectiveness compared to 3D-reconstruction-based approach. Furthermore, it enables real time detection, thereby notifying drivers of the presence of road anomalies prior to encounter, for decisive decision on how navigate through the anomalies. The main contribution of this paper is the survey of some state-of-the-art 2D vision-based approaches for asphalt road surface

condition monitoring. This paper examines the various strengths, limitations, and performance accuracy of these techniques. It highlights possible areas for future research direction towards the development of robust real-time vision-based algorithms for road surface condition monitoring and anomaly detection.

The rest of the paper is organized as follows: Section 2 presents a survey of vision-based approaches for road anomaly detection. Section 3 provides a summary table. While, Conclusion and future research directions are drawn in section 4.

2. LITERATURE REVIEW

This section presents a review of some 2D vision-base approaches for automated road anomalies detection and classification. Specifically, potholes and unsigned speed bumps. We note that most documented techniques proposed are plagued with either of these limitations which include, different lightening or illumination conditions during data acquisition, determining the optimal positioning for placing the onboard camera on test vehicles during data acquisition, used of static manual threshold values for the segmentation and other processing, the supervised manual training with fewer features among others. Furthermore, we also examined the strength of the documented techniques and proffer suggestion for future research direction based on the identified limitations.

The use of 2D vision-based pothole detection approach method was proposed in (Bubenikova *et al.,* 2012), having advantages over 3D approach of high computational cost and equipment. To achieve detection, road image is enhanced using median filter to reduce the noise in the image. Then, image segmentation is implemented on the image, separating the defected and non-defected regions in the image using histogram shape-based thresholding. Due to geometric properties of a defect region, morphological thinning and elliptic regression were used to approximate the potential pothole shape. Subsequently, the texture of the potential defect shape is further extracted and compared with the texture of the surrounding non-defect region, so as to determine if the region of interest (ROI) represents a pothole. The strength of the proposed method in (Bubenikova *et al.,* 2012), recorded accuracy of 86%, precision of 82% and a recall of 86% in detecting road defects. However, additional visual characteristics, when extracting the pothole shape to improve pothole detection was not put into account, and the realization of the algorithm under different weather and light conditions (day/night) is still been tested. Furthermore, improving the detection accuracy rate, by taking additional visual

The Nigerian Society of Engineers
Minna Branch
1st NSE Minna Branch National Conference 2021

Conference theme
Role of Engineering in
Sustainable Development Goals

characteristic into account when extracting the pothole shape, and also the use of machine learning to automatically train and classify potholes and non-potholes pavement textures, are all part of the future work proposed.

Morphological operations which is a tool for noise cancellation in image processing, and better enhancement of important information in images was adopted by (Akarsu *et al.,* 2016) to detect road anomalies in road images. To this effect, a road anomalies detection method using morphological process was proposed in (Buchinger & Silva, 2014). Firstly, image segmentation is carried out on the collected images using Watershed algorithm, and morphological HMAX algorithm is then performed on the segmented image to detect road anomalies in the image. The result of the proposed method has a trade mark of simplicity in implementation, and it is able to detect cracks, but detect potholes more accurately. Out of 229 road defect images, the proposed method detected 211 accurately and 18 wrongly, but the detection accuracy of the method is affected by light and shadowing, the authors did not explicitly state to what degree this affected the detection accuracy but inferred this, because shadows of different objects reflected on the road surface in the images could be detected as a road defect.

Theoretically, potholes are said to be elliptical in shape (Nienaber *et al.,* 2018), but in reality, arbitrary shapes are possible due to irregular wear and tear of road surfaces. Potholes may either contain coarser (dry) or smooth (with water) texture, but the overall surface appearance of potholes can differ due to varying light illumination throughout the day. Due to this limitations which can affect detection accuracy's, the proposed method in (Azhar *et al.,*2016) makes use of Histograms of oriented gradients (HOG) features to compute collected road images. HOG is based on the distribution of edge directions and cumulatively focused on the shape of an object. The collected image features are trained and then classified using Naïve Bayes classifier to different/label the image either as pothole or non-pothole image. The proposed method has a high accuracy of 90%, precision of 86.5% and recall of 94.1%.

A novel based on fast adaptive approach for detecting road anomalies using computer vision was proposed in (Akarsu *et al.,* 2016). The proposed method tries to adapt to various type of roads and detect defects on them. In other to achieve this, the different changes of road colors, had to be put into concentration. To do this, the color of the acquired roads image are been controlled through customization, were, the mean of the RGB image value is calculated and the image is ready for enhancement. To enhance the image, the obtained RGB image is converted

to greyscale, and a blur version of the RGB image is also obtained. The combination of both grey and blur image helps to bring out the crack/ defect structure to the forefront. Binary transform and morphological operation is then carried out to get rid of noise in the image. After the image is enhanced, feature extraction and classification is carried out, and further details can be seen in (Akarsu *et al.,* 2016). Experimental results shows that the proposed algorithm have high accuracy rates in different types of roads via customization, which have an average accuracy while running on all road types, and it has the ability to classify errors on different road surface. However, road color can affect the accuracy rates of the operation.

Using Wavelet Energy to separate potholes from non-potholes regions in road was proposed by (Wang *et al.,* 2017). Although using wavelet energy field and morphological process can accurately detect potholes. To reduce the rate of false detection and increase pothole detection accuracy in an image, two processes (Wavelet energy field model and Markov Random field Model) were adopted to work hand in hand in the proposed method. After the enhancement and retriever of weak signal (potential pothole) among noise (surrounding areas) in the image, using Wavelet energy field by morphological processes and geometric judgment to detect pothole in the image. The detected pothole is then segmented using Markov random field model, where the original image is taken as the feature field, and the wavelet energy field is also taken as the label field. Morphological processing and edge extraction is performed after the pothole segmentation, making the pothole edge to be extracted accurately. The proposed technique is said to be better than that of (Ryu *et al.,* 2015) and (Koch & Brilakis, 2011), having an accuracy of 86.7%, with 83.3% precision and 87.5% recall. It also has a good pothole segmentation results for different kinds of potholes, where about 88.6% of segmented potholes overlap degree is more than 0.85. However, the proposed techniques can be said to be complex, also having a processing time delay which is not suitable for real time implementation. Furthermore, the proposed technique accuracy is affected by light illumination conditions.

Due to the fact that most vision based pothole detection methods / algorithm are complex requiring much data for filtering and training, (Akagic *et al.,* 2017) proposed an algorithm to reduce this complexity by making use of RGB color space. Road image is been pre-processed, followed by image segmentation, to separate the asphalt pavement region from the rest regions in the image. The pothole region is extracted from the pavement image using the first, second and third level seed points, to narrow the search of pothole regions only. The pothole is detected by

The Nigerian Society of Engineers
Minna Branch
1st NSE Minna Branch National Conference 2021

Conference theme
Role of Engineering in
Sustainable Development Goals

comparing the cropped images after Otsu thresholding is applied, and once all the linear and boundary shapes are eliminated in the image, the remaining regions are potential potholes. The proposed algorithm requires less data computation and can be implemented in real time, where the average execution time to detect a pothole from an image is 465.71ms with an average mean error of 7%. Also the accuracy of this method is said to be 82%, which is also suitable as pre-processing step for other supervised methods. However, the effectiveness of the method depends on the extraction of ROI accuracy and it is also affected by light illumination conditions.

The use of Fuzzy c-means clustering and morphological operations has also showed how effective they can be used for image processing. Due to this, a method of detecting potholes through image processing techniques making use of fuzzy clustering and morphological reconstruct was proposed in (Ouma & Hahn, 2017). First, input image is preprocessed and enhanced with median filter to reduce background noise in the image. To detect and recognize pothole in the image, the image is been passed through 2-D discrete wavelet transformation for more filtering. Adaptive soft-thresholding is further applied for detection of candidate defect pixels. Fuzzy c-mean clustering is used for recognition of regions of interest (pothole and non-defect surroundings). The proposed method have an average accuracy of 87.5% using the Dice coefficient of similarity, and average accuracy of 77.7% using Jac card index. However, the method is complex and detection accuracy is affected by lighting conditions and weather conditions.

An improved detection accuracy for the 2D vision-based using Discrete Wavelet Transform (DWT) and Convolution Neural Network (CNN) was proposed in (Oyinbo et al., 2020). Median filter was first applied on the images for denoising, while the edges in the images were enhanced used DWT. The proposed work make use of edge detection as a yardstick for detecting potholes in road images. After DWT, the processed image is then passed through canny edge extraction for segmenting the pothole edges in the images. A resnet50 pre-trained CNN was adopted to detect and classify the road images as either pothole or normal road surface condition. 70% of the road images from the dataset employed, were used for training the algorithm, while the remaining 30% were used in testing and validating the algorithm. The proposed algorithm is said to be working towards a 96% accuracy, 95% precision and about 5% false alarm. However, it is said that the algorithm falls short of real time detection, and a dynamic threshold for segmenting edges in the road images should be explored as future research area.

The use of histogram and closing operation of morphology filter for image segmentation was adopted in (Ryu et al., 2015). Candidate region extraction of potholes are extracted using features such as, size, ellipticity, linearity and compactness. Histogram Shaped-Based Thresholding was also applied to separates both the pothole region and a bright region, such as lane marking from the background region. Finally, Ordered Histogram Intersection (OHI) was used to decide if the image contains a road defect or not. The proposed method, has an accuracy of 73.5% with 80% precision and 73.3% recall in pothole detection. It also has a processing time of average of 46.8sec in processing 10 images. However, it has varying accuracy under different weather condition, vehicular vibration can also affect the detection accuracy. Also, potholes can be falsely detected according to the type of shadow and various shapes of potholes.

The detection of road patches proposed in (Radopoulou & Brilakis, 2015). The method, makes use of histogram equalization for image enhancement. The enhanced image is then converted into binary image using histogram shape-based thresholding algorithm, which allows the separation of darker regions of the pavement image because, patches on pavement are usually darker than its surroundings. Morphological operation is then applied on the binary image. The proposed method makes use of standard deviation of gray-level intensity values to describe texture for both a candidate patch and the healthy pavement around it. The method tackles the problem of reporting the same patch multiple times in a video sequence. It is also cost-effective and has fast processing time. Furthermore, the detection accuracy rate of the method is also affected by weather condition.

3. REVIEW TABLE
Table 1. Gives a summary of the reviewed papers.

Conference theme
Role of Engineering in Sustainable Development Goals

Table 1. A summary of the reviewed papers.

S/N	REFERENCE	TECHNIQUES	STRENGTH	LIMITATION	ACCURACY	PRECISION	RECALL
1	Bubenikova *et al.*, (2012)	Morphological thinning and Elliptic regression	Simplicity.	The proposed work was not tested under different light conditions.	86%	82%	86%
2	Buchinger & Silva. (2014).	Watershed and Morphological HMAX algorithms.	Simplicity in implementation. Detect both cracks and potholes.	Light and shadowing on the road image, affect the detection accuracy.	-	-	-
3	Azhar *et al.*, (2016).	Histograms of oriented gradients (HOG) features.	Computationally efficient. Average processing time.	Not applicable for real time implementation.	90%	86.5%	94.1%
4	Akarsu *et al.*, (2016).	Binary transform and Morphological operation	Ability to classify errors on different road surface. Real time detection system.	Road color can affect the accuracy rates of the operation.	-	-	-
5	Wang *et al.*, (2017).	Wavelet Energy field model and Markor random field model.	Good pothole segmentation results for different kinds of potholes.	High Processing time. Detection accuracy is by light illumination conditions.	86.7%	83.3%	87.5%
6.	Akagic *et al.*, (2017).	RGB color space Image.	Less complex in implementation. Real time implementation.	Detection accuracy is affected by light illumination conditions.	82%	-	-
7.	Ouma & Hahn, (2017).	Fuzzy c-means clustering and morphological reconstruction	Cost Effective	Complexity. Detection accuracy is affected by light illumination and weather conditions	87.5%	-	-
8.	Oyinbo *et al.*, (2020).	Discrete wavelet and Convolution Neural Network.	Detect potholes at different light conditions and pothole filled water.	Not applicable for real time detection.	96%	95%	-
9.	Ryu *et al.*, (2015)	Morphological operation, Histogram Shaped-Based Thresholding, and Ordered Histogram	Average processing time.	Complexity. Not applicable for real time implementation	73.5%	80%	73.3%
10	Radopoulou & Brilakis, (2015)	Histogram equalization for image enhancement, and Standard deviation of gray-level intensity.	Fast processing time. Low implementation cost.	Detection accuracy rate is affected by light and weather conditions	75%	82%	86%

The Nigerian Society of Engineers
Minna Branch
1st NSE Minna Branch National Conference 2021

Conference theme
Role of Engineering in
Sustainable Development Goals

4. CONCLUSION AND FUTURE WORK

This paper present a survey on various 2D vision-based approach for road anomaly detection. Different image processing techniques used in achieving road anomaly detection on asphalt pavements is highlighted. Also, the merits and drawbacks of the various image processing techniques examined were highlighted. Furthermore, the complexity and detection accuracy of various proposed image processing approaches in the literature were analyzed and open research issues are presented. This paper aims to provide researchers with background knowledge required for improving on the 2D vision-based approach for the detection of road anomalies.

From the survey carried out, it can be stated that, the major drawback of the various image processing techniques for the 2D vision-based approach is that they are often characterized by low detection accuracy during foggy weather conditions and at various light intensity. Also, real-time detection of road anomalies from some of the techniques proposed were not achieved. Hence, future research work should explore improving on the existing image processing and segmentation techniques that are robust to different lightening conditions for better detection of road anomalies. Furthermore, real-time detection of road anomalies should be explored.

REFERENCE

Adeniyi, A. M. (2012). *Impact Of Road Transport On Agricultural Development: A Nigerian Example Tunde*. https://doi.org/10.4314/ejesm.v5i3.3

Akagic, A., Buza, E., & Omanovic, S. (2017). Pothole detection: An efficient vision based method using RGB color space image segmentation. *2017 40th International Convention on Information and Communication Technology, Electronics and Microelectronics, MIPRO 2017 - Proceedings*, 1104–1109. https://doi.org/10.23919/MIPRO.2017.7973589

Akarsu, B., Karakose, M., Parlak, K., Akin, E., & Sarimaden, A. (2016). A Fast and Adaptive Road Defect Detection Approach Using Computer Vision with Real Time Implementation. *International Journal of Applied Mathematics, Electronics and Computers*, 4, 290–290. https://doi.org/10.18100/ijamec.270546

Aldagheiri, M. (2009). The role of the transport road network in the economic development of Saudi Arabia. *WIT Transactions on the Built Environment*, 107, 275–285. https://doi.org/10.2495/UT090251

Azhar, K., Murtaza, F., Yousaf, M. H., & Habib, H. A. (2016). Computer vision based detection and localization of potholes in asphalt pavement images. *Canadian Conference on Electrical and Computer Engineering*, 2016-Octob, 1–5. https://doi.org/10.1109/CCECE.2016.7726722

Bello-Salau, H., Aibinu, A. M., Onwuka, E. N., Dukiya, J. J., & Onumanyi, A. J. (2014). Image processing techniques for automated road defect detection: A survey. *Proceedings of the 11th International Conference on Electronics, Computer and Computation, ICECCO 2014*. https://doi.org/10.1109/ICECCO.2014.6997556

Bubenikova, E., Muzikarova, L., & Halgas, J. (2012). Application of Image Processing in Intelligent Transport Systems. *IFAC Proceedings Volumes*, 45(7), 53–56. https://doi.org/10.3182/20120523-3-CZ-3015.00012

Buchinger, D., & Silva, A. G. (2014). Anomalies detection in asphalt pavements: a morphological image processing approach. *Revista Brasileira de Computação Aplicada*, 6(1), 121–129. https://doi.org/10.5335/rbca.2014.3661

Byun, Y., Song, H., & Baek, K. (2018). *Pothole Detection using Machine Learning System View project Pothole Detection using Machine Learning*. https://doi.org/10.14257/astl.2018.150.35

Fan, S., & Chan-Kang, C. (2005). *Road development, economic growth, and poverty reduction in China*. Retrieved from https://books.google.com/books?hl=en&lr=&id=f3c-l4qIYtoC&oi=fnd&pg=PR5&dq=road+reducing+poverty&ots=nNX-QyNmAO&sig=PnX8Gkv_eqMj9e5LRzXmWbaSMrQ

Koch, C., & Brilakis, I. (2011). Pothole detection in asphalt pavement images. *Advanced Engineering Informatics*, 25(3), 507–515. https://doi.org/10.1016/j.aei.2011.01.002

Lemer, A. C. (1999). Building public works infrastructure management systems for

achieving high return on public assets. *Public Works Management and Policy*. https://doi.org/10.1177/1087724X9933007

Nienaber, S., Booysen, M. J., & Kroon, R. S. (2018). *Detecting Potholes Using Simple Image Processing Techniques And Real-World Footage*.

Onoyan-Usina.(2013). Bad drainage and its effects on road pavement conditions in Nigeria. *Cabdirect.Org*. Retrieved from https://www.cabdirect.org/cabdirect/abstract/20133422133

Ouma, Y. O., & Hahn, M. (2017). Pothole detection on asphalt pavements from 2D-colour pothole images using fuzzy c-means clustering and morphological reconstruction. *Automation in Construction*, *83*(October 2016), 196–211. https://doi.org/10.1016/j.autcon.2017.08.017

Oyinbo, A. M., Bello-Salau, H., Mohammed, A. S., Zubair, S., Adejo, A., & Abdulkarim, H. T. (2020). *Towards an Improved Potholes Anomaly Detection Based on Discrete Wavelet Transform and Convolution Neural Network : A Proposal*. *27*(2), 86–91.

Radopoulou, S. C., & Brilakis, I. (2015). Patch detection for pavement assessment. *Automation in Construction*, *53*, 95–104. https://doi.org/10.1016/j.autcon.2015.03.010

Ryu, S. K., Kim, T., & Kim, Y. R. (2015). Image-Based Pothole Detection System for ITS Service and Road Management System. *Mathematical Problems in Engineering*, *2015*. https://doi.org/10.1155/2015/968361

Wang, P., Hu, Y., Dai, Y., & Tian, M. (2017). Asphalt Pavement Pothole Detection and Segmentation Based on Wavelet Energy Field. *Mathematical Problems in Engineering*, *2017*. https://doi.org/10.1155/2017/1604130

540 killed in road crashes in January - FRSC - Premium Times Nigeria. (n.d.). Retrieved March 8, 2020, from https://www.premiumtimesng.com/news/headlines/328229-540-killed-in-road-crashes-in-january-frsc.html

The Nigerian Society of Engineers
Minna Branch
1st NSE Minna Branch National Conference 2021

Conference theme
Role of Engineering in Sustainable Development Goals

A Review on Leach: An Energy Efficient Protocol in Wireless Sensor Networks

P. O. Odeh[1], S. Zubair[2], A. U. Usman[3], and S. Bala[4]

[1,2,3,4] Department of Telecommunication Engineering,
Federal University of Technology Minna – Nigeria.

[1]odehprince@gmail.com, [2]zubairman@futminna.edu.ng, [3]usman.abraham@futmina.edu.ng,
[4]salihu.bala@futminna.edu.ng

ABSTRACT

Wireless sensor networks (WSNs) are networks that comprise of many cheap, low power devices with sensing capability, limited processing and wireless communication capacity. Energy saving is the essential issue in designing efficient wireless sensor networks. The energy consumption of the sensor nodes determines the lifespan of the network. LEACH is a clustering technique that extends a network's lifetime by minimizing the energy consumed and creating efficient energy distribution within the network. In this paper, we review Low Energy Adaptive Clustering Protocol (LEACH) which is a hierarchical protocol which provides solution to energy consumption issues of wireless sensor networks. We analyze several modifications made to LEACH to further curb the energy consumption.

KEYWORDS: *Cluster, Cluster Head, LEACH, M2M, Routing protocol*

1. INTRODUCTION

WSN is an inter-connection of devices that houses sensors with capabilities to detect and respond to some type of physical or environmental input such as pressure, temperature, light, sound, heat etc. the output of these sensors are usually electrical signals that are transmitted through wireless links for onward processing and utilization. These networks are highly distributed and self-organized D. Estrin et al. (2001), Mr. Ankit Gupta et al. (2012). WSN explores different topologies for its communication, these topologies could be star, tree or mesh and the different types of WSN are mainly categorized based on environmental deployment and purpose, which are; Terrestrial, Underwater, multimedia and mobile WSN just to mention a few. The application of WSN technology is endless in areas such as health, transportation, IoT, environmental monitoring, security etc. Wireless sensors are usually tiny in nature but fitted with sensing and computing circuits, a radio transceiver and power element, M. A. Matin et al. (2012). The primary energy source for WSN is a battery with finite life span, so for efficient utilization of the nodes there arose the need for protocols that would ensure efficiency energy utilization of the nodes which will in turn extend the life span of the network.

The two major areas where strategy could be employed to combat this energy efficiency challenge

are physical layer and MAC layer. The physical layer technique deals with designs of circuitry for power storage and dissipation and the quality of materials while the MAC layer involves protocols that coordinates the operation of the devices in the network to achieve the intended purpose Zhihua Lin, et al. (2020).

2. LEACH PROTOCOL

LEACH protocol is a self-organizing protocol that aid efficient utilization of energy. It is hierarchical in characteristics where the parent node of one cluster could be the child node of another cluster as shown in figure 1.1. The position of cluster heads is rotated based on some defined parameters such as residual energy, distance of the node from the sink, position in the cluster etc. It distributes the load in a network and it is assumed that each node in the network has a transmitter with capability of reaching the sink directly. LEACH features in both centralized and decentralized clustering protocol where the activities of the nodes in the network are coordinated by the sink and the nodes respectively Juma W. et al. (2018).

Conference theme

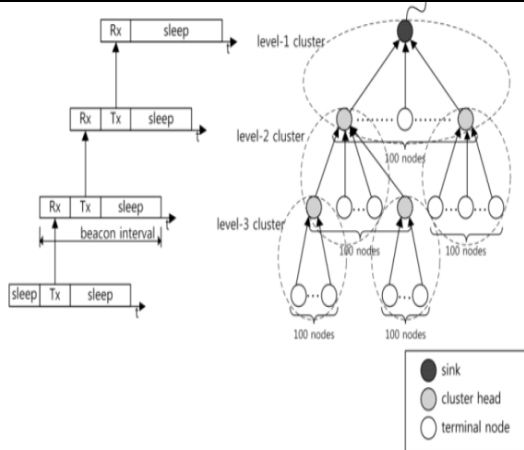# Role of Engineering in Sustainable Development Goals

Figure 1.1 LEACH Cluster Network. Ieryung Park. *et al.* (2014).

LEACH has two phases that describe its operation; the set up phase and the steady state phase, Prabhat Kumar et al. (2012). The cluster is set up and cluster head selection is done under the set up phase whereas the sensor nodes sense their areas and send relevant generated packets to their Cluster Head (CH) in steady state phase. LEACH protocol has several rounds of communication which rotates the responsibility of CH to further balance the energy in the network. A CH is randomly selected. All the nodes in the network pick a number randomly between 0 and 1. The node that select a random number that is less than the threshold for node n then that node becomes the CH for that round. The value for the threshold T (n) can be calculated using the formula.

$$T(n) = \begin{cases} \dfrac{P}{1-P\left(r.\mathrm{mod}\frac{1}{P}\right)}, & \text{if } n \in G \\ 0, & \text{otherwise} \end{cases}$$

Where; P = the desired percentage of the CH node.

r = the number indication the current round of communication.

G = set of nodes that have not been selected as CH node in the previous 1/P rounds.

When CH has been selected successfully, it broadcasts a beacon message to other member nodes. Based on the received signal strength of the beacon message, other nodes decide to which cluster they will join for the current round and send a membership message to their respective CHs. After the exchange, the cluster formation completed.

In the steady state phase, the CHs create TDMA schedule for all the member nodes in their respective clusters. The set of slots assigned to the nodes of a cluster are called frames; Hicham O. et al (2019). The duration of each frame differs according to the number of cluster members of the cluster. When these member nodes generate or sense data they forward to their respective CHs based on the assigned time slot and shut down their radio after successful transmissions. The CHs aggregate the data from the member nodes, compress and forward to the sink. After a predetermined time, the network moves to a new round. This process is repeated until all nodes in the network are elected CH at least once all through the previous rounds. After which the round is reset to back to 0 then the process starts all over again.

The transceiver consumes more of the dissipated energy in the sensors Meenakshi S. et al. (2012). The transceiver is made up of transmitting and receiving circuits embedded in the nodes and the sink. The transmitter circuit uses more energy compared to the receiver circuit. The different power dissipated by the receiver and transmitter is calculated by the following formulas:

Transmitting: Divya Prabha. *et al.* (2018).

$$E_{TX}(k,d) = E_{TX} - \{(E_{elec} * k) + (E_{mp} * k * d)\} \quad (2)$$

$$E_{TX}(k,d) = E_{TX} - \{(E_{elec} * k) + (E_{fs} * k * d)\} \quad (3)$$

$$E_{TX-}(k,d) = \varepsilon fs * d^2 * k \text{ if } d < d0 \quad (4)$$

$$\varepsilon fs * d^4 * k \text{ if } d \geq d0$$

$$d_0 = \sqrt{\frac{\varepsilon_{fs}}{\varepsilon_{amp}}} \quad (5)$$

Receiving: Divya Prabha. *et al.* (2018).

$$E_{RX}(k) = E_{RX} - (E_{elec} + E_{DA}) * k \quad (6)$$

The Nigerian Society of Engineers
Minna Branch
1st NSE Minna Branch National Conference 2021

Conference theme
Role of Engineering in
Sustainable Development Goals

Where, E_{elec} = denotes amount of Energy consumption per bit in the transmitter or receiver circuitry.

E_{mp} = Amount of energy consumption for multipath fading.

E_{fs} = Amount of energy consumption for free space.

E_{DA} = Data aggregation energy.

Where k is the message size and d is the distance.

The novel LEACH has some advantages and disadvantages. These merits and demerit have geared different researches toward improving the protocol's performance in different metrics. Below are some of these advantages and disadvantages.

Advantages: Prashant Maurya *et al.* (2016).

1. LEACH is a completely distributed approach.
2. It does not require any global information of network.
3. It is a powerful and simple routing protocol.
4. It uses random rotation of Cluster-Head, which provides each node to become a cluster head node in a round.
5. It uses TDMA so that each node can participate in rounds simultaneously.
6. Each sensor node communicates only with associated cluster head (CH). It provides localized co-ordination and control for cluster setup and operation.
7. Only a cluster head node (CH) aggregates the data collected by the nodes to minimize the data redundancy.

Disadvantages: Prashant Maurya *et al.* (2016).

1. In LEACH Protocol only cluster head (CH) is responsible for sending data to base station (BS) directly. So, failure of CHs leads to lack of robustness.
2. Single Hop Routing technique is used in LEACH Protocol, which needs high energy for data transmission from CH to BS directly in case of large network.
3. Selection of CH in any round is random and does not consider energy level of node,

which can lead to drainage of a particular node.
4. Dynamic clustering technique is used in LEACH which results in extra overhead like selection of CHs and advertisement.

For the purpose of this paper, we review the different modifications made on different variants of LEACH employed to tackle energy waste due to contention for channel access for network performance through measured metrics such as throughput, packet loss and energy efficiency.

3. LEACH VARIANTS
There are several variants of LEACH protocol based on deployment and node behavior in a given network.

3.1 LEACH-C (CENTRALIZED LEACH)
C-LEACH as it is famously called is a centralized clustering algorithm. The information obtained about the location and energy level of each node in the setup phase is used by the sink to compute the average energy level of the network. The sink runs a simulated annealing algorithm for nodes whose energy level is higher than the threshold to select the CH nodes. The node whose ID matches the advertised ID from sink is selected as CH Gnanambigai J. et al. (2012). The steady state phase is the same as for the novel LEACH. Due to the centralized technique, the sink has the overall knowledge of the network coverage area; hence less energy would be consumed by the entire network. It performs more data transfer per unit of energy. This centralized scheme makes it not suitable for larger network.

3.2 GRID LEACH
The deployment of sensors in this variant of LEACH is done in a grid format; Alireza Firuzbakht. Et al. (2013). The network is separated into independent grids with virtual grids. The node inside the grid with zenith energy level which is also close to the center of the cluster and sink is selected as CH. The data is sensed by a virtual square and forwarded to CH which is then aggregated and transmitted to sink. In this variant, sensor energy is conserved by making the transmitting node only to be the active mode while other nodes will be in sleep mode.

3.3 MULTI-HOP LEACH
The Multi Hop LEACH is akin to novel LEACH protocol except the direct data transmission

to sink. When the desired data is collected by CHs from their cluster nodes, they will transmit them serially through other CHs to the sink. So therefore, the distance between the nodes gets decreased which then conserved energy for data transmission. By raising the number of hops, the lifetime of the network will be improved efficiently Gnanambigai J. et al. (2012). The main tradeoff in this technique is the delay that occurs in the transmission.

4. MODIFICATIONS OF LEACH FOR EFFICIENT ENERGY UTILIZATION

Enhancement of LEACH by application of Radio Frequency through embedding active, ready and sleep communication modes whithin the network was done by Navdeep K. et al. (2016). The active mode was used only to sense data, the ready mode was used to sense and also transmit data from node to the sink whereas the node in sleep mode reduces the energy consumed and also balances the energy loads of the CHs. The term RFID-LEACH was coined as a name for their proposed method. They experienced challenge with clock synchronization which was one of the properties of RFID. This problem was tackled using contention avoidance algorithm (RTS/CTS). This technique described a scenario where CH node send request to send (RTS) packets containing a nonse feed to all its cluster members (CM), the CMs would adapt their clocks to the feed and reply with clear to send (CTS) to achieve synchronization. The RFID-LEACH scheme was simulated on NS2 and graphical results showed better performance than LEACH and RFID protocols in terms of throughput, efficient energy utilization, less end-to-end delay and overhead in the network.

A similar work on a variant of LEACH, where they introduced two new techniques to the novel protocol; the cluster head replacement scheme and dual transmission levels to aid efficient energy utilization Ms. Neha Bhadu, et al (2017). MODLEACH as the protocol was termed does not take into consideration the influence of parameter p which defined the probability of becoming the CH; instead, a mathematical analysis was done to select a nominal value of p. The estimated value of p was also varied and the impact was measured through simulations on MATLAB. MODLEACH performed better than LEACH in terms of network lifetime and packets exchange with base station.

Another work which proposed network efficiency by introduction of vice cluster head, the algorithm allowed one node in the cluster to be selected as VCH in case the CH dies. When this happens, cluster nodes data will always reach base station in an efficient way and no need to elect a new CH for that round of transmission Sasikala S. D. et al. (2015). K-LEACH as the technique was called employed Kmedoids clustering algorithm for uniform clustering, Euclidean distance and Maximum Residual Energy (MRE) was used to select the CH. This modification to CH selection reduced energy consumption by 33% compared with LEACH. This technique has advantages like efficient transmission of data to sink, improved network lifetime and lower energy consumption K. Kishan et al. (2012).

Most of the modification of LEACH focused on cluster head selection methods, inter cluster head communications etc. An improved work on LEACH channeled its effort towards intra-cluster communication in a hierarchical clustering network. The novel LEACH has two stages of operation; the set up state and steady state. IBLEACH in a quest to improve the performance of LEACH introduced a new state between the set-up and steady state called pre-steady state; Ahmed Salim et al. (2014). The main purpose of this new state was to calculate the cluster workload i.e., the aggregation of the sensed data from cluster members and send to the sink in one frame, then elect a CH that can handle the aggregated processes through all frames in that round; Tong M., et al. (2012). This helped to distribute cluster load overhead over the cluster members. This technique improved network lifetime and balanced energy consumption.

H-LEACH described the modification of LEACH which the cluster heads are fixed and chosen dynamically. This protocol utilized the node location coordinate and clusters the area on the basis of this information; Abdul Razaque et al. (2017). It used the maximum energy of the node to select a CH instead of threshold utilized by LEACH. The lifetime of a CH node could be estimated through the number of rounds. Simulation results indicated better performance than Hybrid Energy Efficiency Distributed (HEED).

EEE LEACH an Energy Efficient Extended LEACH is an energy efficient protocol that increase

The Nigerian Society of Engineers
Minna Branch
1st NSE Minna Branch National Conference 2021

Conference theme
Role of Engineering in
Sustainable Development Goals

energy utilization through creation of multilevel clusters and reducing the radio communication distance. This multilevel clustering protocol involves two layers of cluster formation aside having similar one layer formation between the nodes and the sink; Wairagu G. et al. (2009). The formation of clusters and selection of CHs is achieved in the first layer. Then the cluster members transfer their sensed data to their CHs. Using the fuse mechanism, the CHs aggregate the data received from their cluster members. In the next layer, Master Cluster Heads (MCHs) are selected. The CHs locate the nearest MCHs by calculating the distance between them then transfer their aggregate data to the respective MCHs. Meenakshi S. et al. (2012). In the similar fashion, the MCHs accept data from their nearest CHs, aggregate all received data, convert them into a compress format and forward them to the sink.

DD-LEACH (LEACH with Distributed Diffusion) was designed as an improved LEACH Protocol. This technique utilizes multi-hop routing of data from sensor nodes to sink. Nodes and CH serve as relay nodes to forward packets from other nodes towards the sink. In DD-LEACH Protocol data acumulation is done at multiple levels R. K. Kodali et al. (2016) Firstly, data aggregation is carried out at CH level. The CH collects the data from member nodes. While forwarding data to sink, all the median CHs also perform data aggregation at their different levels. In DD-LEACH energy consumed is alleviated through multi-hop routing communication.

LEACH-A (Advanced Low Energy Adaptive Clustering Hierarchy); In this novel LEACH protocol, CH is responsible for sending data directly to sink which expends high amount of energy than other member nodes in the network. M. Usha et al. (2016). In advanced LEACH, a technique called mobile agent is used to process data. This LEACH variant protocol is defined as a heterogeneous energy inclined protocol developed for the purpose of energy conservation, efficient data transfer, reducing the probability of node failure and for improving the time interval before demise of the first node. Hence, both the energy conservation and data transfer reliability is improved in LEACH-A. This scheme also uses synchronized clock, through which

each sensor node gets the beginning of each transmission round. J. Gnanambigai1 et al. (2018).

There is an improved LEACH protocol referred to as MG-LEACH. This modified protocol divides the deployed nodes into sub-groups (G1…. Gk) based on locations of the nodes; where k is a real number. The numbers of groups in this modification are mainly dependent on node density. The groups formation is coordinated by the sink at the time of deployment and after every "r" rounds. Hicham Ouldzira et al. (2019). This is an extra step employed in their algorithm before setup phase and steady state phase called Set building phase. MG-LEACH has three steps. The build phase is utilized during time of deployment after each "r" rounds per sink, and the remaining two are the same as those applied in LEACH such as the set-up phase and steady state phase. This protocol offered better performance than LEACH in terms of energy conservation and efficient utilization. Jong-Yong Lee et al. (2019).

In the same vein of attempt to further reduce the energy consumed in an IoT related environment, this variant of LEACH modified the protocol by initiating a strict threshold for CH selection and retaining the CH position to serve for multiple rounds provided the node has enough residual energy to match up with the task. Siavoshi, S. et al. (2016). The proposed protocol also switches the power between the nodes in a cluster. This protocol focused on the growing demand for IoT devices which the novel LEACH is unable to cater for in terms of energy because of the frequent rotational duties of the CH. This rotation consumes energy. I-LEACH (short for IoT LEACH) maintains a node that has serve as CH in the previous round if the energy threshold value still meets the set criteria. Trupti Mayee et al. (2017). This way the energy wasted during routing information to the new CH in each round can be minimized. The extra energy consumed for the formation of new cluster due to new CH selection can also be mimimized. I-LEACH protocol outperforms LEACH by 67% increase in throughput and extending the lifespan of the network through successful 1750 rounds of communication.

The table 1 summarized the different approach of modification of LEACH, the methods, results, strengths and weaknesses

The Nigerian Society of Engineers
Minna Branch
1st NSE Minna Branch National Conference 2021

Conference theme
Role of Engineering in
Sustainable Development Goals

Table 1 THE DIFFERENT APPROACH TO MODIFICATION OF LEACH

S/N	REFERENCES	PROBLEM ADDRESSED	METHODOLOGY	RESULTS	LIMITATIONS	OPEN AREAS
1.	Navdeep K., Ranbir S. (2016).	Efficient Energy consumption, distributed overhead energy	Embedded active, ready and sleep modes using RFID.	The energy consumed was significantly less compared with LEACH even when the number of nodes connected to the AP increased.	Synchronization problem with the protocol because of the property of RFID.	Ways to improve the performance Through clock synchronization of the cluster heads and members
2.	Ms. Neha Bhadu, Dr. Uma Kumari (2017).	Energy consumption on radio communication by stations in IEEE 802.11 infrastructure WLAN.	Utilized efficient cluster head replacement and dual transmission levels as means to utilize energy efficiently.	Improved energy consumption and longer battery life for sensor nodes. Increase network life span.	Employed only in homogenous networks.	To be implemented in heterogeneous networks
3.	Sasikala S. D., Sangameswaran N.,Aravindh P. (2015).	Failure of selected Cluster Head in the network.	Introduction of Vice Cluster Head (VCH).	Extension of network lifetime in case of cluster Head battery being drained.	Establishment of Vice Cluster Head consumed more energy in the initial set up phase.	Improved technique in selection of Vice Cluster head that will consume less energy in the set up phase.
4.	Ahmed Salim, Walid Osamy, Ahmed M. Khedr. (2014)	Evenly distribution of energy in the network between nodes and the CH.	Used the set up phase. Pre-steady state and the steady state to achieve intra cluster communication.	Reduced rate of energy consumption and energy distribution between CH and Cluster members.	Pre-steady sate introduced complexity to the LEACH process and implementation problem.	Ways to execute pre-steady state with less complexity.
5	Abdul Razaque, Satwic Mudigulam, Kiran Gavini. (2017)	Life time of network and energy consumed per node	Selection of CH by considering residual and maximum energy of nodes, calculation of alive nodes after every round.	Improved energy consumed by individual nodes and lifetime of the network	Loss of nodes with energy below the threshold even when they are yet to die off completely	Ways to utilize nodes with energy below the threshold through assigning minimum energy consumption task.
6	Meenakshi S., Kalpana S. (2012)	Increased Energy efficiency	Used multilevel clusters through radio distance reduction to form MCH which aggregate data from CHs	Increased Energy efficiency and network life time.	Multiple levels of data aggregation that could affect data quality and integrity	Measuring the QoS of data received by the sink efficiently
7	Hicham Ouldzira, Hajar Lagraini,	Energy consumption	Division of the clusters into sub groups depending on	Improved energy conservation and	Added "set building state" as an extra step that	Ways for efficient memory

,

5. OPEN AREAS

So many modifications have been made to LEACH in a quest to further reduce energy consumed and balance the load in the network but there are still areas that are yet to be integrated to LEACH. This novel protocol has potential to last long in the communication space, its unique way of organizing nodes give it an edge in longevity.

One of the basic operations of LEACH is the arrangement of clusters in layers where the child node of one cluster would be the parent node of another cluster, a cluster head in one cluster is a cluster member in another cluster. These are arranged in layers for ease of packet forwarding to

the sink and energy distribution within the network. Contention window adjustment; a technique that devices use to curb contention and collision in communication could be explored in the LEACH space, this has the potential to enable effective Cross-layer communication especially when the number of nodes in one cluster increase astronomically. This would improve the transmission time Sharma M. *et al.* (2012) and throughput of LEACH protocol

6. CONCLUSION AND FUTURE WORK

In this paper, we reviewed the different modification made on LEACH with intention to further reduce energy consumption and improve

network lifetime. We explored the different areas of modification and techniques employed to achieve varying results on energy efficiency, the functionality of the modifications, area of application and comparison of the modification to the novel LEACH and other variants. More parameters could be adjusted to create other modifications that could resolve limitations of current modifications.

7. ACKNOWLEDGMENT

I want to use this opportunity to acknowledge my supervisors in persons of Dr. Suleiman Zubair and Dr. Abraham Usman for the undiluted support through the course of my program and this paper. I want to thank Dr. S. Bala for the push and motivation in actualizing this paper. I want to acknowledge the moral support from my lovely wife Mrs. Sophia Odeh. May God bless you all

REFERENCES

D. Estrin, L. Girod, G. Pottie, and M. Srivastava. (2001) "Instrumenting the World with Wireless Sensor Networks," in International Conference on Acoustics, Speech, and Signal Processing, Salt Lake City, Utah.

M. A. Matin and M. M. Islam. (2012) Overview of wireless sensor networks; technology and protocol, international journal of Advanced Research in Computer Science and Software Engineering, DOI: 10.5772/49376.

Juma W. Raymond, Thomas O. Olwal, and Anish M. Kuren, (2018) "Cooperative Communications in Machine to Machine (M2M): Solutions, Challenges and Future Work". DOI:10.1109/ACCESS.2018.2807583.

Prabhat Kumar, M. P. Singh and U. S. Triar, (2012) "A Review of Routing Protocols in Wireless Sensor Network", International Journal of Engineering Research & Technology (UERT), Vol. 1 Issue 4.

Gnanambigai J., Dr. Rengarajan N., Anbukkarasi K. (2012). "LEACH and Its Descendant Protocols: A Survey", International Journal of Communication and Computer Technologies 01 - No.3, Issue 8.

Alireza Firuzbakht, Asgarali Bouyer. (2013) "An optimal Algorithm based on gridding and clustering for decrease energy consumption in

WSN", international convention on Tele communication and information.

Navdeep K., Ranbir S. (2016) "Energy Optimization of Leach Protocol in WSN Using NS2 Simulator" International Journal of Technology and Computing (IJTC) ISSN-2455-099X, 2, Issue 201.

Mr. Ankit Gupta, Ms. Sangeeta Malik, Ms. Monika Goyal, Dr. Pankaj Gupta (2012) "Clustering Approach for Enhancing Network Energy using LEACH Protocol in WSN" International Journal of Wired and Wireless Communications Vol.2, Issue 1.

Ms. Neha Bhadu, Dr. Uma Kumari (2017) "Performance Enhancement and Analysis of MODLEACH Routing Protocol in WSNs" Advances in Wireless and Mobile Communications. ISSN 0973-6972 10, Number 5, 949-959.

Sasikala S. D., Sangameswaran N., Aravindh P. (2015) "Improving the Energy Efficiency of Leach Protocol Using VCH in Wireless Sensor Network" International Journal of Engineering Development and Research. Volume 3, Issue 2 | ISSN: 2321-9939.

Ahmed Salim, Walid Osamy, Ahmed M. Khedr. (2014) "IBLEACH: intra-balanced LEACH protocol for wireless sensor networks" Springer; Wireless Netw 20:1515–1525. DOI 10.1007/s11276-014-0691-4.

Abdul Razaque, Satwic Mudigulam, Kiran Gavini. (2017) "H-LEACH: Hybrid-Low Energy Adaptive Clustering Hierarchy for Wireless Sensor Networks" International Conference on Systems Engineering and Modeling. 62–71.

Sharma M. (2012) "Transmission Time and Throughput analysis of EEE LEACH, LEACH and Direct Transmission Protocol: A Simulation Based Approach," Advance Computer and International Journal, vol. 3, no. 5, 97–104.

Meenakshi S., Kalpana S. (2012) "An Energy Efficient Extended LEACH (EEE LEACH)" International Conference on Communication Systems and Network Technologies, Rajkot, India. IEEE DOI 10.1109/ CSNT.2012.88.

Wairagu G. Richard, (2009) "Extending LEACH routing algorithm for Wireless Sensor Network,"

Data Communications Engineering, Makerere University.

Hicham O., Hajar L., Ahmed M., Mostafa C., Abdelmoumen T. (2019) "MG-leach: an enhanced leach protocol for wireless sensor network" International Journal of Electrical and Computer Engineering (IJECE) Vol. 9, No. 4, pp. 3139~3145 ISSN: 2088-8708, DOI: 10.11591/ijece. v9i4.pp3139-3145.

Meenakshi S. and Anil K. (2012) "Transmission Time and Throughput analysis of EEE LEACH, LEACH and Direct Transmission Protocol: A Simulation Based Approach" Advanced Computing: An International Journal (ACIJ), Vol.3, No.5, DOI: 10.5121/acij.2012.3511.

R. K. Kodali, and N. Sarma, "Energy efficient routing protocols for WSN's." pp. 1-4.

M. Usha, Dr. N. Sankarram. (2016) "Analysis and operations of variants of LEACH protocol" International Journal of Innovative Research in Computer and Communication Engineering Vol. 2, Special Issue 1.

J. Gnanambigai1, Dr. N. Rengarajan2, K. Anbukkarasi3. (2018) "Leach and Its Descendant Protocols: A Survey" International Journal of Communication and Computer Technologies Vol. 01, No. 3, Issue: 18.

Jong-Yong Lee. (2019) "Improvement of CH election in three-level heterogeneous WSN", Indonesian Journal of Electrical Engineering and Computer Science, Vol. 13, No. 1, pp. 272~278.

Hicham Ouldzira, Hajar Lagraini, Ahmed Mouhsen, Mostafa Chhiba, Abdelmoumen Tabyaoui, (2019) "MG-leach: an enhanced leach protocol for wireless sensor network" International Journal of Electrical and Computer Engineering (IJECE) Vol. 9, No. 4, pp. 3139~3145 ISSN: 2088-8708, DOI: 10.11591/ijece. v9i4.pp3139-3145.

Trupti Mayee Behera, Umesh Chandra Samal, Sushanta Kumar Mohapatra, (2017) "Energy-efficient modified LEACH protocol for IoT application" The Institution of Engineering and Technology. 2018 ISSN 2043-6386 doi: 10.1049/iet-wss.0099 www.ietdl.org.

K. Kishan Chandl, P Vijaya Bharati and B. Seetha Ramanjaneyulu. (2012) "Optimized Energy Efficient Routing Protocol for Life-Time Improvement in Wireless Sensor Networks", IEEE-International Conference on Advances in Engineering, Science And Management.

Tong M., & Tang. (2012) "MLEACH-B: an improved LEACH protocol for wireless sensor network". In 6th international conference on wireless communications networking and mobile computing (WiCOM) (pp. 1–4).

Siavoshi, S., Kavian, Y.S., Sharif, H.: (2016) 'Load-balanced energy efficient clustering protocol for wireless sensor networks', IET Wirel. Sens Syst. 6, (3), pp. 67–73.

Ieryung Park, Dohyun Kim, and Dongsoo Har. (2014) "MAC Achieving Low Latency and Energy Efficiency in Hierarchical M2M Networks with Clustered Nodes" IEEE Sensors. DOI 10.1109/JSEN.2014.2364055.

Prashant Maurya, Amanpreet Kaur. (2016) "A Survey on Descendants of LEACH Protocol" I.J. Information Engineering and Electronic Business, 2016, 2, 46-58 2016 in MECS (http://www.mecs-press.org/) DOI: 10.5815/ijieeb.

Divya Prabha and Vishal Kumar Arora, (2018) "Leach and Its Descendant Protocols in Wireless Sensor Networks: A Survey" International Journal of Communication and Computer Technologies Vol. 01, No. 3, Issue: 02.

Zhihua Lin, Guang Li a, c, Jianqing Li. (2020) "Cross-layer energy optimization in cooperative MISO wireless sensor networks" https://doi.org/10.1016/j.comcom.2020.04.034; 0140-3664/© 2020 Elsevier B.V.

M. Udin Harun Al Rasyid1, Bih-Hwang Lee. (2018). "LEACH Partition Topology for Wireless Sensor Network" IEEE International Conference on Consumer Electronics-Taiwan (ICCE-TW).

Dwi Widodo HK, Adit Kurniawan, M Sigit Arifianto, (2019). "Improving Topology of LEACH Cluster Using Reinforcement Learning Method" IEEE International Conference on Sensors and Nanotechnology, 978-1-5386-5619-8/19/$31.00.

Conference theme
Role of Engineering in Sustainable Development Goals

Finite Element Modelling and Analysis of a 4-Span T-Beam Bridge

*Nyam, J. P.[1] & Sadiku, S. A.[2]
[1] Research Scholar, Department of Civil Engineering
Federal University of Technology, Minna
[2] Professor, Department of Civil Engineering, Federal University of Technology, Minna
*Corresponding author email: joenyam@yahoo.com

ABSTRACT

T-beam bridge is one of the principal types of cast-in place concrete bridge. T-beam bridge consists of a concrete beam called girders and slab decks. The finite element method is a general method of structural analysis in which the solution of a problem in continuum mechanics is approximated by the analysis of an assemblage of smaller sub-structures called finite elements which are interconnected at a finite number of nodal points or in the case 3-D called nodal planes and represent the solution domain of the problem. A 4-span T-beam bridge was analyzed by using BS 5400:2 loadings as a one-dimensional structure. The same T-beam bridge was analysed as a three- dimensional structure using finite element plate for the deck slab and beam elements for the main beam using ANSYS 16.0 software. Both models were subjected to BS 5400:2 Loadings to produce maximum bending moment and extreme shear. The results obtained from the finite element model are lesser than the results obtained from one dimensional analysis, meaning that the results obtained from manual calculations are conservative.

KEYWORDS: *ANSYS, BS 5400, Finite Element Method, T-Beam.*

1 INTRODUCTION

An essential factor in making a sound decision is knowledge of the strength of the bridge in its existing form. The general characteristics of concrete, the inelastic response, distributions of load, and ultimate strength of multi-girder bridges cannot be realistically assessed by use of simplified procedures currently used in design and evaluation. Prediction of this behaviour ultimately requires extensive experimentation or advanced analytical techniques (Shreedhar & Spurti, 2012). In many cases, analytical methods are more economical and expedient than laboratory or field testing, and a number of researchers have extolled the potential of using finite element analysis to predict bridge response with reinforced-concrete deck compositions (Ashour & Morley, 1993; Huria, 1993; Mabsout, 1997).

The development of commercial finite element codes, which provide a unique programme interface with which to analyse a system, has helped practitioners attain a better appreciation for both the usefulness and limitations of finite element modeling of reinforced concrete (Darwin, 1993). Evaluation of specific applications, such as

reinforced-concrete bridge decks, can be handled using these codes. However, to identify possible modeling discrepancies and errors and to verify the accuracy of these computer codes, results from nonlinear finite element analyses need to be compared with those from actual experiments or simple linear methods. This may be achieved only if the analysis can account realistically for the material and geometric properties of the various components of a structure and the interaction among them (Chowdhury, 1995). A definitive technique for analysing reinforced concrete, one of the most used composite materials in construction, has been difficult to develop. Researchers acknowledge that the finite element method works very well for many structural materials such as steel and aluminum, which have well-defined constitutive properties. When the constitutive behaviour is not so straightforward, the task is more difficult. For materials such as concrete, in which discrete cracking occurs, this is certainly the case (Alpesh, 2016).

Linear models were used to analyse structural systems composed of complex materials such as concrete and reinforced concrete in recent times.

The Nigerian Society of Engineers
Minna Branch
1st NSE Minna Branch National Conference 2021

Conference theme
Role of Engineering in
Sustainable Development Goals

Most methods used in the analysis of reinforced concrete structures have not substantially described the behaviour of the structure and load distributed across its span. These methods of analysis are only approximate, hence, the finite element method of analysis which is a more promising method will be used to analyse the T beam bridge as a three-dimensional structure. The analysis will employ a finite element plate for the deck slab and beam elements using the Software Analysis and Systems, ANSYS 16.0.

2 METHODOLOGY

There are many methods available for analyzing bridges. However, of all the available analysis methods, the finite element method is considered to be the most powerful, versatile and flexible method. The 3-D finite-element method is probably the most involved and time consuming, however, the most general and comprehensive technique for static and dynamic analyses, capturing all aspects affecting structural response. The other methods proved to be adequate but limited in scope and applicability.

2.1 FINITE ELEMENT METHOD

The finite-element method is a numerical procedure for solving problems in engineering and mathematical physics. In structural problems, the solution is typically concerned with determining stresses and displacements. Finite element model gives approximate values of unknowns at discrete number of points in a continuum.

This numerical method of analysis starts by discretizing a model. Discretization is the process where a body is divided into an equivalent system of smaller bodies or units called elements. These elements are interconnected with each other by means of certain points called nodes. An equation is then formulated combining all the elements to obtain a solution for one whole body.

In the case of small displacements and linear material response, using a displacement formulation, the stiffness matrix of each element is deduced and the global stiffness matrix of the entire structure can be formulated by assembling the stiffness matrices of all elements using direct stiffness method. This global stiffness matrix, along with the given displacement boundary conditions and applied loads is then solved, thus that the

displacements and stresses for the entire system are determined. The global stiffness matrix represents the nodal force-displacement relationships and can be expressed by the following equilibrium equation in matrix form:

$$[F]=[K][U] \qquad (1)$$

Where,

[K] = global stiffness matrix assembled from the element stiffness matrices,

[U] = nodal displacement vector and

[F] = nodal load vector.

2.2 FINITE ELEMENT PROGRAMME: ANSYS

The finite element modeling and analysis performed in this research were carried using a general purpose, multi-discipline finite element programme, ANSYS. ANSYS is a commercial finite element programme developed by Swanson Analysis Systems, Inc. (SAS IP Inc 16th edition). The programme is available for both PC and UNIX based systems. The analyses presented in this paper were performed using ANSYS version 16.0. ANSYS has an extensive library of truss, beam, shell and solid elements. The brief description of the elements used in the model is presented below:

1. **Shell 63 (elastic shell)**: A four noded element that has both bending and membrane capabilities. The element has six degrees of freedom at each node, translations in the nodal X, Y, and Z directions and rotations about the nodal X, Y, and Z axes. Large deflection capabilities are included in the element. It is stated in ANSYS manual that an assemblage of this flat shell element can produce good results for even curved shell surface provided that each flat element does not extend over more than a 15° arc.

2. **Link 8 (3-D Spar)**: is a two-node, three-dimensional truss element. It is a uniaxial tension-compression element with three degrees of freedom at each node; translations in the nodal X, Y and Z directions. The element is a pin-jointed structure with no bending capabilities. Plasticity and large deflection capabilities are included. The required inputs for this element are the material properties and cross-sectional area.

3. **Beam 188 (3-D Linear Finite Strain Beam):** is a linear (2-node) or quadratic beam element in 3-D. Beam 188 has six or seven degrees of freedom at each node. These include translations in the X, Y, and Z directions and rotations about the X, Y and Z directions. A seventh degree of freedom (warping magnitude) can also be considered. This element is well-suited for linear, large rotation, and/or large strain nonlinear applications. The beam elements are one-dimensional line elements in space. The cross-section details are provided separately using the SECTYPE and SECDATA and commands.

4. **Beam 4 (3-D Elastic Beam):** is a uni-axial element with tension, compression, torsion and bending capabilities. The element has six degrees of freedom at each node, translations in the nodal X, Y and Z directions and rotations about the nodal X, Y and Z axes. Stress stiffening and large deflection capability is included. The required inputs for this element are the cross-sectional properties such as, the moment of inertia, the cross-sectional area and the torsional properties.

2.2.1   VERIFICATION STUDIES OF ANSYS

The finite element model of a concrete beam, simply supported, and subjected to a uniformly distributed load, was initially investigated. The intention of this example was to do the following:

- Analyze standard beam elements using ordinary concrete theory
- Compare finite element results with manual linear hand calculations.

The beam selected for analysis had a span, l of 6.1 m (20 ft), a width, w of 0.25 m (10 in), and a depth of 0.64 m (25 in). The concrete had a strength of 41.4 MPa (6,000 psi) and a modulus, E of 30.5 GPa (4,420 ksi). The loading was a uniform load, w of 62.2 kN/m (4,260 lb/ft), which is close to the ultimate load of the beam. Maximum stresses, displacement, shear force and bending moment attributable to the applied load were calculated in accordance with the code of the British Standard Institute. A finite element model of the beam, consisting of several elements, was also developed, and stresses and deflections were determined. The results are presented and compared under Results and Discussion.

Further verification of the validity of finite element 3-D models of reinforced-concrete components may be demonstrated by comparing the Navier solution for a rectangular plate fixed on all sides results obtained by evaluating a two-way reinforced, fixed concrete slab (Timonshenko, 1959). Load deflection behaviour, stress and distribution, two important results obtained from the model, were compared to values deduced from the linear hand calculation of the fixed slab.

The concrete slab tested had a length, a of 5 m (16.4 ft), a width, b of 5 m (16.4 ft), and a thickness, t of 250 mm (7.87 in); uniformly distributed load w of 12 kN/m^2. The properties of the concrete were the same as those used in the previous simple beam example. The cast-in-place test slab was fixed at its edges.

The success of this analytical model will serve as a precursor to subsequent research of bridge deck analysis.

2.3   DESIGN CONSIDERATION

The structure selected for this work is a four-span continuous T beam bridge (precast) along Karu Road, Abuja-Nigeria. The bridge has a length of 50 m spanning 10 m, 15 m, 15 m and 10 m, and a width of 12.5 m. The doubly reinforced concrete deck is supported by five main girders with a spacing of 2.25 m. For convenience, the girders were labelled A through E. Figure 1 shows a plan view of the deck, which details general dimensions and the spacing of the girders. In order to effect better load distribution cross girders are provided along the transverse direction of the bridge with spacing 5.0 m. The spans from right to left are labelled Span 1 through 4. The cast-in-place T beam bridge deck is made of 24 kN/m^3 concrete and 22 kN/m^3 wearing coarse, with the deck having longitudinal and transverse reinforcement in both the top and bottom. Figure 2 shows the cross section of the bridge, including the main girders, cross girders, footway, and parapets. The main girders are supported by elastomeric bearing resting on a coping bed carried by three piers of equal spacing. Parapets are located on either side of the roadway, are constructed of precast concrete and are fastened to the reinforced concrete deck. Footways are provided at each end of the road made of kerbs and concrete.

Bridge Dimensions:

Clear width of roadway = 12.5 m

Span (centre to centre of bearings) = 10 m, 15 m, 15 m, 10 m = 50 m

Average thickness of wearing coat = 100 mm

Cross section of Deck:

Five main girders are provided at 2.35 m centres.

Thickness of deck slab = 225 mm

Width of main girders = 300 mm

Depth of main girder = 1625 mm

Footway 1200 mm wide by 250 mm deep is provided.

Cross girders are provided at every 5 m interval.

Breadth of cross girder = 300 mm.

The depth of cross girder is taken as equal to the depth of main girder to simplify the computation.
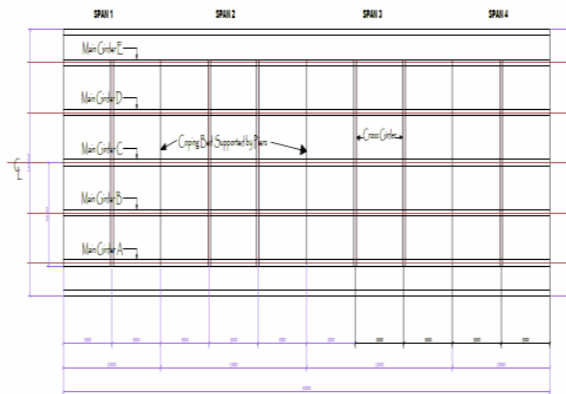
Figure 1: Plan View of 4-Span T-Beam Bridge
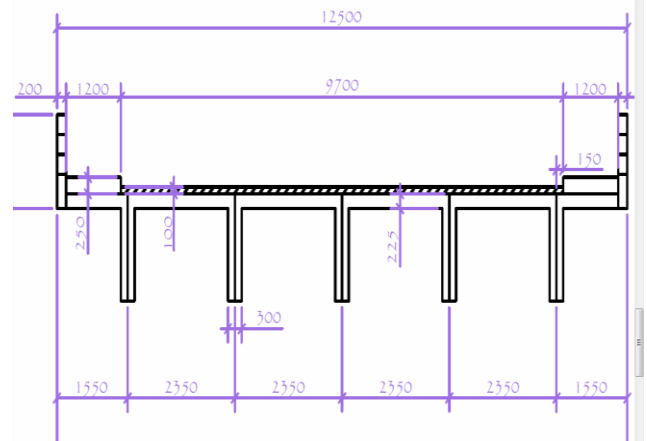
Figure 2: Cross-Sectional View of 4-Span T-Beam Bridge

The material properties of the concrete used for the construction of the bridge by the contractors are reproduced in Table 1 below.

TABLE 1: MATERIAL PROPERTIES, C35/45

Parameter	Description	Value
f_{cu}	Compressive strength of concrete	45 MPa
E_{CM}	Modulus of Elasticity	34077 MPa
γ	Poisson ratio	0.2
ρ	Density	2400 kg/m^3

2.4 LOADING AND BOUNDARY CONDITIONS

The non-composite finite element beam and slab deck bridge models are subjected to the deck load in addition to the permanent self-weight of the deck bridge. The beam element ANSYS models of the bridge is analyzed with boundary conditions using bearings modelled as simply supports at the abutment and piers. In carrying out with the analysis of the T beam bridge the following standards were used for guidance.

BS 8110: Design of Reinforced Concrete Structures.

BS 5400 Part: Loadings for the Design of Bridges

BD37/01: Use of BS 5400:2

These standards laid out the specifications for dead and live loads and their applications on the bridge. It is important to note that Load combination

1 is adopted for analysis of the bridge as provided by BS 5400 and BD 37/01.

2.5 LINEAR ANALYSIS (HAND CALCULATION)

Dead Load

The dead load analysis for ultimate shear force, maximum bending moment and their corresponding diagrams was deduced using:

- The Moment Distribution
- Influence Line Method.

Live loads (Primary)

Standard highway loading consists of HA and HB loading where both loading include impact given by BD37/01.

- HA loading – loading that represent normal traffic
- HB loading – abnormal vehicle unit loading

Clause 6.1.1 states that the structure and its element shall be designed to resists the more severe effects of either:

a) design HA loading, or

b) design HB 30 or 45 units loading, or

c) design HA loading combined with design HB 30 units loading.

The HA loading consist of uniformly distributed load UDL provided by clause 6.2.1 and Table 13 of BD 37/01and a Knife edge load, KEL of 120kN by clause 6.2.2 along the loaded length of the bridge.

Clause 6.3 provides the HB loading, herein 30 units of loading.
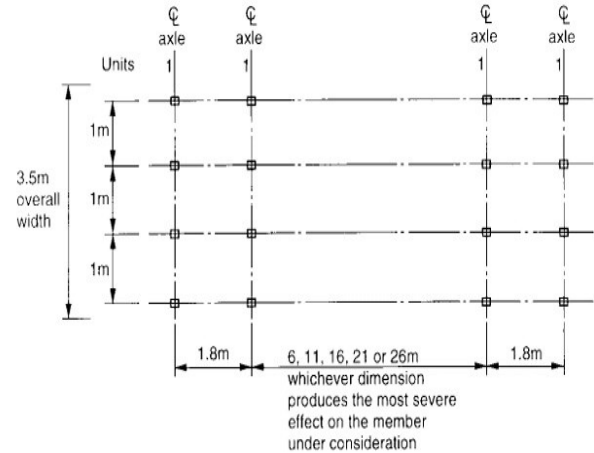
Figure 3: HB Vehicle

Clause 6.4 of BD37/01 provides the applications of live loads. For a carriageway width between 7.5 m to 10.95 m the notional lane is three as provided by clause 3.2.9.3.1 of the code.

The analysis of the bridge due to primary live loads was done using Influence Line Diagram (ILD) of the statically indeterminate beam due to unit load acting along the span under consideration.

Note:

Moment for HB $= \gamma_{FB}$ x 30 units load x sum of y-coordinates of each wheel (2)

Moment for HA UDL $= \gamma_{FA}$ x UDL x area under it on ILD (3)

Moment for HA KEL $= \gamma_{FA}$ x KEL x max. y-coordinate (4)

Where design factor for HB loading, $\gamma_{FB} = 1.3$ and

design load factor for HA loading, $\gamma_{FA} = 1.5$.

3 RESULTS AND DISCUSSION

The results of the analysis are presented below.

3.1 VERIFICATION OF ANSYS

In order to verify the software ANSYS 16.0 as an effective tool for performing the FEM modelling two simple members were modelled as earlier explained in 2.2.1 and the results are presented below.

Simply Supported Beam

The Nigerian Society of Engineers
Minna Branch
1st NSE Minna Branch National Conference 2021

Conference theme
Role of Engineering in
Sustainable Development Goals

Using the description in 2.2.1, by linear methods

a) Reactions

$$R_A = R_B = \frac{wl}{2} \qquad (5)$$

$$= \frac{62.2 \times 6.1}{2} = 189.71 \; kN$$

b) Shear Force, Fv

$$F_V = \frac{wl}{2} \qquad (6)$$

$$= \frac{62.2 \times 6.1}{2} = 189.71 \; kN$$

c) Maximum Bending Moment, Mmax

$$\delta M_{max} = \frac{wl^2}{8} \qquad (7)$$

$$= \frac{62.2 \times 6.1^2}{8} = 289.31 \; kNm$$

d) Deflection, δ

$$\delta_{max} = -\frac{5wl^4}{384EI} \qquad (8)$$

$$= -\frac{5 \times 62.2 \times 6100^4}{384 \times 30500 \times 5.4613 \times 10^9}$$

$$= -6.7321 \; mm$$

e) Maximum Bending Stress, σ_{max}

$$\sigma = \frac{Mmax}{Z} \qquad (9)$$

But modulus of the section, $Z = bh^2/6 = (250 \times 640^2)/6 = 1.7067 \times 10^2 \; mm^3$

$$\sigma = \frac{289.31 \times 10^6}{1.7067 \times 10^7} = 16.9518 \; N/mm^2$$

Results as deduced using ANSYS are shown from Figures 4 through 6;
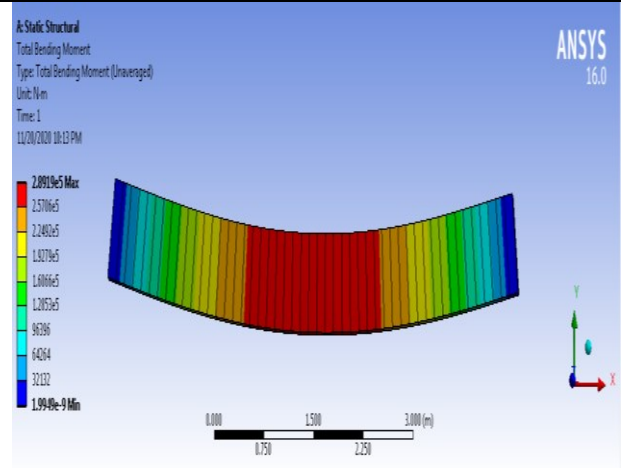
Figure 4: Bending moment of simply supported beam
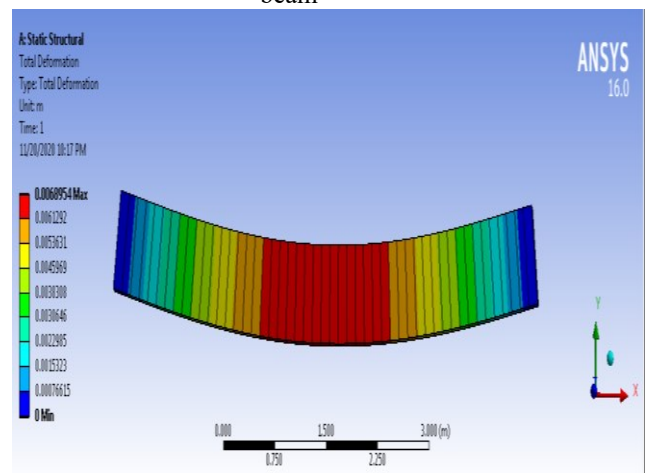
Figure 5: Stress deformation of simply supported beam
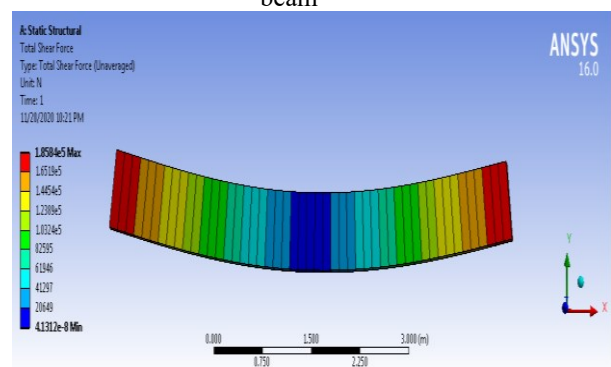
Figure 6: Sheer Force of simply supported beam

Conference theme

Role of Engineering in Sustainable Development Goals

The results of the hand calculation above are compared with finite element analysis computed using ANSYS presented in Table 2.

TABLE 2: VERIFICATION OF SIMPLY SUPPORTED BEAM

	Hand Calculation	ANSYS	% Diff.
Reactions, R_A, R_B (kN)	189.71	189.71	0.00
Shear Force, Fv (kN)	189.71	188.84	0.46
Maximum Bending Moment, Mmax (kNm)	289.31	289.19	0.04
Deflection, δ (mm)	- 6.7321	-6.8954	2.43
Max. Bending stress, σmax (N/mm²)	16.9518	16.9450	0.04

Fixed Slab

Using the description in 2.2.1, the slab was manually calculated using the Navier's solution for thin rectangular plates fixed at all the edges.

Using the Navier's solution

a) Maximum deflection/directional deformation, δ

$$\delta \max(at\ centre) = \frac{0.0284wa^4}{Et^3\left(1.056\left(\frac{a}{b}\right)^5 +1\right)} \quad (10)$$

$$= \frac{0.0284 \times 0.012 \times 5000^4}{30500 \times 250^3\left(1.056\left(\frac{5000}{5000}\right)^5 + 1\right)}$$
$$= 0.2174\ mm$$

b) Maximum bending stress, σmax

$$\sigma_{max} = \frac{wa^2}{2t^2\left(0.623\left(\frac{a}{b}\right)^2 +1\right)} \quad (11)$$

$$= \frac{0.012 \times 5000^2}{2 \times 250^2\left(0.623\left(\frac{5000}{5000}\right)^2 + 1\right)}$$
$$= 1.4787\ N/mm^2$$

Similarly, using same slab description the results as deduced using ANSYS are shown from Figures 7- 8;
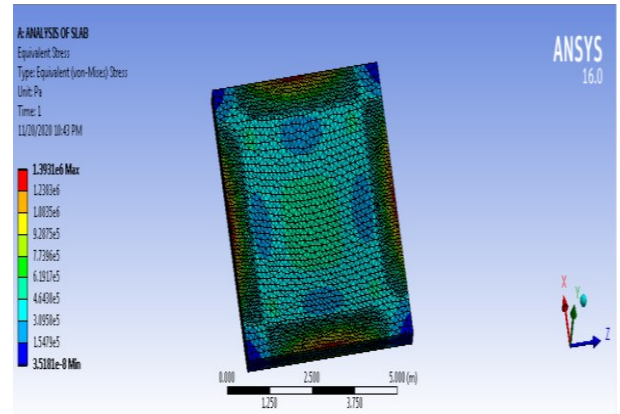
Figure 7: ANSYS Max. Stress of Fixed Slab
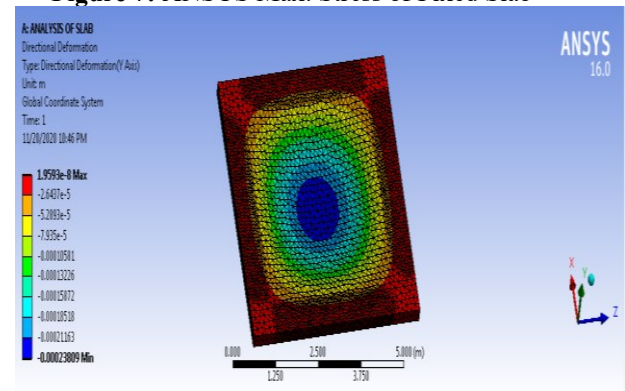
Figure 8: ANSYS Max. Deflection of Fixed Slab

The results of the hand calculation above are compared with finite element analysis computed using ANSYS presented in Table 3 below.

TABLE 3: VERIFICATION OF FIXED SLAB

	Hand Calculation	ANSYS	% Diff.
Deflection, δ (at centre) (mm)	0.2174	0.1959	9.89
Max. Bending stress, σmax (N/mm²)	1.4787	1.3931	5.79

3.2   DEAD LOAD OF T-BEAM BRIDGE

Using BS 5400 loadings, the dead load on the bridge was analysed using moment distribution

method with reference from the left support and presented in Figures 9-12.
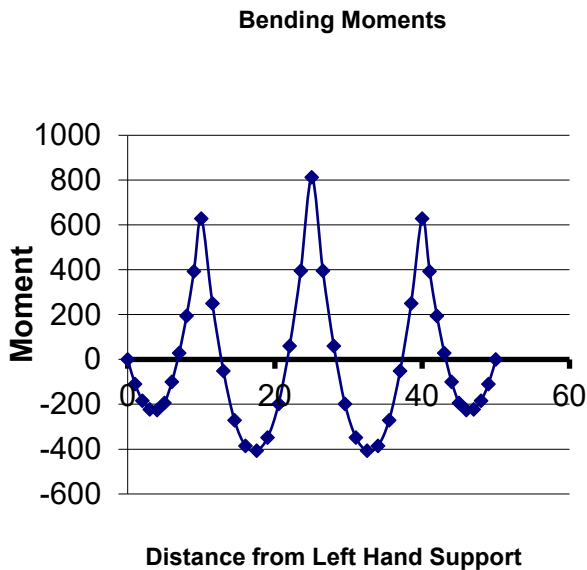
Bending Moments

Figure 9: Bending Moment Diagram for Interior Main Girder (kNm)
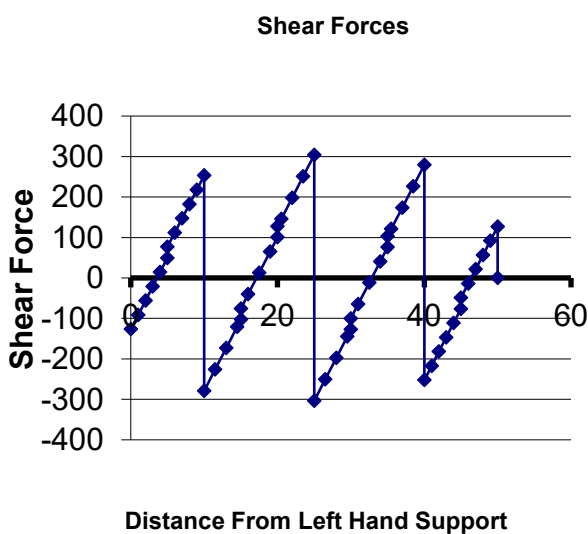
Shear Forces

Figure 10: Shear Force (kN) Diagram for Interior Main Girder
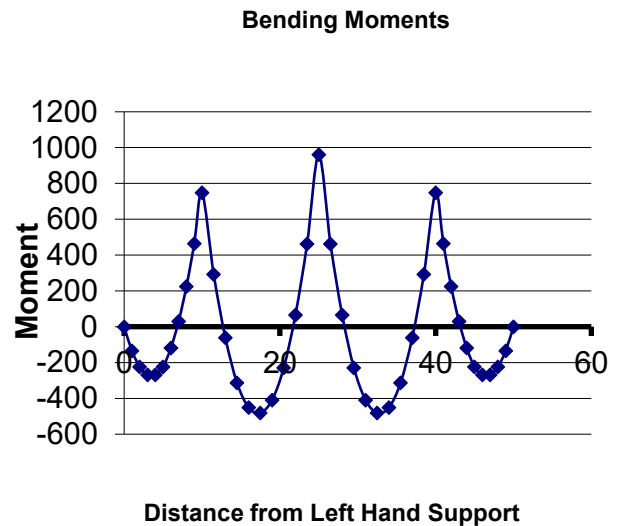
Bending Moments

Figure 11: Bending Moment Diagram for Exterior Main Girder (kNm)
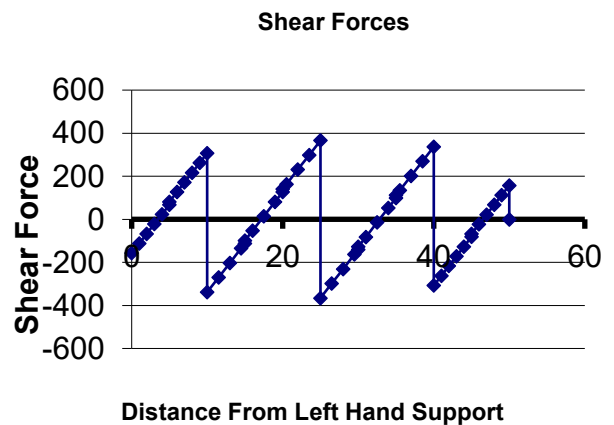
Shear Forces

Figure 12: Shear Force (kN) Diagram for Exterior Main Girder

The dead load of the bridge was also analysed using ANSYS presented from Figures 13-16 as follows;
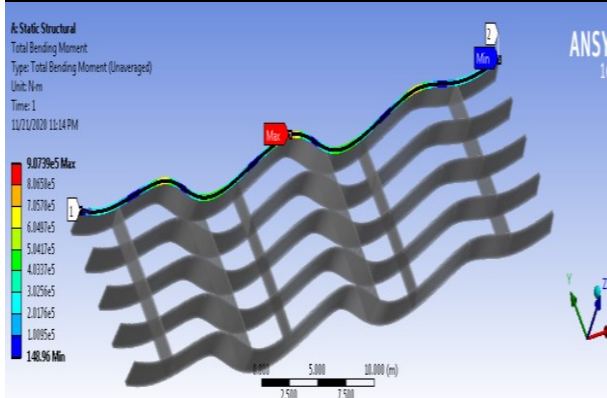
Figure 13: ANSYS Max. Bending Moment of External Girder Due to Dead Load

Figure 14: ANSYS Max. Bending Moment of Internal Girder Due to Dead Load
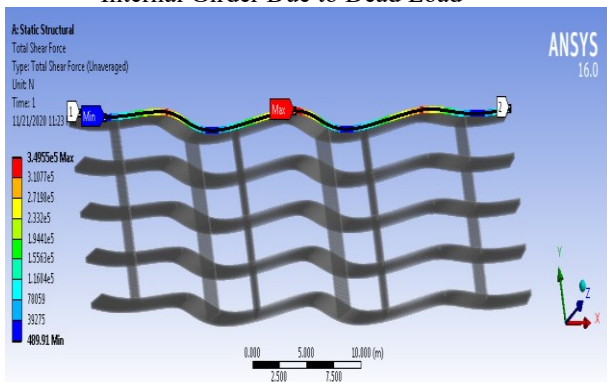
Figure 15: ANSYS Extreme Sheer Force of External Girder Due to Dead Load

Figure 16: ANSYS Extreme Shear Force of Internal Girder Due to Dead Load

The results of the linear (hand calculation) and FEM using ANSYS are compared as shown in Table 4 below.

TABLE 4: RESULT OF DEAD LOAD OF T-BEAM BRIDGE

	Hand Calculation	Position	ANSYS FEM	% Diff.
External Girder				
Max. Moment	965.91 kNm	Support 3	907.39 kNm	6.06
Extreme Shear Force	365.85 kN	Span 2	349.55 kN	4.46
Internal Girder				
Max. Moment	868.83 kNm	Support 3	853.58 kNm	1.76
Extreme Shear Force	323.72 kN	Span 2	314.99 kN	2.70

3.3 LIVE LOAD OF T-BEAM BRIDGE

Using BS 5400 loadings, the live load on the bridge was analysed using moment distribution method and influence line method. HB Vehicles with standard wheel spacing (6m, 11m, 16m, 21m, 26m; see figure 1) were analysed. However, maximum bending moment for the most severe scenario is presented in this paper.

Span 2 (Severe Max. Sag Moment)
Using Moment Distribution method due to unit load the live load was calculated using Influence Line Diagram (ILD) as seen in Figure 1 below.

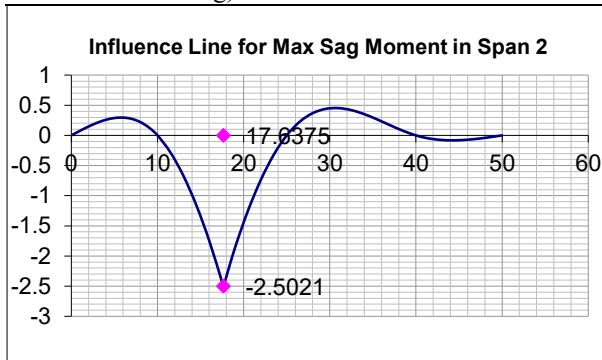|	Hand Calculation	Position	ANSYS FEM	% Diff.
Max. Sag Moment	1776 kNm (HB loading)	Span 2	1698 kNm	4.39
Max. Hog Moment	1890 kNm (HB loading)	Support 3	1813 kNm	4.07

Figure17: ILD for Max Sag Moment in Span 2

The critical application of HB loading with the most severe effect is for wheel spacing 6 m apart.

Maximum sagging moment due to HB loading:

M = 1.3 x 30 x 10 x (0.0849 + 0.3987 + 2.5021 + 1.4923) = **1776 kNm** (HB critical)

Support 3 (Severe Max. Hog Moment)

Using Moment Distribution method due to unit load the live load was calculated using Influence Line Diagram (ILD) as seen in Figure 18 below.
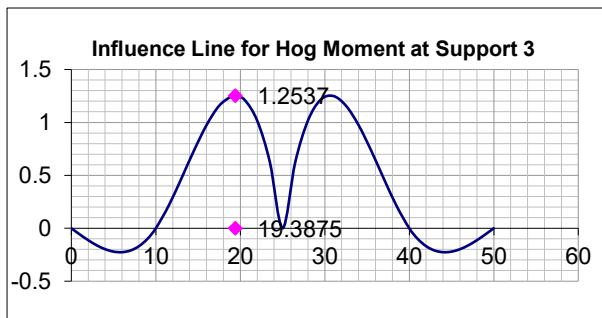
Figure 18: ILD for Max Hog Moment at Support 3

The critical application of HB loading with the most severe effect is for wheel spacing 11 m apart.

Maximum hogging moment due to HB loading:

M = 1.3 x 30 x 10 x (1.148 + 1.2537 + 1.2491 + 1.1950) = **1890 kNm** (HB critical)

TABLE 5: Result of live load of t-beam bridge

The live load of the bridge was analysed using ANSYS Transient (moving) structural as shown in Figures 19 and 20 as follows;
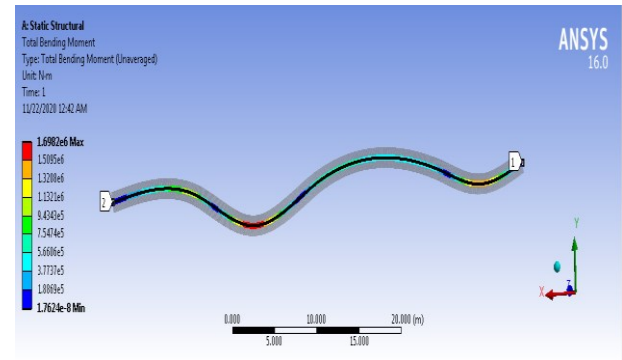

Figure 19: ANSYS Max. Sag Moment of Severe Case (6m Wheel Spacing) Span 2 Due to Live Load
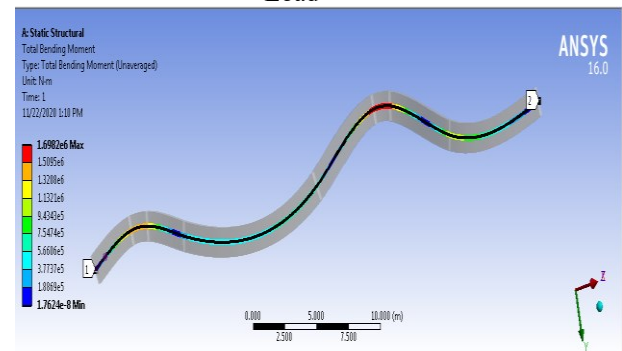

Figure 20: ANSYS Max. Hog Moment of Severe Case (11m Wheel Spacing) Support 3 Due to Live Load

The results of the linear (hand calculation) and FEM using ANSYS are compared as shown in Table 5 below.

4 CONCLUSION

A 4-span T-beam bridge was analysed by using British Standard (BS 5400; BS 8110) specifications and Loading (dead load and live load) as a one

dimensional structure. Finite Element analysis of a three- dimensional structure was carried out using ANSYS 16.0 software. Both models were subjected to BS 5400:2 Loadings to produce maximum bending moment and extreme shear force. The results were analyzed and it was found that the results obtained from the finite element model are lesser than the results obtained from one dimensional analysis, signifying that the results obtained from linear methods of BS 5400 loading are conservative and FEM gives economical design.

The advantage of the approach used in this paper is time saving, economical and user safety. Also, various material properties can easily be defined using the FEM software, with the modal analysis behaving like an actual bridge in three dimensional form, giving simulation results that are quite close to exact solution.

REFERENCES

Alpesh, J. & Vyas, J. N. (2016). Modal Analysis of Bridge Structure Using Finite Element Analysis. *IOSR Journal of Mechanical and Civil Engineering,* Volume 13, Issue 4, pp 06-10.

Ashour, A.F., & Morley, C.T. (1993). Three-dimensional Nonlinear Finite Element Modeling of Reinforced-Concrete Structures. Finite Elements in Analysis and Design, 15: 43-55.

BS 5400: Part 1, 1978. General Statement "Steel,Concrete and Composite Bridges".

BS 5400: Part 2: 1978. Specification for Loads "Steel, Concrete and Composite Bridges".

BS 5400: Part 1- 4: 1990. Code of Practice for Design of Concrete Bridges "Steel, Concrete and Composite Bridges".

BS 5400: Part 5: 1979. Code of practice for design of composite bridges "Steel, Concrete and Composite Bridges".

BS 5400: Part 6: 1999. Specification for material and workmanship, "Steel, Concrete and Composite Bridges".

BS 5400: Part 7: 1978. "Specification for materials and workmanship, concrete, reinforcement and prestressing tendons".

BS 5400: Part 8: 1995. "Recommendations for materials and workmanship, concrete, reinforcement and presetressing tendons".

BS 8110: Part 2: 1985. Design of Reinforced Concrete Structures, "Structural Use of Concrete".

British Design Manual (2001): BD 37/01 Volume 1, Section 3, Part 14, Loads for Highway Bridges "Design Manual for Roads and Bridges".

Chowdhury, M.R. (1995). Further Considerations for Nonlinear Finite-Element Analysis. *Journal of Structural Engineering*, 121: 1377-1379.

Darwin, D. (1993). Reinforced Concrete in Finite Element Analysis of Reinforced-Concrete Structures II: *Proceedings of the International Workshop*. New York: American Society of Civil Engineers, pp. 203-232.

Huria, V. (1993). Nonlinear Finite Element Analysis of RC Slab Bridge. *ASCE Journal of Structural Engineering,* 119(1): 88-107.

Onyia, M. E. (2008). A Finite Element Model for the Analysis of Bridge Decks. *Nigerian Journal of Technology*. Volume 27, No 1.

Sheedhar, R. & Spruti, M. (2012). Analysis of T-beam Bridge Using Finite Element Method. *International Journal and Innovative Technology.* Volume 2, Issue 3.

Conference theme

Role of Engineering in Sustainable Development Goals

Automatic Radio Selection for Data Transfer in Device to Device

C. E. Igbokwe[1], S. Bala[2], M. David[3], and E. MICHAEL[4]

[1,2,3,4] Department of Telecommunication Engineering,

Federal University of Technology Minna – Nigeria.

[1]igbokwe.pg825544@st.futminna.edu.ng, [2]salbala@futminna.edu.ng,

[3]mikeforheaven@futmina.edu.ng, [4]electmike84@gmail.com

ABSTRACT

Over the years, as technology evolves in telecommunication, the choice of the kind of radio to be use for data transfer in a multi radio system at a particular time still remains a challenge especially in D2D communications. This is evident in popular user equipment's such as phones where multiple radio systems such as Bluetooth, WiFi and GSM are present. Despite all these radios in place, the selection of these radios has always been done manually by users which often time, is time wasting before instantaneous data transfer and sometimes fail due to unsimilar radio selection which leads to unsimilar channel operation of the two devices. To mitigate this and to have a smarter system, there is need for D2D to be able to automatically select radio for data transfer based on certain yardstick. One of such yardsticks remains area of coverage as different have different rage of coverage area.to this end, this research presents AUTOMATIC RADIO SELECTION FOR DATA TRANSFER FOR D2D DEVICE. This was used via the use of GPS module, Bluetooth device, Lora module and an Arduino Nano. At the end of the research, the radio selection was possible but with error in distance measurement.

KEYWORDS: *Automated radio selection, Bluetooth, Device discovery, device to device communication, LoRa.*

1   INTRODUCTION

Although, the requirements for the next generation of communication systems referred to as 5G, are still debated by the academics and the industry, fairly broad consensus has been reached pertaining few key requirements such as 1 millisecond end to end round trip delay latency, 1000x bandwidth per unit area, 10-100x number of connected devices, up to 10 years battery life for low power/machine-type devices [1]. Apart from the inevitable increase in bit rates, energy efficiency of the system, the excessive increase of multimedia applications such as High definition (HD) movies, mobile gaming, multimedia file sharing, video conferencing, the requirements agreed to has triggered a rapid advancement in cellular communication and its technology. To aid further development, one of the emerging technologies known as Device to device (D2D) communication, has been proposed to bridge the gap between communicating devices [2]. For instance, in isolated regions, the current networks may offer some level of Quality-of-Service (QoS), but they cannot meet the extreme capacity demands on future wireless systems in areas where they have to handle situations where users are located in close proximity to one another, such as residential environment, stadiums, shopping malls, and even open-air-festivals. These environments are crowded with devices that access the Internet often simultaneously; most (if not all) of them could interconnect and exchange data locally, thus assisting in a better offloading. Instead, currently this usage results in large traffic volumes impacting both the network operation, as well as pricing models [3]. This improves cellular coverage, increases resource utilization and reduces latency [4]. This technology allows devices in close proximity to communicate using a direct link rather than having their radio signal traveling through the base station (BS) [5]. The benefit however, is ultra-low latency due to its short signal traversal path. To achieve the implementation of this D2D technology, various short-range wireless technologies like WiFi direct, Bluetooth and LTE (defined by the Third Generation Partnership Project (3GPP) standardization) is often time suggested [5],[6]. However, it is important to note that these D2D supporting technologies differs in device discovery mechanisms, data rates and coverage distance. Bluetooth as observed by [4] supports a maximum data rate of 50Mbps and a coverage range close to 10m. WiFi direct has data rate of 250Mbps and coverage range of 200m, while, LTE direct has data rates of 13,5Mbps and coverage range of 500m [4]. All these mentioned technologies are

characterized by short-range and consumes energy. However, this may not be applicable to scenarios with larger coverage area. According to [7] LORA (long range radio is characterized with capability to cover 30km surpassing the already mentioned supporting D2D technologies. Furthermore, it is observed that the D2D already in existence usually employ all these supporting technologies manually. In other words, the operator will have to select the technology he or she wishes to use for communication. To improve device discovery in D2D with scenarios of large coverage area, without expending much energy and having the ability to automatically selects the technology to be used for data transfer based on the area of coverage, this research presents Automatic radio selection for data transfer in D2D.

Automated radio selection in D2D has been an issue. In the time past people manually select which radio to use for data transfer in their D2D. this manual selection results to waste of time often regarded as latency in the processes of data transfer. Furthermore, the process involved in initiating data transfer may be regarded as unsmart. All these ills are what necessitated this research. The objective of these study is to

1. Design the hardware of the D2D system
2. Implementation of hardware system

The study will look at establishing an Automatic radio selection for data transfer in D2D device with distance as the yard stick.

2   LITERATURE REVIEW

2.1   D2D DISCOVERY AND CONTROLS USING BLUETOOTH

Over the years D2D has been researched into to achieve cheaper means of data transfer. Bluetooth also known as Bluetooth Low-Energy (BLE), because of its short-range characteristics, was one of the earliest supporting technologies used in D2D. The BLE which operates on the spectrum range of 2.4-2.4835 GHz of the ISM band is designed to provide communication at low power [8]. With this understanding, [9] tracked device in a cooperate building using Bluetooth indoor positioning service (BIPS). The concept which involves the collection of Bluetooth devices that can communicate with each other by sharing a common channel called piconet was used. In his presentation, every mobile BIPS user

is represented on a handheld device equipped with Bluetooth for interacting with a static device. [10], presented a scheme based on carrier sensing in a self-organized BLE network in an effort to avoid collisions during advertisement. This was done so as to achieve lower latency and low energy consumption during the process of discovery in crowded BLE networks. [11] focused on a Bluetooth based automated home using a cell phone. The model was designed on a standalone Arduino BT board and the home appliances are connected to the input/output ports of this board via relays. The Bluetooth based home automated system is designed to be a low cost but yet scalable, allowing variety of devices to be controlled with minimum changes to its core. [12], presented a voice-controlled wheel chair for the physically challenged person, where the voice command controls the movements of the wheelchair. The voice command is given through a cellular device having Bluetooth and the command is transferred and converted to string by the BT voice control for Arduino and is transferred to the Bluetooth Module SR-04 connected to the Arduino board for the control of the wheelchair. [13] developed an android application used as a remote to control the motion of a RC car. The mobile device harboring the android application acts as the car's remote control. The communication between the android application and the controller is enabled by Bluetooth. Another study presented by [14], focused on Blue-Fi, a system that predicts the availability of Wi-Fi connectivity by using a combination of Bluetooth contact patterns and cell tower information. This allows the device to intelligently switch the Wi-Fi interface on only when there is Wi-Fi connectivity available. Therefore; avoiding the long periods in idle state and significantly reducing the number of scans for discovery. [15], in another study presented a water level monitoring and controlling system using Bluetooth in agriculture. A number of sensors were deployed for detecting the water level from testing the soil, and report the detail to farmer's mobile phone. The water level was calculated in digitally and it was displayed on the mobile application in the smart phone. The electric water pump is controlled by the smart phone via Bluetooth.

2.2 LTE D2D DISCOVERY.

The last decade has experienced growth in both the amount of mobile broadband traffic and the user demand for faster data access [16]. Considering that the current 4G technology cannot satisfy the present communication demand and the forthcoming user demand [14], Third Generation Partnership Project (3GPP) developed an enhanced Long-Term Evolution LTE radio interface called LTE-Advanced [17]. [18] modelled two basic scenarios to achieving device discovery using LTE which the first is the broadcasting mode where the device wishing to be discovered broadcasts a message containing its identification information, while devices that want to discover scan and decode the broadcast message and can determine if the device is in its proximity. The second scenario is the Request-Response mode where the device trying to discover another device sends a message containing its identity information to the target device, after the target device is done decoding the message it allows the device trying to be found to discover the target device by configuration, sends a response message to the originating device revealing the proximity. The results of this modelling give efficiency in energy consumption in the first scenario and better interference management. While the request-response mode consumes large energy on the devices if there is no prior information from the discovering device. [19] used LTE as a proximity base to support the Mobile Crowd Sensing (MCS) feature, the MCS feature is installed into smart devices to achieve device discovery. The MCS platform assigns task to participants who are active and generate sensing data. Each task to be completed may include multiple data gathering actions in a given time span within an area of interest; these actions are performed automatically by the MCS app without human interaction (except for initially accepting the task), or may require some active response by the participant. As observed, to provide a detailed user's feedback about an event. The MCS platforms include an MCS server that assigns tasks and gather participants' information from the MCS client app installed on their devices. The result showed efficient location sharing and energy consumption. Limitations was cost of application development and user acceptance. [20], used Timing Advance (TA) to assist the mobile network to determine the distance between two or more devices and they also proposed a direct approach where each device broadcast their discovery signal to determine the other device's location. The result they achieved apart from discovery was efficiency in energy consumption and spectrum utilization. [5] used the parameters of LTE-Advance by introducing the Full Duplex Amplify and Forward (FDAF) Relay Nodes (RNs) to assist cellular network and D2D communication. The result of this experiment was the increase in the coverage probability for both cellular and D2D communication with the relay nodes. [21] proposed a network science approach for adaptive wakeup schedule based on nodes staying asleep when a contact is unlikely to happen and wakes up only when the possibility of successful contact with another node is relatively high. The result was reduction in energy consumption without degrading the performance of the network. In world news, natural disasters occur frequently. [22] takes advantage of 3GPP and D2D communication to help save lives. D2D can be an alternative communication in natural disaster situation with a total or partial absence of network infrastructure. Proposed that a receiver probes all physical resource blocs in a given spectrum band-based LTE networks in order to be able to detect victims. Spreading technique is used when an SOS is transmitted and correlation is analyzed in the receiver side in order to decide whether a victim is using a Resource Bloc to ask for help or not. As well, to multiply the number of receivers in different location to exploit the user's diversity in order to enhance the detection accuracy based on hard information combining. Hence, receivers will cooperate to derive a reliable decision about an SOS transmission. [23] introduced a technique called ROOMMATE which Used the Proximity Based Service (ProSe) to provide the list of available devices and their colocation information and uses the information to help in peering decision process. This model was proposed for a small number of discovery signals and reduce the collision probability of discovery signals.

2.3 WIFI D2D DISCOVERY

The IEEE 802.11 standard for Wireless Local Area Networks (WLANs), commonly known as Wi-Fi [24], has become a choice for short range communication, due to the cost-effective deployment. Its network is implemented in large scale and available for Wi-Fi devices such as smartphones, consumer electronics and industry sensors [25]. In recent time, Wi-Fi direct was released, it' is built upon the IEEE 802.11

infrastructure mode and offers direct, secure and rapid device to device communication. The Wi-Fi direct has become an interesting and suitable technology for communication in several applications [26]. [27], designed a smart home based on the principles of the Wi-Fi technology, embedded the QCA9531 wireless communication module to a STM32F107VCT processor and provided a 5V power for the Wi-Fi wireless module to control the home system through an android platform. The APP user interface contains the welcome interface, login interface, the main interface. Where a user needs to register an account in the APP, set a password and log into the main interface to ensure the privacy of the user. The main interface contains the settings interface and the home control interface. [28], introduced a handheld indoor directory system built on Wi-Fi based positioning techniques. The system consists of three modules, namely mobile phone module, kiosks module and database module. The mobile phone module is the main frontend module which installed on users' mobile devices, whereas the Kiosks and website are to provide supports and maintenances to the main module. User can download maps and application from the Kiosks or website. On the other hand, administrator uses the website to manage the database. The system provides a new way of providing indoor floor directory, which offers capabilities to retrieve customizable information, to navigate interactively, to enable location-awareness computing and most importantly the portability of the directory system. [29], identified several attacks that challenge Wi-Fi Direct based D2D communications. Since pairwise key establishment lies in the area of securing D2D communications, we introduce a short authentication string (SAS) based key agreement protocol and analyze its security performance. The SAS-based key agreement protocol is integrated into the existing Wi-Fi Direct protocol, and implemented in android smartphones. The Wi-Fi Aware was used by some researchers, which enables low power discovery over Wi-Fi and can light up many proximities based used cases. [30] modelled an architecture based on the cellular networks to accommodate non cellular Internet of Things (IoT) devices by device working as relay devices for IoT devices and internet uses. Wi-Fi Aware was also used as a supporting technology for proximity services to discover relay devices. The result of this model reduces energy consumption of devices in IoT.

2.4 LoRa D2D discovery

In recent years, Low-Power Wide Area (LPWA) technologies are becoming popular due to the rapid growth in wireless communication. Supporting technology such as Long Range (LoRa) Technology which is a low-power, low bitrate and wireless technology engaged as an infrastructure solution for Internet of Things [31], [32]. The aim of LoRa is to assess the "worst case" coverage of the technology, by having an estimated number of gateways to cover a city [33]. [34], presented a system used on Internet of Things (IoT). A LoRa based technological platform for the tracking and monitoring of patients with mental disorder. The system consists of the LoRa end device (client side) which is a wearable device attached to the patient, and LoRa gateways, installed in the hospital and other public locations. The LoRa gateways are connected to local server and cloud servers by exploiting both mobile cellular and WiFi networks as the communications media. [35], presented a LoRaWAN tracking system, which is capable of exploiting transmitted packages to calculate the current position without using GPS. This is done using LoRa where the geolocation is calculated applying a multiliterate algorithm on the gateways timestamps from received packages. The whole system consisted of an end-node, four gateways, a server and a java application to store the obtained data in a MySQL database. [36], presented an object tracking system using LoRa, which was deployed on bicycles for location tracking and managing system. The structure is composed of an end device, gateway, server, database and user web and application. For the end device Waspmote is used attached with internal acceleration sensor, GPS sensor and SX1272 of LoRa module. For the gateway, Meshlium is used, which is based on Linux OS, has SX1272 of LoRa Module, and offers Bluemix MQTT API. For the server and database, the data provided by IBM Bluemix and database by Mongo DB are used. IBM Bluemix that serves a role of server, the Broker called IoTF receives data and transfer to Bluemix server. Then the data is saved to Mongo DB, in which data is provided in Cloud form in Bluemix. The Waspmote installed on a bicycle saves data in IBM Bluemix by using gateway and offers services to the mobile APP and website to locate the bicycles. Another study presented by [37], used LoRa for industrial applications compared to the traditional industrial wireless system. With light modifications to the upper layer of LoRaWAN

communication stack. The result of their study shows the feasibility of the approach, which is compatible with the requirements for soft real-time applications in process industry.

All these contributions done by various researchers made contributions on device discovery on D2D with those supporting technologies, which were manually operated. In other words, the operator will have to select the technology he or she wishes to use for communication. To improve device discovery in D2D with scenarios of large coverage area, without expending much energy by designing a sub unit that automatically selects the technology to be used for data transfer based on the area of coverage, this paper presents an Automatic radio selection for data transfer in D2D.

3   METHOD

The section presents the method adopted for the design of the system. This includes hardware and software designs.

3.1   SOFTWARE REQUIREMENT.

To achieve the design of the system, C++ is written on Arduino IDE. The code developed was burned on the controller. Furthermore, for the purpose of presentation in this study, Fritzing was used to achieve the drawing of the design

3.2   HARDWARE ARCHITECTURE

The hardware of the two devices is designed with the architecture shown in Figure 3.1. The battery powered devices consist of a controller which is interfaced with a LoRa radio, Bluetooth module and a GPRS via a multiplexer. The multiplexer is used to expand the universal asynchronous receiver transmitter (UART) communication protocol. Furthermore, the controller is interfaced with an alphanumeric display and a sensor.
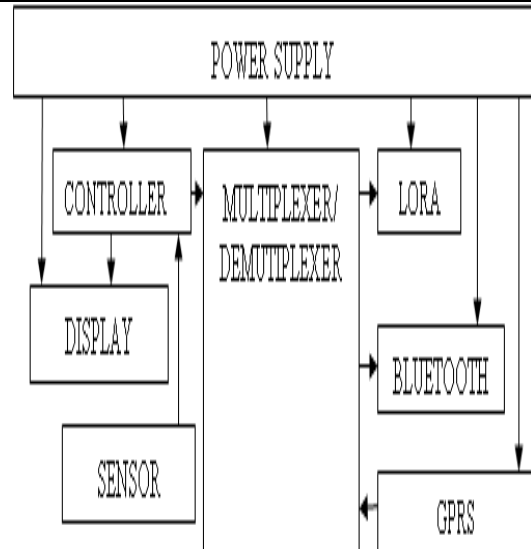

Figure 3.1. Architecture of the system

3.3   POWER SUPPLY

The power supply used in this research consists of two lithium batteries and voltage regulator. The voltage regulators used as shown in Figure 3.2 depends on the voltage requirement of the different devices in the system. According to the data sheet, the controller used needs 3V to 12V to be powered on. Also, the LoRa needs 3.3V which is achieved via the use of LM317 while blue-tooth and the GPRS is powered by 5V regulator. The resistor R1 and RV1 is used to determine the voltage the LM317 outputs. To determine the values of R1 and RV1, the equation (1) is considered

$$V_{out} = 1.25\left[1 + \frac{RV_1}{R_1}\right]$$

(1)

From the datasheet, the voltage at the input must be more than the output voltage by a head voltage. The head voltage as prescribed is 2.5V. Also, the minimum current the regulator can deliver is 10mA. Therefore, to maintain constant reference voltage R1 will be given as

$$R_1 = \frac{1.25V}{10mA} = 120 ohms$$

According datasheet the value of R1 can range from 120Ω to 1kΩ. let the value of R1 in this design be 240Ω. To calculate for RV1

$$V_{out} = 1.25\left[1 + \frac{RV_1}{R_1}\right]$$

$$3.3V + 2.5V = 1.25\left[1 + \frac{RV_1}{240}\right]$$

$$RV_1 = 840 ohms$$

To use a variable resistor one can use 1kΩ which is a little higher than the calculated value.
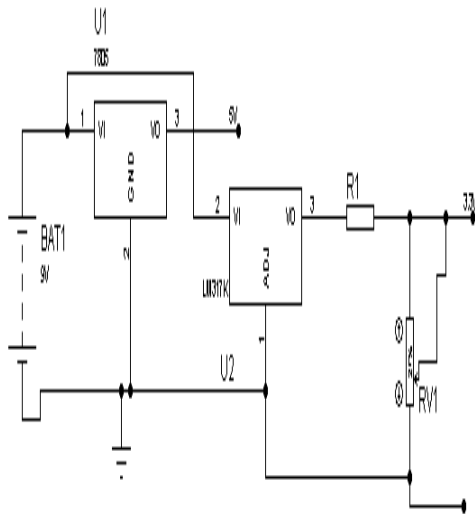

Figure 3.2 Circuit diagram of the power supply

3.4 CONTROLLER:

The controller used in this research is an Arduino Nano. The controller as shown in Figure 3.3 was chosen because of its robust nature as the controller has on board programmer. Furthermore, it is made up of digital input output pins. The controller also has ADC and one UART port which is used to interface the GPS, blue-tooth and the LoRa module.
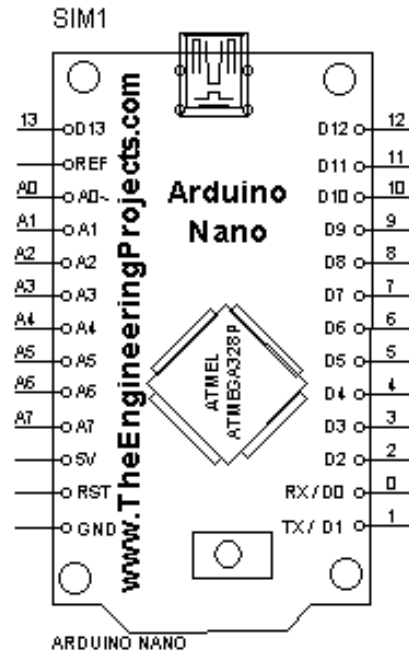

Figure 3.3 schematic representation of the controller

3.5 DISPLAY

The display used in the research is an alpha numeric display. The Liquid crystal display (LCD) 1602 is interfaced with the controller as shown in Figure 3.4 such that the controller communicates with the display via four bits. The number of characters which the LCD displays in total is 32 characters. Sixteen characters are displayed on the upper line and the remaining sixteen on the lower line making 32 characters in total, hence, the name 1602. The display is interfaced to the controller serial port.
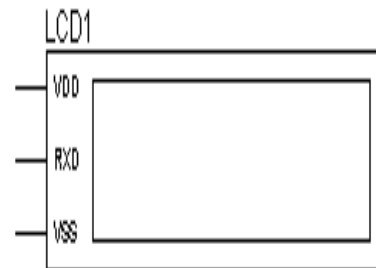

Figure 3.5. circuit description of the display

The Nigerian Society of Engineers
Minna Branch
1st NSE Minna Branch National Conference 2021

Conference theme
Role of Engineering in
Sustainable Development Goals

3.6   SENSOR

The sensor used in this research is a momentary switch (SW). The switch is connected in series with a resistor (R2) as shown in Figure 3.6. This is done to achieve two logics namely logic High which is 5V and logic LOW which is 0V. The LOW logic is achieved when the switch is closed. The reason for the switch in the design is to send a message to the next device.
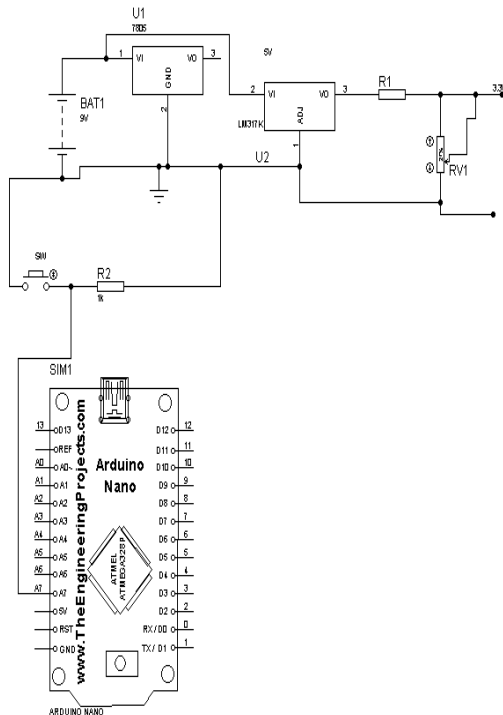

Figure 3.6. circuit diagram of a switch interfaced with the controller

3.7   MULTIPLEXER.

The Multiplexer used is CD4052. The integrated circuit is used to multiplex and de-multiplex signals can be used to select different serial signal channeled to the single serial port of the controller. This is used to interface two devices which are GPS and Bluetooth module which both have Universal Asynchronous Receiver transmitter (UART) port. Figure 3.7 shows the circuit diagram of the multiplexer interfaced with the system.
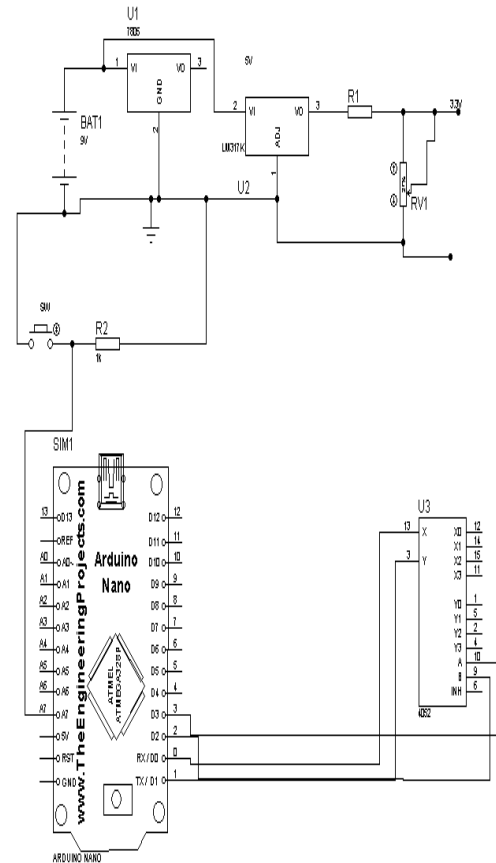

Figure 3.7. Circuit diagram of the multiplexer interfaced with the system

3.8   LORA RADIO

The primary means of communication in this device is the LoRa (long range) module. The module gives the system to communicate in a range of 10km while maintaining low power consumption. The specific LoRa module used is SX1278 which operates at a frequency of 433MHz. Figure 3.8 shows the interface of the of the radio with the system which communicates with the controller via SPI interface

The Nigerian Society of Engineers
Minna Branch
1st NSE Minna Branch National Conference 2021

Conference theme
Role of Engineering in
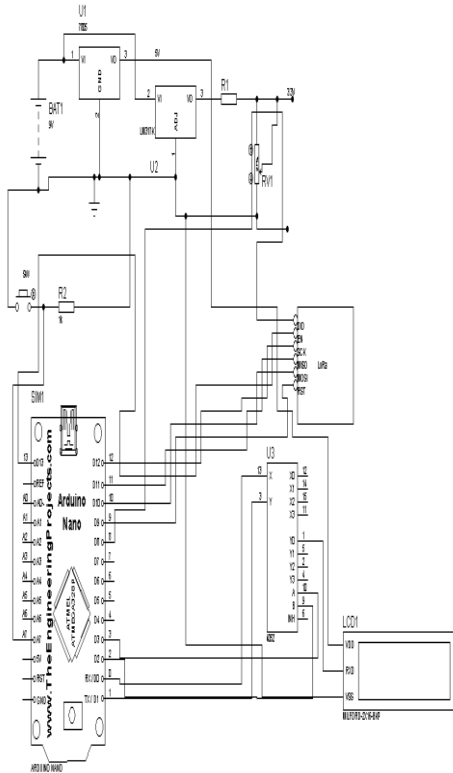Sustainable Development Goals

Figure 3.8. Circuit diagram of the system
interfaced with LoRa.

3.9   BLUETOOTH

The Bluetooth device used is HC05. This is used
in the system so as to aid short distance
communication. The blue-tooth which is interface
with the controller via UART port is powered with
5V. Figure 3.8 illustrates the interconnection of the
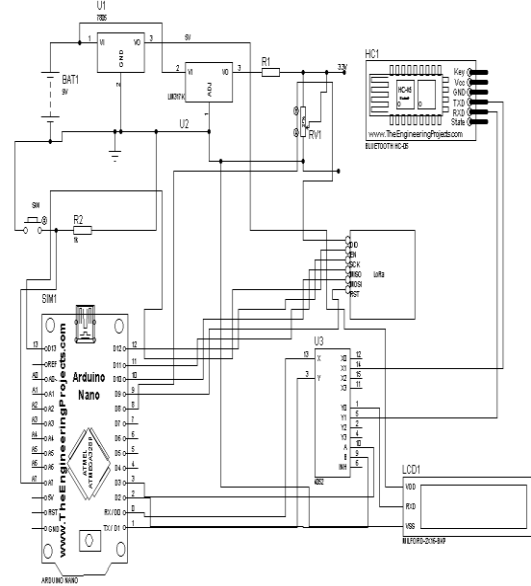device with the system

Figure 3.8 Circuit diagram of the system
interfaced with the Bluetooth radio.

3.10   DISTANCE MEASUREMENT VIA GPS MODULE

The GPS module used in the system was used to
calculate the distance between two devices. This is
achieved via the use of the longitude and the latitude
of the location where the device is. The transmitting
device will take its location and send it to the
receiving device with a request to send using the
LoRa communication. In the request to send is the
location. The receiving device will use this to
determine its distance from the transmitter. Then
advice the system to transmit using LoRa or any other
radio depending on the distance.

Here is the formula for calculating the distance:
The mean circumference of the earth is
$2 \times 6,371,000m \times \pi = 40,030,170m$

$\Delta d \, (lat) = 40,030,170 \times \Delta\Theta \, (lat) \, / \, 360$
(assuming $\Delta\Theta$ is small)

$\Delta d(long) = 40,030,170 \times \Delta\Theta(long) \times \cos\Theta m \, / \, 360$
(Θm: mean latitude between two positions)

Now, the distance is $\sqrt{[\Delta d \, (lat)^2 \, \Delta d \, (long)^2]}$

The Nigerian Society of Engineers
Minna Branch
1st NSE Minna Branch National Conference 2021

Conference theme
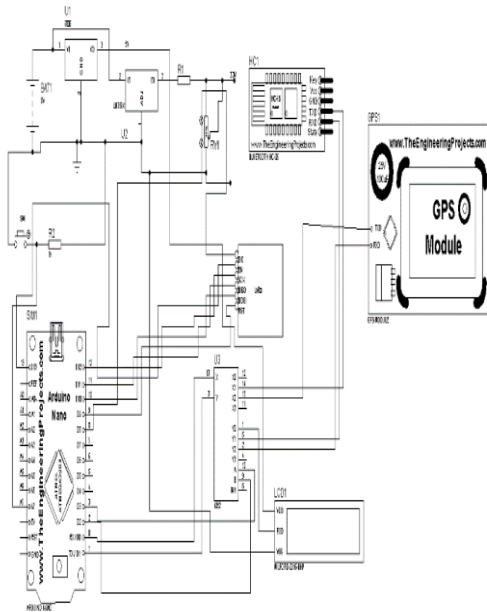Role of Engineering in
Sustainable Development Goals

Figure 3.9 complete circuit diagram of the device

4. RESULTS

As stated earlier we designed an Automated radio selection for data transfer in D2D and tested the distance and which radio it selects automatically for connectivity. Table 4.1 shows us the distance we measured, actual distance measured and the error in distance. Also showed which radio is selected at a certain distance. The result shows us an 87.5% accuracy in radio selection.

Table 4.1 Error in Distance and Error in selection.

S/N	Distance Measured (m)	Actual Distance (m)	Error in Distance (m)	Radio Selected	error in selection
1	1.3	1.28	0.08	BT	Nil
2	3.6	3.54	0.14	BT	Nil
3	5.4	5.5	-0.1	BT	Nil
4	7.7	7.65	0.15	BT	Nil
5	9.9	9.87	0.17	BT	Nil
6	10.13	10	0.13	BT	Error
7	11	10.95	0.05	LoRa	nil
8	12.4	12.2	0.2	LoRa	nil

4.1. CONNECTIVITY

We used an Android smart phone to estimate the time taken to for a device to connect with another from point blank (when the user selects the radio on the device) to when Bluetooth connectivity is achieved. Table 4.2 shows us the time of operation establish connectivity by Bluetooth.

Table 4.2 time of operation on a manually controlled smart phone.

DEVICE SPECIFICATION: RAM – 1GB		
S/N	Trial	Time of operation
1	1	8sec
2	2	5.5sec
3	3	7sec
4	4	6sec
5	5	5.5sec

Table 4.3 shows us the time of operation of our D2D system. We estimated the time taken for our D2D to establish connection from the moment it requests to send till the connection has been established. This active D2D system will initiate a connection via the use of LoRa, then determines the longitude and latitude of the receiving device whose initial reception state is also on LoRa. The receiving device receives the packet, it then takes its longitude and latitude and determine the distance between its device and the Device 1. After that, it sends an acknowledgement to connect and then based on the distance, the radio to be used for communication. Device 1 getting the information will turn off the LoRa (if the distance between the two devices is less than 10m, and if the distance between the devices is more than 10m the Bluetooth will stay off) and use the suggested radio. Note that receiving device has already switch to the radio it advised. Table 4.3 in comparison to Table 4.2 shows that the time taken for connectivity is less in the automated D2D.

Table 4.3 time of operation on the automated device.

DEVICE SPECIFICATION: Our D2D		
S/N	Trial	Time of operation
1	1	6sec
2	2	4sec
3	3	4.5sec
4	4	5sec
5	5	4sec

5. CONCLUSION

In conclusion, the Automated D2D system discovered and established communication automatically between devices in respect to the distance and which radio is best for such communication, i.e. If the device is within the Bluetooth range (0-10m) it connects or as far as the LoRa (10km) range as well, and with lesser time taken compared to a manually controlled smart device.

REFERENCES

Ananthanarayanan, Ganesh, and Ion Stoica. 2009. "Blue-Fi : Enhancing Wi-Fi Performance Using Bluetooth Signals."

Anastasi, Giuseppe et al. 2003. "Experimenting an Indoor Bluetooth-Based Positioning Service." : 480–83.

Asadi, Arash et al. "A Survey on Device-to-Device Communication in Cellular Networks." : 1–18.

Augustin, Aloÿs, Jiazi Yi, Thomas Clausen, and William Mark Townsley. 2016. "A Study of LoRa : Long Range & Low Power Networks for the Internet of Things." : 1–18.

Bellalta, Boris, Luciano Bononi, Raffaele Bruno, and Andreas Kassler. 2015. "Current Status , Future Directions and Open Challenges." *Computer Communications*: 1–25. http://dx.doi.org/10.1016/j.comcom.2015.10.0 07.

Benedetto, Jacopo De, Paolo Bellavista, and Luca Foschini. 2017. "Proximity Discovery and Data Dissemination for Mobile Crowd Sensing Using LTE Direct." *Computer Networks* 0: 1–12. http://dx.doi.org/10.1016/j.comnet.2017.08.00 2.

Burghal, Daoud, Student Member, and Arash Saber Tehrani. "Base Station Assisted Neighbor Discovery in Device to Device Systems."

Centenaro, Marco, Student Member, Lorenzo Vangelista, and Senior Member. 2016. "Long-Range Communications in Unlicensed Bands : The Rising Stars in the IoT and Smart City Scenarios." (October): 1–8.

Ding, Jie, Tian-ran Li, Xue-Li Chen, and China) (Nanjing Normal University, Nanjing. 2018. "The Application of Wifi Technology in Smart Home The Application of Wifi Technology in Smart Home." *IOP Conf. Series: Journal of Physics: Conf. Series 1061 (2018) 012010*.

Fargas, Bernat Carbonés, and Martin Nordal Petersen. 2017. "GPS-Free Geolocation Using LoRa in Low-Power WANs."

Firdose, Saeik. 2017. "Challenges on the Validation of D2D Communications : Availability of Open- Source Tools This Report Relates to Tools and Test-Beds Available and Challenges for Fecilities D2D Communication Within." (January).

Gandotra, Sheetal et al. 2016. "Bluetooth Controlled RC Car Using Arduino." (9): 144–47.

Guo, Jing et al. "Device-to-Device Communication Underlaying a Finite Cellular Network Region." : 1–15.

Gupta, Akhil, Student Member, Rakesh Kumar Jha, and Senior Member. 2015. "A Survey of 5G Network : Architecture and Emerging." 3536(c): 1–26.

Hayati, Ms Nur, and Muhammad Suryanegara. 2017. "The IoT LoRa System Design for Tracking and Monitoring Patient with Mental Disorder." (November 2018).

Ishino, Masanori, Student Member, Yuki Koizumi, and Toru Hasegawa. 2017. "Relay Mobile Device Discovery with Proximity Services for User-Provided IoT Networks." (11): 2038–48.

Jameel, Furqan et al. 2018. "A Survey of Device-to-Device Communications: Research Issues and Challenges." *IEEE Communications Surveys and Tutorials* 20(3): 2133–68.

Jedidi, Linda et al. 2017. "Cooperative D2D Discovery Approach For Public Safety Based On Spreading Technique." : 190–95.

Kar, Udit Narayana, and Debarshi Kumar Sanyal. 2018. "An Overview of Device-to-Device Communication in Cellular Networks." *ICT Express* 4(4): 203–8.

https://doi.org/10.1016/j.icte.2017.08.002.

Khan, Muhammad Asif, Wael Cherif, and Fethi Filali. 2017. "Wi-Fi Direct Research - Current Status and Future Perspectives." *Journal of Network and Computer Applications*. http://dx.doi.org/10.1016/j.jnca.2017.06.004.

Liu, Jia, Canfeng Chen, Yan Ma, and Ying Xu. 2013. "Energy Analysis of Device Discovery for Bluetooth Low Energy." : 1–5.

Liu, Jiajia, Nei Kato, Jianfeng Ma, and Naoto Kadowaki. 2014. "Device-to-Device Communication in LTE-Advanced Networks : A Survey." (c): 1–19.

Lodhi, Deepak Kumar et al. 2016. "Smart Electronic Wheelchair Using Arduino and Bluetooth Module." 5(5): 433–38.

Muthukumaran, S, M Dinesh, and V Panneer Selvam. 2017. "Water Level Monitoring and Controlling Using Bluetooth in Agriculture." 6(11): 22865–68.

Ngo, Thanh-hai, and Younghan Kim. 2015. "Using Timing Advance to Support Proximity Discovery in Network-Assisted D2D Communication." 125(m): 926–28.

Nguyen, Nam Tuan, Kae Won Choi, Lingyang Song, and Zhu Han. 2018. "ROOMMATEs : An Unsupervised Indoor Peer Discovery Approach for LTE D2D Communications." 9545(c).

Piyare, R, and M Tazil. 2011. "BLUETOOTH BASED HOME AUTOMATION SYSTEM USING CELL PHONE." : 1–4.

Rizzi, Mattia et al. 2017. "Using LoRa for Industrial Wireless Networks."

Seo, Jihun et al. 2016. "Journal of Network and Computer Applications A Discovery Scheme Based on Carrier Sensing in Self-Organizing Bluetooth Low Energy Networks." *Journal of Network and Computer Applications*: 1–12. http://dx.doi.org/10.1016/j.jnca.2015.09.015.

Shen, Wenlong et al. 2016. "Secure Device-to-Device Communications over WiFi Direct." (October): 4–9.

Singh, Indrasen, and Niraj Pratap Singh. 2018. "Coverage and Capacity Analysis of Relay-Based Device-to-Device Communications Underlaid Cellular Networks." *Engineering Science and Technology, an International Journal* 21(5): 834–42. https://doi.org/10.1016/j.jestch.2018.07.011.

Sinha, Rashmi Sharan, Yiqiao Wei, and Seung-hoon Hwang. 2017. "A Survey on LPWA Technology : LoRa and NB-IoT." *ICT Express*. http://dx.doi.org/10.1016/j.icte.2017.03.004.

Striegel, Aaron, Shu Liu, Xueheng Hu, and Lei Meng. 2014. "LTE and WiFi : Experiences with Quality and Consumption." *Procedia - Procedia Computer Science* 34: 418–25. http://dx.doi.org/10.1016/j.procs.2014.07.048.

Sun, Shaohui et al. 2015. "Recent Progress of Long-Term Evolution Device-to-Device in Third-Generation Partnership Project Standardisation." 9: 412–20.

Tehrani, Mohsen Nader, Murat Uysal, and Halim Yanikomeroglu. 2014. "Tehrani2014." (May).

Tsolkas, Dimitris, Nikos Passas, and Lazaros Merakos. 2016. "Device Discovery in LTE Networks : A Radio Access Perspective." *Computer Networks* 106: 245–59. http://dx.doi.org/10.1016/j.comnet.2016.07.001.

Vangelista, Lorenzo, Andrea Zanella, and Michele Zorzi. 2015. "Long-Range IoT Technologies : The Dawn of LoRa." 2: 51–58.

Wen, L E E Pieh et al. "Application of WiFi-Based Indoor Positioning System in Handheld Directory System 2 Literature Review." : 21–27.

Xiang, Wei, Kan Zheng, and Xuemin Sherman Shen. 2016. "5G Mobile Communications." *5G Mobile Communications*: 1–691.

Zhang, Bentao, Yong Li, Depeng Jin, and Zhu Han Fellow. 2015. "Network Science Approach for Device Discovery in Mobile Device-to-Device Communications." 9545(c): 1–15.

Zhao, Wenju et al. 2018. "Design and Implementation of Smart Irrigation System Based on LoRa." *2017 IEEE Globecom Workshops, GC Wkshps 2017 - Proceedings* 2018-Janua: 1–6.

Sustainable Development in Construction Industry Using Palm Kernel Shell Ash as Partial Replacement for Cement

S.O. Atuluku and T.E. Adejumo

Civil Engineering Department, Federal University of Technology, Minna, Nigeria

*Corresponding author email: isaiahsurniel@gmail.com +2348137736804

ABSTRACT

The construction sector, in modern times, is faced by multi-faceted challenges primarily due to the increase in the urban population and declining natural resources that facilitates the production of construction materials. The world in general, has turned its focus on environmental effects associated with improper disposal of waste materials which results in excessive accumulation of dirt and pollution. Millions of tons of palm kernel shell are constantly being dumped in the environment through careless disposal and they are mostly resistant to degradability which makes it a problem to the environment. This study presents the sustainable development in construction industry using palm kernel shell ash as partial replacement for cement. All the test procedures were carried out in accordance with British Standard Institution guide. The method adopted in the preparation of concrete was absolute volume method and concrete moulds of 150mm × 150mm × 150mm dimensions were used. The palm kernel shell ash was obtained by burning palm kernel shell at 900^0C, the cement was replaced by palm kernel shell ash at 5, 10 and 15%. The optimum compressive strength of concrete at 28 days curing is 26.53 N/mm^2, which is higher than that of 7, 14 and 21 days. The maximum compressive strength were obtained to be 19.10 N/mm^2, 20.09 N/mm^2, and 22.87 N/mm^2 at 7, 14 and 21 curing respectively. Therefore, the study revealed that the use of agro-waste to develop sustainable construction materials was effective, as the developed materials adhered to established building standards and reduced cost of cement. Therefore, this indicates that palm kernel shell ash has the potential to replace conventional construction materials and hence achieve economic, environmental, and social sustainability in the long run.

KEYWORDS: *Cement; Construction; Palm kernel shell ash; Partial replacement; Sustainable development.*

1   INTRODUCTION

The adoption of new materials in today's construction market is the result of resource constraint, advances in engineering techniques and cost saving measures. There has been so much demand in construction industries on the need for construction materials in many countries around the world. Efforts have equally been made by various researchers to reduce the cost of concrete and hence total construction cost by investigating and ascertaining the usefulness of material which would be classified as agricultural and industrial wastes (Tangchirapat, 2009).

Due to the limited usage of these wastes materials, the rate at which they are disposed as landfill materials are expected to increase consequently leading to potential failure, environmental problems, accumulation, burning and landfill of solid waste disposal which can be expensive and undesirable. When these materials are reused in workable areas such as in the construction industry it is considered as an active area over the entire world which is a current practice (Olowe and Adebayo 2015).

In the early 1960s, Nigeria was the world's largest palm oil producer with global market share of 43%. Today, it is the 5th largest producer with less than 2% of total global market production of 74.08 million MT. In 1966, Malaysia and Indonesia surpassed Nigeria as the world's largest oil producers. Since then, both countries combined produce approximately 80% of total global output, with Indonesia alone responsible for over half i.e., 53.3% of global output. According to the Central Bank of Nigeria (CBN), if Nigeria had maintained its market dominance in the palm oil industry, the country would have been earning approximately $20 billion annually from cultivation and processing of palm oil as at today (PwC Analysis, 2019)

The palm kernel shell (PKS) is a waste material obtained during the extraction of palm oil by crushing the palm nut in the palm oil mills. They are hard, flaky and of irregular shape. These wastes if

properly pulverized has cementitious properties hence making it pozzolanic (Awal and Hussin, 2011). The recycling of these waste into value added products in construction applications will reduce demand on non-renewable natural resources which are fast depleting as well as scarce and costly coupled with the energy required in processing them. This also will further enhance local material research, development, production, utilization and improvement which will enhance a long-term economy by adequately enhancing a cleaner environment and achieving concrete performances with physical tests (Neville, 2011).

Previous researches on the use of palm kernel shell ash focus more on the strength properties rather than its strength, full adoption and sustainability. The underlying objectives of the study is to investigate the strength properties of the palm kernel shell ash, sustainable principles on effectiveness of palm kernel shell ash as partial replacement for cement and a possible reduction of cost in the construction industry.

2 METHODOLOGY

Materials
The materials (raw) required for these research work includes: Dangote brand of Ordinary Portland cement (OPC), fine aggregate, coarse aggregate, palm kernel shell ash (PKSA) and clean water. The palm kernel shells used in this research were obtained at Umomi in Kogi State. The Ordinary Portland cement and aggregates were obtained at Albashiri quarry site along Bida – Minna Road. The palm kernel shell was burnt in an incinerator using a fabricated furnace behind the Civil Engineering Laboratory, after which the ash was sieved using sieve 75µm to obtain a fine powdery form. Tap water free from contaminants was obtained from Civil Engineering Laboratory, Federal University of Technology, Minna, and was used for mixing and also curing of the concrete.

Methods
The production of concrete tests was conducted in Civil Engineering Laboratory, Federal University of Technology, Minna. The materials mentioned in 2.1 above were used, prescribed mix design proportion of 1:2:4 with water cement ratio of 0.6. A total of 48

concrete cubes specimen (150mm X 150mm X 150mm) were cast according to (BS 1881: part 108, 1983), cured according to (BS1881: part 111, 1983) and tested according to (BS 1881: part 116, 1983) at the curing ages of 7, 14, 21, and 28 days respectively.

Tests including sieve analysis according to (BS 812: part 103.1, 1985), specific gravity according to (BS 812: part 107, 1995), bulk density according to (BS 812: part 108, 1995), aggregate impact value test according to (BS 812: part 2, 1995), water absorption test according to (BS 812: part 107, 1995), slump test according to (BS 1881: part 102, 1983) and finally the compressive strength test according to (BS 1881: part 116, 1983) after curing for 7, 14, 21, and 28 days were carried out.

2.1 CASTING AND CURING PROCESS

Casting of concrete cubes
After concrete mixing, slump test precedes casting of concrete cubes. The concrete mould of 150mm × 150mm × 150mm dimensions was used. The moulds were rubbed with black engine oil so as to allow easy removal of the sample. The moulds were placed on a rigid horizontal surface and filled with concrete in such a way as to remove entrapped air as possible and produce full compaction of the concrete with neither segregation nor laitance. The concrete was poured inside the mould in three layers; each layer being given 25 strokes of the 16mm tamping rod. Each layer is of approximately 50mm deep. The test cube was prepared in accordance to (BS 1881: part 108, 1983).

Curing of concrete cube
Curing follows immediately after de-molding of the cubes from the mould. The cubes will be submerged immediately in the curing tank for the required curing age of 7, 14, 21, and 28 days which are the ages to be considered for the purpose of this study. The curing of the cubes was carried out in accordance to (BS 1881: part 111, 1983).

Compressive strength test
Curing is succeeded by crushing of the concrete. Crushing operation was performed on concrete cubes by applying compressive force on them gradually until the cubes starts breaking having attained its supposed maximum strength limit in a compressive strength testing machine. Compressive strength test was carried out on the concrete cubes at

curing age 7, 14, 21, and 28 days respectively, in accordance to (BS 116: part 116, 1963).

Figure 1: Specimen undergoing compressive strength test

2.2 FIGURES AND TABLES

TABLE 1: PARTICLE SIZE DISTRIBUTION OF FINE AGGREGATE

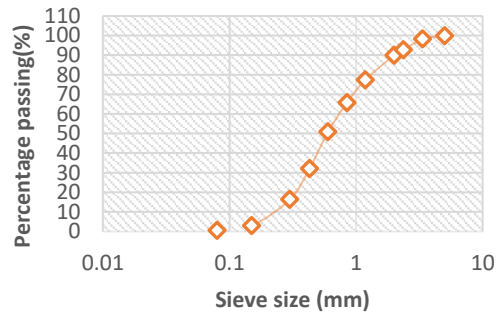| S/No	Sieve sizes (mm)	Weight retained (g)	Cumulative weight retained (g)	Cumulative percentage retained (%)	Cumulative Percentage passing (%)
1	5.00	0.21	0.21	0.042	99.96
2	3.35	8.86	9.07	1.814	98.19
3	2.36	27.75	36.82	7.364	92.64
4	2.00	13.72	50.54	10.108	89.89
5	1.18	62.68	113.22	22.644	77.36
6	0.85	57.75	170.97	34.194	65.81
7	0.60	74.93	245.9	49.180	50.82
8	0.43	93.33	339.23	67.846	32.15
9	0.30	79.08	418.31	83.662	16.34
10	0.15	66.76	485.07	97.014	2.99
11	0.08	12.01	497.08	99.416	0.58
12	0.00	2.92	500.00	100.000	0.00
		Total weight:500g			

Figure 2: Particle size distribution of fine aggregate

Table 2: SIEVE ANALYSIS OF FINE AGGREGATE

S/No	Sieve sizes (mm)	Weight retained (g)	Cumulative weight retained (g)	Cumulative percentage retained (%)	Cumulative percentage passing (%)
1	20.0	2.50	2.50	50.00	50.00
2	14.0	1.80	4.30	86.00	14.00
3	10.0	0.60	4.90	98.00	2.00
4	6.30	0.10	5.00	100.00	0.00
5	0.00	0.00	5.00	0.00	0.00
	Total weight:5kg				
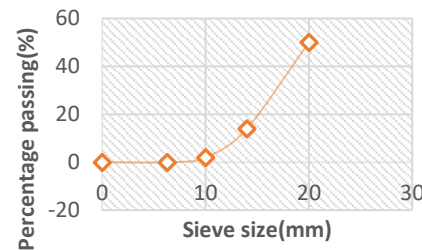
Figure 3: Particle size distribution of coarse aggregate

TABLE 3: SPECIFIC GRAVITY OF PKSA

Trials	1	2	3

Weight of empty vessel	100.8	100.5	100.6	
Weight of sample (g)	106	105	105.4	
Weight of vessel + sample + water (B)(g)	216.4	214.1	215.2	
Weight of vessel + water only (C) (g)	213.2	211.6	212.6	
Specific gravity Gs	2.60	2.25	2.18	
Average specific gravity		**2.34**		

TABLE 4: COMPRESSIVE STRENGTH AT SEVEN (7) DAYS CRUSHING

Replacement level (%)	Cube number	Mass of cube (kg)	Crushing Load (kN)	Compressive strength (N/mm^2)	Average compressive strength (N/mm^2)
0%	1	8.9	483.9	21.51	
	2	9.1	379.5	16.86	**19.10**
	3	9.0	425.5	18.91	
5%	1	8.8	398	17.69	
	2	9.1	315	14.00	**16.02**
	3	9.0	368	16.36	
10%	1	8.9	268	11.91	
	2	9.0	297	13.20	**12.21**
	3	8.9	259	11.51	
15%	1	9.0	230	10.22	
	2	8.9	249	11.07	**10.95**
	3	9.1	260	11.56	

TABLE 5: COMPRESSIVE STRENGTH AT TWENTY-EIGHT (14) DAYS CRUSHING

Replacement level (%)	Cube number	Mass of cube (kg)	Crushing Load (kN)	Compressive strength (N/mm^2)	Average compressive strength (N/mm^2)
0%	1	8.9	454.6	20.20	
	2	8.7	448	19.91	**20.09**
	3	9.0	453.6	20.16	
5%	1	8.8	386	17.16	
	2	9.0	432	19.20	**17.81**
	3	8.9	384	17.07	
10%	1	8.9	285	12.67	
	2	9.0	364	16.18	**14.77**
	3	8.9	348	15.47	
15%	1	9.0	264	11.73	
	2	8.7	240	10.67	**11.69**
	3	9.1	285	12.67	

TABLE 6: COMPRESSIVE STRENGTH AT TWENTY-ONE (21) DAYS CRUSHING

Replacement level (%)	Cube number	Mass of cube (kg)	Crushing Load (kN)	Compressive strength (N/mm^2)	Average compressive strength (N/mm^2)
0%	1	8.75	563.5	25.04	
	2	8.92	561	18.64	**22.87**
	3	8.86	419.5	24.93	
5%	1	8.60	415	18.44	
	2	8.91	436	19.38	**19.33**
	3	8.73	454	20.18	
10%	1	8.91	329	14.62	
	2	8.79	380	16.89	**15.10**
	3	9.00	310	13.78	
15%	1	9.1	280	12.44	
	2	8.7	281	12.48	**12.29**
	3	9.0	269	11.96	

TABLE 7: CHEMICAL COMPOSITION OF PALM KERNEL SHELL ASH

Chemical composition	Concentration (%)
Na_2O	4.928
M_gO	8.529
Al_2O_3	18.991
SiO_2	49.884
P_2O_5	4.561
K_2O	15.049
CaO	3.332
TiO_2	0.668
Fe_2O_3	6.341

TABLE 8: COMPRESSIVE STRENGTH AT TWENTY-EIGHT (28) DAYS CRUSHING

Replacement level (%)	Cube number	Mass of cube (kg)	Crushing Load (kN)	Compressive strength (N/mm^2)	Average compressive strength (N/mm^2)

The Nigerian Society of Engineers
Minna Branch
1st NSE Minna Branch National Conference 2021

Conference theme
Role of Engineering in
Sustainable Development Goals

0%	1	8.92	522.5	23.22
	2	8.78	600	26.67
	3	9.0	667.2	29.65
5%	1	8.79	455	20.22
	2	8.81	468	20.80
	3	8.97	432	19.20
10%	1	8.91	372	16.53
	2	8.86	385	17.11
	3	8.96	340	15.11
15%	1	8.93	312	13.87
	2	9.10	259	11.51
	3	8.86	361	16.04

Figure 4: Compressive strength against Curing days of concrete

3   RESULTS AND DISCUSSION

The sieve analysis test was carried out on aggregates and the fineness modulus of fine aggregate was calculated and obtained to be 2.60 which conforms with the requirement that aggregate fineness modulus must fall within the range of 2.3-3.1. The specific gravity for the aggregates were obtained as 2.66 and 2.66 for fine and coarse aggregate respectively which falls within the standard range of specific gravity 2.5 – 3.0. The specific gravity of the palm kernel shell ash was obtained as 2.34 which is lesser compared to that of ordinary Portland cement of 3.15. The bulk densities of the material were found to be 1534.11 kg/m³ and 1660.82 kg/m³ for un-compacted and compacted fine aggregates respectively, likewise 1481.48 kg/m³ and 1656.92 kg/m³ for un-compacted and compacted coarse aggregates which conforms to the standard range of (1500-1700) kg/m³ and (1300-1800) kg/m³ for fine and coarse aggregate respectively. Percentage porosity of fine aggregate and coarse aggregate was

found to be 7.63 and 10.59 % respectively, and void ratio 0.42 and 0.44 %.

The water absorption of the aggregate were found to be 24.60 %, 2.8 % and 73.24 % for fine aggregate, coarse aggregate and palm kernel shell ash respectively. The aggregate impact value for the coarse aggregate is 24.40 %.

Table 4, shows the compressive strength of the cubes after 7 days of curing age with 0 % having the highest compressive strength of 19.10 N/mm² followed by 5, 10 and 15 % obtained as 16.02 N/mm², 12.21 N/mm², and 10.95 N/mm² respectively.

Table 5, shows the compressive strength for 0, 5, 10 and 15 %, for 14 days curing age and the compressive strength increased than that of 7 days curing ages, the compressive strength obtained are 20.09 N/mm², 17.81 N/mm², 14.77 N/mm² and 11.69 N/mm² respectively.

Table 6, shows the compressive strength for 0, 5, 10 and 15 %, for 21 days curing age and the compressive strength increased than that of 7 days curing ages and 14 days curing ages, the compressive strength obtained are 22.87 N/mm², 19.33 N/mm², 15.10 N/mm² and 12.29 N/mm² respectively.

Table 7, shows the maximum compressive strength for 0, 5, 10 and 15 %, at 28 days of curing ages with the compressive strength which is higher than that of 7-, 14- and 21-days curing ages, the compressive strength obtained are 26.53 N/mm², 20.07 N/mm², 16 N/mm² and 13.81 N/mm² respectively. Figure 5 shows the compressive strength against curing age of concrete specimen3

3.1 ECONOMIC ANALYSIS OF PARTIAL REPLACEMENT OF CEMENT BY PALM KERNEL SHELL ASH

The typical cost analysis was conducted for the optimum replacement that met the value of the target strength which is 15% replacement of palm kernel shell ash compared with the control which is 0% palm kernel shell ash. The various materials needed for casting 1m³ of concrete for both the natural concrete and 15% partially replaced concrete are shown by the following calculations.
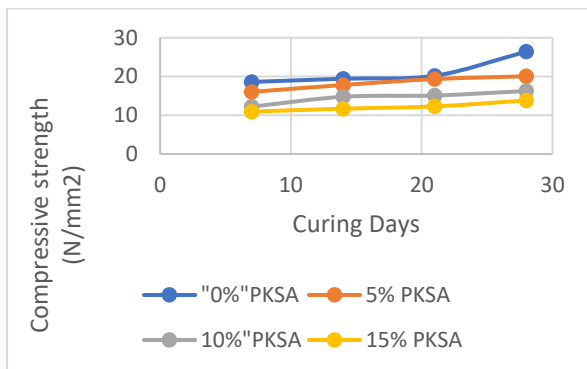
From mix design:

The Nigerian Society of Engineers
Minna Branch
1st NSE Minna Branch National Conference 2021

Conference theme
Role of Engineering in
Sustainable Development Goals

Total material used in kg

Cement = 299.69kg per m^3

Water = 179.82kg per m^3

Fine aggregate = 638.34kg per m^3

Coarse aggregate = 1234.72kg per m^3

For Control Experiment

Volume of 1 cube mould: -0.15 × 0.15 × 0.15 = 0.003375m^3

For 12 cubes: -0.003375m^3 × 12 = 0.0405m^3

Add 15% for compaction and wastage

100 + 15 = 115

1.15 × 0.0405m^3 = 0.047m^3

Calculation for the Total Materials

Cement

1m^3 = 299.69kg/m^3

0.047m^3 = X

X = 14.09kg of cement

Sand (fine aggregate)

1m^3 = 638.34kg/m^3

0.047m^3 = X

X = 30.00kg of sand

Gravel (coarse aggregate)

1m^3 = 1234.72kg/m^3

0.047m^3 = X

X = 58.03kg of gravel

Water

1m^3 = 179.82kg/m^3

0.047m^3 = X

X = 8.45kg of water

Total weight of cement needed = 299.69 × 0.047

= 14.09kg

Total weight of cement replaced by 15% PKSA = $\frac{15}{100}$ × 14.09 = 2.11kg of PKSA

Total weight of cement - 15% PKSA = 14.09 – 2.11
= 11.98kg

Cost of 1 bag of cement 50 kg = N3700

Cost of producing 12 cubes using cement without replacement = $\frac{14.09}{50}$ × 3700 = N1043

Cost of producing 12 cubes using cement with 15% PKSA replacement = $\frac{11.98}{50}$ × 3700 = N887

Cost of saving in cost of cement = 1043 – 887
= N156

Percentage saving in cost of cement = $\frac{156}{1043}$ × 100
= 15%.

4   CONCLUSION

From the results obtained from investigation of sustainable development in construction industry using palm kernel shell ash as partial replacement for cement, the following conclusions were drawn:

1. The sustainability of this development in the construction industry is feasible since over 70% of the states in Nigeria cultivate and harvest oil palm fruit so as to minimize the environmental issues arising from the improper disposal of palm kernel wastes.
2. The total cost required for any construction will be greatly reduced as the use of cement with 15% PKSA replacement will reduce the cost of cement in concrete production to 15% of the total cost.
3. The optimum compressive strength of concrete at 28 days curing age is 26.53 N/mm^2, which is higher than that of 7-, 14- and 21-days curing age with their maximum compressive strength of 19.10 N/mm^2, 20.09 N/mm^2, and 22.87 N/mm^2 respectively.
4. Palm kernel shell ash contains all the main constituents of cement although in varying quantities compared to that of ordinary Portland cement. This implies that it will be a good replacement if the right percentage is used.

4.1 RECOMMENDATIONS

From the investigation of effect of partial replacement of cement with palm kernel shell ash on compressive strength of concrete, the following recommendations are made:

1. Reduced cost of construction arising from the use of locally available agricultural waste materials such as palm kernel shell ash will enhance infrastructural developments.
2. Curing of concrete with palm kernel shell ash (PKSA) as partial replacement of cement should reach 28 days in order to obtain maximum compressive strength.
3. Further studies should be carried out on 0 – 50% replacement of cement with palm kernel shell ash in order to reveal its possibility or otherwise.
   Palm kernel shell ash (PKSA) can be used as pozzolana in concrete production

ACKNOWLEDGEMENTS

REFERENCES

Adama, Y. and Jimoh, Y. A. (2011). Production and classification of Locust Bean Pod Ash as a pozzolana: Project Report, Civil Engineering Portal. Retrieved from http://www.engineeringcivil.com/production-and-classification-of-locust-bean-pod-ash-lbpa-as-a-pozzolana.html 23/02/2020.

American Society for Testing and Materials ASTM C618-92a. (1994) *Chemical and Physical Specifications*, 2 Parks Street, London.

American Society for Testing and Materials ASTM C618, (2005). Specification for coal fly ash and raw or calcined natural pozzolana for use as a mineral admixture in Portland cement concrete. *American Society for Testing and Material*, C618-92a.

Awal, A. S. M. A., and Hussin, M. W. (2011). The Effectiveness of Palm Oil Fuel Ash in preventing expansion due to alkali. *American Journal of Engineering Research*, pp-32-36.

Basel, N. S. and Mohammed, A. R. (2003). Performance of Mortar and Concrete. Construction and Building Materials, 169, pp. 800-818, 2018.

Basri, H. B., Mannan, M. A., and Zain, M. F. M. (1999). Concrete using waste oil palm shell as ash. *Cement and Concrete Research,* 29: 619-622.

BS EN 197:1 (2000). British Standard European Norms 197: Part 1 (2000). Cement-composition, specifications and conformity criteria for common cements. *British Standard Institution*, London.

Basri, H. B., Mannan, M. A., and Zain, M. F. M. (1999). Concrete using waste oil palm shell as ash. *Cement and Concrete Research,* 29: 619-622.

BS 1881 Part 102 (1983). *Method of determination of slump test value of concrete,* British Standard Institute (BSI), 2 Parks Street, London.

BS 1881 Part 103 (1993). *Method of determination of compacting factor test of concrete,* British Standard Institute (BSI), 2 Parks Street, London.

BS 1881 Part 111 (1983). *Method for curing of normal concrete specimens,* British Standard Institute (BSI), 2 Parks Street, London.

BS 1881 Part 114 (1983). *Method for determination of density of hardened concrete cubes,* British Standard Institute (BSI), 2 Parks Street, London.

BS 1881 Part 116 (1983). *Method for determination of compressive strength of concrete cubes,* British Standard Institute (BSI), 2 Parks Street, London.

BS 1881 Part 125 (1983). *Method of sampling fresh concrete in the laboratory,* British Standard Institute (BSI), 2 Parks Street, London.

BS 812 Part 103 (1985). *Method of determination of particle size distribution*, British Standard Institute (BSI), 2 Parks Street, London.

BS 812 Part 103 (1985). *Method of determination of particle size distribution*, British Standard Institute (BSI), 2 Parks Street, London.

BS 812 Part 107 (1995). *Method of determination of specific gravity of aggregates and absorption test*, British Standard Institute (BSI), 2 Parks Street, London.

The Nigerian Society of Engineers
Minna Branch
1st NSE Minna Branch National Conference 2021

Conference theme
Role of Engineering in
Sustainable Development Goals

BS 812 Part 109 (1990). *Method of determination of moisture content of aggregates*, British Standard Institute (BSI), 2 Parks Street, London.

BS 812 Part 2 (1995). *Method of determination of aggregate impact value,* Construction Standard (CS3), North Point, Hong Kong.

BS EN 197:1 (2000). British Standard European Norms 197: Part 1 (2000). Cement-composition, specifications and conformity criteria for common cements. *British Standard Institution*, London.

Camoes, A. and Ferreira, R. M. (2010). Structures and Architecture. University of Mingho, Portugal.

Chen, C., Harbert, G., Bouzidi, Y., Jullien, A. (2010). Environmental impact of production: Details of the different processes and cement plant variability evaluation. *Journal of cleaner production* 18, 478-485

Fadele, O. A. (2016). Compressive strength of concrete containing palm kernel shell ash. *American Journal of Engineering Research.*, Vol-5, issue-12, pp-32-36.

Gworipalan, N., Cabrera, J., Cusens, A. R., and Wainwright, P. J. (1992). Effect of Curing on Durability of Concrete. *ACI Compilation 24. American Concrete Institute*, Farmington Hills, Michgan, USA, pp. 47-54.

https://www.agriculturenigeria.com/manuals/production/crop-production/general-crops/oil-palm/ >

http://www.pwc.com/ng > x-raying the Nigerian palm oil sector.

Jackson, P. J. (1983). Building Materials and construction. Retrieved from https://books.google.com.ng>books 23/02/2020.

Kong, F. H. and Evans, R. H. (1994). Reinforced and Prestressed Concrete, Chapman and Hall, London.

Mamlouk, M. S. and Zaniewski, J. P. (2006). Materials for Civil and Construction Engineers. pp. 8-10.

Mannan, M. A. and Ganapathy, C. (2004). Concrete from an Agricultural waste-oil palm shell (OPS). *Building and Environment*, 39(4), pp. 441-448.

Neville, A. M and Brooks J. J (2011). Concrete Technology, 2nd Edition, Longman.

Neville, A. M. (1996). Properties of Concrete, *ELBS 5th Edition*. Pitman, London.

Neville, A. M., and Brooks, J. J. (2002). Concrete Technology (2nd Indian reprint). *Pearson Education Limited,* Singapore.

Nilson, A. H. (1980). Design of Concrete Structures. Published by McGraw-Hill Inc. pp. 8-9

Olowe, K. O., and Adebayo, V. B. (2015). Investigation of palm kernel ash as partial replacement for high strength concrete. *International Journal of Civil Engineering.,* Vol-2, issue-4, pp-48-50 retrieved from www.internationaljournalssrg.org 22/02/2020.

Palm Kernel Shell p.d.f retrieved from www.indiamart.com/impcat/pks 20/02/2020.

Price, H.W. (1951). Factors influencing concrete strength. *Journal of American Concrete institute.* Vol. 47, pp. 417-32.

Shetty, M. S. (2005). Concrete technology theory and practice. *First Multicolour Illustrative Revised edition.* Indian.

Tangchirapat, W., Jaturapitakkul, C. and Chindaprasirt, P. (2009). Use of palm oil fuel ash as supplementary cementitious materials for producing high strength concrete. *Construction and Building Materials,* 23(7): 2641-2646.

Tay, J. H. (1990). Ash from oil palm waste as concrete material. *Journal of Materials in Civil Engineering,* 2(2): 619-622.

Teo, D. C. L., Mannan, M. A., Kurian, V. J., Ganapathy, C. (2007). Light weight concrete made from oil palm shell: Structural bond and durability properties. *Building and Environ*ment. 42: 2614–2621.

Conference theme

Role of Engineering in Sustainable Development Goals

Effect of Strengthening Vertical Circular Openings with Various Materials on the Behaviour of Reinforced Concrete Beams

[1]PAUL PETER MAIYAMBA and [2]S.M AUTA

Department of Civil Engineering, Federal University of Technolgy,Minna.

maiyambapeter@gmail.com

ABSTRACT

Opening in beam develops cracks around the region where the opening is as a result of stress concentration, this opening causes reduction in the beam strength and load carrying capacity as well. This work presents the effect of strengthening of vertical circular openings with various materials on the behaviour of Reinforced rectangular Concrete beam with dimension of 200mm x230mm x700mm.The effect of strengthening of openings was studied in terms of ultimate failure load, flexural strength and maximum deflection. It was observed that strengthening of vertical circular opening has an increase in load capacity and strength. The solid beam gives an average failure load of 251625N with flexural strength of 16.25N/mm2.The unstrengthen circular opening at L/4 and L/8 distance gives an average decrease in ultimate load of 28% and 32% with strength of 13N/mm2 and 12N/mm2 respectively. With steel plate strengthening of 4mm gauge, the ultimate load carrying capacity of the beam increases by 15% and 17% with flexural strength of 15N/mm2 each at a distance of L/4 and L/8 respectively as compared to beam with un strengthen opening. Using galvanize steel pipe of 2mm thickness increases the ultimate load by 9% and 11% with flexural strength of 14N/mm2 at a distance of L/4 and L/8 respectively. While the use of STM increases ultimate load by 3% and 5% with strength of 13N/mm2 at a distance of L/4 and L/8 respectively.

KEYWORDS: *Beam with Opening, Steel Plate, Steel Pipe, STM, Vertical Opening.*

1. INTRODUCTION

Beam openings in engineering have become a daily routine in the construction industry and this opening is of different shapes, sizes, location and are generally located close to the supports where shear is dominant without considering the engineering implication as it was not designed or planned, Lalramnghaki et, al, (2017). In practical life beam opening is quite often use to provide convenient passage for plumbing pipes and ducts for water supply system, sewage and electrical cables, but this presence of an opening in a reinforced concrete beam leads to many problems in the beam behaviour such as: (i) reduction in the beam stiffness; (ii) excessive cracking; (iii) excessive deflection; and (iv) reduction in the beam strength. Also, the presence of openings leads to a high stress concentration at the opening corners. The reduction in the beam stiffness as a result of the presence of openings changes the beam forces behaviour to a more complex one and leads to a considerable redistribution of the internal forces, Mansur (2006). The degree of change in the beam cross section as a result of the presence of an opening depends on many factors such as; shape and size of the opening; position of the opening; and type of loading. However, it was found that the size of opening and the distance from the support is the most important parameter that affects the beam behaviour, Said

(2015). With all this drawback on the beam, there is need for solution to restore the strength of reinforced concrete beams with openings to the original or high-performance level. Due to this alteration of the beam cross section caused by the presence of openings, strengthening of such beams may be necessary. Strengthening of beams provided with openings may increase the ultimate load capacity of the beam, the stiffness, and reduce deflection and cracking at the opening corners. Those strengthening resist the internal forces that are subjected to. The strengthened openings were compared with their counterparts, the un-strengthened openings. The control beam (solid) served as a reference to assess the performance of the test specimens with un- strengthened and the strengthened vertical circular openings. Since in every civil engineering work, safety is of paramount important, Abeer (2011). Hence, this study presented a clear understanding on the effect of various strengthening of vertical circular openings on the behaviour of reinforced concrete beam. The result of this study may be beneficial to produce an efficient strengthening of vertical circular openings. If the concept of various strengthening of vertical circular opening is commercially accepted, a strengthening process can be conducted much easier with equally satisfactory solutions.
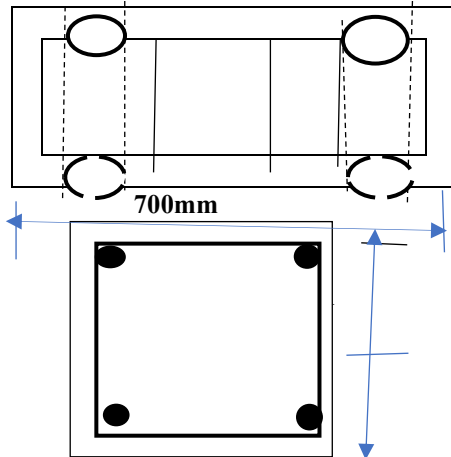
Figure 1.0: Beam details with opening and cross section

2. RELATED WORK

Jamiu, (2019), carried out an investigation on the effect of vertical circular opening on behaviour of reinforced concrete beam experimentally and using ANSYS 19.1, a total of twelve number beam was studied and he concluded that:

RC beams with openings showed a decrease in ultimate load carrying capacity compared to solid beams. The reduction in percentage of load bearing capacity was about 6% for beam with 25mm diameter opening located at 150mm from support, 32% for beam with 25mm diameter opening located at 350mm from support, 28% for beam with 50mm diameter opening located at 150mm from support and 35% for beam with 50mm diameter opening located at 350mm from support when compared with solid beam without opening. Rectangular RC beam with vertical circular opening of diameter more than one - third of the beam width (without special reinforcement in opening zone) with the opening practically located bending zone of the beam reduces the ultimate load capacity of the RC beams by at least 35%, mode of failure is shear at the opening region, maximum compressive stress of the concrete occur at the opening region of the beam for the ultimate load and tensile stress of the longitudinal reinforcement reaches to its yield stress before reaching to the ultimate strength of the beam. The beams that bear openings far away from supports induced less stress to fail when compared with beams that bear opening closer to the support. The most critical position of vertical circular opening to reach the ultimate strength in beams made of normal concrete is near the mid-span and also the best place for the location of opening in these beams is one-third of a distance between the place of applied load and support (close to the support).

khettab et al (2017). Examined the potential use of strengthening reinforced concrete (RC) deep beams that had web openings by steel plates. Experiments were conducted to test thirteen deep beams under two-point loading with square, circular, horizontal and vertical rectangular openings. Two openings, one in each shear span, were placed symmetrically about the midpoint of the inclined compressive strut. It was concluded that the structural behaviour of deep beams that had openings was primarily dependent on the interruption degree of the inclined compressive strut. Constructing square, circular, horizontal and vertical rectangular openings led to decrease ultimate capacity about 20.5 %, 18.3%, 24.7 % and 31.7%, respectively in comparison with the reference solid beam. While strengthening those openings via steel plates was found very effective in upgrading the RC deep beam shear strength. The strength gained in beams that had strengthened square, circular, horizontal and vertical rectangular openings was about 9.3%, 13.2%, 8.8% & 11.88%, respectively in comparison with the unstrengthen openings. Furthermore, adding studs to the strengthening plates caused a strengthening gain in square, circular, horizontal and vertical rectangular openings to be about 16.9%, 17.8%, 14.3% & 26.9%, respectively in comparison with the unstrengthen openings.

Research Significance

Openings adversely affect the overall stability of the structure. To overcome the instability of openings on the structural element, this work studies the incorporation of various strengthening of vertical circular openings using various materials.

3. MATERIAL AND METHODOLOGY EXPERIMENTAL WORK
Experimental Program

The test program consists of fabricating and testing of eighteen reinforced concrete beam with opening using a concrete mix with average cube compressive strength (*fcu*) equal to (18 MPa). All Beam

specimens have the same dimensions (length, width and depth) equal to (700, 200 and 230mm). The variables investigated in this study are the type of opening (with or without strengthening).The specimens are divided into three groups, each of them includes four specimens, the specimens of the first group are with non-strengthened openings while the specimens of second group are strengthened, while the third are the solid with no openings, the nineteen specimen are cast as mass concrete without reinforcement and opening.

Materials Used
Material properties
The materials used in concrete mixture were Portland limestone cement (grade 42.5 Dangote 3x), natural river sand, maximum aggregate size of 20mm (3/4") with specific gravity of 2.70. The tensile strength of concrete is typically 8%-15% of the compressive strength and the Poisson ratio (v) for concrete was assumed to be 0.2, (Amiri and Masaudnia, 2011).The mix was carried out for 28 days with average cube concrete compressive strength f (cu) =18.37N/mm2, the cubes 150mm by 150mm by 150mm were cast at the same time as the specimen and cured alongside the concrete. The mix design proportion of cement, fine aggregate and coarse aggregate were (1:2:4). The water cement ratio by weight was kept in the range of 0.50. The longitudinal steel was high yield steel with nominal yield strength of 400N/mm2.the stirrups was mild steel with nominal yield strength of 240N/mm2, Rezwana, et al (2014). The steel is assumed to be an elastic-plastic material and identical in tension and compression with Poisson ratio of 0.3,Timoshenko, (1961).The main reinforcement bar was 2Ø12 at bottom and 2Ø12 at the top with stirrups of 8mm diameter at 200mm spacing.

Cement
Grade 42.5 Dangote Portland limestone cement (Dangote 3x) was chosen in this work because of its greater fineness which would have effective hydration. The cement which conforms to BS EN, 1971 is used for making concrete. The cement was uniform in colour, grey and was free from any hard lumps. Table 1: Shows the properties of the cement.

Table1: Properties of Cement

S/N	Characteristics	Value
1	Grade cement	42.5
2	Bulk density	1507
3	Initial setting time	65mins
4	Final setting time	160mins
5	Fineness modulus	6%

Fine aggregate
Natural sand was used as fine aggregate. The sand was sieved with sieve size 4.75mm and retained on sieve no.0075 to get rid of coarse aggregate according to BS EN 12620(2002). Which was free from clay or any organic matter or chemical. It has a specific gravity of 2.57 and fineness modulus of 2.25. Moreover, sieve analysis was also conducted on the fine aggregates, in order to identify the gradation of the aggregates and more so, to see if it is suitable for various civil engineering purposes. The grading of the sand complies with BS EN 882, zone II (1992) as shown in Table 2: Also, physical properties of fine aggregate are shown in Table 3:

Table 2: Grading of fine aggregate

BS Sieve size (mm)	Passing (%)
12.7	100
9.52	100
4.75	93.8
2.36	81.1
1.18	61.1
0.60	37.6
0.30	17.1
0.15	8.7
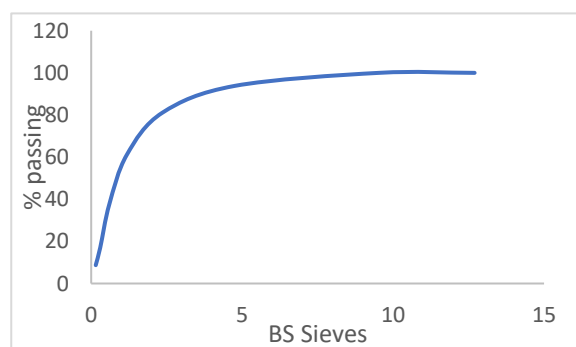
Table3: Physical properties of fine aggregate

Properties	Test results	BS specification limit
Grading Zone	Second	----
Fineness Modulus	2.25	----
Specific gravity	2.57	
Materials finer than sieve No. 200,%	2%	Not greater than 5%
size	Passing 4.75mm	

Coarse aggregate

Coarse aggregate with 20mm nominal (3/4") size was used, sourced from the market, hard and clean, free from organic impurities, free from clay and silt, free from oil coating. The grading of the coarse aggregate complies with the British standard. The preliminary tests such as Aggregate Crushing Value (ACV), Aggregate Impact Value (AIV) and particle size distribution of aggregates were carried out prior to concrete making specify by requirements of British Standards Institution. The grading coarse and particle size curve are shown in table 4 and table 5

Table 4: Grading of coarse aggregate

Sieve size (mm)	Passing (%)
50	100
37.5	100
19.05	90.2
9.52	9.5
4.76	1.2

Table 5: Physical properties of coarse aggregate

Properties	Test Results	BS EN Specification Limits (2002)
Specific Gravity	2.70	----
Bulk Density	1650 kg/m^3	----
ACV	26	23-30

AIV	17	17-21
Materials Finer Than Sieve No. 200,%	3%	Not Greater Than 3%

Mixing Water

Ordinary tap water was used for casting and curing all the specimens which was obtained from the teaching hospital construction site at Baze University, Abuja. According to the Nigerian Industrial Standard (NIS 87, 2004) water play a major role in the strength and workability of concrete when properly used as the water to cement ratio. The water used for mixing and curing was clean, tasteless and odourless and free from injurious amounts of oils, acids, alkali, salts, sugar, organic material or other substances that may be deleterious to concrete or steel.

Materials Used for Strengthening Openings

Steel plates and steel pipe (galvanize GI Pipe) of 4mm and 2mm thickness were used for strengthening the opening regions, these materials were used to strengthened the concrete that was removed due to the construction of the openings, shear connectors were welded to the materials for proper bonding and anchorage between the concrete, also 8mm diameter bar was used to fabricate the STM specimen used to strengthen the opening region. The strengthening materials were placed in the reinforcement cage into the formwork before concreting the beam.

Plate 1: materials used for strengthening the openings

Casting of Beam and Cubes specimen

The beam mould is fabricated with steel with dimension of 200mm x 230mm x 700mm while the mould of 150mm x 150mm x150mm size was used

to produce the test samples in accordance to BS EN 12390 (2002)

Curing of Beam and Cubes Specimen
The samples were completely immersed in water for curing age of 28days in accordance to BS EN 12390(2002)

Experimental Investigation
General
The experimental study consists of casting of eighteen rectangular reinforced concrete beams including beams with and without opening. Circular openings are provided at the shear zone. All the beams cast are tested to failure. The beams are indicated by the label: SOLID, CT1, CT2, PB1, PB1* PB2, PB2*, PB3, PB3*. All beams had the same geometrical dimensions. The behaviour of beams with transverse circular opening under strengthening is carried out. Beams without circular opening are provided (SOLID), two beams with opening at L/4 distance and two beams with opening at L/8 distance from the support without strengthening(CT1 and CT2) all serve as the control beam. The rest are provided with strengthening materials. These beams are tested using 2000kN testing machine under single point loading in the loading frame, the ultimate failure load of the beam and deflection have been recorded and results were compared with the control beam without opening and control beam with unstrengthen opening.
SOLID: Control specimen without opening.
CT1: Beam with two transverse circular opening without strengthening at L/4
CT2: Beam with two transverse circular opening without strengthening at L/8
PB1: Beam with two transverse circular opening with Steel plate strengthening at L/4.
PB1*: Beam with two transverse circular opening with steel plate strengthening at L/8
PB2: Beam with two circular opening with Steel pipe strengthening at L/4.
PB2*: Beam with two opening with steel pipe strengthening at L/4
PB2*: Beam with two transverse opening with steel pipe at L/8
PB3: Beam with two transverse opening with STM at L/4
PB3*: Beam with two transverse opening with STM at L/8

Plate 2: Flexural strength testing machine of 2000kN capacity

Specimens.
The beams consist of eighteen numbers, all the tested beams were rectangular in cross-section having dimension of 200mm width, 230mm height with overall length (L) of 700mm. the beam were cast using steel formwork. The circular openings of 75mm diameter was created by a circular polyvinyl chloride (PVC) pipe inserted in the beam before casting of the concrete which was retracted after the concrete was set for some minutes while the plates and galvanize pipe was left permanent as the means of strengthening the holes. The openings were at two different positions, at the shear zone and above the support.

Mixing, compaction and curing of concrete.
Before mixing, all quantities are weighted and packed in a container, through hand mixing was done. Compaction was done with the help of tamping rod in all the specimens and care was taken to avoid displacement of the reinforcement cage and the strengthening materials inside the formwork after which the surface of the concrete was levelled and smoothened by metal trowel. The curing was done in an open tank to prevent the loss of water which is essential for the process of hydration and hence for hardening.

Plate 3: Cast Beam with Strengthened

The Nigerian Society of Engineers
Minna Branch
1st NSE Minna Branch National Conference 2021

Conference theme
Role of Engineering in
Sustainable Development Goals

Openings

Plate 5: Experimental Setup

Plate 4: Curing of Beam Specimen

Test Setup

The beams were tested 28days after the casting to investigate the effects of the strengthened openings on the flexural behaviour of the concrete beam using an academic Testing Machine of 2000kN maximum capacity. All the specimens were tested for flexural strength under single point flexural load. The specimens were arranged with simply supported conditions. Loads were applied digitally till the ultimate failure of the specimens occurred.

4. RESULT AND DISCUSSION

Engineering Properties of the Hardened Concrete (Compressive Strength Test)

For the purpose of determining the strength of the concrete produced in this study, concrete cubes were cast and compressive strength test was carried out on the cast cubes. The tabulated result for the compressive strength test is given in table 6. The compressive strength test of the specimen is 18Mpa or 18 N/mm^2

Table 6: Compressive Strength Test

speci men	weig ht (kg)	ultim ate failur e load (kN)	compres sive strength N/mm^2	average compres sive strength (N/mm2)
C1	8.01	387.2 1	17.21	
C2	8.04 2	461.9 2	20.53	18.42
C3	8.21 2	389.4 1	17.37	

From the sieve analysis test conducted on the fine aggregate, the fineness modulus of the fine aggregate which was obtained as the ratio of the sum of the cumulative percentage retained on the standard sieve set and an arbitrary number (in this study 100) is 3.01. This implies that the fine aggregate can be said to be a coarse sand and since the fine modulus obtained in this study is lower that the limiting value of 3.2, the fine aggregate can be said to be fit for use in concrete production (Mamlouk and Zaniewski 2006).

The Nigerian Society of Engineers
Minna Branch
1st NSE Minna Branch National Conference 2021

Conference theme
Role of Engineering in
Sustainable Development Goals

Figure 2: Particle size distribution curve for coarse aggregate

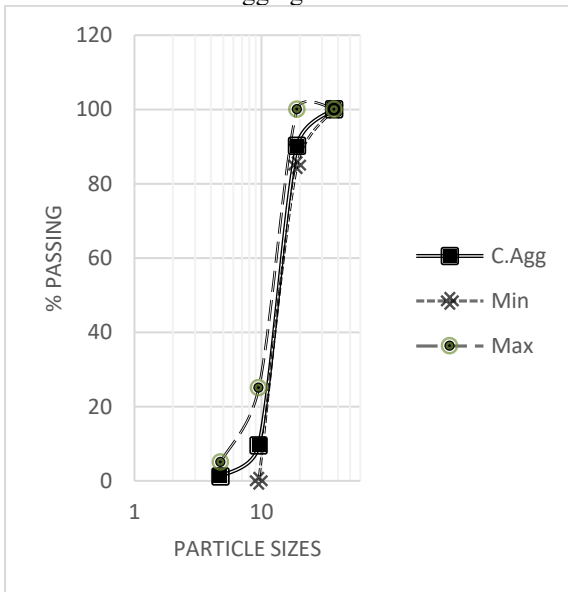
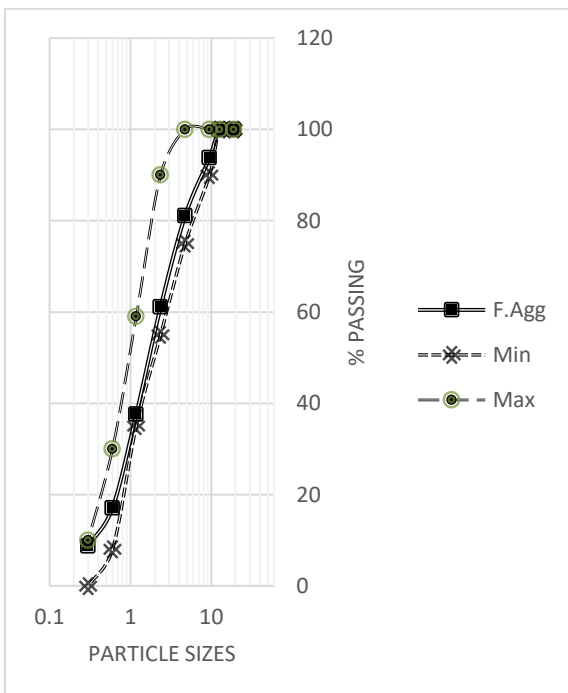**Figure 3:** Particle size distribution for fine aggregate

Table 7. Result of Flexural Strength Obtained

Beam Specimen	Distance of Opening from Support	Ultimate Failure Load(Pu) kN	Maximum deflection (mm)	Flexural Strength (Fs) N/mm2
SOLID		251.625	0.443	16.25
CT1	L/4	196.96	0.347	13.03
CT2	L/8	190.84	0.336	12.62
PB1	L/4	232.31	0.409	15.37
PB1*	L/8	228.92	0.403	15.15
PB2	L/4	217.21	0.383	14.37
PB2*	L/8	214.74	0.378	14.18
PB3	L/4	201.86	0.336	13.36
PB3*	L/8	200.17	0.352	13.24
M.C		88.06	0.155	5.83

Figure 4: Ultimate Load Graph of the Control Beams
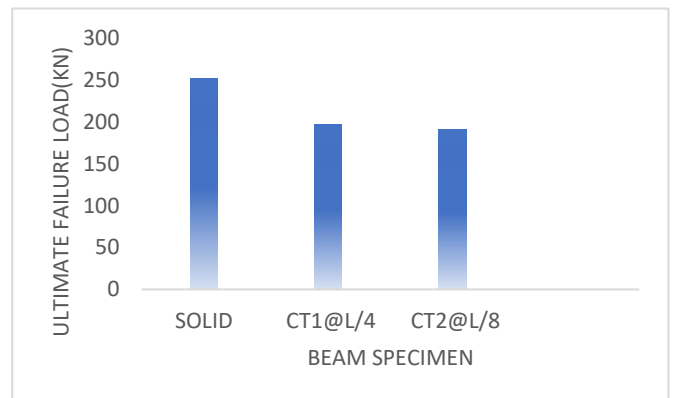
Testing beams CT1@L/4 and CT2@L/8 (Control) revealed the behaviour of un-strengthened beams with openings in comparison to that of a solid beam without opening. Figure 4 shows the effect of vertical circular opening on the beam load carrying capacity, the ultimate bearing capacity of CT1@L/4 and CT2@L/8 decreases by 28% and 32% as a result of the unstrengthen opening of diameter 75mm as compared to the solid beam without opening which has an average ultimate failure load of 251625N. This openings on the beam reduces the ultimate load capacity of the member.
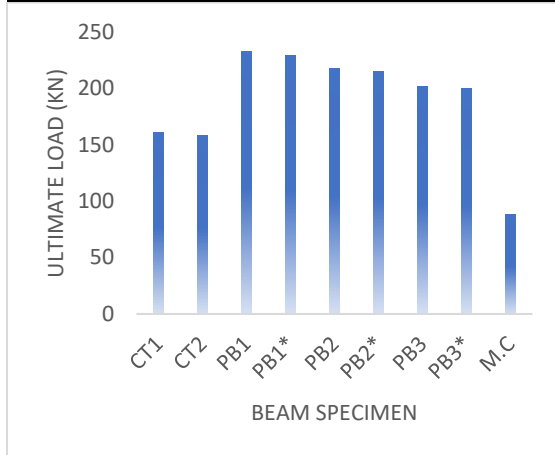
Figure 5: Effect of Strengthening Materials on the Load Carrying Capacity Beam

Figure 5 revealed the significant and noticeable effect of strengthening on the Load capacity of the member, it can be clearly seen that after the openings has been strengthen (PB1-PB3*) the ultimate load also increases as compared to the un-strengthened opening CT1 and CT2 respectively. The use of Steel Plate of 4mm gauge (PB1 and PB1*) as strengthening material increases the load bearing capacity of the beam by 15% at a distance of L/4 and 17% at a distance of L/8 respectively as compared to the unstrengthen opening(CTI and CT2). Using galvanize steel pipe of 2mm gauge (PB2 and PB2*) the ultimate load increases by 11% at a distance of L/4 and 9% at a distance of L/8, while using strut tie method (PB3 and PB3*) it increases the ultimate load by 3% and 5% at a distance of L/4 and L/8 respectively as compared to the control.
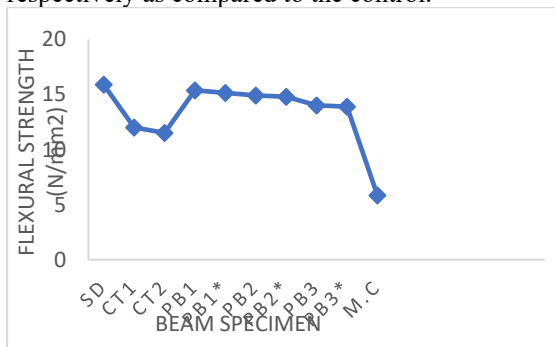

Figure 6: Flexural strength Graph

Figure 6 revealed the relationship between the strength of the beam specimen, it can be observed that the SOLID (SD) beam without opening gain

more strength of 16N/mm2 as compared to CT1 and CT2 which has a strength of 13N/mm2 and 12N/mm2 respectively, this is due to the presence of openings. Observing beam PB1 and PB1* the strength rise to 15N/mm2 at a distance of L/4and L/8 respectively as compared to the unstrengthen opening. Beam PB2 and PB2* also increase in strength by 14.4N/mm2 and 14.2N/mm2 respectively, while STM also increases the strength of the beam by13.4N/mm2 and 13.2N/mm2 respectively. The mass concrete has the least strength of all the beam specimen due to lack of reinforcement.

CONCLUSION

The potential use of selected materials for strengthening circular opening in beams was examined in the current study. Based on the result of this experimental investigation, the following conclusion can be drawn:

The preliminary results were obtained as follows: Compressive strength of concrete cube 18Mpa, AIV 17%, ACV 27%, Specific Gravity for Fine and Coarse are 2.57 and 2.70 respectively, fineness of Cement 6% with 65mins and 160mins Initial and Final Setting time

Using the strengthening techniques, the result showed a noticeable increasing effects on the ultimate load capacity of the beam.

The use of Steel plate increases the ultimate load capacity of the beam by 15% and 17%, galvanize steel pipe increases the ultimate load by 9% and 11%, while the use of STM also increases the ultimate load by 3% and 5% at a distance of L/4 and L/8 from the support respectively as compared to the unstrengthen opening.

Using the three strengthening methods in beam strengthening with vertical openings increases the flexural strength of the beam as compared to the control beams with unstrengthen openings.

Using steel plate and steel pipe for strengthening appear more effective, easy and convenience than STM in beam strengthening.

REFERENCE

Lalramnghaki H, R Raj kumar, N Umamaheswari (2017). behaviour of RC beams with circular openings in the flexural zone strengthened by steel pipe. International journal of civil

The Nigerian Society of Engineers
Minna Branch
1st NSE Minna Branch National Conference 2021

Conference theme
Role of Engineering in
Sustainable Development Goals

engineering and technology (IJCIET) 8 (5) 303-309.

M .A Mansur, (2006) "Design of reinforced concrete beams with Web openings", Proceeding of the 6th Asia-Pacific Structural Engineering and Construction Conference (APSEC 2006), Vol. A, pp.104 – 120.

Said M Allam (2015). strengthening of RC beams with large openings in shear zone. Alexanderia engineering journal 44(1) 59-78.

Oladipo Jamiu, (2019) 'Effect of vertical circular openings on the behaviour of reinforced concrete beam, master research thesis, Federal University of Technology, Minna

Soroush Amiri, Reza Masoudnia (2011) effects of openings on concrete beams without additional reinforcement in opening region using FEM method. Australian journal of basic and applied science 5(5) 617-627.

Rezwana Binte Hafiz, S Ahmed, S Barua .(2014).effects of openings on the behaviour of RC beams.IOSR journal of mechanical and civil engineering 2(2), 52-61.

Khattab Saleem,H Ali, M M Abdul-kareem (2017) a new strengthening techniques for deep beam with openings using steel plates.International journal of applied engineering research.12 (24) 15935- 15947.

Timoshenko, S. P.; Gere, J. M. 1997. *Theory of elastic stability*. 2nd ed. McGraw-Hill.

Mamlouk, M. S. and Zaniewski, J. P. (2006). Materials for Ciivil and Constructi Engineers. London: Pearson Education, Inc

British Standards Institution, BS EN 1971: Cement part 1 composition, specification and conformity criteria for common concretes. BS, London, UK 2002.

British Standards Institution, BS EN 12390 2002: Testing Aggregates of hardened concrete part 2: making and curing specification. British Standards Institution, London, UK 2002.

British Standards Institution, BS EN 882 1992. Specification for aggregate from natural sources for concrete. British Standards Institution, London.UK 1992.

Conference theme
Role of Engineering in Sustainable Development Goals

Opportunities for Engineers in the Solar Energy Value Chain

Mahmud, J. O., *Mustapha, S. A.
[1]NASENI Solar Energy Limited, Karshi, Abuja, *mustapha.ajibola@naseni.org

ABSTRACT

The Nigerian electricity poverty is high due to its rising population leading to high electricity demand. Despite evidence that Solar Energy technology is one of the most viable solutions to the electricity poverty, the professionals have taken the back seat. Bad user experiences rife creating barriers to the adoption of technology due to the proliferation of non-professionals in the industry. This paper therefore calls for the need for Nigerian professionals to rise up to the occasion by taking charge of the different sectors in the solar energy value chain. A literature review was done to establish the diverse prospects and opportunities that abound for professionals in the industry. It is therefore established that the growing demand for energy has opened up opportunities for Nigerian professionals in the solar energy value chain such as: manufacturing, training, research and development some of which have been taken over by non-professionals. This work shows that when indigenous professionals take charge of the industry, the quality of products and services delivered will significantly improve access to quality electricity. More research works are required on ways to ensure sustainable energy for all.

KEYWORDS: *Productivity, Quality Electricity, Solar Energy, Solar PV, Value Chain.*

1 INTRODUCTION

At an average annual growth of 2.6%, the Nigerian population is growing fast. As at the year 2020, the country's population has been estimated to be 210 million people as shown in figure 1 (Worldometer, 2020). Nigeria is adjudged as the most populous black nation in the world with a forecast that it will become the third most populous nation by the year 2050 trailing India and China as depicted in **Figure 2** (Roberts, 2011; United Nations, 2019). As there is continuous rise in population, so are the socio-economic activities of the citizens with attendant increase in energy demand (Olatomiwa, Mekhilef, Huda, & Ohunakin, 2015).
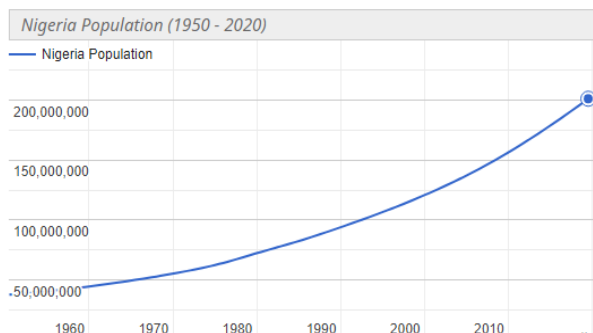

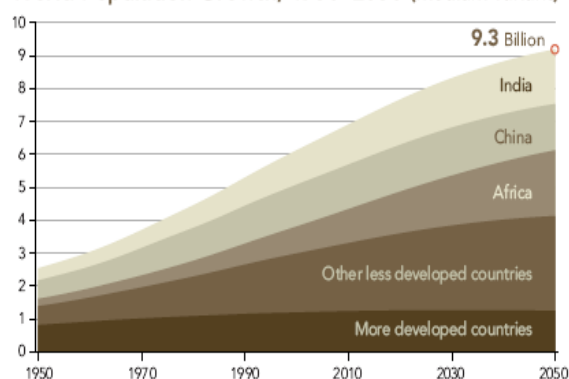**Figure 1:** Year 2020 estimated population for Nigeria (Worldometer, 2020)

Figure 2: Estimated world population towards 2050 (Roberts, 2011; Mahmud, 2020)

The pervasive nature of the electricity poverty in Nigeria has given a huge opportunity for Renewable Energy (RE) practitioners and other stakeholders to take advantage of its deployment in the different sector. RE has been gaining attentions in Nigeria, although with some barriers, in divers' areas of applications especially in electricity generation for residential homes and small businesses (Akinyele, et al., 2019). Sadly, the deployment of RE technologies is still in its nascent stage in Nigeria despite its abundance. Some of the RE technologies available are: Hydro, Solar Photovoltaic (PV) and Solar

The Nigerian Society of Engineers
Minna Branch
1st NSE Minna Branch National Conference 2021

Conference theme
Role of Engineering in
Sustainable Development Goals

Thermal, Wind, Tidal Energy, Geothermal, Biomass, and Solar Hydrogen (National Renewable Energy Laboratory, 2001; Johansson, Kelly, Reddy, & Williams, 1993). Solar PV technology has witnessed a great deal of worldwide acceptance and applications in on-grid and off-grid power systems (Yusuf, Ibikunle, Oluwatosin, & Adeyemi, 2014). Solar PV has achieved this feat due to its continual decline in the cost of Solar PV modules as well as the ease at which its installation is carried as compared to other technologies (Akinyele, Rayudu, K., & Nair, 2015). However, numerous barriers are affecting the effective adoption of RE in Nigeria. The rise in solar power system failures resulting to bad experiences of users have made many researchers to identify some of the causes such as: lack of adequate technical know-how and proliferation of substandard solar PV materials among others as some of the barriers mitigating the adoption of solar PV technology despites its numerous motivating factors (Habib, Idris, Ladan, & Mohammad, 2012).

With the huge potential of the availability of constant and sustainable electricity salvaging the already weakened Nigerian socio-economic activities, there is need for more research on how to get the solar energy sector improved through adequate knowledge sharing among professionals in the industry. Hence, this led to the motivation for this study.

Therefore, this paper presents an overview of different opportunities that abound in the value chain for indigenous professionals in order to salvage the industry for the benefit of Nigeria and its citizens. The rest of this paper presents the Nigeria's energy sector, Renewable energy sources, Solar PV value chain and opportunities for Engineers, Motivating features of Solar PV technology, Barriers to the adoption of Solar PV technology and Conclusion.

2 LITERATURE REVIEW

Some related literatures were reviewed in order to drive home the point that there are numerous opportunities for indigenous Engineers in the solar PV value chain.

2.1 NIGERIA'S POWER SECTOR AND SOLAR ENERGY

Electricity is a very vital component for the development of socio-economic and technological activity of a nation. It is a fact that the electricity demand in Nigeria far outweighs the supply causing it to be epileptic and consequently inhibiting the nation's development (Sambo, 2008). Over the years, Nigeria has been very optimistic to solve the electricity challenge for the country which led to the drafting of various policies and strategies to achieve adequate and sustainable electricity for all. In line of this, some research-based projections were carried out which provided analysis of possible energy demand and supply matching by the year 2030 as shown in Figures 3 & 4 respectively. According to Sambo (2008), at a gross domestic product (GDP) growth rate of 13%, the nation's electricity demand will increase to 297,900MW at 11,686MW/year addition in supply. Sadly, the Nigerian economy's GDP grew at only 0.51% in the first quarter of 2021 following its recent way out of recession (National Bureau of Statistics, 2021). This however has shown the continual rise in the electricity demand with urgent need for a corresponding supply. The Nigerian Government has also perceived solar energy as a key parameter to solving the economic crisis it faces. Its economic recovery growth plan (ERGP) policy document highlighted the strategic adoption of the power sector to save the nation's economy with solar energy as a key component in the energy mix. The objectives ERGP on the power sector is as follows (Ministry of Budget and National Planning, 2017; Central Bank of Nigeria, 2016):

i.   Improve energy efficiency and diversify the energy mix, including greater use of renewable energy.
ii. Facilitate private sector investment in generation, transmission and distribution
iii. Increase rural electrification through the use of off-grid renewable solutions
iv. Improve access to electricity to all Nigerians
v.   Implement a data-driven approach in power sector development planning
vi. Restore financial viability in the electricity market

The Nigerian Society of Engineers
Minna Branch
1st NSE Minna Branch National Conference 2021

Conference theme
Role of Engineering in
Sustainable Development Goals

In line with the ERGP, in 2016, the Nigerian Electricity Regulatory Commission (NERC) approved a regulation targeted at Mini-grid aimed at allowing private electricity companies to generate electricity not more than 1MW to unserved and underserved Nigerian communities (Kemabonta & Kabalan, 2018; Nigerian Electricity Regulatory Commission, 2016). This was aimed at achieving an electricity generating capacity of 10GW by the year 2020 through effective utilization of renewable energy in the energy mix (Ministry of Budget and National Planning, 2017; Kemabonta & Kabalan, 2018; Adebayo, 2017).
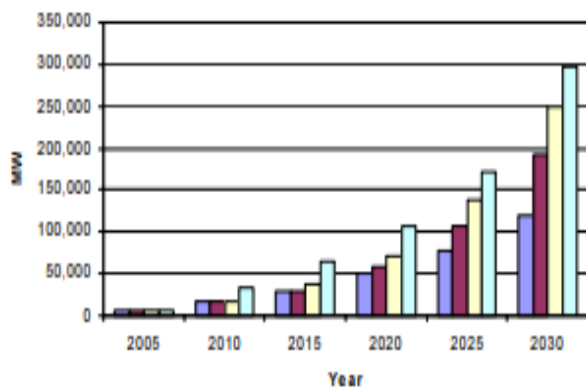
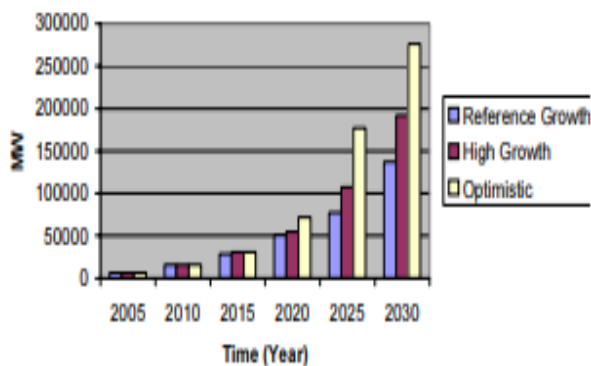**Figure 3:** Nigeria's electricity demand projection (Sambo, 2008)

Figure 3: Nigeria's electricity supply projection (Sambo, 2008)

2.2 SOLAR PHOTOVOLTAIC (PV)

The sun is prominently the primary source of energy in the universe. It continuously sheds its mass through the radiation of electromagnetic waves in the form of light and high energy spatial particles (Cander, 2019). With Nigeria's geographical location, it has been opined by researchers that the best form of alternative source of energy in terms of RE is Solar Energy (Akuru & Animalu, 2009). Solar PV technology converts the light from the sun directly into electricity. This technology has found use in many applications such as for powering rural and urban located homes, small electronics, space vehicles and agriculture. The market for Solar electricity is expanding globally due the continuous advancement in the technology which makes it to be deployed for both on-grid and off-grid connection of homes. Despite the various types of Solar PV systems available, there are three basic components they all have in common which are:

i. Solar PV module: it converts the light from the sun directly into electricity.
ii. Inverter: this transforms the direct current (DC) from the Solar PV module into alternating current (AC) for easy use by many domestic appliances.
iii. Batteries: used as a storage facility for excess electricity by the system.

Some components that may also be included are: charge controller, circuit breakers, wiring and support structure.

2.3 MOTIVATING FEATURES OF SOLAR PV TECHNOLOGY

There are different features of Solar PV technology that is making users and potential users to adopt the technology. This is presented hereunder (Olatomiwa, Mekhilef, Huda, & Ohunakin, 2015; Ugulu, 2019):

i. **Power Stability**: the feature of Solar PV technology is described as the most admiring for its adoption in Nigeria. This is because the reliability enjoyed from the solar PV technology is lacking from the national grid.

The Nigerian Society of Engineers
Minna Branch
1st NSE Minna Branch National Conference 2021

Conference theme
Role of Engineering in
Sustainable Development Goals

ii. **Cost Saving**: the cheapness of the technology in the long run is another motivating feature for the adoption of solar PV technology.

iii. **Familiarity**: awareness level is increasing. This is because potential users are developing interest in the technology as an alternative to the failing national grid.

iv. **Convenience**: the comfort derived from the usage of the technology is very inviting compared to fossil fuel powered generators. Unlike fossil fuel powered generators that requires constant maintenance, noise pollution and rigorous operation, solar PV technology is easier to use.

2.4 BARRIERS TO THE ADOPTION OF SOLAR PV TECHNOLOGY

Despite the inviting features of the technology, some other factors have been creating barriers for its adoption. These are presented hereunder (Yaqoot, P. Diwan, & Kandpal, 2016; Ozoegwu, Mgbemene, & Ozor, 2017; Akinyele, et al., 2019; Ugulu, 2019):

i. **High initial cost of installation**: the seriously high cost of installing Solar PV power system is said to be impeding the use of solar technology in Nigeria.

ii. **Proliferation of substandard products**: the seemingly uncontrolled proliferation of inferior Solar PV products and materials leading to high rate of failures is causing potential users to backtrack on their decision of adopting the technology.

iii. **Inadequate awareness**: it is observed that many intending users of the technology do not have adequate knowledge about solar PV technology. This creates fear for them because they are not sure solar works.

iv. **Inadequate technical know-how**: another factor that is barring intending users of solar PV technology is the incompetence of the system installers. This is due to the high rate of incompetent service providers in the industry.

3 SOLAR PV VALUE CHAIN AND OPPORTUNITIES FOR ENGINEERS

The value chain of solar PV as shown in Figure 3 depicts the different areas of possible intervention and investment by the professionals in the solar PV industry. The value chain comprises of the areas of research and development which leads to the manufacturing of different types of solar PV materials and modules. It also covers innovative areas where solar PV solutions can be applied. Included in the value chain are: Power Service provision; Operation, Maintenance and Training as well as recycling management. These areas are critical areas in the value chain that Engineers can explore for Nigeria to achieve sustainable and clean electricity for all.
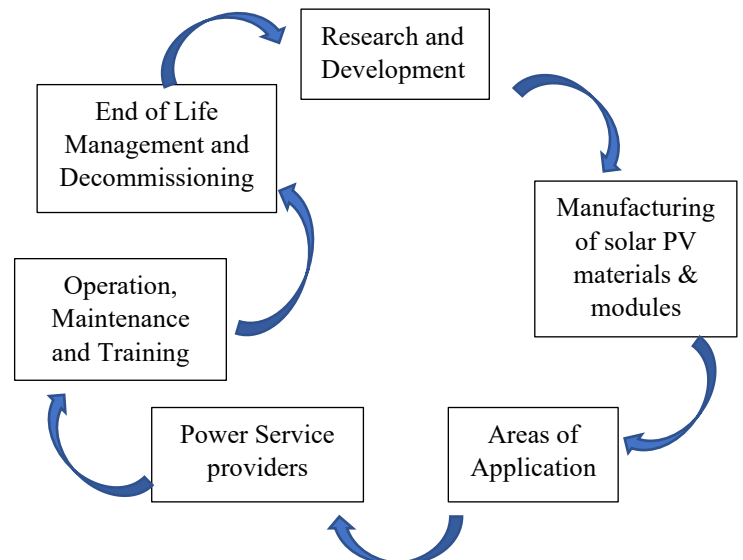

Figure 3: Solar PV Value Chain (Mahmud, 2019; Udayakumar, Anushree, & Manjunathan, 2019)

3.1 RESEARCH AND DEVELOPMENT

All over the world, the solar PV technology industry thrives as a result of intensive research outputs. The outputs are a result of: good data collection and analysis, discovery of available materials for the production of solar cells, cost analysis, efficiency improvements and environmental impacts (Tyagi, Rahiml, Rahim, & Selvaraj, 2013). Apart from data collection, one of the key areas that require further research works is in the indigenous discovery of already known solar cell materials or technologies as in Figure 4 or locally available materials that can be their substitutes. The exploration the research and development sector of the value chain by indigenous Engineers is direly needed as there is still dearth of

intensive research works as it relates to the industry in Nigeria.

3.2   MANUFACTURING OF SOLAR PV MATERIALS AND MODULES

The manufacturing of solar PV module is one of the value chain components in the industry which requires adequate penetration. NASENI Solar Energy Limited (NSEL) has taken a giant stride in this regards with its production of solar PV module as shown in Figure 5. Majority of the local producers focus on the monocrystalline and polycrystalline solar PV modules which are literarily termed conventional of sort. However, there are several others which have not penetrated the market such as: Half cell, Bifacial and Double glass (Daniel, Joao, Hugo, Moreira, & Marcelo, 2019). However, their penetration into the market has been limited due to some factors ranging from high cost of purchase, ruggedness to environmental friendliness issues. It very important that indigenous Engineers begin to look into the direction of producing the solar PV materials and modules locally.
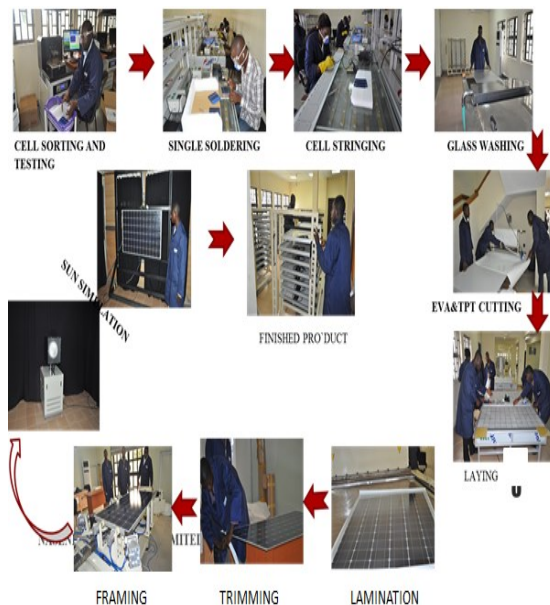

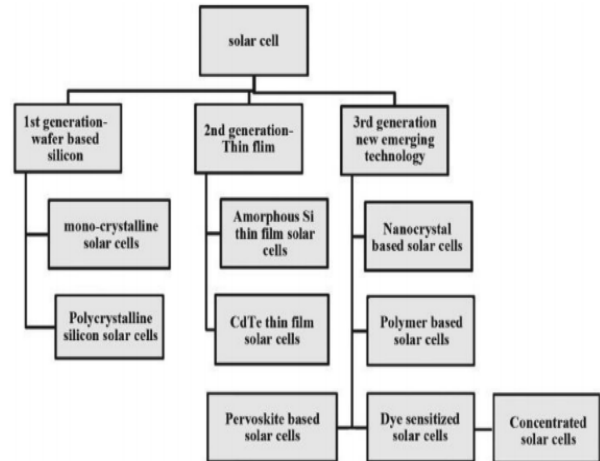**Figure 5:** NASENI Solar Energy Limited old Solar PV Module Manufacturing plant (Mahmud, 2019)

Figure 4: Solar cells technologies (Udayakumar, Anushree, & Manjunathan, 2019)

3.3   AREAS OF APPLICATION

Recently, there are a lot of novelties in the application of solar PV technology in the industry different from the conventional rooftop applications. Emerging areas that can be explored by professionals in the industry include: Building-Integrated PV (BIPV), Solar Powered generators, Agro photovoltaics, Solar carports, Solar trees and Floating PV (Udayakumar, Anushree, & Manjunathan, 2019) . An application is shown in Figure 6. This is a call for Nigerian Engineers to bring about innovative ideas where localized problems can be solved using solar PV solutions.

Figure 6: Deployment of NSEL solar mini generator at a mobile phone charging business center at Karshi, Nigeria (Mahmud, et al., 2020)

The Nigerian Society of Engineers
Minna Branch
1st NSE Minna Branch National Conference 2021

Conference theme
Role of Engineering in
Sustainable Development Goals

3.4 POWER SERVICE PROVIDERS

The solar PV power industry has so far proven to be real alternative to the overwhelmed centralized national grid. This informs the need for the professional players in the industry to take advantage of the NERC 2016 policy to set up independent solar power projects, solar PV power generating companies, off grid rural electrification to adequately compensate for the electricity shortfall from the national grid (Mahmud, 2019).

3.5 OPERATION, MAINTENANCE AND TRAINING

As the market for solar PV is growing, more expertise are required to continue to improve on the life expectancy of solar PV modules and the balance of systems (BoS) via effective operation and maintenance (O&M). Some of the areas in the O&M are intelligent monitoring of solar PV modules and BoS and their outputs using smart data collection techniques, advanced cooling techniques, drones, output forecasting and the likes (Udayakumar, Anushree, & Manjunathan, 2019). There is also the continuous training component that is direly required for personnel in the industry (Mahmud & Mustapha, 2020).

3.6 END OF LIFE MATERIALS RECYCLING

The global acceptance and usage of solar PV modules has equally increased the potential increase of its waste by the end of its life span. It was projected that just by the end of the year 2030, the cumulative waste from solar PV module will amount to 2 million tones which is expected to be tripled by 2048 (Sica, Malandrino, Supino, Testa, & Lucchetti, 2018). It is therefore pertinent that effective ways of disposing the solar PV module wastes as in Figure 7 be adopted while new ways be discovered in order to save the environment. The recycling processes are opportunities to be explored by Nigerian Engineering professionals in the value chain.
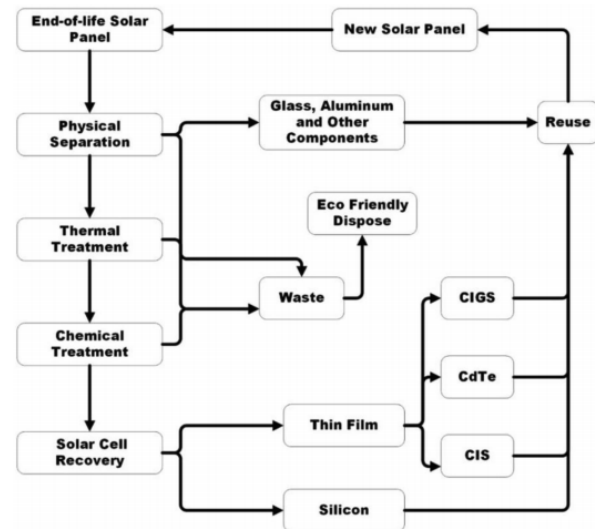

Figure 7: End of Life process of solar PV modules (Sukmin, Sungyeol, Jina, Bonghyun, & Hojin, 2012)

4 CONCLUSION

The solar PV industry in Nigeria is growing and the technologies are becoming accepted. However, non-professionals have taken a larger stake in the industry leading to the incessant bad experiences by unsuspecting users. In this regards, it is very important to bring forth the numerous opportunities and areas in the solar PV value chain that Nigerian Engineering professionals can gain and also utilize their expertise in order to salvage the situation. This paper therefore highlighted the different areas in the value chain as well as the motivating factors and barriers to the adoption of solar PV. This work is expected to charge up the professionals to take charge of the Nigerian solar PV industry.

REFERENCES

Adebayo, H. (2017). *Nigeria launches Economic recovery plan; targets 10GW, Food Security.* Abuja: Premium Times.

Akinyele, D. O., Rayudu, K., R., & Nair, N. K. (2015). Development of Photovoltaic Power Plant for Remote Residential Applications: The Socio-Technical and Economic Perspectives. *Renewable Sustainable Energy Revolution* , 112-139.

Akinyele, D., Babatunde, O., Monyei, C., Olatomiwa, L., Okediji, A., Ighraywe, D., . . . Temikotan, K. (2019). Possibility of Solar Thermal Power Generation Technologies in Nigeria: Challenges and Policy Directions. *Renewable Energy*, 24-41.

Akuru, U. B., & Animalu, A. O. (2009). Alternative Means of Energy Sector Investments in Nigeria. *Proceedings of the First International Seminar on Theoretical Physics and National Development*, (pp. 173-183).

Cander, L. R. (2019). Solar-Terrestrial Interactions in Ionospheric Space Weather. *Springer Geophysics*, 1-297.

Central Bank of Nigeria. (2016). *Annual Report 2016.* Abuja: Central Bank of Nigeria.

Daniel, d. B., Joao, L. d., Hugo, S., Moreira, M., & Marcelo, G. V. (2019). A review and analysis of technologies applied in PV modules. *IEEE PES Innovative Smart Grid Technologies*.

Habib, S. L., Idris, N. A., Ladan, M. J., & Mohammad, A. G. (2012). "Unlocking Nigeria's Solar PV and CSP Potentials for Sustainable Electricity Development. *International Journal for Science & Engineering Research*, 2229-5518.

Johansson, T. B., Kelly, H., Reddy, A. K., & Williams, R. H. (1993). Renewable Energy: Sources for Fuels and Electricity. United States.

Kemabonta, T., & Kabalan, M. (2018). Using what you have, to get what you want – a different approach to electricity market design for local distribution companies (DISCOs) in Nigeria. *IEEE Global Humanitarian Technology Conference*, (pp. 1-2).

Mahmud. (2019, October 15). Renewable Energy-Boosting Generation Capacity Towards Agro Community Commercial Farming Sustainability. *Nigerian Alternative Energy Expo 2019.* Abuja: Nigerian Alternative Energy.

Mahmud, J. O. (2020). Improving Agro Community Commercial Farming Sustainability through Deployment of Renewable Energy. *11th INTERNATIONAL CONFERENCE ON ENERGY AND POWER SYSTEMS OPERATION AND PLANNING (ICEPSOP 2020)*, (pp. 116-119). Abuja.

Mahmud, J. O., & Mustapha, S. A. (2020). DEVELOPING INDIGENOUS INFRASTRUCTURE FOR LOCAL CAPACITY IN SOLAR ENERGY. *National Solar Energy Forum (NASEF 2020)* (p. 35). Sokoto: Solar Energy Society of Nigeria.

Mahmud, J. O., A. O. Nduka, A. O., Acholoson, P. O., Ongbabo, E., Mustapha, S. A., & Akai, Y. (2020). Deployment of Solar Photovoltaic Mini Generators for Small Scale Businesses. *11th INTERNATIONAL CONFERENCE ON ENERGY AND POWER SYSTEMS OPERATION AND PLANNING (ICEPSOP 2020)* (pp. 116-119). Abuja: International Conference on Energy and Power Systems Operation and Planning (ICEPSOP).

Ministry of Budget and National Planning. (2017). *Economic Recovery and Growth Plan 2017 - 2020.* Abuja: Federal Republic of Nigeria.

National Bureau of Statistics. (2021). *National Bureau of Statistics*. Retrieved from https://www.nigerianstat.gov.ng/

National Renewable Energy Laboratory. (2001). Renewable Energy: An Overview. *Energy Efficiency and Renewable Energy Clearing House*, 1-8.

Nigerian Electricity Regulatory Commission. (2016). *Nigerian Electricity Regulatory Commission Mini-Grid Regulation, 2016.* Abuja: NERC.

Olatomiwa, L., Mekhilef, S., Huda, A. S., & Ohunakin, O. S. (2015). Economic Evaluation of Hybrid Energy Systems for Rural Electrification in Six Geo-Political Zones of Nigeria. *Renewable Energy*, 435-446.

Ozoegwu, C. G., Mgbemene, C. A., & Ozor, P. A. (2017). The Status of Solar Energy Integration and Policy in Nigeria. *Renewable and Sustainable Energy Reviews*, 457-471.

Roberts, L. (2011). 9 Billion? *AAAS*, 540-543.

Sambo, A. S. (2008). *Matching Electricity Supply with Demand in Nigeria.* International Association for Energy Economics.

Sica, D., Malandrino, O., Supino, S., Testa, M., & Lucchetti, M. C. (2018). Management of endof-life photovoltaic panels as a step towards a

circular economy. *REnew. Sustain. Energy Rev.*, 2934-2945.

Sukmin, K., Sungyeol, Y., Jina, L., Bonghyun, B., & Hojin, R. (2012). Experimental investigations for recycling of silicon and glass from waste photovoltaic Modules. *Renewable Energy*, 152-159.

Tyagi, V. V., Rahiml, N. A., Rahim, N. A., & Selvaraj, J. A. (2013). Progress in solar PV technology: Research and achievement. *Renewable and Sustainable Energy Reviews*, 433-461.

Udayakumar, M. D., Anushree, G., & Manjunathan, A. (2019). The Impact of Advanced Technological Developments on solar PV Value Chain. *Materials Today*, 1-6.

Ugulu, A. I. (2019). Barriers and Motivations for Solar Photovoltaic (PV) adoption in Urban Nigeria. *International Journal of Sustainable Energy Planning and Management*, 19-34.

United Nations. (2019). *Nigeria to Pass U.S. as World's 3rd most Populous Country by 2050, UN Says.* Associated Press.

Worldometer. (2020). *Worldometer*. Retrieved from Worldometer: https://www.worldometers.info/world-population/nigeria-population/

Yaqoot, M., P. Diwan, P., & Kandpal, T. C. (2016). Review of Barriers to the Dissemination of Decentralized Renewable Energy Systems. *Renewable and Sustainable Energy Reviews*, 477-490.

Yusuf, O. A., Ibikunle, O. O., Oluwatosin, E. I., & Adeyemi, O. A. (2014). A Descriptive Analysis of Public Understanding and Attitudes of Renewable Energy Resources towards Energy Access and Development in Nigeria. *International Journal of Energy Economics and Policy*, 636-646.

The Nigerian Society of Engineers
Minna Branch
1st NSE Minna Branch National Conference 2021

Conference theme
Role of Engineering in Sustainable Development Goals

Development of an electric tricycle with adjustable wheel camber

JAMILU SHEHU MUSAWA and IKECHUKWU C. UGWUOKE
Department of Mechanical Engineering,
Federal University of Technology Minna, Nigeria
E-Mail: Jamilmusawa@gmail.com

ABSTRACT

This research focused on enhancing the stability of tricycles used by the disabled. Tricycles are inherently unstable at high speed and during maneuvers giving rise to safety concerns. As efforts increase to enhance the speed of tricycles used by the disabled, through the use of electric motors, the need to investigate their stability with increase in speed became an important safety concern. Using steady state cornering equations, tire cornering stiffness and understeer gradient, conscious choice of geometric parameters and weight distribution were made to enhance stability. Kinematic bicycle model was modified with application to tricycles with delta design. A tricycle powered by an electric motor was developed having adjustable wheel camber. Quasi static rollover model was used for rollover analyses. Rollover tests were carried out with different radii and different camber angles. Theoretical analyses and practical test results were compared. Constant radius test was carried out with 15m turn radius and with different wheel camber angle adjustments of 0°, 5°, 10° and 15° to determine the handling characteristic. It was observed that at 15m radius, even with maximum camber angle of 15°, only a maximum speed of 17km/h was achieved without the risk of tipping over. As a result, the understeer gradient could not be established due to fewer readings of steering angle measurement and speed that were taken. Wheel camber was seen to improve stability with maximum speed of 10km/h attained at 0° camber angle and 24km/h maximum speed attained at 15° camber angle all tested within a 30m radius turn.

KEYWORDS: *Electric tricycle, Lateral stability, Rollover threshold, Wheel camber*

1 INTRODUCTION

Tricycles are common means of transportation used by people with locomotive disabilities in Nigeria. They are used to access public places like markets, schools, place of work, hospitals.

About 95% of children with disabilities in developing countries are out of school while 90% of them will never have access to education in their life time [1]. In Nigeria, there are an estimated 25 million people living with disabilities as reported in the 2011 world disability report by the World Health Organisation [14]. In Kogi and Niger state alone, 32% of common disabilities involved mobility [2].

Several assistive devices (e.g., wheelchair, tricycles etc.) are being used to enable them perform activities of daily life thereby improving their quality of life, maintain an increasingly independent life style and make them more productive in society [3]. It was reported that below 1% of wheelchair needs in Africa are being met through local production [4].

The sustainable development goals (SDG 11, target11.2) stated that "By 2030, provide access to safe, affordable, accessible and sustainable transport systems for all, improving road safety, notably by expanding public transport, with special attention to the needs of those in vulnerable situations, women, children, persons with disabilities and older persons".

Similarly, in January 2019, the disability rights bill was passed into law in Nigeria which forms the basis for full social inclusion for the disabled. To fully achieve this, development of appropriate home-grown technologies to solve their mobility needs should be considered.

The disabled tricycle, like other three wheeled vehicles, is associated with stability problems as speed increases [13]. These tricycles are very narrow because they are designed to operate indoors and outdoors. This brings limitations to the basic parameters that affect stability such as wheelbase and wheel track. As efforts are made to increase their speed, it is important to design them for stability and also investigate the parameters that govern stability given their narrow configuration.

One of the risk factors related to the use of powered two- and three-wheel vehicles (PTW) is stability and among the key measures and interventions to increase PTW safety is vehicle configuration to enhance stability [5].

The objective of this work is to develop an electric tricycle with enhanced lateral stability. The aim is to determine the understeer gradient as measure of handling response of the tricycle, to evaluate theoretical rollover speeds during lateral acceleration in a turn and while braking in a turn, to improve stability by adjusting wheel camber and to compare theoretical results with field test.

2 METHODOLOGY

2.1 DESIGN CONSIDERATIONS

Bicycle tire properties are insignificant at speed below 21 km/h [6], however previous research has shown that bicycle tire properties, specifically cornering stiffness and camber stiffness, can influence handling and stability [7]. It was mentioned that light alternative vehicles stability and handling depends strongly on tire properties such as cornering stiffness and camber stiffness, though very little data is available on properties of bicycle and tricycle tires currently in the market [8]. The stability of the three wheeled vehicles, such as the tricycle, can be enhanced through thoughtful considerations of the centre of gravity (CG), wheelbase and wheel track [9].

2.2 HANDLING RESPONSE

Proper location of the CG ensures the vehicle is stable by reducing excess yaw rate, reducing weaving at high speed, resist tipping over in turns and changes in road surfaces when sliding, swapping ends in braking due to weight transfer.

Using established relationship between the neutral steer point NSP, the static margin, tire cornering stiffness, steer angle, understeer gradient and steady state cornering equations [9], conscious choice of geometric properties for the tricycle was made to ensure the CG is located to enhance stability.

The Neutral Steer Point (NSP) is a point at which a side load can be applied and not cause a yaw response. The location of the NSP depends upon the total cornering stiffness, C, values at each end of the vehicle. The distance from the front axle line to the NSP is given by:

$$LNSP = \left[\frac{\bar{C}_R}{\bar{C}_F + \bar{C}_R}\right] L \qquad (1)$$

The character of the yaw response is determined by the location of the NSP relative to the CG. The distance from the CG rearward to the NSP divided by the wheelbase is termed "*static margin*" (*SM*), or as measured from the front axle line:

$$SM = \left[\frac{\bar{C}_R}{\bar{C}_F + \bar{C}_R} - \frac{l_1}{L}\right] \qquad (2)$$

The value of *SM* can be positive, negative or zero and its value is an indicator of the yaw response of the vehicle. Consider a special case where the centre of mass is "close" to one half of the wheelbase from the front axle and the same types of tires are used at each end. In that case, $\bar{C}_F = \bar{C}_R$ and equation (3) can be rewritten as:

$$SM = \left[\frac{1}{2} - \frac{l_1}{L}\right] \qquad (3)$$

From equation (3) above, it can be seen that when the centre of mass is at half the wheelbase, $l_1 = \frac{L}{2}$ then $SM = 0$. In this case a load at the CG will not produce a yaw response. The slip angle of the rear and front tires is equal and the vehicle will side slip. This condition is known as neutral steer and is considered stable

SM is positive when $\frac{l_1}{L}$ is less than one half of the wheelbase and when the CG is ahead of the NSP. The rear slip angle is less than the front slip and the vehicle heads up to the direction of the applied force. This condition is termed as understeer.

When the CG is behind the NSP, then $\frac{l_1}{L}$ is larger than one half the wheelbase, the *SM* becomes negative, where the rear slip angle is larger than the front and the vehicles heads against the direction of the applied force. This condition is known as oversteer and is considered unstable.

The above suggests that zero or positive values of *SM* are desirable for stability
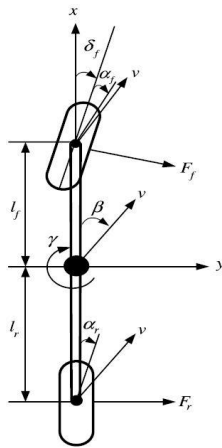
2.2.1 VEHICLE RESPONSE IN A TURN

Figure 1 Steady state handling model

During cornering, tires develop lateral force and also experience lateral slip. The application of Newton's second law along with the equations describing the geometry in turns was used to derive steady state cornering equations [10]. The lateral force, denoted by F_y is known as the cornering force.

$$F_y = C \propto \qquad (4)$$

Consider a vehicle travelling forward with a speed V, the sum of forces in the lateral direction at the tires must equal the mass times the centripetal acceleration (Figure 1).

$$\sum F_{y=} F_y f + F_y r = \frac{MV^2}{R} \qquad (5)$$

For moment equilibrium of the vehicle about its CG, the sum of the moment of the front and rear lateral forces must be zero.

$$F_{yf}b - F_{yr}c = 0 \qquad (6)$$

$$F_{yf} = \frac{F_{yr}c}{b}$$

$$\frac{MV^2}{R} = F_{yr}\left(\frac{c}{b}+1\right) = F_{yr}\frac{(b+c)}{b} = F_{yr}\frac{L}{b}$$

$$F_{yr} = \frac{Mb}{L}\left(\frac{V^2}{R}\right) \qquad (7)$$

Mb/L is the portion of the mass carried by the rear axle *i.e* W_r/g. Equation (7) above implies that the lateral force developed at the rear axle is W_r/g times the lateral acceleration at that time. Solving for F_{yf} in

a similar manner will show that W_f/g times the lateral acceleration at that time is the lateral force at the front axle.

With the lateral forces known, the front and rear slip angles from equation (4) becomes,

$$\propto_f = W_f \frac{V^2}{(C_f gR)} \qquad (8)$$

$$\propto_r = W_f \frac{V^2}{(C_r gR)} \qquad (9)$$

From the geometry of figure 1 it was established that the steering angle, δ, becomes

$$\delta = 57.3 \frac{L}{R} + \propto_F - \propto_R \qquad (10)$$

Substituting equations 9 and 10

$$\delta = 57.3 \frac{L}{R}\left[\frac{W_F}{C_F} + \frac{W_R}{C_R}\right]\frac{V^2}{gR} \qquad (11)$$

The V^2/gR term is the lateral acceleration in terms of the fraction of g's, and is abbreviated as:

$$a_y = \frac{V^2}{gR} \qquad (12)$$

Where V = velocity of CG along the path, *m/s*,

R = radius of the CG path, *m*,

g = acceleration of gravity, *m/s²*

The term in brackets called the "understeer gradient", denoted with symbol K is important to this study.

$$K = \left[\frac{W_F}{C_F} - \frac{W_R}{C_R}\right], \qquad (13)$$

Then equation (11) can be abbreviated as:

$$\delta = 57.3 \frac{L}{R} + (K)(a_y) \qquad (14)$$

The steering angle can also be expressed in terms of the static margin by combining equations (3) and (6) to yield:

$$\delta = 57.3 \frac{L}{R} + (W)\left[\frac{\bar{C}_F + \bar{C}_R}{\bar{C}_F \bar{C}_R}\right](SM)(a_y) \qquad (15)$$

To analyse stability in a turn, it is of interest how steering angle, δ, changes as lateral acceleration, a_y, increases. Each expression for δ is the sum of a constant term, plus an expression involving one of

the following terms, which could be positive, zero, or negative.

From equation (10) $\alpha f - \alpha r$

From equations (13) & (14) $K = \left[\frac{W_F}{C_F} - \frac{W_R}{C_R}\right]$

From equation (2) & (15) $SM = \left[\frac{\bar{C}_R}{\bar{C}_R + \bar{C}_F} - \frac{l_1}{L}\right]$

The conditions that change the signs of these terms are equivalent: for example, when $\alpha_F > \alpha_R$, then $K>0$ and $SM>0$. What determines stability and defines the vehicles steer characteristics is the sign change of these terms.

2.2.2 APPLICATIONS TO THREE WHEELED VEHICLES WITH A DELTA CONFIGURATION

For delta tricycle configuration, Equations 2 and 13 were adjusted for the expressions of *SM* and *K* accordingly, but the $K \geq 0$ and $SM \geq 0$ condition for stability does not change. The expressions that must change are the cornering stiffness values. The cornering stiffness $\bar{C}_F$ value for the front wheel remain single while the rear tire will have its cornering stiffness value doubled denoted as $\bar{C}_R$ .The expressions for *K* and *SM* then becomes:

$$K = \left[\frac{W_F}{C_F} - \frac{W_R}{\bar{c}_R}\right] \qquad (16)$$

$$SM = \left[\frac{\bar{C}_R}{C_F + \bar{c}_R} - \frac{l_1}{L}\right] \qquad (17)$$

If the same tires were used on all three wheels and the weight distribution is equal on all the wheels then the threshold values of K=0 and SM=0 can be obtained. The tires will have the same cornering stiffness and the weight distribution is:

$$W_F = \frac{W}{3}$$

$$W_R = \frac{2W}{3}$$

$$l_1 = \frac{2L}{3}$$

Increasing the value of W_F by moving the load forward will improve the *K* value. Lateral weight transfer has significant design implications for a tricycle with delta configuration. The rear wheels will experience lateral load transfer consequently reducing the $\bar{C}_R$ value. From equation (16), it could be seen that this will produce a negative *K* value. To increase the value of $\bar{C}_R$ rear wheel camber was introduced.

2.3 WHEEL CAMBER CONSIDERATION TO IMPROVE STABILITY

Wheel camber has an influence on the lateral force generated at the contact patch known as camber thrust denoted as $F_y\gamma$ [11]. There is no available data for camber stiffness for the 20 * 2.125 bicycle tire. Four different camber angles, 0, 5, 10 and 15, were used. Limiting the angle to 15 degrees is necessary since excessive camber angle promotes tire wear.

The tricycle was designed with a mechanism to vary the tire camber during testing as seen in Figure 2.

Plate 1 wheel camber adjustment

2.4 DESIGN CONSIDERATION FOR ROLLOVER STABILITY

A quasi-static model was used to identify the level of lateral acceleration, a_y, that causes the inside tires to have zero vertical loads [12]. That level of lateral acceleration is called the rollover threshold. The value for a three-wheeler involves the longitudinal placement of the CG as well as its height, and the vehicle track. The below equations were derived from the geometry of a three-wheel vehicle with delta configuration while negotiating a turn.

$$\sum M_{TT} = -Wl_2 sin\theta + \frac{W}{2.22g} ahcos\theta < 0 \quad (20)$$

The relationship can be re-written

$$\frac{a}{g} < \frac{l_2}{h} tan\theta \quad (21)$$

Note that θ is a function of the geometry of the vehicle; thus, it can be shown that:

$$tan\theta = \frac{b}{2L} \quad (22)$$

Substituting equation 22 into 21 yields:

$$\frac{a}{g} < \frac{b}{2h}\frac{l_1}{L} = F_c \quad (23)$$

Equation (23) above is the condition required to prevent rollover.

The lateral acceleration for a vehicle negotiating a curve of radius R is expressed in terms of the forward speed V, and the turning radius.

$$a = \frac{V^2}{R} \quad (24)$$

Substituting equation (21) into (23) yields equation for the speed at which rollover occurs.

$$V_{ro} = \sqrt{\frac{gRbl_1}{2hL}} \quad (25)$$

2.4.1 ROLLOVER STABILITY DURING LATERAL ACCELERATION IN A TURN

Longitudinal acceleration causes an inertia vector represented with symbol A. The lateral acceleration, resulting from the steady state turn, will cause an inertia vector represented by the symbol E. The symbol Z represents the resultant vector of A and E.

The magnitude of the inertia force vectors A&E can be written as:

$$A = |\vec{A}| = \frac{W}{g} a \quad (26)$$

$$E = |\vec{E}| = \frac{W}{g}\frac{V^2}{R} \quad (27)$$

The resultant expression for the resultant inertia force vector $|\vec{Z}|$ is:

$$\vec{Z} = |\vec{Z}| = [A^2 + E^2 - 2AEsin\gamma]^{\frac{1}{2}} \quad (28)$$

$$\emptyset = tan^{-1}\frac{Esin\gamma - A}{Ecos\gamma} \quad (29)$$

$$\theta = tan^{-1}\left(\frac{b}{2L}\right) \quad (30)$$

The clockwise moment about the axis of tipping axis TT, must be negative to ensure rollover stability while accelerating in a turn. The rollover stability equation governing the three wheeled vehicles with a delta lay out is given as:

$$Z\, cos\beta < \frac{Wb}{2h}\frac{l_1}{\left[L^2 + \left(\frac{b}{2}\right)^2\right]^{\frac{1}{2}}} \quad (31)$$

Where $\beta = \emptyset + \theta$

2.4.2 ROLLOVER STABILITY WHILE BRAKING IN A TURN

Symbol D represents the inertia force vector caused by braking. The magnitude of the vector can be written as:

$$D = |\vec{D}| = \frac{W}{g} d \quad (32)$$

The rollover stability equation when braking in a turn is given by:

$$Zcos\beta < \frac{Wb}{2h}\frac{l_1}{\left[L^2 + \left(\frac{b}{2}\right)^2\right]^{\frac{1}{2}}} \quad (33)$$

Where β = ϕ − θ

To obtain the resultant vector Z and its orientation angle, ϕ, the inertia acceleration force A in equation (28) and (29) was replaced with the negative of the inertia force, D, for braking in a turn.

2.5 TESTING

2.5.1 THE CONSTANT RADIUS TEST

The Constant Radius Test involves driving in a circle of radius R at a steady speed and recording the steering angle, δ, and speed, V. Then incrementally increasing the speed and repeating the measurements until a specified maximum lateral acceleration, a_y, value is attained, or the vehicle is unable to maintain its path. The specified maximum lateral acceleration, a_y, value would be that which corresponds to the "tipping threshold". The velocity

readings were taken from the speed display on the tricycle. A rotary string encoder was used to measure the steering angle, δ, and the readings were displayed on the indicator. The linear displacement was calibrated to correspond to angular displacement of the steering.

The test is based on the equation below.

$$\delta = 57.3 \frac{L}{R} + K(a_y)$$

The a_y value was computed from equation (12) given as:

$$a_y = \frac{V^2}{gR}$$

The understeer gradient K for the tricycle can then be determined from the slope of the steer angle-lateral acceleration curve. From Equation (14), for a constant turning radius, the slope of the curve is given by

$$\frac{d\delta_f}{d\left(a_y/g\right)} = K$$

The K value obtained can be used to obtain motion variable of the tricycle such as yaw velocity response, lateral acceleration response, and curvature response, regarded as outputs to steering inputs from the driver.

2.5.2 ROLLOVER THRESHOLD TEST
The tricycle was tested to determine the actual rollover velocity threshold.

The test was done on an open paved surface area of full circles of 5m, 10m and 15m turning radii and semi circles of 20m, 25m and 30m radii due to space constraint. For each radii the tricycle was driven at different camber angle and the speeds at which the tricycle attempted to rollover were recorded.

2.6 MATERIALS USED

TABLE I: MATERIALS USED IN THE PROJECT.

S/N	Description	Quantity
1	Electric front drive hub motor 1000W, 48V	1
2	Controller 1000W, 48V	1
3	Speed LCD Display, 48V	1
4	Brake disc and caliper	1
5	Throttle with reverse function	1
6	Brake lever	2
7	Bicycle Tires 20*2.125, with load rating of 70 kg each, maximum pressure 60 psi	3
8	Lead acid Batteries, 12V, 7.2 AH	4
9	Linear String Encoder 24VDC, CALT CESI-S1000P for steering angle measurement;	1
10	Indicator, HB961 for readings of steering angle; 24VDC.	1
11	25mm stainless steel round tube	
12	30mm stainless steel round tube	
13	40mm stainless steel round tube	
14	20mm stainless steel square tube	
15	Standard bicycle front fork	
16	Shock Absorber, DNM 165	2

Materials used in this work were all gotten locally except the electric bicycle kit (consisting of items 1 to 6 listed in Table I) and the bike shock absorbers. Stainless steel was selected as the material for the frame because of strength and weight considerations. The batteries were selected due to availability instead of the lithium-ion battery commonly used with electric bicycle.

3 RESULTS AND DISCUSSION
The parameters in table II were used to develop the tricycle and also used in theoretical analyses.

TABLE II: DESIGN PARAMETERS

Parameter	Description	Value
L	Wheel base	1.2 m
l_1	Length from wheel C.G to front axle	0.65m
$l2$	Length from CG rearward to the rear axle	0.55m
b	Wheel track	0.64m
W	Weight of vehicle and rider	120 Kg
h	Height of CG from the ground	0.45m
δ	Steering angle	3°
R	Radius of turn	30 m
V	Velocity	8.33 m/s
g	Acceleration due to gravity	9.82 m/s²
a	Acceleration	6.5 m/s²
d	*deceleration* (according to the United States Consumer Product Safety Commission, the braking requirement for a bicycle is that it must come to complete stop from a speed of 25km/h within 4.57m.)	- 5.27m/s²

Plate 2 Tricycle developed during this work.

3.1   ANALYTICAL RESULT

From theoretical analysis of the rollover threshold, it was established that:

- From equation (23) the design met the conditions for rollover stability
- The rollover velocity from equation (25) was evaluated to be 38.34Km/h
- From equation (31) the design failed to satisfy the conditions for rollover stability while accelerating in a turn
- From equation (33) the design failed to satisfy the conditions for rollover stability while braking in a turn

The analytical calculations do not take into consideration the camber effect on the tricycle wheel.

TABLE III: ROLLOVER VELOCITIES COMPARISON BETWEEN THE CALCULATED AND THE ACTUAL AT DIFFERENT WHEEL CAMBER ANGLES

Radius, R (m)	Rollover Velocity, V_{ro} (Km/h),				
	Calculated	Actual at 0° Camber	Actual at 5° Camber	Actual at 10° Camber	Actual at 15° Camber
5	15.66	6	8	9	9
10	22.14	9	12	13	14
15	27.11	11	14	15	17
20	31.32	14	15	18	19
25	35	17	20	22	24
30	38.34				

From table III, it can be seen that wheel camber increases the rollover velocity threshold. There is significant difference between the actual and the calculated rollover velocity threshold. This could, in part, be attributed to the transient response of the tricycle during lateral acceleration. The speed threshold of 24km/h could not be exceeded during testing. For this reason, no rollover velocity was recorded for the 30m radius. All the camber angles at the 30m radius were tested at the maximum recorded speed of 24km/h with no corresponding risk of rollover. It is noteworthy here to state that the maximum speed recorded in a straight distance was 27 km/h.

As shown in table IV, few readings were obtained for the steering angle due to limited speed and space. Only 15m radius full circle was obtainable. It can be seen that at 15m radius the maximum speed reached was 17km/h and the tricycle could no longer maintain the circular path. Higher speed records, beyond the maximum recorded speed of 27km/h, were required for the constant radius test. Consequently, the handling characteristic could not be ascertained since the understeer gradient, K, could not be determined.

However, the result showed that with low speed and significantly low levels of lateral acceleration the tricycle has tendency for oversteer characteristics and will have poor handling characteristics at higher speeds.

TABLE IV: VELOCITY, LATERAL ACCELERATION AND THE CORRESPONDING STEERING ANGLES

speed Km/h	Lateral acceleration, a_y (g)	Steering angle, δ			
		δ, at 0° Camber	δ, 5° at Camber	δ, at 10° Camber	δ, at 15° Camber
5	0.01332	5	5	5	5
10	0.05328	5	4	4	4
13	0.09004	2	3	3	3
16	0.13639				0
20	0.21311				
23	0.28185				
27	0.3884				

Plate 3 Constant radius test.

4 CONCLUSION

An electric tricycle with variable wheel camber was developed for use by the disabled.

Rollover tests were conducted with the different camber angles at different turn radii. Application of wheel camber improved the rollover stability of the tricycles as shown by the rollover threshold test. There was significant difference between the calculated rollover threshold velocities and the actual.

The understeer coefficient could not be determined from the constant radius test due to fewer readings obtained as a result of speed and space constraint.

Disabled tricycles, both powered and manual, are usually operated within a shorter turn radius. The use of speed limiting devices and use of wheel camber and other means to enhance stability are highly required to enhance stability.

REFERENCES

[1] Factsheet: Inclusive & Basic Education for Children with Disabilities In Nigeria: The role of Federal and state Ministries of Education. Retrieved on January 15, 2019 from www.jonapwd.org

[2] Smith, N., (2011). The Face of Disability in Nigeria: A Disability Survey in Kogi and Niger States. Disability, CBR & Inclusive Development, 22(1), pp.35-47. DOI: http://doi.org/10.5463/dcid.v22i1.11

[3] Ebrahimi A, Kazemi AR, Ebrahimi A. (2016). Wheelchair Design and Its Influence on Physical Activity and Quality of Life Among Disabled Individuals. Iranian Rehabilitation Journal.; 14(2):85-92. https://doi.org/10.18869/nrip.irj.14.2.8

[4] Winters, A., (2006). Wheelchair Design in Developing Countries. Accessed on January 5, 2019 from www.web.mit.edu/winter/public

[5] World Health Organisation (WHO)., 2017. Powered Two- & Three- Wheeler Safety: A Road Safety Manual for Decision-Makers and Practitioners. Accessed on 18 May, 2019 from www.who.int/publications/i/item/powered-two--and-threewheeler-safety

[6] Kooijman, J.D.G., Schwab, A.L., & Meijard, J.P., (2008). Experimental validation of a model of an uncontrolled bicycle. Multibody syst dyn 19, 115-132. https//doi.org/10.1007/s11044-007-9050-x

[7] Dressel, A., & Rahman, A., (2011). Measuring Sideslip and Camber Characteristics of Bicycle Tyres, vehicle system dynamics, 50.8, 1365-1378, DOI: 10.1080/00423114.615408

[8] Windes, P., Archibald, M., (2013). Experimental Determination of Bicycle Tire Stiffness. ASEE North central conference 2013, Retrieved on May 16, 2019 From www.people.cst.cmich.ed

[9] Star, Patrick, J., Prof. (2006). Designing Stable Three Wheeled Vehicles, With Application to Solar Powered Racing Cars. Accessed February 8, 2019, from www.americansolarchallenge.org

[10] Gillespie, T.D., (1992). Fundamentals of Vehicle Dynamics. SAE International

[11] Wong, J.Y., (1993). Theory of ground Vehicles. New York, N.Y.: J. Wiley

[12] Huston, J., Graves, B., & Johnson, D. (1982). Three Wheeled Vehicle Dynamics. SAE Transactions, 91, 591-604. Retrieved May 27, 2019, from http://www.jstor.org/stable/44631967

[13] Haynes, C. D., Stroud, S. D., Thompson, C. E. (1986). The Three-Wheeler (Adult Tricycle): an unstable dangerous machine. The Journal of Trauma: Injury, Infection, and Critical Care. 26 (7) DOI: 10.1097/00005373-198607000-00009

[14] Human rights watch, Nigeria Passes Disability Rights Law | Human Rights Watch (hrw.org). Retrieved on July 7, 2019 from https://www.hrw.org/news

The Nigerian Society of Engineers
Minna Branch
1st NSE Minna Branch National Conference 2021

Conference theme
Role of Engineering in Sustainable Development Goals

Development and Characterisation of Briquettes from Biomass Wastes: A Review

Medashe, Michael Oluwasey[1*] and Abolarin, Mathew Sunda[2]

[1,2]Mechanical Engineering Department

Federal University of Technology, Minna, Nigeria.

*Corresponding Author email: michael.pg917945@st.futminna.edu.ng

ABSTRACT

The energy crisis of the world and other related environmental challenges such as climate change and global warming has paved the way for renewable and sustainable energy sources as a significant field of research. In Nigeria fuel wood is a predominant source of fuel for households, small and medium enterprises. Fuel wood and its use come with inevitable disadvantages: deforestation, desertification, soil erosion and climate change. It is imperative to provide a more efficient substitute for firewood as a source of energy. Briquetting is the process of compression of biomass to produce high bulk density solid which can be used as fuel. Briquette making usually requires a binder to be mixed with crushed feedstocks, a press to compress the mixture into briquette which is then sun dried or dried in the oven. Binders used in briquette making are categorised as organic and inorganic. Different biomasses have been used in briquettes development such as rice husks, corncob, coconut husk, sawdust and so on. Briquette making process is initiated by first collecting the residues followed by sorting, drying, pulverisation, and densification. Briquetting can be carried out either with or without a binder and produced using non-carbonised or carbonised methods. Briquette performance characteristics can be categorised basically into four; material, physical, mechanical and thermal characteristics. One of the ways of controlling deforestation and preserving the environment is by converting biomass wastes to briquettes which could proffer an enduring solution to the problems of waste management and disposal on farms and Nigeria urban areas.

KEYWORDS: *Binder; Biomass; Briquettes; Carbonisation; Characterisation*

1 INTRODUCTION

1.1 BACKGROUND OF THE STUDY

The global trend of energy utilisation growth is on a trajectory and it is anticipated to maintain the course basically because of the population growth expectation in the population of the world and growth in the economy of developing countries. From reports 85% energy needs of the world is met by combustion of fossil fuels which is nonrenewable and the energy needs globally is predicted to grow by about 50% by 2025 with the predominant part of this increase coming from rapidly emerging countries (Agbro and Ogie, 2012). Presently the energy crisis of the world and other related environmental challenges together with increasing prices of fossil fuel has paved way for renewable energy source as an important field of research (Abdeen, 2012). The prevailing trend of energy utilisation has been characterised by huge reliance on mineral and wood fuels, which is not sustainable in the long term due to their environmental impact, global warming and susceptibility to depletion (Agbro and Ogie, 2012). Developing nations are renowned in producing large quantities of biomass waste and agro residues. For instance, Nigeria's total biomass potential consisting of animal and agricultural waste and wood residues was forecasted to be 1.2×10^{15} J in 1990 (Obioh and Fagbenle, 2009). The increase in cost of refined petroleum products and intermittent electricity supply in Nigeria makes fuel wood a major source of fuel for households and small and medium enterprises. In the course of 1989-2000, fuel wood and charcoal composed 32% and 40% of the total primary energy utilisation with 39 million tonnes estimate in national energy need in 2000 (Sambo, 2009). It forms the greatest percentage of the non-commercial energy (about 37.4% of the total energy need) and will continue to take dominance of the non-electricity energy needs for the most of the people in the country (Ohunakin, 2010). The daily average consumption of dry fuelwood for individual is estimated to be between 0.5kg to 1.0 kg utilised domestic purposes and cooking in the country (Ohunakin, 2010).

The Nigerian Society of Engineers
Minna Branch
1st NSE Minna Branch National Conference 2021

Conference theme
Role of Engineering in
Sustainable Development Goals

Consequently, wood and its use come with inevitable disadvantages: deforestation, desertification, soil erosion, and climate change and health issues due to continual exposure to carbon emission when doing domestic cooking indoor domestic cooking. It is imperative to provide a more efficient substitute for firewood as a source of energy that will be economical and affordable to people in rural areas (Lamido, et al., 2018). The use of biomass agroresidue as alternative to fossil fuel(s) is significant considering climate change because biomass has the potential to be CO2 neutral. Raw agricultural residues have numerous disadvantages as an energy raw material. These include: relatively low heating value, difficulty in regulating the rate of burning, large space storage requirement, and transportation and distribution problems. Many of these disadvantages may be ascribed to the low bulk density of agro residues which can be converted into fuel briquettes with high density (Lamido, et al., 2018).

Briquetting sometimes called densification is the process of converting low bulk density biomass wastes into high bulk density fuel briquettes (Ajit et al., 2017). Briquetting is carried out on biomass feedstock for the improvement of density, rate of burning and other energy attributes and to turn it into a size and shape to suit its purpose (Sharma et al., 2015). Briquettes are environmentally friendly and sustainable fuel blocks produced by waste compaction. The performance evaluation of briquettes is by its thermo-physical characteristics which include calorific value, moisture content, volatile matter content, ash content, fixed carbon content and density (Sastry et al., 2013). Depending on the feedstock, the pressure of the press and the speed of compression, additional binders such as cassava starch may also be needed to bind the raw materials together. Briquettes can be produced on a small scale and large scale. Although, different types of scales of machines and equipment can be employed, the main processing procedures remain the same (Lamido, et al., 2018). Another viable opportunity is the supply of fuel to small scale industries and rural industries using raw biomass as fuel for boilers and biomass cogeneration plants (Agbro and Ogie, 2012). In industries, briquettes could be used in heating plants, boiler plants, , power stations and thermal power stations, as well as by individual customers for domestic use. It is also possible to use fuel briquettes in conventional boilers and fireplaces that are previously using fire woods (for instance local bakeries use firewood for their oven) because of the efficient, superior and well controlled burning characteristics they offer.

1.2 AIM AND FOCUS OF THE REVIEW

This review aims to holistically look at how various biomass raw materials that are otherwise been dumped indiscriminately and burnt inefficiently can be developed into briquettes that can serve as alternative renewable source of energy and the characterisation of developed briquettes that will in turn help to combat deforestation, desertification, and by extension mitigate climate change and global warming.

1.3 LIMITATIONS IDENTIFIED FROM THE REVIEW

Briquetting technology is relatively new in African countries, but well developed in Asia, America, and Europe. In such developed nations, much gain have been achieved in the production and utilisation of briquettes, but these account cannot be given in many developing countries including Nigeria. The enlargement of compaction of biomass fundamentally relies on three factors, which include biomass wastes and agro residue availability, adequate technologies, and the ready market for sales of briquettes. Developing countries in the third world, biomass availability does not constitute a problem, however the optimisation of the physicochemical and mechanical treatments needed for most of the abundant raw materials remains a challenge. Considering the rural areas where power is either inadequate or not available, a suitable method of pre-processing will be the type that requires minimum energy input. Most of the technologies that produce high-quality briquettes, as reviewed, are expensive and require a high energy input.

2 LITERATURE REVIEW

2.1 BIOMASS

Biomass is ranked as the third global main source of energy closely behind coal and fossil fuel and is set to become a critical contributor to the energy mix of the world (Sugumaran & Seshadri, 2010). Biomass are non-fossil decomposable organic material from plant, animal and microbial origin. Biomass materials are made up of products, by-products, agroresidues and wastes from forestry activities; non-fossil and decomposable fractions from municipal and industrial wastes. Typical examples are, grasses, remnant from agricultural crops, agricultural wastes, waste products from

processing trees and wood and their derivatives, bagasse, waste paper, municipal solid waste, waste from food processing as well as aquatic plants and algae animal wastes. Biomass resources are categorised as renewable as they occur naturally and when properly handled, may be harvested without substantial depletion of their sources (Demirbas, 2010). Biomass as a typical energy feedstock may be harnessed directly as solid fuel, or converted through a variety of techniques such as pyrolysis, gasification and combustion into liquid or gaseous forms for generation of electricity, heating processes, steam generation, and mechanical or shaft power applications as well for production of biofuel. In Nigeria, the large deposits of agricultural waste been generated yearly, coupled with the dwindling availability of wood fuel has engendered cooperative efforts to seek for efficient ways to utilise this waste for sustainable and renewable energy generation (Zubairu and Gana, 2014). Combustion of agricultural waste as fuel raw materials directly comes with inevitable disadvantages among which is difficulty in regulating the rate of burning of the biomass, challenging mechanized feeding supply, low calorific value, difficulty in feedstock handling and transportation as well as large storage space problems. These problems are predominantly accompanied with the low bulk density of the agro waste. To address these drawbacks and utilise efficiently the agricultural wastes as fuel source is by their compression to produce briquettes (Zubairu and Gana, 2014).

2.2 BRIQUETTES

A briquette mostly refers to a pellet of highly flammable solid material utilised as fuel to start and maintain a fire. The usual types of briquettes are charcoal briquettes and biomass briquettes (Zubairu and Gana, 2014). Briquetting sometimes called densification is the process of developing low bulk density biomass into high density fuel briquettes with high energy concentration (Ajit et al., 2017). Briquette making process is carried out on biomass feedstocks to increase the density, rate of burning and other energy properties and to turn it into a size and shape to suit its purpose (Sharma et al., 2015). Briquettes are ecofriendly and sustainable fuel blocks developed by waste densification. The properties of a briquette affect its performance can be determined by its thermo-physical characteristics, including calorific value, volatile matter content, ash content, moisture content, fixed carbon content and density (Sastry et al., 2013). Depending on the feedstock, the pressure of the press and the speed of compression, additional binders such as cassava starch may also be needed to bind the raw materials together. Briquettes can be made on small scale and industrial scale. Briquettes can be produced on a small scale and large scale. Although, different types of scales of machines and equipment can be employed, the main processing procedures remain the same (Lamido, et al., 2018).

2.3 BIOMASS BRIQUETTING PROCESS AND TECHNOLOGIES

Briquetting is the process of compaction of biomass to develop similar, uniformly sized solid pellets of high bulk density which can be easily utilised as a fuel. Biomass densification can be carried out by any method from the following: (i) Carbonised densification using a binder, (ii) Direct densification of biomass using binders and (iii) Briquetting without binder (Kathuria, 2012).

Briquetting technologies are processes which develop light weight agro residues into high bulk density solid fuels. These solid fuels can be utilised for heating and burning purposes with improved efficiency and pollution reduction. The primary types of briquetting technologies are screw press, piston press, hydraulic press, roller press, pellet press and low pressure or manual presses (Kathuria, 2012).

2.4 BINDER

Binding is the process of sticking together the compressed feedstock. If subjected to significantly high temperature and pressure biomass feedstocks can bind together naturally, without the aid of additional binding agents. High temperature can melt a substance lignin which occurs naturally and under pressure this can act as binder (Hamish, 2012). Briquetting process therefore, needs binder to be added to the mixture of crushed raw materials, a press to compress the mixture into briquette which is then sun dried or dried in the oven. The addition of binder helps to strengthen the biomass particles strongly together in place, so that the briquette is significantly strong enough to hold desirably in the

fire. It is desirable essentially for the binder material to be combustible, although a binder that is non-combustible is also suitable and effective at low concentrations. The best binder for a given application depends on the locality and the kind of biomass being compressed and also the purpose the briquette made is intended. However, there is a wide range of reports that starch as a binder is the most effective material (Zubairu and Gana, 2014).

2.4.1 TYPES OF BINDER USED IN MAKING BRIQUETTES

There are numerous binding agents in use which can be divided into two major groups: organic and inorganic binders. Organic binders include; - starch, molasses, and resin while inorganic binders may include; - clay, cement, lime and sulphite liquor (Kakooza, 2017). Binders' addition is done to feedstocks that cannot be densified alone to form strong briquettes. The binder addition results in improved bonding and more stable characteristics in the briquettes developed (Asamoah et al., 2016). The quantity of binder added usually depends on the binding capabilities of the feedstocks and the binding agent. The compacting and binding ability of the briquette machine also shows whether a binding agent is necessary or not. Thuis, using a briquette making machine with high pressure would ultimately reduce the need for a binding agent (Asamoah et al., 2016; Okegbile et al., 2014).

2.4.2 ORGANIC BINDERS

Organic binders are naturally occurring binding agents used in development of briquettes. Examples of organic binders include starch, cassava starch, wheat starch, cassava flour, wheat flour, molasses, lignin, gum arabic, corn starch, sweet potato stems sap, banana stem pulp, banana peel and cassava peel gel (Aransiola *et al*., 2019; Kakooza, 2017; Lubwama and Yiga, 2017; Okegbile *et al*., 2014; Idah and Mopah, 2013).

2.4.3 INORGANIC BINDERS

Inorganic binders are chemical based binding agents employed in development of briquettes. For example, inorganic binders include; cement, lime, clay, sulphite liquor, sodium silicate, bentonite, magnesium chloride, iron oxides, magnesium oxides and calcium oxides (Zhang et al., 2018 ; Das et al., 2018; Kakooza, 2017).

3 MATERIALS AND METHODS OF BRIQUETTES DEVELOPMENT

3.1 MATERIALS FOR BRIQUETTES

In Nigeria different materials have been used in briquettes development. Olugbade and Mohammed (2015) worked on the development of briquettes from rice bran and palm kernel shells mixtures. The rice bran was crushed to a semi pulverised form. The palm kernel shells were crushed into three different particle sizes (2 mm, 4 mm, and 6mm diameters). The three particle sizes of palm kernel shells were separately mixed with rice bran, each in ratios of 1:9, 2:8, 3:7, 4:6, and 5:5 of palm kernel shell to rice bran. The briquettes were formed by compacting the rice bran and palm kernel shells mixtures in the moulds of a briquette-making machine operated manually with sixteen moulds at the optimum pressure of 3.5 N/mm2, which produced briquettes with a density of 524 kg/m2. The higher colorific value of the briquettes was 14.25 MJ/kg. The heating value increased with a decrease in palm kernel shell grain size, and the maximum heating values was obtained in the 3:7 ratio (palm kernel shell to rice bran). The briquettes were produced with a rice bran-palm kernel shell to starch ratio of 6:1.

Oladeji (2010) developed briquette from agro residues using corncob and rice husk with a focus to determining which of the two feedstocks investigated can be utilised more effectively as fuel. Ultimate and proximate analyses of the samples were carried out to find out the average composition of their constituents. A simple prototype briquette making machine was constructed to facilitate compaction of the residues into briquettes. The results of this work show that briquettes developed from these two feedstocks would make good biomass fuels. Nonetheless, reports show that corncob briquette has more positive attributes of biomass fuel than rice husk briquette. It has an optimum moisture content of 13.47%, higher density of 650 kg/m3 and lower relaxation ratio of 1.70. Other positive characteristics of corncob briquette over rice husk are long after glow time of 370 seconds and slow propagation rate of 0.12 cm/s. It also has higher volatile matter of 86.53%, higher heating value of 20,890 kJ/kg and compressive strength of 2.34 kN/m2 compared to

rice husk which are 67.98%, 13,389 kJ/kg, and 1.07 kN/m2, respectively.

In another work by Oyelaran (2016), he developed briquettes from groundnut shell and sugar cane bagasse. Different samples of briquettes were developed by mixing varying composition of the coal with the biomasses in the ratio of 100:0; 90:10, 80:20, 70:30, 60:40, 50:50, 40:60 and 0: 100, using calcium carbonate as a desulfurizing agent and cassava starch binder. A manually operated hydraulic briquetting making machine was employed with constant pressure of 5MPa. The results of the performance evaluation shows that biomass increases the burning efficiency of briquettes with increase in the biomass feedstocks, increasing rate of combustion, faster ignition, producing lesser ash and fewer pollutants. Results obtained shows that the heating value of briquettes developed from coal-groundnut shells and coal-sugarcane bagasse ranges from 16.94 - 20.81 and 17.31 – 21.03 MJ/kg respectively. The time taken for ignition ranges from 6.9 – 12.5 minutes for coal-groundnut shells briquettes while that of coal-sugarcane bagasse ranges from 6.5 – 11.1 minutes. The bio-coal blends with sugarcane bagasse were better than that of groundnut shells. In contrast, both sugarcane bagasse and groundnut shells produce bio-coal briquettes that are very effective, giving adequate heat as at the time necessary, generated less smoke and gases (e.g., Sulphur) that are harmful to environment, and generated less ash which all have adverse effect during cooking.

Other feedstocks that have been established as suitable for briquettes development in Nigeria include but not limited to: Saw dust of Daniellia oliveri; Palm Kernel Shell, mixture of waste paper and coconut husk; yam peels; rice husks, coconut shell, groundnut shells, and maize cobs; corncob; groundnut shell, melon shell, cassava peels and charcoal particles and sawdust agglomerates (Ugwu and Agbo, 2011; Oladeji, 2012; Idah and Mopah, 2013; Tembe et al., 2014; Ajimotokan et al., 2019; Sarpong et al., 2019).

3.2 METHODS OF BRIQUETTES DEVELOPMENT

Briquettes can broadly be categorised into two types based on the process of briquettes development as non-carbonised briquettes and carbonised briquettes (Asamoah et al., 2016)

Briquette making process is usually initiated by first collecting the residues followed by sorting, drying,

pulverisation, and densification. Briquetting can be carried out either with or without a binder. Briquetting without a binder is relatively easy, but it needs costly and sophisticated presses and drying equipment (Sharma et al., 2015). According to the type of briquettes to be produced, that is, non-carbonised and carbonised briquettes can be developed using the following methods.

3.2.1 NON-CARBONISED BRIQUETTING METHOD

In the works of (Arewa et al., 2016) using no-carbonised briquetting method, rice husk in different ratios was mixed with the binder with the total weight of the mixture kept constant at 200g. Fourteen samples of briquette were developed: one was without using binder, five using cassava starch binder and the remaining eight using cassava peels as the binder. The percentage composition of binder utiliseed was between the range to 10%. For instance, briquettes samples of rice husk was 2% binder ratio had 196 g of rice husk to 4 g of the binder: 4 g of the binder was used to prepare a solution in 15 ml cold water to form a paste; 385 ml of boiling water was then added to the paste and mixed thoroughly to obtain a gelatinous starch solution; in the hot state, 196 g of the sieved sample of rice husk was gradually added and mixed properly with the aid of a stirring rod until a homogenously thick composite was formed; the mixture was introduced into the briquette mould and compacted with a constructed hydraulic press briquette making machine at a constant pressure of 80x105N/m2 for 3 minutes before ejecting the briquette from the mould; the briquette was thereafter dried in the sun while recording the weight daily until a uniform weight was obtained. The briquettes were formed by compacting the mixture of the rice bran and palm kernel shells into the moulds of a briquette making machine operated manually designed by (Adegoke et al., 2006). The machine operated on principle of hydraulics and was made up of sixteen moulds in which the mixture of the biomass was introduced. The pressure was between the range 1.5 Nmm-2 to 7.5 Nmm-2 (with optimum pressure of 3.5 N/mm2), which produced briquettes with densities between 200 kg/mm3 and 550 kg/mm3. The piston was lowered, to compact the mixture, until the desired suitable pressure was attained. The briquettes were produced in the ratio of 6:1, rice bran-palm kernel shells to starch. The briquettes were thereafter dried in the sun for about a week. The briquette-making machine is shown in Figure 3.1.

Conference theme

Role of Engineering in Sustainable Development Goals

Figure 3.1: Manually operated briquetting making machine *Source*: (Olugbade and Mohammed, 2015)

Figure 3.2: Carbonising kiln *Source:* (Kakooza, 2017)

3.2.2 CARBONISED BRIQUETTING METHOD

Another method that is employed is the carbonisation of the agro residues before their compaction. In this method the agro residues are first being placed directly into a carbonising kiln before being pulverised and developed into briquettes (Chaney, 2010). To carry out charring or carbonising process on the dried raw materials, a Top-Lit Updraft (TLUD) kiln with a chimney is used. A top-lit updraft kiln is a drum used to produce charcoal, especially in biochar. At the bottom of the drum, many 2mm holes were cut at an evenly spaced distance to serve as intake vents. With this kiln, fire is set on top of the raw material to be charred – in that way forcing combustion to the bottom. The drum stood upright with the open-end up with 2/3 of its inner space filled with the prepared raw material. Fire was then started on top of the raw material in the drum. The fire burned from the top which eventually spread to the bottom gradually and the open end of the drum is covered. The cover used in this study had a chimney (Sarpong et al., 2019). The top was cut out to introduce the chimney. For evidence of carbonisation of the biomass raw materials, the black smoke coming out of chimney will fade away, the raw materials became brittle and easy to grind and were totally black (Aransiola et al., 2019). The experimental set up is shown in the figure below.

4 CHARACTERISATION OF BRIQUETTES

Biomass briquette performance characteristics from various research works can be categorised basically into four namely; material characteristics, physical, mechanical and thermal (combustion) properties, depending on the parameters desired to be measured.

4.1 MATERIAL CHARACTERISTICS

Material characteristics that affect the performance of briquettes include basically particle size and shape of biomass and moisture content of the biomass.

4.1.1 PARTICLE SIZE OF BIOMASS

Particle size is significant for briquettes densification. Biomass feedstocks of 6-8 mm size with 10-20 %composition of powder (< 4 mesh) usually gives the best results for screw press technology. Smaller particle size produces briquettes with higher density with relatively slow rate of burning (Grover and Mishra, 1996). Finely grain particles (about 1.75mm and 2.00mm) had low heating values as the grinding briought about loss of some heat and made the sample susceptible to oxidation by air (Zakari et al., 2013). In a work by Tokan et al., (2014) to investigate the calorific value of feedstocks from sawdust, corncobs and prosopis Africana charcoal increased as the particle size increases. They observed that for all the feedstocks considered, particle size increase was accompanied by higher calorific value. Research results have

shown that particles size <3mm although produces briquettes with higher values of physical properties but produces briquettes with lower calorific value.

4.1.2 MOISTURE CONTENT OF BIOMASS

The moisture content in biomass feedstock is a very vital characteristic. Generally, it has been discovered that when the moisture content of the material is 8-10 %, the briquettes usually have moisture range between 6-8% moisture (Grover and Mishra, 1996). This percentage moisture content produces strong briquettes that are cracks and a smooth briquetting process. However, when the moisture content exceeds 10 %, poor and weak briquettes are produced and the briquetting operation will be erratic (Ajikashile, 2017). High moisture content usually produces excessive steam thereby resulting to the blockage of incoming materials from the hopper, and can sometimes shoots the briquettes out from the die. Therefore, it is essential to ensure optimal moisture content is maintained (Grover and Mishra, 1996).

4.2 PHYSICAL CHARACTERISTICS

Physical properties of briquettes include density (compressed and relaxed), relaxation ratio, and shattered Index.

4.2.1 DENSITY

The density of briquettes is determined immediately it is removed from the mold by equation below:

$$\rho = \frac{\text{mass of briquette}}{\text{volume of briquette}} \qquad 1$$

The mass of the briquette can be determined by weighing the sample in digital weighing balance while the volume can be evaluated through linear measurement of the diameter and height of the briquette. The volume is then calculated. The ratio of mass to volume gives the density (Huko, 2016). Density is measured as compressed and relaxed density. Compressed density (also called maximum density) is expressed as the ratio of the mass of the briquette immediately after it is extracted to calculated volume. FAO (1990) asserted that the compressed density of a briquette depends to some degree on a wide range of factors including the nature of the original material, the machine employed and the working condition, and other factors. The maximum density of a briquette from almost all materials usually varies between 1,200 - 1,400 kg/m³ for high pressure briquetting processes (Ajikashile,

2017). Relaxed density is expressed ratio of mass of a briquette to its volume, determined 30 days after removal from the press (ASAE., 2003). Drawing from the works of Obi et al., (2013), Bamgboye and Bolufawi, (2008) relaxed density of a briquette depends large extent on the compressed density of the briquette.

4.2.2 RELAXATION RATIO

Relaxation ratio is expressed as the ratio of the compressed density to the relaxed density of developed briquettes (Oyelaran et al., 2014). Relaxed density indicates how stable a briquette is when exposed to atmospheric conditions. Although there is no information on acceptable values of relaxation ratio for a quality briquette established yet but reports from research have shown that a low value of relaxation ratio suggests a more stable briquette, while higher value shows high propensity towards relaxation. Oladeji, (2012) reported the relaxation ratio of briquette from groundnut shell, corncob, melon shell, cassava and yam peel to be 2.20, 1.60, 1.95, 1.92 and 1.78, respectively.

4.2.3 SHATTERED INDEX

Shattered index is used to measure the durability of briquette. It is a critical factor affecting the ability of briquettes to withstand extreme handling during transportation, storage, and adverse conditions of the locations where the products are transported, stored or exposed. Therefore, the measurement of durability is vital in describing briquette quality, considering the fact that it helps to determine aforetime briquette performance in transportation, storage and adverse conditions (Ajikashile, 2017). Shattered index is evaluated by dropping the briquette samples repeatedly from a given height of about 1.5m to a rigid base. The fraction of the briquette retained was used as an index of briquette breakability. The percentage weight loss of briquettes was expressed as a percentage of the initial mass of the material remaining on the solid base, while the shatter resistance was obtained by subtracting the percentage weight loss from 100 (Tembe et al., 2014).

4.3 MECHANICAL CHARACTERISTICS

Effective densification process to produce strong and durable bonding in densified products such as pellets, briquettes, and cubes can be achieved by testing the strength (i.e., compressive resistance, impact resistance, and water resistance), and durability (i.e., abrasion resistance) of the densified products. These tests can indicate the maximum

force/stress that the densified products can withstand, and the amount of fines produced during handling, transportation, and storage (Kaliyan and Morey, 2009).

The mechanical property of briquette is measured in terms of the compressive strength, which expresses the strength of the briquettes. Low breaking strength briquettes are weak, crumble easily during burning and very brittle during transportation to potential end users. Also, these briquettes rate of burning is fast and produce less heat. High compressive strength shows increased volume displacement which is good for handling, storage and transportation and also it is an indication of quality briquettes because of the strong bond between the inter-particle (Kaliyan and Morey, 2009).

4.3.1 COMPRESSIVE STRENGTH
Compressive resistance (or crushing resistance or hardness) gives the maximum crushing load a briquette can resist before breaking. Compressive resistance of the compressed briquettes is evaluated by diametrical compression test. Test for Compression strength simulates the compressive stress due to weight of the top blocks on the lower blocks when storing them in bins or silos and crushing of the pellets in a screw conveyor (Zafari and Kianmehr, 2014).

4.3.2 DURABILITY
Durability or test for abrasive resistance simulates either mechanical or pneumatic handling. These tests can help control the compression process and the quality of pellets in the feed manufacturing industry. In the feed industry, high durability means high pellets quality. Durability is the prevalent form of measurement and expression of pellet quality in the feed pelleting industry (Kaliyan and Morey, 2009).

4.4 THERMAL CHARACTERISTICS
The thermal properties that determine the performance characteristics of briquettes falls under proximate analysis and are majorly percentage volatile matter, percentage ash content, percentage fixed carbon and heating or calorific value of biomass briquettes. These characteristics also depend on the biomass feedstocks employed.

4.4.1 VOLATILE MATTER IN BIOMASS
Volatile matter constitutes the composition of carbon, hydrogen and oxygen present in the biomass that usually turn to vapour when heated, usually a mixture of short and long chain hydrocarbons (Chaney, 2010). High degree of organic matter in a biomass feedstock results in high level of volatile matter. Feedstocks with relatively high volatile matter usually ignite easily, rate of burning is fast and commensurate increase in the length of flame. Some biomass generally consists of high volatile matter of about 70 - 80% with low char content (Akowuah et al., 2012).

4.4.2 ASH CONTENT OF BIOMASS
Ash is the residue of non-combustible constituent of biomass and it affects the heat transfer to the surface of briquette fuel and the permeation of oxygen through the fuel surface during char combustion. High ash content produces dust emissions which can cause air pollution and influences the combustion volume and efficiency. The higher the ash content of the fuel, the lower its heating or calorific value because ash content affects the rate of burning of the fuel because heat transfer to the internal part of the fuel and penetration of oxygen to the briquette surface during char combustion is minimised (Katimbo et al., 2014).

4.4.3 FIXED CARBON
Fixed carbon of the briquette represents the percentage of carbon (solid fuel) available for char combustion after volatile matter is sublimated off or evaporated to the atmosphere. Thus, fixed carbon gives a rough approximate of the calorific value of the fuel and represents the main heat generator constituents during combustion (Akowuah et al., 2012).

4.4.4 CALORIFIC VALUE
Calorific value is the measure of heat generated and released by the combustion of the biomass fuel. The calorific or heating value of briquettes largely depends on the process conditions and parameters such as particle size, temperature, and pretreatment of the feedstock. Generally, briquettes with higher calorific value also have higher density. Fuel with smaller particle sizes give more rapid and complete combustion process. This is due to the increase in surface area exposure. Fuel with large particle size requires a longer time in the combustion chamber at a specified temperature compared to the smaller particles (Obi, 2013). According to Katimbo et al., (2014) the calorific or heating value of biomass-briquette is increased by the type of binder used. It is further stated that the type of binder used is one of the essential factors to be considered in briquetting in order to achieve substantial heat generation.

5 CONCLUSION AND RECOMMENDATION

5.1 CONCLUSION

The use of wood fuel for domestic and industrial purposes is a major contributor to our environmental problems which has resulted to desertification in the arid-climate regions and deforestation in the rainforest regions of the country. Deforestation and desertification expose the top soil to erosion, land degradation, resulting in wood fuel crisis and ecosystem instability. One of the ways of controlling deforestation and preserving the environment is by converting biomass wastes to briquettes. Biomass gives an alternative chance to reduce our continual reliance on fossil fuels. The drawback with biomass is because of its low bulk energy density, which presents challenges such as difficulty in handling, transportation, and storage. These challenges are therefore addressed by converting the biomass to briquettes, which results in improved biomass density, burning time, and the calorific or heating value. Briquettes are flammable feedstocks produced from the compaction or densification of biomass matter into solids that can be utilised as fuel for domestic and industrial purposes, which burn more efficiently than wood. This paper reviewed various studies on briquetting of biomass. From the review the type of biomass feedstock, pre-processing, process parameter in making briquettes, and technology employed affect the overall quality of briquettes that will be produced. In addition, compressing biomass wastes to briquette could proffer an enduring solution to the problems of waste management and disposal on farms and Nigeria urban areas.

5.2 RECOMMENDATION

Briquettes production on an industrial scale involves significant capital investment requirement. This poses a barrier to further expand densification of biomass. To address high capital investment requirement and high energy input in briquettes production, research efforts should be directed towards the design of more user-friendly technologies that are cost and energy effective at various scales for briquettes development.

REFERENCES

Abdeen, M. O. (2012). The Energy Crisis, the Role of Renewable and Global Warming, *Greener Journal of Environment Management and Public Safety ISSN: 2354-2276 Vol. 1 (1), pp. 038-070.*

Agbro, E. B.. and Ogie, N. A. (2012). A Comprehensive Review of Biomass Resources and Biofuel Production Potential in Nigeria. *Research Journal in Engineering and Applied Sciences 1(3) 149-155.*

Ajit Kaur, Madhuka Roy, Krishnendu, Kundu. Densification of Biomass by Briquetting: A Review. *International Journal of Recent Scientific Research Vol. 8, Issue,10,pp.20561-20568, DOI:10.24327/ijrsr.2017.0810.0916. (2017).*

Akowuah, J., Kemausuor F., and Mitchual, J. S. (2012). Physiochemical characteristics and market potential of sawdust charcoal briquettes. *International Journal of Energy and Environmental Engineering, 3(20): 1−6.*

ASAE, (2003). Cubes, pellets and crumbles – definitions and methods for determining density, durability and moisture content. 567 – 569. *St. Joseph, Mich.: U.S.A*

Bamgboye, A. and Bolufawi, S. (2008). Physical Characteristics of Briquettes from Guinea Corn (sorghum bi-color) Residue. *Agricultural Engineering International: the CIGR Ejournal, Manuscript 1364*

FAO (1990). The briquetting of agricultural wastes for fuel: *environment and energy paper, vol. 11. Rome*

Hamish, F. (2012). The Potential for Briquette Enterprises to Address the Sustainability of the Ugandan Biomass Fuel Market. *GVEP International London.*

Kaliyan, N., and Morey, R. V. (2009). Factors Affecting Strength and Durability of Densified Biomass Products. PhD. Dissertation. *University of Minnesota, USA.*

Katimbo, A., Kiggundu, N., Kizito, S., Kivumbi, H.B., and Tumutegyereize, T. (2014). Potential of Densification of Mango Waste and Effect of Binders on Produced Briquettes. *Agric Eng Int: CIGR Journal. Vol. 16, No.4.*

Lamido, S.I., Lawal, M., and Salami, H., (2018). Briquetting Business in Nigeria: A Solution to Unemployment. *International Journal of Engineering Development and Research 6(4) 101-106*

Maninder, S. Rupinderjit, S. K., Sonia, G. (2012). Using Agricultural Residues as a Biomass Briquetting: An Alternative Source of Energy. *IOSR Journal of Electrical and Electronics Engineering (IOSRJEEE). Volume 1, Issue 5.*

Nordiana, J. O. (2010). Development and Performance Evaluation of an Electrically Operated Biomass Briquetting Machine. *International Journal of Natural and Applied Sciences, 5(2):120-124*

Obi, O. F., Akubuo, C. O. and Okonkwo, W. I. (2013). Development of an Appropriate Briquetting Machine for Use in Rural Communities. *International Journal of Engineering and Advanced Technology (IJEAT) ISSN: 2249 – 8958, Volume-2, Issue-4.*

Obioh, I. and Fagbenle, R. O. (2009). Energy Systems: *Vulnerability Adaptation Resilience (VAR). Helio International/Nigeria.*

Ohunakin, S. O. (2010). Energy Utilization and Renewable Energy Sources in Nigeria. *Journal of Engineering and Applied Sciences, Vol 5, Issue 2, pp 171-177.*

Oyedepo, S. O. (2012). Energy and sustainable development in Nigeria: the way forward. *Energy, Sustainability and Society, Springer Open Journal 2:15.*

Oyelaran, O. A., Bolaji, B. O., Waheed, M. A. and Adekunle, M. F. (2014). Effects of Binding Ratios on Some Densification Characteristics of Groundnut Shell Briquettes. *Iranica Journal of Energy & Environment 5 (2): 167-172.*

Sambo, A. S. (2009). Strategic Developments in Renewable Energy in Nigeria. International Association for Energy Economics.

Sastry, M. K., Bridge, J., Brown, A., and Williams, R. (2013). Biomass Briquette: A Sustainable and Environment Friendly Energy Option for the Caribbean. In *Fifth International Symposium on Energy, Puerto Rico Energy Center-Laccei Puerto Rico*.

Sharma, M. K., Priyank, G., and Nikita, S. (2015). Biomass Briquette Production: A Propagation of Non-Convention Technology and Future of Pollution Free Thermal Energy Sources, *American Journal of Engineering Research (AJER) e-ISSN: 2320-0847 p-ISSN: 2320-0936 Volume-04, Issue-02, pp-44-50* www.ajer.org

Sugumaran, P., and Seshadri, S. (2010). Biomass charcoal briquetting. Technology for Alternative Energy Based Income Generation in Rural Areas, 4-22. Palavakkam, Chennai 600041: *JR Designing, Printing and Advertisement Solutions.*

Tokan, A., Sambo, A. S., Jatau, J. S. and Kyauta, E. E. (2014). Effects of Particle Size on the Thermal Properties of Sawdust, Corncobs and Prosopis Africana Charcoal Briquettes. *American Journal of Engineering Research (AJER). Volume-03, Issue-08, pp-369-374.*

Zakari, I. Y., Ismaila, A., Sadiq, U. and Nasiru, R. (2013). Investigation on the Effects of Addition of Binder and Particle Size on the High Calorific Value of Solid Biofuel Briquettes. *Journal of Natural Sciences Research.Vol.3, No.12*

Treatment of Industrial Waste Water to Remove Heavy Metal (Zinc) Using Palm Flower Activated Carbon as Adsorbent

Samson Adeiza OKEJI[1], Patience Oshuare SEDEMOGUN[1]
[1]Department of Chemical Engineering,
Federal University of Technology, Minna, Nigeria
pilalokhoin@futminna.edu.ng

ABSTRACT

This study was carried out to treat zinc heavy metal present in industrial wastewater (effluent from Scientific Equipment Development Institute, Minna, Niger state, Nigeria) using activated carbon prepared from palm flower, a low-cost agricultural material. Though zinc is useful in the body, higher concentration of zinc in the body is a major contributing factor in kidney stones. The concentration of Zinc present in the wastewater was shown to be 12.3mg/l. BET results for the prepared palm flower activated carbon showed a surface area of 9.55m2/s. Adsorbent dosage, contact time, and adsorption temperature were varied in a batch adsorption process. The optimum conditions for the adsorption process were; 5g of adsorbent in 100ml of waste water sample, temperature of 1200C and contact time of 120minutes giving 93.8% removal from 12.3mg/l to 0.76mg/l. It was noted that the adsorption increased with increase in contact time as well adsorbent dosage and temperature. It was also observed that the adsorption of zinc metal on the adsorbent fits more to the Freundlich adsorption isotherm. The studies reveal that the activated carbon from palm flower is effective for the removal of Zinc ions in any industrial effluent where zinc is present.

KEYWORDS: *Activated carbon, Heavy metal, Palm flower, wastewater, Zinc.*

1 INTRODUCTION

Recent advances in science and technology have brought about tremendous progress in many areas of development, but this has also contributed to the degradation of the environment. Industrial pollution continues to be a potential threat to fresh water globally. Domestic and industrial wastes are mostly channeled to seas, lakes, oceans and other large water bodies. These wastes are either organic or inorganic, with organic wastes mostly coming from domestic wastes and inorganic from industries. Accumulation of these wastes in water bodies makes water harmful and unsafe for use by man. Inorganic wastes, which contains heavy metals stands to be of greater risk to cells of living organisms and hence constitute a major ecological menace. Waste streams containing heavy metals such as Zinc, Lead, Nickel, Copper, Cadmium and Chromium are often encountered in various chemical industries. The discharge of these non-biodegradable heavy metals into water bodies is hazardous because the consumption of such polluted water causes various health problems (Okeji, 2019). The major source of these heavy metals is the effluent of industries. Chemicals used by industries during production are mixed with water and are later discharged into water

bodies. The major factors which distinguish other pollutants from heavy metals are their non-biodegradable nature and their unpropitious inclination to accrue in living things (Abdunnasar et al., 2014). This has made the removal of such metals a thing of consideration. Techniques such as ion exchange, membrane filtration, co-precipitation, chemical precipitation and carbon adsorption have been contrived for the deportation of these heavy ferrous materials. These techniques have been limited to effluents of low heavy metal concentrations and have stood to be expensive. To reduce costs, naturally occurring materials can be used for this purpose.

The emergence of bio-adsorbents as potential alternatives for the removal of heavy metals has given a projection of these limitations being checked. Rice husk, palm flower, palm kernel husks, coconut husks, peanut shells, dry tree leaves and barks as well as activated carbon has been used as bio-adsorbents.

Adsorption of heavy metal ions occur as a result of physicochemical interaction, mainly ion exchange or complex formation between metal ions and the functional groups present on the cell surface.

Adsorption is one of the established unit operations used for the treatment of contaminated water i.e., raw water and/or wastewater. Adsorption studies are usually conducted over batch studies and column studies (Desta, 2013).

Activated carbon is one of the most used adsorbents. Researchers are currently turning towards the use of alternative and non-conventional, low-cost adsorbents for use due to the high cost of treatment and considering the enormous quantity of effluent produced by industries. Adsorption process is present in many natural physical, biological, and chemical systems, and is widely used in industrial applications such as activated charcoal, capturing and using waste heat to provide cold water for air conditioning and other process requirements (adsorption chillers), synthetic resins, increase storage capacity of carbide-derived carbons for tenable nonporous carbon, and water purification (Chavan, et al., 2019).

Based on the contributions made by many researchers who have used various materials derived from agricultural source such as orange peel, rice husk, sugarcane bagasse, coconut husk, palm flower and so on to produce adsorbents, it can be said that they are the best suitable, economical and yet effective method for treating polluted water (Kumar et al., 2008).

African palm flower which is a material from agricultural source is known to be abundantly available in Nigeria. The present study looked into the removal of zinc heavy metal as encountered in industrial and domestic waste water by adsorption using a low-cost adsorbent developed from abundantly available palm flower, a plant material.

2   METHODOLOGY
2.1 Preparation of activated carbon
The palm flower used was collected from Government Day Secondary School farm, Ihima, Kogi State. They were then taken to the Department of Water Aquaculture and Fishery Technology, Federal University of Technology, Minna and was washed using distilled water. It was then sun dried for 5 days and later crushed using the hammer mill. The crushed dried palm flower was then sieved to a desired particle size and further dried in an oven at a temperature of $105^{0}C$ for 48 hours to eliminate all the water content in the palm flower before usage.

The *palm flower* was calcined at a temperature of $200^{o}C$ for one hour using a furnace situated in Step-B Bosso campus after which it was impregnated with sulphuric acid (H_2SO_4) in the ratio 1:1. The pH was corrected by washing the sample with distilled water.

2.2 Characterization of activated carbon
Brunauer-Emmett-Teller (BET) characterization was carried out on the adsorbent (PFAC) to obtain the surface area, Pore Volume and pore width.

2.2 Preparation of the Industrial Effluent for Adsorption
The effluent used in this analysis was obtained from Scientific Equipment Development Institutes (SEDI), Minna, Niger state, Nigeria. Atomic Absorption Spectrophotometric analysis was carried out to determine the concentration of heavy metal present in the sample. It was carried out to ascertain the amount of selected elements in the wastewater sample. From the results obtained, Zinc metal, Zn^{2+} was found to be the most dominant metal present in the industrial effluent with a concentration of 12.3 mg/l. This necessitated and prompted the choice of metal removal from industrial waste water.

2.3 Equilibrium adsorption studies
2.3.1 Effect of Dosage
Adsorption dosage was varied during the first stage of the adsorption process. 1g, 2g, 3g, 4g and 5g of the adsorbent were introduced into four different conical flasks containing 100ml of the effluent each and then placed in a water bath with constant agitation. A constant contact time of 30 minutes, temperature of $30^{o}C$ and effluent volume of 100ml was used.
2.3.2 Effect of contact time
Contact time between the adsorbent and the effluent was varied to ascertain the optimum time of contact of the system. The variation was done for a total period of 2 hours starting from 20 minutes, 40, 60, 80 and 120minutes. This was done by introducing 1g of the adsorbent into five different conical flasks containing 100ml of the effluent and they were placed in a water bath with constant agitation. Each conical flask was removed after each

variation time is completed and then filtered with a filter paper, then the resulting effluent was stored in a sample bottle and taken for final analysis of the effluent using the Atomic Absorption Spectrophotometer at step-B bosso. All other parameters such as adsorbent dosage, effluent volume and temperature we kept constant with values of 1g, 100ml, and 30°C respectively, while the contact time was varied.

2.3.3 Effect of Temperature

To ascertain the effect of temperature on the adsorption process of heavy metals using activated carbon obtained from palm flower, the temperature was varied from 30°C to 120°C. This was done by placing 1g of the adsorbent into four different conical flask and each conical flask with varying temperature i.e., 30, 60, 75, 100 and 120°C was taken at a time into the water bath with constant agitation for constant time of 30 minutes. The volume of effluent, adsorbent dosage and contact time were kept constant at 100ml, 1g and 30 minutes respectively.

3 RESULTS AND DISCUSSION

3.1 BET characterization BET Characterization of *palm flowerActivated carbon* (PFAC).

Table 3.1 Characterization of *palm flower Activated carbon (PFAC).*

S/N	Data Reduction Parameter	Values obtained from analysis
1	Surface Area	$9.55 m^2/g$
2	Pore Volume	$0.0788 cm^3/g$
3	Pore width	245.65nm

3.1.1 Effect of Dosage Adsorption capacity of adsorbent on industrial effluent

Table 3.2 Adsorption with varying adsorbent dosage

Heavy metal	Adsorbent dosage (g)	Zn^+ (initial conc.)(mg/l)	Zn^+ (final conc.)(mg/l)	Removal ration (%)	Contact time (min)
Zn	1	12.3	2.75	77.64	30
	2	12.3	2.43	80.24	30
	3	12.3	1.85	84.96	30
	4	12.3	1.63	86.75	30
	5	12.3	0.89	92.76	30

The figure 1 below show that the more the adsorbent dosage, the more the percentage removal of zinc metal. This was proved experimentally by varying the adsorbent dosage from 1 – 5g in 100ml of effluent at a temperature of 30oC and a time of 30minutes. The calculated percentage removal of the zinc metal was plotted against the adsorbent dosage to obtain Figure 1. It can then be said from the figure that the maximum percentage removal was obtained at 5g which was the maximum adsorbent dosage used. The curve shows that the higher the adsorbent dosage, the higher the percentage removal.
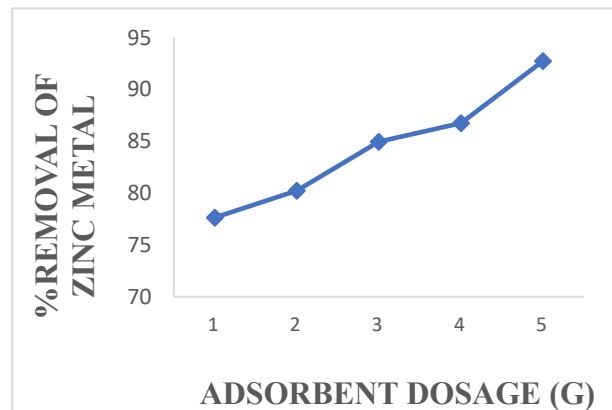

Figure 1 Effect of Adsorbent Dosage

3.1.2 Effect of contact time

Table 3.3 Adsorption with varying Contact Time

Heavy metal	Adsorbent dosage (g)	Zn^+ (initial conc.)(mg/l)	Zn^+ (final conc.)(mg/l)	Removal ratio (%)	Contact time (min)
Zn⁺	1	12.3	2.53	79.43	20
	1	12.3	2.41	80.41	40
	1	12.3	1.89	84.63	60
	1	12.3	1.52	87.64	80
	1	12.3	0.76	93.82	120

The figure 2 below shows a plot of percentage removal of heavy metal at different contact time.

This was conducted experimentally to know the equilibrium contact time of the adsorbate between liquid and solid regions. The plot shows an increase in the percentage removal of the metallic ions as the contact time is increased. The graph shows that 120minutes was the optimum time for the highest percentage removal of zinc which was 93.82% from effluent. Equilibrium is reached when no more metal ions can be housed on the adsorbent. The amount of adsorbate adsorbed at this time shows the maximum capacity of the adsorbent under this specific condition.

With this, it can be propounded that the percentage removal of zinc metallic ions is directly proportional to the contact time.
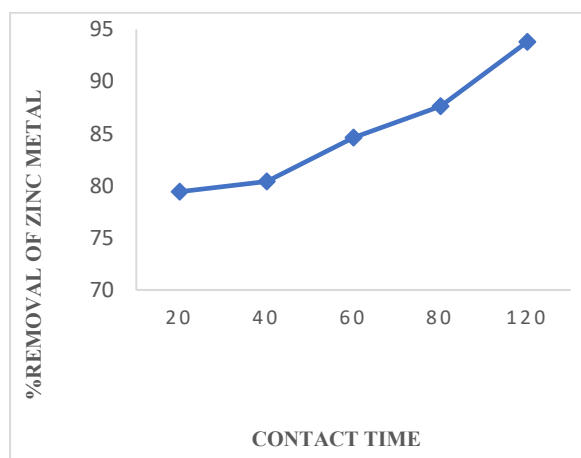
Figure 2: Effect of Contact Time

Table 3.4 Adsorption with varying temperature

Heavy metal	Adsorbent dosage (g)	Temperature (min)	Zn^+ Initial conc (mg/l)	$Zn+$ Final Conc. (mg/l)	Removal ratio (%)
Zn^+	1	30	12.3	2.45	80.08
	1	6	12.3	2.32	81.14
	1	75	12.3	1,76	85.69
	1	100	12.3	1.32	89.27
	1	120	12.3	1.02	91.71

The figure 3 shows that at 30°C, the percentage of zinc was found to be 80.08% and at 60°C, there was no much significant difference in the percentage removal. Significant increase is however noticed at 75°C, with a percentage of 85.69%. It can thus be deduced that there is increase in the amount of heavy metal removal as operating temperature increases.

The optimal operating temperature for the process was found to be 120oC.
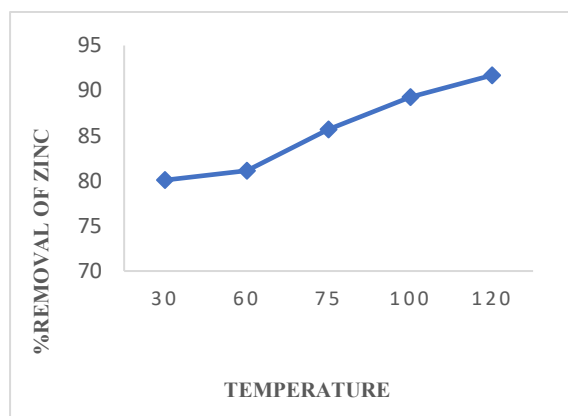
Figure 3: Effect of Temperature

3.5 Adsorption Isotherms

A better understanding of adsorption is gotten by studying the adsorption isotherms. These isotherms show the distribution of solutes in the adsorption phases. Various models help in explain this distribution but, but based on the scope of work, the Freundlich and Langmuir linearized adsorption isotherms were considered. The figure 4 and 5 shows the plots and the R-squared values are also stated. The R-squared values clearly show that the adsorption of Zinc ion is best explained by the Freundlich adsorption isotherm.

3.5.1 Isotherm data

Table 3.5 Isotherm data

Ce (mg/L)	q(mg)	Q (mg/g)	L0G Ce	LOG Q	1/Qe	1/Ce
2.75	0.955	0.955	0.439333	-0.02	1.04712	0.363636
2.43	0.987	0.4935	0.385606	-0.30671	2.026342	0.411523
1.85	1.045	0.34833	0.267172	-0.458	2.870813	0.540541
1.63	1.067	0.26675	0.212188	-0.5739	3.748828	0.613497
0.89	1.141	0.2282	-0.05061	-0.64168	4.382121	1.123596

3.5.2 Langmuir adsorption isotherm for Zinc (Zn) by plotting 1/Q against 1/Ce.
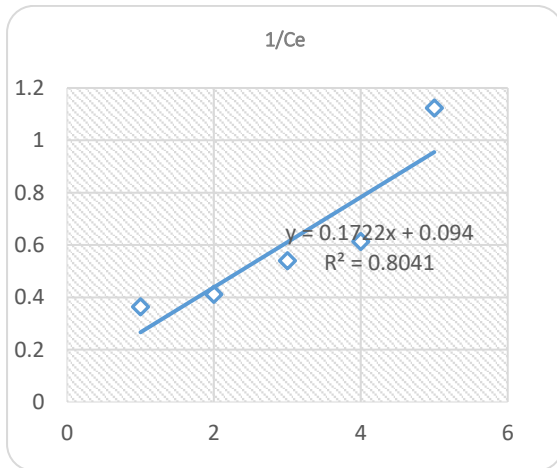
3.5.3

FIGURE 4: Graph of Langmuir Adsorption Isotherm

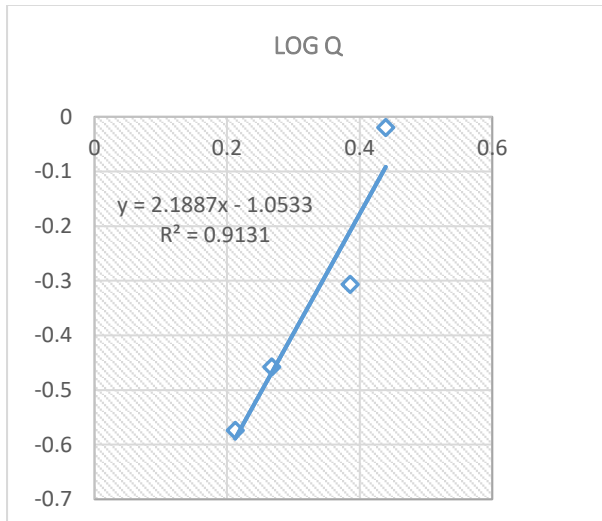### 3.5.3 Freundlich adsorption isotherm for Zinc (Zn) by plotting 1/Q against 1/Ce.

FIGURE 5: Graph of Freundlich Adsorption Isotherm

3.5.4 Comparative studies between Langmuir and Freundlich adsorption isotherm

3.5.5 Langmuir adsorption isotherm

From the plot, Figure 2.0

y = 0.1722x + 0.094

Comparing with Langmuir's equation, Table 1.4 was obtained.

$$\frac{1}{q_e} = \frac{1}{a_L} \times \frac{1}{C_e} + \frac{k_L}{a_L} \qquad (1)$$

$$y = \frac{1}{q_e} \; ; \; x = \frac{1}{C_e} \qquad (2),$$

TABLE 3.6: Langmuir adsorption isotherm

1/ a_L	a_L	K1 / a_L	K1	R^2	a_L / k1	R_L
0.1722	5.807201	0.094	0.545877	0.7381	10.6383	0.12963

3.5.6 Freundlich adsorption isotherm

Comparing with Freundlich's equation, Table 3 was obtained

From the plot,

y = 2.1887x - 1.0533

Comparing with Freundlich's equation;

$$\log q_e = \log K_F + \frac{1}{n} \log C_e \qquad (1)$$

$$y = \log q_e \; ; \; x = \log C_e \qquad (2)$$

Table 3.7: Freundlich adsorption isotherm

1/n	N	R^2	log k	k
2.1887	0.456892	0.8688	-1.0533	0.348785

Kinetic studies

TABLE 3.8: Kinetic data

Co	t(min)	Ce	qt	(qe − qt)	Log(qe − qt)
12.3	20	2.53	97.7	17.7	1.247973
	30	2.41	98.9	16.5	1.217484
	60	1.89	104.1	11.3	1.0 53078
	80	1.52	107.8	7.6	0.880814
	120	0.76	115.4	0	0

First order Model for Zinc (Zn) is obtained by plotting log (qe-qt) against t.
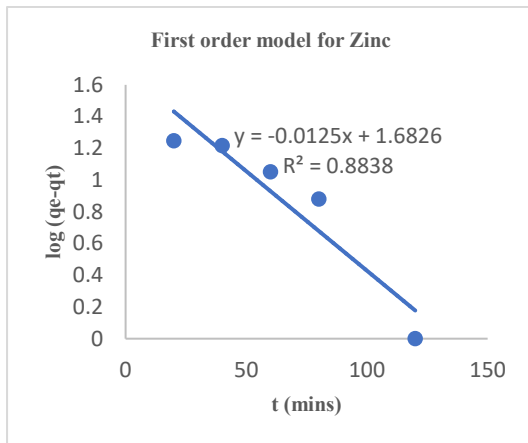
Figure 6: First order diffusion models.

3.5.8 Comparing with First Order Model equation and figure 4.6, the first order constants was obtained

From the plot,

y = -0.0125x + 1.6826

$$\frac{dq}{dt} = k_1(q_e - q)$$

(4)

$$Log(q_e - q) = log(q_e) - \frac{k_1}{2.303}t$$

(5)

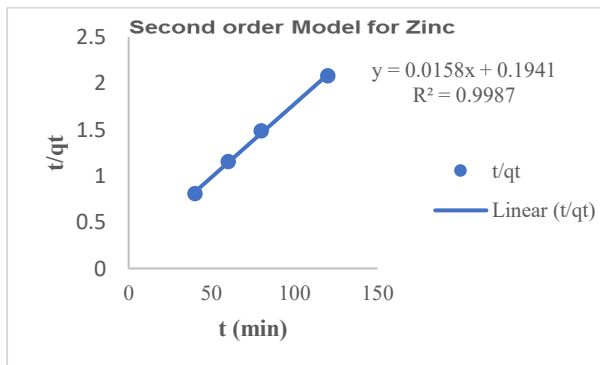**Second order Model for Zinc (Zn) is obtained by plotting t/qt against t.**

Figure 7: Second order diffusion models.

3.5.9 Comparing with second Order Model equation and figure 4.7, the second order constants was obtained

From the plot,

y = 0.0158x + 0.1941,

Comparing with second Order Model equations

$$\frac{dq}{dt} = k_1(q_e - q)^2$$

(6)

This expression can be re-written in a linearized form as

$$\frac{t}{q} = \frac{1}{k_2\,q_e^2} + \frac{t}{q_e}$$

(7)

3.5.10 First and Second order model constant

First order constants in relation to first order model equation 4 and 5, while second order constants in relation to second order model equation 6 and 7.

Table 5: First and Second order model constant

Kinetic Parameters	Zinc
First Order	
$K_1(min^{-1})$	0.028788
$q_e(mg/g)$	4674.122
R^2	0.8838
Second Order	
K_2	4.850005
$q_e(mg/g)$	63.29114
R^2	0.9987

CONCLUSION

This study shows that the adsorption of zinc metal Zn2+, onto the palm flower activated carbon treated with sulphuric acid was effective. From the experimental results obtained, it is noted that an adsorbent dosage of 5g was obtained as the optimum dosage in 100ml of the solution. The optimum temperature was gotten to be 1200C while the optimum time was 120 minutes.

The adsorption isotherm data fitted well with the Freundlich adsorption equilibrium models. The separation factor of the Langmuir isotherm R1 lies well in between 0 and 1. The Freundlich constant (n) fell between 1 and 10 which indicated that the process is favourable. The analysis carried out by the Atomic Adsorption Spectrophotometer (AAS), showed that the effluent gotten from the Scientific Equipment development Institute (SEDI) had a higher concentration of Zinc metal (i.e., 12.3mg/l), hence making it a point of interest for this experiment, while other metals such as iron, manganese were found in lower concentrations. These heavy metals were present beyond their threshold values (acceptable limits) and hence, needs treatment before being disposed into the environment. The results obtained from the adsorption study shows that adsorption as a process is dependent on key factors such as adsorbent dosage, contact time between the adsorbate and adsorbent, and the temperature of the process. With an encouraging removal percentage obtained from the experiment, it can hence be concluded that palm flower activated carbon (PFAC) is a low-cost agricultural source material based activated carbon and it is a recommendable and suitable adsorbent to be sort after when it comes to carrying out a viable adsorption study which can be employed for the removal of heavy metals from wastewater or any industrial effluent.

REFERENCES

Abdunnasar, M. E, Mahmoud, E, Mohamed, T. M. (2014). Removal of some heavy metals from waste water using Fava beans. 225-226.

Alen Gabelman P. C. (2017). Adsorption Basic part 1, Gabelman process solution LLC, American institute of chemical engineers.

Alloway B. J (2013). Source of heavy metals and metalloids in soil. In: Alloway B (eds) Heavy metal in soils. Environmental pollution, volume 22 Springer, Dordrecht.

Amana T., Kazi A. A., Sabir M. U., Banao Q., (2008). Potato peals as solid waste for the removal of heavy metals copper II from waste water/industrial effluent. Colloids surf. B; Biointerfaces 63, 166-181.

Barakat M., (2011). New trends in removing heavy metals from industrial waste water. *Arabian Journal of chemistry*, 361-377.

Bharathi K. S. and Ramesh S.T. (2013). Removal of dyes using agricultural waste as low-cost adsorbents: A review, *Applied Water Science 3(4)* December 2013, DOI: 1110.1007/s13201-013-0117-y

Chen G. H. (2004), Electrochemical technologies in waste water treatment. *Sep. purifies. Technol.* 38 (1).11-41.

Crini G., Lichtfouse E., Wilson L., Nadia Morin-Crini. (2019). Conventional and non-conventional adsorbents for wastewater treatment. *Environmental Chemistry Letters*, Springer Verlag, 17(1),195-213. DOI:10.1007/s10311-018-0786-8

Desta M. B., (2013). Batch Sorption Experiments: Langmuir and Freundlich Isotherm Studies for the Adsorption of Textile Metal Ions onto Teff Straw (*Eragrostis tef*) Agricultural Waste, *Journal of Thermodynamics*, vol. 2013, Article ID 375830, 6 pages, 2013. https://doi.org/10.1155/2013/375830

Ebuka, O. (2017). 59,000 children in Nigeria die yearly of water related diseases, Nigerian government. Premium times publications.

Fenglianfu, Q. W. (2010). Removal of metal ions from waste water: A review, *Journal of environmental management*.

Fu F, Wang Q. (2011). Removal of heavy metal ions from wastewaters: a review. *Journal of Environmental Management*. 92(3):407-418. DOI: 10.1016/j.jenvman.2010.11.011.

Gulson B. L. Mahaffey K. R., Mizon K. J., Korsch M. J., Cameron M. A., Vimpani G. (1995). Contribution of Tissue Lead to Blood Lead in adult female subjects based on stable lead isotope method. [Retrieved from http://www.ncbi.nlm.nih-gov/pubmed/77693643]: J. lab clin med 125; 703-712.

Gupta V. K., Jain R., Saleh T., Nayak AA., Malathi S. and Agarwal S. (2011). Equilibrium and thermodynamic studies on the removal and recovery of safranine-T dye from industrial effluents. *Separation science and technology*, 46 (5), 839-846.

Kumar S. P., Senthamaria C., Durgadevi A. (2012). Adsorption kinetics, mechanism, isotherm and

thermodynamics analysis of copper ions onto the surface modified agricultural waste. *America institute of chemical environ prog*, 33: pg 28-37.

Laxmi G. S., Ahmaruzzaman M. (2014). Phenotic waste water treatment: Development and application of new absorbent materials" *Industrial Wastewater Treatment Recycling and Reuse*, volume 1.

Lim A.P. and Aris A.Z., (2014). A review on economically adsorbents on heavy metals removal in water and wastewater. Reviews in Environmental Science and Bio/Technology, 13(2), 163-181.

Mousa W. M., Soliman S. I., El-Baily A. B. and Hanaa A. S., (2013). Removal of some heavy metal from aqueous solution rice straw, *Journal of Applied Science Research* 9(3); 1696-1700.

Nalenthiran P., Sambandam A., and Muthu Pandian A. (2015). Removal of heavy metals from waste water An alternative green sonochemical process optimization and pathway studies. *Hand book of ultrasonic and sonochemistry,* Springer science business media, Singapore.

Nimibofa A., Augustus N. E. and Donbebe W. (2017). Modeling and interpretation of adsorption isotherms. *Journal of chemistry department of chemical science*, Niger Delta University, 11.

Ptiha E. H., Hidayat y. and Firdaus M. (2016). The Langmuir isotherm adsorption equation; the monolayer approach. *Iop conference series: material science and engineering* volume 107, conference 1.

Rana S. V. S. (2006). Environmental pollution; health and toxicology *Alpha science international technology limited U.K.*, 172.

Raymond A. Wuana, Felix E. Okieimen, (2011). Heavy Metals in Contaminated Soils: A Review of Sources, Chemistry, Risks and Best Available Strategies for Remediation, *International Scholarly Research Notices*, vol. 2011, Article ID 402647, 20 pages, 2011. https://doi.org/10.5402/2011/402647

Ruan C. A. Moura, Daniel A. B., Carlos A. F. Franco D. R. Amado (2012). Study of chromium removal by the electrodialysis of Tannery and metal-finishing effluents. *International journal of chemical engineering,* volume 2012, article ID 179312. Brazil.

Shende, A., and Main, J. S. (2014). Effect of Contact Time on Adsorption of Nitrates and Phosphates. *International Journal of Advanced Technology in Engineering and Science*, pp 117-122.

Tchounwou, P. B., Yedjou, C. G., Patlolla, A. K., & Sutton, D. J. (2012). Heavy metal toxicity and the environment. *Experientia supplementum*, *101*, 133–164. https://doi.org/10.1007/978-3-7643-8340-4_6

UNEP (1991). Impact of lead toxicity in social ecosystem UNEP, 1991.

Veli, S and Alyüz, B. (2007). Adsorption of copper and zinc from aqueous solutions by using natural clay. *Journal of Hazardous Materials*, 149(1), 226-233.

Wang H., and Farhang S. (2012) "Effect of particle size on the adsorption and desorption properties of oxide nano particles". *American Institute of chemical engineers* 59: 1502-1510.

Wang L. K., Vaccari, D. A., Li, Y., Shammas N. K.., (2004). Chemical precipitation. In Wang L. K., Hung Y. J., Shammas N. K. (Eds), *Physicochemical Treatment Processes*, volume 3. Humana press, New Jersey, pp. 141-198

The Nigerian Society of Engineers
Minna Branch
1st NSE Minna Branch National Conference 2021

Conference theme
Role of Engineering in Sustainable Development Goals

Irrigation with Unsafe Industrial Wastewater and Associated Health Risks: An Emerging Technology for Heavy Metals Removal

A. S. Mohammed[a,c*], E. Danso-Boateng[b], G. Sanda[c], A.D. Wheatley[c], M.I. Animashaun[d], I.A. Kuti[c], H.I. Mustapha[d], M.Y. Otache, J.J. Musa[d]

[a,d]Department of Agricultural and Bioresources Engineering, School of Infrastructure, Process Engineering and Technology, Federal University of Technology, Minna, Nigeria
[b]School of Chemical, Energy and Process Engineering, University of Leeds, Leeds, LS2 9JT, UK.
[c]School of Architecture, Building and Civil Engineering, Loughborough University, Loughb., LE11 3TU, UK.
[*]Corresponding email: ask4sadeeq@futminna.edu.ng

GRAPHICAL ABSTRACT
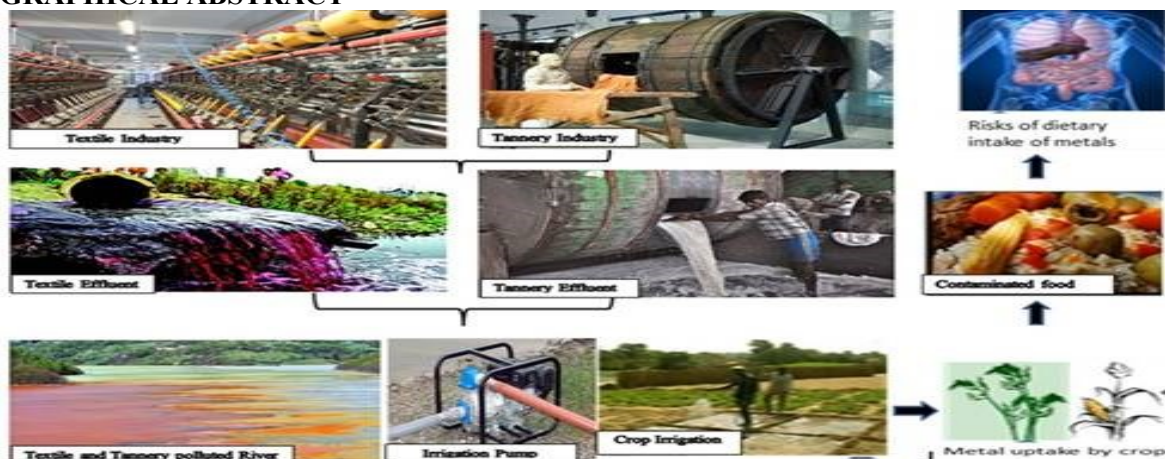
ABSTRACT

The scarcity of freshwater resources, being currently experienced in water-stressed countries has prompted millions of smaller farming communities to depend on wastewater for crop irrigation, drinking, bathing and fishing. However, in this context, the treatment of wastewater from textile and tannery industries is the subject of interest, this paper aim to address. The rule of thumb suggests, wastewater to constitute beneficial nutrients recycling due to rich organic matter content. Inherently, the same kind of wastewater has been investigated and analysed by several researchers and found to contain micro-pollutants such as inorganics (heavy metals, salts) and organics (dyestuff, starch). Regrettably, the presence of these pollutants in wastewater used for irrigation is of concern particularly as it relates human health. Although, several conventional wastewater treatment technologies exist; their applications are now hamstrung by high procurement, operation and maintenance costs. Recent studies on cheap and readily available biomass wastes have confirmed their high sorption potential and can therefore, be used as adsorbents for micro-pollutants removal from industrial wastewater. In this study, chicken eggshell, coconut peat, coconut shell, rice husk and lemon peel were all used for the wastewater treatment. Hydrothermal carbonisation (HTC), was used to change the surface functional characteristics of the adsorbents for enhanced adsorption. To achieve this, batch experiments using raw biomass were carried out in triplicates at 3 different contact times and pH values. After 2 hr of contact time at pH9, the coco-peat was proven to have Cr removal efficiency of 91.6% against 73.2% using a bonechar; and 95.0% for Pb (II) against 91.2% for the bonechar. The outcome of this study suggests that coconut-peat and eggshell even without been carbonised can provide a cost-effective means for metal removal from industrial wastewaters.

KEYWORDS: *Adsorption, biomass waste, crop irrigation, freshwater scarcity, wastewater reuse*

The Nigerian Society of Engineers
Minna Branch
1st NSE Minna Branch National Conference 2021

Conference theme

Role of Engineering in
Sustainable Development Goals

1 INTRODUCTION

One-third of the world's population currently live in developing and water-deficit countries, with overall water need is expected to rise by 2025 (Gu, et al., 2019; Dubey and Swain 2019). As a consequence of the resource exploitation, about two-third of the global population would suffer from water shortages (Mahfooz, et al., 2020). Scarcity of freshwater resources may limit food production and supply, as about 70% of all freshwater withdrawals go to irrigated agriculture (≈ 2800 km3 of freshwater/year). Scarcity of freshwater resources may limit food production and supply, as about 70% of all freshwater withdrawals go to irrigated agriculture (≈ 2800 km3 of freshwater/year) (UN-Water, 2012). Water is an essential resource for the sustenance of life and plays a cardinal role in agriculture and allied industries, consequently, it also receives a variety of wastes from different sources (Merchant and Painter, 2019; Kennedy,et al., 2018). Studies have shown that there is global decline in the amount of available freshwater resources due to intensified agricultural practices such as excessive application of fertilizers, pesticides, insecticides and herbicides (Gu, et al., 2019) as well as climate change and increasing urbanization but its severity is mostly experienced in developing and water-stressed countries (Mahfooz, et al., 2020). The economic contributions of peasants farmers especially in developing and water-stressed countries are now hamstrung by freshwater scarcity, and this is observed to affect the expansion of crop yields and their quality. As a consequence of artificial scarcity of freshwater resources, wastewater stem to provide a great deal of relieve to farmers for year-round production of crops (Dubey and Swain, 2019). The use of wastewater for agriculture permits the cultivation of wide range of crops in multiple cycles, thereby promoting potentials for high yields.

Surmise to the above, reuse of wastewater for agriculture has become a norm and its practical application in developing and water-stressed countries has historical precedence which is likely to increase in the near future (Bougnom and Piddock, 2017). Although, several benefits of wastewater reuse, particularly in agriculture have been widely reported; it's practical application is most beneficial and cost-effective in developing nations (Drechsel, et al., 2009). However, despite the huge economic benefits of wastewater reuse, it is apparent that this important resource is recording varying concentrations of heavy metals and pigments due to uncontrolled discharge of industrial effluents into waterways (Becerra-Castro et al., 2015; Mohammed et al., 2020).

Regrettably, the peasant farmers along the fringes of these waterways utilize such resource for crop irrigation, hence compromising crop quality and food safety (Dickson, et al., 2016). There are several documented articles from developing countries reporting varying concentrations of organic and inorganic chemical substances in agricultural soils and crops that have been receiving perpetual wastewater (Qu, et al., 2019). Ironically, the concentrations of these pollutants in wastewater, agricultural soils and crops usually exceeds the FAO/WHO recommended thresholds. Seemingly, prolong exposure to wastewater pollutants are impediments that hinders safe agricultural practice and farmers' productivity, which culminate to pervasive health implications on humans through food supply chain. There are several research articles establishing the epidemiological and carcinogenic links between the consumption of poorly irrigated crops with individual or societal illnesses (Qu, et al., 2019; El-Azazy et al., 2019). Other likely ailments resulting from excessive exposure to heavy metals and metalloids include mutagenicity, carcinogenicity and teratogenicity. Mutagenicity is the alteration of genetic structure, while carcinogenicity causes damage to specific regions of the genome, Carcinogenic substances can get into a biological tissue through inhalation, ingestion and contact with skin. Teratogenicity on the other hand, is a specific mutagen that cause damage to the genome which then causes abnormality in the developing foetus (Tong et al., 2000). It's worthy to know, that humans, animals and plants do not have good mechanisms for fixing or excreting heavy metals; hence bio-ccumulate and remain for life (Zhuang et al., 2009 QU, et al., 2012).

Policymaking bodies such as World Health Organisation (WHO), Food and Agriculture Organisation (FAO), International Commission on

Irrigation and Drainage (ICID), among others have been exploring modalities to safeguard humans and environment from excessive exposure to micro-pollutants found in wastewater used for irrigation. In a quest to define these modalities, these international bodies jointly issued some guidelines to regulate the concentrations of micro-pollutants in irrigation water worldwide. Adoption of these guidelines is highly desirable; but in reality, their implementation is hard to achieve practically, particularly in developing countries (Chang et al., 2002). The probable reasons for the unsuccessful implementation of those guidelines may be due to any or combination of the following: 1) high procurement and installation costs for modern wastewater treatment facilities; 2) non-compliance with policy guidelines governing effluent discharge into waterways and environment by industries; and 3) poor monitoring and enforcement strategy.

The essence of these guidelines is to safeguard agricultural soils, plants and humans from excessive exposure to organic and inorganic chemical substances (Dickson, et al., 2016). Although, application of these guidelines has recorded tremendous success in developed nations; regrettably, their effective implementation in developing countries is still looming and unsuccessful (Ensink and Van Der Hoek, 2009). Proffering an alternative wastewater treatment method is the purpose for which this paper is anchored.

Over the years, chemical precipitation, ion-exchange, electro-dialysis, reverse-osmosis, membrane and adsorption using activated carbon and other industrial by-products have been the most widely treatment technique for wastewater (Geetha and Belagali, 2013; Bhattacharjee et. al., 2020; Ajiboye, et. al., 2021). Of all the treatment methods mentioned, activated carbon is reported to be the most commonly used for the removal of ions and pigments from industrial wastewater at much lower concentrations (Phadtare and Patil, 2015; Bhattacharjee, et al., 2020). However, the major limitation with the use of activated carbon is that its procurement is quite expensive.

Furthermore, limitations of conventional wastewater treatment methods mentioned above, other than activated carbon include high initial operating cost and generation of secondary toxic wastes which may require additional cost of treatment. The toxic wastes generated are mostly non-environmentally friendly. Against these backdrops, researchers are now exploring cheaper, sustainable and more effective method for the removal of organic and inorganic pollutants in wastewaters (Bhattacharjee, et al., 2020).

To this end, the work herein, explores the potentials of biomass wastes that comprise rice husk, coconut shell, coconut peat otherwise called coir, chicken eggshell and lemon peel. All these wastes are readily available in Nigeria. The raw biomass wastes are needed for the preliminary adsorption tests. However, for column tests, the biomass wastes were carbonised to produce hydrochar. The technology used for the conversion of biomass wastes into hydrochar is called hydrothermal carbonisation (HTC). Hydrochar is mainly composed of 40–45wt% cellulose, 25–35wt% hemicellulose, 15–30wt% lignin and up to 10wt% for other compounds (Sevilla and Fuertes, 2009).

Hydrothermal carbonisation is an exothermic process that takes place in water at temperature between $180 – 250\ °C$ within a time period ranging from 30–500 min to produce a carbon-rich coal-like derivative commonly called hydrochar at saturated pressure of $15 – 20$ bar which releases CO_2 and other volatiles (Titirici et al., 2007; Funke and Ziegler, 2010; Libra et al., 2011). The HTC involves dehydration and decarboxylation of biomass in order to raise the carbon content which enhances sorption characteristics and increases hydrochar energy values (Libra et al., 2011). For the purpose of his paper, only raw biomass wastes are used to investigate the effectiveness of the metal ions removal.

2   MATERIALS AND METHODS

2.1   RAW MATERIALS

All the materials used herewith were obtained locally; these include the following: the chicken eggshell were gotten from the Loughborough University kitchen; lemon from a street market in Loughborough town, Leicestershire; the coconuts bought from a supermarket also in Loughborough;

the coconut peat was purchased from Fertile Fibre, Withington Hereford; and rice husk from E-Coco Products, Tewkesbury, all in the UK.

2.2 PREPARATION OF THE ADSORBENT

Commercial activated bonechar (BS) was supplied by Jaret Limited, 4 Birch groves, Houston, Johnstone, Renfrewshire, Scotland. The bonechar was meant to serve as the reference adsorbent material to the raw biomass wastes and their corresponding hydrochars used for the adsorption. See Figure 1.
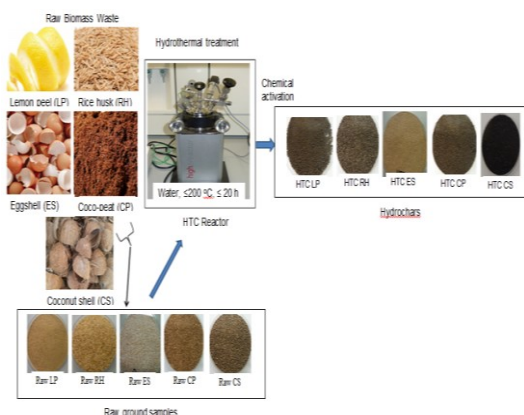

Figure 1: A graphical illustration of hydrochar production from biomass wastes using HTC

2.3 REAGENTS AND INITIAL CONCENTRATION OF SIMULATED WASTEWATER

All reagents used in this study were of analytical grade, supplied by Fisher Scientific Equipment Laboratories Ltd., Loughborough, United Kingdom. The standard ICP solution was prepared in nitric acid with concentration of 10,000 mg/L for $CuSO_4$ and $Pb(NO_3)_2$, and 1000 mg/L for K_2CrO_4 and $FeSO_4$. Procedure for the synthetic wastewater preparation was based on the method outlined in Standard Methods for the Examination of Water and Wastewater (APHA, 2012). To prepare the required 5 mg/L of the standard solution needed for the adsorption studies, approximately 0.5 ml of $Pb(NO_3)_2$ and $CuSO_4$ were withdrawn and poured into an empty 1000 ml (1 L) volumetric flask,

followed by addition of 5.0 ml of K_2CrO_4 and $FeSO_4$. Deionise water was added to the flask to make up to 1 litre. The stock solutions of the synthetic wastewater on the other hand, was meant to contain a mixture of Cr(VI), Cu(II), Fe(II) and Pb(II) at six different concentrations (0.5, 1.0, 2.0, 3.0, 4.0 and 5.0 mg/L); given initial concentration, C_1 as 100 mg/L; initial volume, V_1 (0.5, 1.0, 2.0, 3.0, 4.0 and 5.0 ml) and final volume, V_2 (100 ml). The mixture was poured into separate volumetric flasks and labelled according to the concentrations. In order, to produce a fair representation of a typical textile and tannery wastewater, 2 g/kg of corn starch, 6.13 g/kg of anhydrous sodium sulphate (Na_2SO_4) and 0.09466 g/kg of methylene blue were added to the undiluted constituents in each volumetric flask before deionised water was added to make-up 1 litre. The dosages of corn starch, salt and methylene blue stated above were chosen and used based on the recommendations of Awomeso *et al.* (2010), Ong *et al.* (2010) and Randall *et. al.* (2014).

2.4. Adsorbent dosage

Batch adsorption tests were conducted by starting with measuring 1.5 g of each raw biomass waste (eggshell, rice husk, coconut shell, coconut peat and lemon peel) in a conical flask before adding 50 mL of ordinary deionised water. The purpose for this is to determine a baseline concentration of each inherent analyte of interest and pH in the aqueous samples. The conical flasks were then placed on a pH meter incorporated with magnetic stirrer (pH-8+ DHS Benchtop meter, Czech Republic) and various sample pH taken. Then the conical flasks were transferred to a mechanical shaker (Gallenkamp Orbital Incubator-cooled Shaker, INR-200 INR-250, Netherlands) for thorough mixing. The incubator was pre-set at room temperature (25 ± 2 °C) and speed of 150 rpm. At each time lap (10, 20, 30, 40, 50, 60, 120, 240 and 360) mins, a corresponding flask was withdrawn from the shaker, filtered using Whatman paper No. 42 (2.5 μm) membrane filter to separate treated water from the solid sorbents. The filtrates were analysed for the baseline concentrations of Cr(VI), Cu(II), Fe(II) and Pb(II). The baseline concentrations served as the controls for the experiments and were deducted from the sample analysed using wastewater. Similarly, the

procedure was followed using the same adsorbent dosage, operating conditions and volume of wastewater.

2.5. Effect of contact time on adsorption.

At the preliminary stage of this study, the effect of three (3) different contact times (2, 4, and 6) h on adsorption were examined using the raw biomass wastes. The chosen contact time were for the purpose of optimisation in order to explore to shortest possible time to achieve maximum adsorption yield.

2.6 Effect of pH

A polygon F371220040 spin bar was dropped into each volumetric flask containing ordinary water different adsorbent and placed on magnetic stirrer to examine the effect of solution pH on adsorption. While the magnetic stirrer is switched ON, the mixture begins to stir, and the initial pH taken. and that was repeated after adjustment with 1M NaOH. Based on typical scenarios as documented in several literature, textile and tannery wastewaters are known to be alkaline in nature with pH values ranging from 9 to 11. Hence, this justifies the choice of pH9 and pH11 for alkalinity medium used in this study. Whereas, the pH of solutions that contain hydrochar in natural state ranges from 4 to 6, which is relatively acidic. However, in order to adjust the acidic pH to alkalinity, 1M of sodium hydroxide (NaOH) was gradually added to the solution until the desired pH for each mixture was attained.

2.7 Heavy metal removal efficiency

To determine the percentage adsorption of heavy metals by the adsorbents, the following equation as described by (Chen and Wang, 2008) was used.

$$R\% = \left[\frac{C_i - C_f}{C_i} \right] \times 100$$

(1)

Where;

C_i is initial metal concentration (mg/L) and
C_f is the final metal concentration (mg/L).

2.8 CHARACTERISATION OF BIOMASS WASTE

The analytical method used in carrying surface characterisation are as follows: (i) Scanning Electron Microscopy (SEM); (ii) Energy Dispersive X-Ray Spectroscopy (EDS); (iii) Brunauer, Emmett and Teller (BET), (vi) Fourier transformed Infrared Ray (FTIR).

2.9 BATCH ADSORPTION TESTS

At the end of the batch adsorption tests after, the filtrates (treated water) were all collected in 50 mL labelled plastic bottles and stored at 4 oC to analyse and determine the residual concentration of each interacting heavy metals and pigment in the synthetic textile and tannery wastewater.

3. RESULTS AND DISCUSSION

3.1 CHARACTERISATION OF RAW BIOMASS AND CORRESPONDING HYDROCHAR

Details on surface characterization, including morphology, pore volume, pore size and Fourier Transform Infrared Ray (FTIR) of both raw biomass wastes and the corresponding hydrochar can be found in the author's recent publication by Danso-Boateng et al. (2021)

3.2 EFFECT OF CONTACT TIME ON METAL ADSORPTION BY RAW BIOMASS WASTE

The effect of contact time on adsorption of Cr(VI), Cu(II), Fe(II) and Pb(II) ions from an aqueous textile and tannery wastewater by various raw biomass wastes (ES, RH, CP and LP) was investigated. The preliminary results of the batch tests that were carried out using only raw biomass wastes are presented in Figure 8. To start with, a careful study of Figure 8 (b), (c) and (e) displayed very low uptake of Cr(VI) ions. This implies that the surface chemistry of the raw ES, RH, LP have poor sorption affinity for the Cr(VI) ion and even with progressive increased in contact time, there is no significant change on the amount of Cr(VI) ions removed. However, Figure 8 (a) and (d) indicates removal of about 80% and 90% of Cr(VI) by BC and CP respectively after the first 2 h.

Conference theme
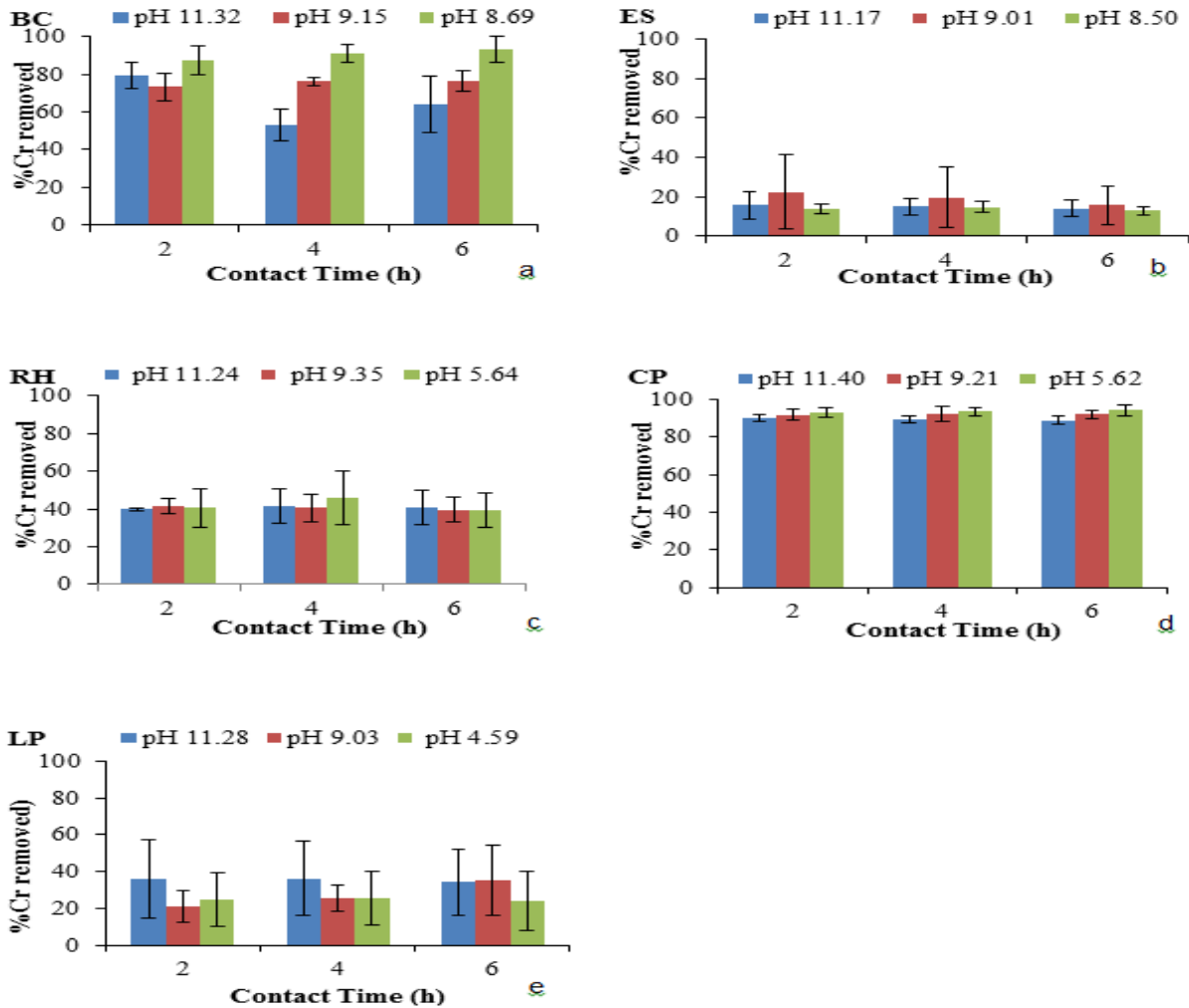**Role of Engineering in Sustainable Development Goals**

Figure 2 shows the effect of contact time on % removal of Cr(VI) by: (a) BC (b) ES (c) RH (d) CP and (e) LP

Surprisingly, Figure 3 (d) the raw CP appears to have sorption ability almost equal the reference adsorbent, though the BC has been a derivative of a pyrolytic process and characterised with larger surface area than the CP. In Figure 9 over 95% Cu(II) was removed by ES and CP as shown in Figure 3(b) and (d) respectively within the first 2 h and the adsorption rate remain constant. This shows that increase in contact time did not affect the amount of Cu ions adsorbed. About 50% of Cu ions was removed by RH and LP as shown in Figure 3 (c) and (e) after 2 h of contact; thereafter the percent adsorption decreased.

The Nigerian Society of Engineers
Minna Branch
1st NSE Minna Branch National Conference 2021
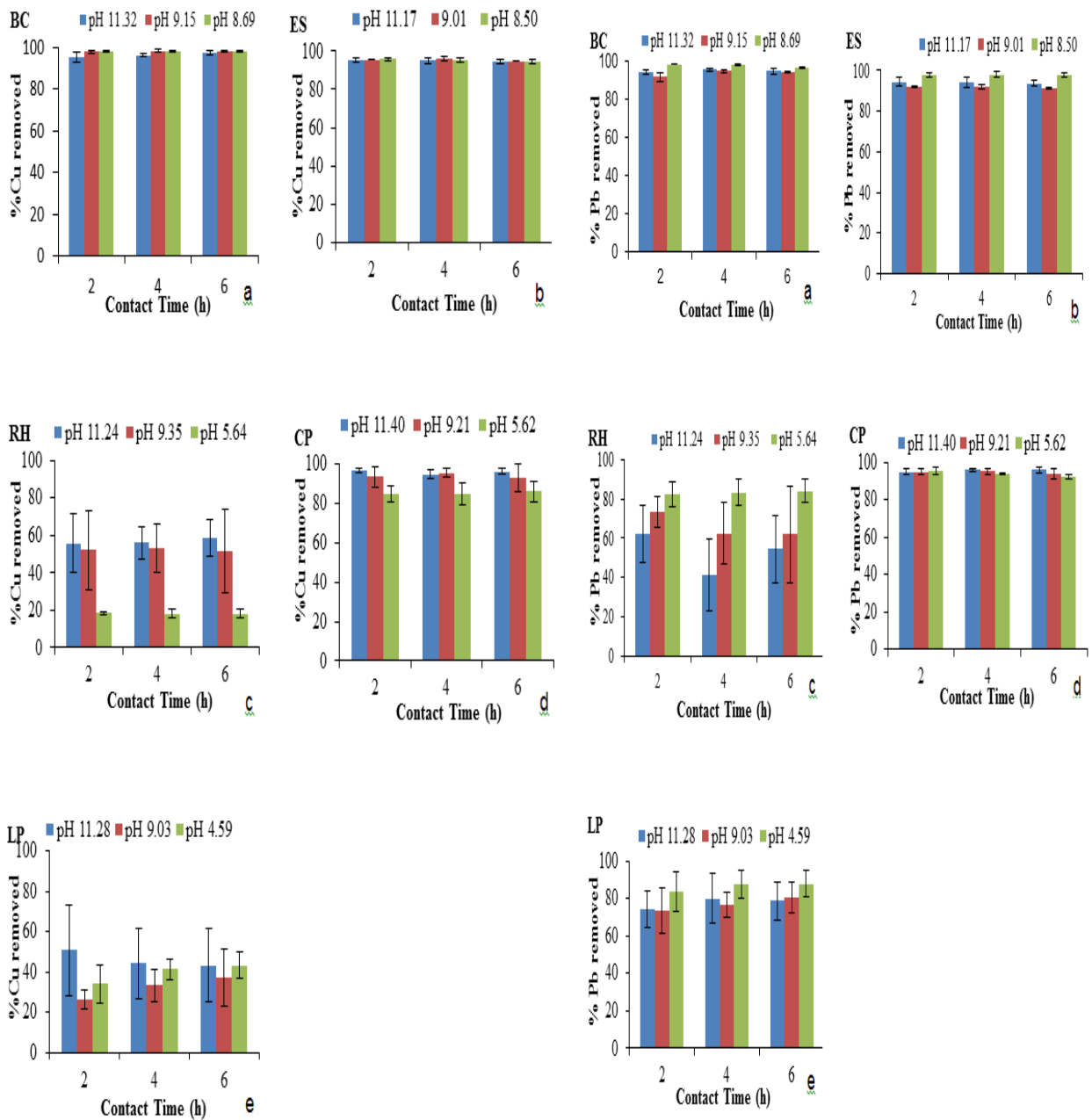
Conference theme
Role of Engineering in
Sustainable Development Goals
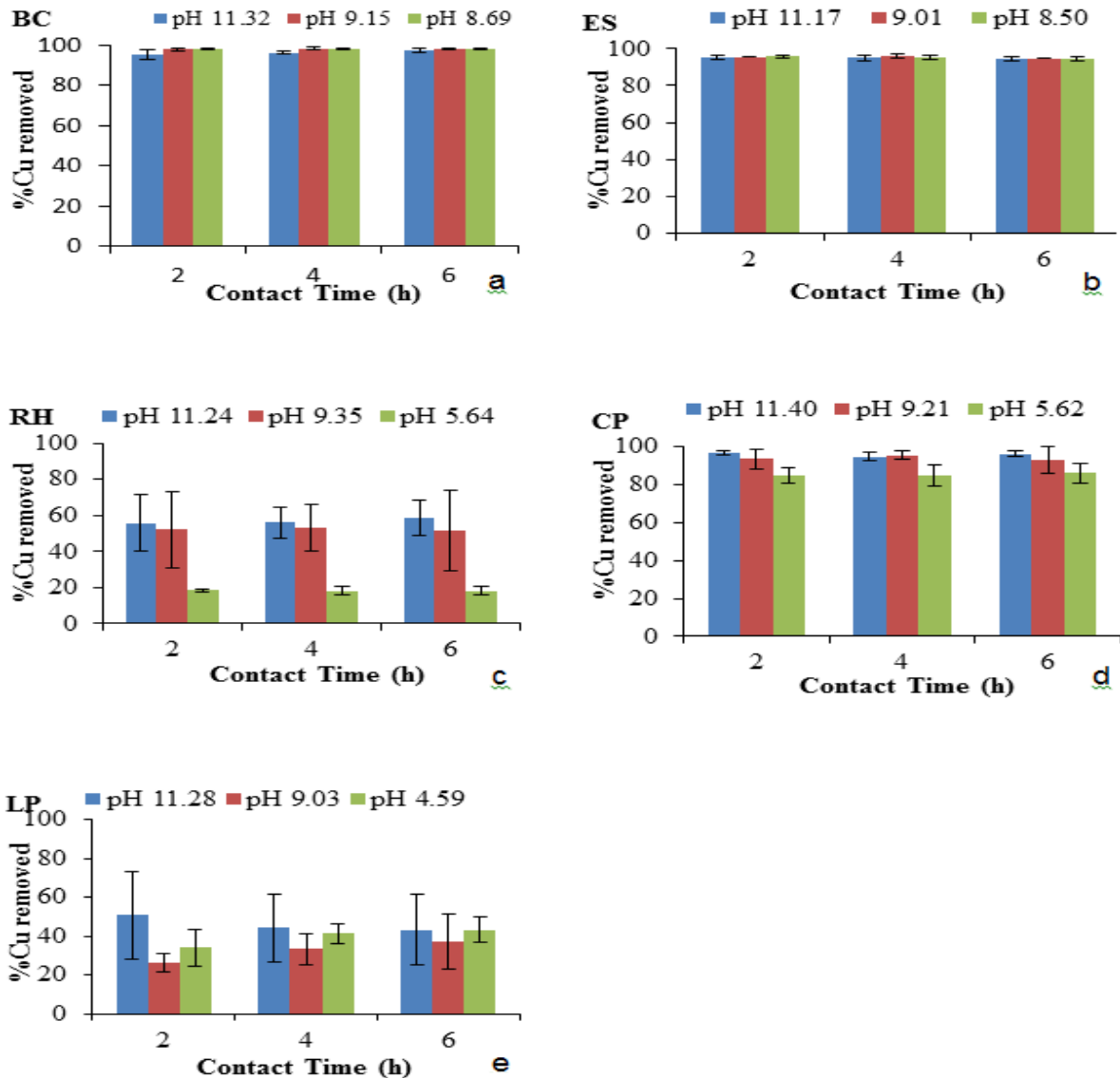
Figure 3 shows the effect of contact time on % removal of Cu by: (a) BC compared (b) ES (c) RH (d) CP and (e) LP

On the other hand, Figure 4 (a) and (b) showed that about 100% of Fe ions was removed by BC and ES after 2 h, same with CP as illustrated in (d). Thereafter, the adsorption rate became practically constant through the remaining period. ES and CP respectively after 2 h; further contact time did not have any significant effect.

Likewise, Figures 5 (a), (b) and (d) demonstrate that over 90% of Pb(II) was removed by BC. It can then be concluded that the rate of metal binding with adsorbent was more rapid during the initial stages (2 h), and this may be due to the presence of large number of active sites for metal binding, which became saturated with time and gradually decreased

and remain constant. Observation on the effect of contact time on adsorption in this study is supported by other researchers that examined and heavy metals removal by biomass wastes.

Figure 3 shows the effect of contact time on % removal of Cu by: (a) BC compared (b) ES (c) RH (d) CP and (e) LP

Figure 4 shows the effect of contact time on % adsorption of Fe by (a) BC compared (b) ES (c) RH (d) CP and (e) LP

The Nigerian Society of Engineers
Minna Branch
1st NSE Minna Branch National Conference 2021

Conference theme
Role of Engineering in
Sustainable Development Goals

Seemingly, based on the trend observed from Figures (2 – 5), The % removal of metal ions by different adsorbents (raw biomass waste) increased after 2 h. This may be due to availability of large active sites for binding, which becomes saturated with time and subsequently reducing in decreasing efficiency with time. In conclusion, findings from this study is in agreement with those reported by Azouaou et al.(2010) and Han et al. (2017).
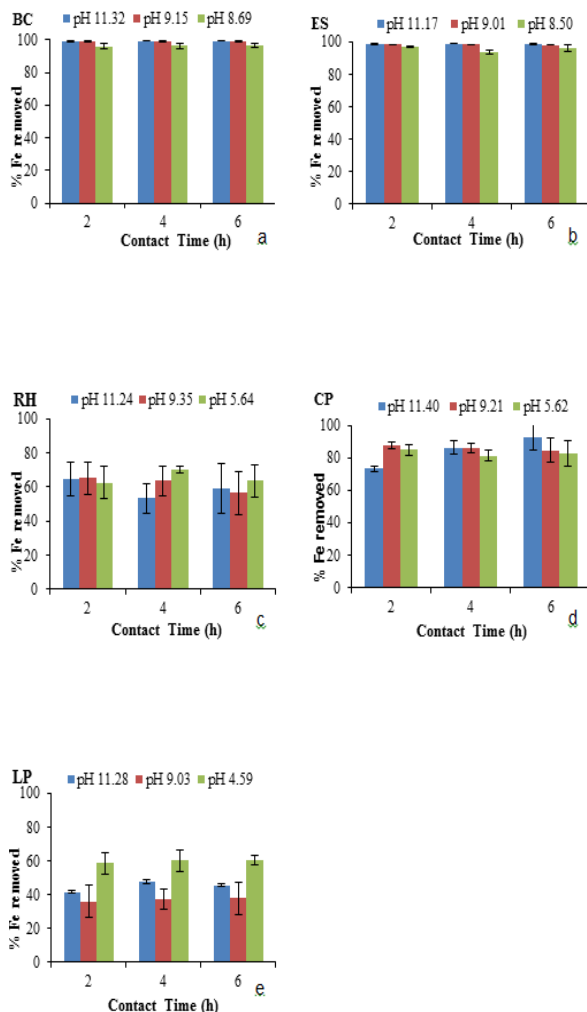
Figure 5 shows the effect of contact time on % removal of Pb(II) by: (a) BC (b) ES (c) RH (d) CP and (e) LP

3.2 EFFECT OF pH ON METAL ADSORPTION BY RAW BIOMASS WASTE

As expected, the varying pH considered in this study appears to have influenced on adsorption rate, since it governs the speciation metal ions and dissociation of the active sites of the sorbents. The effect of pH on removal of Cr(VI), Cu(II), Fe(II) and Pb(II) ions by BC and raw biomass of the following: ES, RH, CP and LP was investigated and results linked to Figure 8 to Figure 11. By observing Figure 8, the natural pH5.62 which indicates acidity, appears to explore the potentials of CP by removing over 90% of Cr(VI) ions. The sterling observation made on CP, revealed a better adsorption when compared to the reference adsorbent BC, which is barely 90% at pH8.69 (slightly basic). However, in Figure 8, pH4.59 and pH5.64 were only able to favour the removal of 40% and 20% of Cu(II) by LP and RH respectively. At pH9.01 and 11.0, ES and CP were able to remove about 100% of Cu(II) relatively better than the BC. On the other hand, at natural pH8, adjusted pH 9 and 11, ES was able to remove 100% of Fe(II); hence, equating the performance pollutant adsorption BC. Furthermore, almost 100% of Pb(II) were completely adsorbed by CP, ES compared BC irrespective of their media pH conditions which ranged from weakly acidic pH5.62 through pH8.69 to pH11.32. At high pH values, the surface of these adsorbents become negatively charged (anions); hence, resulting in very high affinity for cations attraction. The effect of pH on metal adsorption found in the present study are in agreement with the results obtained by other researchers that used biomass wastes such as coffee residues (Oliveira *et al.*, 2008), orange waste (Azouaou *et al.*, 2013), tea waste (Amarasinghe and Williams, 2007), banana peel (Anwar *et al.*, 2010) and coconut shell (Pino *et al.*, 2006).

Surmise to the above, the lemon peel used in its raw state in this work did not perform well in the adsorptions of Cr(VI), Cu(II) and Fe(II) at different pH conditions. This may be due to the presence of lipids, fats, oils and lignin in the peels, and when in aqueous media, these constituents are released into the solution. Therefore, to effectively utilise LP for adsorption, it is essential to subject the peels to a

thermochemical treatment in order to denature the organic constituents and increase its surface area for adsorption. The thermochemical process is termed hydrothermal carbonisation (HTC), which produces a product called hydrochar.

4 CONCLUSIONS

Biomass wastes consisting of coco-peat (CP), coconut shell (CS), rice husk (RH), lemon peel (LP) and eggshell (ES) were hydrothermally treated at 200 °C for 20 h in order to investigate their sorption ability for pollutant adsorption. The study demonstrated that the raw biomass wastes have the potential to be used as adsorbents. However, hydrochar would be better due to changes in surface characteristics of the adsorbents. The SEM images showed that the hydrochars have more porous structures, which resulted from denaturing of biomass structures due to carbonisation. The surface area of the hydrochars were significantly higher than the corresponding raw biomass, with CS hydrochar having the largest surface area (21.82 m²/g), whilst ES hydrochar the smallest (0.5 m²/g). The enhanced porosity and surface area of the hydrochars result in more characteristics active sites for sorption of pollutants. Therefore, the abundance of these biomass waste materials in developing countries and the moderate HTC temperature required make these produced hydrochars suitable for potential practical applications, especially in developing countries.

REFERENCES

Akan, J. C., Abdulrahman, F. I., Ayodele, J. T., & Ogugbuaja, V. O. (2009). Impact of tannery and textile effluent on the chemical characteristics of Challawa river, Kano state, Nigeria. *Electronic Journal of Environmental, Agricultural and Food Chemistry*, *8*(10), 1008–1032.

Ajiboye, Timothy O, Opeyemi A Oyewo, and Damian C Onwudiwe. 2021. "Simultaneous removal of organics and heavy metals from industrial wastewater: A review." *Chemosphere* 262: 128379-128399. doi:10.1016/j.chemosphere.2020.128379.

Alaoui, N. S., Laghdach, A. E., Correa, E. M., Stitou, M., Yousfi, F. E. and Jbari, N. (2014) 'Preparation of bone chars by calcination in traditional furnace', *J. Mater. and Environ. Sci.*, 5(2), pp. 476–483.

Amarasinghe, B. M. W. P. K. and Williams, R. A. (2007) 'Tea waste as a low cost adsorbent for the removal of Cu and Pb from wastewater', *Chem. Eng. J.*, 132(1–3), pp. 299–309. doi: 10.1016/j.cej.2007.01.016.

Anwar, J., Shafique, U., Waheed-uz-Zaman, Salman, M., Dar, A. and Anwar, S. (2010) 'Removal of Pb(II) and Cd(II) from water by adsorption on peels of banana.', *Bioresource technology*, 101(6), pp. 1752–5. doi: 10.1016/j.biortech.2009.10.021.

APHA. (2012). *Standard Methods for the Examination of Water and Wastewater*. (E. W. Rice, R. B. Baird, A. D. Eaton, & L. S. Clesceri, Eds.) (22nd ed.). Washington, DC: American Public Health Association, American Water Works Association,Water Environment Federation.

ASTM (2008) 'American Standard Test Methods for Instrumental Determination of Carbon, Hydrogen, and Nitrogen in Laboratory Samples of Coal: D5373-08', *A Standard - ASTM International, West Conshohocken*.

Azouaou, N., Belmedani, M., Mokaddem, H. and Sadaoui, Z. (2013) 'Adsorption of lead from aqueous solution onto untreated orange barks', *Chemical Engineering Transactions*, 32, pp. 55–60. doi: 10.3303/CET1332010.

Barrett EP, Joyner LG, Halenda PP (1951) The determination of pore volume and area

distributions in porous substances.I. Computations from nitrogen isotherms. J Am Chem Soc 1896(1948):373–380

Becerra-Castro, C., Lopes, A. R., Vaz-Moreira, I., Silva, E. F., Manaia, C. M., & Nunes, O. C. (2015). Wastewater reuse in irrigation: A microbiological perspective on implications in soil fertility and human and environmental health. *Environment International*, *75*, 117–135. https://doi.org/10.1016/j.envint.2014.11.001.

Bhattacharjee, Chiranjit, Suman Dutta, and Vinod K Saxena. 2020. "A review on biosorptive removal of dyes and heavy metals from wastewater using watermelon rind as biosorbent." *Environmental Advances* 2: 100007-. doi:10.1016/j.envadv.2020.100007.

Blumenthal, U., & Peasey, A. (2002). Critical review of epidemiological evidence of the health effects of wastewater and excreta use in agriculture, (December), 1–42.

Bougnom, Blaise P, and Laura J.V Piddock. 2017. "Wastewater for Urban Agriculture: A Significant Factor in Dissemination of Antibiotic Resistance." *Environmental Science and Technology* (American Chemical Society) 51: 5863-5864. doi:10.1021/acs.est.7b01852.

Chen, C., & Wang, J. (2008). Removal of Pb^{2+}, Ag^+, Cs^+ and Sr^{2+} from aqueous solution by brewery's waste biomass. *Journal of Hazardous Materials*, *151*(1), 65–70. https://doi.org/10.1016/j.jhazmat.2007.05.046 .

Chhikara, S., & Rana, L. (2013). Physico-chemical Characterization of Textile Mill Effluent : A Case Study of Haryana , India. *International Journal of Science and Technology*, *8*, 19–23.

Danso-Boateng, E., Holdich, R. G., Wheatley, A. D. and Martin, S. J. (2015) 'Hydrothermal Carbonization of Primary Sewage Sludge and Synthetic Faeces : Effect of Reaction Temperature and Time on Filterability', *AlChE Journal*, 34(5), pp. 1279–1290. doi: 10.1002/ep.

Danso-Boateng, E., Mohammed, A.S., Sander, G.C., Wheatley, A.D., Nyktari, E. and Usen, I.C. (2021). Production and characterisation

of adsorbents synthesised by hydrothermal carbonisation of biomass wastes. Springer Nature (SN) Applied Sciences 3:257 https://doi.org/10.1007/s42452-021-04273-5

Dickin, S. K, C.J Schuster-Wallace, M Qadir, and K Pizzacalla. 2016. "A Review of Health Risks and Pathways for Exposure to Wastewater Use in Agriculture." *Environmental Health Perspectives* 124 (7): 900-909. http://dx.doi.org/10.1289/ehp.1509995.

Drechsel, P., Scott, C. A., Raschid-Sally, L., Redwood, M., & BAHRI, A. (2009). *Wastewater Irrigation and Health: Assessing and Mitigating Risk in Low-income Countries*. Retrieved from http://www.amazon.com/Wastewater-Irrigation-Health-Mitigating-Low-income/dp/1844077969

Dubey, Rachana, and Subhasis Swain. 2019. "Wastewater use in agriculture: issues and prospects."

Dubey, Rachana, and Subhasis Swain. 2019. "Wastewater use in agriculture: issues and prospects." *Agriclture & Food: e- Newsletter* 1 (10): 254-257.

El-Azazy, M, A. S El-Shafie, A. A Issa, M Al-Sulaiti, J Al-Yafie, B Shomar, and K Al-Saad. 2019. "Potato Peels as an Adsorbent for Heavy Metals from Aqueous Solutions: Eco-Structuring of a Green Adsorbent

Ensink, J. H. J., & Van Der Hoek, W. (2009). Implementation of the WHO guidelines for the safe use of wastewater in Pakistan: Balancing risks and benefits. *Journal of Water and Health*, *7*(3), 464–468. https://doi.org/10.2166/wh.2009.061.

Fang, J., Zhan, L., Ok, Y. S. and Gao, B. (2017) 'Minireview of potential applications of hydrochar derived from hydrothermal carbonization of biomass. Available online 24 August 2017', *Journal of Industrial and Engineering Chemistry*. doi: 10.1016/j.jiec.2017.08.026

FAO/WHO. (2006). Guidelines for the Safe use of Wastewater, Excreta and Greywater 2: Wastewater Use in Agriculture (Vol. II). Geneva, Switzerland

Funke, A. and Ziegler, F. (2010b) 'Hydrothermal carbonization of biomass : A summary and discussion of chemical mechanisms for process engineering', *Biofuel, Bioproducts and Biorefining*, 4, pp. 160–177. doi: 10.1002/bbb.198.

Geetha, K. S., & Belagali, S. L. (2013). Removal of Heavy Metals and Ss Using Low Cost Adsorbents from Aqueous Medium- , A Review, *4*(3), 56–68..

Gu, Shiquing, Xiaonan Kang, Lan Wang, E Lichtfouse, and Chuanyi Wang. (2019). "Clay mineral adsorbents for heavy metal removal from wastewater: a review." *Environmental Chemistry Letters, Springer Verlag,* (Springer Verlag) 17 (2): 629-654. doi:10.1007/s10311-018-0813-9.

Han, L., Sun, H., Ro, K. S., Sun, K., Libra, J. A. and Xing, B. (2017) 'Removal of Antimony(III) and Cadmium(II) from Aqueous Solution using Animal Manure-derived Hydrochars and Pyrochars Bioresource Technology Removal of antimony (III) and cadmium (II) from aqueous solution using animal manure-derived hydrochars an', *Bioresource Technology*. Elsevier Ltd, 234(March), pp. 77–85. doi: 10.1016/j.biortech.2017.02.130.

Heilmann, S. M., Davis, H. T., Jader, L. R., Lefebvre, P. A., Sadowsky, M. J., Schendel, F. J., Keitz, M. G. . and Valentas, K. J. (2010) 'Hydrothermal carbonization of microalgae', *Biomass and Bioenergy*. Elsevier Ltd, 34(6), pp. 875–882. doi: 10.1016/j.biombioe.2010.01.032.

Hunton P (2005) Research on eggshell structure and quality: an historical overview. Braz J Poult Sci 7(2):67–71

Islam, S., Islam, F., Bakar, M. A., Das, S., & Bhuiyan, H. R. (2013). Heavy Metals Concentration at Different Tannery Wastewater Canal of Chittagong City in Bangladesh. *International Journal of Agriculture, Environment and Biotechnology*, *6*(3), 355. https://doi.org/10.5958/j.2230-732X.6.3.003.

Ji-lu, Z. (2007) 'Bio-oil from fast pyrolysis of rice husk: Yields and related properties and improvement of the pyrolysis system', *J. Anal and Appl Pyrolsis*, 80, pp. 30–35. doi: 10.1016/j.jaap.2006.12.030.

Kamsonlian, S., Suresh, S., Majumder, C. B. and Chand, S. (2011) 'Characterization of Banana and Orange Peels: Biosorption Mechanism', *Int. J. Sci Technol and Manag.*, 2(4).

Kennedy, K. K, K. J Maseka, and M. Mbulo. (2018). "Selected Adsorbents for Removal of Contaminants from Wastewater: Towards Engineering Clay Minerals." *Open Journal of Applied Sciences* 8: 355-369. http://www.scirp.org/journal/ojapps.

Khan, K., Lu, Y., Khan, H., Ishtiaq, M., Khan, S., Waqas, M., Wang, T. (2013). Heavy metals in agricultural soils and crops and their health risks in Swat District, northern Pakistan. *Food and Chemical Toxicology*, *58*, 449–458. https://doi.org/10.1016/j.fct.2013.05.014

Lima, I. M. and Marshall, W. E. (2005) 'Granular activated carbons from broiler manure: physical, chemical and adsorptive properties', *Bioresour Technol*, 96, pp. 699–706. doi: 10.1016/j.biortech.2004.06.021.

Liyanage, C. D. and Pieris, M. (2015) 'A Physico-Chemical Analysis of Coconut Shell Powder', *Procedia Chemistry*, 16, pp. 222–228. doi: 10.1016/j.proche.2015.12.045.

Merchant, R.R, and Z. Z Painter. (2019). "Study of Removal of Heavy Metals from Waste Water by Adsorption." *International Journal of Applied Engineering Research* (Research India Publications.) 14 (1): 63-68.

Mumme, J., Eckervogt, L., Pielert, J., Diakité, M., Rupp, F. and Kern, J. (2011) 'Bioresource Technology Hydrothermal carbonization of anaerobically digested maize silage', *Bioresour. Technol.* Elsevier Ltd, 102(19), pp. 9255–9260. doi: 10.1016/j.biortech.2011.06.099.

Oliveira, W. E., Franca, A. S., Oliveira, L. S. and Rocha, S. D. (2008) 'Untreated coffee husks as biosorbents for the removal of heavy metals from aqueous solutions.', *Journal of hazardous materials*, 152(3), pp. 1073–81. doi: 10.1016/j.jhazmat.2007.07.085.

Phadtare, Madhukar J, and S. T Patil. (2015). "Removal of Heavy Metal from Industrial Waste water." International Journal of Advanced Engineering Research and Studies 4 (3): 4-8.

The Nigerian Society of Engineers
Minna Branch
1st NSE Minna Branch National Conference 2021

Conference theme
Role of Engineering in
Sustainable Development Goals

Pilon G, Lavoie J (2014) Biomass char production at low severity conditions under CO_2 and N_2 environments. Biomass Biofuels, WIT Trans State Art Sci Eng 83:67–78. https://doi.org/10.2495/978-1-78466-034-5/007

Pino, G. H., De-Mesquita, L. M., Torem, M. L. and Pinto, G. A. (2006) 'Biosorption of cadmium by green coconut shell powder', *Mineral Eng.*, 19, pp. 380–387. doi: 10.1016/j.mineng.2005.12.003.

Qiang, L., Xu-lai, Y. and Xi-Feng, Z. (2008) 'Analytical and Applied Pyrolysis Analysis on chemical and physical properties of bio-oil pyrolyzed from rice husk', *J. Anal. and Appl Pyrol.*, 82, pp. 191–198. doi: 10.1016/j.jaap.2008.03.003.

Qu, Xiaoyan, Yuanyuan Zhao, Ruoren Yu, Yuan Li, Charles Falzone, Gregory Smith, and Keisuke Ikehata. (2016). "Health Effects Associated with Wastewater Treatment, Reuse, and Disposal." *Water Environment Research* 88 (10): 1823-1855.
doi:10.2175/106143016X14696400495776.

Rencoret, J., Ralph, J., Marques, G., Gutiérrez, A., Martínez, A. T. and Del-Río, J. C. (2013) 'Structural Characterization of Lignin Isolated from Coconut (Cocos nucifera) Coir Fibers', *Journal of agricultural and food chemistry*, 61(10), pp. 2434–45. doi: 10.1021/jf304686x.

Robbins, R. (2013) 'Scanning Electron Microscope Operation Zeiss'. Texas at Dallas: The University of Texas at Dallas.

Schneider, D., Escala, M., Supawittayayothin, K. and Tippayawong, N. (2011) 'Characterization of biochar from hydrothermal carbonization of bamboo', *Int. J. Energy and Environ.*, 2(4), pp. 647–652.

Titirici, M. M., Thomas, A., Yu, S. H., Muller, J. O. and Antonietti, M. (2007) 'A direct synthesis of mesoporous carbons with bicontinuous pore morphology from crude plant material by hydrothermal carbonization', *J. Chem. of Mater.*, 19(17), pp. 4205–4212. doi: 10.1021/cm0707408.

Zaman, T., Mostari, M. S., Mahmood, M. A. and Rahman, M. S. (2018) 'Evolution and characterization of eggshell as a potential candidate of raw material', *Cerâmica*, 64(370), pp. 236–241. doi: 10.1590/0366-69132018643702349.

Formulation of Cutting Oil Using Green Base Extract (Soya-Bean and Groundnut)

Oketa A.J and Okoro U.G
Mechanical Engineering Department,
Federal University of Technology PMB 65 Minna, Niger State Nigeria
Corresponding author's email: oketaalexander@gmail.com

ABSTRACT

This is an ongoing project aimed at formulating Metal Working Fluid (MWF) from green materials. The green base oil was improved by adding additives to it so as to attain the properties of commercial Metal Working Fluid (MWF). This was important because it reduces dependence on the regular cutting fluid which is mostly petroleum base, which is non-biodegradable and also has hazardous effect on machinist. All green materials used here wee Tobacco extract (antioxidants and Extreme Pressure (EP) Additives), Garlic Extract (Biocide and Extreme Pressure (EP) Additives), soya bean extract (base oil), groundnut extract (base oil), and Neem Extract (Anti corrosive agent), all oil extract went through physiochemical analysis such as Percentage yield, Refractive Index, Pour point, Flash point, PH value, Kinematic viscosity, Saponification test, Free fatty acidic, density, and Iodine value test. All values were tabulated and compared with the properties of the commercial metal Working Fluid. All parts of the analysis exhibited excellent qualities, which is an indication that the bio extract will produce a sustainable and a healthy cutting fluid.

KEYWORDS: *Extreme Pressure Additive (EP), Green Material, Commercial Metal Working Fluid (CMWF), Metal working fluid (MEF) and Base oil.*

1 INTRODUCTION

Cutting fluid known as coolant, lubricant, metal working fluid (MWF) designed specifically for metalworking processes, such as machining, stamping etc. Cutting fluids are used to reduce the negative effects of heat and friction on both tool and work piece [1]. Taylor historically reported the use of cutting fluids in metal cutting in 1894. He observed that cutting speed could be increased up to 33% without reducing tool life by applying large amounts of water in the cutting zone [2].

Cutting fluids produce three positive effects in the process of machining, and these effects are heat evacuation, lubrication on the chip–tool interface and chip removal [3]). Higher surface finish, quality and better dimensional accuracy are also obtained from cutting fluid [4]. Cutting fluids are widely used throughout industry in machining operation such as milling, grinding, boring, and turning. Estimations shows that over 320 thousand tonnes of metalworking fluids are used annually [5]. Cutting fluid may act as coolant, lubricant or both depending on the type of machining operation. During machining heat is generated and this has adverse effect on the work piece, surface finish, dimensional accuracy, tool Wear as well as production rate [6]. The need to quickly remove heat, lubricate, reduce friction during grinding, machining, cutting process among many others justifies the use of metalworking fluids. Therefore, applying metalworking fluids in a system is crucial, especially to reduce wear of the materials employed in the system. Cutting fluid used in lubrication system can be in different forms, such as solid, gas and liquid [7].

2 METHODOLOGY

Soya bean, groundnut, garlic and tobacco seed were obtained from Nigerian markets and their oil extracted from their respective seeds using the Soxhlet extractor. Determination of some specific physiochemical properties (flash point, pour point, kinematic viscosity, PH test, iodine value, free fatty acid, refractive index Density, saponification and specific gravity) were determined.

Procedure for solvent-based extraction of vegetable oil The seeds were first cleaned by removing contaminants; common contaminants often associated with the (soya-bean) seeds are sticks, strains, leaves, sands and dirt. The seeds were crushed into fine particles, powdered materials were rolled up in a filter paper and then loaded into the Soxhlet extractor, but remember the Soxhlet extractor consist of three major parts which are the condenser, the extractor, the flask. The condenser condenses the vaporized mixture of the Solvent and oil into the extractor, the extractor basically holds the grinded material rolled up in a filtered paper, the flask contains the solvent which is being heated. Hexane was the solvent used for the extra action. Hexane was filled to more than half of the flask, water was also added to the water bath container in which the flask was placed and then stirred continuous as heat was applied to enhance the leaching process. Hexane solvent has a boiling point of 69°c. The solvent was heated until its vapor

climbs through the outer tube and then enters the extraction chamber, the chamber then begins to be filled with the solvent, also the level of solvent rises in the inner tube too. When the extractor is full enough,the inner tube sends the solvent containing the extract back to the flask. The extraction process goes on till there was nothing left. After the extraction process has been concluded the extraction solvent (hexane) can be improved using distillation process [8].Care is taken to store vegetable oil extract in contaminant-free and air tight condition. The amount of extract obtained is calculated using the equation below :

2.1 Procedure for Solvent-Based Extraction of Vegetable oil

The seeds were first cleaned by removing contaminants; common contaminants often associated with the (soya-bean) seeds are sticks, strains, leaves, sands and dirt. The seeds were crushed into fine particles, powdered materials were rolled up in a filter paper and then loaded into the Soxhlet extractor, but remember the Soxhlet extractor consist of three major parts which are the condenser, the extractor, the flask. The condenser condenses the vaporized mixture of the Solvent and oil into the extractor, the extractor basically holds the grinded material rolled up in a filtered paper, the flask contains the solvent which is being heated.

Hexane was the solvent used for the extra action. Hexane was filled to more than half of the flask, water was also added to the water bath container in which the flask was placed and then stirred continuous as heat was applied to enhance the leaching process. Hexane solvent has a boiling point of 69°c. The solvent was heated until its vapor climbs through the outer tube and then enters the extraction chamber, the chamber then begins to be filled with the solvent, also the level of solvent rises in the inner tube too. When the extractor is full enough, the inner tube sends the solvent containing the extract back to the flask.

The extraction process goes on till there was nothing left. After the extraction process has been concluded the extraction solvent (hexane) can be improved using distillation process [8].

Care is taken to store vegetable oil extract in contaminant-free and air tight condition. The amount of extract obtained is calculated using the equation below:

$$Oil\ Content(\%) = \frac{Weight\ of\ the\ oil}{Weight\ (g)\ of\ sample} x100$$

The entire extraction processes were carried out at Chemical Engineering Department, Federal University of Technology Minna, Niger Stare Nigeria.

Figure 1 and Figure 2 shows Soxhlet Extractor loaded with sample and Flask containing a mixture of condensed solvent and the oil

2.2 Physiochemical Analysis of Soya-bean, Groundnut, Tobacco, and Garlic Oil

(a) Determination of Kinematic Viscosity

In this work, the kinematic viscosity of the oil samples is determined using ASTM D 445 standard. The same standard has been used in the works of Didam (2016).

The determination of the kinematic viscosity of oil based on ASTM D 445 begins with determination of the velocity of flow of the oil, However the apparatus has to be prepared first to ensure the fidelity of the result. The conditions necessary for a high fidelity result stipulates; surrounding temperature of 40°c as used in [9].

The temperature of the viscometer bath was adjusted to 40oC. A calibrated thermometer was held in upright position and inserted into the bath by a holder. A clean dry calibrated viscometer was selected and carefully flushed with a dry nitrogen gas to remove the moist room air. A sample of the vegetable oil was drawn up into the working capillary of the viscometer and the timing bulb was then allowed to drain back as an additional safeguard against moisture condensing or freezing on the walls. The charged viscometer was inserted into the bath at a depth such that at no time during the measurement of the flow time was any portion of the sample in the viscometer less than 20mm below the surface of the bath as used in [10].

The viscometer together with its content was allowed to remain in the bath for 30minutes to reach the test temperature (40oC). A suction bulb was used to adjust the Head level of the vegetable oil sample to about 7mm above the first timing mark in the capillary arm of the viscometer. The vegetable oil sample is then allowed to flow freely from the first to the second marks and timing using the stop watch. The procedure was repeated to make a second measurement of flow time and the average of these determinations was used to calculate the kinematic viscosity. The procedure is repeated for the other

samples as prescribed by ASTM D 445 [9]. The equation used is shown in Table 2

(b) Determination of Density of Oil
The densities of the oils were determined using the procedure of ASTM method D-1298 The sample was brought to a specified temperature and a test portion was transferred to a hydrometer cylinder which had been brought to approximately the same temperature. The appropriate hydrometer also at a similar temperature was lowered into the test portion and allowed to settle. After which temperature equilibrium was reached. The hydrometer scale reading and temperature of test portion were taken. The observed hydrometer reading was reduced to the reference temperature by means of oil measurement table. An hydrometer correction was applied to the observed reading and the corrected hydrometer scale reading recorded to the nearest 0.1kg/m3 as density [11].

(c) Determination of Pour Point
 The procedure for the determination of the Pour point followed the description contained in ASTM method (ASTM D – 97).

Oil sample was poured into the test jar to the level mark. The test jar was closed with a cork carrying high – pour thermometer. Position of the cork and thermometer were adjusted for the cork to fit tightly, the thermometer and the jar were coaxial and the thermometer bulb was immersed 3mm below the surface of the sample. After this, the test jar was placed into the cooling medium. Sample was cooled at a specified rate and examined at interval of 3oC for flow characteristics until a point was reached at which the sample showed no movement when test jar was held in a horizontal position for 5seconds. Observed reading of thermometer was recorded. 3oC was added to the recorded temperature and the result was observed as the pour point. [9]

(d) Determination of Flash Point
The pensky-Martens Closed Cup Test (ASTM D93) method was used to determine the flash point of oil under investigation. The test cup was filled with about 75ml of each sample of oil under investigation. It was ensured that the test flask and test sample were at least below the expected flash point of 18. The automated apparatus was started and heat was applied at a rate that temperature as indicated by temperature measuring device increased 5 oC to 6 oC. The stirring device was turn at between 100 to 110 rpm stirring downward direction. The ignition source was applied when the test sample was 23 ± 5 below the expected flash point and each time afterward at a temperature reading that was in multiple of 1. Stirring of test sample was discontinued and the ignition source was applied by operating the mechanism on the test cover which controlled the shutter so that the ignition source was lowered into the vapor space of the test cup in 0.5 and left it in lowered position for 1sec and quickly raised again to it upward position. The observed flash point reading on the temperature measuring device was recorded accordingly [12].

(e) pH Test
The pH for the test sample of the oils was measured with a pH meter. The pH meter was first calibrated with standard solution. After each reading, the electrode was cleaned with distilled water before taking another reading. This was replicated for each run. This procedure was repeated for all test samples and their pH value was read.

(f) Determination of Saponification
The saponification of the oils was determined using the procedure of ASTM method D464 This method is used to determine the total acid content, both free and combined, of all oil. (Acid number only measures the free acid). The combined acids are primarily esters formed by reaction with the neutral components present in the original oil. The saponification value is therefore a measure of all oil quality. It is determined by measuring the alkali required to saponify the combined acids and neutralize the free acids.

(g) Determination of Free Fatty Acid
Acid values of the vegetable oils were each determined by ASTM method (ASTM – D 974). 0.2 – 0.5g of sample were weighed into 250ml conical flask. 50ml of neutralized ethyl alcohol was added. The mixture was heated on a water bath to dissolve sample. The solution was titrated against 0.1M KOH using phenolphthalein as indicator.

(h) Determination of Iodine Value
The protocol for iodine value determination usually comprises a titration procedure, such as the Wijs method. In this procedure, iodine chloride was used for double-bond saturation analysis, and the content of consumed iodine was measured by titration with 0.1 mol L− 1 sodium thiosulfate solution [14].

2.3 Selection of Extreme Pressure Additives
Tobacco and Garlic were selected as additive because they are sulphur containing non-hazardous substance, though this compound is present in combined state. Sulphur is used as an extreme pressure additive in lubricant and cutting fluids [15]. The performance of MWFs was improved by adding substances that contain phosphorus, sulphur, and chlorine as EP additives [16]. Tobacco and Garlic shown good tribological properties when it was added to Neem and jatropha oil as EP additive [17]. As result shows better performance in term of tool

wear, temperature and surface finish as quantity of tobacco.

2.4 Cutting Oil Formation
Base oils are;

Groundnut oil and Soya beans oil, (petroleum base oil being replaces with the vegetable oil due to its bio degradability)

Additives

Liquid soap as an emulsifier (morning fresh), Neem as anti-corrosive agent, Tobacco seed as anti-oxidant, Garlic as biocide

pH of the base oil

The pH of Groundnut oil is between 6.59 - 6.79 (weakly acidic)

The pH of Soya beans oil is between 6.80 - 6.90 (weakly acidic)

According to [18]. Green alkaline base cutting fluid is non toxic, biodegradable and cause no harm to the environment being a sustainable product derived from renewable source. The Green alkaline base cutting fluid is cost effective, stable and with better machining properties. It promotes the healthy work environment and prevent work place injuries and illnesses compared to the ide effect of conventional mineral oil base cutting fluid.

pH of Additives

Garlic oil 6.3 (weakly acidic)

Tobacco oil 7.5 (weakly alkaline)

Neem extract 7.7 (weakly alkaline)

Emulsifier (Morning Fresh) 7.3 (weakly alkaline)

These values were all obtained using the hand-held pH meter

For typical steel/iron/cast iron, when the pH is less than about 4, protective oxide films tend to dissolve and corrosion rates increase that's is to say a low pH promoted corrosion. However, Metals typically develop a passivation layer in moderately alkaline (high pH) solutions, which lowers the corrosion rate as compared to acidic (low pH) solution.

Note that as the pH increases from 5.5 to 7.0, corrosion rate starts to decrease before gradually gaining the momentum of growth beyond pH 7.0 and reaching the maximum rate of pH 9.5. [19].

2.5 Formulation of Cutting Oil
-Base oil 100%

-Tobacco oil 5% of base oil

-Neem extract 2.5% of base oil

-Garlic oil 5% of base oil

-Emulsifier 2% of base oil.[20].

These was thoroughly agitated to ensure proper mixing, also this formulation gives good lubricity and it was in accordance with ASTM standard for cutting fluid/oil which is ASTM D7455 – 19. Standard Practice for Sample Preparation of Petroleum and Lubricant Products for Elemental Analysis.

2.6 MATERIALS
The work piece to be used was a medium carbon steel. In this study, medium carbon steel was used by virtue of its availability, properties and relatively cheap cost. Soya bean, and groundnut seed were obtained from Tunga market in Minna, also some of the additives such as neem and garlic were obtained at Gidan Mangoro, the tobacco seed was obtained from Dukku village in Gombe. The extraction and analysis of oils from the two vegetable oil seeds were carried out at Chemical Engineering Department Federal University of Technology Minna Niger State.

3 FIGURES AND TABLES
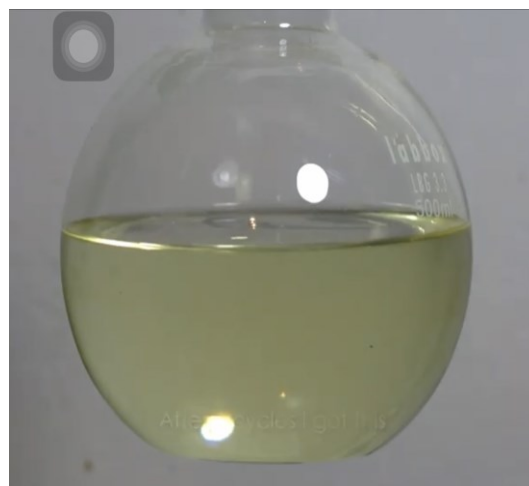The laboratory and workshop equipment used during the physiochemical analysis include the following

Figure 1: Soxhlate extractor loaded with sample

Figure 2: Flask containing a mixture of condensed solvent and the oil

TABLE 1: Summary of Materials

S/N	Equipment (Model)	Function
1	XL400-Excel Lathe Machine	The machine tool that rotates the work piece about an axis of rotation to perform various operations
2	135-Surface Roughness Tester	Test for the surface roughness of a material
3	IR-66Infrared Thermometer	for the work piece and work tool temperature
4	Pycometer:	Laboratory device use for measuring the density or more accurately, the volume of solid.
5	Gas mask	used to protect the machining operator from inhaling toxic gases and airborne pollutant.
6	Heating mantle	laboratory device used to apply heat to containers
7	Graduated Baker	laboratory glassware used for measuring volume of liquids.
8	Electronic Weighing Balance	device for measuring weight or mass of a substance
9	Bunsen Burner	laboratory equipment that produces a gas flame which is use for heating.
10	Tri-pot Stand	three-legged frame used for supporting and maintaining the stability of other object.
11	Test sieve	used to determine the particle size of granular materials
12	Hack saw	hand tool used for cutting metals to size
13	Digital Venier Capillar	precision instrument that can be used to measure internal and external distance accurately.
14	Viscometer	an instrument used to measure the viscosity of a fluid
15	Mild steel round bar	Work piece
16	Rotary viscometer	For measuring the viscosity of the oils
17	Mortar	For crushing the seeds
18	Refractometer	For refractive index of oil

Table 2: Formulas and Descriptions

S/N	Physiochemical Analysis	Formulae	Description
1	Kinematic Viscosity	$V = C \times t$	Where V= Kinematic Viscosity (mm2/s) C= Calibration coolant of the viscosity (mm2/s)/S
2	Free Fatty Acid or Acid Value.	$A \times M \times 56.1(f)/w$	Where A=ml of 0.1m of KOH consumed by sample

The Nigerian Society of Engineers
Minna Branch
1st NSE Minna Branch National Conference 2021

Conference theme
Role of Engineering in
Sustainable Development Goals

No	Property	Formula	Description
			M= Molarity of KOH w=weight in grams of sample Source: ASTM D974
3	Saponification Value	$SV=(A-B)\times N\times 56.1/w$	Where A=H2SO, for blank ml B=H2SO, for sample ml w=weight of sample N=Normality H2SO4 solution 56.1= Equivalent weight of Potassium Hydroxide Source: ASTM D464
4	Specific Gravity	$SG=Do/DA$	Where Do=Density of oil DA=Density of Air

3. RESULTS AND DISCUSSIONS

Table 3: Comparison of the Physiochemical Analysis of Extract with the Commercial Metal Working Fluid (CNC COOLANT)

Physiochemical Analysis	Tobacco Oil/Extract	Soyabean Oil/Extract	Groundnut Oil/Extract	Garlic Oil/Extract	Commercial Metal Working Fluid (CNC Coolant)
Iodine Value gl2/100g of Oil	130.2	73	38.6	100	28
Density g/ml at 25°C	0.923	0.917	0.926	1.083	0.932
Specific Gravity	1.79	0.917	0.901	0.894	0.932
(gram/mole)					
Flash Point °C	220	303	315	47	175
Free Fatty Acid or Acid Value (mg KOH/g oil)	15.05	0.60	4.00	12.69	16.92
pH	6.5-7.2	6.8-6.9	6.6-6.8	6.3-6.7	8.5
Kinematic Viscosity (mm2/s)	38.21	35.00	38.00	32.1	29
Pour Point °C	-5	-20	-23	-7	-22
Refractive Index at (40°C)	1.452	1.459	1.463	1.471	1.482
Saponification Value (mg KOH/g oil)	102.5	187	184	166	142.5

Oils with iodine values higher than 115g are considered to be drying oil and also highly unsaturated in nature, this high saturation also makes it oxidative [21]. Comparing the gotten values of the base oil and addictive, it could be seen that all oil are saturated and also falls within range. This further shows that all extract has a good quality as compared with the commercial metal working fluid

Comparing the densities of the base oil with the control, it could be seen that the base oil (soya bean and ground nut oil) are fairly in the same range as the control with a value of +or – 0.006.

The specific gravity is used alternatively with the density valve., it could be seen that the base oil falls within same rage too with a value of +or- 0.02.

The Nigerian Society of Engineers
Minna Branch
1st NSE Minna Branch National Conference 2021

Conference theme

Role of Engineering in
Sustainable Development Goals

The flash points of these extracts are the lowest temperature at which its vapor ignites if given an ignition source, however comparing these temperatures gotten with the control, it therefore showed that the flash point for both base oils are higher when compared with the control which makes using these set of base oil safer. But the high value of the garlic extract will have no effect with the cutting oil formulation because it is an addictive and would be added in a very low quantity therefore it will pose no hazard during Machining operation, the area of flash point concern is only on the base oil

The more the content of fatty acid in any fluid or oils the more oxidation and rancidity it will experience, therefore affecting the shell life of such fluid or oil [22] [23]. From the values of free fatty acids gotten from the table, it was observed that all values fell below the control value which then means that all extracts will have less oxidation, better shell life and also act resistance to rancidity as compared with the commercial cutting oil.

Most cutting fluids have a pH of 8.5 -9.6, but there are also products that have a lower pH during use due to contamination [24]. Although the base oil here showed weakly acidic values tending towards complete alkalinity which can be manageable, considering that all other analyses carried out showed excellent values on the use of the base oil.

Viscosity has considerable influence on the properties of a cutting fluid. Higher viscosity improves the lubrication abilities of the fluid, but decreases the cooling performance. Lower viscosity provides better cooling performance and easier removal of solid particles. On the other hand, this may lead to a lack of lubrication between tool edge and work piece, especially at higher production speed. Poor surface quality and increased tool wear can occur. So, viscosity affects the speed, at which the liquid fills the contact zone between cutting tool and work piece, and the thickness of the liquid film. Viscosity measurement helps to find a balance between fastest possible machine parameters and best possible surface quality of the work piece.[25] lubricants range from 5 to 50, the lower the number, the more readily the oil flows.[26] Comparing the gotten values of the base oil with these standards, it can be seen that all extracts are within range and suitable for use.

The pour point is the lowest temperature at which the oil will pour or flow when it is cooled, without stirring, under standard cooling conditions. Pour point represents the lowest temperature at which oil is capable of flowing under gravity. Major attention and comparison here would be the base oil against the control fluid which was observed to be in the

same range of +1or -1, which make the base oil suitable for use.

The higher the refractive index, the closer to the normal direction the light will travel. When passing into a medium with lower refractive index, the light will instead be refracted away from the normal, towards the surface. Furthermore, the more or higher the refractive index the more room it gives for the growth of microbial organisms [27]. The corresponding values of extracts compared with the control are all in the same range which is also another reason these green materials can be used.

The higher the saponification value, the lower the fatty acids, the lighter the mean molecular weight of triglycerides and vice-versa. [28][29]. Practically, oils with high saponification values are more preferable when it comes to cutting fluid, because the more the content of fatty acid in any fluid or oils the more oxidation and rancidity it will experience, thereby affecting the shell life of such fluid or oil [22] [23]. Comparing values gotten it could be seen that all extracts have higher saponification values when compared with the control which makes it veritable for use.

4. CONCLUSION

All physiochemical analysis carried out in this study showed an excellent characteristic when compared with the CNC coolant, except for the pH value of the base oil which fell into the weakly acidic range but was compensated by other analysis carried out, therefore making it suitable for the formulation of a Green Metal working Fluid

REFERENCES
Jamiu O., and Sharafadeen k. 2013) "Performance Evaluation of Vegetable oil based cutting fluid in Mild Steel Machining"

De Avila R.F and Abrao A.M. (2001). "The Effect of Cutting Fluid on the Machining of Hardened AISI 4340 Steel".*Journal of Material Processing Technology 119(1):21-26.*

Lopez L.N, Angulo C., Lamikiz A., and Sanchez J.A (2006). "Experimental and Numerical Investigation of the Effect of Spray Cutting Fluids in High speed milling" *Journal of*

Materials Processing Technology 172 (1), 11-15, 2006

Sokovic, M. and Mijanovic, K. (2001) Ecological Aspects of Cutting Fluids and Its Influence on Quantifiable Parameters of the Cutting Processes. *Journal of Materials Processing Technology, 109, 181-189.*

Abdalla,H.S., Baines W., McIntyre G., and Slade C (2007).Development of novel sustain- able neat-oil metalworking fluids for stainless steel and titanium alloy machining. Part 1. Formulation development, J. Adv. Manuf. Technol. 34 (2007) 21–33.

Lawal S.A., Sunday A.M., Ugheoke B.I., Onche E. (2007). "Performance Evaluation of Cutting Fluids Developed from Fixed Oils".

Leonard Electronic Journal of Practices and Technology 6(10)

Ahmad U., Azman A.H., and Maidin N.A., (2020). " The Significant Study of Using Vegetable Oil as Lubricant on Conventional Lathe Machune.

IOP Conference Series Materials Science and Engineering 834:012014

Benedikt A., Weggler.,Frank L., Dorman. (2020). "Basis Multi Dimensional Gas Chromatography") Separation Science and Technology

Ademoh A.N., Didam J.H,. Garba D. K (2016). "Investigation of Neem Seed oil as an Alternative Metal cutting Fluid"

American journal of Mechanical Engineering

Stanchu I., (2014)."Methods of Determination of viscosity index for sunflower"n*International Journal of Scientific Research 3(11):55-56*

Komintarachat C., Sawangkeaw R., Ngamprasertsith S., (2015). "Density Determination of Ethyl Acetate Palm oil Mixture in Super Critical Conditions" *Engineering journal 19(2):29-39*

Ateeq E.A. L, Ashqer I., Musameh S., (2015). "Biodiesel Viscosity and Flash Point Determination"

Conference: The Eighth Palestinian International Chemistry Conference (PICC 2015) " Chemical Sciences Towards Knowledge Based Economy " Tue - Wed 21 - 22/4/2015 At: An Najah University, Nablus Palestine

ASTM D464 "Saponification Number of Naval Stores Products Including Tall Oil and Other Related Products."

Oliveira W.S., and Ballus A.C., (2019). Mature Chemical Analysis Methods for Food Chemical Properties evaluation

Lawal S.A., Abolatin M.S., Ugheoke B. I., and Onche E.O., (2003) "Performance evaluation of cutting fluids developed from fixed oil"

Leonado electronic journal of practices and technology; Retrieved from http://www.lejpt.academicdirect.

Brinksmeier E., Meyer D., Huesmann-Cordes A.G., Hermann C. (2015). "Metal Working Fluids-Mechanism and Performance"

CIRP Annals - Manufacturing Technology 57(2)

Nwadinobi C.P., and Okoli U. (2018)." Development of Cutting Fluid from Spent Engine Oil"

Nigerian Journal of Technology Vol 37, No.4 pp 950-956

Rakesh Somashekaraiah 1), Suvin P S 2), Divya P G3), Satish V K1)*, Dipshikha C 2)*

"Eco-Friendly, Non-toxic Fluid for Sustainable Manufacturing and Machine Processes"

Department of Mechanical Engineering, Indian institute of Science CNR Rao Circle Mallaeswaram, 5600112 BANGALORA, Indian.

Center For Product Design and Manufacturing, Indian institute of Science CNR Rao Circle Mallaeswaram, 5600112 BAN GALORA,Indian.

Department of Microbiology and Cell Biology, Indian institute of Science

CNR Rao Circle Mallaeswaram, 5600112 BANGA LORA,Indian.

* Corresponding authors: sativk@mecheng.iisc.ernst.in, dipa@mcbl.iisc.ernst.in

Eliyan F.F., and Alfantazi A.,(2014). "Effect of Bicarbonate Concentration on Corrosion of Hight Strength Steel"

Corrosion Engineering Science and Technology 50(3).

The Prospects of Vegetable based Oil as Metal Working Fluids in Manufacturing Application.

International Journal of Engineering Research and Technology

ISSN 2278 -0181

Vol. 3.

Naumov A.G., Latyshev V.N., and Naumoba O.A., (2015). "Tribological Properties of Iodine as a Cutting-Fluid Component Durinh Metal Cutting".

Journal for Friction and Wear 36, 184-188

Christie W.W., and Han X., (2012). "Analysis of Simple Lipid Classes Lipid Analysis Fourth Edition.

Mahesar S.A., Sherazi S.T.H., khashkheli A.R., Kandhro A. A and Udim S., (2014) "Analytical Approaches for the Assessment of Free Fatty Acids in Fats Na Oil". From the Journal Analytical Method.

Valaki J., (2015). "Vegetable Beased Metal cutting fluid for sustainable marching Process" *International Journal of Engineering Technologies and Applications in Engineering Technology and Sciences Volume 7.*

Viscosity of Metal Working Fliud in cutting Processes Determined with SVM 3001 and SVM 4001Viscometer. Accessed date 25 May, 2021.

Curley R.,(2020). "SAE Number, Code for specifying the Viscosity of Lubricating Oil

established by the U.S. Society of Automotive Engineers.

Hecht E., (2002). Optics. Addison-Wesley. ISBN 978-0-321-18878-6.

"Saponification Value of Fats and Oils". Retrieved May 24, 2021

"Saponification value of Fat and Oil" (PDF). kyoto-kem.com. Retrieved May 24, 2021

The Nigerian Society of Engineers
Minna Branch
1st NSE Minna Branch National Conference 2021

Conference theme
Role of Engineering in Sustainable Development Goals

Friction Stir Welding of Some Selected High Strength Aluminium Alloys- A Review

B. I . Attah[1], S. A Lawal[1], E.T Akinlabi[2], K. C Bala[1], O. Adedikpe[1] O. M Ikumapayi[3]
1. Mechanical Engineering Department, Federal University of Technology, Minna- Nigeria
2. Directorate, Pan African University for Life and Earth Sciences Institute, Ibadan-Nigeria
3. Department of Mechanical and Mechatronics Engineering, Afe Babalola University Ado-Ekiti
Corresponding author: benilehttah@yahoo.com

ABSTRACT

Friction stir welding is a solid-state joining technique which involves the plastic deformation of materials to create a solid joint. The tool generates the temperature and pressure to create the solid joints. The process can be used for joining both similar and dissimilar materials. This review addressed the friction stir welding of some selected high strength aluminium alloys. These alloys are used for applications where premium is placed on high strength to weight ratio, thus making them suitable for the aerospace industry where weight reduction is of great importance.

KEYWORDS: *Welded joints, Structural, Rotational speed*

1 INTRODUCTION

Friction stir welding was invented in the U.K in December 1991 at the weld institute. It is a technique used for joining materials in their solid state after undergoing plastic deformation to create a solid joint. The automobile and aerospace industries have found this technique very attractive in light weighting as joints are formed without riveting or bolts and nuts and also without filler metals as is the case with fusion (conventional welding technique) in order to improve vehicle and aircraft performance respectively. The high strength aluminium alloys can withstand stress under service condition making them suitable for structural and other applications in the aircraft industry (TWI, 2015).

The technology has been used to produce vehicle bonnets, wheel rims (Smith et al., 2012) and vessels bulkheads and decks (Gesto et al, 2008) and freezing plants (Midling et al. 1999). It has been used in joining metals in both similar and dissimilar manner and also considered as the most significant improvement in the metal joining processes as it is unharful to the environment, efficient in energy utilisation and with wider areas of application (Akinlabi et al. 2012).The benefits of this welding technique is that it does not generate harmful fumes, no cracking after it has solidified, results in less distortions and improvement in weld quality for the proper conditions, adaptable to all positions and is a relatively noiseless process (Hussain, 2010).

The joining of aluminium however can only be successful when the process parameters are properly selected as mechanical properties are used to qualify the soundness of a weldment and also ascertain the integrity of the welded portion (Attah et al., 2021). Figure 1.0 by Attah et al., (2021) is a schematic representation of the friction stir welding process indicating the advancing and retreating sides (AS and Rs) and the dissimilar alloys pairs of AA1200 and AA 7075 been joined in a butt-welding configuration arrangement.
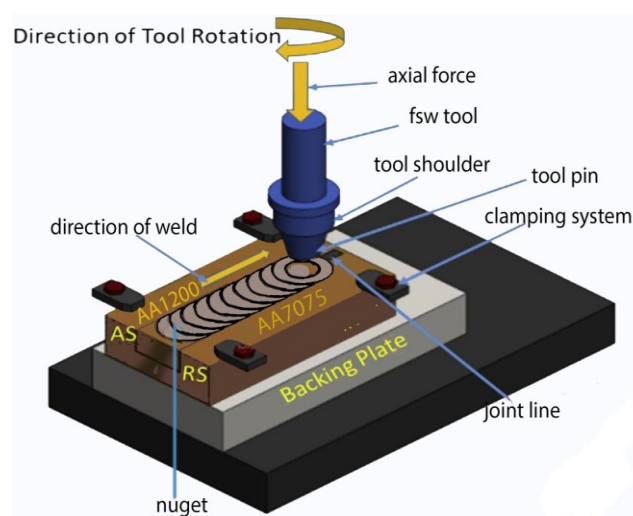

Figure 1.0: Schematic Representation of the friction stir welding Process

2 OPTIMISATION OF OPERATIONAL PARAMETERS IN FRICTION STIR WELDING OF AA7075-T6 ALUMINIUM ALLOYS USING RESPONSE SURFACE METHODOLOGY.

The welding of AA7075 was conducted by applying the response surface methodology approach at five levels of three process variables (Farazadi et al. 2017). The rotational, welding speeds and tool diameter were varied from 350-650 rpm, 35-95 mm/min, 12-18 mm tool diameter respectively and pin length of 4-6 mm and represents the parameters for consideration.

It was observed that the optimal range of the process parameters required to produce the joint with efficiency of 85 % is 380–530 rpm, 90–95 mm/min, 14.2–17.8 and 5–6 mm. It was also observed that the highest value of 458.9 MPa was obtained as the UTS when the spindle speed was varied between 350-500 rpm and at above 500 rpm it begins to decrease. It was also observed that the UTS is mostly affected by both the transverse and rotational speeds as well as pin and shoulder diameters with welding speed been the major factor of influence.

2.1 Microstructural Features of Friction stir Welded dissimilar Aluminium Alloys AA2219-O - AA7475- T761

Dissimilar welding of the alloys both of plate thickness 2.5 mm was performed by Noor et al., (2018) in butt configuration to examine the effect of spindle speed on micro-hardness distribution and microstructure of the dissimilar alloy's joints. The process parameters used are tool rotational speeds of 710, 900 and 1120 rpm. The dimensions of the workpieces are 180 x 50 x 2.5 mm. Micro hardness; microstructural analysis and optical microscopy were done on the materials. The softer material AA 2219-O was positioned on the advancing side while the harder material AA7475 was positioned on the retreating side; high carbon die steel tool was used with pin length of 2.2 mm, pin diameter of 4mm and 10mm shoulder diameter. The results showed the highest value of micro- hardness of 168.8HV at the nugget zone at a spindle speed of 1120 rpm on the retreating side.

The results also revealed that spindle speed significantly affects hardness due to increase in grain size, coarsening and dissolution of strengthening precipitates and re-precipitation. It was observed that as a result of refined grains at the stir zone, there was higher micro-hardness value at the zone. There was proper mixing of the workpieces (along the stir zone) at both advancing and retreating sides for all set of chosen parameters. Microhardness values at the advancing side are reduced by increase in spindle speed due to coarsening of grains. At high rotational speeds at nuggets, precipitates were dissolved and re-precipitation occurred. Hardness value increased with increase in rotational speed on retreating side and decreased on Advancing side.

2.2 Multiscale Electrochemical Study of Welded Al Alloys Joined by Friction Stir Welding

Dissimilar AA7475-T651 and AA 2024-T3 were butt-joined using friction stir welding by Caio-Palumbo et al., (2017) and the properties of the joints were evaluated.

The corrosion behavior of the two alloys was investigated using global and local electrochemical methods and SEM analysis before and after exposure to 0.1 M Na_2SO_4 + 0.001 M NaCl solution. Corrosion of the system results from the attainment of a galvanic coupling in which the AA7475 acted as anode with regards to the AA2024. The results of the anodic polarisation curves and of the global EIS diagrams displayed much lower corrosion resistance for the FSW affected zones compared to the two aluminum alloys tested seperatey. Local pH measurement allowed demonstration of the location of the enhanced reactivity for the welded system.

2.3 Effect of process parameters on the tensile strength of friction stir welded dissimilar Aluminium Alloy joints

The effects of tool rotational and welding speeds on the tensile strength of dissimilar weldment of AA2024-AA7075 joints were examined by Padmanaban et al. (2017). The two plates each of size 150 mm x 60 mm x 5 mm were used along with cylindrical threaded tool, having a shoulder and pin diameter of 17.5 mm and 5 mm respectively and height 4.65 mm was used with the tool rotational speed varied from 900 to 1200 rpm at10-20 mm/min welding speed, the tensile strength of the weldment is measured.

Mathematical model was developed for tensile strength in terms of tool rotational and welding speed. The results revealed higher tensile strength

for the base metals as compared to that of the weldment. Lower tensile strength is recorded at low tool rotational speeds as a result of insufficient heat required for mixing. It was observed that the tensile strength increased when the tool spindle speed increased from 900 rpm to around 1100 rpm. This is because higher rotational speed generates higher amount of heat, better material flow and good mixing. Increasing tool rotational speed above 1100 rpm led to lower tensile strength which may be due to increase in grain size resulting from grain growth at higher peak temperature. However, higher tool spindle speed (beyond 1100 rpm) produces flash and tunnel defects probably due to stirring effect of the pin at high speed. Elangovan and Balasubramanian (2008) obtained a similar result. They reported flash and tunnel defects at tool rotational speeds above 1100 rpm and can be attributed to increased turbulence in the weld zone as reported by Elangovan et al. (2009). It was observed that the change in tensile strength remains constant regardless of weld speed and that the joints made at a tool spindle speed of around 1050 rpm gave the peak tensile strength for a given weld speed.

It was concluded that both the tool spindle and travel speeds affect the tensile strength of the weldment. That tensile strength increases with increase in tool spindle speed up to a value of 1050 rpm but reduces upon further increase. Also, that the tensile strength increases with increase in weld speed up to 15 mm/min and with additional increment decreased. Surface and contour plots revealed that when tool travel and spindle speeds are within 1075 rpm and 1125 rpm, and weld speed are within 13 mm/min to 15 mm/min that the tensile strength would be very near to highest.

2.4 Influences of processing parameters on induced energy, mechanical and corrosion properties of friction stir welded joints of AA 7475 Aluminium Alloys

Butt welding was done by Rajesh et al. (2011) on the alloy plate of 9 mm thickness under the following parameters: travel speed of 50 mm/min, spindle speed was varied between 300-100 rpm, plunge depth of 865 mm, tilt angle of . Tensile, microhardness and corrosion tests were performed

The result revealed that hardness increases from base material to a maximum at the stir zone regardless of the rotational speed due to finer grains. It was observed that a joint efficiency of 89.5 % can be obtained from the welding of the alloy. It was also observed that highest tensile strength of 355 MPa can be attained at a tool spindle speed of 400 rpm, and 50 mm/min travel speed. Also, corrosion resistance from potentiostatic polarisation for both SZ and TMAZ increase with increase in rotational speed from 300-1000 rpm with a maximum corrosion resistance obtained at 1000 rpm and welding speed of 50 mm/min with the stir zone having the highest resistance to corrosion.

3 MULTI-OBJECTIVE OPTIMISATION OF FRICTION STIR WELDING PROCESS PARAMETERS OF AA6061-T6 AND AA7075-T6 USING A BIOGEOGRAPHY BASED OPTIMISATION ALGORITHM

In this study by Mehran et al. (2017), dissimilar welding of the two alloys was conducted on the weldment in butt configuration with dimensions 100 x 50 x 6 mm. The ultimate tensile strength and elongation of AA 6061 and AA7075 are 310 MPa, 524 MPa and 12% and 11% respectively as determined before welding. Experiment was performed on UTS, % elongation and hardness of the weldment, the result was employed in developing a mathematical regression model which was validated.

Analysis of the experimental data by the developed model indicates that it can be employed predicting the stated mechanical properties of the weldment within 9% of their experimental values at a 95% confidence limit. They developed a multi objective optimization algorithm based on two phases: generation of a Pareto set by MOBBO, and the use of two different decision-making methods (Shannon's entropy and TOPSIS) to achieve the best compromise solution from the Pareto set.

The result shows that multi-response algorithm along with mathematical model can be used in friction stir welding to attain maximum mechanical properties. The optimal values for spindle and travel speeds and tilt angle which gave the UTS value of 252.23 MPa, elongation of 8.1% and 72.11 HV were 1002.14 rpm, 149.73 mm/min and 1.92 % respectively at -0.74 mm tool offset. Setting these parameters closely within those of theoretical and milling machine, the experimental values achieved are 253 MPa, 8.2 % and 71.4 HV respectively.

3.1 Characteristics of AA7075-T6 and AA6061-T6 Friction Stir Welded Joints

Dissimilar AA7075-T6 and AA6061-T6 were friction stir welded by Sathish and Vaddi (2015). The metal is in cylindrical form with a cross section of 23 mm diameter and 75 mm length. The process parameter was in three levels and varied from 1000 to 1500rpm at 250rpm interval. Mechanical and metallographic characterizations were performed on the weldments. Taguchi method was used for experimental design.

The result obtained from the experiment gave a range of values for the ultimate tensile strength as 53-203MPa with the highest elongation of the strain rate of 11.56 %. It was noticed that increasing the upset and frictional pressure while decreasing the spindle speed resulted in better tensile strength and ductility.

3.2 Mechanical Strength of Dissimilar AA7075 and AA6061 Aluminium Alloys Using Friction Stir Welding

Sathari et, al (2015) studied the effects of material location and tool spindle speed on the tensile strength of the dissimilar weldment with dimensions 100 x 50 x 2 mm. The tool rotational speeds were varied from 800-1400 rpm while welding speed and tilt angle were kept fixed at 100 mm/min and 3° respectively and by changing the fixed position of the material on the advancing and retreating sides. A total of 10 weldment were made.

From the result, a maximum value 207 MPa was obtained as tensile strength when AA6061 alloys were positioned on the advancing side at a spindle speed of 1000 rpm with good surface features and non-defective internally across the weld area, while the least tensile strength of 160 MPa was attained when AA6061 was located on the retreating side with acute tunnel defects across the weld area leading to crack propagation.

3.3 Experimental Study and Analysis of the Wear Properties of Friction-Stir-Welded AA7075-T6 and A384.0-T6 Dissimilar Aluminium Alloys of Butt Joints

The workpieces with dimensions 100 x 50 x 6.35 mm were joined by Karruppannan et al., (2017). The ultimate tensile strengths of the joints were tested to obtain their highest and a lowest level of these specimens and wear analysis was conducted on them. Their results were compared with the wear resistance of the parent metals. Before obtaining the

results, the tool rotational speed, time and weld speed were held constant at 500 rpm, 300s and 3.141m/s respectively while the applied load was varied as 20, 40 and 60 N.

Wear analysis was conducted and 92 and 35.8 HRB were respectively obtained as hardness for AA7075 and A384.0 while for wear rate, A384.0 was higher and those for the weldment were within the wear rate values of the base metals. The hardness of the weldment was between 35.8 and 92 HRB. They concluded that the hardness of materials and the level of wear are inter-related parameters.

3.4 Optimization of the friction-stir-welding process and tool parameters to attain a maximum tensile strength of AA7075–T6 aluminium alloy

Welding was done in a butt joint arrangement using 300 mm x 150 mm x 5 mm thick plate to derive a relationship empirically between the friction stir welding process and tool variables (spindle and travel speeds, axial load, shoulder and pin diameters, and hardness of the tool) and the joints tensile strength. Empirical relationship was developed using experimental design, ANOVA, and regression analysis. The developed model was applied in predicting the tensile strength of the weldment confidently at 95% limit, employing friction stir welding process and tool variables.

Highest tensile strength of 375 MPa was recorded by the weldment produced with the optimised conditions of 1438 rpm, 67.64mm/min, 8.29 kN axial load, shoulder and pin diameters of 15.54 and 5.13 mm, and tool material hardness of 600 HV. It was concluded that higher sensitivity was displayed by rotational speed compared to other variables followed by travel speed then others. Rajkumar *et al.* (2010).

3.5 Study on mechanical, macro and microstructural characteristics of friction stir welding of AA7075-T6 to AA6061-T6 aluminium alloys

Dissimilar joining of the alloys both of 5mm thick plates was done in a butt arrangement by Pouya et al. (2010). Welding was done at travel speeds of 80,100, 120 and 60 mm/min. The rotational speed and tilt angle were fixed at 900 rpm. Temperature readings were taken at 5mm apart and range of 10-

The Nigerian Society of Engineers
Minna Branch
1st NSE Minna Branch National Conference 2021

Conference theme
Role of Engineering in
Sustainable Development Goals

30mm from the 7075 side. Harness and tensile strength of the weldment were investigated.

The result revealed a steady increase in tensile strength while increasing the travel speed to a level and then starts declining. 255 MPa was obtained for UTS at peak value at travel speed of 120 mm/min and thereafter begins to decrease while the hardness increased with increase in travel speed and the highest value obtained at around 127 HV at 160 mm/min travel speed.

Conclusion

In conclusion, a review of friction stir welding of some selected high strength aluminium alloys has been undertaken. This review has shown that significant progress has been made in both similar and dissimilar welding using friction stir welding process. Most of the cited literature were directed at understanding the appropriate process parameters, Mechanical and microstructural properties as well as microstructure and corrosion characteristics of the weldment. The knowledge of friction stir welding technology can be utilised in fabricating joints of both similar and dissimilar materials in order to maximize their benefits and minimize their drawbacks. The technology is suitable for aerospace, railway and electrical industries amongst others.

REFERENCES

Akinlabi, E.T., Annelize, E & Patrick, J. M (2012). Effect of Travel speed on Joint Properties of Dissimilar Metal Friction Stir Welds. *Second International Conference on Advances in Engineering and Technology*

Attah, B.I., Lawal, S.A., E.T Akinlabi & K. C Bala (2021) Evaluation of mechanical properties of dissimilar aluminium alloys during friction stir welding using tapered tool. Volume 8 issue 1:1909520.
https://doi.org/10.108023311916.2021.1909520

Caio Palumbo D. A., Isolda Costa., Hercilio Gomes D. M, Nadine, P., Bernard T. and Vincent, V. (2017). Multiscale Electrochemical Study of Welded Aluminium Alloys Joined by Friction Stir Welding. *HAL Achievers- ouvertes HAL Id: hal 01611642* https://hal.sorbonneuniversite.fr/hal-01611642.

Divya, D. D., Anuj. S, & Charit, V. (2014): Optimisation of Friction Stir Welding Parameters for AA 6061 and AA 703 Aluminium Alloys by

Response Surface Methodology (RSM). *International Journal of Advanced Mechanical Engineering. ISSN 2250-3234 Volume 4, Number5 (2014), pp. 565-571 © Research India Publications* http://www.ripublication.com

Elangovan, K.; & Balasubramanian, V. (2008).

Influences of tool pin profile and welding speed on the formation of friction stir processing zone in AA2219 aluminium alloy. *Journal of Materials Processing Technology*, 200(1-3), 163175.

Elangovan, K.; Balasubramanian, V.; & Babu, S. (2009). Predicting tensile strength of friction stir welded AA6061 aluminium alloy joints by a mathematical model. *Materials & Design*, 30(1), 188-193.

Farzadi1, A., Bahmani, M. & Haghshenas, D.F (2017). Optimisation of Operational Parameters in Friction Stir Welding of AA7075-T6 Aluminium Alloys Using Response Surface Methodology. *Arab Journal of Science and Engineering 42:4905 4916 DOI 10.1007/s13369-0172741-6.*

Gesto, D., Pintos, .V., Vazquez, .J. Rasilla J., & Barreras, S. (2008). Application of Friction stir welding in ship building. Proceedings of TWI,s 7th Int. Sympsium on Friction stir welding', May 4th-7th 2008, Awaji Island, Japan.

Hussain, A.K. (2000). Evaluation of parameters of friction stir welding for aluminium AA6351Alloy, *International journal of engineering science and technology*, 2(10),59775984.

Mehran, T., Hang, B. T., Baharudin, T., Shahla, P., Khamirul, A. M.,Shamsuddin, S & Firouz,

F.(2017). Multi-Objective Optimisation of Friction Stir Welding Process Parameters of AA6061-T6 & AA7075-T6 Using a

Biogeography Based Optimisation Algorithm Midling, O. T., Kvåle, J. S. & Dahl, O. (1999). Industrialisation of the Friction Stir Welding Technology in Panels Production for the Maritime Sector. Proceedings of TWI 1st International Symposium on 'Friction stir welding', June 2nd- 5th 1999, Thousand Oaks, CA, USA.

Noor, Z. K., Mohammed, U., Arshad, N. S., Zahid, A. K.., Abdulrahman, A. A, Xizhang, C & Mustufa, H. A . (2018) :Microstructural Features Of Friction Stir Welded Dissimilar Aluminium Alloys Aa2219 AA7475. *Journal of material research express* Vol (5) https://doi.org/10.1088/2053-1591/aac4e1.

Pouya, B., Mohammad, H., Mohammad, K. B. G & Sahand, A. (2010). Study on mechanical, macro and microstructural characteristics of friction stir welding of AA7075-T6 to AA6061-T6 aluminium alloys . *Proceedings of the Institution of Mechanical Engineers part B journal of Engineering Manufacture* 1:1-12. DOI: 10.1243/09544054JEM1959

Rajkumar, S., Muralidharan, C & Balasubramanian, V. (2010). Optimisation of the friction-stir Welding process and tool parameters to attain a maximum tensile strength of AA707-T6 aluminium alloy. *Proceedings of the Institution of Mechanical Engineers part B journal of Engineering Manufacture* 1:1-12. DOI: 10.1243/09544054JEM1959

Rajesh, K .G., Hrishikesh D., & Tapan K. P. (2012) Influence of Processing Parameters on Induced Energy, Mechanical and Corrosion Properties of FSW Butt Joint of 7475 AA. *Journal of Materials Engineering Performance* 21:1645–1654 _ASM International. DOI: 10.1007/s11665-011-0074-21

Karruppanan, A., Subramaniam, P & Mayakrishnan, M (2017) Experimental Study and Analysis of the Wear Properties of Friction-Stir-Welded AA7075-T6 and A384.0-T6 Dissimilar Aluminium Alloys of Butt Joints. UDK 620.1:620.178.16:669.715

Sathish R & Vaddi S. R. (2014). Characteristics Of AA7075-T6 and AA6061-T6 Friction Welded Joints. *Transactions of the Canadian Society for Mechanical Engineering*, Vol. 39, No. 4, 2015

Smith, C. B,, Hinrichs, J. F., & Ruehl, P. C. (2012). Friction Stir and Friction Stir Spot Welding – Lean, Mean and Green. Retrieved on October 20 2017 from: www.frictionstirlink/Pub14AwssmcLeanMean Geen-UnitedStates

TWI, (2015). What is welding? Definition, processes and types of welds. Retrieved on 25th March, 2021 from www.twi-global.com.

Padmanaban, R.V., Balusamy, V. & Nouranga, K.. N.(2015): Effect of Process Parameters on the tensile strength of friction stir welded dissimilar aluminum joints. *Journal of Engineering Science and Technology Vol. 10, No. 6. 790 – 801 © School of Engineering, Taylor's University*

Conference theme
Role of Engineering in Sustainable Development Goals

The Failure Analysis in Steel Reinforced Beams with different Reinforcement Ratio

*Ayandokun W. A[1], Balogun B. T[1], and Abdulrahman A. S[2]
[1]Department of Mechanical Engineering,
[2]Department of Materials and Metallurgical Engineering
Federal University of Technology, Minna.
*08030999791, ayandokun.pg915448@st.futminna.edu.ng

ABSTRACT

This research paper presents the failure analysis in reinforced steel concrete through experimental investigation. The experiment set-up used the flexural cracks in strainedsamples of steel reinforced beams in separate three (3) plains and three (3) reinforced steel concretes with reinforcement ratio 0.12% and theeffects was investigated and analyzed through the crack behaviours in fracture mode. The samples were loaded with two applied forces in one third of the length. The loading by force displacement allowed reducing the failure and observing the development of the crack using controlled hydraulic jacks and gauges. The compressive strength and young's modulus were tested on reinforced concrete with cylinders of 150 mm diameter and height of 300 mm, and the average values recorded were 20.4 and 22,118 MPa respectively. The strength (tensile)was tested on mode of cubes with length (150 mm), breadth (150 mm) and height (150 mm) at a separate test and average value recorded was 1.64 MPa while the corresponding tensile strength (axial) was recorded as 1.48 MPa. The average cracking moment was 5.08 kNm in plain and 5.39 kNm in reinforced steel concretes. The experimented sample beams of differential ratio of 0.6% failed at the applied load of 44 kN and the maximum bending moment reached was 4.07 kNm. The experimental results recorded in the reinforced beam of ratio 1.5%, the shear force of cracking experienced was recorded as 4.2 kN, but the maximum shear force reached was higher at 5.14 kN. Whereas in the sample reinforced beam of ratio 2.1%, the shear force of cracking experienced was recorded as 5.07 kN and the maximum shear force reached was 5. 96kN.Conclusively, the inference observed that the maximum shear forces reached were numerically advantage to cracking forces (shear). Hence, the inclined effect crack behaviours did not occur rapidly but influenced by tensile strain, elongation, deformation mechanics, impact, and reinforcementstiffness.

KEYWORDS: *Failure analysis; Flexural crack; Reinforcement ratio; Reinforced steel.*

1 INTRODUCTION

With a long history of technical development behind it, the steel industry is firmly established as a heavy reliable industrial product of great utility. However, the diversity in today's society and economy leads to continuity demand for steel, better performance, and for novel design features in building constructions. This in turn presents new technical research into the load capacity of building structures supported by reinforced steels, tends to be defected through the deformation behaviour of reinforced beams. Most researches proved that the compressive test (strength) of reinforced beams are usually varies from 17 to 28 MPa and higher in residential and commercial structures,(about 10 times)higher than its tensile strength around 2 to 5 MPa. This means, an average, the tension averages about10% of the compressive strength (Ajagbe et al., 2018). Though, concrete belongs to the composite regarded as brittle but it isimperfection in nature (quasi-brittle). Two major parameters are required to analyze the effects of quasi-brittle nature of concrete on cracking. These are referred to as tensile strength and tensile toughness (Abdullahi, 2012). In a course to measure the effect of tensile toughness in concrete, fracture energyapplication tends to be analyzed (Akinleye and Tijani, 2017). Moreover, the characteristics of fracture toughness in reinforced beams application have no direct impact tothe conventional design of structures, while considering the British standards, (BSI, 2009).

This research paper highlights failure investigation of reinforced steel with different reinforcement ratio through most of the reinforced materials formed and contributed to the initiation of cracks in a flexure. Nonetheless, it can either be in plain or reinforced beams which are of great importance to analysis the effect of failure in crack propagation.A stable propagation of several flexural cracks is develop in moderately reinforced concrete beams, and the load carrying capability is supported with reaching the yield stress of reinforcing steel in

the compression zone. In advanced set-up of reinforced concrete beams without transverse reinforcement, brittle failure can easily occur due to shear forces and the development of diagonal cracks (Alaneme et al., 2019). From structural appearance, consideration should be given to the sampled steel reinforced beams when investigated, brittle failure due to occur when the martensiticrepeated bending stress which must be stable by the reinforced beams. It is possible for overload fractures to occur when the excessive loads being applied (Das et al., 2014).

Since a fatigue fracture is progressive in reinforced beams, all types of contaminants developing over a long period of time, the fracture surface usually shows characteristic "beach" markings. In this case the fracture showed discontinuity on the surface and, proceeded nearly across the section before final separation. Fatigue fractures initiate in shear by a mechanism involving slip and work hardening, eventually forming microscopic discontinuities which develop into cracks (Hari and Moga, 2009).

Once a crack is formed, its rate of growth depends upon the stress magnitude, stress gradient, endurance limit of the material, notch sensitivity, and the presence or absence of structural flaws and inclusions. After the crack has formed, the stress is reduced to below the value necessary to initiate it, the crack may not propagate any further. This is probably caused by an increase in strength due to strain hardening at the crack tip. If the applied load is large enough, the crack will advance perpendicular to the maximum tensile stress. They indicate the position of root of the advancing crack at weakens; the crack grows faster, apart, larger, and more distinct. Therefore, specifications and control measures require when these markings are plenty, they provide a means of locating the origin of fracture (Taber et al., 2002). When reinforcing steel bars are not designed properly, the structure willcrack and eventually fail (Xiaoke et al., 2020).

The failure behaviour of cracks in concrete has demonstrated the need for a better understanding of the mechanisms of fracture in reinforced steel concretes under flexure. Series of researchers worked over the past decades have led to the evolution of the field of the steel reinforcement in concretes. This subject proved series of numerical analysis on quantification of the relationship between the properties of the materials such as stress, crack-producing flaws and crack propagation (Fernandez et al., 2016). The design engineers should be better equipped to perform and thus prevent structural failures (Fernandez et al., 2018).

As a result of this, failure analysis can focus on increases in deflections, determination of the location, type, and source of the crack-initiating flaw. Also, reduction of bearing capacity, which is normally a part of analysis, involvesexamining the path of crack propagation as well as microscopic features of the fracture surface in relation to transverse reinforcement and, eventually cyclic stresses such axial (tension-compression), flexural (bending), or torsional (twisting) in nature.

2 FAILURE ANALYSIS OF PLAIN AND REINFORCED STEEL CONCRETES

2.1 PLAIN CONCRETE AND REINFORCED STEEL CONCRETE

A series of earlier set of the technological tests proved that buildup to failure effect parameters include specimen fabrication and surface preparation, metallurgical variables, specimen alignment, mean stress, and test frequency, especially inslightly reinforced steel concretes. These techniques have been developedto specify the structures of plain and reinforced concretes in terms of crack initiations and propagations, at a maximum stress expecting 0.12% of the reinforcement ratio. The sample structures wereclassified into two categories, one is associated with plain concretes, that produce not only elastic strain but also some plastic strain during failure.For the other category, reinforced steel concrete wherein deformation are totally elastic, longer lives results in as much as relatively large numbers of cracks were appeared to cause failure.The loading as a result of statistical treatment were based on fatigue life and fatigue limits.

Consequently, sample structures set up by aggregate composite of cement, sand, steel bars and required water for the 40mm dimension mould loaded with two bearing forces appliedfrom bottom to top at about 33% of the length. The standard methods employed to test the basic concrete properties throughforce displacement using jacks and gauges.

The compressive strength and young's modulus were tested on reinforced concrete with cylinders of

150 mm diameter and height of 300 mm, and the average values recorded were 20.4 and 22,118 MPa respectively. The stress (tensile) was tested on mode of cubes with length (150 mm), breadth (150 mm) and height (150 mm) at a separate test and average value recorded was 1.64 MPa while the corresponding tensile strength (tension-compression) was recorded as 1.48 MPa and the yield stress was 275 MPa. The average cracking moment was 5.08 kNm in plain and 5.39 kNm in reinforced steel concretes. The experimented sample beams of reinforcement ratio of 0.6% failed at the applied load of 44 kN and the maximum bending moment reached was 4.07 kNm. The experimental results recorded in the reinforced beam of ratio 1.5%, the shear force of cracking experienced was recorded as 4.2 kN, but the maximum shear force reached was higher at 5.14 kN. Whereas in the sample reinforced beam of ratio 2.1%, the shear force of cracking experienced was recorded as 5.07 kN and the maximum shear force reached was 5.96 kN. Location of steel bars is presented in Figure 1.
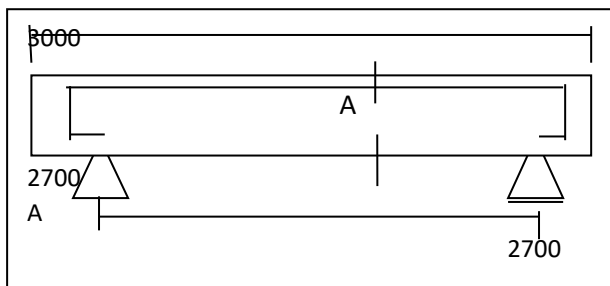
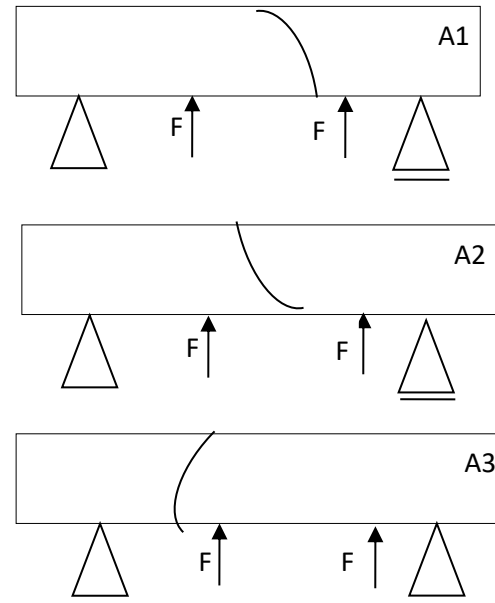in reinforced steel concretes continued developing two or three cracks as is presented in Figure 2 and 3.

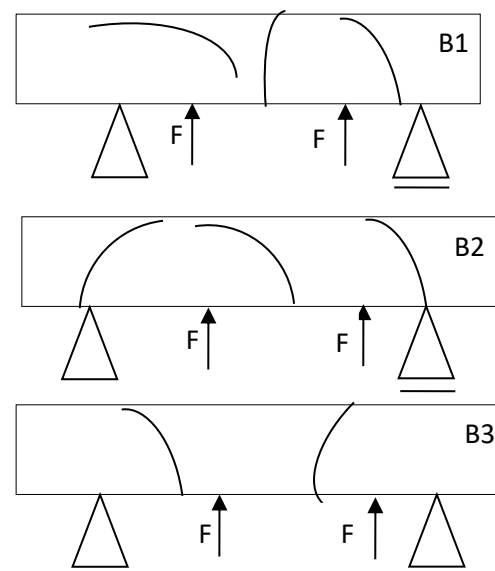
Figure 2 The location of cracks in plain concretes

Figure 1: Location of Reinforcement on the reinforced steel concrete

A brittle character of failure was observed in all tested reinforced concretes during the experiment, but size elongation in failure process were noticed and a higher cracking resistance was obtained in reinforced steel concretes in comparison to that measured in plain concrete samples. In plain concrete sample, a brittle and sudden failure was noticed right after the appearance of the first flexural crack. In reinforced steel concrete sample of the reinforcement ratio 0.12%, the failure was also caused by the main flexural crack but the concretes' damage was noticed at higher load level than in plain concrete samples. The failure crack did not occur as rapidly as in concretes, and the destructive process

Figure 3 The location of cracks in slightly reinforced steel concretes

2.2 BENDING MOMENTS

Cranks in fracture behaviour of materials can be determined using bending momenttechniques. On the basis of the fracture surface, it is possible to ascertain whether or not a material experiences a ductile to brittle transition and the elongation range over which such a transition occurs. The calculated mean values of cracking moments were 5.08 kNm in plain concrete and 5.39 kNm in reinforced steel concrete samples

The need often arises for engineering fracture energy data that are practical to collect from normal laboratory tests to be input into the formula. This is true for prolonged exposure tests in excess of the requirements, for shorter time periods and at a comparable stress level, and then making a suitable to the service condition. Hence, the situation of cracking moment affects the load capacity of plain and reinforced steel concrete appeared to be higher in both cases than the theoretical cracking moment (BSI, 2009).

Crack's initiation exists in micro-cracks start to grow into nucleated coalescence. For the fracture energy, the energy absorbed per unit crack area during crack's formation. Fracture energy relationship is due to the area under the stress crack opening curve σ – w (Slowik and Blazik-Borowa, 2011). In the process of this, the normal stress distribution in the fracture obtained in the plain concrete as presented in Table 2 and figure 4.

$$GF = \int \omega l \sigma \partial \omega \qquad (1)$$

TABLE 1: GAUGE READINGS FOR THE PLAIN AND REINFORCED STEEL CONCRETES

Gauge Readings (kN)	1	2	3	Average
Plain concrete (A)	5.10	5.51	4.45	5.02
Reinforced steel concrete (B)	5.59	5.44	5.21	5.41

TABLE 2: THE DISTRIBUTION OF NORMAL STRESS IN THE FRACTURE PROCESS ZONE OF PLAIN CONCRETE

Load (kN)	Reinforcement Ratio (%)					
	1.0	1.9	3.1	4.0	4.96	5.19
0.03	- 2650	- 2300	- 1800	- 1400	-900	- 600
0.06	- 1800	- 1700	- 1300	- 1000	-700	- 400
0.09	- 1100	- 1100	-900	-700	-450	- 300
0.12	-400	-500	-400	400	-300	- 200
0.15	400	400	0	0	0	0
0.18	1400	900	500	300	200	100
0.21	1300	1500	1000	700	500	300
0.24	1100	1300	1500	1100	700	500
0.27	800	1200	1400	1400	900	600
0.30	700	1100	1300	1500	1100	700

The distribution of normal stress in the fracture process zone was obtained in the reinforced steel concrete with reinforcement ratio 0.12% in the following steps of loading as shown in figure 4 and 5.
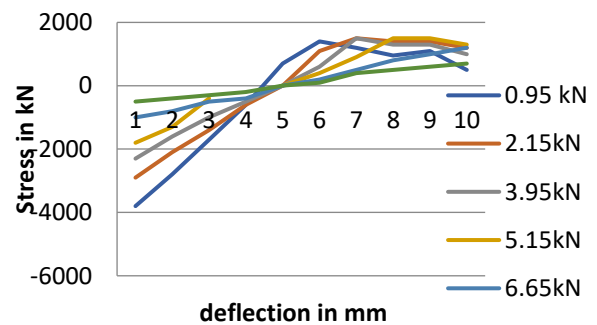

Figure 4: Normal stress distribution in concrete in the fracture process zone in plain concrete beam

TABLE 3: THE DISTRIBUTION OF NORMAL STRESS IN THE FRACTURE PROCESS ZONE OF REINFORCED STEEL CONCRETE

Load (kN)	Reinforcement Ratio (%)					
	0.9	2.15	3.95	5.15	6.65	8.45
		--				
0.03	-3800	2900	-2300	-1800	-1000	-500
0.06	-2800	-2100	-1600	-1300	-800	-400
0.09	-1700	-1400	-1000	-400	-500	-300
0.12	-600	-600	-500	-	-400	-200
0.15	700	0	0	0	0	0
0.18	1400	1100	600	400	200	100
0.21	1200	1500	1100	900	500	400
0.24	950	1400	1300	1500	800	500
0.27	1100	1400	1300	1000	1000	600
0.30	500	1200	1000	1300	1200	700

The Nigerian Society of Engineers
Minna Branch
1st NSE Minna Branch National Conference 2021

Conference theme
Role of Engineering in
Sustainable Development Goals

TABLE 4: NORMAL STRESS
DISTRIBUTION IN THE SAME LOAD LEVEL
FOR PLAIN CONCRETE AND REINFORCED
STEEL CONCRETE BEAMS

Load (kN)	0.15	0.18	0.21	0.24	0.27	0.30
Plain	400	1400	1350	1100	800	400
Reinforced Steel	100	700	1350	1400	1450	1200

be observed when compare the normal stress the
same load distribution of plain and reinforced steel
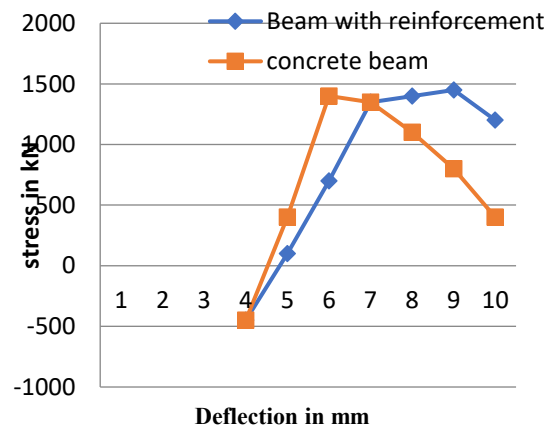beams as shown in table 4 and figure 6.

Figure 6: Comparison of normal stress distribution
in the fracture process zone at the same level

The numerical simulation permits to explain a
less brittle character of the crack formation in
reinforced steel concretes comparing to plain
concrete beams

Figure 5: Normal stress distribution in concrete
in the fracture process zone in reinforced steel
concrete

The analyzing of the crack development in
normal stress, experienced the fracture effectwhich
is significantly related to tensile strain in concrete.
The flow of stress distribution proved a linear
character until tensile stress reaches the maximum
tensile strength in the extremeupper edge of the
tension. As concrete is perfectly inelastic and brittle,
it shows aprogressive cracking influence that leads
to the nucleated crack formation. For the extreme
edge of the fracture, the distribution of the normal
stress reaches the level of the tensile strength in such
concrete, whereas in the lower level oftension, the
tensile stress decreases to zero. Moreover, the
presence of steel reinforcement in beams causes
significant increase in failure resistance. The
concrete and steel bars influence the bond within the
vicinity ofstress intensity of reinforcement. Also, it
reduces the process of crack propagation. The
characteristics difference in the crack formation can

3 STABLE AND HIGHER RATIO OF REINFORCED BEAMS

In the course of this research, experimental
investigation of the longitudinal reinforcement in
stable beams with high reinforcement ratio proved
the tendency of cracks accumulation. The
experiment set-up considered on longitudinally
reinforced beams, that the reinforcement ratio was
0.6%, 1.5% and 2.1%. It is clearly noticed that
transverse reinforcement was not used in the beams.
The load bearing capacity was applied directly from
the testing machine. The concrete beams were 2.05
m long, and the beams' effective span during the test
was 1.8 m. Beams were made of concrete with the
maximum aggregatesize of 16 mm. The basic
concrete properties were tested by standard
methods. The stress (tensile) were tested on mode of
cubes with length (150 mm), breadth (150 mm) and
height (150 mm) at a separate test and average value
recorded was 4.79 MPa while the corresponding
tensile strength was recorded as 3.5 MPa, and the
axial (tension-compression) tensile strength was

The Nigerian Society of Engineers
Minna Branch
1st NSE Minna Branch National Conference 2021

Conference theme
Role of Engineering in
Sustainable Development Goals

calculated as 3.15 MPa. The young's modulus was measured on to be 41400 MPa. As a longitudinal reinforcement, steel bars of the diameter 12 mm were used. The characteristic yield stress of steel bars was 460 MPa.

From the analysis of the sample structures, the initiation of cracks at similar load level in the mid-span fracture, and propagated into the transverse direction. Consequently, the increment in load applied caused the corresponding increased in flexural cracks within the structures. But, the effect of the cracks was more significant toward the supports. It can be deduced that the resulted vertical cracks became wider and deeper. Moreover, with the increase in applied loads, the resulted vertical cracks also moved toward the edge of the supports and tend to change their orientations. It finally becomes the inclined failure cracks (Ferreira et al., 2013). The reinforcement ratio determines the distribution, number of cracks and their width as well as length, which varied accordingly. The distribution cracks is as presented in Figure 7.
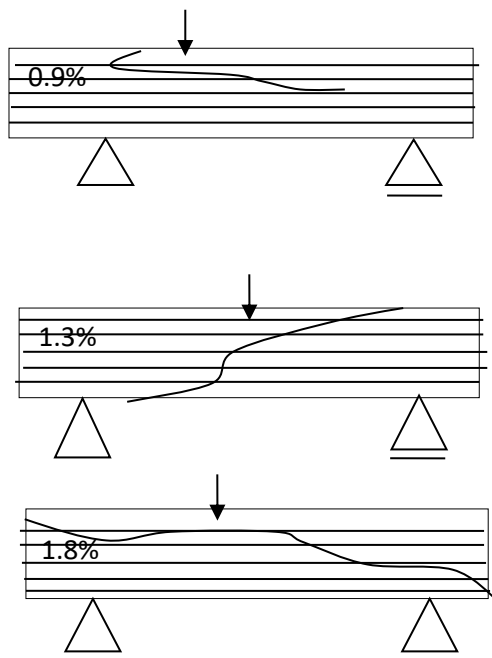

Figure 7: The Failure crack distribution in the beams

In most cases, the reinforcement ratios depend on different levels of failures when observing the tested beams. The procedure to be followed in the preparation of a specimen is comparatively simple and involves a technique which is developed only after constant practice. The ultimate objective is to produce a stable growth of resulted cracks from the moderately reinforced concrete beam of reinforcement ratio 0.6%. If a failure is to be investigated, the sample should be close as possible to the area of failure and compared with one taken from the normal section, which prevented against a sudden failure. The developments of flexural cracks were noticed, and the failure from the flexure then confirmed. The specimen beam failed and recorded the value of the applied load as 9.04 kN. Numerically, its maximum bending moment recorded was 4.11 kNm.

In furtherance of the research, the specimen reinforced steel beams of 1.5% and 2.1% while reinforcement ratios were being considered, after nucleated flexural crack formation. Also, the resulted diagonal crack propagated in the support area of the specimen beams. Under certain circumstances, the resulted diagonal crack formed from the flexural crack was due to stresses (shear) that change its orientation and eventually become a diagonal crack. Although in principle, the specimen beams tend to not use the transverse reinforcement, since the propagation of inclined cracks through the shear, caused brittle failure. Instantly, the failures of the specimen beams occur after the formation of the diagonal crack. The various shear forces controlled the failure in sample reinforced beams, with the utmost flexural capacity due to the inability of achieving the required longitudinal reinforcement. When it is increased, the reinforcement ratios cause the corresponding increase in failure cracking of shear force. In many cases, particularly appearance of diagonal crack and maximum shear force at failure cracking were observed. From the application of specimen beam of reinforcement ratio 1.5%, the cracking shear forces was 4.11 kN and the maximum shear force was 5.14 kN. While, considering the specimen beam of reinforcement ratio 2.1%, the cracking shear force was 5.07 kN and the maximum shear force recorded as 5.96 kN. The most commonly observed from the results of this research showed that maximum shear forces were numerically higher to the cracking shear forces. Therefore, the process of failure propagated by resulted inclined cracks did not show in a rapid way.

This analysis, fortunately, is the failure process of cracking in the beams. From the properties, this

The Nigerian Society of Engineers
Minna Branch
1st NSE Minna Branch National Conference 2021

Conference theme
Role of Engineering in
Sustainable Development Goals

can be concluded that the development of the flexural cracks were somehow slow as observed to the zone of crack failure in uniformly reinforced steel concretes. Hence, in highly reinforced specimen, diagonal cracks appear after the stabilization of flexural cracking. The start up of inclined cracks is affected by strained tensile concrete, but in the accumulation of nucleated diagonal cracks such procedures as an aggregate interlock. Consider the steel bars, appearance is predominating. From the description of this, the increase in the capacity of shear stress results in corresponding increase in reinforcement ratio. The results are importantly to show that more crack failure in shear transfer formed in highly reinforced steel concrete beam (Abdullahi, 2012; ASTM, 1997).

4   CONCLUSIONS

The effect of failure cracks of steel reinforced concrete beams in relation to different reinforcement ratio changes accordingly in terms of longitudinal reinforcement ratio:

Flexural strength reached its full capacity with the bearing capacity, and improves on steel yielding through the axial stress in the zone.

The propagation of the failure crack with the applied bearing capacity do follow the process of an aggregate interlock of steels.

The analyzed results proved that transverse reinforcement do play a major role in reducing shear failure (brittle), when considering concrete beams with high longitudinal reinforcement ratio.

5   ACKNOWLEDGEMENTS

REFERENCES

Abdullahi M. (2012). "The effect of aggregate type on compressive strength of concrete". *International Journal of civil and structural engineering*, 2(3).

Ajagbe O. W., Tijani A. M., and Agbede O. A. (2018). "Comprehensive strength of concrete made from aggregate of different sources", *Journal of research information in civil engineering*, 5(1).

Akinleye M. T., and Tijani M. A. (2017). "Assessment of quality of Asphalt concrete used in road construction in southwest Nigeria", *Nigeria Journal of Technological Development*, 14(2).

Alaneme K. K., Fajemisin A. V., and Maledi B. N., (2019). "Development of Aluminum-based composite reinforced with steel and graphite particles, Structural, Mechanical and Wear characterization", *Journal of material research and technology*, 8(1), 670-682.

ASTM A944-95, "*Standard Test Method for Comparing Bond Strength of Steel Reinforcing Bars to Concrete Using Beam-End Specimens*," 1997 Annual Book of ASTM Standards, Vol. 1.04, American Society for Testing and Materials, West Conshohocken, PA. 1997, pp. 514-517.

British Standards Institution (2009). "*Testing hardened concrete; compressive strength of test specimens BS EN 12390 parts*", London, Uk.

Fernandez I., Herrador M. F., Mari A. R., and Bairan J. M., (2016). "Structural effects of steel reinforcement corrosion on statically indeterminate reinforced concrete members", *Journal of Materials and structures*, 49(12).

Fernandez I., Herrador M. F., Mari A. R., and Bairan J. M., (2018). "Ultimate capacity of corroded statically indeterminate reinforced concrete members*", International Journal of concrete, Structures and Materials,* 12(75).

Ferreira D., Bairán J., Marí A., and Faria R., (2013). "Nonlinear analysis of RC beams using a hybrid shear-flexural fibre beam model". *Engineering and Computer* 31:1444–1483. doi: 10.1108/EC-04-2013-0114

Hari W., and Moga N., (2009). "Bending of reinforcing bars testing methods and influence on structures". *International Journal of Structural Engineering.*

MacGregor, J. (1997). "*Reinforced Concrete*". Mechanics and Design, 3rd Ed., Prentice Hall, 1997.

Malumbela G., Alexander M., and Moyo P. (2009). "Steel corrosion on RC structures under

sustained service loads — A critical review". *Engineering Structures*, 31:2518–2525. doi: 10.1016/j.engstruct.2009.07.016.

Shivayya M., and Bhavi I. G., (2015). "Experimental and Finite element analysis of bending strength of various structural cross sections of conventional and composite", *Material science*, 4(4).

SlowikM.,andBlazik-Borowa E.,(2011). "Numerical study of fracture process zone width in concrete members",*Journal of Architecture, civil engineering and environmental*, 2, 73-78

Slowik M., (2014). "Shear failure mechanism in concrete beams", *Journal of Process, and Material sciences*, 3, 1977-1982

Souvik D., Jitendra M. Tanmay B., and Sandip B., (2014). "Failure analysis of re-bars during bending operations", *Case study in Engineering Failure Analysis*, 2, 51-53.

Taber L. H., Belarbi A., and Richardson D. N., (2002). "Effect of reforcing bar contamination on steel-concrete bond during concrete construction"*, Journal of Performance of constructed facilities*, 24(3).

Tribune 14 May 2012, News Headline, Building collapse, COREN proposes death penalty for perpetrator, http//:www.tribunenews.ng

Xiaoke L., Songwie P., Kunpeng F., Habin G., and Fenglan L., (2020). "Bending performance of steel fibre reinforced concrete beams based on composite-recycled aggregate and matched with 500 MPa Rebars", *Materials science*, 13, 930.

Oxidative Stability and Cold Flow Properties of Non-Edible Vegetable Oil for Industrial Biolubricant Applications

*Timothy Yakubu Woma[1,2], Sunday Albert Lawal,[1] Asipita Salawu Abdulrahman,[3] M.A. Olutoye,[4] and A.A. Abdullahi,[1]

1. Department of Mechanical Engineering,
3. Department of Metallurgical and Materials Engineering,
4. Department of Chemical Engineering,
Federal University of Technology Minna P.M.B 65 Minna, Niger State, Nigeria
2. Department of Physics, Federal University Wukari, P.M.B 1020 Wukari, Taraba State, Nigeria

ABSTRACT

The use of mineral oil-based lubricants is attracting increasing environmental concern. Additionally, mineral oil is non- renewable and subject to high price fluctuation. There is therefore a need to seek alternative sustainable and renewable lubricant base stock. Vegetable oil are thought of as good substitute for mineral oil -based lubricants, but their use suffers setback due to their poor cold flow characteristics and thermo-oxidative instability. The oxidative stability, flash point and cold flow behaviour of castor oil were measured and compared to commercially available mineral oil -based lubricant SAE 20/W50. The castor oil had peroxide value of 8.92 meq/kg, flash point of 2820C, cloud point of -12.40C and pour point of 23.20C. The commercially available mineral oil- based lubricant SAE 20/W50 had peroxide value of 0.99 meq/kg, flash point of 2550C, cloud-point temperature of -18.90C and pour-point temperature of 24.10C. The castor oil has poor oxidative stability but excellent fire safety and cold flow properties. The - castor oil is a good sustainable and renewable alternative to petroleum oil -based lubricant, however its oxidative stability needs to be improved to increase its shelf life and service life as a lubricant.

KEYWORDS: *Biolubricant, castor oil, cold flow, flash point, Peroxide.*

1   INTRODUCTION

Virtually every industry consumes lubricating solids, oils or gases. Within the last decade the annual worldwide consumption of lubricants is over 40 billion kilograms. The final destination of 30% of lubricants consumed is the ecosystem, the base oil used for the formulation of most lubricants is environmentally dangerous petroleum oil (Bartz, 2006; Ajithkumar, 2009).

However, petroleum oil reserve is finishing and the environmental outcry about the damaging impact of mineral oil is growing. The search for environmentally friendly alternatives to petroleum oils as base oils in lubricants has become a novel area of research in the lubricant industry. Oils from plants and animals are perceived to be alternatives to mineral oils for lubricant base oils due to certain their inbuilt technical behaviour and their ability to be biodegradable. Previously, detail review of the prospects and challenges of plant-based oils as lubricants for industrial applications was reviewed by Woma, et al., (2019).

Vegetable oils in general compared to petroleum oils possess high flash point, high viscosity index, high lubricity and low evaporative loss (Erhan and Asadauskas, 2000; Adhvaryu and Erhan, 2002; Mercurio, et al., 2004). During disposal or accidental spillage, oils have been found to be less dangerous to the soil, water, flora and fauna compared to mineral oil (Mercurio et al. 2004; Awoyale et al. 2011). Erhan and Asadaukas, (2000); as well as Adhvaryu et al. (2005) reported that poor oxidative and hydrolytic stability, high temperature sensitivity of tribological behaviour and poor cold flow properties are reckoned to be the limitations of vegetable oils for their use as base oils for industrial lubricants.

Based on findings from low temperature studies, most vegetable oils undergo cloudiness, precipitation, poor flow, and solidification at $-10\ ^\circ C$ upon long-term exposure to cold temperature (Rhee et al., 1995; Kassfeldt and Goran, 1997). Not all vegetable oils possess equivalent chemical and performance properties (Erhan et al; 2006).

The flash-point of the lubricant is the temperature at which its gaseous-state will ignite. Flash and fire points are very important from the safety view point since they constitute the only factors which define the fire hazard of a lubricant. In general, the flash point of oils increases as their molecular weight increases.

For systems exposed to low temperature, the pour point of oil is an important property in their lubrication. When oil ceases to flow this indicates that sufficient wax crystallization has occurred or that the oil has reached a highly viscous state. At this stage waxes or high molecular weight paraffins precipitate from the oil forming the interlocking crystals which prevent the remaining oil from flowing. The continuous supply of oil to the moving parts of machines is a critical issue because the successful operation of a machine depends on it. Thus pour point is very important.

Oxidation stability (ASTM D943) is the lubricant ability to resist molecular breakdown or rearrangement at elevated temperatures in the ordinary air environment (ASTM; 2004). Exposing lubricating oils to air can oxidize them, particularly at elevated temperatures, and this has a very strong influence on the life of the oil. According to Demian (1990), the peroxide value is essentially used as the basis for studying the stability of vegetable oils. The peroxide value is majorly a characteristic of the conventional oils and is a measure of its oxygen; it is usually less than 10 mEQO2/kg (Codex, 1993). A rancid taste begins to appear between 20 mEQO2/kg and 40 mEQO2/kg (Onuoha, 2015).

Castor oil is gotten by pressing the castor beans obtained from the castor plant. The castor bean is shown in Figure 1. Nigeria is rated at between 950-1,500 kg/ha yield of castor seed (Gana et al., 2014), and virtually every part of the country is suitable for castor plantation Bingfa et al; (2015). Half of the dry weight of castor bean seed is made of oil (Brigham, 1993). This has attracted the investigation of the lubrication properties of this oil. This work investigated the oxidative stability, flash point and cold flow properties of castor oil for its possible industrial biolubricant applications. The properties of a mineral oil based commercial lubricant (SAE 20/W50) was also measured for comparison with the castor oil.

Figure 1: Castor bean

2 METHODOLOGY

Castor oil that is cold pressed obtained from Agrienergy Kano, Nigeria and commercially available mineral oil-based lubricant from Kano were used for this research. The castor oil was a colourles to a very pale-yellow liquid with a distinct-bland taste and odour. Digital infra-red thermometer, open cup crucible and refrigerator were also used. distilled water, starch, powdered potassium iodide and 98 % purity sodium thiosulphate obtained from JHD Chemical Reagents Co. Ltd, Guangzhou China were used for the research.

2.1 DETERMINATION OF OXIDATIVE STABILITY (PEROXIDE VALUE)

The peroxide value was measured according to American Oil Chemist Society (AOCS) C/8 53 standard. Firstly, 0.001 kg of oil was weighed into a clean drying boiling tube, 0.001 kg of powdered potassium iodide and 20ml of solvent mixture (2volume of glacial acetic acid + 1volume of chloroform) was added, the tube was placed in boiling water so that the liquid boils within 30 seconds and was also allowed to boil vigorously for not more than 30seconds. The content was quickly emptied into a glass flask containing 20ml of potassium iodide solution; the tube was washed out with 25ml of distilled water and was titrated with 0.02M sodium thiosulphate solution using starch as indicator. A blank was also carried out at the same time. The peroxide value (PV) of the castor oil and lubricant was determined by calculation using (1).

$$PV = \frac{(A-B)XNX1000}{Woil} \qquad (1)$$

Where   B= volume of sodium thiosulphate used in blank titration. A= volume of sodium thiosulpate used in titration with oil. N= normality of sodium thiosulphate (which is 0.02). Woil= weight of oil used

2.2   MEASUREMENT OF CLOUD POINT AND POUR POINT

The cloud point was measured according to the ASTM D2500 standard using a refrigerator and digital infra-red thermometer with measuring range from -50^{0}C to 380^{0}C shown in Figure 2. The oil was first heated to 50^{0}C to ensure solution of all ingredients and elimination of any influence of past thermal treatment. It was then cooled at a specific rate in the refrigerator and observed for the onset of wax precipitation in the form of a distinctive cloud or haze. The temperature at the onset of the cloudiness was measured using the digital infra-red thermometer and recorded as the cloud point.

The pour point was determined according to the ASTM D97 standard (ASTM., 2002a). The same procedure and equipment as that of the cloud point was employed. The decrease in the temperature of the oil at 3^{0}C was monitored while the test container was tilted to check for movement. The temperature 3°C above the point at which the oil stopped moving was recorded as the pour point.

Figure 2: Digital infra-red thermometer

2.3   MEASUREMENT OF FLASH POINT

The flash point was measured according to the ASTM D92 standard (ASTM 2002b). 30mls of the oil was poured into an open cup apparatus and heated at atmospheric pressure while the temperature was being monitored with the digital infra-red thermometer. The set up was carried out in a fume chamber where air was being supplied to the heated oil until it ignited. The temperature at which it ignited was noted and recorded as the flash point of the oil.

3   RESULTS AND DISCUSSION

The result gotten from the various tests carried out and detail discussion of the results are presented in subsections 3.1 -3.3.

3.1   OXIDATIVE STABILITY CHARACTERISATION OF CASTOR OIL AND MINERAL BASED LUBRICANT

The peroxide value is the usual method of assessment of primary oxidation products. Peroxide value of any oil gives an indication of its oxidative and thermal stability. The peroxide value of the jatropha and castor oil is shown in Table 1. The peroxide value of castor oil was 8.92 meq/kg, while that of the mineral based lubricant SAE 20/W50 was 0.99 meq/kg. The peroxide value of the castor oil was too high showing that the oil has poor oxidative and thermal stability. The SAE 20/W50 had desirable oxidative and thermal stability.

This result is consistent with the findings of all other researchers that had studied the thermo-oxidative stabilities of vegetable oils (Gunstone, 2004; Adhvaryu *et al;* 2005). The poor thermal and oxidation stability of the castor oil implies that lubricants formulated from castor oil will have a low shelf life as degradation of the oil will take place very fast. The poor thermo-oxidative stability of castor oil is a major hindrance for its application as industrial lubricant; thus, the oil must be modified for it to be useful in the production of industrial lubricants.

Table 1: PEROXIDE VALUE OF CASTOR OIL AND MINERAL BASED LUBRICANT SAE 20/50

Oil/Lubricant	Peroxide value (meq02/kg)	Oxidative stability
Castor oil	8.92	unstable

SAE 20/W50	0.99	Very stable

3.2 COLD FLOW PROPERTIES OF CASTOR OIL AND MINERAL BASED LUBRICANT

The cold flow properties (cloud point and pour point) of the castor oil and the mineral based oil SAE 20/W50 are shown in Figure 3. The pour point of the castor oil was -23.2^0 C which is very low and desirable. The pour point of SAE 20/W50 was -24.1^0 C. the castor oil had cloud point of -12.4^0 C while the SAE 20/W50 had a cloud point of -18.9^0 C. The pour point of the castor oil is very similar to that of the SAE 20/W50; thus, castor oil can be used as a lubricant in the same cold areas where SAE 20/W50 is being used.

Castor oil had good cold flow properties (cloud point and pour point) which have been what is lacking in most vegetable oils that hinder their applications in systems exposed to low temperatures. Thus, castor oil can be used for lubrication of machines exposed to low temperatures such as automotive engines, construction machines, military and for space applications.
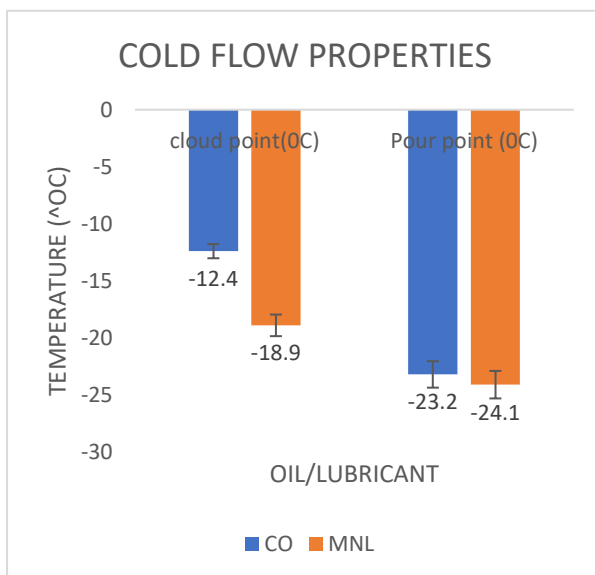

Figure 3: Cloud point and pour point of castor oil and mineral oil- based lubricant SAE 20/W50.

3.3 FLASH POINT AND FIRE SAFETY OF CASTOR OIL AND MINERAL BASED LUBRICANT

The flash point of the castor oil and the SAE 20/W50 is shown in Figure 4. The flash point of the castor oil was 282^0 C which is higher than that of the SAE 20/W50 (255^0 C). The flash point of the castor oil might be higher than that of the SAE 20/W50 because the castor oil has a higher molecular weight than the SAE 20/W50. Both oils have very high flash points which is desirable for a lubricant from the safety point of view. Castor oil is safer to be used at high temperatures as lubricant than most lubricanting oils with flash point of 210^0 C and fire point of about 230^0 C (Stachowiak, and Batchelor, 2000). The fire hazard while using castor oil as lubricants is lower than the fire hazard of using commercially available mineral based oil lubricant SAE 20/50.
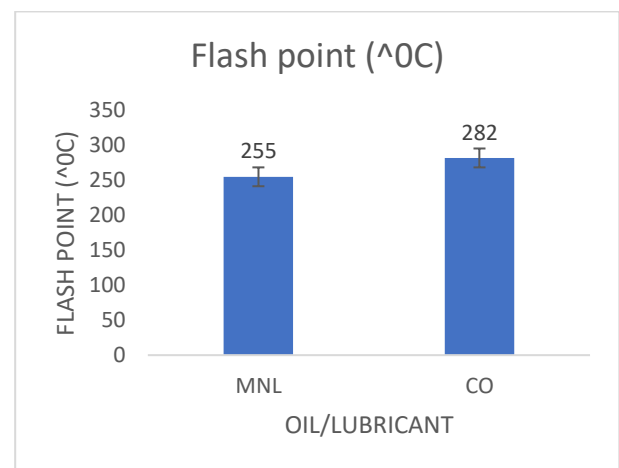

Figure 4: Flash point of castor oil and mineral based lubricant SAE 20/W50

4 CONCLUSION

The environmental issues associated with the use of mineral based lubricants as well as the fluctuation in price of crude coupled with the depletion of oil reserves has made it necessary to look for alternatives. The oxidative stability, flash point and cold flow properties of castor oil has been studied and compared to commercially available mineral oil-based lubricant SAE 20/W50. The castor

oil had poor oxidative stability compared to the SAE 20/W50 which implies that its shelf and service life as a lubricant is low

The castor oil had a higher flash point than the SAE 20/W50, thus, in applications where fire safety is of out most consideration the castor oil will be preferred lubricant. Both the castor oil and SAE 20/W50 had good fire safety compared to most lubricant oil base stock. The castor oil had a pour point similar to that of the SAE 20/W50 lubricant and competed favourable with the mineral oil-based lubricant in cloud point. Thus, the castor oil has excellent cold flow property and can be used for lubrication of machines exposed to low temperatures such as automotive engines, construction machines, military and for space applications. Castor oil can be a good renewable, environmentally friendly and sustainable substitute for mineral oil-based lubricants.

ACKNOWLEDGEMENTS

REFERENCES

Adhvaryu, A., & Erhan, S. Z., (2002), Epoxidized Soybean Oil as a Potential Source of High-Temperature Lubricants, *Ind. Crops Prod.,* 15: 247–254.

Adhvaryu, A., Liu, Z., & Erhan, S. Z., (2005), Synthesis of Novel Alkoxylated Triacylglycerols and Their Lubricant Base Oil Properties, *Ind. Crops Prod.,* 21, 113–119.

Ajithkumar, G., (2009). Analysis, Modification and Evaluation of the Cold Flow Poperties of Vegetable Oils as Base Oils for Industrial Lubricants, PhD thesis submitted to the Faculty of Engineering, Cochin University of Science & TechnologyKochi-22, India: 38 - 79

American Society for Testing and Materials (2004).

ASTM D943-04a, Standard Test Method for Oxidation Characteristics of Inhibited Mineral Oils, ASTM International, West Conshohocken, PA, USA.

American Society for Testing and Materials, (2002a).

ASTM D97–02, Standard Test Method for Pour Point of Petroleum Products, ASTM International, West Conshohocken, PA, USA.

American Society for Testing and Materials (2002b).

ASTM D92-02b, Standard Test Method for Flash and Fire Point by Cleveland Open Cup Tester, ASTM International, West Conshohocken, PA, USA.

Awoyale, A.A; Odubiyi,O. A. & Eloka-Eboka, A. C. (2011). Production and Testing of Biodegradable Grease from Black-Date (Canarium schweinfurthii) *Oil, Journal of Innovative Research in Engineering and Sciences* 2(4), 223-233

Bartz, W. J., (2006). Ecotribology: Environmentally Acceptable Tribological Practices, *Tribol. Int*., 39 (8), 728-733.

Binfa, B; Atabor, P.A; Barnabas, A;and Adeoti,M.O; (2015). Comparison of lubricant properties of Castor oil and commercial engine oil. *Jurnal Tribologi* 5, 1-10.

Brigham, R.D. 1993. Castor: Return of an old crop. New Crops, Wiley, New York, 380- 383.

Codex Alimentairus Commission (1993). *Graisses et huiles vegetales*, Division 11, version abregee FAO/WHO, Codex Stan.

Demian, M. J., (1990). Principles of Food Chemistry, 2nd edition, London: Van Nostrond Reinhold International Company Limited

Erhan, S. Z., & Asadauskas, S., (2000), Lubricant Base Stocks from Vegetable Oils, *Ind. Crops Prod*., 11: 277-282.

Erhan, S.Z; Sharma, B.K. & Perez, J. M. (2006). Oxidation and low temperature stability of vegetableoil-based lubricants, *Industrial Crops and Products*, 24: 292-299.

Gana, A., Amosun, A., Alhaji, B.B. 2014. Determination of Number of Manual Hoe Weeding for Optimal Yield of Castor (Ricinus communis

L., Euphorbiaceae) in Nigeria. Global Journal of Botanical Science, 2, 21-25.

Gunstone, F.D. 2004. *Rapeseed and Canola Oil: Production,Processing, properties and uses*. London: Blackwell Publishing Ltd

Kassfeldt, E., & Goran, D., (1997). Environmentally Adapted Hydraulic Oils, *Wear*, 207:41–45.

Mercurio, P., Burns, K. A., & Negri, A., (2004), "Testing the Ecotoxicology of Vegetable Versus Mineral Based Lubricating Oils: 1. Degradation Rates Using Tropical Marine Microbes", *Environ. Pollut.,*129 (2): 165-73.

Onuoha, O.J., (2015). Suitability of Vegetable Based

Oils in Orthorgonal Machining of AISI 1330 Carbon Steel Using Taguchi Method, PhD thesis submitted to the Department of Mechanical Engineering, Federal University of Technology Minna, Niger State, Nigeria: 85 - 89

Rhee, I.S., Valez, C., & Bernewitz, K., (1995). Evaluation of Environmentally Adapted Hydraulic Fluids, *TARDEC Tech Report* 13640, US Army Tank Automotive Command Research, Development and Engineering Center, Warren, MI, 1–15.

Stachowiak, G.W. & Batchelor, A. W., (2000). Engineering Tribology, Second Edition. Butterworth-Henemann, Boston: 3-616.

Woma, T.Y; Lawal, S.A; Abdurahman, A.S; Olutoye, M. A; & Ojapah, M .M;(2019) ."Vegetable Oil Based Lubricants: Challenges and Prospects," Tribology Online, vol. 14(2). Pp.60-70

Effect of Turning Process Parameters on Surface Roughness of AISI 1045 Medium Carbon Steel Using Aluminum Coated Carbide Tool

Salawu Morufu Ajibola and Sunday Albert Lawal
Corresponding Author's email: masalawu@gmail.com
Department of Mechanical Engineering, School of Infrastructure, Process Engineering and Technology,
Federal University of Technology, P.M.B 65, Minna, Nigeria

ABSTRACT

This work investigated effects of turning process parameters on surface roughness of AISI 1045 medium carbon steel using aluminum coated carbide tool. The experiments were conducted on CNC lathe using Duratomic, alpha-base aluminum oxide (Al_2O_3) coated carbide tool. The material was turned at five different cutting speeds and three different feed rates at a constant depth of cut, under wet condition. One variable at a time method of analyses was used to illustrate the influence of cutting parameters on surface roughness. Cutting speed variation between 355 m/min and 435 m/min at the feed rate of 0.15 mm/rev gave the optimum surface roughness.

KEYWORDS: Surface roughness, depth of cut, carbide tool and feed rate.

1 INTRODUCTION

Efficient manufacturing process is required for producing parts of acceptable quality [1]. Machining, one of the most widely used manufacturing processes is done by removing unwanted material from a workpiece in the form of chips such that the desired shape and size in conformity with the specifications laid in the relevant engineering drawings is achieved. Machining surpassed every other manufacturing processes in that hardly is there any product that does not directly or indirectly involve metal cutting. It provides dimensional accuracy and surface quality to a pre-formed blank for it to fulfill its functional requirements. However, investigation into the metal cutting process appears to be very difficult due to the complexity arising from the many variables involved [2]. Nevertheless, the need to fulfill increasing demand of machine parts that fit into sensitive and sophisticated areas, requires the principle to be well understood for it to have economical application.

Surface roughness plays vital roles in metal cutting and is one of the factors of great importance in the evaluation of machining accuracy [3]. It has a significant impact on characteristics such as fatigue

strength, corrosion resistance and aesthetics of the finished product [4]. Not only that, it is a factor that greatly influences manufacturing cost. Be that as it may, so much attention is being devoted to machine parts surface finish and dimensional accuracy. Therefore, proper selection of process parameters (the cutting speed, the feed and depth of cut) is very much crucial [5] otherwise; it could result in surfaces with high roughness and dimensional inaccuracy. The current trend to optimize production rate at shorter time and at minimum machining cost, without affecting product quality has not been achieved, because of the inability to find appropriate parameters that influence the machining characteristics of workpiece material.

. Machining operations often performed in conjunction with turning are drilling, reaming, tapping, threading and knurling. In turning, the workpiece is rotated about its axis while cutting tool is fed into it [6-9]. The unwanted material is sheared away and the desired part is created. What is involved here are the workpiece, the tool including the holding devises, the chips and the cutting fluid. The tool is thus constrained to move relative to the workpiece in such a way that it removes the metal in the form of chips. Thus, the results of the research

The Nigerian Society of Engineers
Minna Branch
1st NSE Minna Branch National Conference 2021

Conference theme
Role of Engineering in
Sustainable Development Goals

investigation will be helpful in cutting tools selection combines with appropriate process parameters for machining process such that optimum production at low cost is achieved.

2   METHODOLOGY

The material used in this investigation is AISI 1045, medium carbon steel rod of diameter 70 mm × 3500 mm length. AISI 1045 medium carbon steel is widely used for industrial applications requiring more wear-resistance and strength such as gears, axles, bolt, nuts, stud, connecting rods, crankshafts and pins. Duratomic, Alpha-base aluminium oxide (Al_2O_3) coated carbide insert was the cutting tool used for this study. The cutting tool was employed for its toughness and wear resistance which result in stable machining. One Variable at a Time (OVAT) method was adopted for the experimental design of the machining operation. OVAT, ease in the analysis of data, revealing by how much a single change affect the results of the experiment.

2.1 Methods of Experimentation

Spectrometric analysis test was conducted on the workpiece material to determine the elemental composition of the workpiece materials. The turning process was conducted under wet condition on Computer Numerically Controlled (CNC) lathe, that is regularised by a menu-type interface on a computer. The machine code fed into the machine contained information on cutting speed, feed rate, depth of cut, workpiece material and the cutting tool. The workpiece was cut to 70 mm diameter by 232 mm length, 15 in number, using CNC band saw. One piece at a time, the workpiece was face turned at both ends to diameter 70 mm by 230 mm length and predrilled at one end on the CNC lathe before the actual machining test. Workpiece materials were turned at five different cutting speed and three different feed rate at a constant depth of cut, 2.0 mm. Cutting speed was varied from 355 m/min – 435 m/min, Feed rate from 0.15 – 0.45 mm/rev in steps of 0.15 mm/rev, while depth of cut (DoC) was fixed at a value of 2.0 mm as presented in Table 1.

Table 1: Experimental design for the turning operation

Experimental Run No.	Cutting Speed (m/min)	Feed Rate (mm/rev)
1	355	0.15
2	375	0.15
3	395	0.15
4	415	0.15
5	435	0.15
6	355	0.3
7	375	0.3
8	395	0.3
9	415	0.3
10	435	0.3
11	355	0.45
12	375	0.45
13	395	0.45
14	415	0.45
15	435	0.45

On the workpiece material, a length of 100mm length. was turned, one piece at a time. Machining time, as captured by the machine and gotten via the visual display unit of the computer interface was married with the stop watch reading, recorded and the average value was calculated. The procedure was repeated on all the 15 workpiece materials.

2.2 Determination of Surface Roughness

For every machined surface it was measured surface roughness using Mitutoyo, Portable Surface roughness tester shown in Plate I. Along the machined surface, three readings were taken. Average of the three R_a values measured, was calculated and recorded for each experimental run.

The Nigerian Society of Engineers
Minna Branch
1st NSE Minna Branch National Conference 2021

Conference theme
Role of Engineering in
Sustainable Development Goals
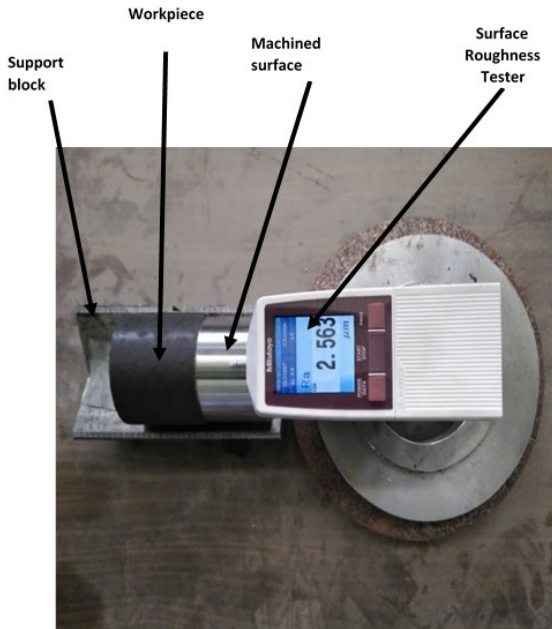
Plate I: Set up arrangement for surface roughness measurement

3 RESULTS AND DISCUSSION

3.1 Spectrometry Analysis

Experimental result of the spectrometric analysis test conducted on the workpiece material showed that it contained 0.409% carbon content as shown in Table 2. The obtained value of 0.409% of carbon in this study quantitatively agreed with the literature thus affirming the classification of the workpiece as belonging to the group of AISI 1045 steel.

Table 2: Chemical composition of element in the workpiece sample

Element	Symbol	Percentage composition
Carbon	C	0.409
Iron	Fe	98.08
Silicon	Si	0.350
Manganese	Mn	0.636
Phosphorous	P	< 0.005
Sulphur	S	< 0.003
Chromium	Cr	0.186
Molybdenum	Mo	< 0.005
Nickel	Ni	0.025

Source: (Nigeria Machine Tools, Oshogbo 2020)

3.2 Effect of cutting Speed on Surface Roughness

Figure .1 showed the influence of cutting speed on surface roughness. It could be observed that the best parameter combination to achieve smooth surface finish, were the cutting speed variation between 355 m/min and 435 m/min at the feed rate of 0.15 mm/rev and a depth of cut of 2.0 mm while, the optimal combination of process parameters for minimum surface roughness were the cutting speed of 355 m/min, Feed rate of 0.15 mm/rev, at a constant depth of cut of 2.0 mm.
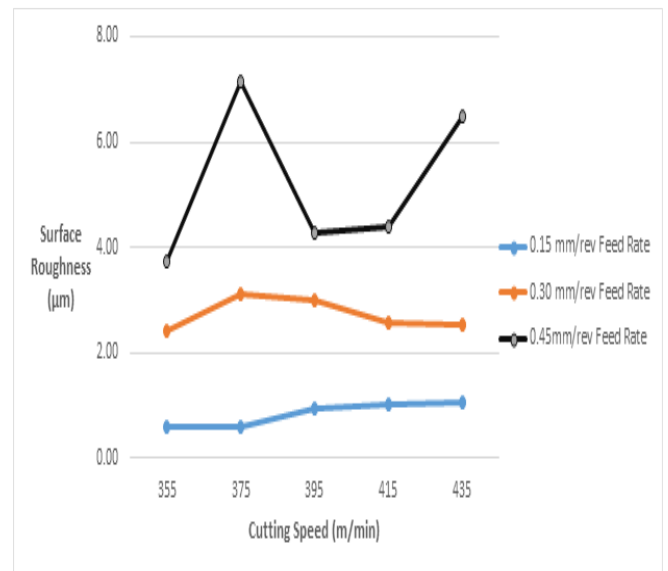

Figure 1: Effect of cutting speed on Surface roughness at various feed rate

Profuse application of cutting fluid, low feed rate, sharp cutting edge of the tool, and low friction at the tool-chip-workpiece interface contributed to fine workpiece surface finish.

3.2 Effect of Feed Rate on Surface Roughness

Figure 2 showed the effect of feed rate on surface roughness while depth of cut was constant at a value of 2.0mm.
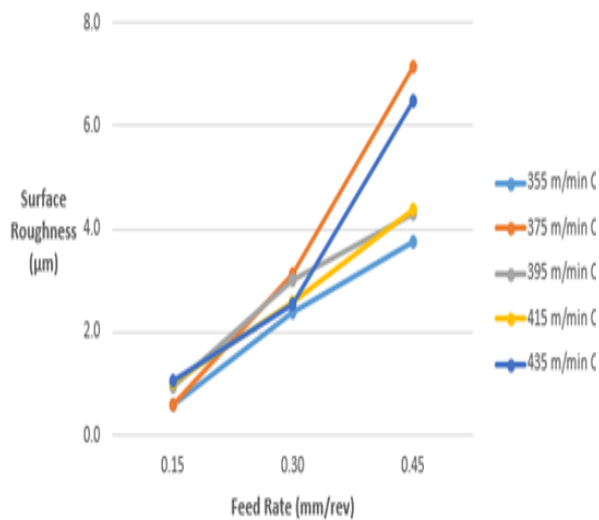

Figure 2 Effect of feed rate on surface roughness at various cutting speed

Considerable rise in surface roughness with increase in feed rate was observed. This showed that feed rate has more influence on surface roughness than cutting speed. Thus increase in feed rate resulted into increase in temperature, that translated to a high heat generation at the tool-workpiece interface and thus led to rough machined surface.

4 CONCLUSIONS

The carbon content of the workpiece materials obtained from spectrometric analysis showed 0.409% which is within the acceptable carbon content of medium carbon steel. The parameter combination to achieve smooth surface finish, were the cutting speed variation between 355 m/min and 435 m/min at the feed rate of 0.15 mm/rev, while the optimal combination of process parameters for minimum surface roughness were the cutting speed of 355 m/min, Feed rate of 0.15 mm/rev

REFERENCES

Abu, J. O. (2011). Manufacturing Engineering and Production Management. (1st edition) Makurdi, Benue State: Aboki Publishers

Olugboji, O. A, Matthew, S. A., Jiya, J. Y., Popoola, S. O., and Ajani, C. K. (2015). Effect of Cutting Speed and Feed Rate on Tool Wear Rate and Surface Roughness in Lathe Turning. *International Journal of Engineering Trends and Technology (IJETT)*. 22(3), 1 – 9.

Nurhaniza, M., Ariffin, M. K. A. F., Mustapha, F., and Baharudin, B.T.H.T. (2016*). Analyzing the* Effect of Machining Parameters Setting to the Surface Roughness during End Milling of CFRP-Aluminium Composite Laminates International Journal of Manufacturing Engineering, (2016), 1 – 9. doi:10.1155/2016/4680380.

Mgbemena, C., Etebenumeh, G., and Ashiedu, F. (2016). Effect of Turning Parameters on Metal Removal and Tool Wear Rates of AISI 1018 Low Carbon Steel. *Nigerian Journal of Technology (NIJOTECH),* 35(4), 1 – 7.

Cini, B., Kumar, N. S., Vijavan, K., Rao, G. N., and Joji, J. C. (2017). Effect of Machining Parameters on Surface Roughness and Material Removal Rate during Rotary Ultrasonic Machining of Silicon Carbide. *International Research Journal of Engineering and Technology (IRJET)*, 4(6), 1 – 9

Ogundimu, O., Lawal, S. A., and I. P. Okokpujie (2018). Experimental study and Analysis of Variance of Material Removal Rate in High Speed Turning of AISI 304L Alloy Steel. *IOP Conference Series: Materials Science and Engineering*, 413, 012030. doi:10.1088/1757-899X/413/1/012030

Didit, S., Sri, E. S., and Anton, C. (2018). Effect of Cutting Parameter on Surface Roughness of Carbon Steel S45C. *Journal of Mechanical Engineering and Automation*, 8(1), 1- 6, DOI: 10.5923/j.jmea.20180801.01.

Gowd, G. H., Vali, S. S., Ajay, V., and Mahesh, G. G. (2014). Experimental Investigations and Effects of Cutting Variables on MRR and Tool Wear for AISI S2 Tool Steel. *International Conference on Advances in Manufacturing and*

Material Engineering, 5(2014), 1398 – 1407, doi: 10.1016/j.mspro.2014.07.458

Vaykhinde, A. S., Bhor, U. B., Sachhe, V. V., Valte, S. P., and Deokar, S. B. (2017). Review of Effect of Tool Nose Radius on Cutting Force and Surface Roughness. *International Research Journal of Engineering and Technology (IRJET)*, 457- 464

Conference theme

Role of Engineering in Sustainable Development Goals

Thermal and Physicochemical Characterization of Locally Sourced Lignite Coal

C. O. Emenike, P. E. Dim and J. O. Okafor
Department of Chemical Engineering
School of Infrastructure Process Engineering and Technology
Federal University of Technology Minna Nigeria

ABSTRACT

Coal as a solid mineralized substance consumed to provide was composed in ecosystems where remains of animal or plant were conserved by wood and fine-grained sediment from oxidation and decomposition by biological activities. The aim of this study is to examine the properties of locally sourced lignite coal. The characterization method used were thermogravimetric analyses and physicochemical analyses. The results of the physicochemical analyses obtained shows high carbon (C) and hydrogen (H) content of 90 % and 8.38 %; high fixed carbon of 81.3 % with low sulphur, oxygen and nitrogen content of 0.79 %, 0.67 % and 0.16 %; low moisture content, low ash content and low volatile matter of 1.45 %, 1.78 % and 15.84 % respectively. The low moisture content, ash content and volatile matter shows that the lignite coal is of good quality with 16.113 MJ/kg as the high heating value, (HHV). However, this coal has nitrogen and sulphur content less than 1 % which is an indication of the environmental friendliness of coal relative to potential NOx and SOx pollutant emissions. This coal can be used in power generation, iron and steel making, pharmaceutical industries.

KEYWORDS: *Lignite, Thermal, Ultimate, Proximate*

1 INTRODUCTION

Coal is a combustible form of rock made by the deposition and compression of small particles which contains both compounds of carbon minerals and compounds of non-carbon materials, it is the world's most sufficient and commonly dispensed mineralized energy given substance (Idris and Ahmed, 2019). Coal and coal-derived energy given substance have been used in residential, commercial, and industrial applications such as generation of electricity, iron and steel making, chemical and pharmaceutical productions, cement production and paper manufacturing (Bodude et al., 2018). Coal as a solid mineralized substance consumed to provide energy was composed in ecosystems where remains of animal or plant were conserved by wood and fine-grained sediment from oxidation and decomposition by biological activities a layer of dead plants and animals at the bottom of the wetland was covered by layers of water and dirt, snare the energy of the dead plants and animals for millions of years (Bizualem and Busha, 2017). The pressure and heat from the top layers enhanced the dead plants and animals turn into coal, it takes millions of years to form thereby became nonrenewable energy source. However, the energy in coal is obtained from the energy stored by dead plants and animals over hundreds of millions of years ago, when the earth was not completely covered with wetland forests. Coal is an easily combustible black or brownish-black form of rock made by the deposition and compression of small particles composed mainly of carbon and hydrocarbons, with little amount of other elements, like oxygen, nitrogen and sulfur (Wolde-Rufael, 2010). Coal seem to possess the most entreat of all the possible options for short-term development suitable for the national necessity of energy (Vasireddy et al., 2011). Coal and its products, play an important role in satisfying the energy necessity of the wester society. The quantity of coal deposits estimated all over the word was approximately ten times greater than that of other carbon yielding resources. The availability of coal resources was a main support to the economic expansion of many nations like the US, China, India, and Australia (Mehran et al., 2015). Coals can be classified into two: hard coals (the bituminous and anthracite) which is associated with high carbon and energy content and soft coals (the lignite and subbituminous) which is also associated with high moisture content, both hard coals and soft coals can be used in transportation, generation of electricity and cement manufacturing because quality of coals is not pre-requisite (Chukwu, 2015). Matsumoto et

al., (2016), reported that researching on physicochemical characterization of coal sample would provide an enhanced information on the use and application of coal samples. The aim of this study is the thermal and physicochemical characterization of locally sourced lignite coal.

2 METHODOLOGY

The lignite coal was collected from Ogwashi Azagba in Delta state, Nigeria.

2.1 CHARACTERIZATION

Physicochemical Analyses involved ultimate and proximate analyses. The ultimate analysis was done using the method adopted from (Bodude *et al.,* 2018). Proximate analysis consists of the following parameters: moisture content, ash content, volatile matter and fixed carbon content.

Moisture Content (MC):

0.3 g of sample was placed on a dish. Weight of dish with sample was recorded before placing the sample in the tray dryer. Temperature of the dryer was adjusted to 60^OC, and sample was then dried to constant weight and final weight was recorded. Moisture content was calculated using:

$$MC\ (\%) = \left(\frac{Wet\ Weight - Dry\ Weight}{Wet\ Weight}\right) \times 100\ \%$$
(1)

Ash Content (AC):

0.2 g of coal sample was placed into tarred crucible. The sample was preheated to 600 OC for 3 h. The crucibles were allowed to cool in the furnace to less than 100 ºC and then placed into desiccators with a vented top.

$$AC\ (\%) = \left(\frac{Weight\ of\ Residue}{Weight\ of\ Sample}\right) \times 100\ \%$$
(2)

Volatile Matter (VM):

Volatile matter (VM) was determined by heating the dry sample in a covered crucible in a furnace at 930 °C for 7 min. The sample was then weighed after cooling in a desiccator. The VM was then calculated using the equation below:

$$VM\ (\%) = \left(\frac{B-C}{B}\right) \times 100\ \%$$
(3)

Where B is the weight of the oven dried sample and C is the weight of the sample after heating in the furnace at 930 °C.

Percentage Fixed Carbon:

The percentage fixed carbon (FC) was computed by subtracting the sum of VM and AC from 100 as shown in
the equation below:

FC = 100 % − (MC + AC + VM)
(4)

Determination of Calorific Value

1.0g of coal sample in a nickel-chromium crucible was placed in an atmospheric environment of high-pressure known as Combustion Vessel, surrounded by water. The sample was then ignited. The calorimeter jacket was held at a constant temperature by regulating the fan speed while the heat produced by the burning sample caused the bomb and bucket temperature to increase. The temperature of the water was determined by an electronic thermometer with a resolution of 1/10000 of a degree. Any minute heat flow between the jacket and the surrounding during the test was continuously monitored by a microprocessor and necessary corrections of any heat leak applied automatically. Heat evolved is proportional to the gross calorific value (air-dried basis) of the sample and displayed automatically by the instrument. Duration of each run was 10 min.

Thermogravimetric Analysis

The lignite coal was heated from 25 ºC to 1000 ºC in air with an an air flow rate of 50 ml/min at a heating rate of 10 ºC/min. The weight change of the sample was recorded automatically until there was no further weight change. The residue in the crucible represents the ash content of the sample. Typical run time of the test was about 3.5 h.

3 RESULTS AND DISCUSSION

3.1 PHYSICOCHEMICAL ANALYSES AND THERMOGRAVIMETRIC ANALYESS

Ultimate Analyses: The data generated from ultimate analysis, were elemental parameters (such as carbon, hydrogen, sulphur, oxygen and nitrogen), which are used to determine the quality of coal. From Table 1, the coal sample possess high carbon content followed by hydrogen content of about 90 % and 8.38 % with low values of sulphur, oxygen and nitrogen content of about 0.79 %, 0.67 % and 0.16 % from the elemental analysis obtained. Among these elements, the carbon and hydrogen content of

coals determines the maturity (rank), calorific value and chemical reactivity during thermal conversion of coals. From this analysis, the sulphur and nitrogen contents of the lignite coal examined were very low, are such, little or no NO_x and SO_y gases will be released during combustion to the environment (Bodude et al., 2018). However, this lignite coal will be friendly to the environment and the equipment because of the little percentage composition of sulphur and nitrogen contents obtained from the analysis.

Table 1: Ultimate Analyses of Lignite Coal

Parameters	Values (%)
Carbon	90.00
Hydrogen	8.38
Sulphur	0.79
Oxygen	0.67
Nitrogen	0.16

Carbon and hydrogen are the main combustion constituents of coal and these two constituents are high in this lignite coal as compared with other elements such sulphur, oxygen and nitrogen. The type and ranking of coal are determined by the amount of carbon, from lignite to anthracite. Meanwhile, the carbon content in coal is used for classifications of coal, the higher the carbon content, the higher is the calorific value and the better is the quality of the coal. Hydrogen is commonly attached with volatile matter to determine the use to which the coal will be engaged. (Solomon and Aliyu, 2013), also concluded, that a good coal sample should possess high carbon content as compared with quantity of hydrogen, nitrogen and oxygen, as in the case of the result obtained for this lignite coal in Table 1.

The moisture content is a useful property of coal as all coals are mined wet. The groundwater and other non-essential moisture which are known as external sourced moisture is easily evolved while the moisture held within the coal itself is inherent moisture that is analyzed quantitatively. Most coals, as they are dug from the ground, have some quantity of moisture associated with them. The degree of maturity of coal, depends on the quantity of moisture content (Idris and Ahmed., 2019). The quality of coal is also determined by moisture content because it affects the calorific value, the higher the moisture content, the lesser the calorific value which causes reduction of the coal capacity and the lower the moisture content, the higher calorific value. 1.5 % moisture content is required in a good coking coal (Solomon and Aliyu., 2013). The value recorded for moisture content of this lignite coal in Table 2 was very closed to the stipulated value (1.5 %) for a good coking coal, this is an indication that the coal is a good coking coal which can be used for different applications where coking coal are needed. The ash content of coal is the remains residue that will not readily ignite left after the burning of coal, this represent the size of mineral matter when the Volatile Matter, moisture content, carbon, oxygen and sulphur are burnt off during combustion, it also indicates the rank of coal. The ash content of this coal used in this research work is about 1.78 % from the proximate analysis carried out (Table 2).

Table 2: Proximate Analyses on Coal Sample

Parameters	Values (%)
Moisture Content	1.45
Ash Content	1.78
Volatile Matter	15.84
Fixed Carbon	81.30
HHV	16.113 MJ/kg

The high yield of ash content is usually a signed by the mutually sufficient supply of disintegrated materials in wetland, while the fusing materials govern mainly with low yield ash content of coals, whereas the part of disintegrated materials increases and the organically bound elements concentration decreases with increased ash yield. However, these observations seem valid majorly for coals ranking, lignite majorly consist of fusing mineralization, moisture, pyrite and calcite and organically bound C and S are common (Rasheed et al., 2015). This observation is also in agreement with the statement that some low yield ash content (<10%) coals contain mainly fusing and biogenic inorganic matter, whereas those with higher ash yield (>10%) show simultaneous enrichment in disintegrated and fusing inorganic matters (Sahni et al., 2013). The volatile matter is also a coal component which are evolved at high temperature when air is absence, at the temperature where volatile matter is evolved, the moisture content is as well totally liberated. Except

for the fixed carbon and ash content which exceed that temperature, thereby required more high temperature. Volatile matter is mostly a combination of short and long chain hydrocarbons, aromatic hydrocarbons and some Sulphur. Volatile matter ranging from 2 % to about 50 % (Rasheed et al., 2015). in this research work, the volatile matter of the coal sample used is found to be about 15.84 % from the proximate analysis carried out (Table 2). The coal that contain high volatile matter are readily ignite, it burns fast and freqently burn with a long smoky fire because of high percentage of a combination of short and long chain hydrocarbons, aromatic hydrocarbons and some Sulphur present, the high volatile matter of coal is an indication of low ranked coal while low volatile matter content in a coal is more typical of higher-rank coal (Speight, 2013). In coal, the carbon found remaining after which volatile materials are driven off is known as fixed carbon content of coal. Fixed carbon is determined by subtracting the mass of volatiles material from the original mass of the coal sample, it helps in estimating the quantity of coke that will be produced from a coal sample. The fixed carbon contents are different from carbon content determined from ultimate analysis, because some carbon is evolved in hydrocarbons with the volatiles. The fixed carbon content of coals, excluding the ash and moisture, ranges from 50 % to about 98 % (Rasheed et al., 2015). However, the value of carbon content of coal determines the fixed carbon value of coal, in this research work, the fixed carbon of this lignite coal used is found to be about 81.30 % from the proximate analysis carried out (Table 2). Heating Value indicates the extent of heat content of coal this lignite coal is good for heating and power generation.

Table 3 shows the comparisons between this work and other reported work in literature. The present work has high carbon and hydrogen content as compared with the previous work, the more the carbon content, the better the quality of coal. Meanwhile, the previous work has high oxygen and nitrogen content as compared with the present work.

Table 3: Comparative Ultimate Analyses between this and previous work

Parameters	A Values (%)	B Values (%)	C Values (%)	D Values (%)
Carbon	90.00	70.42	68.24	60.21
Hydrogen	8.38	5.42	6.48	5.89
Sulphur	0.79	0.88	0.97	0.58
Oxygen	0.67	10.48	10.43	9.46
Nitrogen	0.16	1.09	1.67	1.07

A (present study); B, C and D-(Idris and Ahmed., 2019)

Table 4: Comparative Proximate Analysis between this and previous works

Parameters	A Values (%)	B Values (%)
Moisture Content	1.45	12.78
Ash Content	1.78	19.83
Volatile Matter	15.84	41.24
Fixed Carbon	81.30	26.15
HHV	16.113 MJ/kg	16.02 MJ/kg

A (present study) and B-(Mehran *et al.,* 2015).
Table 4 shows the comparisons between this work and other reported work in literature. However, the HHV were similar, the previous work has high volatile matter, ash content and moisture content as compared with the present work.

Thermogravimetric Analyses
The decomposition curves of TG and DTA of the locally sourced lignite coal from Ogwashi Azagba in nitrogen atmosphere determined at the heating rates of 10.00 oC /min are shown in Figures 1 and 2, respectively. The TG curve indicates the percentage weight loss of a coal sample at the temperature range from 27.00 oC to 950 oC. The rate at which weight is loss depends on temperature: the more the temperature, the more the weight is loss because, pyrolysis process proceeds slowly at lower temperatures. There were three stages involved in TG curve shown in Figure 1, the first stage

characterized by weight loss at the temperature range (27–266) oC was ascribed to the loss of moisture or water vapor. The second stage characterized by weight loss at the temperature range (266-580) oC was typically ascribed to the loss of volatile matter or devolatilization process. The last stage characterized the degradation from temperature range (580-820) oC was attributed to the slow process of coke formation.
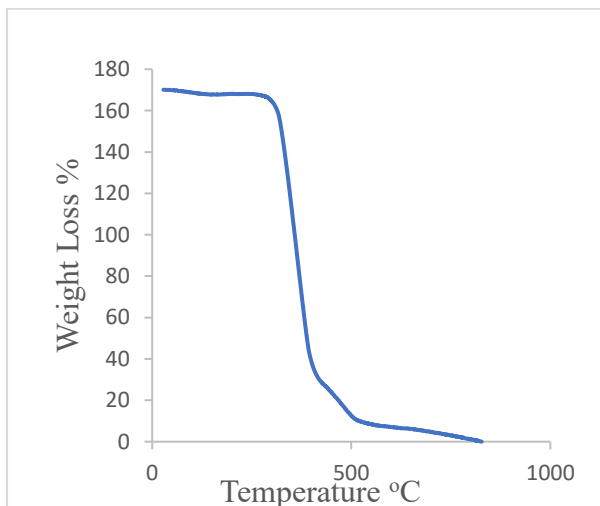

Figure 1: TGA properties of Lignite Coal

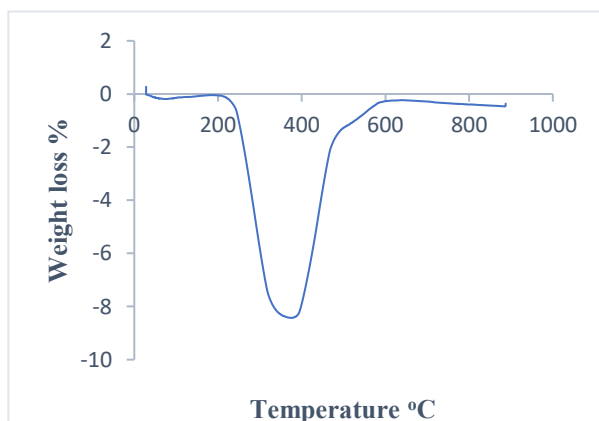The DTA curve of sample at the heating rates of 10.00 oC /min is shown in Figure 2.

Figure 2: DTA properties of Lignite Coal

This DTA curve display two peaks which described evaporation of moisture and primary breakdown, and secondary breakdown. The small peak represents the evaporation of moisture content which take place at temperature between 30-183.92 oC. The second peak occurred at the temperature between 183.92 - 576.02 oC indicating devolatilization process in this coal sample which involved the liberation of volatile matter content and thermal breakdown of some covalent bond like ether bonds and methylene group which will produce gases like hydrogen, carbon monoxide, and lighter hydrocarbons. This region is the most important region to investigate since the main weight loss and complicated chemical reaction, like release of tar and gaseous products and semi coke formation, take place in this temperature range (Aboyade et al., 2013). The peak temperature (TP) from Figure 2 is 379.88 oC which is the main important point on the DTA curve. In addition, the peak temperature represents where the rate of weight loss is at a maximum. This parameter is used in the assessment of combustibility (Mehran et al., 2015).

4   CONCLUSION

The physicochemical analyses carried out shows high carbon content of the locally sourced lignite coal. The carbon content and HHV indicate its use in generation of electricity, iron and steel making, cement production and raw material for chemicals. This analysis also shows that the coal sample possess relatively low sulphur, oxygen and nitrogen contents which is an indication of environmental friendliness of coal relative to potential NOx and SOx pollutant emissions. However, the locally sourced lignite coal sample is easy to process, it burns slowly and does not burn with long smoky fire because of its low percentage of a combination of short and long chain hydrocarbons, aromatic hydrocarbons and some sulphur present.

REFERENCES
Aboyade, A. O., Gorgens, J. F., Carrier, M., Meye, E. L. and Knoetze, J. H. (2013). "Thermogravmetric study of the pyrolysis characteristics andkinetics of coal blends with corn and sugarcane rsidues," *Fuel Processing Technology*, 106: 310–20.

Applications of Some Nigerian Coals ABUAD Journal of Engineering Research and Development. 2(1): 20 -25.

Bizualem, W. and Busha A (2017). Physicochemical Characterization of Coal and its alternaas a

Source of Energy (in case of Yayo Coal Mining Journal of Environmental Science, Toxicology and Food Technolog. 11(5): 44-50.

Bodude, M. A., Ayoola, W. A., Oyetunji, A., Baba, Y.D., Odukoya, A. L., Onifade, O. A. and Olugbile, O. O. (2018). Proximate, Ultimate Analysis and Industrial Application of Some Nigerian Coals. Journal of Engineering Research and Development. 2(1): 20-25.

Chukwu, M. (2015). Characterization of Some Nigerian Coals for Power Generation. M.Eng. Thesis published. Ahmadu Bello University Zaria, Nigeria

Idris, M. N. and Ahmed, Z. D. (2019). Qualitative Characterisation of Coal Minerals Selected From 5 Different Locations in Nigeria For Possible Studies on Gasification Technology. International Journal of Engineering and Modern Technology. 5(2): 55-69.

Matsumoto, S., Ogata, S., Shimada, H., Sasaoka, T., Kusuma, G. J. and Gautama, R. S. (2016). Application of Coal Ash to Postmine Land for Prevention of Soil Erosion in Coal Mine in Indonesia: Utilization of Fly Ash and Bottom Ash. Advances in Materials Science and Engineering, 1–8. doi:10.1155/2016/8386598.

Mehran, H., Moshfiqur, R. and Rajender, G. (2015). Kinetic Study and Thermal Decomposition Behavior of Lignite Coal. International Journal of Chemical Engineering
http://dx.doi.org/10.1155/2015/481739

Rasheed, M. A., Srinivasa Rao, P. L., Annapurna, B., Syed, Z. H., Arpit, P. V. and Velani, K. P. (2015). Geochemical Characterization of Coals Using Proximate and Ultimate Analysis of Tadkeshwar Coals, Gujarat. Geosciences, 5(4): 113-1 DOI:10.5923/j.geo.20150504.01

Sahni, A., Saraswati, P.K., Rana, R.S., Kumar, K., Singh, H., Alimohammadian, H., Sahni, N., Rose, Kd, Singh, L. And Smith, T. (2013). Palynostratigraphy and Depositional Environment of Vastan Lignite Mine Gujarat, Western India. Journal of Earth System Science. 122(1): 289-307.

Solomon, A. R. and Aliyu, J. (2013). Proximate analysis, rheological properties and technological applications of some Nigerian coals. Ryemshak and Jauro International Journal of Industrial Chemistry 4(7): 1-7.

Speight, J. G, (2013). *The chemistry and technology of coal*. 3rd ed. Boca Raton: CRC Press, 2013. ISBN 978-14398-3648-4.

Vasireddy, S., Morreale, B., Cugini, A., Song, C. and Spivey, J. J. (2011). "Clean Liquid Fuels from Direct Coal Liquefaction: Chemistry, Catalysis, Technological Status and Challenges," Journal of Energy and Environmental Science. 4(2): 311–345.

Worde-Rufael Y. (2010). Coal Consumption and Economic Growth Revisited. Journal of Applied Energy 87(1): 160-167.

Thermal and Physicochemical Characterization of Biochar Produced from Waste Bamboo

E. Daniel, P.E. Dim and J.O. Okafor

Department of Chemical Engineering, Federal University of Technology, Minna, Nigeria.

ABSTRACT

This study is aimed at the characterization of biochar produced from waste bamboo using physicochemical and thermal analysis method. The physicochemical result shows that bamboo contains 73.8 % cellulose, 12.49 % hemicellulose, 10.50 % lignin, 0.4 % pectin and 3.20 % aqueous extracts. Thermogravimetric analysis (TGA) was done on raw bamboo waste to determine the temperature of decomposition of bamboo and pyrolysis was done in an inert atmosphere (pure nitrogen) at temperatures of 400 ºC, 450 ºC and 500 ºC to produce the biochar. Proximate and ultimate analysis of the raw bamboo and biochar was carried out and the results showed that the physicochemical properties of the biochar slightly changes as the pyrolysis temperature was increased.

KEYWORDS: *Bamboo; Biochar; Carbon; Proximate analysis; Pyrolysis*

1   INTRODUCTION

Bamboo is one of the strongest and quickest growing trees in the world and have been gaining increasing interest due to its high strength to weight ratio, requires less water, little or no use of pesticides or herbicides and is harvested at its base, leaving the root complete. Also, the tree surface is round and smooth. It is light, harder and stronger than other woods (Pecas et al., 2018). Bamboo has been used in processing abundant and high-quality cellulose fibers for a long time, and has become a major feedstock for weaving, pulp, paper, and in the manufacture of fiber-based composite. The main chemical compositions of bamboo include cellulose, hemicellulose, lignin, all kinds of extracts, a little ash, and silicon dioxide. All of these constituents and properties contribute to bamboo's high strength, bending ductility, toughness and low density (Wang and Chen, 2017). Bamboo is mainly composed of cellulose, hemicellulose and lignocellulose that can be processed into higher value-added products by pyrolysis processes. Furthermore, it possesses many other advantages such as easy cultivation, fast development and low ash content (Mena et al., 2014). Biochar is a carbon-rich solid derived by pyrolysis of biomass with little or no oxygen, Biochar is usually produced from plant residues, wood biomass, animal litters, and solid wastes through various thermochemical processes, including slow pyrolysis, fast pyrolysis,

hydrothermal carbonization, flash carbonization, torrefaction and gasification (Tan., et al., 2016). Biochar gotten from biomass is typically 20-40 % of dry lignocellulose biomass. Nonetheless, the yield and chemical properties of the pyrolysis products are firmly impacted by operating conditions during pyrolysis such as temperature, heating rate, holding times, particle size, atmosphere and feedstock. Depending on the final use of biochar, the required properties of the material may be different (Mena et al., 2014). Pyrolysis which is a thermochemical decomposition process, takes place in the absence of oxygen to produce a liquid phase (tar or hydrocarbon liquids and water), a carbon rich solid phase (charcoal) and non-condensable gases (CH4, CO2, CO, H2,), (Mena et al., 2014). Thermo-chemical conversion of biomass is one of the many methods that can be used to convert biomass into valuable products. Pyrolysis, a thermo-chemical process is an effective method with less emission to produce alternative fuels from biomass (Oyedun et al., 2012). The objective of this study is to investigate the thermal and physicochemical analysis of biomass and its product of thermal treatment.

2   METHODOLOGY

2.1. BAMBOO COMPOSITION

The percentage composition of cellulose, hemicellulose, lignocellulose, pectin and aqueous extracts of bamboo waste was determined by acid

The Nigerian Society of Engineers
Minna Branch
1st NSE Minna Branch National Conference 2021

Conference theme
Role of Engineering in
Sustainable Development Goals

digestion using a fibre Analyzer. The standard acid digestion fibre (ADF), neutral detergent fibre (NDF) and acid detergent lignin (ADL) analysis were carried out using Ankom 200 Method 5, Method 6 and Method 8 respectively. 0.5 g of ground fibres was used for each analysis. The percentage of cellulose, hemicellulose and lignin content were then determined.

TABLE 1: COMPOSITION OF RAW BAMBOO

CONSTITUENT	COMPOSITION (%)
Cellulose	73.83
Lignin	10.50
Hemicellulose	12.49
Pectin	0.40
Aqueous extracts	3.20

2.2. THERMOGRAVIMETRIC ANALYSIS (TGA)

The TGA of raw bamboo was done using a PerkinElmer TGA 4000 thermogravimetric analyzer and at a heating rate of 10.00 $^{\circ}$C/min to determine the stability temperatures of bamboo during pyrolysis and to determine the temperatures of transitions and reactions of raw bamboo

2.3. PREPARATION OF BIOCHAR

Bamboo was collected from a building site in Minna, Niger state. The sample was cut into small pieces of 6-8 cm in length and washed thoroughly with running water followed with distilled water to remove impurities. The sample was dried in an electric oven at 100 oC for 24 h to reduce moisture content. The dried Bamboo was crushed using a club hammer, it was then reduced further into smaller sizes of length 8-10 mm using a grinding machine. 25 g of the crushed Bamboo was weighed into a crucible and charged into the pyrolysis reactor. The air-lock was closed to avoid the introduction of oxygen. The cylinder containing nitrogen gas was then connected to the pyrolysis reactor and the valve opened with gas flow rate set at 1cm/min. Pyrolysis was done at temperatures of 400 oC, 450 oC and 500 oC for 2 h. The char was then removed from the

reactor, air-cooled, weighed and kept for further analysis.

2.4. PROXIMATE AND ULTIMATE ANALYSIS

The proximate and ultimate analysis of Bamboo and Biochar was done to determine their physical and chemical properties. Proximate analysis carried out includes; moisture content (ASTM E1358-97), ash content (ASTM E1755-01), volatile matter (E872-82) and fixed carbon content (ASTM D1762-84) while the elemental analysis includes; percentage carbon, Nitrogen, Hydrogen and Oxygen (C, N, H and O).

3 RESULTS AND DISCUSSION

3.1 COMPOSITION OF BAMBOO

Analysis on the structural composition of Bamboo was carried out on waste stem samples and results showed that the bamboo stem has a very high cellulose content of 73.83 %. Percentage contents of Lignin, Hemicellulose, Pectin and aqueous extracts are 10.50 %, 12.49 %, 0.40 % and 3.20 % respectively as shown in table 1. These are in the range of hard wood biomass as reported by (Amaral and Leite., 2014). A high percentage of cellulose in biomass suggests more volatilization during pyrolysis as both the polysaccharide structures are broken down at a lower temperature range of 200-400 oc. This is in conformity with the findings of (Sahoo et al., 2021).

3.2 THERMOGRAVIMETRIC ANALYSIS (TGA)

Thermal analysis was carried out using 10 mg of raw bamboo samples at a constant heating rate of 10 oC/min from room temperature up to 850 oC. The TGA shows the thermal degradation steps, the first TG curve corresponds to drying and dehydration between the temperature range of 30 – 100 oC. The second curve between the temperature range of 250-400 oC corresponding to weight losses as a result of Hemicellulose and cellulose degradation (Mena et al., 2014). At temperatures higher than 400 oC, almost all cellulose was pyrolyzed. Lignin decomposes slowly all through the temperature range from room temperature to 850 oC which correlates with the findings of (Mahanim et al., 2011). In general, pyrolysis of wood biomass takes place in a step-wise manner with Hemicellulose

The Nigerian Society of Engineers
Minna Branch
1st NSE Minna Branch National Conference 2021

Conference theme
Role of Engineering in
Sustainable Development Goals

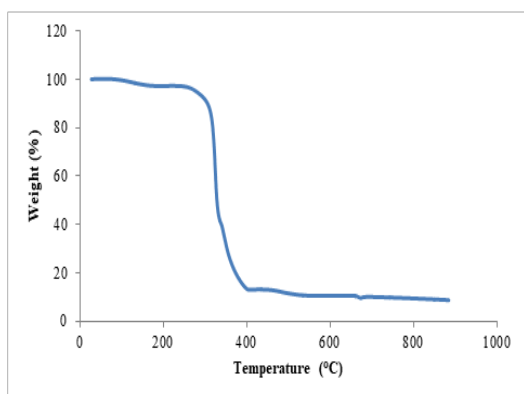breaking down first, cellulose next and then Lignin. This is shown on figure 1.

FIGURE 1: TGA THERMOGRAM OF RAW BAMBOO

3.3. PROXIMATE AND ULTIMATE ANALYSIS

The proximate analysis of raw bamboo was based on the ASTM standards methods (ASTM E871-82, ASTM E1755-01, and ASTM E872-82). This was to determine the moisture content, ash content, volatile matter and fixed carbon. The proximate and ultimate analysis of bamboo is shown in Table 2, the high percentage of Volatile matter, high fixed carbon, low moisture and ash content meets the criteria of bamboo to be utilized as feedstock for the production of biochar. Lower moisture contained in the bamboo implies less energy requirement, low biomass consumption for the pyrolysis process and greater biochar yield. So biomass with a low percentage of moisture content is the most preferable feedstock for the production of biochar which correlates with the findings of (Canal et al., 2020). The biochars produced at pyrolysis temperature of 400 oc had a somewhat higher volatile matter as a result of incomplete carbonization. The percentage ash content in the biochars slightly increased as the pyrolysis temperature is increased. However, the percentage fixed carbon had no significant difference in all the biochars. This may be as a result of escape of some carbon in the form of volatile matter as the pyrolysis temperature is increased. These results are in conformity with the findings of (Sahoo et al., 2021). It can be observed that raw bamboo contained predominantly volatile matter which is expected to decompose during pyrolysis. Low percentage of moisture content was as a result of the samples being dried before pyrolysis. Elemental analysis of raw bamboo as shown in Table 2 indicates a high percentage of oxygen and carbon which are the main constituents of plant fibres. Proximate and ultimate analysis of biochar was conducted at reactor temperatures 400 oc, 450 oc and 500 oc. There is a decrease in moisture content and volatile matter as a result of continuous decomposition of these components as the pyrolysis temperature is increased, this invariably lead to an increase in the percentage ash content.

TABLE 2: PROXIMATE AND ULTIMATE ANALYSIS OF RAW BAMBOO

Proximate and Ultimate analysis	Composition (%)
Moisture Content	10.24
Ash content	1.85
Volatile Matter	74.15
Fixed Carbon	14.73
Carbon	38.50
Nitrogen	0.52
Hydrogen	5.40
Oxygen	53.50

TABLE 3: PROXIMATE ANALYSIS OF BIOCHAR

Pyrolysis Temp ºC	Moisture content (%)	Ash content (%)	Volatile Matter (%)	Fixed Carbon (%)
400	1.90	3.05	49.40	45.65
450	1.54	3.26	49.30	45.60
500	1.38	3.56	49.10	46.96

TABLE 4: ULTIMATE ANALYSIS OF BIOCHAR

Temp. ºC	C (%)	H (%)	N (%)	O (%)
400	54.82	6.18	0.24	15.06
450	50.62	5.03	0.25	10.45
500	56.48	3.88	0.22	6.37

4 CONCLUSION

Biochar from bamboo waste was subjected to pyrolysis at different temperatures of 400 ºc, 450 ºc and 500 ºc. Physicochemical analysis showed a slight change in properties with increase in pyrolysis temperature. The waste bamboo biochars shows

suitable properties for its application in reinforcements, as energy source and agricultural applications.

REFERENCES

Amaral, S., & Leite, L. (2014). Comparative Study for Hardwood and Softwood forest Biomass; Chemical Characterization, combustion phases and gas and Particulate Matter Emissions. Bioresource Technology, Vol. 164, pp. 55-63.

Canal, W.D., Carvalho, A.M.M., Figueiro, C.G., Carneiro, A.D.C.O., Fialho, L.D.F., Donato, D.B. (2020). Impact of wood moisture in charcoal production and quality. Florest. Ambient. 27 http://doi.org/10.1590/2179-8087.099917.

Mahanim, S.M.A., Asma, I.W., Rafidah, J., Puad, E., & Shaharuddin, H. (2011). Production of Activated carbon from Industrial bamboo wastes. Journal of Tropical Forest Science 23(4): 417-424

Mena. L., Pecora. A., & Beraldo. A. (2014). Slow pyrolysis of Bamboo Biomass: Analysis of Biochar properties. Chemical Engineering Transactions, 37, 115-120. DOI:10.3303/CET1437020

Oyedun, A., Gebreegziabher. T., & Hui. C. (2012). Mechanism and Modeling of bamboo pyrolysis. Fuel processing Technology. DOI:10.1016/j.fuproc.2012.09.031

Pecas, S., Carvalho. H., Salman. H. & Leite. M. (2018). Natural fibre composites and their Applications: A Review. Singh, A.P., Causin, V., Nuryawan, A., & Park, B. (2014). Morphological, chemical and crystalline features of Journal of composites science 2,66.

Phuakpunk, K., Chalermsinsuwan, B., & Assabumrungrat, S. (2020). Pyrolysis Kinetic Analysis of Biomasses: Sugarcane Residue, Corn Cob, Napier grass and their mixture. ENGINEERING JOURNAL Volume 24 Issue 4. DOI: 10.4186.

Sahoo, S., Vijay, V., Chandra, R., & Kumar, H. (2021). Production and Characterization of Biochar produced from slow Pyrolysis of Pigeon pea stalk and bamboo. Cleaner Engineering and Technology 3(2021) 100101.

Tan, x., Liu, Y., Gu, Y., Xu, Y., Zeng, G., Hu, X., Liu, S., Wang, X., Liu, S., & Li, J., (2016). Biochar based nano composites for the decontamination of wastewater: A review. Bioresource Technology (2016), doi:http://dx.doi.org/10.1016/j.biortech.2016.04.093.

Wang. G. & Chen. F.(2017). Development of Bamboo fibre-based composites. International centre for Bamboo and Rattan, Beijing, China.

The Nigerian Society of Engineers
Minna Branch
1st NSE Minna Branch National Conference 2021

Conference theme
Role of Engineering in Sustainable Development Goals

Synthesis of Ni-Al2O3 Nanocatalyst for Low Temperature Production of Carbon Nanotubes (CNTs)

Yerima, M. L[1]., Abdulkareem A. S[2]., Abubakre, O. K[3], Ndaliman, M. B[4]. Khan, R. H.[5], and Muriana, R.A.[6]

Material and Metallurgical Department, Federal University of Technology, Minna, Nigeria[1, 6]
Chemical Engineering Department, Federal University of Technology Minna, Nigeria[2]
Mechanical Engineering Department, Baze University, Abuja, Nigeria[5]
Mechanical Engineering Department, Federal University of Technology, Minna, Nigeria[3, 4,]

ABSTRACT

This study focused on the synthesis of nickel - aluminium oxide support (Ni-Al$_2$O$_3$) nanocatalyst by wet impregnation method. The catalyst yield of 86.00 % was obtained at temperature of 400 ^{O}C for 3 hours after calcination. The catalyst was characterized to determine the thermal property, Morphology, crystalinity, pore volume/particle size and surface area using TGA, SEM/EDX, XRD, DLS and BET respectively. Results obtained revealed that the catalyst produced has an average particle size of 82.24 nm. It was highly crystalline with BET surface area of 428.352 m^2/g, pore size of 0.2817 Å and pore volume of 0.1779 cc/g. Analysis of the results also shows that the catalyst developed is thermally stable with about 0.5% wt loss at 800 ^{O}C, which makes the catalyst suitable for CNTs production. The catalyst developed was used to produce carbon nanotubes at operating temperature of 600 ^{O}C with argon flow rate of 30ml/min, acetylene flow rate of 300 ml/min and production time of 55 minutes. The results obtained revealed that the yield of 135 % was obtained. The CNTs produced was characterized and the results shows that the produced CNTs is thermally stable with BET surface area of 833.64 m^2/g, pore volume of 0.3286 cc/g and pore size of 0.3148 Å. This study demonstrated that employing Ni-Al$_2$O$_3$ nanocatalyst provides suitable route for efficient low temperature production of CNTs.

KEYWORDS: Nickel, Aluminium oxide, characterization, CVD, CNTs

1 INTRODUCTION

Since its discovery, Carbon nanotubes (CNTs) has continued to attract research interest worldwide. After its discovery by Sumio Iijima in 1991, this novel nanostructure material has gained recognition due to its wonderful physical properties that makes it suitable for many unique applications (Toussi *et al.,* 2011) in many fields of engineering. CNTs are nanoscale carbon structure that could be described as graphene sheets rolled up into the shape like of a cylinder (Bondi *et al.,* 2005) with one end covered with hemisphere of the fullerene structure (Arranz-Andréas and Blau, 2010). Regardless of the type of CNTs which are single walled carbon nanotube and multiwalled carbon nanotube (Werner and Andreas 2004); they generally have common methods of synthesis. Owing to its many intriguing properties, the production of CNT has turn out to be a significant subject of worldwide research. Carbon nanotubes (CNTs) are especially promising over various existing materials inferable from their interesting unique/ anisotropic extraordinary

chemical, electrical, thermal and mechanical properties (Afolabi *et al.*, 2014) that have caught creative energy of scientists globally since their revelation by Sumio Iijima in (1991). Owing to these remarkable electrical properties and very extraordinary thermal conductivity, CNTs was utilized for energy storage, functional fillers in composites field-emission displays, some biomedical devices and electronics (Muhammad *et al.,* 2011; Ajayan*,* 2001; Baughman *et al.,* 2002). Additionally, CNTs have great flexible moduli (>1TPa), huge expandable straining length equal to 5 percent, with huge breaking strain up to 20 percent (Esfarjani, 2013). It's their outstanding mechanical properties may conceivably pilot an excess of many uses. For instance, with their noteworthy stiffness and strength and adding to the advantage of lightness, standpoint prospect applications of CNTs are in progressive plane design (aerospace engineering), biomedical engineering (virtual bio-devices) and other disciplines.

Different support materials such as Al_2O_3, zeolite, MgO, SiO_2, and $CaCO_3$ have been applied as a carrier in supported-catalysts for CNT (Kathyayini *et al., 2008;* Willems*et al.,* 2000; *Mao-Lin et al.,* 2012 and Couteau*et al.,* 2003). Several researchers have reported high purity multi-walled carbon nanotubes obtained from Co-Mo supported MgO catalyst via CVD Pelech*et al.,* 2009; Quian*et al.,*2003; Yeoh*et al.,*2009). Awadallah*et al. (*2012) demonstrated the synthesis of CNTs prepared via CVD methods from Ni-Mo and Co-Mo supported on Al2O3 catalyst. Studies have shown that alumina supported catalysts for CNTs synthesis appeared more promising due creation of a high surface areas and mesoporous materials which promote catalysis (Kathyayini*et al., 2008*). In addition, Al_2O_3 has good thermal stability and can be easily removed after the synthesis via acid purification. In this present study, bi-metallic Fe-Ni catalyst supported on aluminium oxide were developed and utilised to prepare CNT through CVD method. The choice Ni as an active part of the catalyst is due to it availability and cheapness (Uddin *et al., 2008*).

2.0 METHODOLOGY

2.1 Materials
The chemicals used in this work are of high grade with high purity, ranging from 98.5- 99.99 %. These chemicals include nickel nitrate hexahydrate (Ni $(NO_3)_2.6H_2O$), alumina (Al_2O_3), distilled water and concentrated hydrochloric acid (H_2SO_4) were supplied by Aldrich. The carbon source (acetylene) and carrier gas (argon) are also of analytical grade with 99.99% purity supplier by BOC Nigeria.

2.1.1 Catalyst Synthesis
The catalyst was prepared by wet impregnation methods. A 0.22 mol/dm³ aqueous solution of Ni $(NO_3)_2.6H_2O$ with IUPAC Name Nickel (II) nitrate hexahydrate (salt solution) was made by impregnating support material (Al_2O_3 powder) in the salt solution. For single metallic Ni based catalysts, Ni $(NO_3)_2.6H_2O$/aqueous solution was used. Molar ratio of Ni: Al_2O_3) 1:2 was used in preparing the catalyst systems. The following describes the detailed procedure for preparing a Ni/Al_2O_3 catalyst.

Support material (5-6 g) was suspended in 50 ml of deionized water with stirring, followed by the addition of 3.198 g of a green Ni $(NO_3)_2.6H_2O$. The mixture was allowed to stir for 20 min. and the resulting slurry was dried in an oven at $120\ ^0C - 125\ ^0C$ for 5 to 7 hrs. After drying, the material was grinded with an agate mortal to obtain fine light green powder. It was then calcined in muffle furnace at $400\ ^0C$ for 2hr, cooled to room temperature, and re-grinded prior to CVD growth. The calcined material (grey) was sieved using a sieve of 150 micrometer and the desired catalyst was collected as fine particles. The percentage yield of the catalyst before oven drying (Yield Dried), and after calcination (Yield Calcined) is calculated using equation 1 and 2;

$$Yield\ (\%) = \left(\frac{Mass\ of\ catalyst\ after\ oven-drying}{Mass\ after\ oven\ drying}\right) \times 100 \qquad 1$$

$$Yield\ (\%) = \left(\frac{Mass\ of\ catalyst\ after\ calcination-drying}{Mass\ after\ oven\ drying}\right) \times 100 \qquad 2$$

2.1.2 Synthesis of CNTs
The horizontal CVD reactor equipment shown in Plate 1was used for the CNTs synthesis. It has a length of 1010 mm with internal and external diameter of 52 mm and 60 mm respectively. 1.0 g of the supported bimetallic catalyst (Ni/Al_2O_3) was weighed and spread evenly on a quartz boat placed at the central part of the horizontal tube.

Plate 1: The horizontal CVD set up for the synthesis of carbon nanotubes

The Nigerian Society of Engineers
Minna Branch
1st NSE Minna Branch National Conference 2021

Conference theme

Role of Engineering in
Sustainable Development Goals

The heating rate, temperature, gas flow rates were maintained at the desired rate. The entrapped gases in the quartz tube were expelled using argon as the carrier gas at a flow rate of 30 ml/min. At a temperature of 600 0C, the flow of acetylene was released into the quartz tube of catalytic reactor at 100 ml/min for 55 min with immediate increment in the flow rate of the carrier gas (argon) to 300 ml/min. As the residence time (45 minutes) of the reaction was attained, the flow of acetylene was stopped and the argon gas was left flowing at 30 ml/min until the reactor cooled to room temperature. The sample was removed, weighed and analysed. The yield of the deposited carbon was therefore determined using Equation (3) (Yeoh*et al.,* 2009; Taleshi, 2012).

$$CNTs\ Yield\ (\%) = \left(\frac{MTotal - MCatalyst}{MCatalyst}\right) \times 100 \qquad 1$$

2.2 Characterization
2.2.1 Thermo Gravimetric Analysis (TGA) and Differential Thermal Analysis (DTA)
The thermal stability, compositional and percentage purity of materials were determined using TGA 4000 (PerkinElmer). Samples were analyzed in nitrogen environment at a volumetric flow rate of 20 ml/min, pressure of 2.5 bars and heating rate of 10 ^{O}C/min. The thermal balance was zeroed, the sample was recorded and placed into the equipment utilizing pyris manager software. When constant weight was observed utilizing the formed heating profile, the analysis was then commenced. The test effects were then studied using pyris manager for proximate and compositional analysis.

2.2.2 X-Ray Diffraction Patterns (XRD)
Crystal phase identification of the catalyst and CNTs materials were studied utilising Bruker AXS D8 X-ray diffractometer system which was linked to Cu-Kα radiation of 40 kV and a current of 40 mA. The λ for Kα was 0.1541 nm, scanning rate was 1.5 º/min, The step width of 0.05° was used over 2θ range value of 20 – 80º.

2.2.3 High Resolution Scanning Electron Microscope (HRSEM)
The surface topology and the microstructure of the catalyst and CNTs was studied using Zeiss Auriga HRSEM. The HRSEM was equipped with EDS and it was used to obtain the elemental composition of the produced materials. A small quantity of the materials was sprinkled on a sample holder and sputter coated with Au-Pd using Quorum T15OT for 5 minutes before the analysis. The sputter coated samples was firmly attached to the carbon adhesive tape and studied using ZeissAuriga HRSEM equipped with In-lens standard detector at 30 kV.

2.2.4 BET Surface Area
The surface area of the synthesized catalyst was investigated by means of BET method in Nova e-series equipment. A sample weighing 300 mg was degassed at 150 o - 250 OC for 4 hrs in order to remove moisture. The degassed sample was then examined for physisorption of the adsorbate (nitrogen) by the adsorbent in liquid nitrogen environment.

2.2.5 Particle Size Analysis (DLS Technique)
In order to determine the particle size and the hydrodynamic diameter, Zeta Nanosizer was used at scattering angle of 173 ^{O} operating at 25 ^{O}C with equilibrating time of 120 secs. 1 mg of the samples were dispersed in 10 ml of ethanol then transferred into a polystyrene cuvette using a syringe with 0.22 µm filter coupled to it.

3 RESULTS AND DISCUSSION
The suitability of the nickel catalyst material for CNTs growth at CVD reaction temperature of about 600 ^{O}C was investigated by thermogravimetric analysis (TGA) and the thermal differential analysis (DTA) presented in Figure 1. The results as presented in Figure 1 shows that there were four regimes of weight losses in the TGA graph of the catalyst sample. The sample had continuous loss in weight from the initial temperature until 400 ºC. According to the differential thermogravimetric (DTG) curves this process is endothermic and can be attributed to elimination of water. In the regime of 400– 550 ºC the sample loss of weight was observed to be faster. This can be ascribed to the thermal decomposition of nickel nitrate hexahydrate as well as the formation of metal oxides (Lobiak *et al.,* 2014).
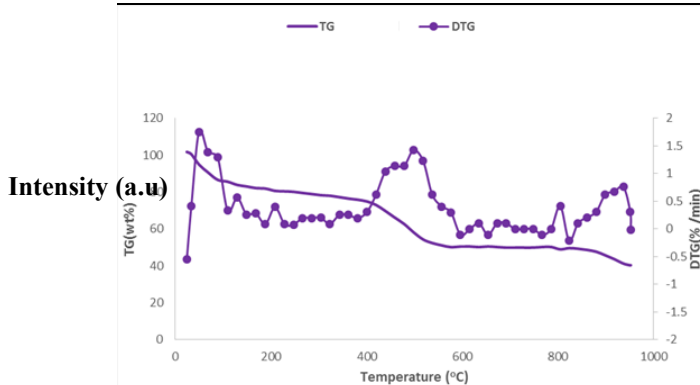
Figure 1: TGA and DTA curves of nickel catalyst obtained at 10 ºC /min heating

Moreover, within these temperature ranges the DTG curves show the peaks corresponded to crystallization processes of metal oxides. In the following regime of 600 -850 ºC the change of weight was not significant until 850 ⁰C and above which exhibited another regime of steady weight loss.

The XRD analysis pattern of the calcined catalyst sample is presented in Figure 2, showed sharpened diffraction peaks that indicates that a growth has occurred in the crystallite size of NiO. This also suggests that the prepared catalyst is highly crystalline, an indication of orderly distribution of the metallic ions on the pore of the alumina support. Deep peaks matching the alumina support are detected for the catalysts. The aluminium oxide existed in the both α -Al_2O_3 and ⅄ - Al_2O_3 form or as a combination of both. Metal oxide peaks were detected in catalyst

The major characteristics peak position appearing at 2θ= 19.1º, 27º, 31º, 36º, 37.10º, 43º.30º, 45º, 55º, 62.87º, 76.50º and 79.22º value respectively. The characteristics peak at 2θ value of 35. 23º suggest the presence of alpha alumina (α-Al_2O_3) (Kathyayini *et al.,* 2008) explaining that the pattern showed primarily the presence of peaks Al_2O_3 due to Nickel particles well dispersed on the surface of the Al_2O_3. This infers that the metal nanoparticles might have very small particle sizes in amorphous state and therefore unable to cause a Bragg reflection (Scherrer, 1918). This also conformed to the findings of (Tran *et al.,* 2007) who observed similar occurrence during the analysis of the XRD spectra

obtained on the characterization of Ni/Al_2O_3.The sharpness and intensity of the peaks designates the well crystalline nature of the developed catalyst.
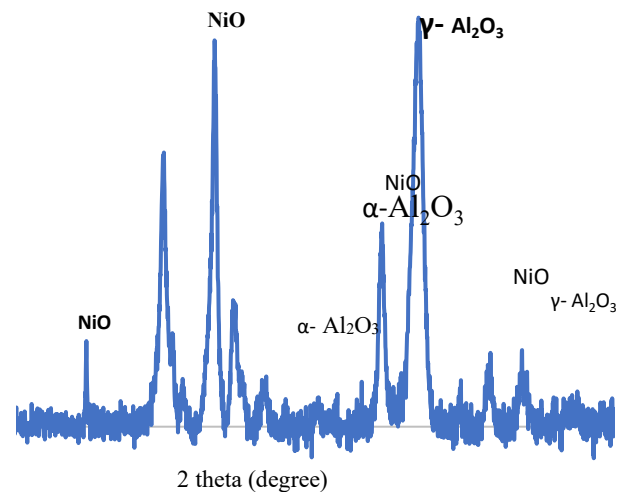

Figure 2: XRD spectra of Fe-Ni/Al_2O_3 catalyst

The particle size distribution of the synthesized supported catalyst based on the respective identified peaks in the XRD pattern is presented in Figure 2 In order to properly establish the phases that are present in the catalyst sample, comparison is made between peaks in its XRD pattern and peak positions reported by other researchers in literature.

The average crystallite particle size was examined to be 41.5 nm from the XRD patterns of the developed catalyst using Scherer equation 2 (Chen *et al.,* 2006) and the percentage abundance is shown in Figure 3.

$$D = \frac{K\lambda}{\beta COS\theta} \qquad 2$$

Where D is the particle size diameter,β is the full width at half maximum, λ is the wave length of X-ray, θ is the diffraction angle and K is the Scherer constant.
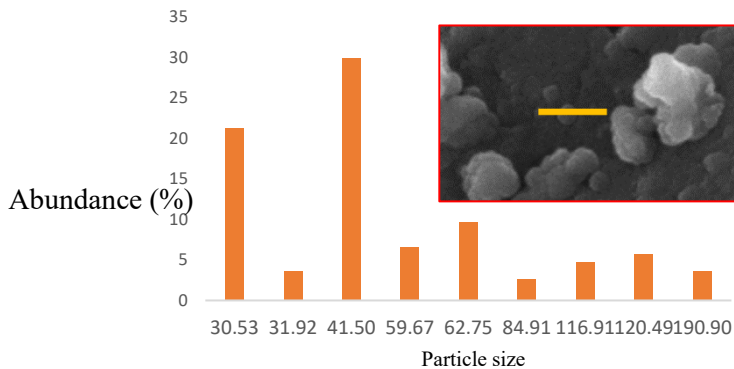
Figure 3: Percentage Crystallite Size Population Density of Catalyst

From Figure 3 it can be seen that majority of the particle fall within 41.50 nm which confirmed that the size of the prepared monometallic catalyst is nanostructure in nature and as such the catalyst is a good template for CNTs production. The result of the average crystalline particle obtained (82.18 nm) shows a quite deviation from that obtained by kariim *et al.* (2015) with obtained average particle size of 42.24 nm from their XRD analysis.

The HRSEM image presented in Figure 4 indicates that the clustered solid catalyst material is near spherical in geometry and is of high crystallinity. The agglomerates seen in the SEM images could be ascribed to the drying process in sample preparation. The micropores can be recognized in the catalyst, a property showing that there was appropriate dispersion of Ni nanoparticles on the Al_2O_3 support material with tiny spaces inside the composite. The Al_2O_3 matrix sites were homogeneously occupied by the oxides of Ni that was formed during calcination of the catalyst sample. The SEM image of the catalyst also indicates that the nickel nanoparticles that were dispersed on the Al_2O_3 support material are suitably less than 50 nm in size (red arrow, concentric square). The results also show that nitrates of nickel nitrate salts were effectively removed by converting them to oxides during calcination. Though, there are little clusters of nanoparticles (red arrow, lower right-hand corner) and lumps of catalyst (yellow arrow). These might be responsible for the growth of CNTs of varying diameter, which is one of the existing challenges in producing nanotubes of uniformly distributed diameter from catalyst prepared by wet impregnation.
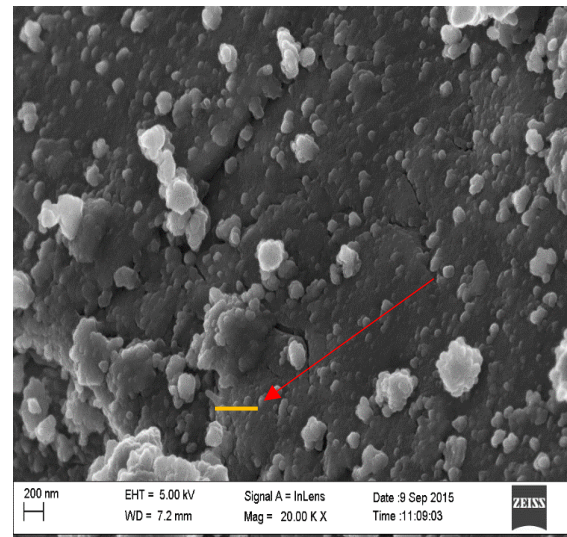

Figure 4: SEM image showing nanoparticles of Ni dispersed on Al_2O_3 support

The surface area analysis was carried out on the developed monometallic nickel catalyst (Ni/Al_2O_3) by BET method. The SBET surface area of the developed monometallic catalyst was determined to be 428.352 m^2/g using the multipoint equation under nitrogen condition, with micropore volume of 0.1779 cc/g and micropore half pore width of 28.17 Â. This surface area is little less than those reported by (Abassi *et al.,* 2014). This may be due to the presence of weak bond that exist between $Ni-Al_2O_3$ (Zhang *et al.,* 2006).

The HRTEM micrograph of the produced CNTs is presented in Figure 5. The micrograph shows a densely populated strand of CNTs with high degree of homogeneity covering the impurity present. The morphology of the CNTs illustrates that the CNTs formed under these conditions are entangled with each other and possess curved, hollow, and tubular shapes, with diameters in the range of 15 – 45 nm. Also, some catalyst particles appear to be encapsulated within the nanotubes hollow core. Encapsulated metal nanoparticles are also detected along the inside diameter of the nanotubes samples which were introduced by the metal catalysts utilized for CNTs growth.
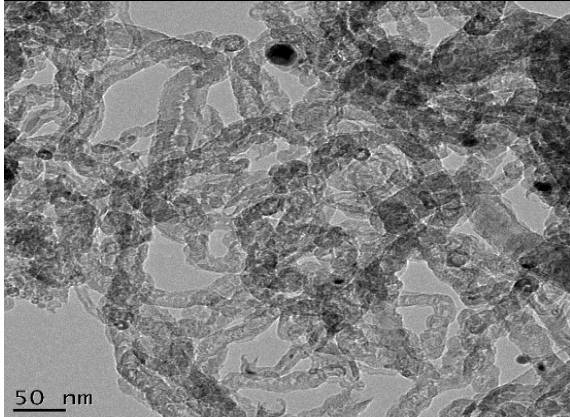
Figure 5: TEM image of as-synthesized MWCNTs

Figures 6 represents the TGA and DTA profile of as-produced MWCNTs which were attained under N_2 environment and heating rate of 10 ^{0}C /min up to 900 ^{O}C. It can be deduced from the result that the loss of absorbed moisture on the as-synthesized CNTs was responsible for the weight loss between 30 -100 ^{o}C, while the reduction observed at the temperature of 100 - 400 ^{o}C depicts the removal of crystal water of nitrates and elimination of volatile products. Between 400 -800 ^{o}C, the change of weight was not significant beyond which the CNTs exhibited another regime of steady weight loss. The percentage weight loss of the as-synthesized CNTs observed are 10 % (30 -100 ^{o}C), 20 % (100 – 400 ^{o}C), 21 % (400 – 800 ^{o}C) and 40 % (800 – 950 ^{o}C).
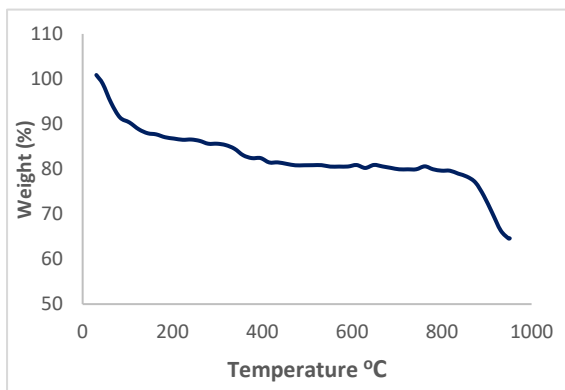

Figure 6: TGA Profile of As-synthesiseed CNTsobtained at 10 ^{O}C/min heating rate under Nitrogen atmosphere.

The loss in weight of the as-synthesized MWCNTs is associated to the presence of impurities that oxidizes at temperatures lower than that of nanotubes which accompany the synthesis of the CNTs (Ebbensen *et al.,* 1994; Eftehari *et al.,* 2005) and these impurities are in the form of amorphous carbon and metals.

Utilizing the hydrodynamic diameter of the sample as obtained by DLS, the literature values of aspect ratio of MWCNT was used to correlate length and diameter of this single CNT sample. Z-average (or hydrodynamic diameter) of the sample represents neither the diameter nor the length of the nanotube. The correlated equation utilized for the determination of length and diameter based on these aspect ratios is (Nair *et al.*, 2008; Horiba Ltd, 2015).

$$Dh = \frac{L}{In(\text{L/d}) + 0.32}$$

Aspect ratio of MWCNTs produced by CVD process as reported by Abu Al-Rub, Ashour & Tyson (2012), ranges from 157 to 3,750. These values of aspect ratio (L/d), along with Z-average from DLS were substituted to find the corresponding lengths and diameters of the as-grown MWCNT produced in the current work. This analyses provides a correlation between the diameter, length and aspect ratio, for this MWCNT sample, as shown in the charts of Figures 7.
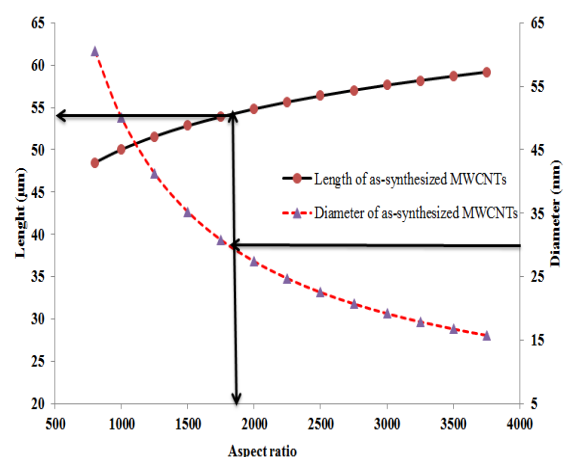

Figure 7: Correlation chart between the aspect ratio, length and diameter of the as – grown MWCNT sample.

Specific surface area m_2/g of the synthesized is presented in Table 1 the SBET surface area of the as synthesized CNTs was determined to be 833.64 m^2/g

The Nigerian Society of Engineers
Minna Branch
1st NSE Minna Branch National Conference 2021

Conference theme
Role of Engineering in
Sustainable Development Goals

using the multipoint equation under nitrogen condition, with micro pore volume of 0.3286 m^3/g and micro pore half pore width of 31.48 Å. This surface area is a little high than those reported by (Abassi *et al.,* 2014). This may be due to the presence of weak bond that exist between Ni-Al$_2$O$_3$ (Zhang *et al.,* 2006). Peigney *et al.* (2001) also showed that the surface area of MWNTs decreases with increasing walls and nanotube diameters. However, the trend of the surface area obtained in this work do not strictly obey the observation made by Peigney and co-workers because the average sizes are affected by contribution from sizes of impurities present in varying quantities in the samples.

Table 1: Result showing BET-Surface area Analysis

Surface area, pore volume, pore size of synthesized CNTs and average particle size

BET surface area			(m^2/g)
833.641			
Pore volume			(m^3/g)
0.3286			
Pore size			(Å)
0.3148			
Average Particle size (DLS)			nm
82.24			

The SAED patterns of the CNTs sample confirmed the graphitic nature of MWCNTs especially the innermost ring which is due to the usual strongest reflection plane (002) of graphite (Das e*t al.*, 2015). As illustrated in Figure 8. The occurrence of the sharp rings at reciprocal lattice spacing (1/*d*) of 2.9, 4.8, 5.7 and 8.5 nm^{-1} are in good agreement with those reported for graphite. Kariim, (2015) also collected SAED pattern of MWCNTs and observed sharp rings attributable to the MWCNT at reciprocal lattice spacing of 3.1, 5.0, 6.0 and 8.5 nm^{-1}.
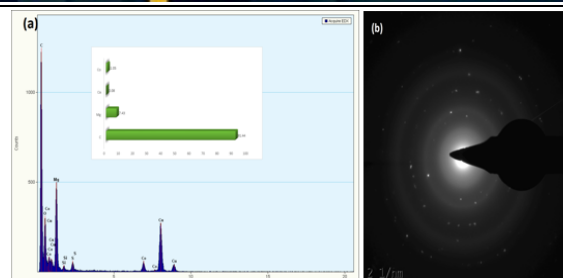

Figure 8: (a) EDS and (b) SAED pattern of as-synthesized MWCNTs

Again, it can be observed from the SAED that the CVD reaction parameters affect the crystallinity of MWCNTs and it present a low crystallinity which as it displayed diffuse rings in its SAED pattern, which is typical of amorphous substances. The single bright spots are reflections from certain individual crystals.

4.0 CONCLUSION

In this study, multi-walled carbon nanotubes were successfully produced from nickel supported alumina catalyst via wet impregnation followed by CVD technique. The CNTs was successfully synthesized at reaction time of 45 minutes, temperature of 600 ºC, argon flow rate of 200 ml/min and acetylene flow rate 100 ml/min. The average diameter of the as-produced multiwalled carbon nanotubes obtained from bimetallic Ni/Al$_2$O$_3$ catalyst was 28.89 nm whereas; the bimetallic catalyst had average particle size of 46.24 nm. The correlation chart showed that the MWCNTs produced was a long-tube multiwall carbon nanotubes with aspect ratio of 1250. Thus, the nickel catalyst on alumina support developed via incipient wet impregnation method is suitable for CNTs production by CVD method.

REFERENCE

Abbasi, N., and Mahdavifar, Z. (2014). The influence of

Cu-doping on aluminum nitride, silicon carbide and boron nitride nanotubes' ability to detect carbon dioxide; DFT study. *Physica E: Low-dimensional Systems and Nanostructures*, *56*, 268-276.

Abbasi, S. A., Loan, S. A., Nizamuddin, M., Bashir, F., Shabir, H., Murshid, A. M., R., and Alamoud, A. (2014). Design of a novel high gain carbon

The Nigerian Society of Engineers
Minna Branch
1st NSE Minna Branch National Conference 2021

Conference theme
Role of Engineering in
Sustainable Development Goals

nanotube based operational transconductance amplifier. In *Proc. of the International MultiConference of Engineers and Computer Scientists 2014-IMECS 2014*.

Afolabi, A. S., Abdulkareem, A. S., Mhlanga, S. D. and Iyuke, S. E. (2011) "Synthesis and purification of bimetallic catalysed carbon nanotubes in a horizontal CVD reactor", *Journal of Experimental Nanoscience, vol. 6(3), 248-262*

Ajayan, P.M. and Zhou, O.Z. (2001), Applications of carbon nanotubes. *Carbon Nanotubes (Topics in Applied Physics), ed Dresselhaus, M.S., Avouris, Ph. 80, 391-425*, Berlin: Springer Verlag.

Arranz-Andréas, J., and Blau, W. J. (2010). Enhanced device performance using different carbon nanotube types in polymer photovoltaic devices. *Carbon*, *46*(15), 2067-2075.

Awadallah, A. A., Mina, A. N., Phillips, A. H., and Ahmed, R. R. (2012, February). Simulation of the Band Structure of Graphene and Carbon Nanotube. In *Journal of Physics: Conference Series* (Vol. 343, No. 1, p. 012076). IOP Publishing.

Baughman, R. H., Zakhidov, A. A., Heer, W. A. (2002) Carbon nanotubes-the route toward applications. Science, 297 pp.787-792.

Bondi, S. N., Lackey, W. J., Johnson, R. W., Wang, X. and Wang, Z. L. (2005), Laser assisted chemical vapour deposition synthesis of carbon nanotubes and their characterization, *Carbon* 44 (2006) 1393–1403. doi:10.1016/j.carbon.2005.11.023

Chen, G. Z., Shaffer, M. S., Coleby, D., Dixon, G., Zhou, W., Fray, D. J., and Windle, A. H. (2006). Carbon nanotube and polypyrrole composites: coating and doping. *Advanced Materials*, *12*(7), 522-526.

Ebbesen, T. W., Treacy, M. J., and Gibson, J. M. (1996). Exceptionally high Young's modulus observed for individual carbon nanotubes.

Esfarjani S.A (2013). A Modeling Framework for the Synthesis of Carbon Nanotubes by Plasma Technology. Published PhD Thesis. University of Toronto, Canada.

Horiba Scientific Ltd (2015), "Carbon nanotube particle size". Available online at http//www.horiba.com/scientific/products/partic le-characterization/applications/carbon-nanotubes/. Retrieved May, 2015.

Kariim I, Abdulkareem, A.S., Abubakre O.K., Mohammed, T.A., Bankole, M.T and Jimoh T. (2015). Suitability of Alumina (Al_2O_3) as Bimetallic Catalyst Support for MWCNT Growth. *Journal of Nanotechnology*, 1 - 16.

Kathyayini, H., Reddy, K. V., Nagy, J. B., and Nagaraju, N. (2008). Synthesis of carbon nanotubes over transition metal ions supported on Al (OH) 3. *Indian journal of chemistry. Section A, Inorganic, bio-inorganic, physical, theoretical & analytical chemistry*, *47*(5), 663.

Muhammad M. A., Javed I., (2011). Production of Carbon Nanotubes by Different Routes— A Review. *Journal of Encapsulation and Adsorption Sciences, 2011, 1, 29-34*, 29-34

Nair, N., Kim, W., Braatz, R., and Strano, M. (2008) *Langmuir*, 24, 1790 – 1795

Peigney, A., Laurent, C., Flahaut, E., Bacsa, R. R., & Rousset, A. (2001). Specific surface area of carbon nanotubes and bundles of carbon nanotubes. *Carbon*, *39*(4), 507-514.

Qian, D., Liu, W. K., & Ruoff, R. S. (2009). Load transfer mechanism in carbon nanotube ropes. *Composites Science and Technology*, *63*(11), 1561-1569.quantumdotled. html. Accessed July 10, 2006

Toussi, S. M., Fakhru'l-Razi, A., Chuah, A., and Suraya, A. (2011). Effect of synthesis condition on the growth of SWCNTs via catalytic chemical vapour deposition. *Sains Malaysiana*, *40*(3), 197-201.

Uddin, M. A., Tsuda, H., and Sasaoka, E. (2008). "Catalytic Decomposition of Biomass Tars with Iron oxides Catalyst", Fuel, Vol. 87, No (4), pp. 451-459.

Yeoh, Wei-Ming; Lee, Kim-Yang; Chai, Siang-Piao; Lee, Keat-Teong; & Mohamed, A. (2009). Synthesis of high purity multi-walled carbon nanotubes over Co-Mo/MgO catalyst by the

Zhang, Q., Yu, H., Zhang, Q., Wang, Q., Ning, G., Luo, G. and Wei, F. (2006), "Effect of the reaction atmosphere on the diameter of single-walled carbon nanotubes produced by chemical vapour deposition". *Carbon, 44, pp. 1706–1712.*

The Nigerian Society of Engineers
Minna Branch
1st NSE Minna Branch National Conference 2021

Conference theme
Role of Engineering in Sustainable Development Goals

Evaluation of Strength Properties of Lateritic Soil Stabilizer with Cement Kiln Dust

T.E. Adejumo and F.A. Okeshola

Civil Engineering Department, Federal University of Technology, Minna, Nigeria

*Corresponding author email: faithokeshola@gmail.com +2348133884436

ABSTRACT

In this study, the strength properties of Lapai-Gwarri lateritic soil stabilized with cement kiln dust was evaluated. The scope includes determination of the physical composition, index properties, compaction and strength characteristics of laterite soil-cement kiln dust mix. From the results obtained, soil sample encountered was classified as A-7-6 corresponding to CL, it is organic silts and organic silty-clays of very low to medium plasticity, gravelly clays, silty clays and lean clays according to AASHTO and USCS system of soil classification respectively. There was to sharp reduction of plasticity index from 22.20% to 11.09%, with increased in quantity of cement kiln dust, the Compaction characteristics of cement kiln dust soil mixed from 0 and 16% gives the Optimum Moisture Content (OMC) values which decreased from 19.69 - 13.02%. The Maximum Dry Density (MDD) increase in value from 1.50 - 1.79 g/cm³. The Unconfined Compressive Strength test at 7, 14 and 28 days of curing for Cement kiln dust of 0, 4, 8, 12 and 16% obtained average values of 170, 369,511, 461 and 347 (kN/m^2) respectively. The addition of 8% cement kiln dust to samples of laterite soil significantly improves its compressive strength characteristics and is considered as the Optimum percentage of cement kiln dust present and reduces construction costs.

KEYWORDS: *Cement Kiln Dust; Index Properties; Lateritic Soil; Stabilization; Strength Properties.*

1. INTRODUCTION

In general construction, stable subgrade and base layers are essential for engineering structure, the need to reduce the dilemmas in geotechnical engineering during design and construction in terms of the variable nature of soil and rock properties and other in-situ conditions has become a major challenge because of the issues in reliability of design and construction methods, and problems in the costs and benefits of proposed designs policies. The geotechnical properties like strength and volume stability of the subgrade have significant influence on the overall performance and durability of constructions (William, 2003).

For road construction, soils encountered mostly during construction are unable to respond to the imposed stresses, which has become a dominant factor responsible for the failure of road pavement especially in Nigeria (Aigbedion,2007; Okechukwu *et al.* 2011) identified inadequacy of construction materials and poor attribute of construction as other factors responsible for road failure. Improving the properties of these soils by the addition of chemical and cementitious additives becomes not only a

necessity but an important factor to make them suitable for construction.

Chemical additives vary from waste products to the manufactured materials which include lime, Portland cement, proprietary chemical stabilizers, class C fly ash, bitumen and recent technology like NANO technology (Parson and Kneebone, 2004).

Soil stabilization is the process of improving the engineering properties of soil and thus making it more suitable. It is also the treatment of soil with modifier to enable their strength and durability to improve such that they become completely suitable for construction beyond their original classification (Hausmann, 1990). Lots of consideration has been given mainly to the problems encountered in the engineering use of laterite soils. This might give the impression that all laterites and lateritic soils give trouble (Christophe, 1949).

Cement kiln dust is a waste product from the manufacturing of cement. The quantities, nature and characteristics of CKD generated depends on the number of operational factors and the characteristics

The Nigerian Society of Engineers
Minna Branch
1st NSE Minna Branch National Conference 2021

Conference theme
Role of Engineering in
Sustainable Development Goals

of inputs to the manufacturing process, including the raw fed, fuel used, and the design and operation of the cement kiln. This by-product has desirable properties that make it satisfactory for variety of beneficial use and application including soil improvement (Abeln *et al.* 1993).

The evaluation of possible change in characteristics of lateritic soil when treated with additive such as cement kiln dust can be an important task in the prevention of natural disasters on our road pavements and even buildings. Cement kiln dust provides a cheaper alternative to Portland cement and lime in soil improvement by stabilization. Miller *et al.* (2003) showed that soil improvement by stabilization using CKD is cheaper than lime especially when problematic soils are encountered.

Cement kiln dust is also available in Nigeria and if this is realized, it can find lasting solution to the failure of road and buildings due to weak sub-grade and foundation arising from substandard construction materials. This work lead to improvement without incurring excessive cost in the construction industry.

2. METHODOLOGY

Materials
The soil used was obtained at Lapai-Gwarri area of Minna, using the disturbed sampling technique. Sample was obtained at 1.5m depths and classified according to AASTHO and UCSC soil classification system. Cement Kiln Dust which is a greyish black material is the byproduct of cement and one of the essential materials needed for this work. It was obtained from Obajana Cement Plant Kogi. The material was sieved appropriately and finally stored in an air-tight container pending the time for sample preparations, this is done so it maintains its value.

Methods
The production of concrete tests was conducted in Civil Engineering Laboratory, Federal University of Technology, Minna. The materials mentioned in 2.1 above were used, the collected soil was air – dried and stored. Laboratory tests were carried out on two different samples (the natural lateritic soil and one treated with Cement Kiln Dust). The treatment with

cement kiln dust was done at 4, 8, 12 and 16% dry weight content in accordance to BS 1377 (1990).

Index properties of fill materials: Natural moisture content, specific gravities, particle size analysis and Atterberg limits tests were conducted in accordance with tests procedures specified in BS 1377 (1990).

Compaction characteristics: Compaction of the samples was conducted in accordance with the guidelines specified in BS 1377 (1990) to compute the required parameters. The Reduced British Standard Heavy (RBSH) compactive effort was used. The RBSH compaction is the energy resulting from 4.5 kg rammer falling through a height of 30 cm onto three layers, each receiving 25 blows to determine MDD and OMC of the sample according to ASTM D-698 (1992) and ASTM D-1557 (1992).

Unconfined compressive strength (CCS): The test was conducted in accordance with the procedure specified in BS, 1377 (1990), to determine the compressive strength characteristic using the values of OMC obtained during compaction results from Reduced British Standard Heavy compaction method.

2.1 FIGURES AND TABLES

TABLE 1: NATURAL MOISTURE CONTENT OF SOIL SAMPLE

Trial	1	2	3
Can No	M4	PQ4	A21
Weight of can (g)	34.80	38.20	38.20
Weight of can + wet soil (g)	55.30	58.60	54.80
Weight of can + dry soil (g)	51.40	54.70	51.50
Weight of dry soil (g)	16.60	16.65	13.30
Moisture Content (%)	23.50	23.63	24.80
Average Moisture Content (%)		23.97	

TABLE 2: SPECIFIC GRAVITY OF SOIL SAMPLE

Trial	1	2	3
Weight of Cylinder (g)	46.0	46.0	43.6
Weight of Sample + Cylinder (g)	97.4	88.0	87.9
Weight of Sample + Cylinder + Water (g)	170.8	168.1	167.1
Weight of Cylinder + Water (g)	144.9	145.0	142.4
Specific Gravity	2.04	2.21	2.31
Average Specific Gravity		2.2	

TABLE 3: SUMMARY OF INDEX PROSPERTIES OF SOIL AND SOIL MIX

CKD(%)	Liquid Limit (%)	Plastic Limit (%)	Plasticity Index
0	45	22.80	22.2
4	43	24.92	18.08
8	41	27.08	13.92
12	44	31.01	12.99
16	45	33.91	11.09

TABLE 4: COMPACTION STRENGTH CHARACTERISTIC OF SOIL SAMPLE AND SOIL MIXTURE

CKD%	Maximum Dry Density (g/cm³)	Optimum Moisture Content (%)
0	1.50	19.69
4	1.71	15.95
8	1.74	15.66
12	1.77	15.52
16	1.79	13.02
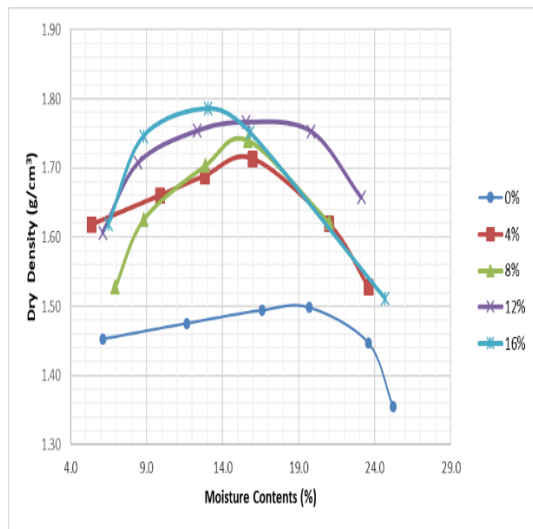
Figure 1: Compaction Graph
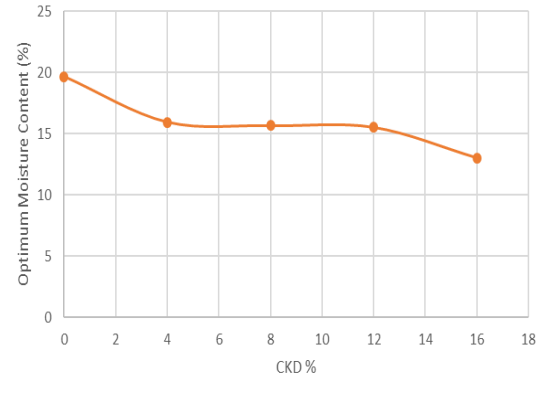
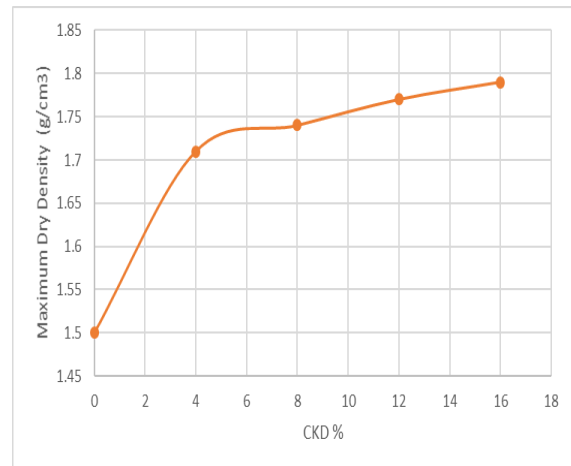**FIGURE 2:** RELATIONSHIP BETWEEN OPTIMUM MOISTURE CONTENT AND CKD STABILIZED SOIL

FIGURE 3: RELATIONSHIP BETWEEN MAXIMUM DRY DENSITY AND CKD STABILZED SOIL

TABLE 5: COMPRESSIVE STRENGTH CHARACTERISTICS

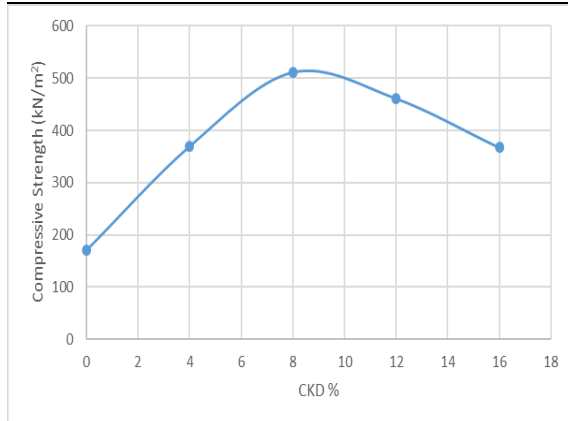| CKD (%)	UCS (kN/m²) 7days Curing	UCS (kN/m²) 14days Curing	UCS (kN/m²) 28days Curing	Average (kN/m²)
0	163	174	174	170
4	314	384	407	369
8	452	500	581	511
12	442	458	484	461
16	336	377	393	367

FIGURE 4: RELATIONSHIP BETWEEN COMPRESSIVE STRENGTH AND CKD

3. RESULTS AND DISCUSSION

The natural moisture content of lateritic soil gotten from the laboratory test after taking 3 trials was gotten to be an average of 23.97% of NMC as shown in Table 1.

Specific Gravity Test was carried out in accordance to BS1377 (1990). Three trials were carried out to get the average specific gravity of the soil, which was gotten to be 2.2 which is satisfactory for a fine aggregate specific gravity. Results are shown in Table 2.

The liquid limit decreased with the addition of CKD up to 8% and then increased slightly with further increase in the addition of CKD. This initial reduction in the liquid limit according to (Talal and Awad 1998) is accredited to cementitious properties of CKD due to high content of calcium oxide (CaO) which aid flocculation and aggregation of soil particles. The increased in liquid limit beyond 8% CKD content is attributed to the extra water required to turn the soil-CDK mix to fluid. The plastic index increased with the addition of cement kiln dust, this is due to the increase in cementitious property from cement kiln dust.

Therefore, the plasticity index reduced with increase in CKD content from 0% to 16%. This may be due to the replacement of the finer soil particles by CKD with consequent reduction in plasticity index (Miller et al;1997). Summary of Index properties of soil and soil mix is shown in Table 3.

Compaction reduces further settlement, increases shear strength and decreases permeability by placing soils in a denser state. Consolidation, permeability can be exhibited if the dry density and moisture content are controlled (Gidigasu, 1976).

The results indicate that between 0% and 16% CKD content, the MDD increased from $1.50 mg/m^3$ to $1.79 Mg/m^3$ respectively while the OMC decreased from 19.69% to 13.02, hence it is safe to say that MDD is inversely proportional to OMC. This is as a result of CKD occupying the void within the soil matrix. The compaction characteristic is shown in Table 4, Figure 1. Figure 2 and Figure 3 shows how the OMC and MDD is affected with the addition of CKD.

The most common and adaptive method or test required for the evaluation of strength of stabilized soil is Unconfined compressive strength (UCS). It is the main test recommended for the determination of the amount of additive required to be used in stabilization of soil (Singh and Singh 1991).

The Unconfined Compressive Strength increased from 0% to 8% CKD and decreased gradually from 12% to 16% CKD, the increase in the UCS is attributed to the formation of cementitious compound between CaOH present in the soil and the CKD, the decrease in attributed to the slowing down of the hydration process of Cement. A summary of the compressive strength characteristics is shown Table 5 and the relationship between the cement kiln dust and compressive strength is shown in Figure 4.

4. CONCLUSION

From the Evaluation of Strength Properties of Lateritic Soil Stabilized with Cement Kiln Dust, the following conclusions were drawn:

1. The Lateritic Soil obtained from Lapai-Gwari was classified as A-7-6 and CL an organic silts and organic clay of very low to medium plasticity according to AASHTO and USCS respectively.
2. Atterberg Limit Test was done at percentage of replacement method. The liquid limit decreased with the addition of CKD up to 8% and then increased slightly with further increase in the addition of CKD, Plastic Limit increased with addition of CKD ranges from 22.80% to 33.91%

while Plasticity Index reduced progressively from 22.2 to 11.09.

3. Compaction test was done at percentage of 0%, 4%, 8%, 12% and 16% of CKD using replacement method having Optimum Moisture Content between 13.02% and 19.69, also a Maximum dry density between 1.5g/cm3 and 1.79g/cm3.

4. Unconfined Compressive Strength was done at 0%, 4%, 8%, 12% and 16%, of CKD Compressive Strength increased with increase in CKD from 0% to 8%, then decreased progressively, Compressive Strength ranged between 170 kN/m2 to 511 kN/m2 8% of CKD replacement is gotten to be the Optimum compressive strength because it is more economical.

4.1 RECOMMENDATIONS

From the Evaluation carried out on the strength properties of lateric soil stabilized with Cement Kiln Dust, the following Recommendations were made:

1. Due to practical work on field where heavy weight of soil will be used, more research should be carried out using additional method instead of replacement method in order to ascertain the best percentage of CKD to add in such case.

2. The work can be furthered by implementing other soil parameters such as California Bearing Ration (CBR) and consolidation.

3. Cement kiln dust (CKD) can be used to improve Unconfined Compressive Strength (UCS) of soils. The improvement would make it more suitable and economical to use as stabilizer for sub-base and base course material in highway construction, thereby reducing construction cost.

4. Stabilization of other soil type in Nigeria for improvement with Cement Kiln Dust should be investigated.

REFERENCES

AASHTO (1986). American Association of State Highway and Transport Officials. Standard Specifications for Transport Materials and Methods of Sampling and Testing. 14th Edition, AASHTO, Washington, D.C.

ASTM, D - 698 (1992). American Standards Testing Methods. Standard Proctor Compaction Test of ASTM standards, Vol. 05.03, 1992. Philadelphia.

ASTM, D - 1557 (1992). American Standards Testing Methods. Modified Standard Proctor Compaction Test of ASTM standards, Vol. 05.05, 1992. Philadelphia

Abeln, D.L., Hastings, R.J., Scxhreiber, R.J., and Yonley, C. (1993).DetailedIllustration of Contingent Management Practices for Cement Kiln Dust,*Researchand Development Bulletin,* SP115T, Portland cement Association, Skokie, IL.

Aigbedion,I. (2007). Geophysical Investigation of Road failure using ElectromagneticProfile along Opoji-Uwenlenbo and Illeh in Ekpoma-Nigeria,*Middle –East Journalof Scientific Research 2(3-4) pp 111-1115.*

BS 1377 (1990). Methods of Testing Soils for Civil Engineering Purpose,*British StandardInstitution*, London.

Christophe, L., (1949). Les Laterites et leur Utilization Comme Materiau de Construction des Routes, Rev. Gen. des Routes et des Aerodromrs, Paris, France, No.212, 38-50.

Gidigasu, M.D., (1976)Laterite soil engineering: pedogenesis and engineering principles. Elsevier, Amsterddam

The Nigerian Society of Engineers
Minna Branch
1st NSE Minna Branch National Conference 2021

Conference theme
Role of Engineering in
Sustainable Development Goals

Hausmann, M.R.(1990). Engineering principles of ground modification, McGraw-Hill, Maidenheach.

Miller, G.A., Zaman M., Rahman, J., and Tan, K.N. (2003). Laboratory and Field Evaluation of Soil Stabilization Using Cement Kiln Dust, Final Report, No. ORA 125-5693, Planning and Research Division, Oklahoma Department of Transportation.

Okechukwu, P. A., and Celestine O. O., (2011): " Geotechnical Assessment of Road Failure in Abakalike Area, Southeastern Nigeria". International Journal of Civil and Environmental Engineering, Vol. II No 2 pp 12-24

Parson, R. L. and Kneebone E. (2004). Use of cement kiln dust for subgrade stabilization, Kansas Department of Transportation. Final Report No 364.

Singh G., Singh J., (1991): "Highway Engineering" Standard Publisher Distributions, Nai Sarak, India, pp 608-610

Talal, O.A., and Awad A.A., (1999) Experimental study on the utilization of cement kiln dust for ground modification. J. King Saud Univ (JKSU) 11:218-230

William, W.H., (2003): Encyclopedia of Physical Science and Technology (Third Edition)

The Nigerian Society of Engineers
Minna Branch
1st NSE Minna Branch National Conference 2021

Conference theme
Role of Engineering in Sustainable Development Goals

Development of A Low-Cost Briquette Making Machine

[1]Abdullahi A., [2]Abolarin. M. S., [3]Olugboji. O. A
[1,2,3]Mechanical Engineering Department, Federal University of Technology, Minna, Niger State
Corresponding Author: [1]abdoolkobbos2001@gmail.com

ABSTRACT

The work focuses on the development of a low-cost briquette making machine using Rice husks and Sugarcane baggase as selected materials. In developing this briquetting machine, mild steel was used in preference to other available materials because of its rigidity and strength to support the weight of the component parts put together, widely available, easily machined, improved surface finish and has low carbon content of about 0.15% - 0.25%.The developed briquette machine is based on power screw concept technique which operates in such a way that once the electric motor is plugged into an electricity source and it is switched on, the power being transmitted by the motor drives and rotates the screw shaft of the machine through the V-belt. As the power from the electric motor drives the shaft, it forces the screw shaft to rotate and force the prepared material either sugar cane baggase or Rice husks which has been properly mixed with binder to move into the briquetting die after the compression. The moment the compressed briquette comes out of the briquetting die, it then moved to the collection tray attached to the frame of the machine for proper collection of the briquettes to avoid being scattered. In evaluating the performance of the designed machine, the rice husks and sugarcane baggase were used with starch as a binder. The machine efficiency was found to be 66%. The calorific values of rice husks briquette and sugar cane baggase briquette were found to be 18.978MJ/kg and 15.578MJ/kg respectively.

KEYWORDS: *Rice husks, Sugar cane baggasse, Binder*

1.0 INTRODUCTION

Briquetting can be regarded as an attempt to link up two large and complex words: that of agriculture and that of fuel supply and use.

The realization that deforestation and wood fuel shortages are likely to become pressing problems in many countries has turned attention to other types of biomass fuel. Agricultural residues are, in principle, one of the most important of these. They arise in large volumes and in the rural areas which are often subject to some of the worst pressures of wood shortage.

However, residues are often bulky and difficult to burn so various conversion techniques have been developed. As the population of the world continues to grow, the demand for energy is becoming critical challenge for the world's energy leaders (Christoph, 2012). Global energy consumption has about doubled in the last three decades of the past century. In 2004, about 77.8% of the primary energy consumption was from fossil fuels (32.8% oil, 21.1% natural gas, 24.1% coal), 5.4% from nuclear fuels, 16.5% from renewable resources, of which the main one was hydro (5.5%) whereas the remaining 11% consisted of non-commercial biomasses such as wood, hay, and other types of fodder, that in rural-economies still constitute the main resource (BP-Amoco, 2005). With improvements in energy efficiency, it is expected that global energy demand doubles by 2050. This is the consequence of global population growth, global economic growth, continued urbanization, as well as the resulting increased demand on mobility and other energy dependent services (Christoph *et al.,* 2013).

The selected materials for making briquettes from this briquette making machine for rural areas are:
1. Rice husks
2. Sugar cane bargasse

Briquettes produced from briquetting of biomass are good substitute for coal, lignite, fire wood with numerous advantages. Briquetting is one of the alternative methods to save the consumption and dependency on fire wood, the densities of these fuels can be easily handled, transported and stored. (Jeng *et al.,* 2012)

2.0 MATERIALS AND METHODS
2.1 Materials

The materials used for the development of briquette making machine are;

(i) Mild steel (ii) Angle Iron (iii) Solid Shaft (iv) Barrel (v) Pulley (vi) Electric Motor (vii) Bearings (viii) Bearing house (ix) Rod (x) V-belt (xi) Bolts and Nuts

2.2 Methods

(i)   Development of a briquette making machine
(ii)   Preparation of selected materials such as Rice husks and Sugar cane baggase
(iii)   Mixing the selected materials with binder
(iv)   Production of briquette from two selected materials
(v)   Drying of the briquettes
(vi)   Briquettes storage

2.3   Preparation of Selected Materials

A known quantity of Sugar cane baggase and Rice husks were sourced from Sugar cane market, Wuya, along Mokwa road, Gbako Local Government Area, Niger State and Rice Mill at Ciriko Junction, Bida Niger respectively. The materials were carbonized and sieved in order to increase the surface area and to enhance the binding efficiency. 1 kg of each selected materials were mixed thoroughly with cassava starch together with 0.5 litre of water. The cassava starch was used as a binder because of the following reasons; it is easily accessible, it is cheap and burns lightly without smoke when used in required quantity. The sugarcane bagasse was carbonized which is shown in Plate I and then mixed with the binder prepared to put into the machine show in Plate II. This was also done for the rice husk which is shown in Plate III and IV.
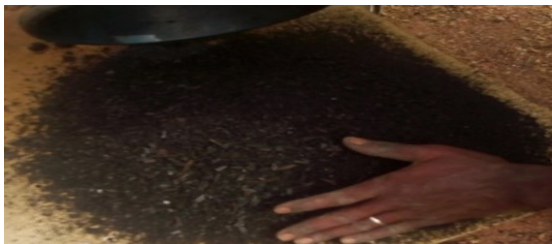

Plate I: Carbonized sugarcane bagasse

Plate II: Carbonized sugarcane bagasse mixed with binder

Plate III: Carbonized rice husk

Plate IV: Carbonized rice husk mixed with binder

2.4 Production process

The electric motor was connected to a power source and it was switched on then the prepared materials were poured into the hopper and as the electric motor drives the rotating screw shaft or conveyor, it forced the material into the briquetting die in which the compression took place. The compressed briquette being ejected from the die was cut with a knife and the process continues for another briquette production. After the production of the briquettes produced, they were sundried for used, in which the process is shown in Figure 2.4
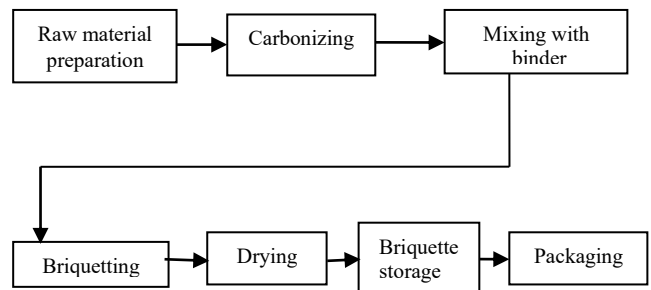

Figure 2.4: Schematic sketch of the process

The production process shown in plate V, the packaging process of the briquette produced shown in plate VI and the drying process of the briquette produced shown in plate VII.

Conference theme

Role of Engineering in Sustainable Development Goals

Plate V: Production process

Plate VI: Packing process of the briquette produced

Plate VII: Drying process of the briquettes produced

3.0 RESULTS AND DISCUSSIONS

3.1 Results

Table 3.1 and table 3.2 shown the Results drawn after testing for the chemical composition of the briquettes produced.

The proximate and ultimate analysis was employed for the test to know the constituents and calorific value of the briquettes produced.

Table 3.1: Proximate Analysis test

Proximate				
Sample	Moisture content	Ash content	Volatile Matter	Fix Carbon
Rice husks (%)	6.2	1.48	66.22	33.76
Sugar cane baggasse (%)	4.2	0.84	72.0	22.96

Table 3.2: Ultimate Analysis test

Ultimate					
Sample	Carbon	Hydrogen	Sulphur	Nitrogen	Oxygen
Rice husks (%)	59.34	4.0	0.2	1.04	35.42
Sugar cane baggasse (%)	54.92	6.0	0.3	0.86	37.92

The calorific values of Rice husks and Sugar cane baggase briquettes produced were 18.978MJ/kg and 15.578MJ/kg respectively using bomb calorimeter test at Central Service Laboratory, National Cereals Research Institute, Baddegi, Niger State-Nigeria.

3.2 Discussions

Proximate Analysis: The proximate Analysis classifies the briquette fuel produced in terms of its moisture content (M), volatile matter (VM), fixed carbon (FC) and ash content.

By comparison between the two results obtained from table 4.1 and 4.2 using proximate analysis, the rice husks briquette produced moisture content of about 6.2% and sugar cane baggase produced moisture content of 4.2%. These values were low and the effect on the calorific value were minimize. Therefore, the rice husks briquette produced high heating value and excessive energy not required for drying since its moisture content falls within the range of 5-15%.

Moisture content should be as low as possible, generally in the range of 5-15 percent. High moisture content will pose problems in grinding and

excessive energy is required for drying. (FAO, 1996).

Ultimate Analysis: The ultimate analysis generally reports the elemental Carbon (C), Hydrogen (H), Sulphur (S), Nitrogen (N), and Oxygen (O) very often by difference in solid fuel. From the table 3.2 of the ultimate analysis of rice husks briquette produced and sugarcane bagasse briquette produced validates the values stated for rice husks and sugar cane baggasse in the literature view; Stahl *et al* (2004). The values in brackets are from literature review (Stahl *et al*, 2004).

Table 3.2: Ultimate Analysis of rice husks briquette and sugarcane baggase

	Rice Husks	Sugar cane baggasse
C	59.34 (49)	54.92 (49)
H	4.0 (7)	6.0 (6)
O	35.42 (41)	37.92 (41)
N	1.04 (1)	0.86 (2)
S	0.2 (0-7)	0.3 (0-3)

4.0 CONCLUSION

The briquette making machine developed is based on power screw concept, and is suitable for the briquetting of the carbonized selected materials of rice husk and sugar cane baggase.

The machine developed is a technique which can be easily operated by a single person and machine is capable of producing briquettes from rice husks and sugar cane baggase.

Therefore, with availability of this developed machine technique, it will help in solving problems of waste management, environmental pollution, over dependent on fossil fuels, over dependency on fire wood which lead to deforestation problems through the conversion and recycling of Agricultural wastes to solid fuel.

REFERENCES

BP-Amoco, (2005). Statistical Review of World Energy.

Christoph. F (2012). Official publication of the World Energy Council to mark the World Energy leaders' Summit, Istanbul.

Christoph F. *et al.* World Energy Council (2013). World Energy issues monitor report, p. 2.

FAO, (1996). Food and Agricultural Organization of the United Nations Bangkok

FAO (2009). Biomass briquettes for Green Electricity Production, Briquetting of Agricultural waste for fuel: Food and Agriculture Organisation of the United Nations, Bangkok.

FAO (1990). The briquetting of agricultural wastes for fuel. Food and Agriculture Organization of the United Nations, Via delle Treme di Caracalla, 00100 Rome, Italy, pp 2-33.

Jeng S. L., Zainuddin A. M., Sharifah R.W., and Haslends A. (2012). A review on Utilization of Biomass from Rice Industry as a source of Renewable Energy, Vol. 16, Pp 3084-3094.

Stahl R., Enrich E., Gehrmann H.J., Vodegel S., and Coch M. (2004). Report prepared.